

LOUGHBOROUGH
UNIVERSITY OF TECHNOLOGY
LIBRARY

| | | |
|---------------------|------------|--|
| AUTHOR/FILING TITLE | | |
| FLETCHER, N | | |
| ACCESSION/COPY NO | | |
| 089718/01 | | |
| VOL NO | CLASS MARK | |
| | ARCHIVES | |
| | COPY | |
| FOR REFERENCE ONLY | | |

| | |
|-------------------------|-----------|
| Loughborough University | |
| of Technology | |
| Date | Nov. 76 |
| Class | |
| File No | 089718/01 |

CHAPTER 7

DISCUSSION OF THE EXPERIMENTAL WORK AND RESULTS

7.1 INTRODUCTION

In this chapter the discussion of the experimental work is undertaken in two parts. The first part covers the dressing of grinding wheels using single point diamond tools, in which the influence of the dressing variables on the dressing process and ensuing grinding wheel condition are discussed. In the second part, the influence of dressing conditions on the cylindrical grinding process are discussed for both rough and finish grinding. General conclusions drawn from the above discussion are stated in Chapter 8.

7.2 DISCUSSION OF THE GRINDING WHEEL DRESSING TESTS AND RESULTS

7.2.1 Tests 1 to 3 inclusive.

This series of tests was designed to investigate the effect of drag angle on dressing tool performance by observing the dressing action of the diamond tool through dressing force analysis.

Three components of dressing force were recorded, these being the radial (F_r), tangential (F_t) and axial (F_a) components of force being measured relative to the grinding wheel face and direction of rotation. From the tests conducted, the radial component of force was seen to be predominant, with a value of between 2 to 6 times that of the tangential component, (the highest force recorded being of the order of 4 Newton), and the axial component being of least significance. It was expected that F_a would be small in comparison with F_r and F_t since the ratio of the peripheral wheel speed to the cross-feed rate when dressing was in the order of 1,900:1 for the extreme conditions used, i.e. wheel diameter 305 mm, wheel speed 30 rev/sec and cross-feed rate of .5 mm/rev of grinding wheel.

Test 1.

The diamond used for this test is shown in fig. 6.2, and its orientation relative to the grinding wheel is depicted in fig. 2.5. At this setting it presented a cutting edge to the grinding wheel face which had a rake angle of -60 degrees for a drag angle of 0 degrees. As the drag angle was increased or decreased about this datum, the rake angle became more or less negative respectively. (The rake angle of the diamond is taken as being negative to conform with metal-cutting tool nomenclature.)

Fig. 7.1 shows the variation of the radial component of force with diamond drag angle (and rake angle). The four force curves are in the order of the test sequence, working from the bottom of the figure upwards. All the curves depicted are basically the same shape and show an initial reduction in force as the drag angle decreased from a maximum value of +15 degrees. In each case, at some particular value of drag angle the value of F_r increased sharply. After this point, for further decreases in drag angle, the dressing process was seen to become unstable due to diamond vibration. For each elevated force curve, the turning point occurred at a higher positive value of drag angle. This was due to the influence of wear on the diamond tip, which caused an increase in diamond area in contact with the wheel face. In fig. 7.1 the drag angle range has been divided into three regions, namely, a stable region in which the dressing process was stable and F_r increased for an increase in drag angle; a critical region which covers a narrow band of drag angle values in which the dressing process was stable and F_r was a minimum, and an unstable region in which the dressing process was unstable and F_r increased rapidly for further decreases in drag angle.

In order to analyse the dressing action of the diamond tool it is necessary to show the relationship between the diamond geometry and the dressing force.

Figs. 7.2 to 7.8 show the resolution of dressing

force for test 1. Although the diamond is shown as being sharp, a small natural flat was apparent at its tip. The figures (7.2 to 7.8 inclusive) show the effect of decreasing the value of drag angle in steps of 5 degrees from a starting point of +15 degrees. Two components of force have been resolved for each drag angle value that are normal to, and parallel with, the diamond cutting edge (rake face). These are termed F_n and F_p respectively. The second of these force components F_p shows the tendency for the diamond tool to be pushed away from, or drawn into the grinding wheel face. At a drag angle of +15 degrees there is a tendency for the diamond tool to be pushed away from the wheel face, thereby maintaining stable conditions. As the drag angle is reduced, both F_p and F_n are reduced in value until F_p becomes zero and F_n takes on a minimum value. At this point, F_n is equal in magnitude and direction to F_{res} , which is the vector sum of F_r and F_t . This condition corresponds to the critical region depicted in fig. 7.1. For a reduction in drag angle beyond this point, the diamond is drawn into the wheel face and the dressing process becomes unstable. At this critical point for this particular set of dressing conditions, the drag angle was between +5 to +10 degrees, and the rake angle was between -65 to -70 degrees.

The diamond wear which resulted from test 1. is shown in the upper half of fig. 7.9. It can be seen that the greatest amount of wear occurred when the diamond was subjected to drag angles in the range -5 to -15 degrees.

Test 2.

Test 2 was a continuation of test 1 with the cross-feed reduced from .5 mm/rev to .1 mm/rev, all other conditions remaining as before. This was done in an attempt to reduce the rate of diamond wear. The results of this test are used to show how the drag angle influences diamond tool wear, and the corresponding effect on dressing force.

Fig. 7.9 shows the mode of diamond tool wear for the same drag angle sequence used in test 1, with each dressing cycle repeated fifteen times. Two wear areas were noticed on the diamond, and are denoted by the letters A and B. As before, the dressing cycles using negative values of drag angle gave rise to increased diamond wear over and above that experienced when using positive values. This increased wear is possibly due to a combination of shock loading received by the diamond, and attrition. The greater wear area is denoted by the letter B. It is interesting to note that the angle subtended by the wear face A and a normal to the wear face B is approximately 69 degrees, and suggests that the line of contact between the two wear areas A and B corresponds to the critical point, where there is no sliding component of force acting on the rake face, i.e. $F_p = 0$. (The rake face at this point is the wear face A.) This condition occurs at a lower value of drag angle than was the case in test 1. This further suggests that a sharp diamond which is subjected to unstable conditions may become stable for the same conditions after it has become partially worn.

Fig. 7.10 shows the range of values of F_r and F_t obtained for the conditions stated above. It can be seen that the tangential component of force F_r , increased as the drag angle was reduced. Unlike the results shown in fig. 7.1, there is no turning point for F_r . This is because of the change in diamond condition, i.e. a transition from line or point contact to area contact as the diamond wore. Although there was an increase in F_r for any reduction in drag angle, the dressing process remained stable until a value of 0 degrees was reached. For further reductions in drag angle, unstable conditions again prevailed.

Values of the force ratio F_r/F_t , are shown in fig. 7.11, and vary from 3 to 6 as the drag angle was reduced from +15 to -15 degrees. The range 3 to 4.5 was obtained for stable conditions, whilst greater values

represent unstable conditions. This suggests that the higher force ratios are caused by a combination of two events, namely, an increase in wear area of the diamond tool, and diamond vibration. For the case of the sharp diamond (test 1), a force ratio as low as 2.5 was recorded for conditions in the critical region.

Test 3.

In test 3 a combination of four different grinding wheels were used in conjunction with two diamonds of different geometry, to test further the influence of drag angle (and rake angle) on dressing conditions. The diamonds used were classified as dodecahedrons and had included angles of 143 degrees and 95 degrees respectively, these being measured in the vertical plane. The diamonds were set so that for a drag angle of 0 degrees, the corresponding rake angles presented to the grinding wheel were -69 degrees and - 45 degrees respectively. Their orientations were such that the more obtuse angled diamond made point contact with the grinding wheel face, due to its well formed sharp point, whilst the other diamond presented a chisel edge to the grinding wheel, with the line of contact running in the horizontal plane across the wheel face. This setting is shown in fig. 7.16. The orientations were as depicted in figs. 2.5 and 2.6 respectively.

Fig 7.12 shows the variation of the radial component of force F_r , with drag angle (and rake angle) when dressing the four grinding wheels with the more obtuse angled diamond tool. The force curves shown are similar to those plotted in fig.7.1, except that the critical region is displaced by 5 degrees to the right. The curves are identified in the order of test sequence followed, and form a family of curves that increase in the same order. Since the grinding wheels having different grit sizes were used in a random order, it is reasonable to assume that the increases in force from curve to curve are due to diamond wear and not variation in the grinding

wheels themselves. For each elevated force curve, the turning point occurred at a higher positive value of drag angle, this being a trend similar to that depicted in fig. 7.1. It was also noticed when dressing, that instability occurred for drag angles less than 0 degrees.

Fig. 7.13 shows the variation of the radial component of force F_r , with drag angle (and rake angle), when dressing the four grinding wheels with the less obtuse angled diamond tool. The figure shows a rapid increase in force for each curve when the drag angle was reduced from the initial condition of +15 degrees, and the complete range of drag angles are depicted as giving unstable conditions. It was found in practice that when using this particular diamond, instability was encountered for all dressing conditions used.

This phenomenon is shown more clearly in figs. 7.14 and 7.15 in which the dressing force components F_r and F_t are resolved. Fig. 7.14 shows that minimum values of F_r and F_t occur for the more obtuse angled diamond when the resultant force $F_{res} = F_n$, and $F_p = 0$. This occurs for a drag angle of 0 degrees and corresponding rake angle of -69 degrees. For further reductions in drag angle, the diamond was drawn into the grinding wheel. This was seen to occur irrespective of the particular grinding wheel used. Fig. 7.15 shows that for any value of drag angle in the range used, there was a tendency for the less obtuse angled diamond to be drawn into the grinding wheel, as depicted by the force component F_p . Again, this occurred for all four grinding wheels. Values of the force ratio recorded for the more obtuse angled diamond were between 2.6 and 5.8, whilst those for the other diamond were between 3.1 and 6.9. These values are similar to the range established for the diamond used in the previous two tests. The results show that the radial component of force F_r , is influenced more by changes in drag angle than the tangential component F_t , this being due to the influence of drag angle (and rake angle) on diamond wear and instability.

This is in keeping with the observations made for test 2.

Diamond wear is depicted in fig. 7.17 for the more obtuse angled diamond, and figs. 7.16 and 7.18 for the other diamond. Considering fig. 7.17 first. This particular diamond was similar in form to that used in tests 1 and 2, and had the same orientation. In terms of angular presentation, a larger value of rake angle was apparent for the same drag angle setting. It can be seen that two wear flats were formed at its tip (front view), and that they correspond to those shown in fig. 7.9. This would suggest that similar dressing conditions prevailed in both cases, and that the analysis of the dressing action for the diamond in test 2 holds true for this diamond tool. When looking at the diamond in plan view, the wear faces were seen to run parallel to the grinding wheel face, i.e. parallel to the cross-feed motion. In fig. 7.18 it is seen that a single wear flat was formed at the tip of this diamond tool, resulting from the unstable dressing conditions encountered. A better view of this is shown in fig. 7.16, where it can also be seen that diamond flaking or attritious wear was apparent on the diamond rake face. Like the previous diamond, the wear face when viewed in plan runs parallel to the cross-feed motion.

One of the most important features of any dressing operation is the surface condition produced at the grinding wheel face, since this affects directly the surface finish of the ground component. Figs. 7.19 and 7.20 show the surface finish obtained on a plunge ground specimen, using a grinding wheel that had been dressed with both diamonds over the full range of drag angles. Fig. 7.19 shows the surface finish traces obtained for the more obtuse angled diamond tool. It can be seen that for the stable conditions encountered, i.e. +15 degrees to +5 degrees, a reasonably smooth surface was obtained. In the critical region, i.e. 0 degrees (verge of instability), the specimen surface showed signs of instability with occasional rifts in the surface. For drag angles of less than 0 degrees, instability was present and is

shown in the irregular surfaces produced. Fig. 7.20 shows the surface finish traces obtained for the less obtuse angled diamond. It is seen that all the traces produced show irregular surface patterns, which have high surface finish values. This was to be expected since all conditions produced instability in the dressing process.

It was noted when dressing in the unstable region that the wheel surfaces were penetrated to a depth of at least 150 μm by all the diamonds used. This depth is approximately equal to half the diameter of the grit sizes used in the grinding wheels. For these cases, the resulting surface damage to the grinding wheel would impair its ability to grind efficiently.

The results of these three tests would suggest that the rake angle presented to the grinding wheel face by the dressing diamond, is a more important parameter when considering the dressing action of the diamond tool, than that of drag angle. This finding will be discussed more fully in the summary (statement 7.3).

7.2.2 Tests 4 to 7 inclusive.

This series of tests was designed to investigate the effects of drag angle, diamond wear, in-feed and cross-feed on dressing force and grinding wheel surface roughness, when dressing four grinding wheels with an initially sharp diamond.

The tests covered a wide range of dressing conditions, involving a 5 x 5 matrix of in-feed and cross-feed values, with three values of drag angle. The dressing diamond used throughout this series of tests is shown in fig. 6.1, and was classified as an octahedron diamond. Its orientation relative to the grinding wheel was as depicted in fig. 2.5. At this setting it presented a cutting edge to the grinding wheel face which had a rake angle of -64 degrees for a drag angle of +5 degrees. This rake angle was modified as the diamond wore.

Test 4

A grinding wheel of the type 32A60-K8VBE, which had a relatively fine grit and an open structure, was used for this test.

Fig. 7.22 shows in a three dimensional form, the variation of the radial component of dressing force F_r with in-feed and cross-feed for all three values of drag angle used. It can be seen that increases in both in-feed and cross-feed brought about an increase in F_r for all values of drag angle, up to a maximum value of about 4.5 Newtons (1 lbf) for the most severe dressing condition tested. This force value is low compared with those obtained for the other tests in this series, and is accounted for by the fact that the diamond tool was initially sharp and presented a smaller area of contact to the grinding wheel than for the later tests. Variations in drag angle caused little overall change in the value of F_r , and the force trends were the same for each drag angle setting. This observation is explained by the fact that any increase in the value of F_r for the lower drag angle setting, due to instability in the dressing process, was balanced by an increase in F_r for the higher drag angle settings as the diamond wore.

Values of the force ratio F_r/F_t are shown in Appendix VI, pages 265 to 267 inclusive. These show that for low values of in-feed, the value of the force ratio dropped from around 3 to 2.2 as the drag angle was increased from +5 to +15 degrees, irrespective of the cross-feed value. This is explained by the fact that at the drag angle setting of +5 degrees, the diamond, which was in a sharp condition, presented a rake angle to the grinding wheel which gave unstable dressing conditions. Hence the observed reduction in the force ratio for an increase in drag angle suggests that more stable dressing conditions were brought into being. As the in-feed and cross-feed were increased at the higher drag angle settings, the force ratio also increased. This was a direct result of an increase in diamond wear.

Simplified diagrams showing the variation of

dressing force (F_r and F_t components) with cross-feed and in-feed are depicted in figs. 7.23 and 7.24 respectively. Values have been plotted for the +15 degree drag angle setting. It is seen from fig. 7.23 that a linear relationship exists between the dressing force and cross-feed rate (in-feed remaining constant), and that there is a family of curves ascending in the order of increasing in-feed. At the lowest cross-feed rate (.1 mm/rev) the diamond cut each grit at least twice, since the grit for the type of grinding wheel used can be considered to be approximately spheroidal in shape, and having a mean diameter of .25 mm. In the mid range (.3 mm/rev) each grit was cut once, and at the highest cross-feed rate (.5 mm/rev), the diamond missed each alternate grit. If the diamond is considered as only cutting the grits, it could be expected that the rate of increase of force with increase in cross-feed would decrease, or that the force would remain constant as the cross-feed exceeded the mean grit diameter. This is disproved as shown by the above linear relationship between force and cross-feed, and suggests that the diamond cut through both grit and bond at the same time. A further conclusion to be drawn is that the abrasive grits and bond considered at any depth from the wheel face are distributed in a uniform manner at that level, and that an increase in cross-feed rate causes a proportional increase in diamond-grit/bond contact. Fig. 7.24 shows that the relationship between dressing force and in-feed (cross-feed remaining constant) is non-linear, and that a family of "S" shaped curves exist, ascending in the order of increasing cross-feed. The shape of the force curves suggest that at the lower depths of cut ($< 7.5 \mu\text{m}$) the grit density was less than that encountered further into the wheel surface, i.e. a greater void density. This is highlighted by the fact that at the lower values of in-feed, the dressing force is seen to vary very little with changes in cross-feed rate. A further point of note is that for an increase in depth of cut (cross-feed constant) a point is

reached where the dressing force tends towards a plateau value, this being elevated for each higher cross-feed rate. The inference here is that a depth of cut was reached for each cross-feed rate at which an optimum value of dressing force was generated for splintering through the grit and bond around the dressing tool.

The above conclusion drawn from figs. 7.23 and 7.24 are upheld by the similarity in results obtained for the other tests in this series, as will be shown.

A substantial proportion of this test was devoted to the measurement of the grinding wheel surface condition after dressing, since this directly affects the grinding characteristics of the wheel, particularly at the start of grinding. Figs. 7.25 to 7.39 inclusive, show "Talysurf" traces of the grinding wheel surface roughness for each dressing condition covered, as represented by the surface of a plunge ground testpiece. (N.B. It had been noted in the past⁸ that a direct analysis of the wheel surface with stylus type instruments, after dressing, proved to be meaningless when analysing dressing parameters.) Figs. 7.25 to 7.29 inclusive, show surface roughness traces recorded when dressing with a drag angle of +5 degrees. It can be seen that when using the lower values of in-feed in conjunction with the first two cross-feed rates (.1 and .2 mm/rev), the surface finishes obtained were reasonably smooth and show no discernable signs of the diamond profile in them. A possible reason for this is that because the diamond was sharp and on the verge of instability when set at the +5 degree drag angle, rapid wear took place at the diamond tip for the initial dressing conditions, resulting in the ensuing surface profiles being representative of the pre-test wheel surface roughness. At the higher values of in-feed for the same cross-feed rates, the surface finish traces show much coarser profiles, having higher surface finish values. This suggests that the dressing action of the relatively sharp diamond had a splintering effect on the grit and bond, causing a random profile to be

generated. For an increase in traverse rate it is seen that a modified form of the diamond shape is discernable in the surface finish traces, particularly at the higher depths of cut.

Increasing the drag angle brought greater stability to the dressing process, and the "modified" diamond shape is seen with increasing clarity in the traces at both high and low cross-traverse rates, in either triangular or trapezoidal form (figs. 7.35 and 7.38).

The in-feed when dressing is shown to have a limited effect on the surface roughness depth (peak to valley height), as seen clearly at the higher cross-feed rates (figs. 7.29, 7.34 and 7.39), where an increase in depth of cut from 5 μm to 25 μm brought about changes in the surface roughness depth of approximately 5 μm . This was to be expected since initial rapid wear of the diamond at the +5 degree drag angle setting caused substantial blunting at its tip, hence increasing the possibility of diamond overlap for the range of cross-feed values used, and thereby causing a corresponding reduction in surface roughness height. Another possible reason for low peak to valley height values is that the nature of the abrasive is such, that the grits in the wheel surface remain obtuse after dressing, and present relatively shallow cutting points with which to grind.

Fig. 7.35 shows the limiting effect on dressed profile depth when assigning a low value to the cross-feed (.1 mm/rev), even when the diamond presented a relatively sharp cutting edge to the grinding wheel (sharp edge presented by the diamond when set initially at +15 degree drag angle). It is seen that at this cross-feed rate, increases in depth of cut from 5 μm to 25 μm produced little or no change in either the surface roughness depth or the corresponding value of average arithmetic roughness, R_a . This can again be attributed to the influence of diamond overlap as mentioned above.

To obtain an overall view of the effects of in-feed, cross-feed and diamond geometry on wheel surface

roughness when dressing, values of grinding wheel average arithmetic roughness have been presented in both tabular and graphical form in figs. 7.40 to 7.43 inclusive. The experimental results are presented in three tables in fig. 7.40 according to the drag angle setting, with an accompanying set of "equivalent" theoretical values. In figs. 7.41 to 7.43 inclusive, the experimental values are plotted in a three-dimensional arrangement with in-feed and cross-feed.

Figs. 7.41 to 7.43 show that whilst equations 3.5, 3.7 and 3.9 in chapter 3 give some indication of the effects of in-feed, cross-feed and diamond geometry on grinding wheel surface roughness (specimen values plotted in figs. 3.17 to 3.21 inclusive), the theoretical values calculated are far greater than those obtained in practice under similar dressing conditions. The main discrepancy lies in the fact that one of the four assumptions made in order to set up the initial equations has since been proved to be incorrect. This is the assumption that the dressed wheel takes on the same shape as the diamond tool producing it. Figs. 7.41 to 7.43 do not give a clear indication of the effects of in-feed, cross-feed and drag angle on grinding wheel surface roughness for the particular diamond used, but show a range of values of average arithmetic roughness that could be expected in practice. Fig 7.40 gives more meaningful information.

The "equivalent" theoretical values of average arithmetic roughness in fig. 7.40 have been calculated from parameters taken from actual "Talysurf" traces, by likening the traces to a series of equilateral triangles having a base length equal to the particular values of cross-feed considered, and a height equal to the mean peak to valley height of the particular profile. It is shown that by using the above method, values of average arithmetic roughness are obtained which are close to the recorded values. This analysis however, could not be used for the initial dressing conditions tried at the +5 degree drag angle setting because of the

irregular traces being recorded due to dressing instability.

To complete the analysis, values of the included angle (β) for each approximated triangular form seen in the surface roughness traces, have been calculated from the above information and entered into, fig. 7.40. These values of β show that the triangular "screw thread" form generated in the wheel surface for the majority of dressing conditions, was obtuse, with values in excess of 158 degrees even when the diamond was in a relatively sharp condition (the initial values of the included angle of the diamond being 94 degrees, measured in the horizontal plane). The trend, as seen from fig. 7.40, is that the greatest change in β occurred for an increase in cross-feed from .1 to .2 mm/rev, irrespective of the drag angle setting, and that for further increases in cross-feed up to .5 mm/rev, the value of β was increased up to a maximum value of 177.5 degrees. Increases in depth of cut from 5 μ m to 25 μ m for any cross-feed value caused a small decrease in the value of β .

These values of the included angle β considered in conjunction with the "Talysurf" traces (Figs. 7.28 to 7.39 inclusive) suggest that as the diamond tool ploughed through the wheel surface, the grit and bond on either side of the diamond dressing tool were dislodged as well as that immediately in front, even for those dressing conditions using high cross-feed rates with low depths of cut.

The final wear recorded for the diamond dressing tool at the end of test 4 is shown in fig. 7.21. It can be seen that two wear flats were generated at the diamond tip, as depicted in the profile view (2). The smaller wear flat was caused by the conditions operating at the +5 degree drag angle setting, and the upper wear flat, adjacent to the original diamond rake face, was caused by the conditions operating at the +10 and +15 degree drag angle settings, which gave the more stable dressing conditions. The wear faces as seen in plan view (2), run at a small angle to the cross-feed motion, and show that

for this particular diamond, most wear was encountered on the diamond's approach side to the grinding wheel.

Tests 5, 6 and 7

These remaining three tests in this series are discussed together, since the results from each test were similar in nature for each different grinding wheel employed. The diamond dressing tool was the same one as used in test 4 except that it was in a more worn condition at the start of test 5 due to intermediate use.

Figs. 7.44 to 7.46 inclusive, show in three-dimensional form, the variation of the radial component of dressing force F_r with in-feed, cross-feed and drag angle for the three grinding wheels used.

The general trend depicted is that increases in both in-feed and cross-feed brought increases in dressing force F_r , up to a maximum value of about 13 Newtons (approx. 3 lbf), with an overall difference in force between any of the grinding wheels used being of the order of 3.5 Newtons (.7 lbf) for the same maximum cross-feed and in-feed values. Since this was the difference recorded for two similar wheels (46 grit) dressed with the same diamond under different wear conditions, it is reasonable to assume that the difference in force readings were due more to differences in dressing conditions than in wheel characteristics.

Increases in drag angle from +5 to +15 degrees caused reductions in dressing force F_r to be recorded for all three grinding wheels, particularly for the higher values of in-feed and cross-feed used. This trend is best explained with reference to fig. 7.21, which shows the diamond wear at the end of each test. It can be seen from the diamond profile views that as each dressing test progressed, the wear flat generated at the lowest drag angle setting of +5 degrees, increased more in size relative to that generated for the two higher settings. This may be due to a combination of the diamond's natural wear characteristics, and increased

dressing stability as the drag angle was increased. The greatest change in dressing force F_r , due to changes in drag angle, is seen in fig. 7.46, where the maximum force recorded for the final test in this series at the +5 degree setting was approximately 1.8 times that of either of the forces recorded at the +10 and +15 degree settings, these being of almost equal value. This result is explained by referring to fig. 7.21 again, where it is seen for the final diamond condition in profile (5), that the wear flat generated at the +5 degree drag angle setting covered almost the entire diamond tip, whilst that for the +10 and +15 degree drag angle setting was small in comparison. The views of diamond wear in plan show that as the dressing tests progressed, the wear faces changed from being at a slight angle to the cross-feed motion (on the diamond's approach side to the grinding wheel) to being parallel with it. The overall reduction in dressing force F_r in test 7 (fig. 7.46) as compared with tests 5 and 6 (figs. 7.44 and 7.45 respectively) may be due in part to the influence of a flaw uncovered in the main wear face, which increased in size during test 7. The upper edge of the flaw (which ran diagonally across the wear face) is seen at the bottom side of the wear face in plan views (3), (4) and (5).

Figs. 7.44 to 7.46 inclusive, show similar trends to those seen initially in figs. 7.23 and 7.24, from which the relationships between in-feed and cross-feed with the dressing force component F_r were drawn for test 4. The force component F_r is again seen to have increased linearly with increases in cross-feed (in-feed constant), and non-linearly with increases in in-feed (cross-feed constant), this being the same for all tests conducted. The families of curves produced for increases in one parameter, the other being held constant, are of the same form as those shown for test 4, irrespective of wheel grit size (46 and 60 grit used) or increases in diamond wear. This suggests that the analysis made of dressing force with changes in cross-feed and in-feed

for test 4 (page 154) holds true for tests 5, 6 and 7.

Values of the force ratio F_r/F_t , which are tabulated in Appendix 1V pages 268 to 276 inclusive, for tests 5, 6 and 7, show that the variation in the force ratio for each test is smaller for changes in drag angle and cross-feed than for changes in in-feed; with a range of values of between 2.6 to 3.8 being recorded. In general, increases in force ratio were due to increased diamond area of contact through wear (influenced by drag angle), and increased diamond-grit/bond contact (influenced by in-feed and cross-feed). The average force ratios recorded of F_r/F_a were in the range of 18:1 up to 40:1, showing that the axial component of force F_a was small in comparison with F_r and F_t . The above range of values were recorded for stable dressing conditions.

The influence of in-feed cross-feed and drag angle on grinding wheel surface roughness when dressing were again represented by "Talysurf" recordings made of the plunge ground surface of a test piece (plastic strip) after wheel dressing. A selection of these traces from tests 5, 6 and 7 are shown in figs. 7.47 to 7.57 respectively.

At the lower drag angle setting of +5 degrees a greater wear area of the diamond dressing tool was presented to each grinding wheel, with the result that fairly smooth surface finish traces were obtained at the lowest cross-feed rate (.1 mm/rev) for any in-feed value, particularly in test 5 (fig. 7.47) in which the finer 60 grit wheel was used. Similar conditions for tests 6 and 7 (figs. 7.50 and 7.53) caused rougher surface finishes due to the coarser 46 grit wheels being used. At the same drag angle setting and the highest cross-feed rate (.5 mm/rev), the diamond shape was again discernable in the surface roughness profiles in a modified form (fig. 7.57). These traces also show that the coarser 46 grit wheels sustained deeper profiles (peak to valley height) than the finer 60 grit wheel under similar dressing conditions.

As the drag angle was increased in value, the

diamond shape was seen more clearly in the surface roughness profiles, even at the lowest value of cross-feed (fig. 7.54). This was due to the diamond tool presenting a smaller wear area to the grinding wheel at this setting. It can be seen from fig. 7.54 that increases in depth of cut produced little effect on the peak to valley height values of the wheel profiles (and corresponding values of average arithmetic roughness), even for the "sharper acting" diamond condition. This again highlights the limiting effect of low cross-feed rates on grinding wheel surface roughness, irrespective of depth of cut. As the tests progressed, the initial "sharp acting" condition of the diamond at the higher drag angle settings was cancelled out by the increasing diamond wear, and the "modified" diamond shape seen in the "Talysurf" traces became more obtuse, with increases in profile apex angle from 165 degrees (fig. 7.54) to 174 degrees (fig. 7.55). (N.B. The apex angles as depicted in the surface roughness profiles can be misleading, since the ratio of the vertical to the horizontal magnification is 40:1).

It can be seen again by reference to the surface roughness profiles, that throughout the tests, the in-feed had limited effect on surface roughness, even at the highest cross-feed rate of .5 mm/rev. (figs. 7.49, 7.52, 7.56 and 7.57) with a maximum depth of profile of 15 μm being recorded for a depth of cut of 25 μm (fig. 7.52) when using the A46KV grinding wheel. This was due in part to the obtuse geometry of the diamond tool, caused by wear; and was probably affected by the way in which the grit fractured when dressed, this being a natural characteristic of the grit itself.

In order to see the overall effects of in-feed, cross-feed and drag angle on grinding wheel surface roughness for tests 5, 6 and 7, values of average arithmetic roughness have been presented in a similar manner to that in test 4, in both graphical and tabular form in figs. 7.58 to 7.69 inclusive.

In the tables of results (figs. 7.58, 7.62 and 7.66), experimentally obtained values of grinding wheel average arithmetic roughness have been presented in three tables per figure according to the drag angle setting, and are accompanied by sets of "equivalent" theoretical values. These were calculated on the basis that the surface roughness profiles were composed of a series of triangular forms (modified diamond shape), whose base length was equal in value to the cross-feed rate considered, and height equal to the average peak to valley height of the particular profile. Also tabulated is the profile apex angle β , which was an approximate theoretical value of the included angle of each triangular form

From the tables of results it can be seen that the theoretical and experimental values of average arithmetic roughness compare favourably with each other for all three sets of results, showing that the theoretical analysis of wheel surface roughness derived from test 4 and applied here is a good approximation to the real situation. The trend shown by the changes in the calculated values of β is similar for each test and compares well with that seen in test 4 for the stable dressing conditions. This is that increases in cross-feed in the range .1 to .5 mm/rev (in-feed constant) caused increases in the value of β in the range 163 degrees to 178 degrees, with the greatest increase occurring at the lower values of cross-feed. This range of values quoted for β is a collective range for tests 5, 6 and 7. The above trend is seen to a lesser degree for test 5 (60 grit wheel) at the lower drag angle settings, than for tests 6 and 7 (46 grit wheels). The increase in β , as seen for all tests, gives credence to the earlier postulation that increases in cross-feed (in-feed constant) caused greater sideways grit/bond cleavage by the dressing diamond. Variations in in-feed had less influence on β than cross-feed, with increases of between 1 to 4 degrees being recorded in the above mentioned range for reductions in in-feed from 25 μm to 5 μm .

In general it can be seen that the sharp condition of the diamond existed for a relatively short period of time (test 4), and that the values of $\sqrt{3}$ evaluated when the diamond was sharp, and operating under stable dressing conditions, varied very little with those evaluated when the diamond was blunt (tests 5, 6 and 7).

Figs. 7.59 to 7.61, 7.63 to 7.65 and 7.67 to 7.69 show in a three dimensional form, the variation of grinding wheel surface roughness with in-feed, cross-feed and drag angle, and supplement the tabulated results. These figures give a much better indication of the effects of the above dressing variables on wheel surface roughness than those plotted for test 4. This is most probably due to the change from semi-stable conditions encountered in test 4, for the initially sharp diamond, to the fully stable conditions of the latter three tests, when the dressing diamond had become worn.

The above figures show clearly the tendency of the lower cross-feed rates (.1 and .2 mm/rev) to limit the values of wheel surface roughness irrespective of in-feed, drag angle, diamond condition or wheel type (grit size), as seen by the low plateaux depicted for each test. A similar trend is shown to a lesser degree, for changes in the cross-feed rate at the lowest in-feed value (5 μm), where again, lower values of surface roughness were recorded than for other conditions. In general, increasing the values of in-feed and cross-feed above 5 μm and .2 mm/rev respectively, caused increases in wheel surface roughness. The exception is seen in test 5 (60 grit wheel) at the lowest drag angle setting where increases in cross-feed and in-feed caused little change in values of surface roughness.

The effect of changes in drag angle on wheel surface roughness is less evident than that of in-feed and cross-feed, as shown by the variations in trend from test to test. As stated previously, changes in drag angle had little effect on surface roughness at the lower values of in-feed and cross-feed, but did appear to have some

effect at the higher values of these two variables. The results of test 5 (60 grit wheel) showed an increase in average arithmetic roughness from $1.70\text{ }\mu\text{m}$ to $2.73\text{ }\mu\text{m}$ for an increase in drag angle from $+5$ to $+15$ degrees, whilst test 6 (46 grit wheel) showed a decrease from $3.82\text{ }\mu\text{m}$ to $2.18\text{ }\mu\text{m}$ when using the same range and sequence of drag angle values. The conclusion to be drawn is that once the dressing diamond had become worn, changes in drag angle influenced the wheel surface roughness in as much, as greater or lesser worn areas of the diamond tool were presented to the grinding wheel.

From the values of average arithmetic roughness recorded for tests 5, 6 and 7 it is seen that at the lower end of the scale, i.e. $.75\text{ }\mu\text{m}$ to $1.1\text{ }\mu\text{m}$, values varied very little within each test, whilst at the higher end of the scale, i.e. $1.70\text{ }\mu\text{m}$ to $3.82\text{ }\mu\text{m}$, values varied considerably for similar dressing conditions. Overall, higher values of average arithmetic roughness were recorded for the coarser grit wheels (46 grit) than for the finer grit wheel (60 grit).

7.2.3 Test 8.

This test was designed to investigate the effects of in-feed and cross-feed on dressing force and grinding wheel surface roughness, when dressing the four grinding wheels with a blunt diamond, at a fixed value of drag angle. The test procedure followed the same pattern as that for tests 4 to 7 inclusive, and the results are presented in a similar manner.

The diamond dressing tool used, had a large wear flat at its tip, which covered an initial area of approximately 1.2 mm^2 before the start of the test. This was considered as being the limit of useful life for a dressing diamond before it was either reset or discarded. Views of the diamond showing its condition before and after dressing are depicted in figs. 7.70 and 7.71. The original worn face was presented parallel to the grinding wheel face for a drag angle setting of $+5$ degrees, and was seen to remain in a "polished" condition throughout

the test, with very little sign of wear occurring on it. The majority of wear which did occur, took place on the diamond rake face and at the trailing edges relative to the cross-feed motion. This was seen in the form of diamond flaking and was probably caused by a combination of attritious wear and vibration. It was found necessary to play coolant onto the tip of the dressing tool throughout the test, since the diamond was seen to glow "white" hot when dressing without coolant. This suggests that the friction generated between the grinding wheel face and the dressing tool was quite considerable.

The variation of dressing force (F_r and F_t components) with in-feed and cross-feed for the four grinding wheels used, is presented in a three-dimensional form in figs. 7.72 to 7.75 inclusive. The trends shown for each grinding wheel are similar and will be discussed collectively.

It is seen that variations in the depth of cut had a greater influence on the magnitude of the dressing force generated, than variations in the cross-feed rate, and was due in part to the obtuse nature of the dressing diamond. At each depth of cut, the dressing force increased marginally in value as the cross-feed was increased from .1 to .5 mm/rev. This suggests that a constant area of contact existed between the grinding wheel and diamond, producing a constant pressure for each in-feed value which was not affected by changes in cross-feed. Increases in depth of cut from 5 μ m to 25 μ m (cross-feed constant) caused substantial increases in dressing force, with final values of between 17 to 20 Newtons (3.8 to 4.5 lbf) being recorded for the four grinding wheels used. The maximum diamond width in contact with each grinding wheel was of the order of 1.6 mm, which corresponds to an average linear grit contact of between 4 to 5 for the 60 grit wheels, and between 3 to 4 for the 46 grit wheels, and explains to some extent why little overall variation in force was noticed from wheel to wheel.

The curves depicting the increase in dressing force for increases in depth of cut are similar to those first shown in test 4 (fig. 7.24), where the greatest increase in force was seen for changes in depth of cut at the lower end of the scale used. Similarly, the rate of increase of force at the higher depths of cut was again seen to diminish as before. These trends uphold the earlier speculation that, firstly the grit density was greater just inside the wheel surface compared with that at the wheel periphery; and secondly that as the depth of cut was increased, the force required for rupturing the grit and bond at the wheel face tended towards a plateau value.

Values of the force ratio F_r/F_t are tabulated in Appendix IV, pages 277 to 280 inclusive for the four grinding wheels used, and show that as the in-feed was increased from 5 μm to a maximum value of 25 μm , the force ratio increased in value from 4 to 6. The direction in which the resultant force acted, as derived from these ratios, was at an angle of between 76 and 81 degrees to the plane of dressing, which suggests that the mode of grit/bond removal was predominately one of crushing as the in-feed was increased. The force ratio derived for each depth of cut changed little in value as the cross-feed was increased from .1 mm/rev up to .5 mm/rev, and was to be expected for the prevailing condition of a constant contact area between the grinding wheel and dressing diamond.

The "as-dressed" condition of the four grinding wheels has been presented in two ways to show the effects of diamond shape (degree of bluntness), and in-feed and cross-feed on wheel surface roughness. Figs. 7.76 to 7.79 inclusive show a selection of "Talysurf" traces of wheel surface roughness which were obtained in the same manner as those for the previous tests. All the traces show that the profiles produced were of a random form in which the diamond shape was not discernable, and was caused by several grits being dressed at once by the

blunt diamond. Although vibration was present throughout the dressing cycles, the surface roughness was not so pronounced as that obtained for the sharp diamond in test 4 (figs. 7.26 and 7.27 at the higher in-feed values), and suggests that the large wear face of the blunt diamond was responsible for this.

The variation of average arithmetic roughness for changes in cross-feed and in-feed are depicted in three-dimensional form for all four grinding wheels in figs. 7.80 and 7.81. It is seen that the in-feed and cross-feed had limited effect on surface roughness when dressing with the blunt diamond, particularly for the A46KV and A60KV grinding wheels, where values of average arithmetic roughness varied in the ranges $1.10\text{ }\mu\text{m}$ to $1.28\text{ }\mu\text{m}$ and $.70\text{ }\mu\text{m}$ to $.98\text{ }\mu\text{m}$ respectively. At the lower in-feed and cross-feed settings there was a tendency for lower surface roughness values to be recorded for the 38A46-K5VBE and 32A60-K8VBE grinding wheels than at the higher settings, with values ranging from $.78\text{ }\mu\text{m}$ to $1.43\text{ }\mu\text{m}$ and $.35\text{ }\mu\text{m}$ to $1.25\text{ }\mu\text{m}$ respectively. In general, the 60 grit wheels displayed lower surface roughness than the 46 grit wheels, for similar dressing conditions, as would be expected.

7.2.4 Test 9.

This test was designed to investigate the effects of the continual dressing of a grinding wheel over a long period of time on dressing force, diamond wear, volume of grinding wheel dressed away and wheel surface roughness when the diamond was initially set to dress in the critical region at a fixed depth of cut and traverse rate.

The dressing diamond, which was sharp at the start of the test, was classed as an octahedron diamond and was presented to the grinding wheel in the manner depicted in fig. 2.6, such that its rake face was set at a rake angle of -69 degrees, this corresponding to a drag angle of $+15$ degrees for this particular diamond. Profile and plan views of the diamond are shown in fig. 7.82. A 46 grit grinding wheel was chosen in preference to a

60 grit wheel as it was felt that the coarser grit would show variations in wheel surface roughness better than the finer grit, this being based on the results of the previous experiments. The cross-feed was maintained constant at .1 mm/rev thus ensuring that diamond overlap would occur during the initial stages when the diamond was sharp. This was to prevent in-feed build up on successive cuts, which might have led to dressing instability. An average depth of cut was chosen of 12.5 μm (.0005 in.), which remained constant for each dressing cycle.

The resolution of dressing force is shown in Fig. 7.83, where the initial and final force readings are depicted in vector form relative to the diamond and the plane of dressing. This analysis shows that stable dressing conditions prevailed throughout the test, with the diamond tending to be pushed away from the wheel face. The directions of the force components (F_p and F_n) as depicted for the final stage of the test is rationalized in fig. 7.82, in which the wear face generated at the diamond tip is shown to lie at an angle of approximately 3 degrees to the plane of dressing, giving a radial penetration into the wheel face equal to the depth of cut. This suggests that at this stage of the test, grit/bond fracture took place along this face and was totally independent of the original rake face. The force ratio F_r/F_t (tabulated in Appendix VI page 281), was seen to increase steadily from a value of 2 for the initial sharp diamond condition to a value of 4.8 after the completion of 300 passes when the diamond had attained a wear area of .348 mm^2 , and suggests a possible change from grit/bond removal by splintering to that of crushing as diamond wear increased.

The effect of the cross-feed rate on diamond wear is seen in the plan view of fig. 7.82 in the form of a step generated in the rightward side of the wear face. This phenomenon, however, did not occur at the leftward side, even though dressing was conducted in both cross-feed directions, and the wear face, considered overall, was seen to run parallel with the cross-feed motion. This

step did not appear to affect the relationship between the radial component of force and the generated wear area as seen in fig. 7.84, in which the dressing force is shown as increasing in direct proportion to the diamond wear. The resulting pressure between the dressing diamond and the grinding wheel is tabulated in fig. 7.85, and remained approximately constant throughout the test, with a mean value of $21.2 \mu\text{Pa}$ (1.35 Tons/in^2). This was to be expected since the grinding wheel had a high grit density (low structure number) and was dressed at a low traverse rate ($.1 \text{ mm/rev}$).

The changes in wheel surface roughness for increasing diamond wear is given in both qualitative and quantitative form in figs. 7.86 and 7.87 respectively. In fig. 7.86 the as-dressed surface roughness of the grinding wheel is represented for all dressing conditions by the equivalent surface roughness of a plunge ground test piece. After the 1st pass of the initially sharp diamond, its shape was easily detected in the "Talysurf" trace, and gave an equivalent triangular form having an apex angle of 171 degrees, as compared with the diamond included angle of 110 degrees, this result comparing favourably with those obtained for similar conditions in tests 4 to 7 inclusive. After the 10th pass, the diamond shape was hardly discernable in the "Talysurf" trace, and from the 25th pass onwards, the surface roughness profiles were of random form, and were independent of the diamond shape. (N.B. At the 25th pass, the wear area generated was approximately 36% of that at the 300th pass). It is seen in fig. 7.87 where values of average arithmetic roughness are plotted against the number of diamond passes, that the maximum variation in surface roughness was of the order of $.27 \mu\text{m}$, with an average value of $1.26 \mu\text{m}$. The greatest changes were seen in the initial stages of the test, e.g. up to the 50th pass, and suggest as stated earlier, that grit/bond fracture caused by the relatively sharp diamond was probably brought about by splintering as opposed to crushing. After the 50th pass when the

diamond had a substantial wear face, the values of average arithmetic roughness were seen to vary very little, which suggests that grit/bond fracture in this case was the result of crushing. See figs. 7.82 and 7.83.

An important parameter in any dressing operation is the rate of diamond wear for the particular dressing conditions, since this directly affects the amount of useful wheel dressing that can be accomplished before the diamond tool becomes unusable. In fig. 7.88 the volume of diamond wear has been plotted against the number of diamond passes, along with the ratio of the volume of wheel dressed away to the volume of diamond worn away in the same time. It is seen that as the number of diamond passes increased, the initial rapid rate of diamond wear decreased as would be expected for reasons stated by Pahlitzsch⁵, these being related to the diamond's geometry and physical properties. The more practical dressing ratio shows that after an initial period of rapid increase in value, lasting for the first 25 passes, a linear relationship existed for the remaining 275 passes during which time the volume of diamond wear reduced relative to the volume of grinding wheel dressed away. At the end of the test, the dressing ratio approached a value of 2.8×10^6 for a diamond wear area of $.35 \text{ mm}^2$, this being equal to a third of the diamond's estimated useful life (maximum value of 1 mm^2), and highlights the diamond's resistance to abrasion when set relative to the grinding wheel for dressing in the stable region. It is expected that the dressing ratio would vary in value according to the prevailing dressing condition.

7.3 SUMMARY OF THE DRESSING TEST RESULTS

The results of the experimental work have shown the importance of dressing force measurement both as a tool in assessing the variables associated with the dressing process, and as a means of analysing the dressing process itself. Prior to this research, little evidence could be found of any notable work in which dressing force had

been used to any great extent, and for the limited cases found, conflicting views were put forward. Pahlitzsch⁶² cites work conducted independently by Taher and Schwartz concerning the magnitude of dressing force, in which Taher stated that the ratio between the radial and tangential force is between 2 and 4, whilst Schwartz found much greater ratio values. Pahlitzsch concluded that further work was necessary to elucidate their differences.

The results of this work have shown that both Taher and Schwartz were correct, and that the force ratio is dependent in the first instance on the diamond presentation to the grinding wheel, and the diamond condition, i.e. sharp or blunt, as these factors affect the dressing force through both increased diamond wear and dressing instability.

The following conditions have been proven:-

1. For a sharp diamond presented to the grinding wheel such that dressing is conducted in the critical region, $F_r/F_t \geq 2$.
2. For the same diamond presented in the stable region, and depending on diamond wear, $F_r/F_t \leq 4$.
3. For the same diamond presented in the unstable region, and depending on diamond wear and degree of instability, $F_r/F_t \leq 7$.
4. For a very blunt diamond (approx. wear area of 1 mm^2) presented in the stable region, $F_r/F_t \leq 6$.

In terms of importance, the radial component of force was predominant with a value of between 2 and 7 times that of the tangential component, and the axial component of force was least significant with a value of between .025 and .1 times that of the radial component.

The values of force generated whilst dressing, depended very much upon the stability of the process, the diamond condition, and the cross-feed and in-feed values (and possibly the wheel properties, e.g. bond hardness etc., although no significant difference was noticed between the 46 grit and 60 grit wheels), with a maximum individual value of 20 Newtons (4.5 lbf) being recorded for a blunt

diamond having a wear area of 1 mm^2 . It is thought that as the force ratio increased due to diamond wear, the dressing action of the diamond tool changed from one of splintering the grit and bond, to one of crushing.

Due to a lack of information on the subject, the overall force range obtained for this research cannot be compared directly with similar work, but can be compared with results obtained from work conducted in the field of dynamic and static hardness testing of grinding wheels. Peklenik et al.,^{63,64} have measured the force required to shear grit and bond material away from the body of a grinding wheel using a vee-shaped tool which was traversed over the wheel face at a small depth of cut of approximately one grit diameter. From their research, they found that the force required to shear the grit from a 46 or 60 grit wheel of K hardness, was of the order of 18 to 27 Newtons (4 to 6 lbf) which compares favourably with the above result for dressing force. Although their form of testing was done under quasi-static conditions, Colwell et al.,⁶⁵ who conducted similar work, found that crushing force varied very little with change in wheel peripheral speed from an initial static condition, hence justifying the above comparison.

Analysis of the forces acting on the diamond during dressing has shown the need for an unambiguous definition of the geometry which at the present time is somewhat inadequately covered by the term "drag angle". This is defined as the angle between the axis of the diamond holder and a radial line passing through the point of contact with the wheel face. What is important, is the angle between the upper surface of the diamond (rake face) and a radial line passing through the point of contact with the wheel face. This is defined as "rake angle". Thus it may be said that "drag angle" takes no account of the variable geometry of the dressing diamond, which has been found to be an important factor influencing diamond wear and dressing stability.

It has been shown that three dressing regions exist which may be classified according to the angle of presentation between the diamond and the grinding wheel, i.e. rake angle, and that this angle itself is modified by the onset of diamond wear. The most efficient dressing was conducted in the critical region with a sharp diamond at a rake angle of between -65 to -70 degrees, this giving stable conditions. For higher rake angles, i.e. more negative values, dressing was conducted in the stable region but with higher forces; and for lower rake angles, i.e. less negative values, dressing became unstable with the diamond digging into the wheel face. It was seen that in the critical region, the resultant force and the force normal to the rake face were coincidental with no sliding component along the rake face, and that a force ratio (F_r/F_t) of the order of 2 to 2.8 existed. To explain this, it is necessary to consider the grit shape and its reluctance to cleavage. It has been suggested by many researchers^{33,43,45} that the grit in the wheel face presents rake angles of between -30 to -60 degrees or higher, showing that there is a general agreement that the grits have high negative values of rake angle. If the rake angles of the grit and dressing diamond were coincidental in the critical region, then grit cleavage may have occurred instantaneously on contacting the diamond rake face without sliding taking place. Another possible explanation can be drawn from work conducted by Graham and Rubenstein⁶⁶ in which the grinding grit has been likened to a wedge, the base of which is held in the wheel by the bonding material. Although this work was on grinding, the conditions were analogous to the dressing situation. They suggest that for a low force ratio, it is highly probable that tensile stress exists on the grit rake face causing fracture failure to occur at a high rate, even for a relatively small magnitude of tensile stress. For higher force ratios there is less likelihood of tensile stress existing within the grit, and hence a greater reluctance of the grit^{to} fracture. This condition may have existed

in the unstable region where very high force ratios were evident, resulting in grit/bond rupture to a depth 12 times greater than the original depth of cut.

These findings show the importance of correct presentation of the dressing tool to the grinding wheel, particularly where shaped single point diamonds are to be used, since rapid wear through unstable conditions will occur for incorrect settings.

Relationships between in-feed, cross-feed and dressing force have been established from which inference has been made concerning their influence on the dressing process within the confines of the conditions tested.

It has been shown that a linear relationship existed between the cross-traverse rate and the force generated when dressing grinding wheels of the same bond hardness and different grit size; and that the constant of proportionality was governed by the degree of bluntness of the diamond, and the volume of grit encountered at different depths of cut.

The relationship between in-feed and dressing force established for the above grinding wheels has been shown to be non-linear, with a decaying increase of force for increase in depth of cut. Similar trends were observed for both sharp and blunt diamonds operating over the same range of cross-feed rates.

The results of the work conducted into assessing the relative importance of cross-feed and in-feed in wheel dressing have shown that cross-feed has a greater influence on wheel surface roughness than in-feed, and corroborates the earlier findings of other researchers^{2,3,4,8,19,20}. At low traverse rates (.1 mm/rev) the roughness depth (peak to valley height) was limited by diamond overlap with only marginal changes occurring as the in-feed was increased; whilst at high traverse rates (.5 mm/rev) the roughness depth was limited by the obtuse nature of the grits after dressing, with maximum measured values equal

to half the in-feed value being recorded. Similar trends were seen for both sharp and worn diamond conditions.

It has been shown that the action of a grinding wheel dressed with a sharp or part worn diamond tool produced a saw-tooth profile on a plunge ground workpiece which could be likened to a series of triangular forms of base length equal to the cross-feed rate, and height equal to the mean peak to valley height of the profile considered. Values of profile apex angle based on the triangular forms, showed that variations in drag angle within the stable region, and changes in diamond condition, had limited effect on surface roughness for the same in-feed and cross-feed settings.

Information derived from the above analysis coupled with grinding data, has enabled equations to be formulated from which the surface roughness of a cylindrically traverse ground workpiece can be predicted with reasonable accuracy, this being verified from grinding results.

An overall review of the factors influencing diamond wear has revealed that most wear occurred for diamonds presenting rake angles of less than -69 degrees to the grinding wheel, and that wear was reduced as the rake angle was increased above this value, i.e. greater negative values. It was seen that wear at the diamond tip was rapid even for stable conditions, and that the wear faces generated were either parallel to the cross-feed motion and direction of wheel rotation, or formed at some small angle to them, i.e. < 3 degrees, with greater wear at the leading edges.

It is thought that the nature of the diamond wear was basically one of attrition for the stable dressing conditions, and attrition coupled with diamond chipping for the unstable conditions caused by non-preferred diamond settings, and large wear areas being presented to the grinding wheel.

7.4 DISCUSSION OF THE CYLINDRICAL GRINDING TESTS AND RESULTS

7.4.1 Tests 1 to 4 inclusive.

This short series of grinding tests was designed to investigate the effects of cross-feed (traverse rate) in grinding, on the volume of wheel wear encountered for a set volume of metal removed, and hence determine grinding ratio; and its effects on wheel and workpiece surface roughness for constant dressing and grinding conditions. From the results of these four tests, the value of cross-feed in grinding and test duration (volume of metal removed) were decided for the programme of "rough-grinding" experiments.

The diamond dressing tool chosen for this series of tests and for the "rough-grinding" experiments was a dodecahedron diamond of one carat weight, which was set relative to the grinding wheel as depicted in fig. 2.6, at a drag angle of +15 degrees, giving a rake angle of approximately -69 degrees. A plan view of the diamond is shown in the upper half of fig. 7.89 where it can be seen that the diamond had a small nose radius of approximately 10 μm giving a stabilising effect at the tip, and hence reducing the tendency for initial rapid wear when dressing. A dressing cross-feed of .3 mm/rev was chosen, being in the mid-range of the values used in the dressing tests, with an in-feed of 25 μm . It was thought that the severity of this dressing condition would highlight changes in the measured parameters due to changes in grinding cross-feed. Its effect on the workpiece surface roughness (and wheel surface roughness for little overlap, i.e. $v_t/nN = .75$) is shown in the bottom half of fig. 7.89.

The grinding wheel used for tests 1 to 4, and throughout the grinding programme, was of the type 32A60-K8VBE and was chosen because of its ability to generate finer surface finishes when grinding, than the coarser 46 grit wheels for similar dressing conditions. This was of extreme importance when considering "fine-grinding"

(precision grinding), as was the case later in the programme of tests.

The grinding wheel and workpiece rotational speeds were maintained constant for tests 1 to 4, and throughout the grinding programme, at 30 rev/sec (1800 rev/min) and 1.5 rev/sec (90 rev/min) respectively, giving peripheral speeds of 29 m/sec for the grinding wheel, and a maximum value of .24 m/sec for the workpiece. This value of workspeed was considered to be adequate in the absence of any hard and fast rules for determining this parameter, and was chosen to give easily maintainable cross-feed rates in the range selected when grinding.

Cross-feed values were chosen to give a range of values of the ratio v_t/nW within the band width zero to unity, this being the parameter governing the amount of grinding wheel width actively engaged in grinding. The following values were chosen on the basis of a wheel having a maximum grinding width available of 18 mm:-

| | | | | |
|--------------|------|------|-----|-----|
| v_t mm/sec | 20.5 | 13.5 | 6.5 | 2.5 |
| v_t/nW | .75 | .50 | .25 | .09 |

These values were used in conjunction with a radial in-feed when grinding, of 12.5 μm (.0005 in.), which was considered as being an average depth of cut.

The variation of grinding wheel wear with volume of metal removed for the various grinding cross-feed rates is depicted in fig. 7.90, and follows the general pattern as shown initially in fig. 2.15. It can be seen that the initial breakdown of the grinding wheel followed the same path irrespective of the value of v_t (cross-feed rate), until a point was reached after about 3.5 cm^3 of metal had been removed, corresponding to a value of .3 cm^3 of wheel wear, beyond which the rate of wheel wear differed for each of the four test conditions. At the change over point (25th pass), the loss of wheel height was approximately equal to the dressing depth of cut, i.e. 25 μm , this being the same value for each test condition, and shows that the

initial rapid rate of wear extended beyond the measured profile depth as shown in fig. 7.89. This suggests that the dressing action of the diamond tool caused damage to the wheel surface to a depth greater than the initial in-feed value.

After the initial rapid^t breakdown of the wheel surface, conditions stabilized, and further wheel wear was governed by the particular value of v_t employed. For the condition $v_t/nW = .75$, the uniform wear region existed for a relatively short period of time before vibrations were observed between the wheel and workpiece, and the grinding process became unstable. This happened around the 40th pass (position C in fig. 7.90). After this point wheel wear increased rapidly. For reducing values of v_t/nW , e.g. .50, .25 and .09 (all other conditions being the same), the rate of wheel wear decreased for similar increases in metal removal, with stable grinding conditions being observed throughout.

Values of grinding ratio are tabulated in Appendix VII pages 286 to 289 inclusive, and show a range of peak values from 12.7 to 30.8 over the range of conditions used. For test 1 ($v_t = 20.5$ mm/sec) the grinding ratio was seen to decline after the 50th pass from a steady state value of around 12.7, and heralded the onset of catastrophic wheel wear. Values from the remaining three tests indicated that the grinding ratio was still in a state of increase after 100 passes of the workpiece, and that the effect of reducing v_t , and hence v_t/nW , was to delay the point at which the grinding ratio attained a steady state value. Similar final values of around 30 were recorded for the cases where $v_t = 6.3$ mm/sec and 2.5 mm/sec. The overall results showed that for test 1, the wheel wear had progressed through all three wear stages (see fig. 2.15), whilst for test 2 the wheel was part way into the second stage of wear, and that for tests 3 and 4, the wheel was on the verge of entering the second stage of wear.

The effect of grinding cross-traverse rate on wheel and workpiece surface roughness are shown in figs. 7.91

and 7.92 for tests 1 and 4 respectively. The "Talysurf" traces show the deterioration of the as-dressed surface roughness of the grinding wheel as the number of work passes increased, and the corresponding effect on workpiece surface roughness. In fig. 7.91 only traces of the workpiece surface are shown, since these were indicative of both wheel and workpiece surface roughness due to the limited effect of grinding overlap for the case $v_t/nW = .75$. After the first pass of the workpiece, the effect of the diamond cross-feed was clearly seen in the work surface trace, which had a maximum peak to valley height of $17.5 \mu\text{m}$. This suggests that the initial depth of cut on the first grinding pass was greater than the set depth of $12.5 \mu\text{m}$. The traces show that as the number of passes increased, the peaks on the wheel surface were broken down and became more obtuse, whilst still retaining the dressing cross-feed effect. At the 20th pass, the peak to valley height of the work surface trace had been reduced to $6 \mu\text{m}$, and was approaching the change over point from a rapid to a uniform wheel wear rate. By the 50th pass, the surface roughness had become more random in form, whilst retaining the same value of average arithmetic roughness as that recorded at the 20th pass, and at the 100th pass had attained a completely random form relative to that of the original condition. In fig. 7.92, traces are shown for both the wheel and workpiece surfaces since grinding overlap caused by the condition $v_t/nW = .09$, modified the workpiece surface roughness relative to that of the grinding wheel. The trend shown for the grinding wheel breakdown up to the 20th pass, i.e. approaching the change over point, was similar to that shown for test 1, with slightly lower values of average arithmetic roughness being recorded. After the 20th pass, the value of average arithmetic roughness for the grinding wheel surface remained fairly constant up to the end of the test, at which point the effect of the dressing cross-feed rate was still visible within the surface trace. The effect of the grinding wheel overlap due to the low value of

v_t is shown clearly in the traces of the workpiece surface, where values of average arithmetic roughness ranged from $\frac{1}{2}$ to $\frac{3}{4}$ of the value of the wheel producing the particular condition. This shows that for the fairly coarse dressing condition used, the reduction in workpiece surface roughness relative to that of the grinding wheel, for a degree of grinding wheel overlap of 9, (i.e. $\frac{nW}{v_t} - 1 = 9$), was at the best only 50%.

An overall view of the variation of workpiece surface roughness with the volume of metal removed at the various grinding cross-feed rates, is shown in fig. 7.93. It can be seen that there was an initial rapid decrease in workpiece surface roughness for all cross-feed rates until 3 to 4 cm³ of metal had been removed, this point corresponding to the change over from rapid to uniform wheel wear, after which the values of workpiece surface roughness remained constant for further increases in metal removal. The four plots show that the final steady state values of workpiece surface roughness decreased in the order of decreasing cross-feed rate, as would be expected, and suggest that the steady state conditions were governed by the grinding process, and were independent of the original dressing operation.

The results of tests 1 to 4 suggest that great care must be taken when selecting values for grinding cross-feed since this parameter has been shown to be a powerful variable which influences both the rate of grinding wheel wear (and grinding stability), and the workpiece surface roughness, particularly after the initial period of rapid wheel wear has ended. When selecting an optimum value of v_t to give the best conditions under which to test the influence of dressing variables on the grinding process, the following three criteria needed to be satisfied.

1. The rate of wheel wear must be neither too rapid, causing grinding instability to occur prematurely, nor too slow, thereby rendering the grinding process insensible to changes in dressing condition.

2. The workpiece surface roughness should, if possible, be representative of the wheel surface, with minimum grinding overlap occurring.
3. The grinding wheel should wear uniformly across its face width.

Considering the results of tests 1 to 4, the value of grinding cross-feed rate which fulfilled the three criteria adequately was 13.5 mm/sec, giving a value of $v_t/nW = .5$ for a grinding wheel width of 18 mm, and was therefore used throughout the "rough-grinding" experiments.

The test duration was increased by four times, giving a final volume of metal removed for each test of approximately 60 cm³, in an attempt to determine at which point the dressing conditions ceased to influence the grinding process.

7.4.2 Tests 5 to 16 inclusive.

This series of tests was designed to observe the effects of dressing in-feed and cross-feed on the cylindrical traverse grinding process, through the measurement of grinding ratio, grinding force and workpiece surface roughness for constant grinding conditions. In all, twelve separate tests were performed in which a combination of three cross-feed rates and four in-feed values were used to cover a wide range of dressing conditions. The diamond tool and grinding conditions employed were as described previously.

The experimental results were grouped initially to show the influence of the dressing in-feed for each of the three dressing cross-feed rates in the order .3, .1 and .5 mm/rev. The values of wheel wear were then regrouped to show the influence of the cross-feed rate with the in-feed constant, and finally all the recorded parameters were plotted simultaneously to show the overall trends for each set of dressing conditions.

One of the main criteria in any "rough-grinding" operation is the volume of metal which can be removed

from the workpiece before the process becomes unstable, since the final size and geometric form of the workpiece depend very much upon the condition of the grinding wheel. Figs. 7.94 to 7.100 inclusive, show the variation of grinding wheel wear with volume of metal removed for the various wheel dressing conditions. In fig. 7.94 values have been plotted for the mid-range cross-feed rate of .3 mm/rev, and show a family of curves similar in form to that described initially in fig. 2.15. It is seen that the curves increased in order of increasing in-feed, showing that for this particular cross-feed rate, the greater the depth of cut, the greater was the influence on the initial stage of wheel wear. The explanation for this order is found by observing the as-dressed condition of the grinding wheel face, which is shown in figs. 7.101 and 7.102 for the maximum and minimum in-feed values respectively. For the maximum depth of cut, the combination of dressing variables were sufficient to generate a screw thread effect in the grinding wheel face with minimum overlap occurring, thereby producing relatively sharp cutting points with which to grind. The initial rapid wear which ensued was limited to a wheel depth approximately equal to the dressing depth of cut, and was completed after about 130 grinding passes, i.e. 15 cm^3 of metal removed. After this point, the dressing conditions were no longer visible in the workpiece surface. For the minimum depth of cut condition, the dressing cross-feed was again seen in the as-dressed wheel face, but in this case, not all the wheel surface was effectively dressed, resulting in relatively blunt cutting points being formed. It is thought that the cutting edges of the grits were partly formed from the original pre-dressed wheel surface, and were stronger, due to the lighter dressing conditions. The initial wheel wear was much less than that encountered at the highest in-feed value for the same volume of metal removed, and the change over point from the primary to the secondary stage of wear was less definable. The effect of the dressing cross-feed was still discernable in the workpiece surface at the

end of the test, and suggests that under certain conditions, the dressing process can influence the wheel wear after the primary wear stage has finished. The other two dressing conditions caused wheel wear rates which lie in between those obtained for the upper and lower in-feed values. At some point during the secondary wear stage for each of the four wheel conditions, the wear rate was seen to increase, but not sufficiently to be termed catastrophic wear. At this point vibrations were noted in the grinding process, which started in the earliest case ($a = 25 \mu\text{m}$) after about 280 grinding passes, i.e. 30 cm^3 of metal removed.

Fig. 7.95 shows similar wheel wear trends for the lower dressing cross-feed rate of $.1 \text{ mm/rev}$ with the same range of dressing in-feed values, except that the curves plotted show a bunching together of values, which lie in the mid-range of those plotted for the above mentioned tests. For an explanation, it is necessary to look again at the as-dressed condition of the grinding wheel, which was reflected in the ground workpiece surface, and is shown for the maximum and minimum in-feed values in figs. 7.103 and 7.104 respectively. The limiting effect of the low cross-feed rate is seen in both figures, which show similar as-dressed wheel surfaces for both the high and low depths of cut, suggesting a high degree of diamond overlap. In both cases, the effect of the dressing cross-feed disappeared from the workpiece surface after about 30 grinding passes (approximately 3.5 cm^3 of metal removed), although the primary wear stages continued until at least 6 cm^3 of metal had been ground away. The wheel wear rates again increased for all conditions at some point in the secondary stage of wear (fig. 7.95), and were heralded by the onset of vibrations between the grinding wheel and workpiece. This was particularly pronounced for the cases of maximum and minimum dressing depth of cut, but for different reasons. For the condition: $a = 25 \mu\text{m}$, vibrations were encountered after a relatively short period of secondary wheel wear, when about 18 cm^3 of metal had been removed, and was probably due to damage

caused to the grinding wheel well inside its surface, by the dressing action of the diamond at that depth of cut. For the condition: $a = 5 \mu\text{m}$, the initial wheel wear was low compared with the other three conditions, and vibrations were not encountered in the grinding process until the grinding wheel was restarted after stalling, when approximately 30 cm^3 of metal had been removed. This sequence of events suggests that little damage was caused to the grinding wheel by the dressing action of the diamond for this dressing condition, resulting in insufficient grit breakdown for efficient grinding to take place. It is highly probable that the grinding wheel became unbalanced on stalling, thereby causing adverse grinding conditions to become operable when re-started, leading to the greatly increased wear rate.

Fig. 7.96 depicts the variation of grinding wheel wear for the coarsest dressing cross-feed rate of $.5 \text{ mm/rev}$ used in conjunction with the same range of in-feed values mentioned previously. It is seen that catastrophic wheel wear (tertiary wear stage) was encountered for all conditions early on in the grinding tests (8 to 20 cm^3 of metal removed), and was again heralded by vibrations between the grinding wheel and workpiece. The significant difference between the wheel wear characteristics for these dressing conditions and those discussed earlier, is that the primary and secondary wear stages occurred as one, and were of relatively short duration, terminating in extremely rapid wheel wear. An interesting point noted from the four curves is that at some point after the start of the tertiary stage of wear, the wheel wear rate decayed, and suggests a recovery of the wheel surface. A possible explanation is that the initial damage caused to the active wheel surface by the adverse grinding conditions, extended to a depth equal to one or two grit diameters before sound grit and bond material were uncovered.

The behaviour of the grinding wheel can best be explained with reference to figs. 7.105 and 7.106, which show traces of the workpiece surface after grinding, for the

highest and lowest values of dressing in-feed respectively. Both these figures show that the wheel dressing conditions were insufficient to cause the whole wheel face to be dressed adequately with the sharp diamond, resulting in part of the surface remaining in the pre-dressed condition. The cutting edges so generated were few, and rendered the grinding wheel ineffective as an efficient cutting tool. The reluctance of the as-dressed wheel face to breakdown, is demonstrated by the minimal change in the measured peak to valley height of the surface profiles (and average arithmetic roughness values), until at least the 10th grinding pass had been accomplished. This implies that the coarse dressing traverse rate (.5 mm/rev) caused limited local damage to the wheel face, even for the highest depth of cut (25 μ m), as shown by the subsequent tenacity of the grit when grinding. The workpiece surface roughness traces show that once the grinding wheel had entered the tertiary stage of wear, the ensuing wheel surface bore no resemblance to the original as-dressed surface condition, and was of random form.

In figs. 7.97 to 7.100 respectively, the variation of grinding wheel wear with volume of metal removed has been re-plotted to show to better advantage the influence of the dressing cross-feed rate for each of the dressing depths of cut, in reducing order. The wheel wear curves in fig. 7.97 show clearly that for these particular dressing conditions, the higher the initial wear rate in the primary wear stage, the longer the secondary wear stage became in which useful work was done, resulting in a lower wear rate on entry to the tertiary wear stage. The most efficient dressing conditions occurred for the mid-range cross-feed rate of .3 mm/rev, in which the dressing parameters were just sufficient to effectively dress the whole wheel face (fig. 7.101); whilst the lower cross-feed rate created conditions that were too severe, and the higher cross-feed rate created conditions which were not severe enough. Figs. 7.98 to 7.100 inclusive, highlight the inability of the highest dressing cross-feed rate to

create efficient conditions for grinding, whatever the in-feed value, and show that overall, the best conditions (lowest wheel wear) were created by the mid-range cross-feed rate of .3 mm/rev.

The influence of the dressing conditions on workpiece circularity when grinding, are depicted in figs. 7.107 to 7.110 inclusive, for the highest and lowest cross-feed rates, combined with the highest and lowest in-feed values. The as-dressed screw thread effect on the grinding wheel was visible around the circumference of the workpiece for both in-feed values at the coarsest cross-feed rate (figs. 7.107 and 7.108), and persisted to about the 140th grinding pass for the case of the lower in-feed value. At the higher in-feed value (fig. 107) the screw thread effect was short lived, due to vibrations occurring between the grinding wheel and workpiece, with their influence on the workpiece circularity being seen clearly at the 60th grinding pass. By the 180th pass, this effect had diminished, indicating a recovery on the part of the grinding wheel. The traces of workpiece circularity depicted in figs. 7.109 and 7.110, show that at the lower cross-feed rate, no screw thread effect was visible around the workpiece circumference at either depth of cut. These figures do show, however, the coarsening effect of the grinding wheel breakdown on workpiece circularity up to the tertiary wear stage of the grinding wheel. At this point, the effect of the grinding vibration was seen clearly in the workpiece surface. Allowing for discrepancies in the wheel and workpiece rotational speeds, the final traces in figs. 7.107 to 7.110, show the formation of 18 lobes around the workpiece circumference, which can be attributed to the out-of-balance of the grinding wheel.

Another important parameter in grinding, is the resulting surface finish of the workpiece, since this may influence its useful life in service. Figs. 7.111 to 7.113 inclusive, show the variation of workpiece surface roughness, with the volume of metal removed for the various wheel dressing conditions. The trend depicted

for all dressing conditions was the same, and shows that irrespective of the initial as-dressed condition of the grinding wheel, the workpiece surface tended towards the same final steady state value of average arithmetic roughness after the grinding wheel had entered its secondary stage of wear, with this value being governed by the grinding conditions. This finding verifies that stated earlier for grinding tests 1 to 4. Although it was seen that the final value of workpiece average arithmetic roughness fell within the limits of 1 to 1.5 μm (40 to 60 $\mu\text{in.}$), which could be classed as a reasonable rough-ground surface, the workpiece circularity traces have shown that for certain dressing conditions, the final workpiece roundness was not acceptable, due to excessive lobing.

The force generated when grinding has been used as a means of comparing the efficiency of the grinding wheel after dressing under different conditions, through a macro analysis of the cylindrical traverse grinding process, and was subsequently found to be useful in determining the points in the grinding tests at which the wheel entered the various wear stages. The general range of force values recorded were from a maximum value of 79 Newtons, i.e. 17.8 lbf for F_R , to a minimum value of 11 Newtons, i.e. 2.5 lbf for F_T ; with force ratios of the order of 1.7 to 2.3.

The variation of the radial and tangential components of grinding force with the volume of metal removed, have been shown in figs. 7.114 to 7.116 inclusive, for each dressing cross-feed rate over the range of dressing depths of cut. Several trends were apparent from all three figures, which were in agreement. Firstly, the general pattern of force variation was as follows:-

An initial increase in force whilst the grinding wheel passed through its primary wear stage, terminating in a peak value; followed by a dwell period during the wheel's secondary wear stage; with a final decrease in force as the tertiary wear stage was entered. It was noted that in all cases, the final grinding force tended

towards the same value. If it is taken that the dwell period represented the most efficient removal of metal, then it is seen clearly that for the coarsest dressing cross-feed (fig. 7.116), little useful work was done by the grinding wheel.

A second trend to emerge from the force analysis was that by increasing the dressing depth of cut at any cross-feed rate, the resulting force, when grinding, was decreased. This supports the argument that the greater dressing depths of cut caused more damage to the wheel surface than the finer ones, and produced sharper cutting edges, thereby requiring less force to grind and to remove dulled grits. Another effect of increasing the dressing depth of cut, which was less obvious, was the increase in the initial grinding period before the peak force value was reached. This is shown clearly in fig. 7.116.

An overall view of the grinding force analysis shows that the grinding wheel dressed at the mid-range cross-feed rate of .3 mm/rev, and the higher in-feed values (12.5 to 25 μ m), needed less force to grind than when dressed at either the higher or lower cross-feed rate for similar depths of cut, and therefore gave the most efficient wheel conditions from a grinding force point of view.

The usefulness of the two parameters, grinding ratio, and force ratio (F_R/F_T), in determining the boundaries of each wheel wear stage for the different dressing conditions are shown in figures 7.117 to 7.140 inclusive, and have been plotted against volume of metal removed along with grinding force, wheel wear and workpiece surface roughness, to show the influence of the dressing process on these grinding parameters collectively.

It was noted that at the end of the more clearly defined primary wheel wear stages, obtained for certain of the dressing conditions, the force ratio value increased from one level to another, due to a falling off of the tangential component of grinding force relative to the

radial component. This change in force ratio, however, was not instantaneous, and shows that a relatively short transition period existed between the primary and secondary wear stages. A good example is shown in fig. 7.117 for the mid-range dressing cross-feed rate of .3 mm/rev at the highest dressing in-feed value of 25 μ m. For conditions giving less definable change over points on the wheel wear curves, e.g. fig. 7.123, the force ratio was used to advantage. It was also noted that in certain cases, a second increase in the force ratio was apparent, e.g. figs. 7.123, 7.129 and 7.131, which corresponded to the end point of the secondary wear stage. This trend, however, was not encountered for all wheel conditions, and called for another method of determining this point in the grinding wheel life cycle. This was established through the parameter, grinding ratio.

Normally, the grinding ratio is determined for the secondary wheel wear stage only (assuming that this stage has been previously defined), where a constant value is obtained, giving a wheel performance rating against which other grinding conditions can be compared. From the results of this programme of research, the grinding ratio has been plotted for all three wear stages, giving a continual wheel rating which has proved to be useful when comparing the influence of the various dressing conditions on the grinding process. By superimposing fig. 7.123 onto fig. 7.124, fig. 7.129 onto fig. 7.130 and fig. 7.131 onto fig. 7.132, it was seen that the second increase in force ratio corresponded to the maximum turning point value of the grinding ratio. It was found that this second parameter could be used to determine the end point of the secondary stage of wheel wear for those conditions giving less definable change over points on the wheel wear curves, or in the absence of a second force ratio change, e.g. figs. 7.126 and 7.128.

Using the two above mentioned grinding parameters

several observations were made. In the cases where the highest dressing cross-feed rate of .5 mm/rev was used, it was noted that for all dressing depths of cut, an initial decrease in grinding ratio occurred (figs. 7.134, 7.136, 7.138 and 7.140), which suggests, as stated previously, that for these conditions, the initial rapid wheel wear was much reduced or non-existent, leading to a relatively short secondary wear stage before the onset of tertiary wear. In general, a reduction in grinding ratio heralded the start of adverse grinding conditions. The variation of force ratio with volume of metal removed, showed that the duration of the primary stage of wheel wear was influenced by the dressing conditions, with a longer period being observed for the wheel dressed at the mid-range cross-feed rate, as compared with that for the combinations of in-feed with the lower cross-feed rate.

Overall, the best rough-grinding conditions were obtained for the wheel dressed at the mid-range cross-feed rate of .3 mm/rev, with grinding ratios of between 49 and 157 being recorded in the order of decreasing in-feed. The second best conditions were obtained for the wheel dressed at the lower cross-feed rate of .1 mm/rev for the same in-feed values, giving grinding ratios of between 49 and 90; and the worst conditions were obtained for the wheel dressed at the highest cross-feed rate of .5 mm/rev, with grinding ratios as low as 11 being recorded after only 20 cm³ of metal had been removed.

7.4.3 Tests 17 and 18 (with a comparison of tests 7 and 11)

To ascertain the effect of varying the grinding depth of cut (traverse rate constant) on wheel wear, grinding ratio and workpiece surface roughness, for selected dressing conditions, two further rough-grinding tests were conducted in which the grinding in-feed (radial) was reduced to 5 μ m. The measured parameters were then compared with those obtained from similar previous tests in which a grinding in-feed of 12.5 μ m had been used.

The dressing conditions chosen had previously resulted in relatively stable wheel breakdown occurring during the grinding period, and were considered to be ideal standards against which to test other grinding conditions. These were dressing cross-feed rates of .3 and .1 mm/rev, used in conjunction with a dressing in-feed value of 12.5 μm . The diamond dressing tool used was the same one as described previously.

In fig. 7.141 the influence of the combined dressing and grinding conditions on grinding wheel wear has been shown when removing a volume of between 50 to 60 cm^3 of metal from each workpiece.

It was seen from this figure that the initial grinding wheel breakdown in the primary stage of wheel wear was dependent in all cases upon the dressing conditions, with the same initial rates of wheel wear being observed for similar dressed wheels, irrespective of the grinding depth of cut; but varying according to the dressing cross-feed rate. It was noted, however, that as wheel wear progressed, the rate of wear was reduced for those conditions involving the lower grinding depth of cut, particularly for the wheel dressed at the finer cross-feed rate. This influenced the point at which the primary wear stage ended, and the depth to which the wheel had worn during this period of time.

These effects can best be explained with reference to figs. 7.142 and 7.143, where traces of the ground workpiece surface roughness have been presented for surface conditions resulting from coarse and fine dressed wheels respectively, used at both grinding depths of cut. The traces have been paired for similar amounts of metal removed, and reflect the surface condition of the grinding wheel throughout the tests.

The ground profile resulting from the as-dressed wheel surface for the coarse dressing condition (1st pass, fig. 7.142) had a measured peak to valley height equal to the dressing depth of cut (12.5 μm), showing that the dressing variables selected, gave efficient conditions

without diamond overlap occurring. This had been shown previously to produce a strongly cohesive wheel surface. In the case of the finely dressed wheel, an as-dressed ground profile was produced, whose peak to valley height was less than half the dressing depth of cut (1st pass, fig. 7.143). This showed a high degree of diamond overlap, which suggested that greater surface damage had been caused to the grinding wheel, as compared with the previous condition. By reducing the value of the grinding in-feed, the wheel surface was subjected to less stress when grinding metal, resulting in a substantial reduction in primary wheel wear for the finely dressed wheel, and a marginal reduction for the coarsely dressed wheel. This less-stressed condition was seen when comparing traces produced for similar volumes of metal removed at both grinding depths of cut, by the more uniform, and less rugged surface contours generated at the lower in-feed value.

When using the coarsely dressed grinding wheel, the dressing cross-feed was seen in the workpiece profile up to the end of the primary wear stage for both grinding depths of cut, at which point, the loss of wheel height was approximately equal to the original as-dressed profile depth. This occurred after the removal of about 16 cm^3 of metal, and showed the limited effect of change of grinding in-feed for this dressing condition, i.e. 360 passes for $a_g = 5 \text{ }\mu\text{m}$, and 120 passes for $a_g = 12.5 \text{ }\mu\text{m}$. In the case of the finely dressed wheel, the dressing cross-feed disappeared from the profile contour towards the end of the initial wear periods; and a total loss of wheel height of between $2\frac{1}{2}$ to 3 times the original as-dressed profile depth was recorded at the end of the primary wear stage, for the lower and higher grinding in-feed conditions respectively. (End point = 100 passes for $a_g = 12.5 \text{ }\mu\text{m}$, and 350 passes for $a_g = 5 \text{ }\mu\text{m}$). This highlights the severity of the dressing condition for the finely dressed wheel, and shows that whilst a reduction in grinding in-feed of 250% caused a substantial

reduction in wheel wear, the final primary wear depth was still greater than the original as-dressed profile depth.

The grinding ratio calculated for each set of conditions in the secondary wear stage (fig. 7.141) gave similar values of around 190, showing that once the primary stage of wheel wear had ended, the following rate of wheel breakdown was a function of the grinding conditions coupled with the natural characteristics of the grinding wheel, and was independent of the original dressing conditions. The reduction in grinding depth of cut caused a longer period of secondary wheel wear for both wheel conditions, with the wheel remaining in the secondary stage of wear until 75 cm^3 of metal had been removed for the finely dressed wheel; and to the end of the test for the coarsely dressed wheel, after the removal of 53 cm^3 of metal.

The effect of the dressing and grinding conditions on workpiece circularity are shown in figs. 7.144 and 7.145 for the coarse and finely dressed wheel conditions respectively. In all cases the as-dressed wheel condition was seen around the workpiece circumferences in the early stages of the tests, but disappeared during the primary stage of wheel wear. The subsequent circular profiles portrayed random surfaces, until the onset of grinding vibrations, when the lobing effect became pronounced. This occurred for all cases except the coarser dressed wheel, subjected to the lower grinding depth of cut.

In fig. 7.146, the variation of workpiece surface roughness with volume of metal removed is depicted for the combination of dressing and grinding conditions.

At the beginning of each test, the influence of the dressing conditions on workpiece surface roughness were seen clearly, with the coarser dressing cross-feed giving rise to higher initial values of average arithmetic roughness. As the primary stage of wheel wear progressed, the surface finishes created by the coarsely dressed grinding wheel were reduced, and tended towards a steady value after the wheel had entered the secondary stage of

wear. It was seen that the steady state value was different for each grinding depth of cut, and was lower for the reduced in-feed value. In the case of the finely dressed grinding wheel, the low initial values of workpiece surface roughness varied marginally as the wheel progressed through its primary wear stage, with the value of average arithmetic roughness increasing slightly for the higher grinding depth of cut, and reducing for the lower depth of cut. Again, as the wheel entered its secondary stage of wear, the surface finish values tended towards a steady state value which was the same as that reached previously for the same grinding depth of cut.

These events showed that the dressing conditions only influenced the workpiece surface roughness during the primary stage of wheel wear, and that the final surface finish value was dependent on the grinding conditions.

7.4.4 Tests 19 to 30 inclusive.

This last series of tests was designed to observe the effects of the dressing in-feed and cross-feed rate, coupled with the grinding cross-feed rate, on the cylindrical traverse grinding process when fine grinding. The parameters measured were the workpiece surface finish and circularity, and the grinding force. The results of these experiments have been used to test the reliability of equation 3.44 (and the preceding theoretical work), which predicts the final ground surface roughness (R_a) for known dressing and grinding conditions.

Dressing was conducted with a blunt diamond tool which had a wear flat of approximately 1.09 mm width, and is shown in fig. 7.147. This diamond was used in conjunction with the fine-grained grinding wheel mentioned in the previous grinding experiments, to give conditions suitable for fine (precision) grinding. In all, 60 different situations were covered through a combination of 12 dressing, and 5 grinding conditions, with the grinding in-feed remaining constant at 5 $\mu\text{m/pass}$ (radial).

As seen in fig. 7.147, the as-dressed surface roughness of the grinding wheel was reflected in the traces taken from the ground surface of the workpieces. In each of the three cases shown, the dressing cross-feed was clearly visible in the traces, which highlighted its influence on surface roughness when using a blunt diamond. Also, its limiting effect on profile depth was noted for reductions in value from .5 to .1 mm/rev when compared with the initial dressing in-feed, which was 25 μ m in each case. The profiles portrayed, were for the case of no grinding overlap, and showed that in the first instance, the surface roughness could be represented as a series of triangular forms having a base length equal to the dressing cross-feed rate. This was the premise upon which equation 3.44 was based.

In Chapter 3, it has been shown through analysis of the cylindrical traverse grinding process from a theoretical point of view, that the surface pattern produced by the grinding process is dependent in the first instance upon the dressing conditions, and secondly, upon the grinding traverse rate. Fig. 7.148 shows as a precursor to tests 19 to 30, the effect of these parameters on a typical cylindrical traverse ground workpiece. The "Talysurf" traces depict the influence of both dressing and grinding conditions on surface roughness, whilst the photograph shows clearly the influence of the grinding traverse rate for conditions producing grinding overlap, i.e. $nW/v_t > 1$, and $b \neq 0$.

Analysis of the test results is made easier by first observing the table of calculated parameters for tests 19 to 30 inclusive in fig. 7.149. The inset at the top of the figure is a common table, in which the degree of wheel overlap is predicted for the particular values of grinding traverse rate and rotational workspeed, i.e. the number of values of interference E to be expected. This number is dependent upon the ratio nW/v_t , and is given by the terms $(A + b)$, where A is an integer, and b is a fraction. (See Chapter 3, page 75). Row (1)

gives the number of values of interference E at the trailing edge of the feed band, and Row (2) gives the number of values at the leading edge, assuming $b \neq 0$.

This common table shows that for the grinding conditions chosen, each ground workpiece should have two final surface conditions per feed width, i.e. $b \neq 0$ for any case, and that for grinding traverse rates greater than 10 mm/sec., i.e. $nW/v_t = 2.70$, the surface roughness at the trailing edge of the feed band should be equal to the as-dressed condition of the grinding wheel.

The three tables below the common table show the values of interference E to be expected for each dressing cross-feed rate h , and profile depth a^* (average peak to valley height for the as-dressed surface roughness); and the corresponding values of average arithmetic roughness. These tables all show that the greatest reductions in average arithmetic roughness R_a are dependent primarily on reductions in the dressing cross-feed rate h , and should occur for values of $v_t < 10$ mm/sec, i.e. $v_t/nW < .4$. No great improvement can be expected for values of $v_t > 10$ mm/sec, i.e. $v_t/nW > .4$.

The test results will now be discussed in the light of this analysis. Figs. 7.150 to 7.152 inclusive, show in trace form, the variation of the workpiece surface roughness with the grinding traverse rate for dressing conditions taken in the order of $h = .5, .3$ and $.1$ mm/rev, when combined with values of a , of 25 and 5 μm respectively.

The first two points to be noted were, that as h was reduced, the as-dressed surface roughness depth changed to a lesser degree for changes in a ; and that the grinding depth of cut of 5 μm did not limit the roughness height (7.5 to 10 μm) for h max., as would have been expected. The first effect was due to the obtuse nature of the dressing diamond, which had a greater influence when coupled with reduced values of h , and will be demonstrated later; and the second effect was due to the passage of several grinding passes with in-feed being applied, before recordings of the workpiece surface

roughness were taken. This caused higher values of R_a than would be expected.

Values of the parameter E/h , which were deduced from the tables in fig. 7.149 for the occurrence of single values of E , i.e. for $v_t > 10$ mm/sec, are verified in figs. 7.150 and 7.151, by the grinding overlap present. This is emphasized when comparing these traces with the addressed condition for each case in fig. 7.147. For the cases where single values of E existed, i.e. limited overlap, the greatest reductions in surface roughness should have occurred for values of E/h of around .5, resulting in values of R_a of approximately $\alpha^*/8$ units. The experimental results showed that values of R_a of between $\alpha^*/5$ and $\alpha^*/6$ units were prevalent, with little difference being noted over the range of values of E/h between .22 and .88. The discrepancy between the experimental and theoretical values was in the triangular approximation approach. For values of $v_t < 10$ mm/sec, the reduction in workpiece surface roughness was clearly visible in the traces, particularly in figs. 7.150 and 7.151 at the higher dressing cross-feed rates, and was due to the increased grinding overlap, as depicted by the increase in the number of values of E .

The overall effect of the dressing and grinding conditions on the workpiece surface roughness for fine grinding are shown in a three-dimensional form in figs. 7.153 to 7.155 inclusive, for the three dressing cross-feed rates in reducing order. The lower values of average arithmetic roughness obtained for each set of experimental and theoretical conditions have been plotted together. The discrepancies between these values are due to several factors, i.e. the inability of equation 3.44 to take account of the degree of randomness generated in the wheel face when dressing, and differences between the actual and stated values of the dressing and grinding parameters.

The inset table at the top of each diagram emphasizes the limiting effect on the workpiece roughness

depth a^* , of the diamond geometry combined with the cross-feed rate h . These tables show that when the grinding wheel was dressed for fine grinding, the ensuing as-dressed surface roughness was primarily a function of the parameters β and h , and was independent of the depth of cut a , except at the highest cross-feed rate of .5 mm/rev. This trend was reflected in the starting values of R_a .

The general trends depicted bore out the previously stated predictions of equation 3.44, with the greatest reductions in surface roughness being recorded when $v_t < 10$ mm/sec, for the conditions involving the higher values of h . For conditions at the lowest value of h (fig. 7.155), little change was noted, with predicted values of R_a being 50% lower than the actual values by the time v_t had reached 5 mm/sec. This suggests that a point may have been reached after which the natural characteristics of the wheel influenced the workpiece surface roughness, e.g. the grit size and spacing.

Comparing the experimentally obtained values of workpiece surface roughness with those considered as being acceptable for fine grinding⁵⁹, e.g. .25 to .64 μm (A.A), showed that a high degree of grinding overlap was necessary for those conditions incorporating the higher values of h , before favourable results were obtained. This demonstrates the importance of using low values of dressing cross-feed rate when dressing for fine grinding.

Traces showing the influence of the dressing and grinding conditions on workpiece circularity have been presented in figs. 7.156 to 7.158 inclusive. The severity of the coarse dressing conditions for both the high and low dressing depths of cut were seen clearly in the circular traces of fig. 7.156, with the cross-feed rate being discernable in the workpiece circumference until the grinding traverse rate had been reduced to 7.5 mm/sec. From this point onwards, the circularity of the workpiece improved, due to increased grinding overlap. The same effect was observed for the mid-range dressing conditions, to a lesser degree, but disappeared completely for the

fine dressing conditions , with no noticeable change occurring in workpiece circularity over the range of grinding traverse rate used. These observations strengthen the previous finding that fine dressing cross-feed rates are needed to obtain the best overall conditions for good surface finish, and circularity.

To compare the efficiency of the different dressing conditions when fine grinding over the range of traverse rates specified, the grinding force was measured in the form of its radial and tangential components. The variation of grinding force is portrayed in figs. 7.159 to 7.161 inclusive, in the order of reducing dressing severity. The main trend depicted in each figure is the same, and shows that a linear relationship existed between the grinding force and traverse rate (v_t) for each dressing condition used. This trend implies that as v_t was reduced, only part of the wheel width was engaged in grinding, i.e. an amount v_t/n mm or greater, with the trailing edge having a smoothing effect on the workpiece surface, whilst removing little metal.

Extrapolating the mean lines representing the force variation, gives implied conditions of zero force at some value of v_t , which is improbable. A possible explanation is that the measured force values were low, due to a sideways deflection of the wheel tending to lift the trailing edge away from the workpiece, although this cannot be substantiated.

The force trends showed that the influence of the dressing in-feed on grinding efficiency was limited, and depended upon the particular dressing cross-feed rate chosen. For the cases when $h = .5$ mm/rev (fig. 7.159), diamond overlap did not occur, which resulted in sharper wheel profiles being formed at the greater depths of cut. The improved efficiency of the wheel for these conditions was reflected in the subsequent reduction in the grinding force. The lowest overall values of force were generated when using the wheel dressed at the mid-range cross-feed rate of .3 mm/rev, with a relatively narrow band of

values of F_T being recorded (fig. 7.160). This emphasized the limited effect of the dressing in-feed when diamond overlap was encountered, and showed that an improvement in grinding efficiency was brought about by the reduction in h . An exception was noted for conditions embracing the lowest dressing in-feed, where a substantially higher value of force was recorded. It was possible that relatively blunt cutting edges were formed at this dressing condition, thereby impairing the grinding action of the wheel. Similar trends were noted when using the wheel dressed at the lowest cross-feed rate (fig. 7.161), except that the overall force values were higher, showing a reduction in grinding efficiency.

The increase in the tangential component of force relative to the radial component for fine grinding, is seen when comparing values of the force ratio obtained from the rough grinding tests, i.e. 1.5 to 2.0 and 1.7 to 2.3 respectively. This shows the reduction in grinding efficiency caused by the dressing action of the relatively blunt diamond tool.

7.5 SUMMARY OF THE GRINDING TEST RESULTS

The results of this work have shown the importance of the correct selection of dressing variables when preparing the grinding wheel for both rough and finish cylindrical traverse grinding operations, since they influenced both the useful working life of the wheel when rough grinding, and the resulting workpiece surface finish when fine grinding.

The dressing variable having the greatest influence on both rough and finish grinding conditions was the cross-feed rate, with the depth of cut being of secondary importance. This finding was in accordance with that of many previous researchers,^{2,3,4,8,19,20,45} whose work was mainly conducted in the field of surface grinding. The ideal dressing conditions for rough grinding were found to be those giving minimum diamond overlap, which highlighted the importance of the diamond geometry,

through the angle β , when coupled with the cross-feed rate. Conditions resulting in excessive, diamond overlap, caused reductions in grinding efficiency by impairing the grinding action of the wheel. Similar trends were observed when fine grinding, after dressing with the relatively blunt diamond. These observations are in agreement with those made by others,⁵⁰ after conducting work in the field of internal grinding.

The grinding parameters Force Ratio,^{42,57} and Grinding Ratio,^{34,45} have been shown in this work to be useful in assessing the influence of the dressing variables on the grinding process, through their ability to pin-point the various stages of wheel wear.

For those dressing conditions giving optimum, or near optimum wheel performance, it has been shown that their influence was restricted to the initial period of rapid wheel wear, and that the following period of uniform wear, in which useful work was done, was governed solely by the prevailing grinding conditions. This trend follows a generally accepted pattern. It was seen that in the cases of inefficient wheel dressing caused by too great a traverse rate, the useful working life of the wheel was severely affected by the onset of grinding vibrations after a relatively short period of primary wear. This highlighted the adverse conditions possible when using cross-feed rates greater than the mean grit diameter .

The grinding force has been shown to be a more appropriate parameter than force ratio when assessing the severity of dressing on wheel performance at the start of grinding. It was noted that the grinding force resulting from increased dressing depths of cut was reduced, and suggests that sharper cutting edges were produced for these conditions. The ensuing primary wheel wear was seen to extend to depths greater than the mean peak to valley height of the as-dressed surface roughness, and supports the argument that the greater depths of cut

caused more damage to the wheel face than the finer ones.

The influence of the dressing variables on the workpiece surface roughness has been shown to depend upon the type of grinding being considered.

In the case of rough-grinding, where a relatively high grinding traverse rate was employed, the trend depicted for all dressing conditions was the same, with their influence on workpiece surface roughness being limited to the period of primary wheel wear only. It was seen that irrespective of the as-dressed condition of the grinding wheel, the workpiece surface roughness tended towards the same final steady state value after the wheel had entered its secondary stage of wear, with this value being governed by the grinding conditions.

In the case of fine-grinding, the dressing cross-feed rate has been shown to have a highly significant effect on workpiece surface roughness. For those conditions employing high values of this variable, a high degree of grinding wheel overlap was required to reduce the surface roughness to an acceptable level. The results of the fine grinding experiments corroborate the predictions made from the theoretical analysis of this process, and have shown the usefulness of such an approach.

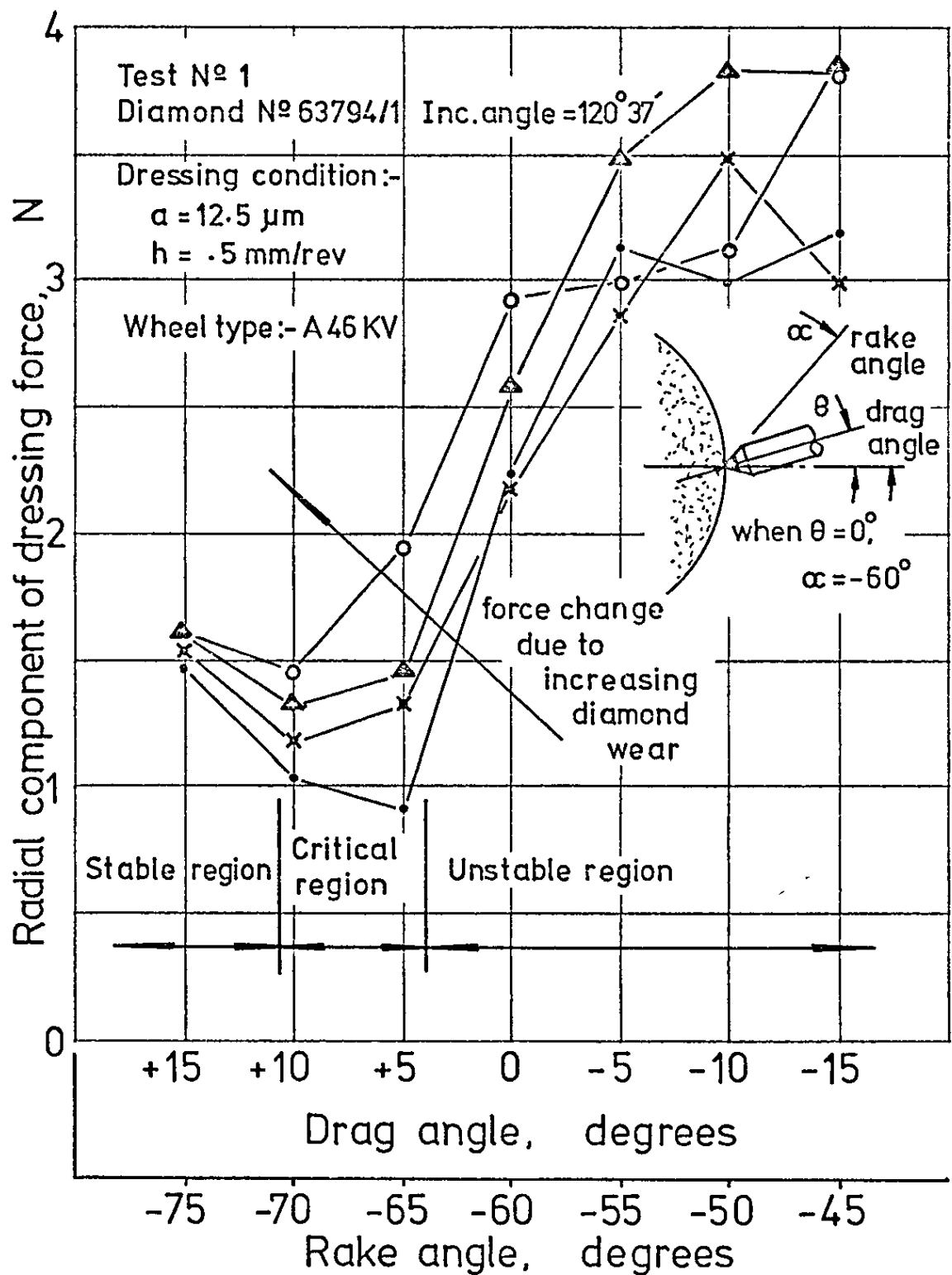
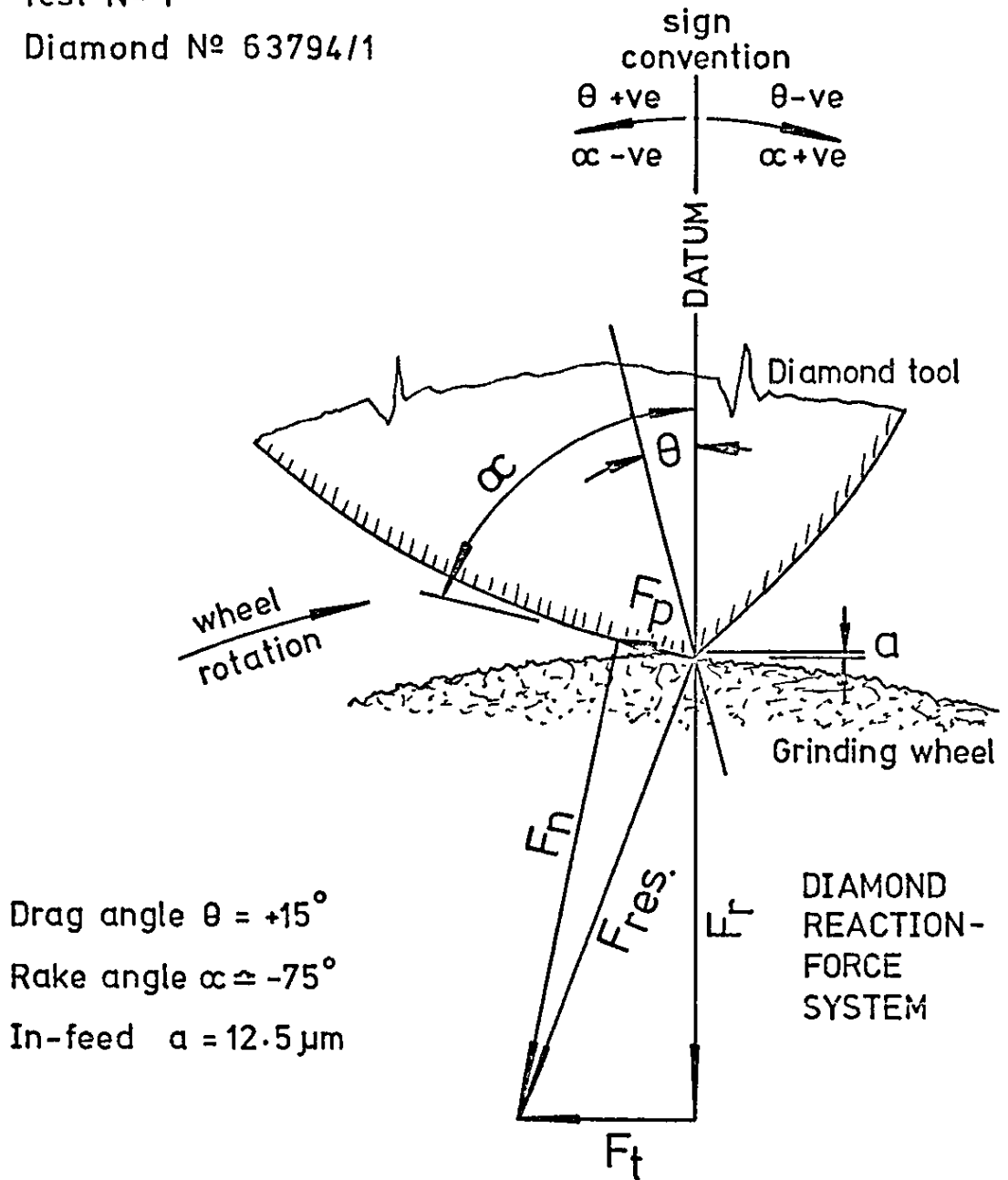


Fig.7.1 Variation of the radial component of dressing force with diamond tool drag & rake angles, for increasing diamond wear.

Test N^o 1

Diamond N^o 63794/1



Drag angle $\theta = +15^\circ$

Rake angle $\alpha \cong -75^\circ$

In-feed $a = 12.5 \mu m$

Dressing force components(recorded) :-

$$F_r = 1.45 \text{ N}$$

$$F_t = .55 \text{ N}$$

F_h = force component normal to the rake face of the diamond tool.

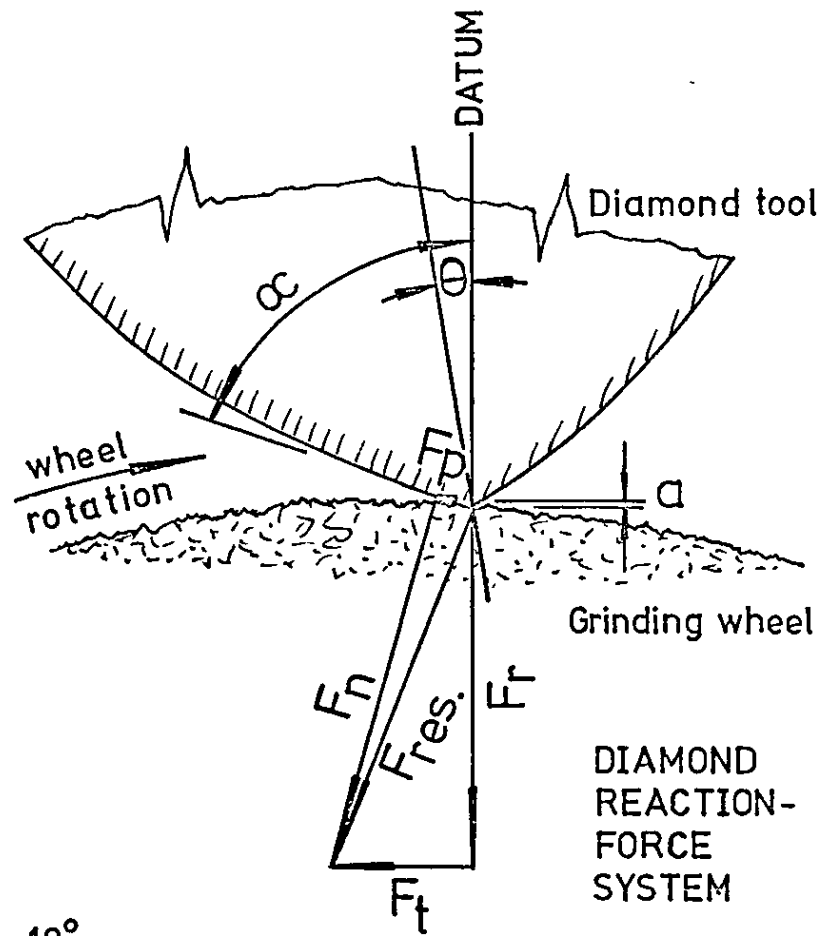
F_p = force component acting along the rake face of the diamond tool.

$F_{res.}$ = resultant force.

Fig. 7.2 Resolution of Dressing Force

Test №1

Diamond № 63794/1



$$\theta = +10^\circ$$

$$\alpha \approx -70^\circ$$

$$a = 12.5 \mu\text{m}$$

Dressing force components (recorded):-

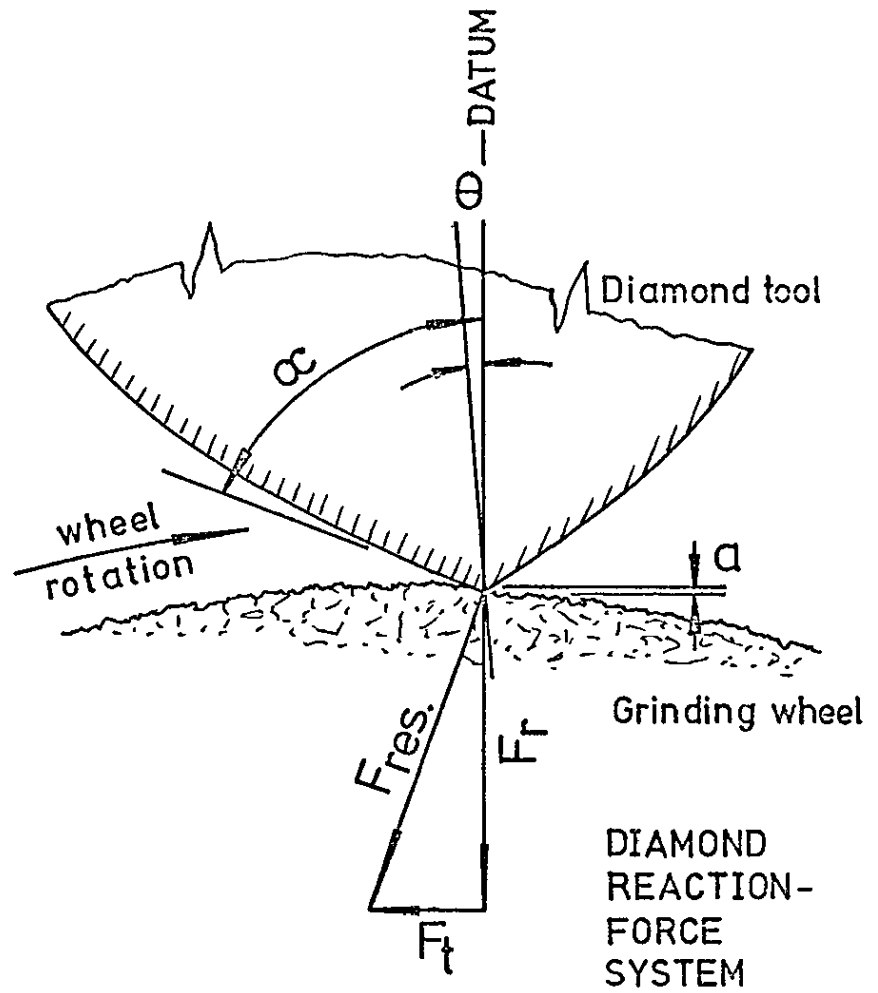
$$F_r = 1.04 \text{ N}$$

$$F_t = .41 \text{ N}$$

Fig. 7.3 Resolution of Dressing Force

Test N° 1

Diamond N° 63794/1



$$\theta = +5^\circ$$

$$\alpha \approx -65^\circ$$

$$a = 12.5 \mu\text{m}$$

Dressing force components (recorded)

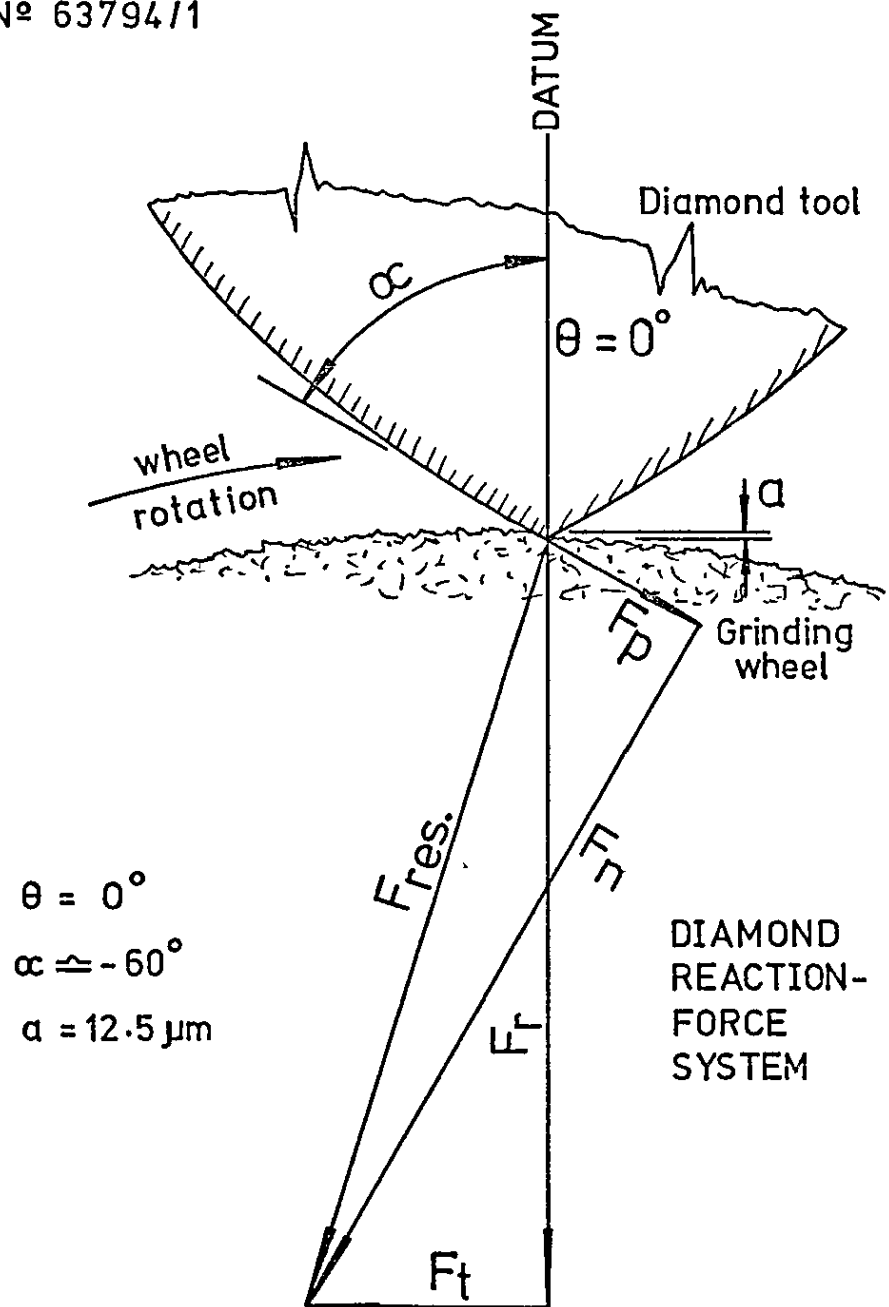
$$F_r = .90 \text{ N}$$

$$F_t = .34 \text{ N}$$

Fig.7.4 Resolution of Dressing Force

Test № 1

Diamond № 63794/1



Dressing force components (recorded)

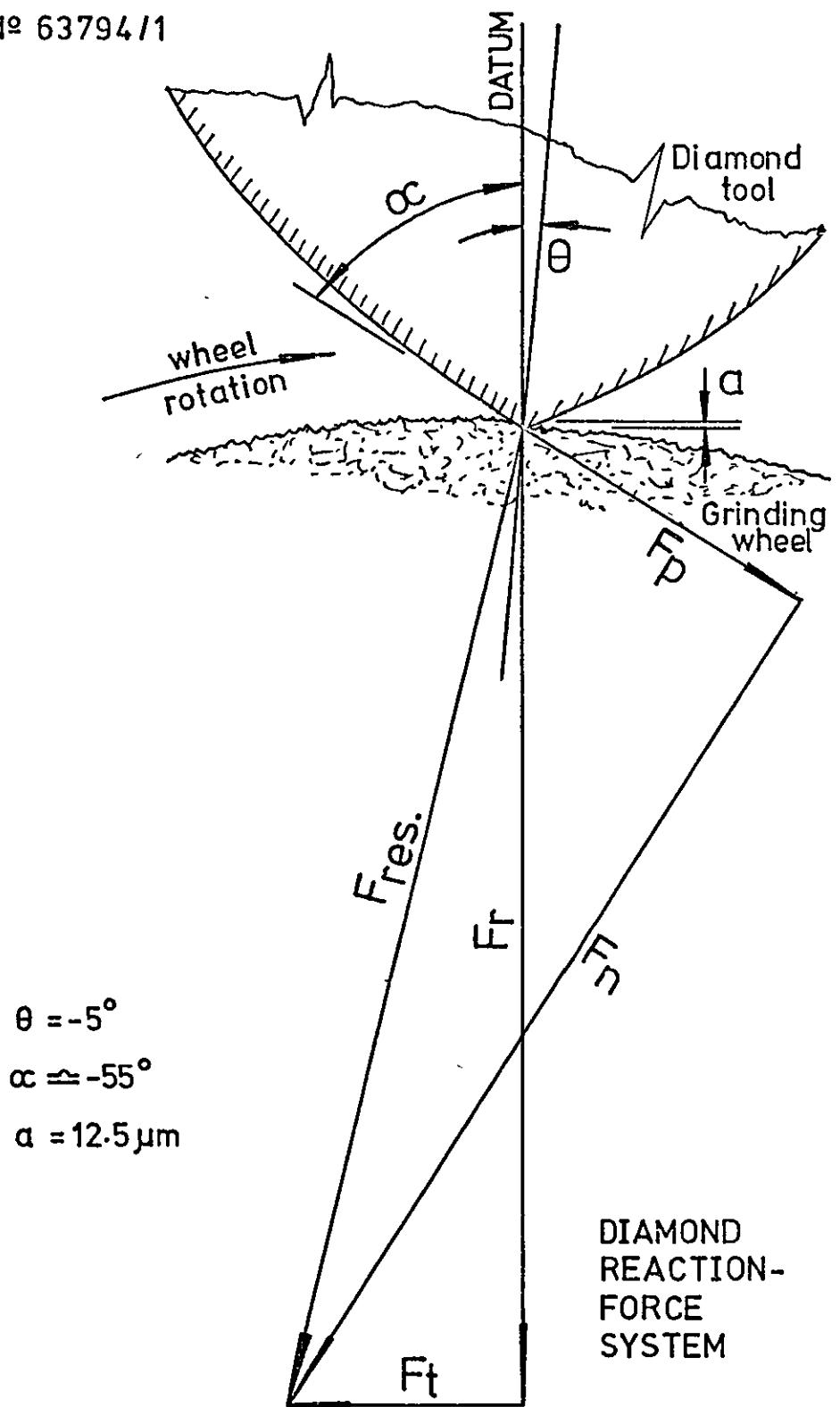
$$F_r = 2.22 \text{ N}$$

$$F_t = .69 \text{ N}$$

Fig. 7.5 Resolution of Dressing Force

Test № 1

Diamond № 63794/1



Dressing force components (recorded)

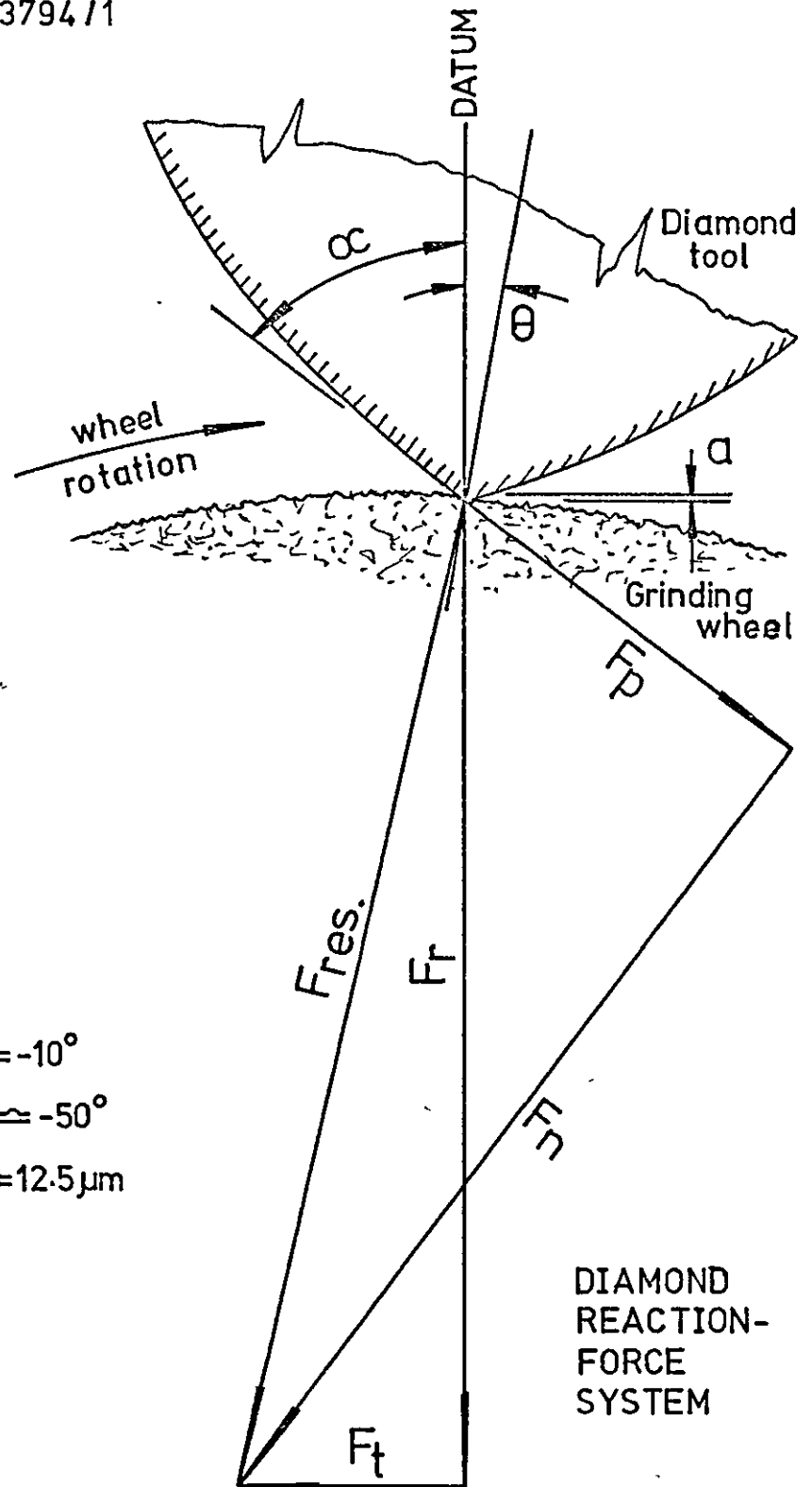
$$F_r = 3.12 \text{ N}$$

$$F_t = .76 \text{ N}$$

Fig. 7.6 Resolution of Dressing Force

Test № 1

Diamond № 63794/11



Dressing force components (recorded)

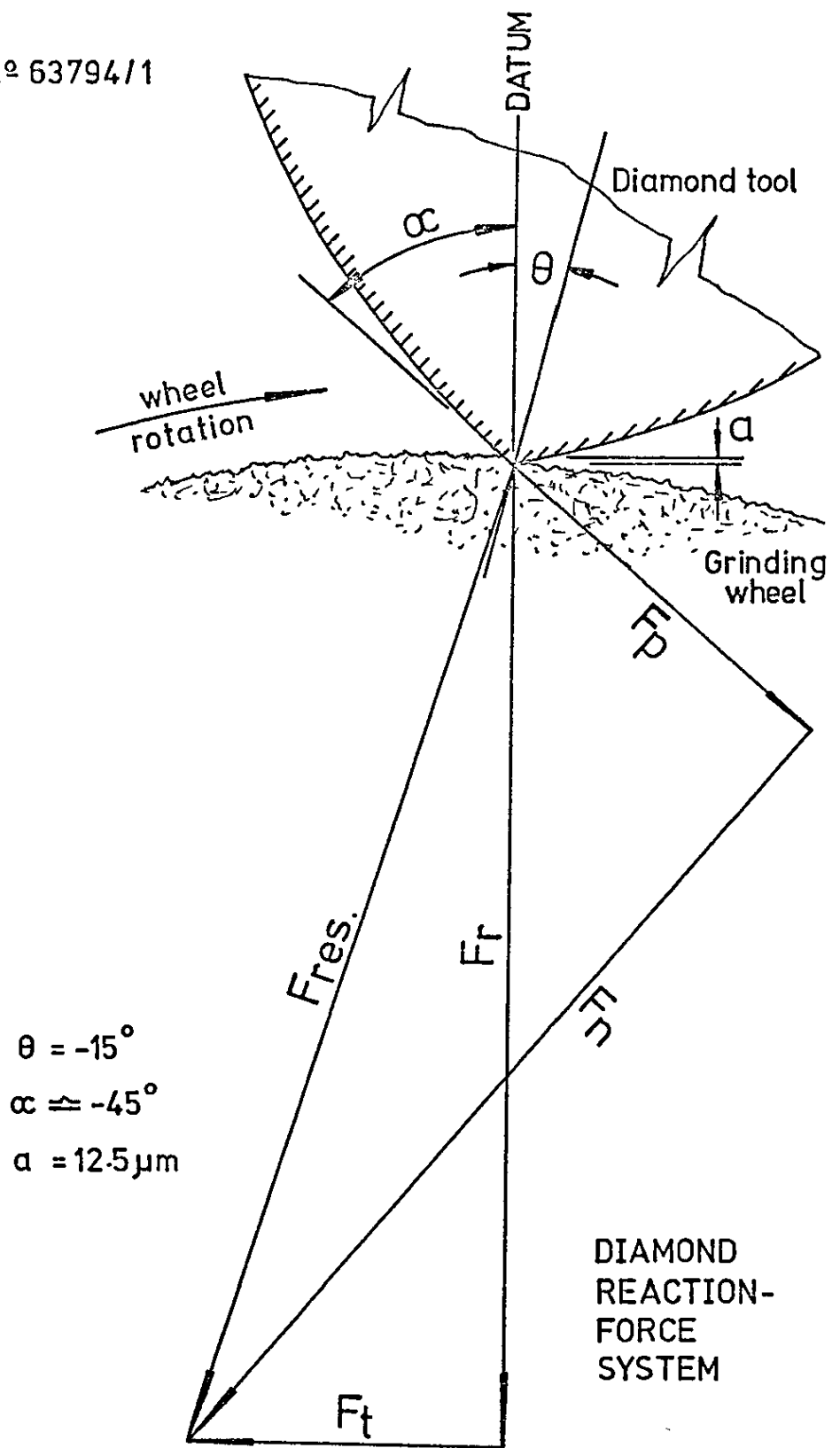
$F_r = 2.98 \text{ N}$

$F_t = .69 \text{ N}$

Fig. 7.7 Resolution of Dressing Force

Test № 1

Diamond № 63794/1



Dressing force components (recorded)

$F_r = 3.19 \text{ N}$

$F_t = 1.04 \text{ N}$

Fig. 7.8 Resolution of Dressing Force

Test N^o 2
Diamond N^o 63794/1

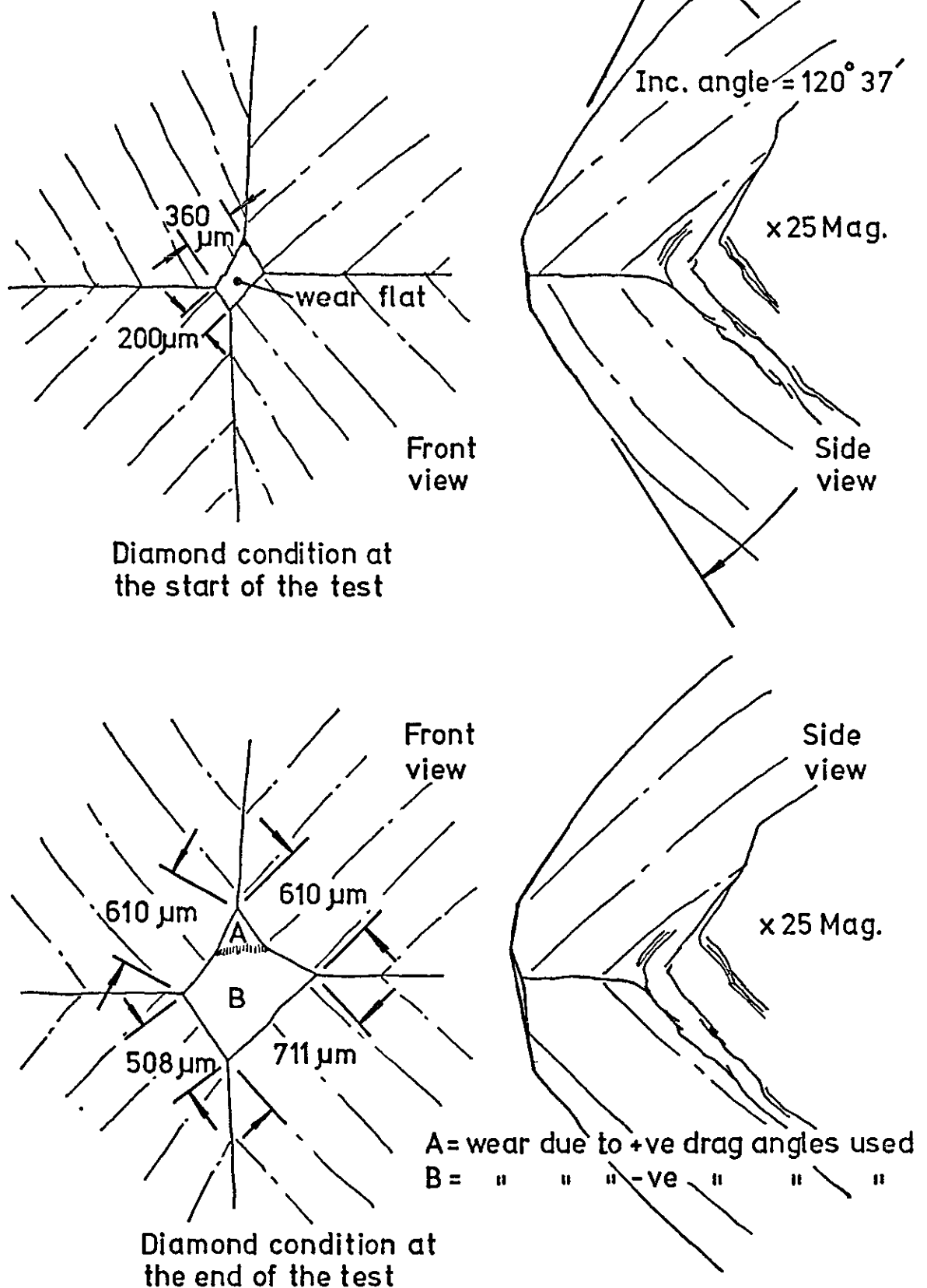


Fig. 7.9 Pictorial representation of the effect of drag angle on diamond wear when dressing.

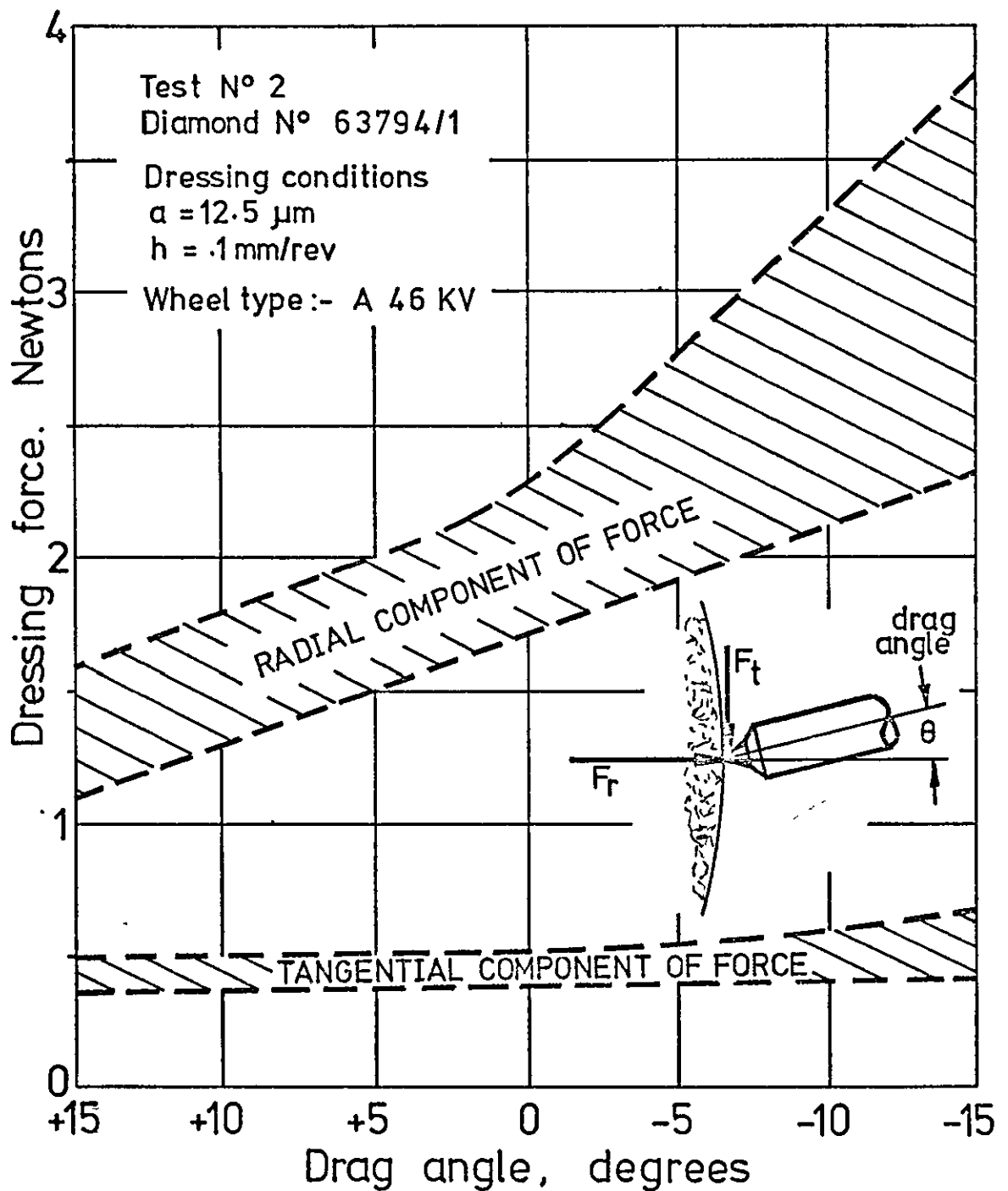


Fig. 7.10 Variation of the radial and tangential components of dressing force with diamond tool drag angle, showing the range of values obtained for a repeated test.

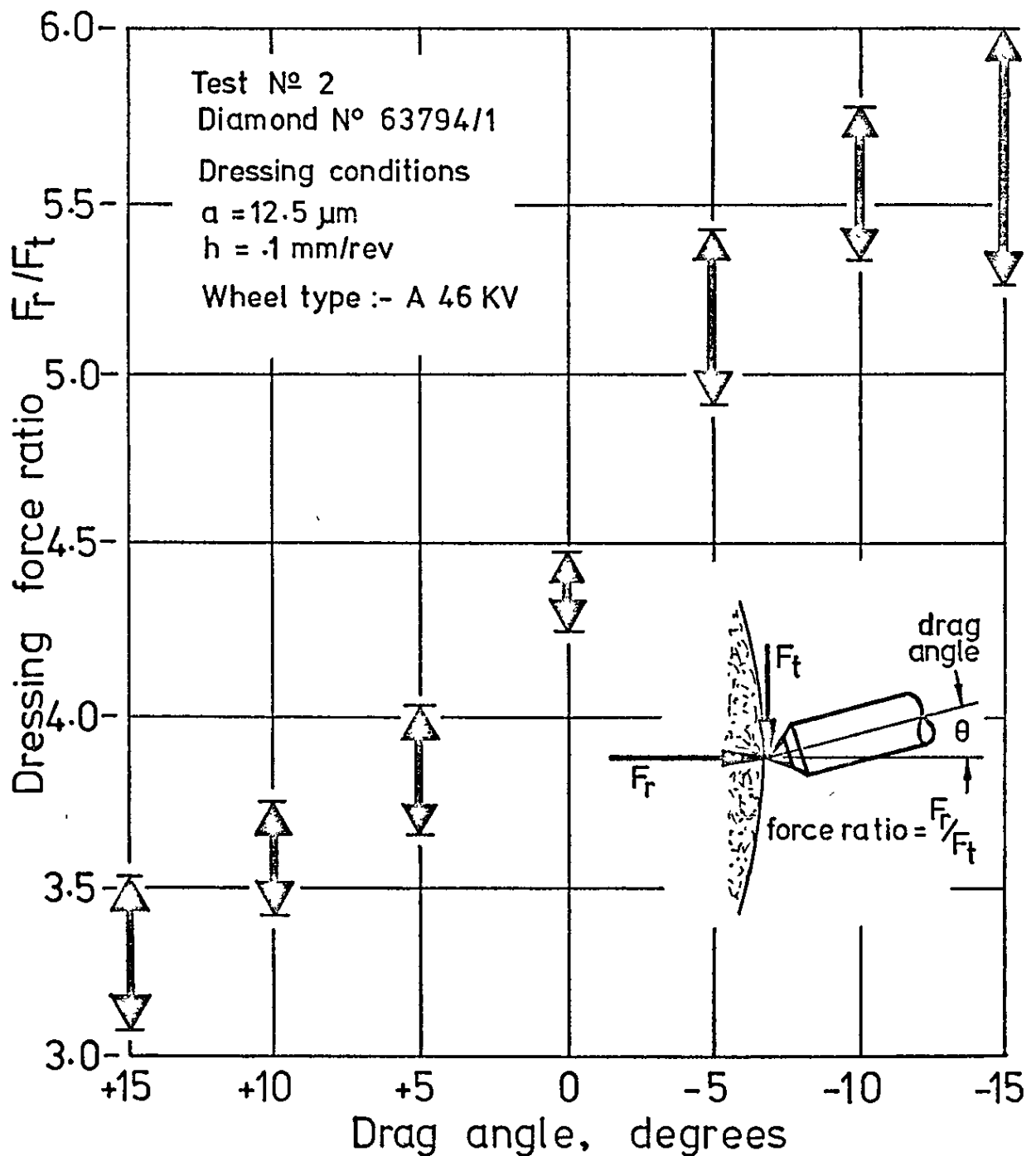


Fig. 7.11 Variation of dressing force ratio, F_r/F_t with diamond tool drag angle, showing the range of values obtained for a repeated test.

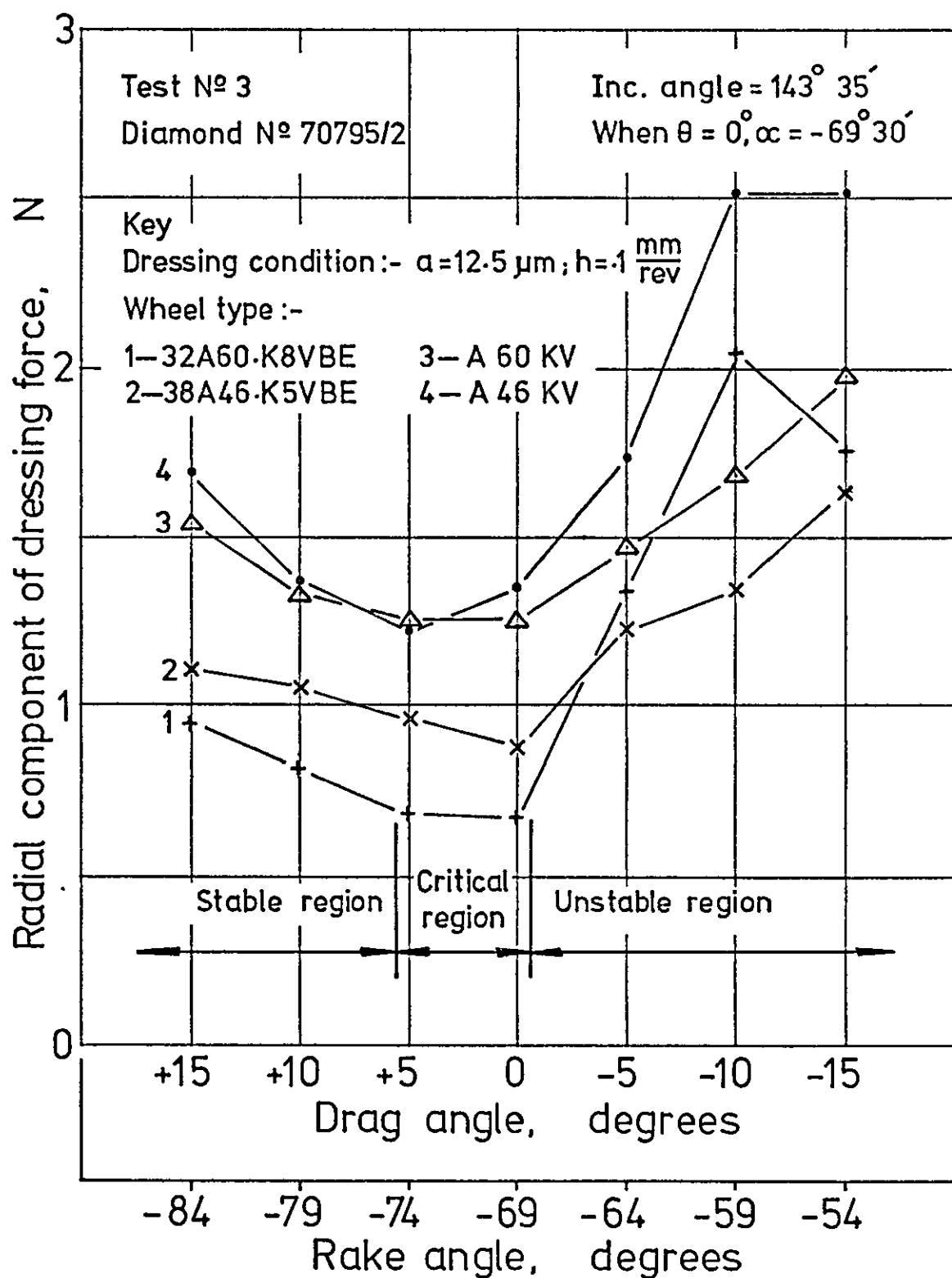


Fig. 7.12 Variation of the radial component of dressing force with the drag angle & rake angle of the diamond dressing tool for four different grinding wheels.

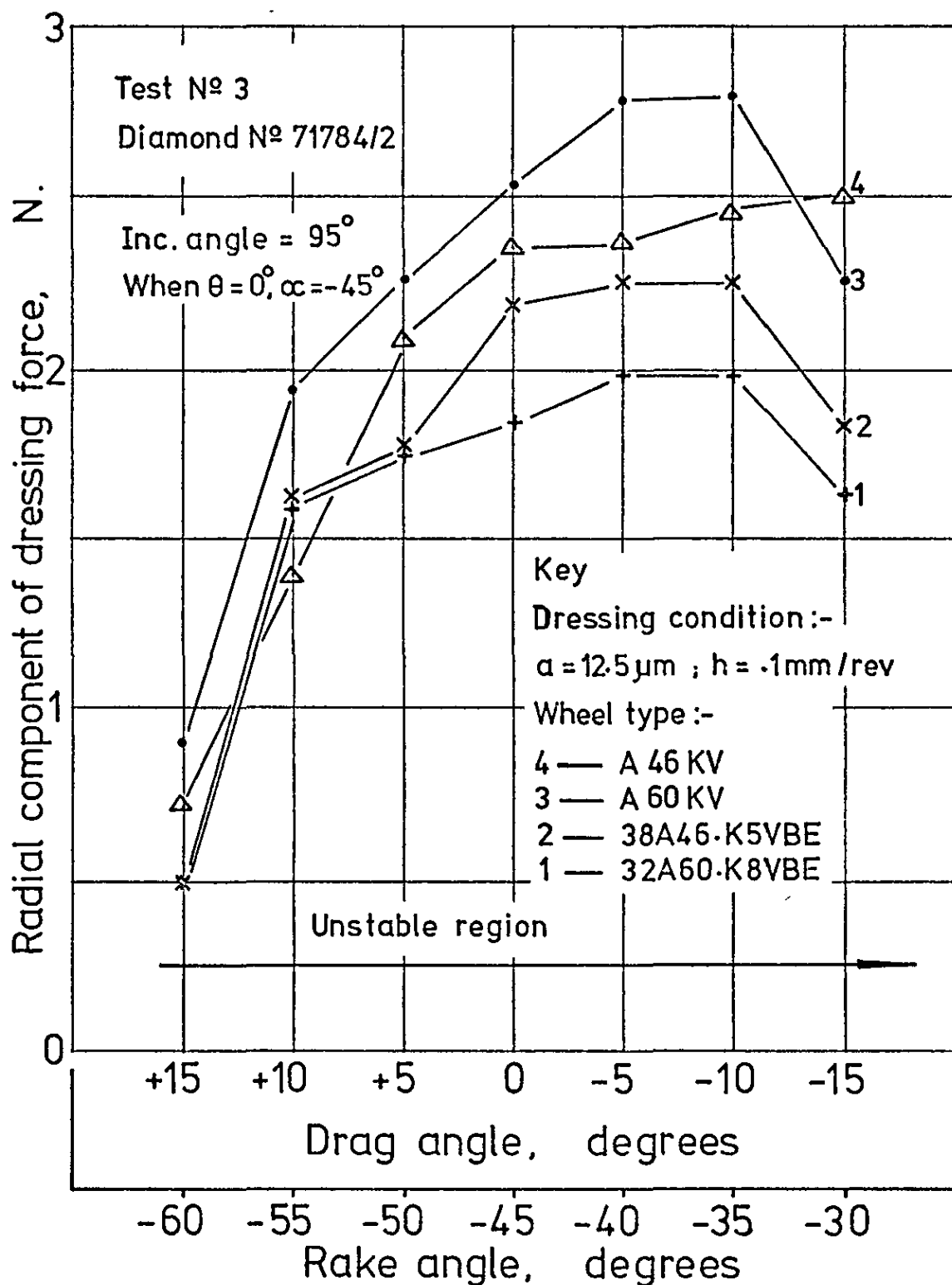


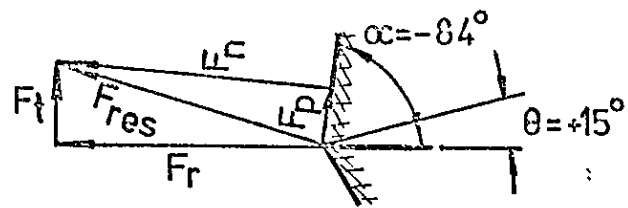
Fig. 7.13 Variation of the radial component of dressing force with the drag angle & rake angle of the diamond dressing tool for four different grinding wheels.

Test N^o 3

Diamond N^o 70795/2

Inc. angle. = $143^{\circ}35'$

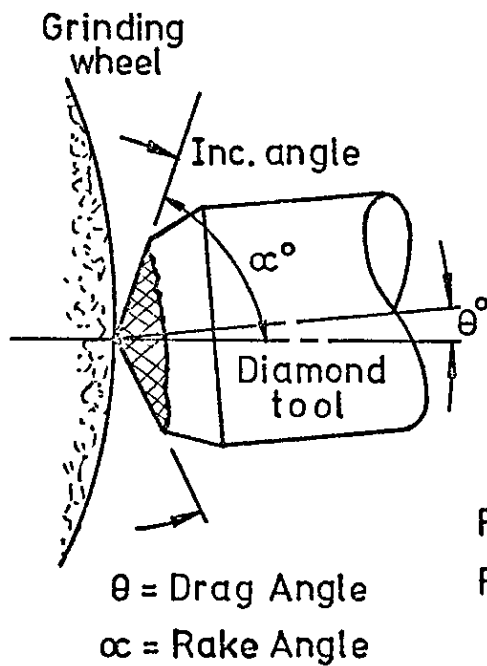
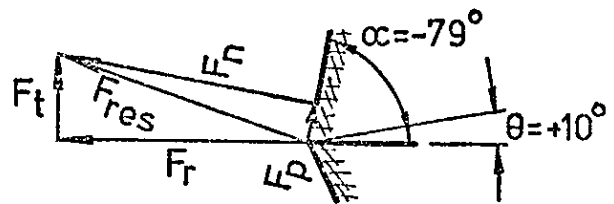
$$\left. \begin{array}{l} F_r = 1.11 \text{ N} \\ F_t = .35 \text{ N} \end{array} \right\}$$



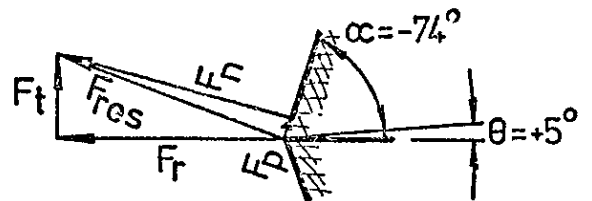
Wheel type:-

38A 46-K 5 VBE

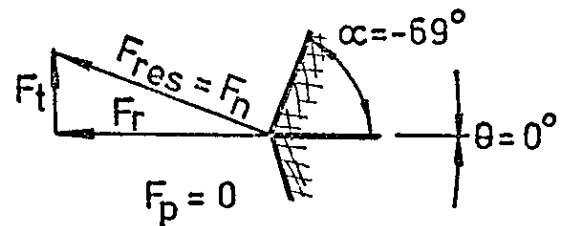
$$\left. \begin{array}{l} F_r = 1.04 \text{ N} \\ F_t = .35 \text{ N} \end{array} \right\}$$



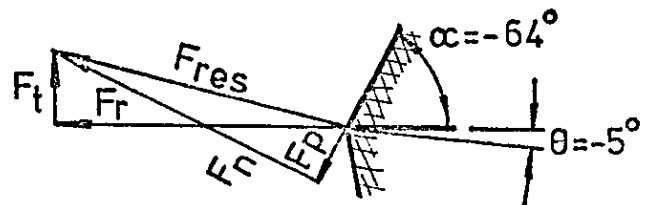
$$\left. \begin{array}{l} F_r = .96 \text{ N} \\ F_t = .33 \text{ N} \end{array} \right\}$$



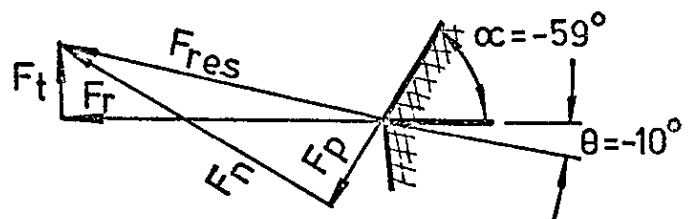
$$\left. \begin{array}{l} F_r = .88 \text{ N} \\ F_t = .31 \text{ N} \end{array} \right\}$$



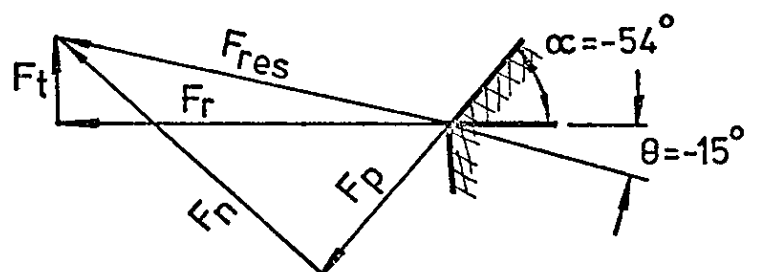
$$\left. \begin{array}{l} F_r = 1.22 \text{ N} \\ F_t = .32 \text{ N} \end{array} \right\}$$



$$\left. \begin{array}{l} F_r = 1.33 \text{ N} \\ F_t = .32 \text{ N} \end{array} \right\}$$



$$\left. \begin{array}{l} F_r = 1.63 \text{ N} \\ F_t = .33 \text{ N} \end{array} \right\}$$



Scale: 10 mm represents .3 N

Fig. 7.14 Resolution of dressing force

Test N^o 3
Diamond N^o 71784/2
Inc. angle = 95°

$F_r = 1.93 \text{ N}$
 $F_t = .41 \text{ N}$

Wheel type:- A 46 KV

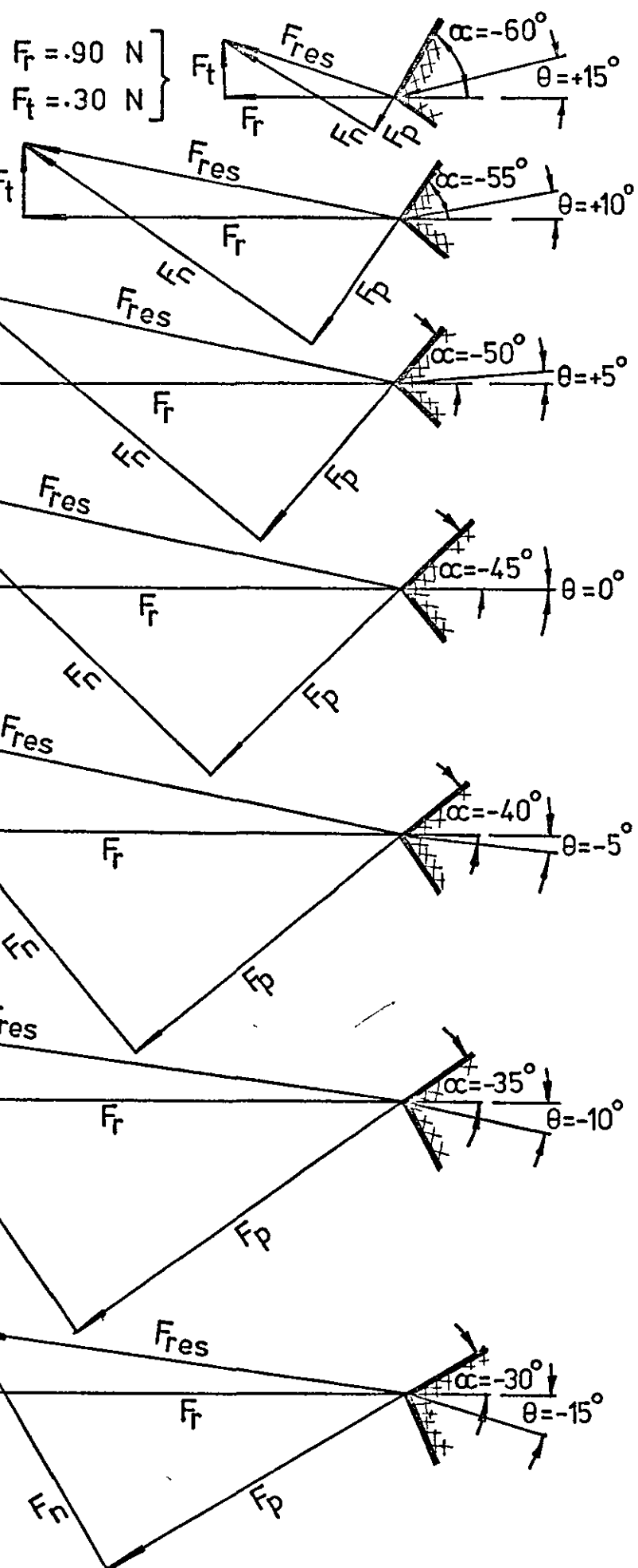
$F_r = 2.25 \text{ N}$
 $F_t = .51 \text{ N}$

$F_r = 2.52 \text{ N}$
 $F_t = .55 \text{ N}$

$F_r = 2.78 \text{ N}$
 $F_t = .54 \text{ N}$

$F_r = 2.79 \text{ N}$
 $F_t = .40 \text{ N}$

$F_r = 2.25 \text{ N}$
 $F_t = .33 \text{ N}$

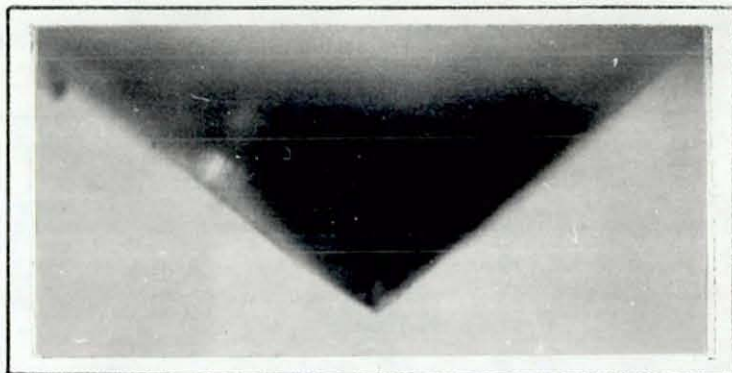


Scale: 10mm represents .3 N

Fig. 7.15 Resolution of dressing force

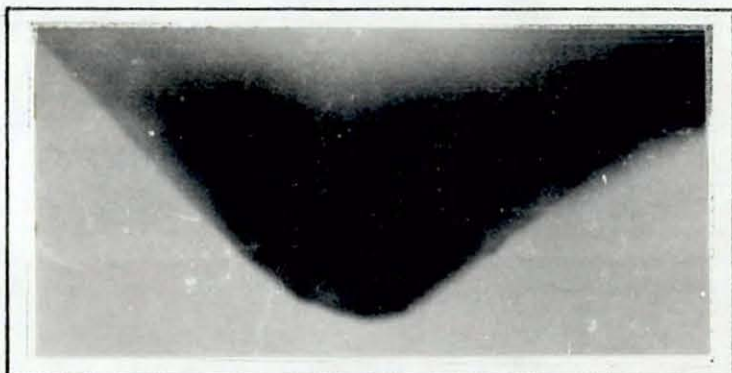
Pre-test plan view of
diamond N° 70795 / 2

Inc. angle (vertical plane)
 $143^{\circ} 35'$



Pre-test plan view of
diamond N° 71784 / 2

Inc. angle (vertical plane)
 95°



Pre-test front view of
diamond N° 71784 / 2

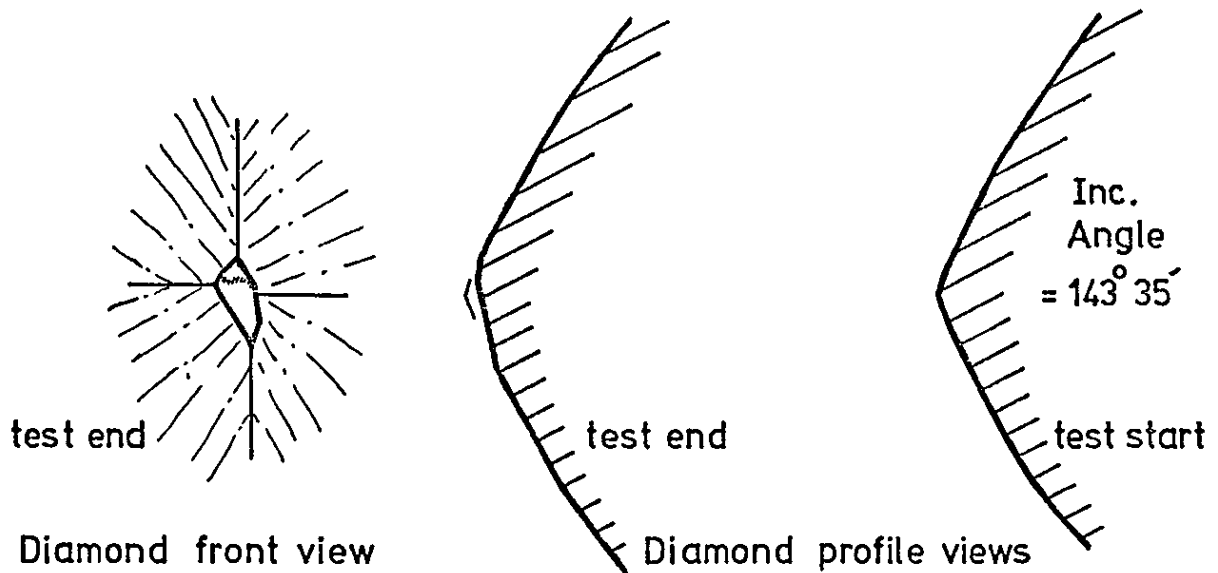


Post-test front view of
diamond N° 71784 / 2
showing the degree of
diamond wear on the tip

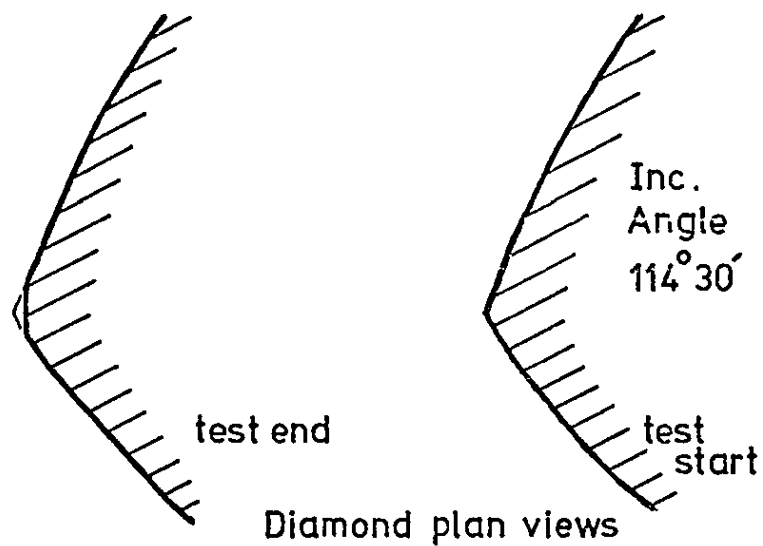
NB. Abrasion can be
seen on the diamond
rake face



Fig. 7.16 Plan views of two diamond tools before dressing, and front views of one of the diamonds before and after dressing.



All views x25 mag.



When $\theta = 0^{\circ}$, $\alpha = -69^{\circ} 30'$

Fig. 7.17 Views of wear on a diamond after dressing four grinding wheels at different values of drag angle; in-feed & cross-feed constant.

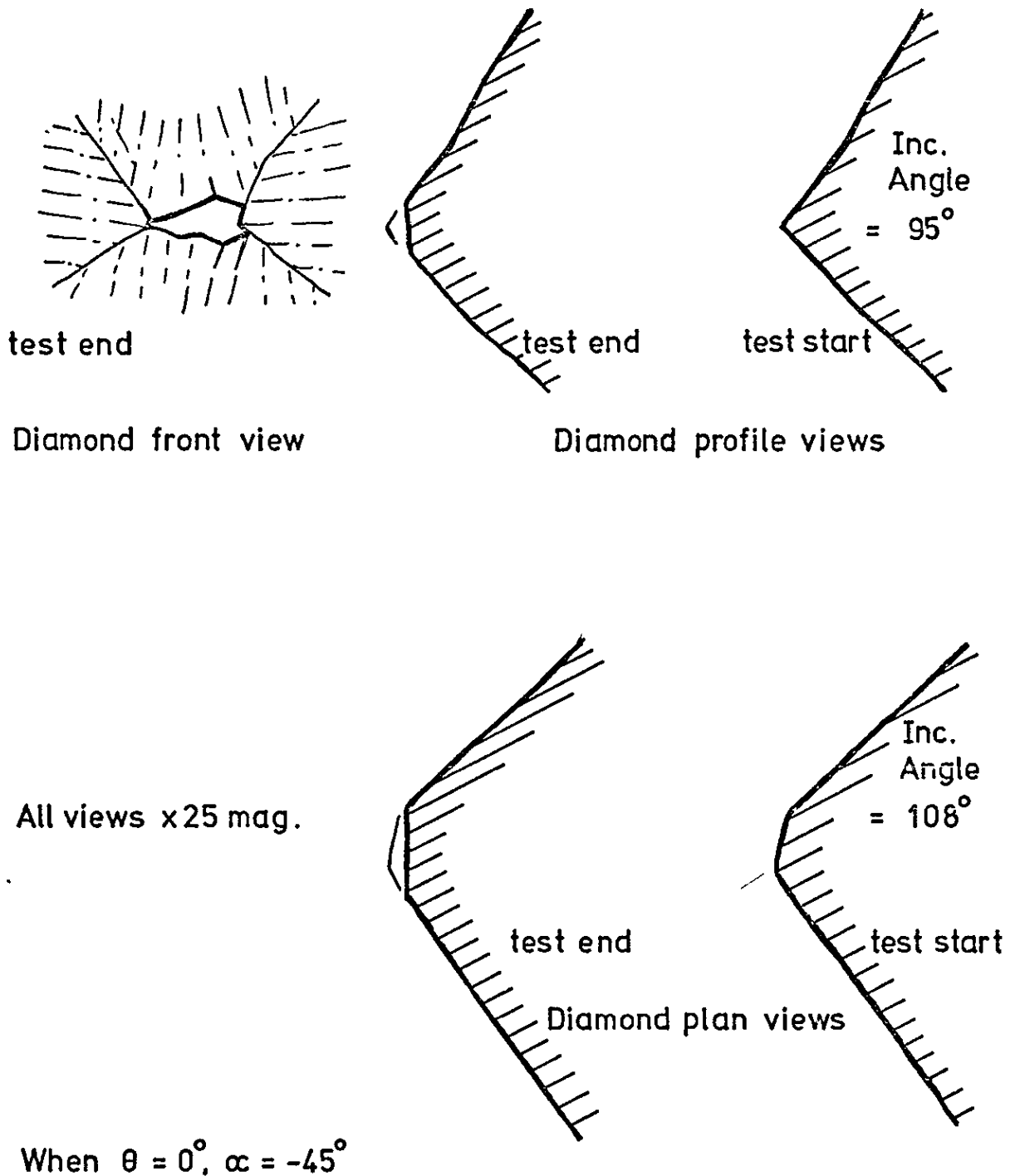
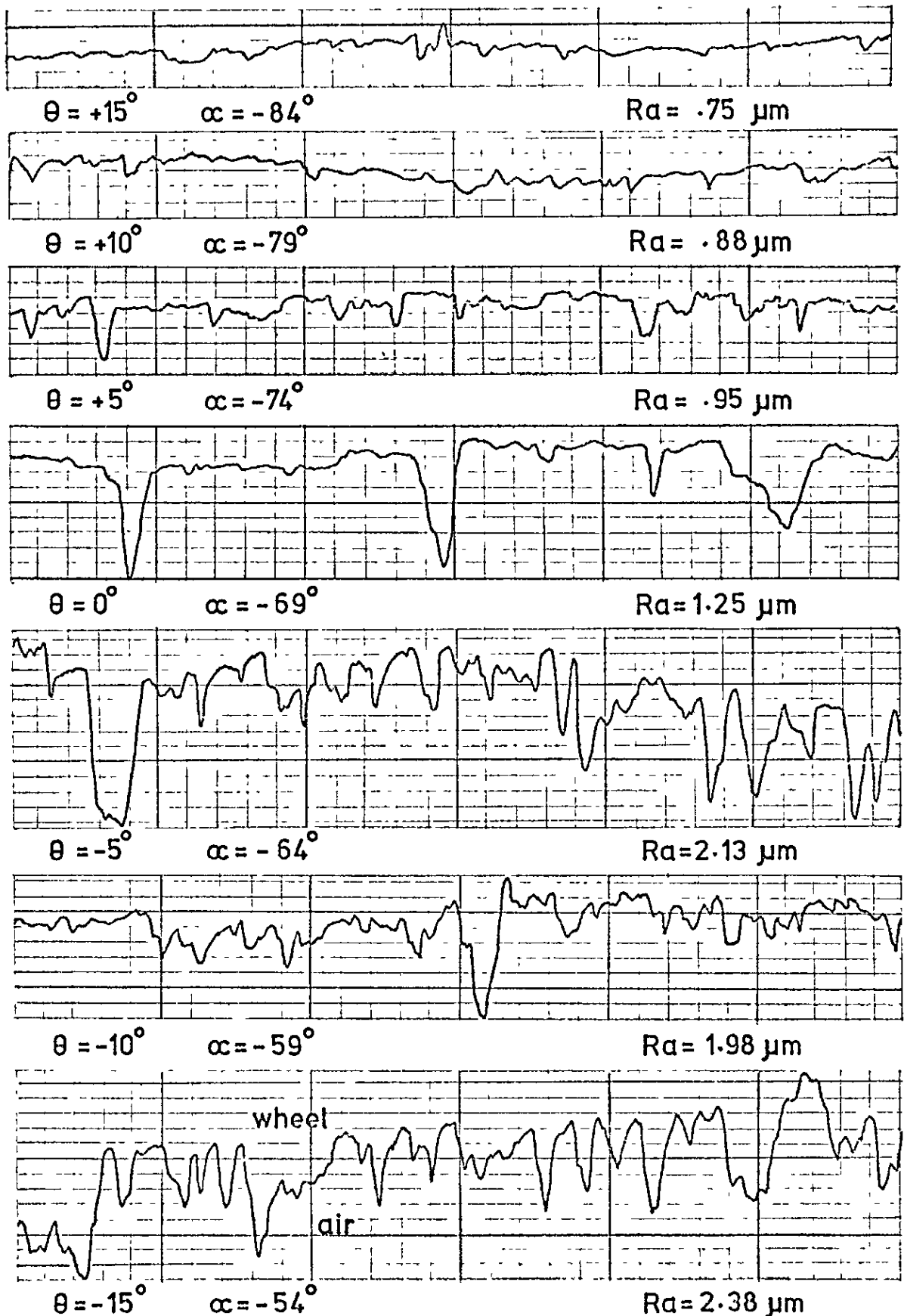


Fig. 7.18 Views of wear on a diamond after dressing four grinding wheels at different values of drag angle, in-feed & cross-feed constant.

Test N° 3: Wheel type:- A 60 KV :Diamond N° 70795/2(sharp)

Vertical mag.: 1 scale div.=1.25 μ m Horiz.mag.: 1 scale div.=50 μ m



cross-feed h , constant at .1mm/rev :: in-feed a , constant at 12.5 μ m

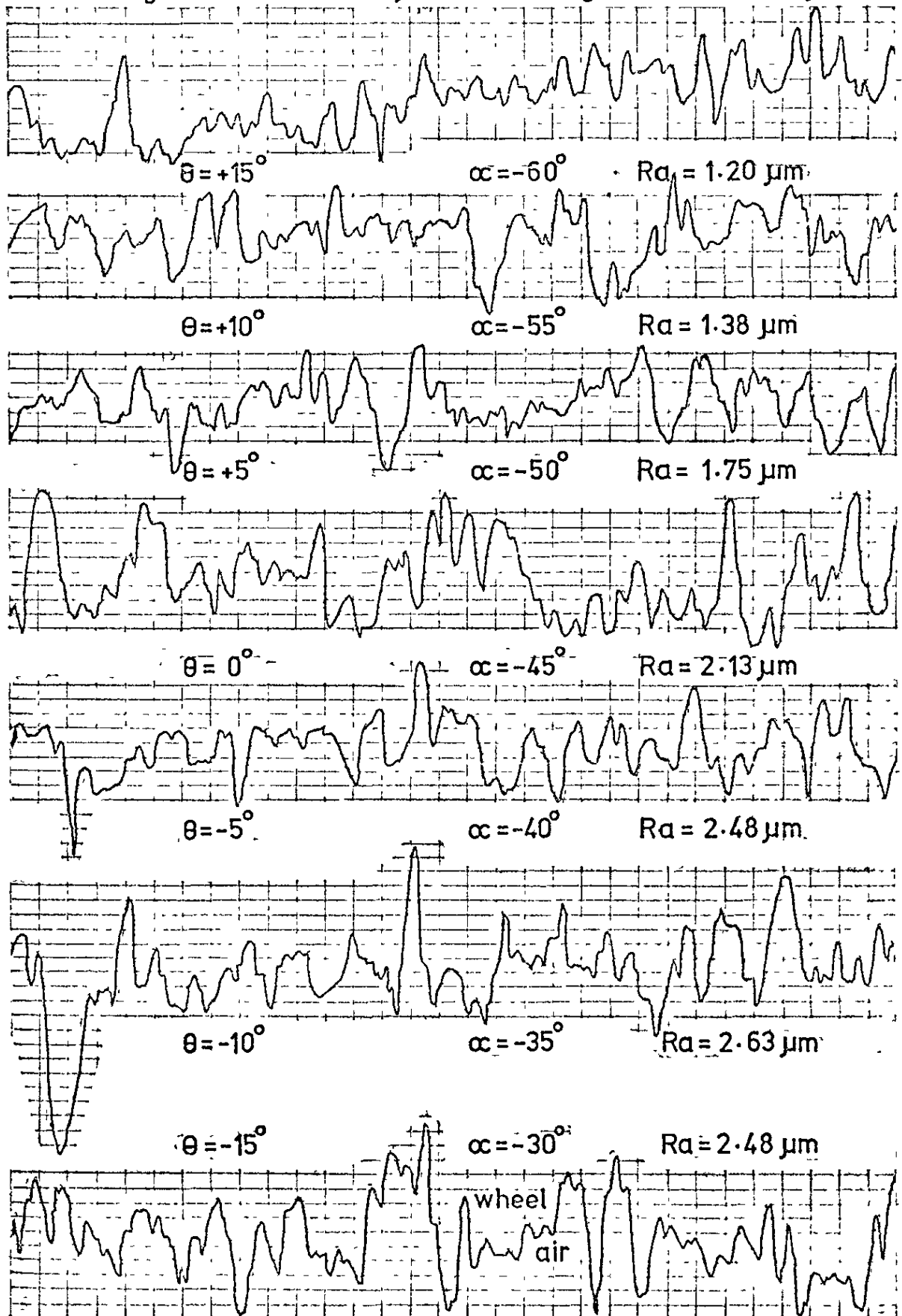
θ = Drag angle (degrees) :: α = Rake angle (degrees)

Fig. 7.19 "Talysurf" traces showing the influence of diamond drag angle (& rake angle) on grinding wheel surface roughness R_a , when dressing.

Test N° 3 : Wheel type:- A 60 KV

:Diamond N° 71784/2(sharp)

Vertical mag.: 1 scale div. = 1.25 μm Horiz. mag.: 1 scale div. = 50 μm



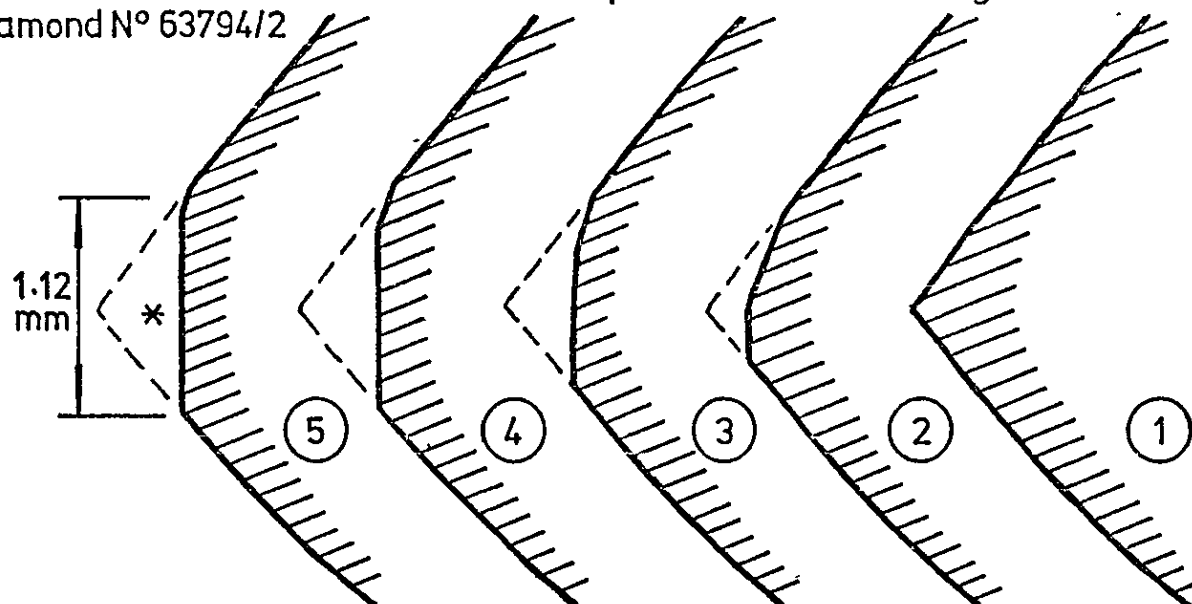
cross-feed h , constant at .1mm/rev :: in-feed a , constant at 12.5 μm

θ = Drag angle (degrees) :: α = Rake angle (degrees)

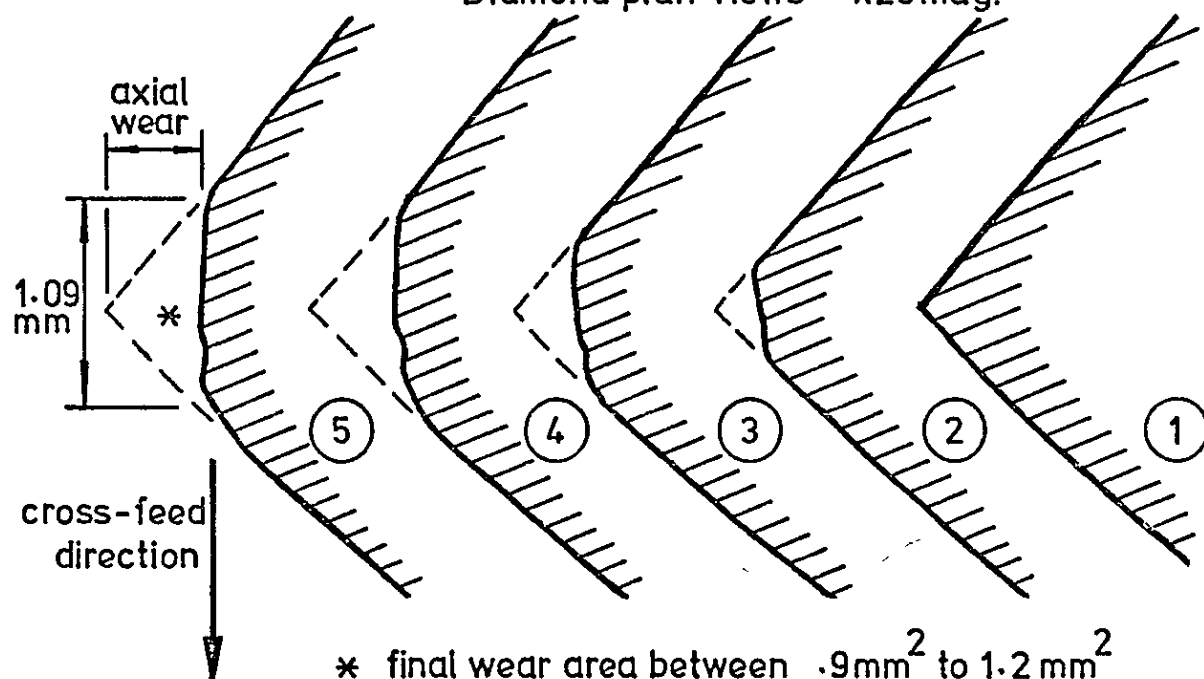
Fig. 7.20 "Talysurf" traces showing the influence of diamond drag angle (& rake angle) on grinding wheel surface roughness R_a , when dressing

Test Nos 4 to 7 inc.
Diamond N° 63794/2

Diamond profile views x25mag.



Diamond plan views x25mag.



| Diamond condition | comment | Axial wear µm | Difference µm |
|-------------------|------------------------------|------------------|------------------|
| (1) | New diamond - no wear | 0 | 200 |
| (2) | Wear at the end of Test N° 4 | 200 | 140 |
| (3) | " " " " " " " 5 | 340 | 95 |
| (4) | " " " " " " " 6 | 435 | 60 |
| (5) | " " " " " " " 7 | 495 | |

Fig. 7.21 Profile and plan views of a diamond showing the extent of diamond wear after dressing four grinding wheels at various values of in-feed, cross-feed and drag angle.

Test N^o 4
 Diamond N^o 63794/2 (sharp)
 Wheel type:- 32 A 60 - K 8 VBE

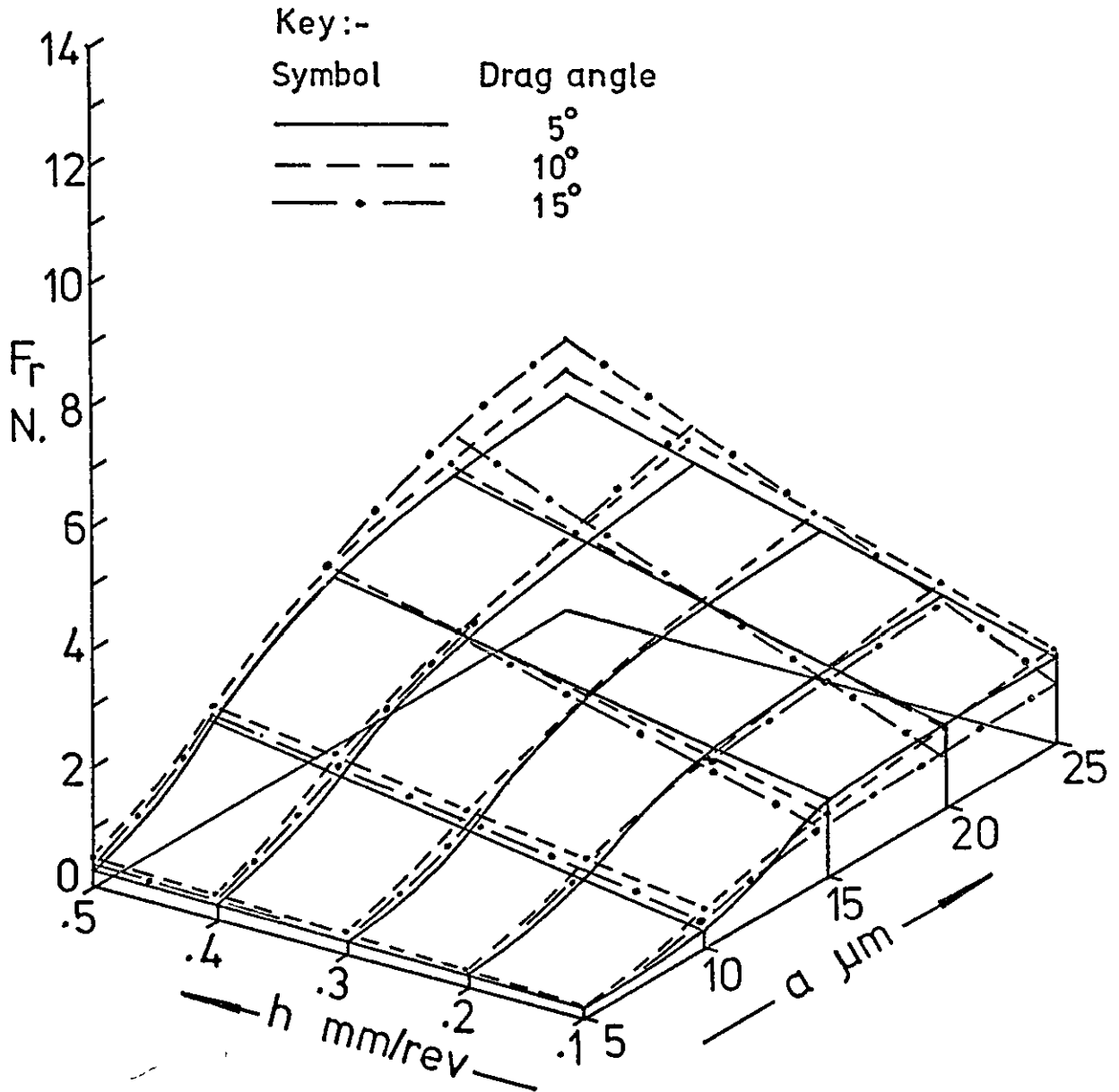


Fig. 7.22 Variation of dressing force (radial component) with dressing depth of cut and traverse rate for a range of values of drag angle.

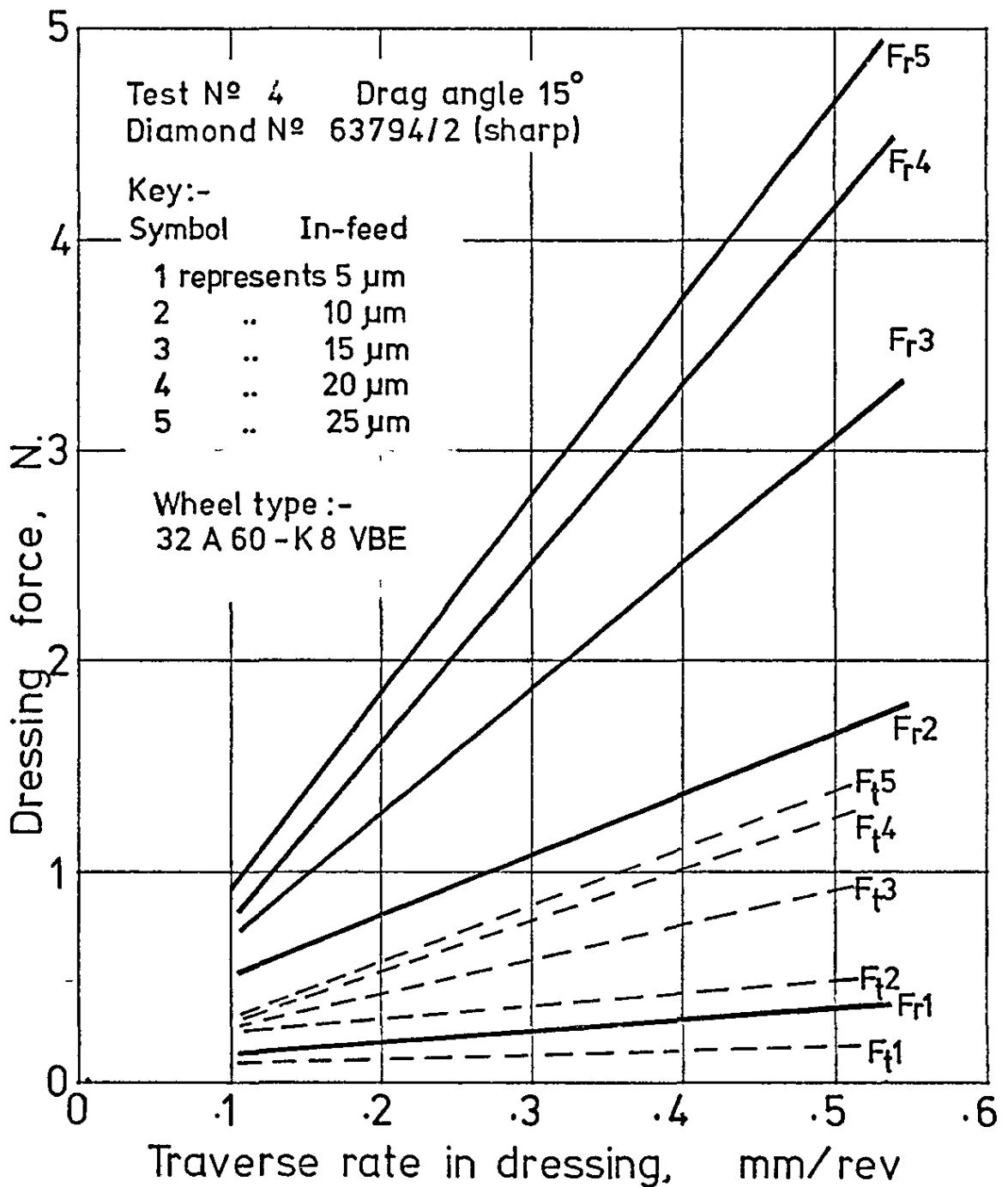


Fig. 7.23 Variation of the radial & tangential components of dressing force, namely F_r & F_t respectively, with traverse rate in dressing. for different depths of cut.

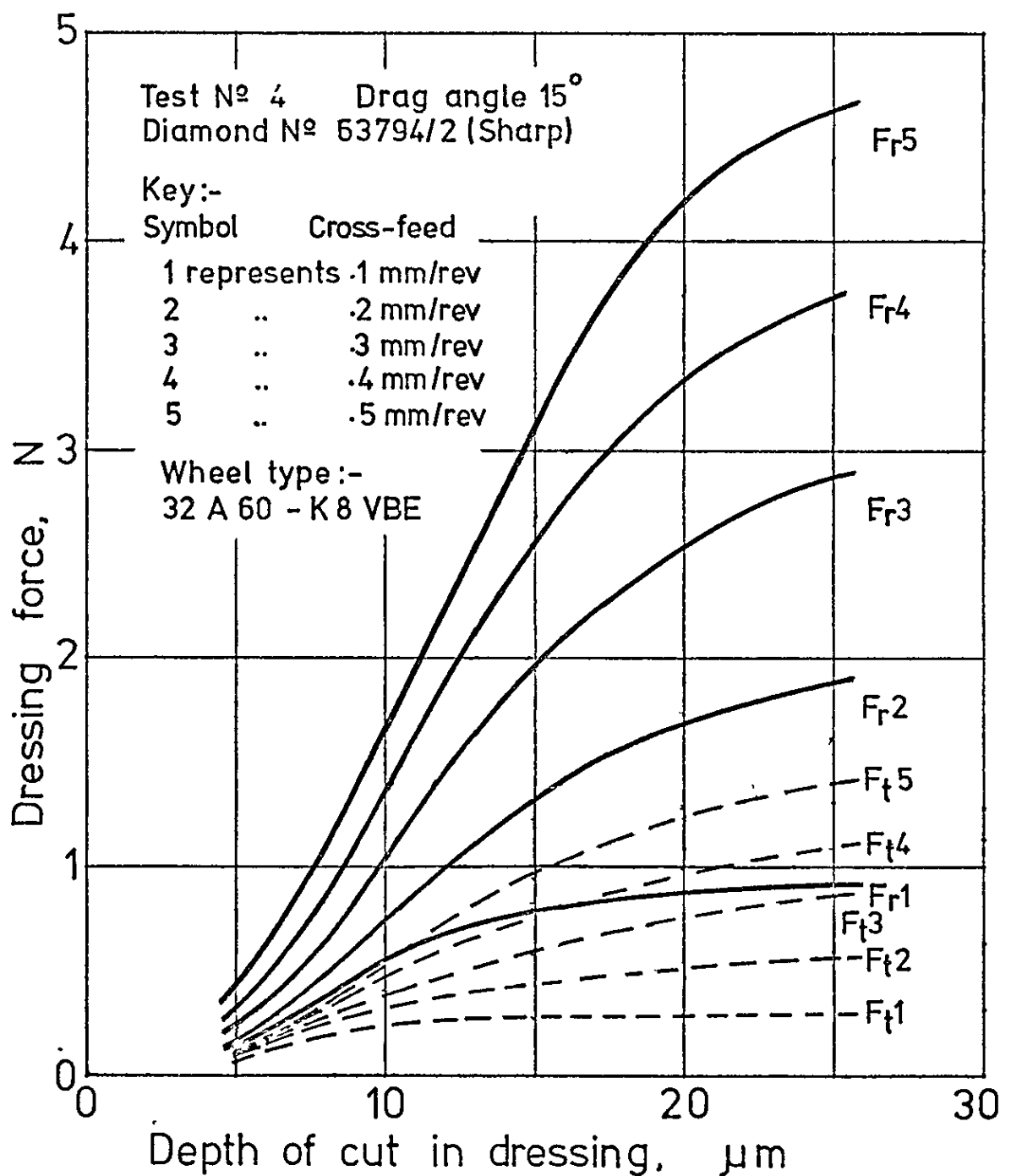
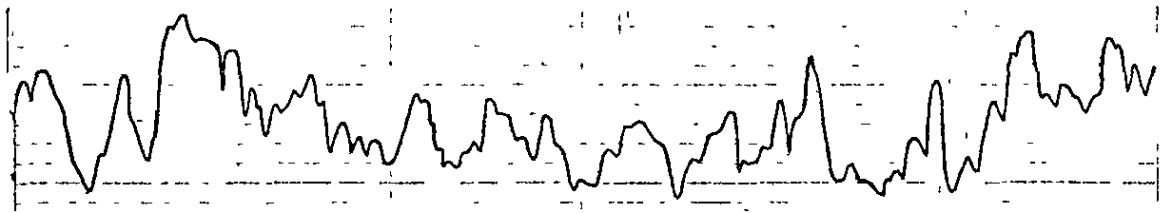


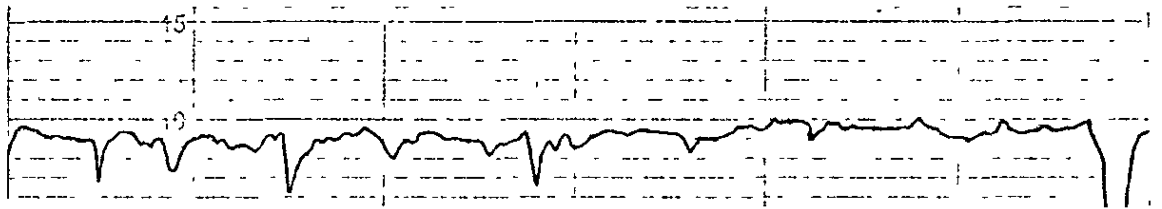
Fig. 7.24 Variation of the radial & tangential components of dressing force, namely F_r & F_t respectively, with depth of cut in dressing for different traverse rates.

Test № 4: Wheel type:- 32 A 60-K8 VBE: Diamond № 63794/2 (sharp)
 Vertical mag.: 1 scale div. = 1.25 μm Horiz. mag.: 1 scale div. = 50 μm



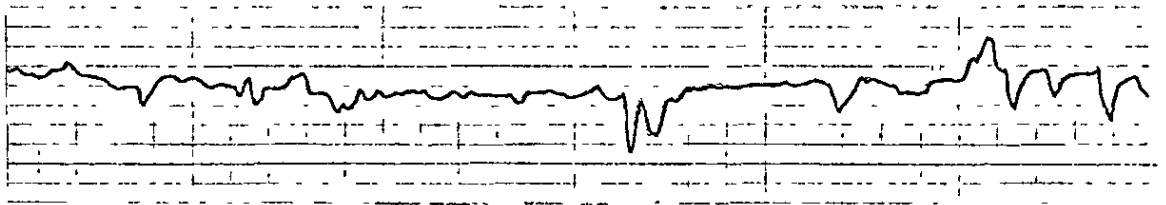
$a = 25 \mu\text{m}$

$Ra = 2.36 \mu\text{m}$



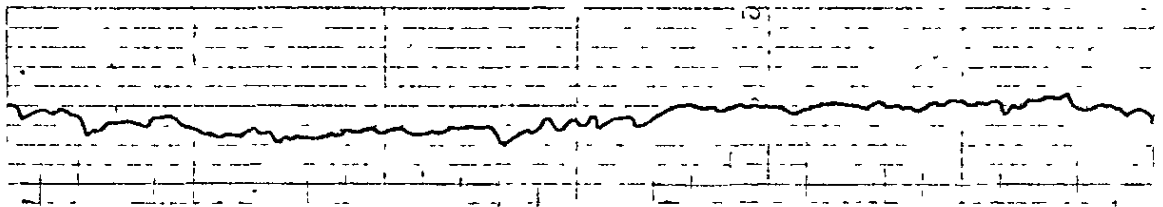
$a = 20 \mu\text{m}$

$Ra = 1.45 \mu\text{m}$



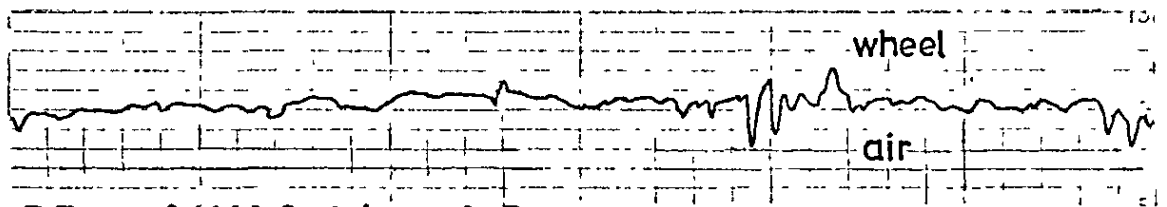
$a = 15 \mu\text{m}$

$Ra = .90 \mu\text{m}$



$a = 10 \mu\text{m}$

$Ra = .75 \mu\text{m}$



$a = 5 \mu\text{m}$

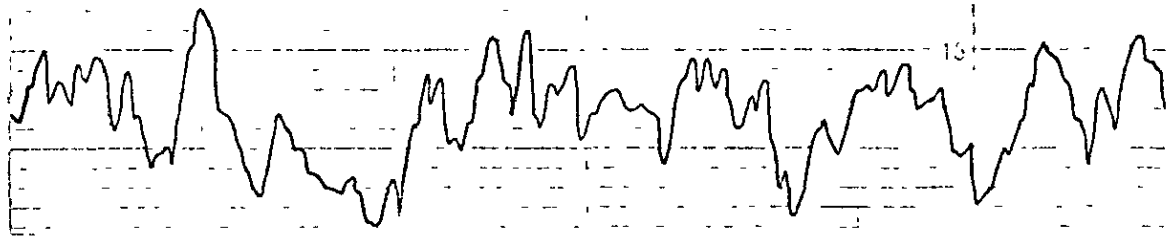
$Ra = .50 \mu\text{m}$

h constant at .1 mm/rev

θ constant at 5°

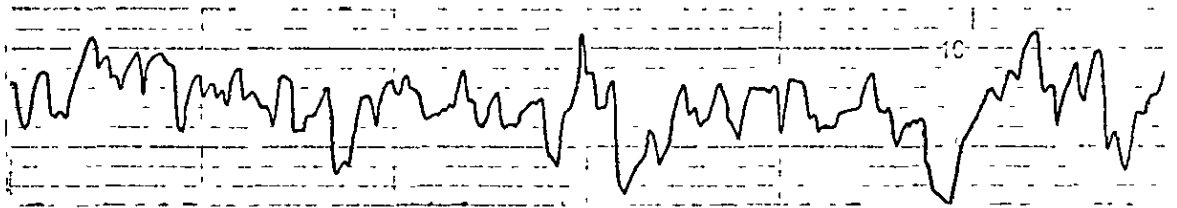
Fig. 7.25 "Talysurf" traces of grinding wheel surface roughness Ra when dressing with a fixed diamond drag angle θ , constant cross-feed h and variable in-feed a .

Test N° 4 : Wheel type:-32A60-K8VBE : Diamond N° 63794/2 (sharp)
 Vertical mag.: 1 scale div.=1.25 μm Horiz.mag.: 1 scale div.= 50 μm



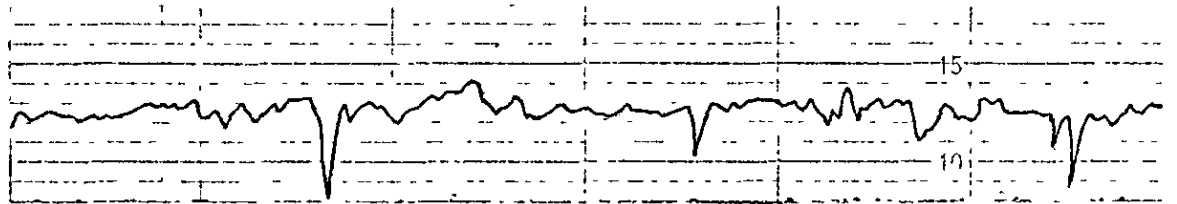
$\alpha = 25 \mu\text{m}$

$Ra = 2.42 \mu\text{m}$



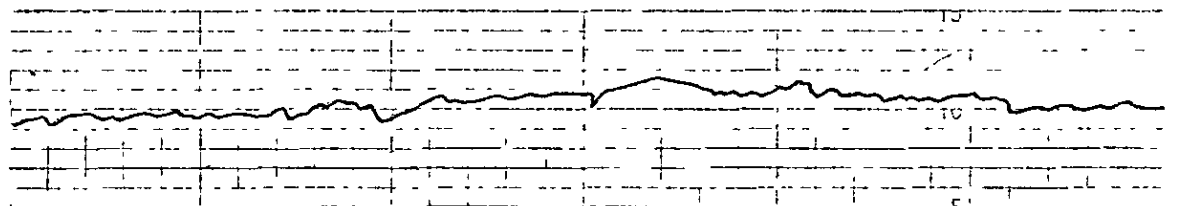
$\alpha = 20 \mu\text{m}$

$Ra = 1.80 \mu\text{m}$



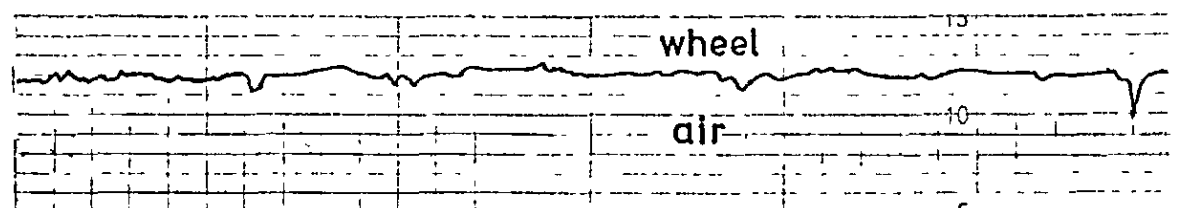
$\alpha = 15 \mu\text{m}$

$Ra = 1.05 \mu\text{m}$



$\alpha = 10 \mu\text{m}$

$Ra = .75 \mu\text{m}$



$\alpha = 5 \mu\text{m}$

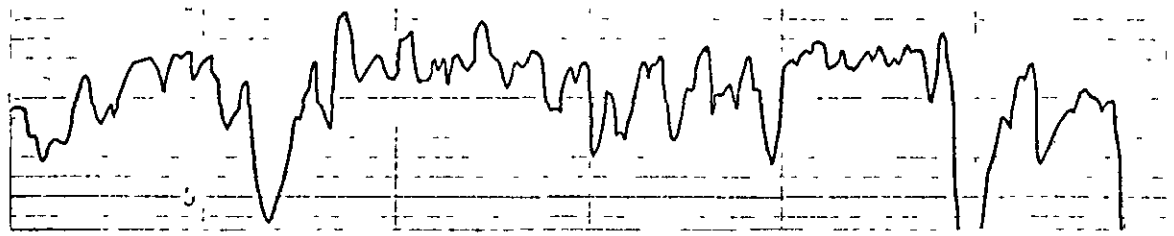
$Ra = .70 \mu\text{m}$

h constant at .2 mm/rev

θ constant at 5°

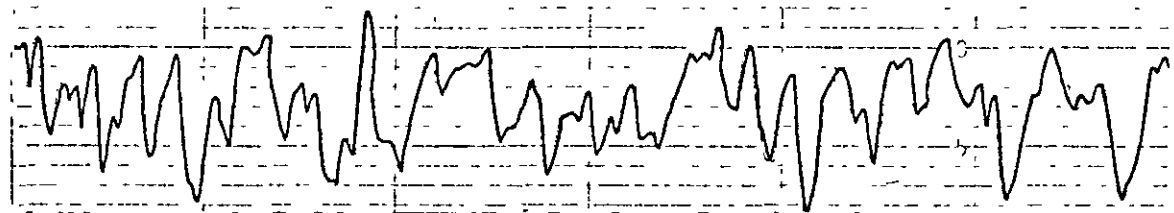
Fig. 7.26 "Talysurf" traces of grinding wheel surface roughness Ra when dressing with a fixed diamond drag angle θ , constant cross-feed h and variable in-feed α .

Test N° 4 : Wheel type: -32 A60-K8VBE : Diamond N° 63794/2 (sharp)
 Vertical mag.: 1 scale div. = 1.25 μm Horiz. mag.: 1 scale div. = 50 μm



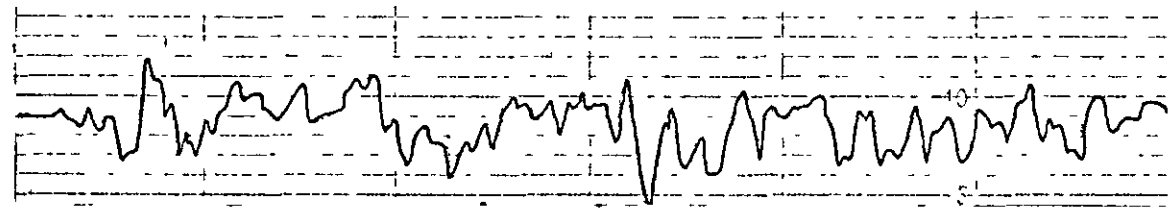
$\alpha = 25 \mu\text{m}$

$Ra = 2.50 \mu\text{m}$



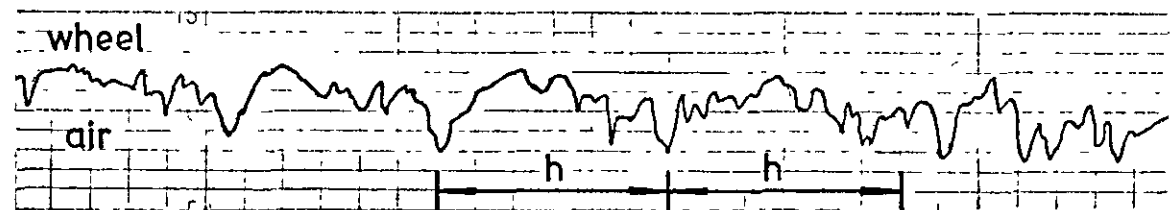
$\alpha = 20 \mu\text{m}$

$Ra = 2.30 \mu\text{m}$



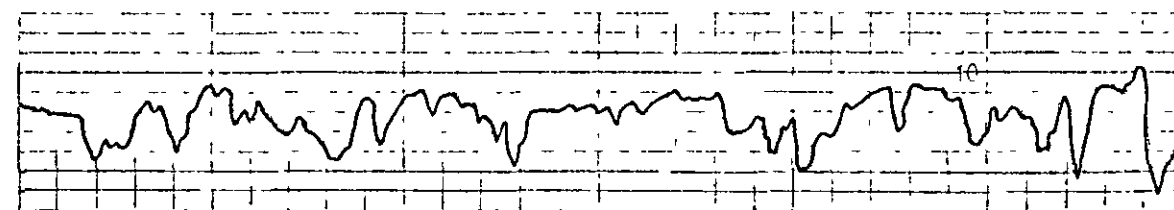
$\alpha = 15 \mu\text{m}$

$Ra = 1.25 \mu\text{m}$



$\alpha = 10 \mu\text{m}$

$Ra = 1.05 \mu\text{m}$



$\alpha = 5 \mu\text{m}$

$Ra = 1.00 \mu\text{m}$

h constant at .3 mm/rev

θ constant at 5°

Fig. 7.27 "Talysurf" traces of grinding wheel surface roughness Ra when dressing with a fixed diamond drag angle θ , constant cross-feed h and variable in-feed α .

Test N° 4 : Wheel type:- 32A60-K8VBE : Diamond N° 63794/2 (sharp)
 Vertical mag.: 1 scale div.=1.25 μm Horiz.mag.: 1 scale div.= 50 μm

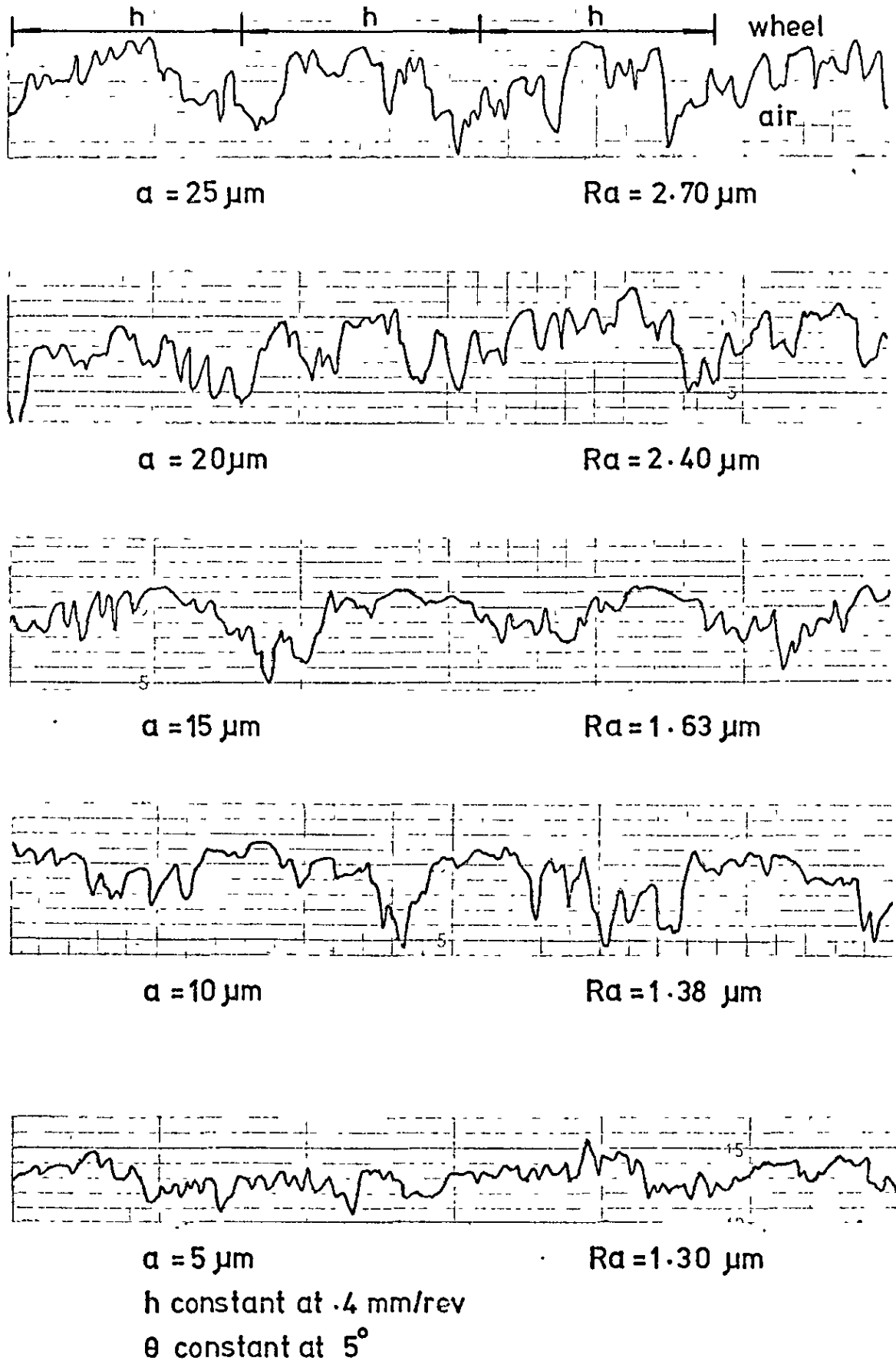


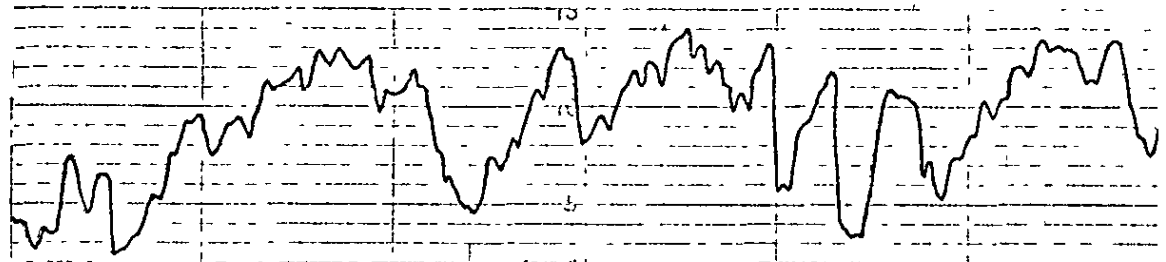
Fig. 7.28 "Talysurf" traces of grinding wheel surface roughness Ra when dressing with a fixed diamond drag angle θ , constant cross-feed h and variable in-feed a .

Test N° 4 : Wheel type:- 32 A 60-K8VBE: Diamond N° 63794/2 (sharp)
 Vertical mag.: 1 scale div.=1.25 μm Horiz.mag.: 1 scale div.= 50 μm



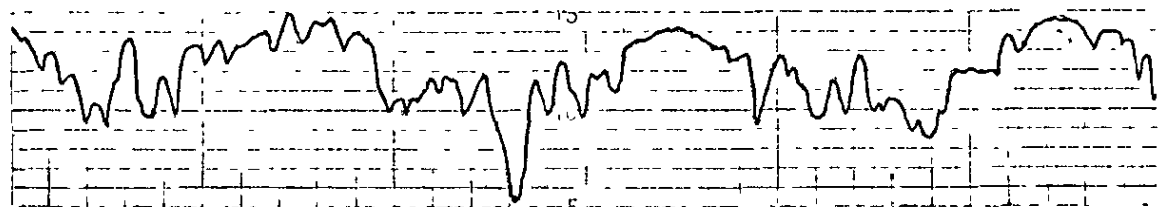
$\alpha = 25 \mu\text{m}$

$Ra = 2.98 \mu\text{m}$



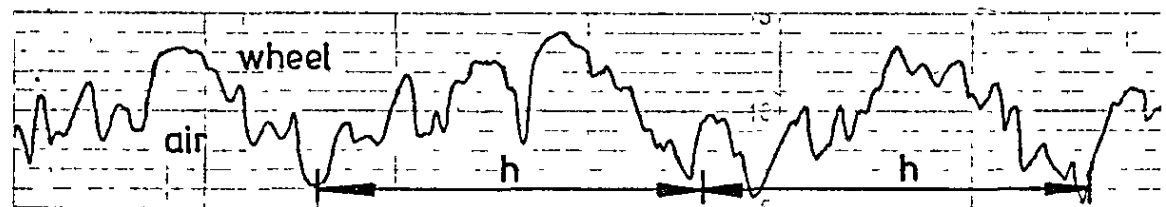
$\alpha = 20 \mu\text{m}$

$Ra = 2.88 \mu\text{m}$



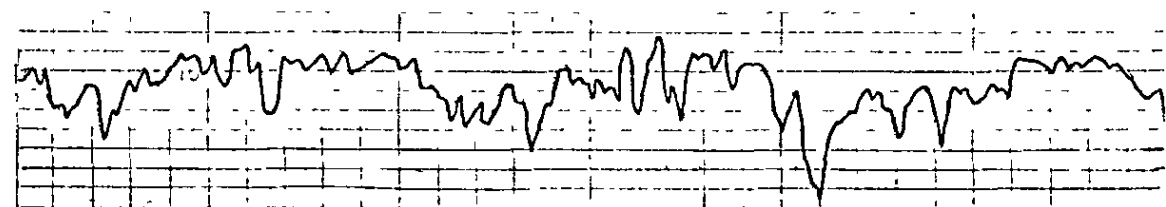
$\alpha = 15 \mu\text{m}$

$Ra = 2.70 \mu\text{m}$



$\alpha = 10 \mu\text{m}$

$Ra = 2.10 \mu\text{m}$



$\alpha = 5 \mu\text{m}$

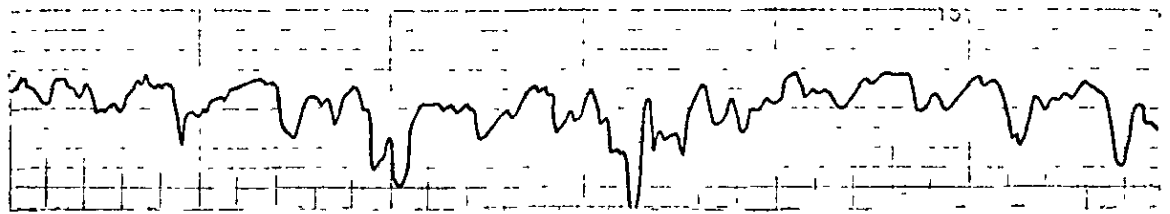
$Ra = 1.65 \mu\text{m}$

h constant at .5 mm/rev

θ constant at 5°

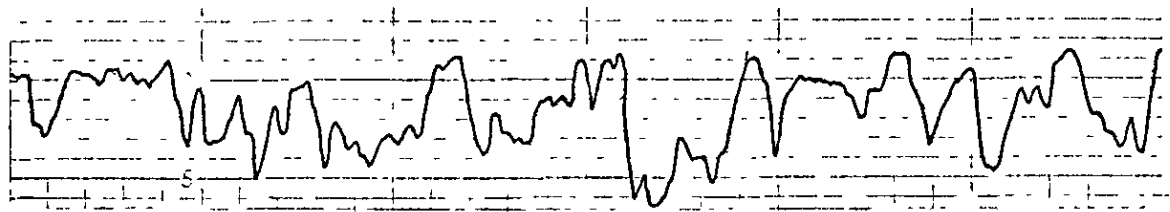
Fig. 7.29 "Talysurf" traces of grinding wheel surface roughness Ra when dressing with a fixed diamond drag angle θ , constant cross-feed h and variable in-feed α .

Test N° 4 : Wheel type :-32 A60-K8VBE : Diamond N° 63794/2 (sharp)
 Vertical mag.: 1 scale div.=1.25 μm Horiz.mag.: 1 scale div.= 50 μm



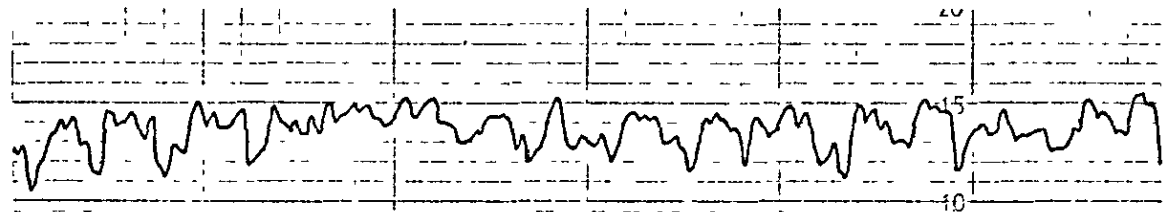
$\alpha = 25 \mu\text{m}$

$Ra = 1.70 \mu\text{m}$



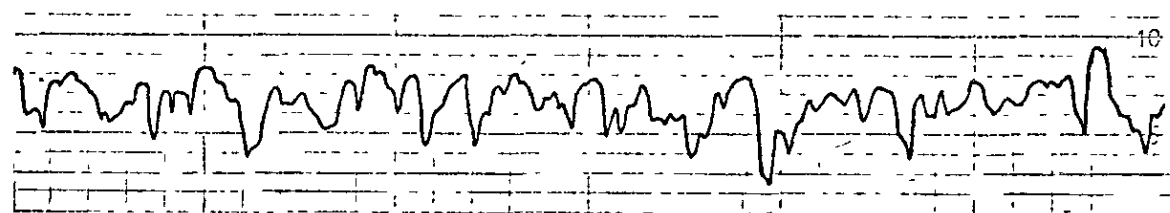
$\alpha = 20 \mu\text{m}$

$Ra = 1.63 \mu\text{m}$



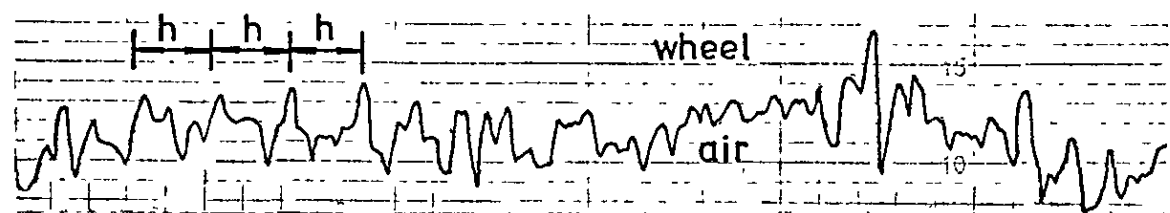
$\alpha = 15 \mu\text{m}$

$Ra = 1.25 \mu\text{m}$



$\alpha = 10 \mu\text{m}$

$Ra = 1.33 \mu\text{m}$



$\alpha = 5 \mu\text{m}$

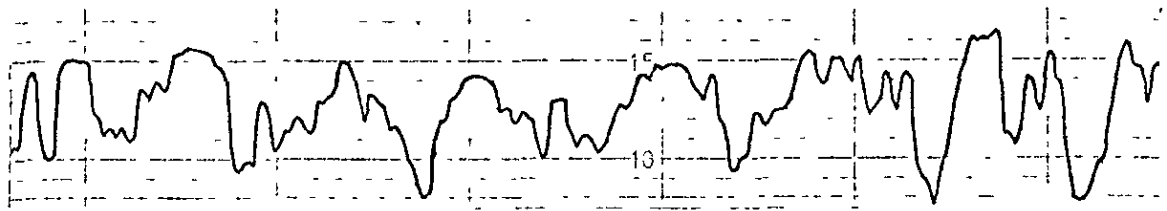
$Ra = 1.00 \mu\text{m}$

h constant at .1 mm/rev

θ constant at 10°

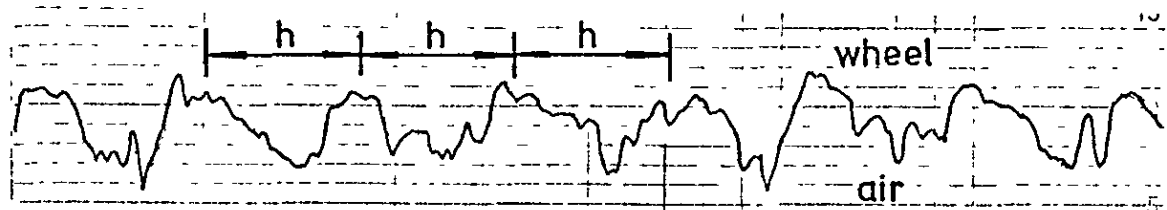
Fig. 7.30 "Talysurf" traces of grinding wheel surface roughness Ra when dressing with a fixed diamond drag angle θ , constant cross-feed h and variable in-feed α .

Test N° 4 : Wheel type :- 32A60-K8VBE: Diamond N° 63794/2 (sharp)
 Vertical mag.: 1 scale div. = 1.25 μm Horiz. mag.: 1 scale div. = 50 μm



$\alpha = 25 \mu\text{m}$

$Ra = 1.80 \mu\text{m}$



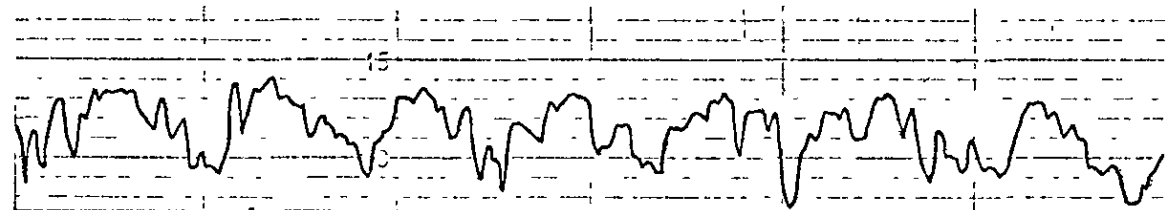
$\alpha = 20 \mu\text{m}$

$Ra = 1.75 \mu\text{m}$



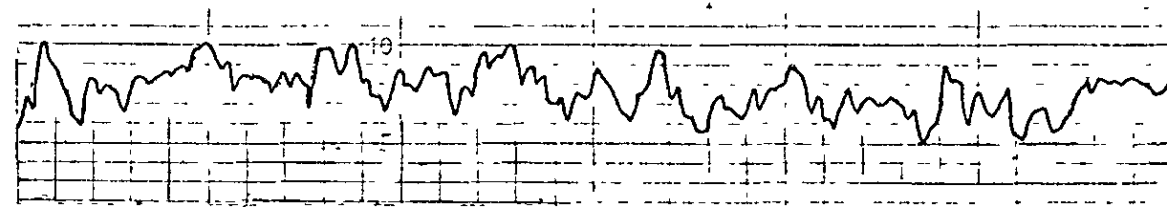
$\alpha = 15 \mu\text{m}$

$Ra = 1.75 \mu\text{m}$



$\alpha = 10 \mu\text{m}$

$Ra = 1.55 \mu\text{m}$



$\alpha = 5 \mu\text{m}$

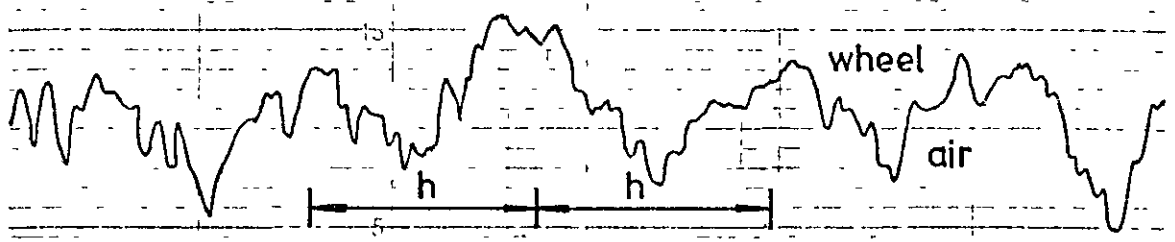
$Ra = 1.25 \mu\text{m}$

h constant at .2 mm/rev

θ constant at 10°

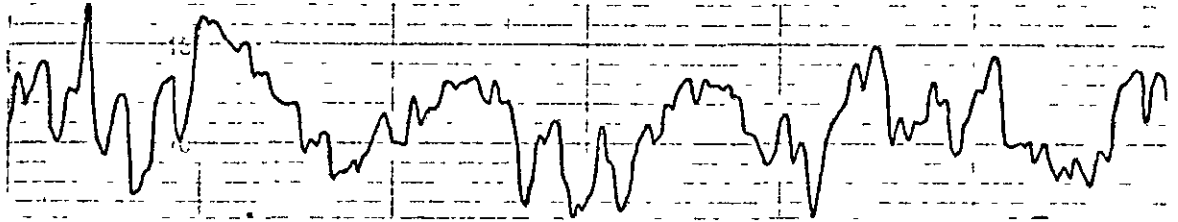
Fig. 7.31 "Talysurf" traces of grinding wheel surface roughness Ra when dressing with a fixed diamond drag angle θ , constant cross-feed h and variable in-feed a .

Test N° 4 : Wheel type:-32A60-K8VBE : Diamond N° 63794/2 (sharp)
 Vertical mag.: 1 scale div.=1.25 μm Horiz.mag.: 1 scale div.= 50 μm



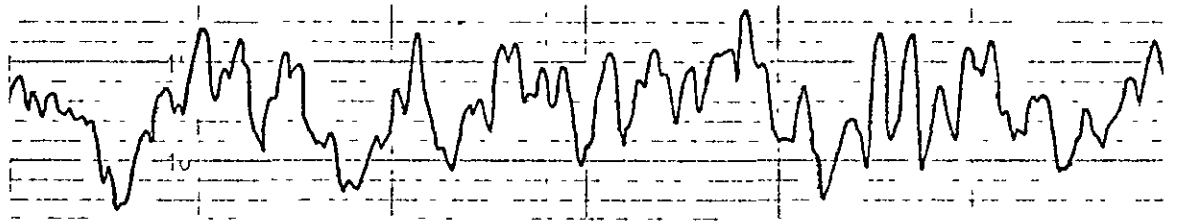
$a = 25 \mu\text{m}$

$Ra = 2.63 \mu\text{m}$



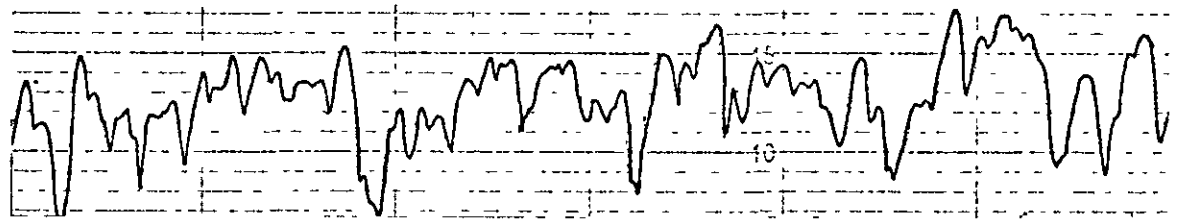
$a = 20 \mu\text{m}$

$Ra = 2.38 \mu\text{m}$



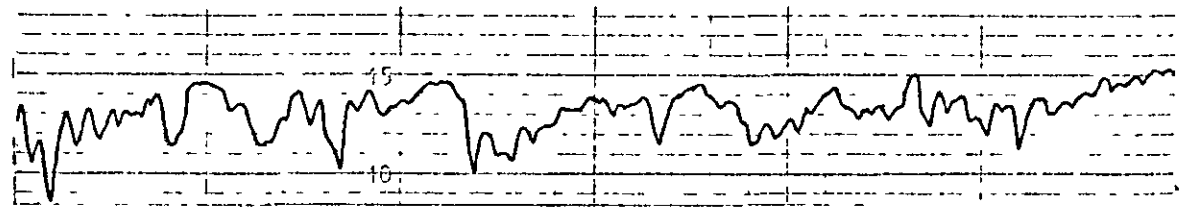
$a = 15 \mu\text{m}$

$Ra = 2.13 \mu\text{m}$



$a = 10 \mu\text{m}$

$Ra = 2.00 \mu\text{m}$



$a = 5 \mu\text{m}$

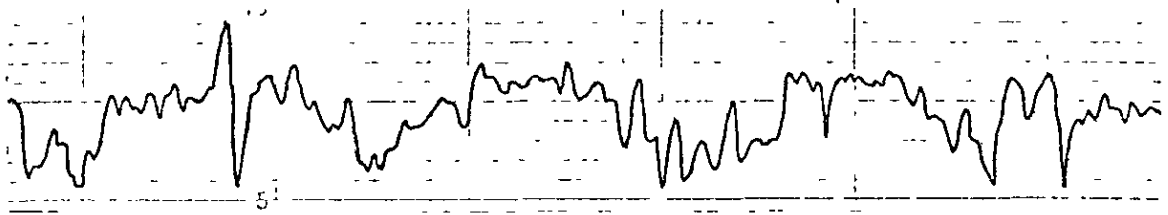
$Ra = 1.55 \mu\text{m}$

h constant at .3 mm/rev

θ constant at 10°

Fig. 7.32 "Talysurf" traces of grinding wheel surface roughness Ra when dressing with a fixed diamond drag angle θ , constant cross-feed h and variable in-feed a .

Test N° 4 : Wheel type :- 32A60-K8VBE : Diamond N° 63794/2 (sharp)
 Vertical mag.: 1 scale div.=1.25 μm Horiz.mag.: 1 scale div.= 50 μm



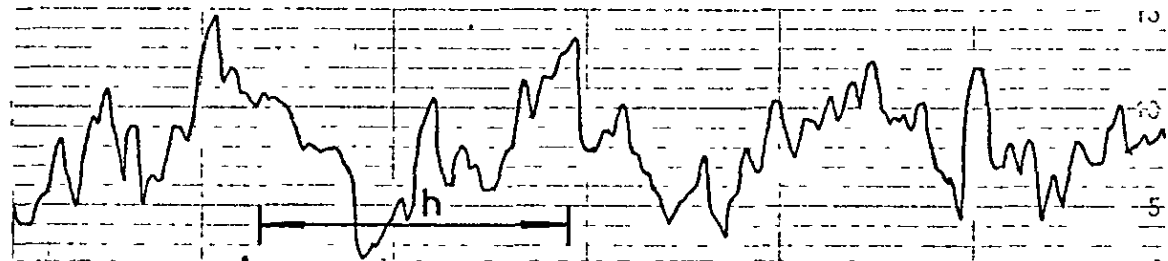
$\alpha = 25 \mu\text{m}$

$Ra = 1.98 \mu\text{m}$



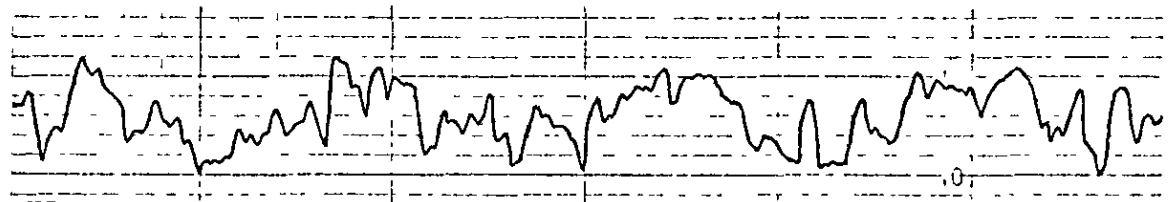
$\alpha = 20 \mu\text{m}$

$Ra = 1.98 \mu\text{m}$



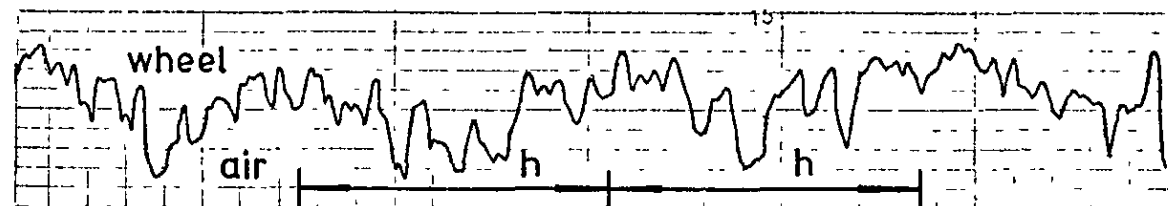
$\alpha = 15 \mu\text{m}$

$Ra = 2.05 \mu\text{m}$



$\alpha = 10 \mu\text{m}$

$Ra = 1.70 \mu\text{m}$



$\alpha = 5 \mu\text{m}$

$Ra = 1.50 \mu\text{m}$

h constant at .4 mm/rev

θ constant at 10°

Fig. 7.33 "Talysurf" traces of grinding wheel surface roughness Ra when dressing with a fixed diamond drag angle θ , constant cross-feed h and variable in-feed α .

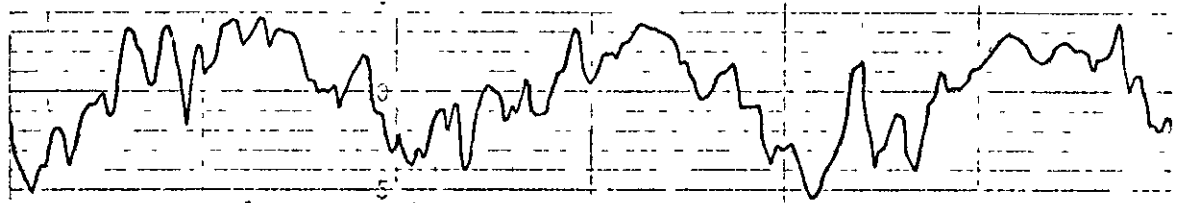
Test N° 4 : Wheel type:-32A60-K8VBE :Diamond N° 63794/2 (sharp)

Vertical mag.: 1 scale div.=1.25 μm Horiz.mag.: 1 scale div.= 50 μm



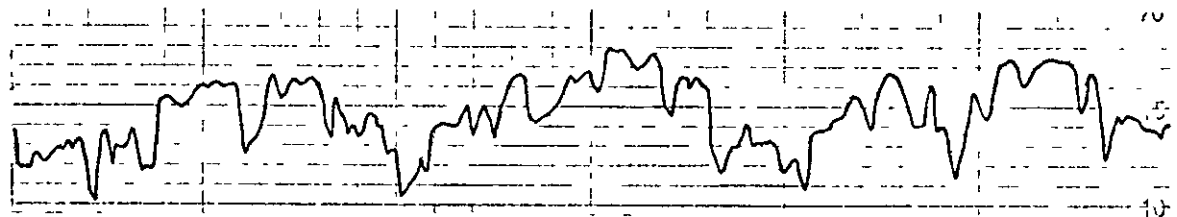
$a = 25 \mu\text{m}$

$R_a = 2.70 \mu\text{m}$



$a = 20 \mu\text{m}$

$R_a = 2.08 \mu\text{m}$



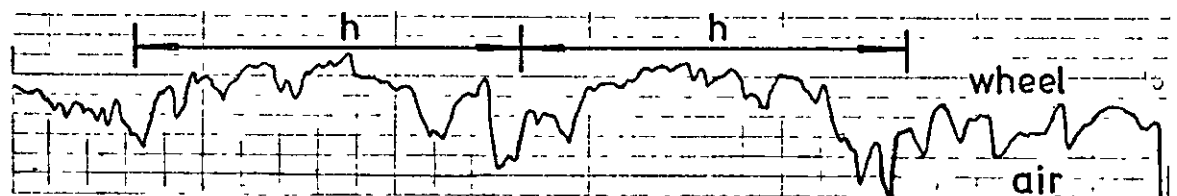
$a = 15 \mu\text{m}$

$R_a = 1.93 \mu\text{m}$



$a = 10 \mu\text{m}$

$R_a = 1.88 \mu\text{m}$



$a = 5 \mu\text{m}$

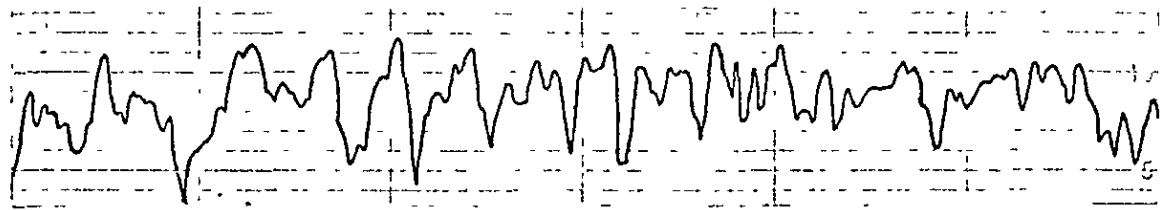
$R_a = 1.50 \mu\text{m}$

h constant at .5 mm/rev

θ constant at 10°

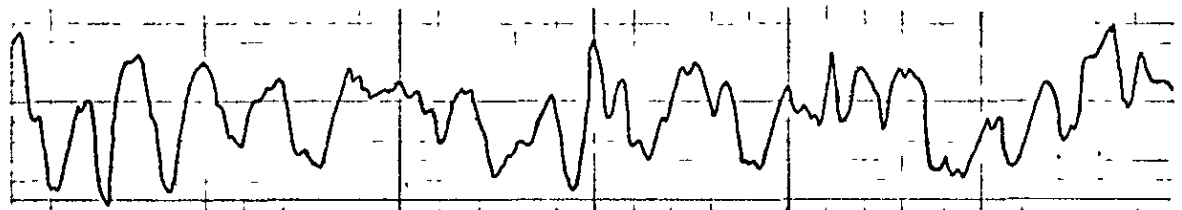
Fig. 7.34 "Talysurf" traces of grinding wheel surface roughness R_a when dressing with a fixed diamond drag angle θ , constant cross-feed h and variable in-feed a .

Test N° 4 : Wheel type:- 32A60-K8VBE : Diamond N° 63794/2 (sharp)
 Vertical mag.: 1 scale div.=1.25 μm Horiz.mag.: 1 scale div.= 50 μm



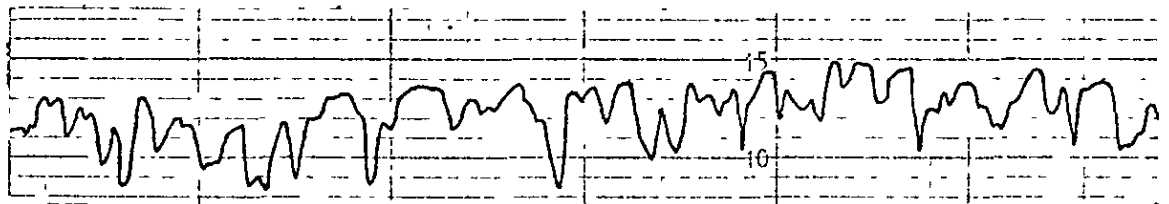
$\alpha = 25 \mu\text{m}$

$Ra = 1.63 \mu\text{m}$



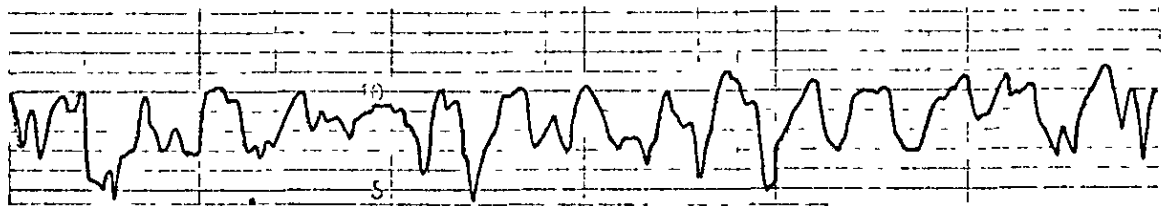
$\alpha = 20 \mu\text{m}$

$Ra = 1.68 \mu\text{m}$



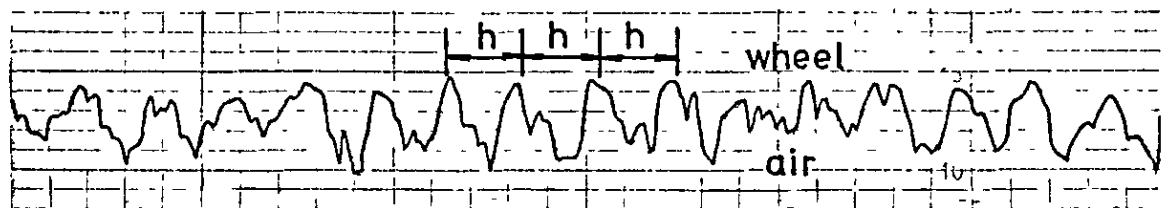
$\alpha = 15 \mu\text{m}$

$Ra = 1.63 \mu\text{m}$



$\alpha = 10 \mu\text{m}$

$Ra = 1.30 \mu\text{m}$



$\alpha = 5 \mu\text{m}$

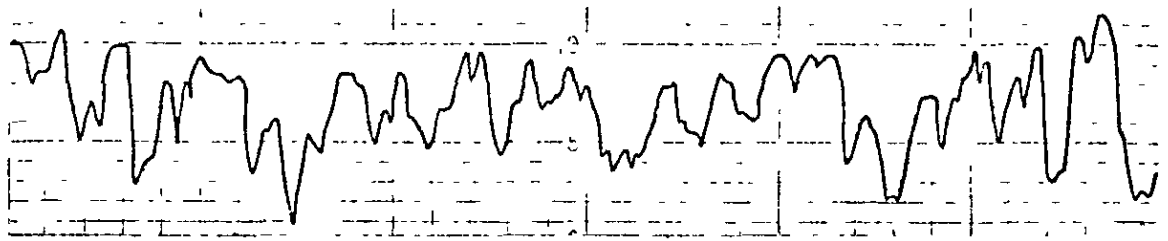
$Ra = 1.63 \mu\text{m}$

h constant at .1 mm/rev

θ constant at 15°

Fig. 7.35 "Talysurf" traces of grinding wheel surface
 roughness Ra when dressing with a fixed diamond drag
 angle θ , constant cross-feed h and variable in-feed α .

Test N° 4 : Wheel type:-32A60-K8VBE :Diamond N° 63794/2 (sharp)
 Vertical mag.: 1 scale div.=1.25 μm Horiz.mag.: 1 scale div.= 50 μm



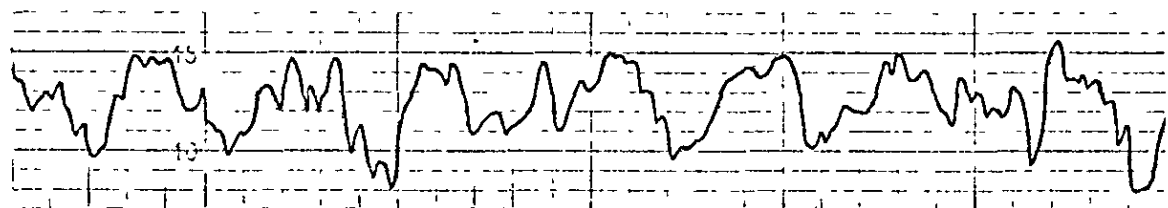
$a = 25 \mu\text{m}$

$Ra = 1.88 \mu\text{m}$



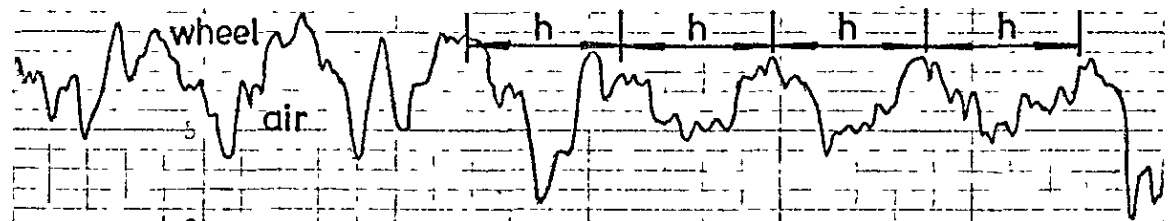
$a = 20 \mu\text{m}$

$Ra = 1.75 \mu\text{m}$



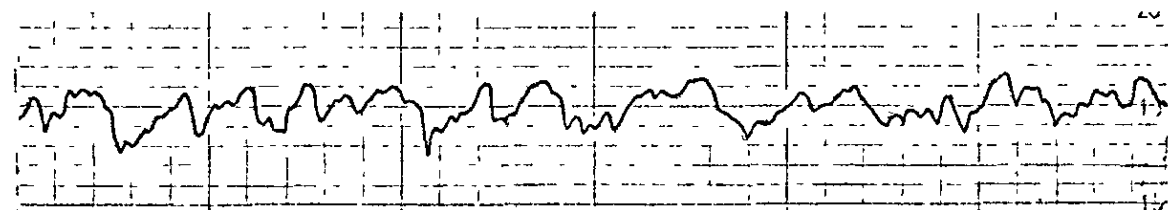
$a = 15 \mu\text{m}$

$Ra = 1.55 \mu\text{m}$



$a = 10 \mu\text{m}$

$Ra = 1.83 \mu\text{m}$



$a = 5 \mu\text{m}$

$Ra = 1.00 \mu\text{m}$

h constant at .2 mm/rev

θ constant at 15°

Fig. 7.36 "Talysurf" traces of grinding wheel surface roughness Ra when dressing with a fixed diamond drag angle θ , constant cross-feed h and variable in-feed a .

Test N° 4 : Wheel type:- 32A60-K8VBE: Diamond N° 63794/2 (sharp)
 Vertical mag.: 1 scale div.=1.25 μm Horiz.mag.: 1 scale div.= 50 μm

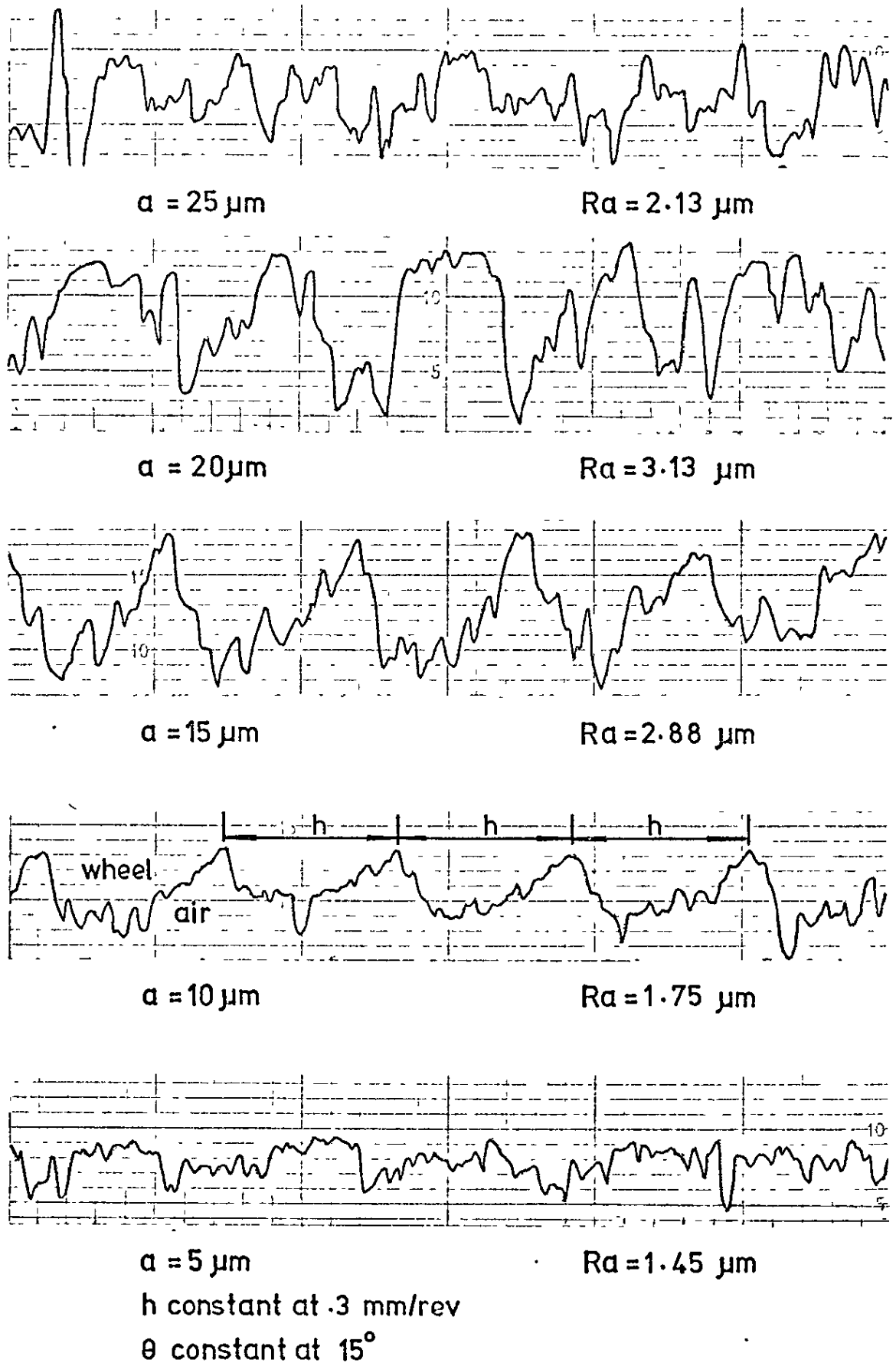
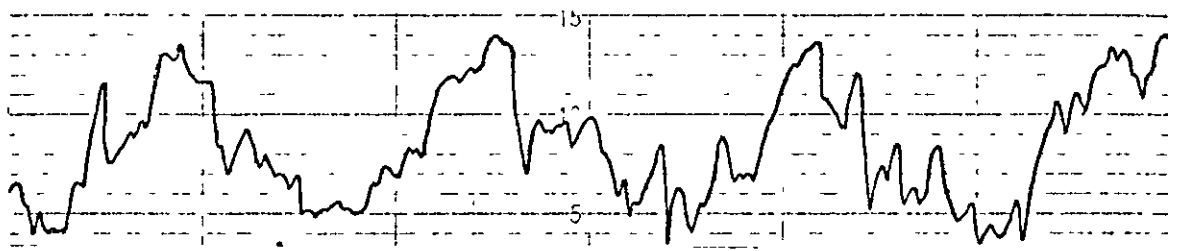


Fig. 7.37 "Talysurf" traces of grinding wheel surface roughness R_a when dressing with a fixed diamond drag angle θ , constant cross-feed h and variable in-feed α .

Test N° 4 : Wheel type: -32 A60-K8VBE : Diamond N° 63794/2 (sharp)
 Vertical mag.: 1 scale div. = $1.25 \mu\text{m}$ Horiz. mag.: 1 scale div. = $50 \mu\text{m}$



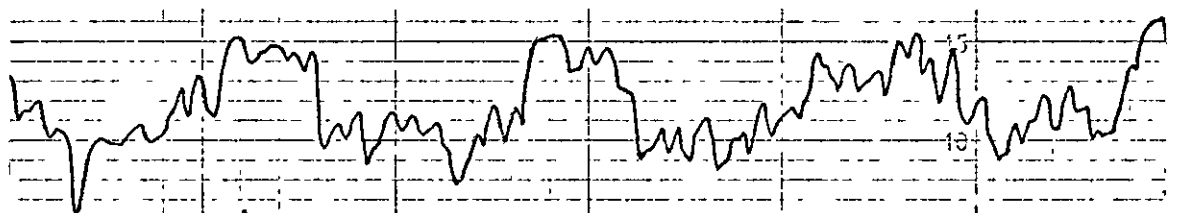
$a = 25 \mu\text{m}$

$Ra = 3.00 \mu\text{m}$



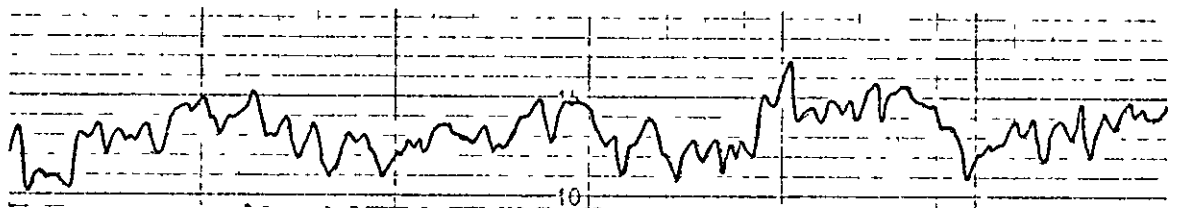
$a = 20 \mu\text{m}$

$Ra = 2.88 \mu\text{m}$



$a = 15 \mu\text{m}$

$Ra = 2.25 \mu\text{m}$



$a = 10 \mu\text{m}$

$Ra = 2.13 \mu\text{m}$



$a = 5 \mu\text{m}$

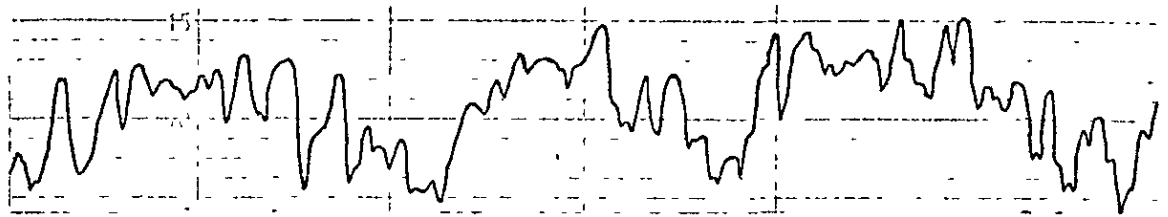
$Ra = 1.88 \mu\text{m}$

h constant at $.4 \text{ mm/rev}$

θ constant at 15°

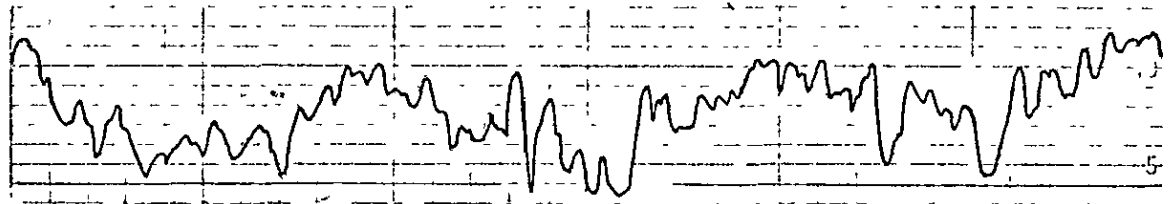
Fig. 7.38 "Talysurf" traces of grinding wheel surface roughness Ra when dressing with a fixed diamond drag angle θ , constant cross-feed h and variable in-feed a .

Test N° 4 : Wheel type:- 32A60-K8VBE : Diamond N° 63794/2 (sharp)
 Vertical mag.: 1 scale div.=1.25 μm Horiz.mag.: 1 scale div.= 50 μm



$\alpha = 25 \mu\text{m}$

$Ra = 2.13 \mu\text{m}$



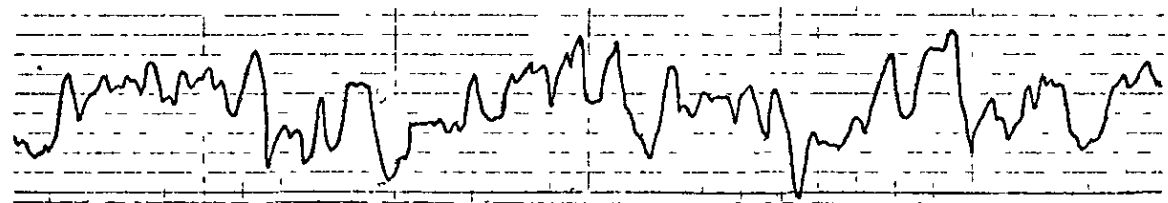
$\alpha = 20 \mu\text{m}$

$Ra = 1.88 \mu\text{m}$



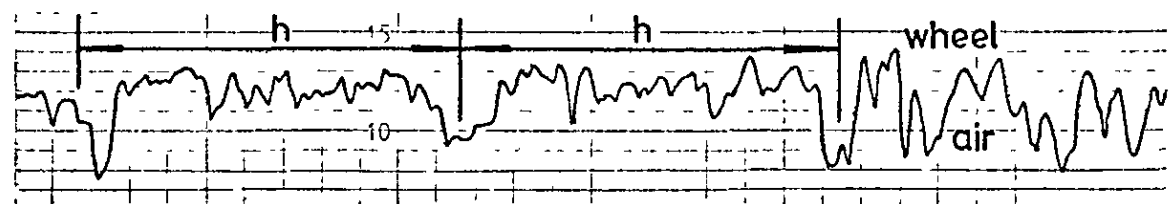
$\alpha = 15 \mu\text{m}$

$Ra = 1.70 \mu\text{m}$



$\alpha = 10 \mu\text{m}$

$Ra = 2.13 \mu\text{m}$



$\alpha = 5 \mu\text{m}$

$Ra = 1.30 \mu\text{m}$

h constant at .5 mm/rev

θ constant at 15°

Fig. 7.39 "Talysurf" traces of grinding wheel surface roughness Ra when dressing with a fixed diamond drag angle θ , constant cross-feed h and variable in-feed α .

Test No 4
Diamond No 63794/2 (sharp)
Wheel type 32 A 60-K 8 VBE

Key:-
Row 1. Ra actual (µm)
Row 2. Ra theoretical (µm)
Row 3. β theoretical (degrees)

| Drag angle 5° | | Cross-feed h mm/rev | | | | | | | | | |
|---------------|----|---------------------|-------|------|------|------|------|-------|------|-------|-------|
| row | | .1 | | .2 | | .3 | | .4 | | .5 | |
| In-feed a µm | 5 | 1 | .50 | — | .70 | — | 1.00 | .98 | 1.30 | 1.31 | 1.65 |
| | | 2 | — | — | — | — | — | — | — | — | 1.46 |
| | | 3 | — | — | — | 177 | — | 177 | — | 177 | — |
| | 10 | 1 | .75 | — | .75 | — | 1.05 | .98 | 1.38 | 1.31 | 2.10 |
| | | 2 | — | — | — | — | — | — | — | — | 2.18 |
| | | 3 | — | — | — | 177 | — | 177 | — | 176 | — |
| | 15 | 1 | .90 | — | 1.05 | — | 1.25 | .98 | 1.63 | 1.75 | 2.70 |
| | | 2 | — | — | — | — | — | — | — | — | 2.73 |
| | | 3 | — | — | — | 176 | — | 176 | — | 175 | — |
| | 20 | 1 | 1.45 | — | 1.80 | — | 2.30 | .98 | 2.40 | 2.40 | 2.88 |
| | | 2 | — | — | — | — | — | — | — | — | 3.00 |
| | | 3 | — | — | — | 173 | — | 174.5 | — | 174.5 | — |
| | 25 | 1 | 2.38 | — | 2.42 | — | 2.50 | .98 | 2.70 | 2.62 | 2.98 |
| | | 2 | — | — | — | — | — | — | — | — | 3.00 |
| | | 3 | 158.5 | 2.38 | 169 | 2.40 | 172 | 2.63 | 174 | 2.62 | 174.5 |

| Drag angle 10° | | Cross-feed h mm/rev | | | | | | | | | |
|----------------|----|---------------------|------|------|------|------|-------|------|-------|------|-------|
| row | | .1 | | .2 | | .3 | | .4 | | .5 | |
| In-feed a µm | 5 | 1 | 1.00 | — | 1.25 | — | 1.55 | .98 | 1.50 | 1.48 | 1.50 |
| | | 2 | — | — | — | — | — | — | — | — | 1.46 |
| | | 3 | 171 | .98 | 174 | 1.31 | 174 | 1.48 | 176 | 1.48 | 176 |
| | 10 | 1 | 1.33 | — | 1.55 | — | 2.00 | .98 | 1.70 | 1.75 | 1.88 |
| | | 2 | — | — | — | — | — | — | — | — | 1.91 |
| | | 3 | 168 | 1.32 | 173 | 1.53 | 174 | 1.97 | 176 | 1.75 | 176.5 |
| | 15 | 1 | 1.25 | — | 1.75 | — | 2.13 | .98 | 2.05 | 1.96 | 1.93 |
| | | 2 | — | — | — | — | — | — | — | — | 1.91 |
| | | 3 | 168 | 1.32 | 172 | 1.75 | 173.5 | 2.13 | 175.5 | 1.96 | 176.5 |
| | 20 | 1 | 1.63 | — | 1.75 | — | 2.38 | .98 | 1.98 | 1.96 | 2.08 |
| | | 2 | — | — | — | — | — | — | — | — | 2.18 |
| | | 3 | 165 | 1.65 | 172 | 1.75 | 173 | 2.29 | 175.5 | 1.96 | 176 |
| | 25 | 1 | 1.70 | — | 1.80 | — | 2.63 | .98 | 1.98 | 1.96 | 2.70 |
| | | 2 | — | — | — | — | — | — | — | — | 2.70 |
| | | 3 | 165 | 1.65 | 172 | 1.75 | 172 | 2.63 | 175.5 | 1.96 | 175 |

| Drag angle 15° | | Cross-feed h mm/rev | | | | | | | | | |
|----------------|----|---------------------|------|------|-------|------|-------|------|-------|------|-------|
| row | | .1 | | .2 | | .3 | | .4 | | .5 | |
| In-feed a µm | 5 | 1 | 1.63 | — | 1.00 | — | 1.45 | .98 | 1.88 | 1.48 | 1.30 |
| | | 2 | — | — | — | — | — | — | — | — | 1.46 |
| | | 3 | 165 | 1.46 | 175 | 1.09 | 175 | 1.46 | 176 | 1.48 | 177.5 |
| | 10 | 1 | 1.30 | — | 1.83 | — | 1.75 | .98 | 2.13 | 2.18 | 2.13 |
| | | 2 | — | — | — | — | — | — | — | — | 2.18 |
| | | 3 | 168 | 1.32 | 171.5 | 1.86 | 174.5 | 1.80 | 175 | 2.18 | 176 |
| | 15 | 1 | 1.63 | — | 1.55 | — | 2.88 | .98 | 2.25 | 2.18 | 1.70 |
| | | 2 | — | — | — | — | — | — | — | — | 1.64 |
| | | 3 | 165 | 1.65 | 173 | 1.53 | 171 | 2.95 | 175 | 2.18 | 177 |
| | 20 | 1 | 1.68 | — | 1.75 | — | 3.13 | .98 | 2.88 | 2.84 | 1.88 |
| | | 2 | — | — | — | — | — | — | — | — | 1.91 |
| | | 3 | 165 | 1.65 | 172 | 1.75 | 170.5 | 3.12 | 173.5 | 2.84 | 176.5 |
| | 25 | 1 | 1.63 | — | 1.88 | — | 2.13 | .98 | 3.00 | 3.06 | 2.13 |
| | | 2 | — | — | — | — | — | — | — | — | 2.18 |
| | | 3 | 165 | 1.65 | 171 | 1.97 | 173.5 | 2.13 | 173 | 3.06 | 176 |

Fig. 7.40

Table of actual and theoretical values of grinding wheel surface roughness Ra for different dressing conditions.

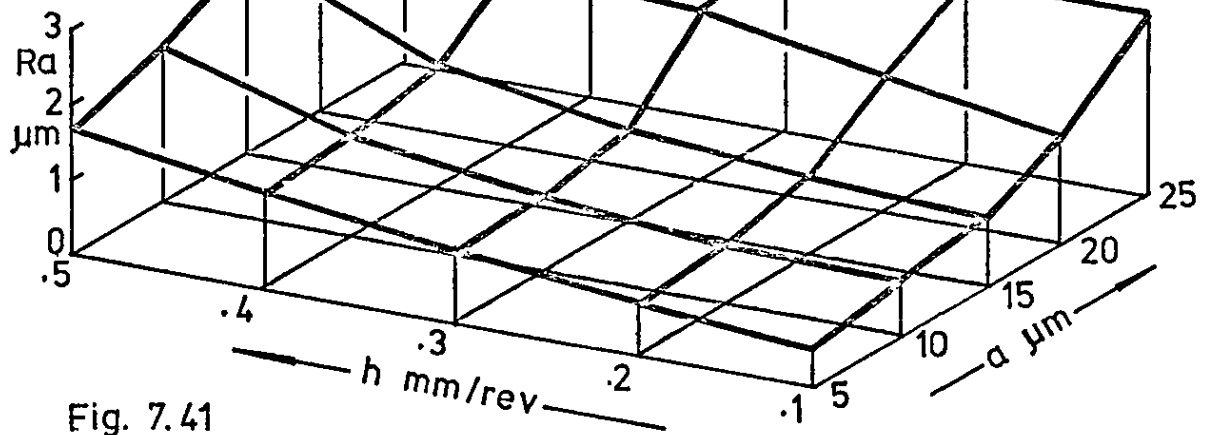


Fig. 7.41

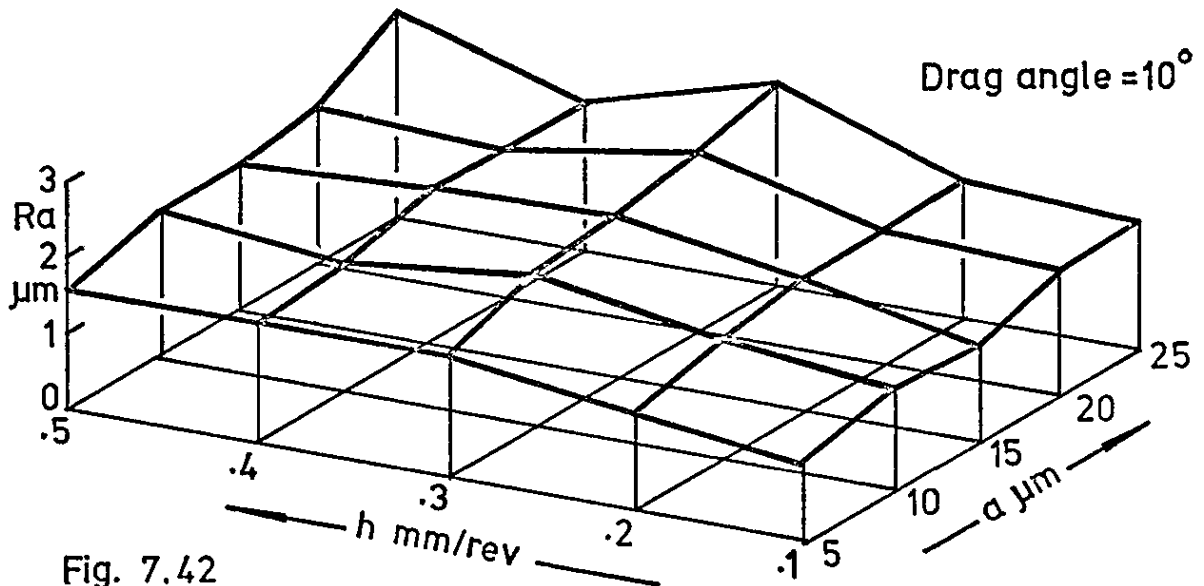


Fig. 7.42

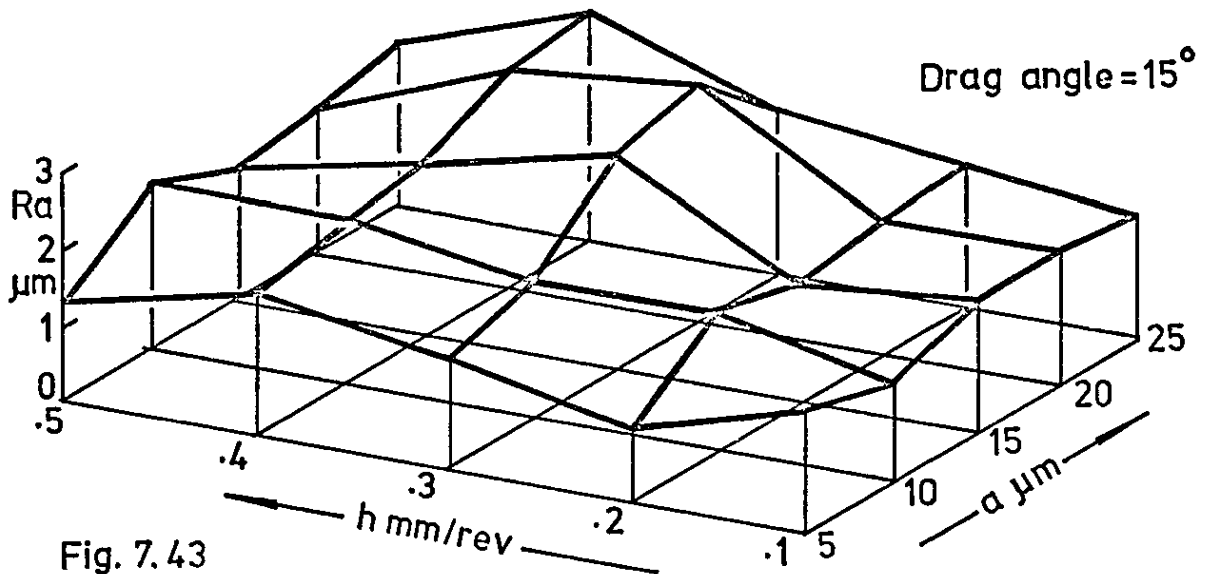


Fig. 7.43

Figs. 7.41 to 7.43 inc. Variation of grinding wheel surface roughness with depth of cut and traverse rate when dressing with a sharp diamond set at different values of drag angle.

Test N^o 5
 Diamond N^o 63794/2 (worn)
 Wheel type:- A 60 KV

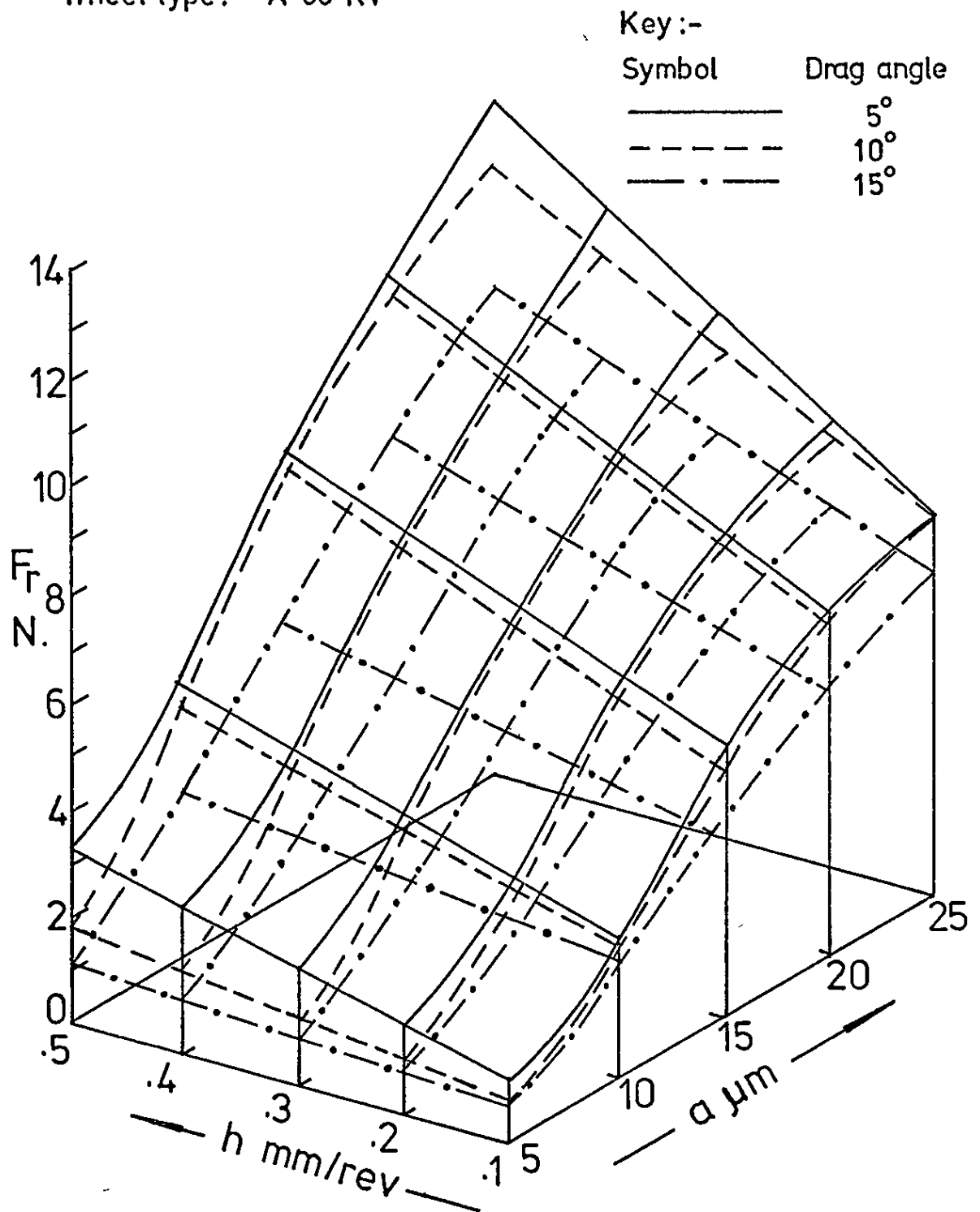


Fig. 7.44 Variation of dressing force (radial component) with dressing depth of cut and traverse rate for a range of values of drag angle .

Test N^o 6
 Diamond N^o 63794/2 (worn)
 Wheel type:- A 46 KV

Key:-

| Symbol | Drag angle |
|---------|------------|
| ———— | 5° |
| ----- | 10° |
| — · — · | 15° |

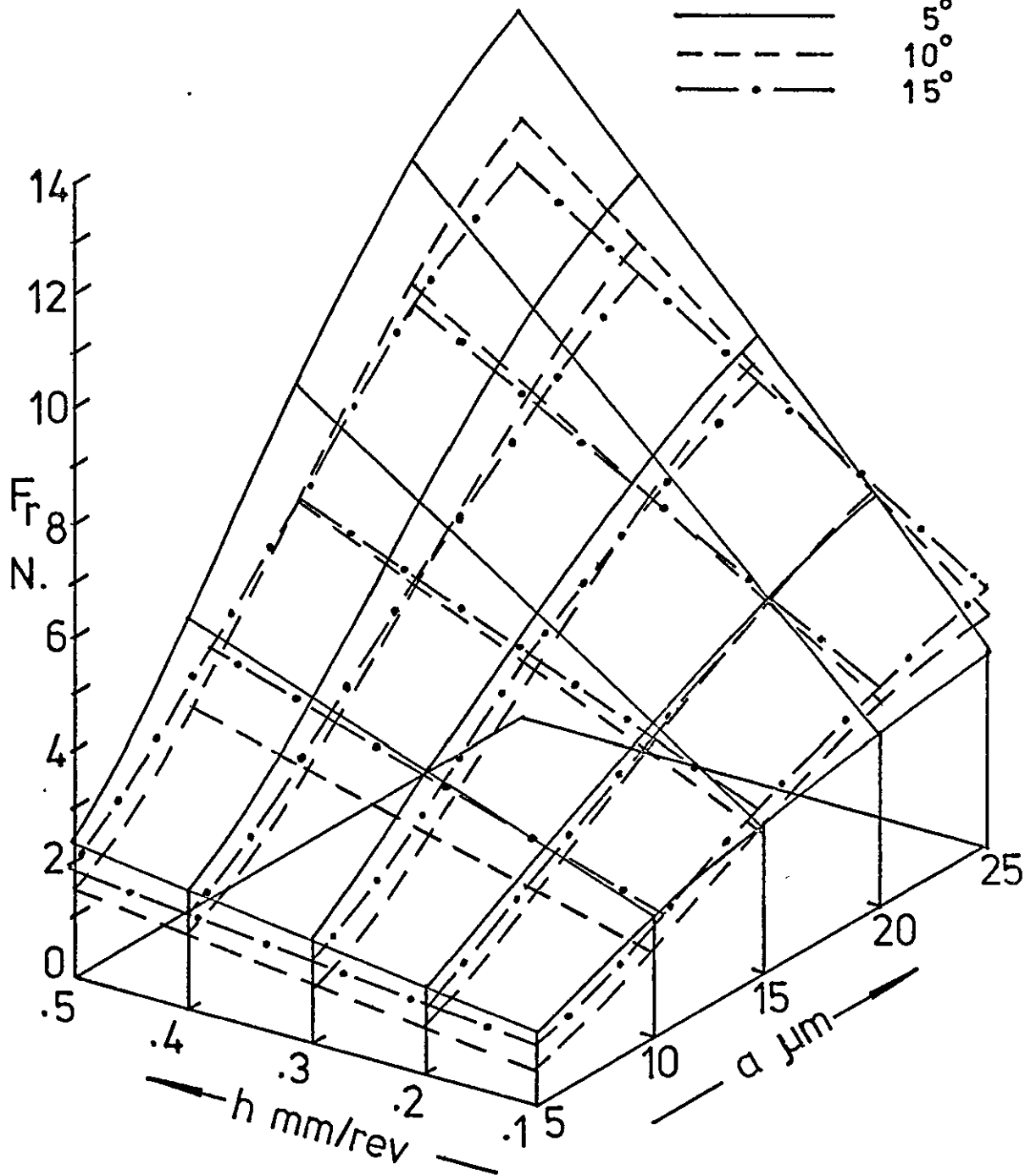


Fig. 7.45 Variation of dressing force (radial component) with dressing depth of cut and traverse rate for a range of values of drag angle.

Test N^o 7
 Diamond N^o 63794/2 (worn)
 Wheel type:- 38 A 46-K5 VBE

Key:-

| Symbol | Drag angle |
|---------|------------|
| ———— | 5° |
| ----- | 10° |
| — . — . | 15° |

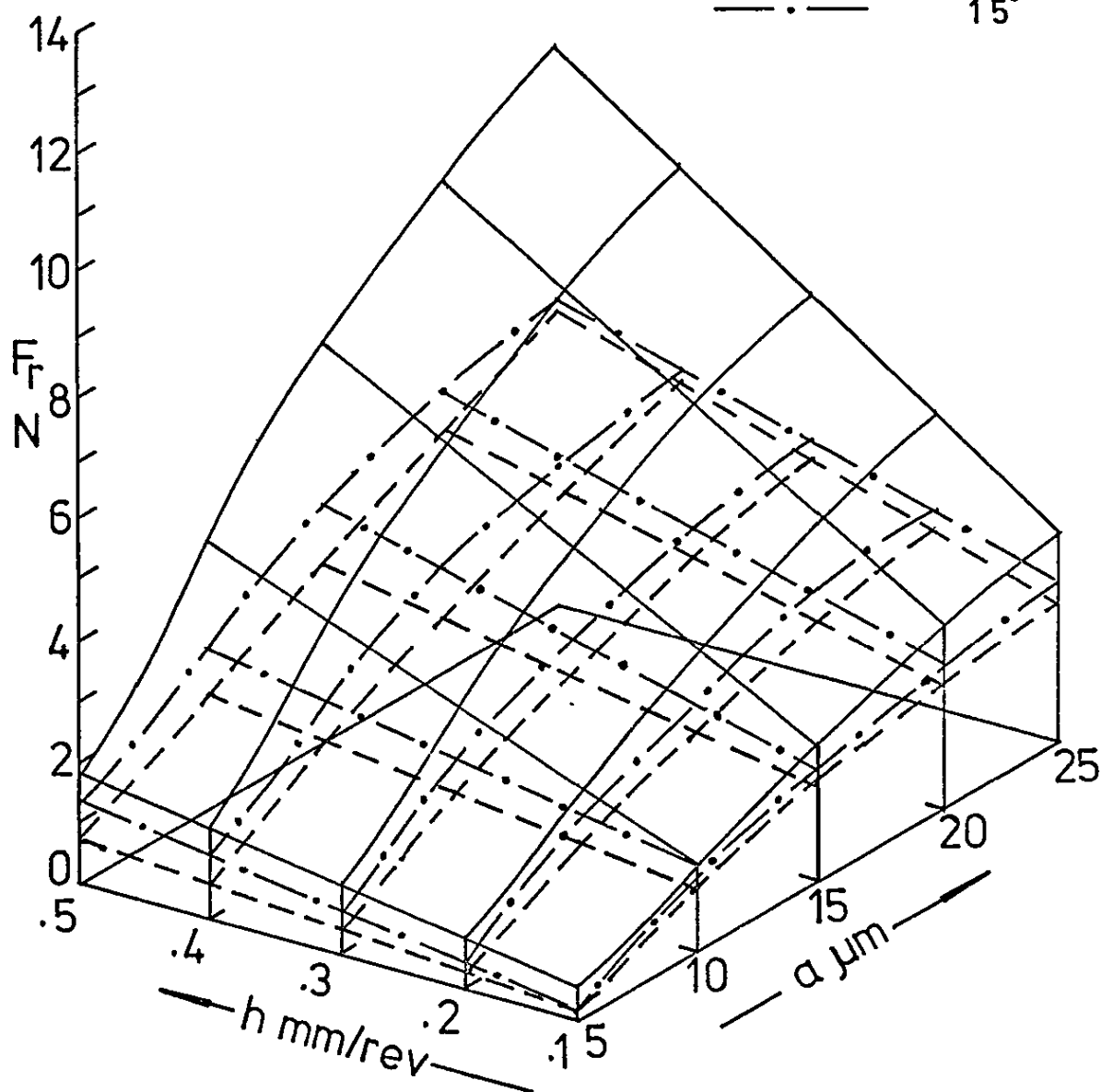
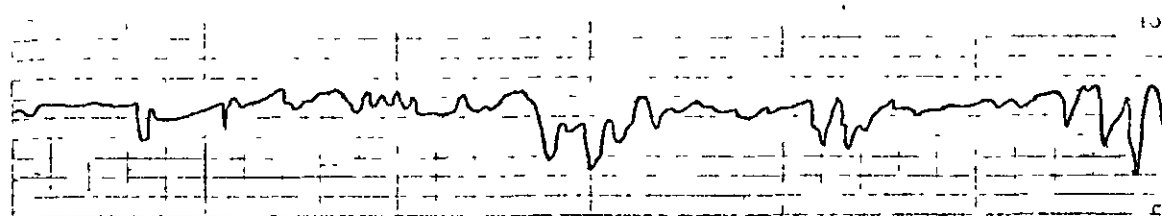


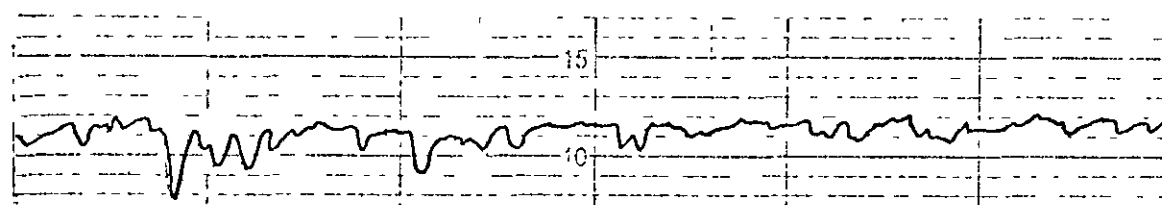
Fig.7.46 Variation of dressing force (radial component) with dressing depth of cut and traverse rate for a range of values of drag angle.

Test N° 5 : Wheel type:- A 60 KV :Diamond N° 63794/2 (worn)
 Vertical mag.: 1 scale div.=1.25 μm Horiz.mag.: 1 scale div.= 50 μm



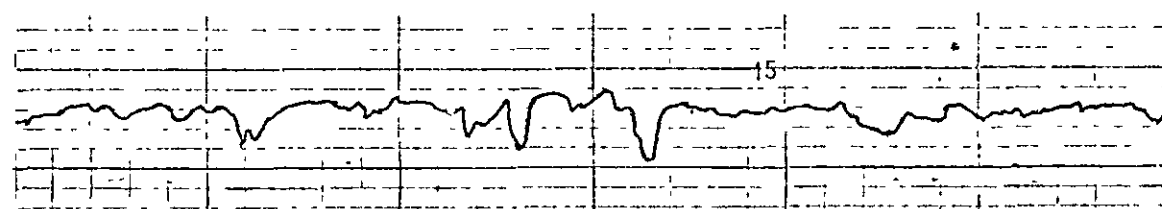
$\alpha = 25 \mu\text{m}$

$Ra = .88 \mu\text{m}$



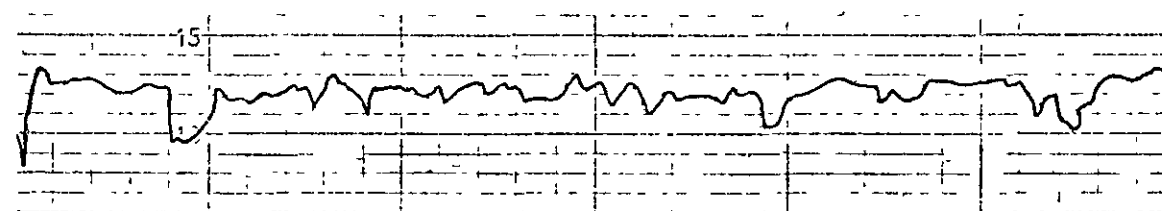
$\alpha = 20 \mu\text{m}$

$Ra = .88 \mu\text{m}$



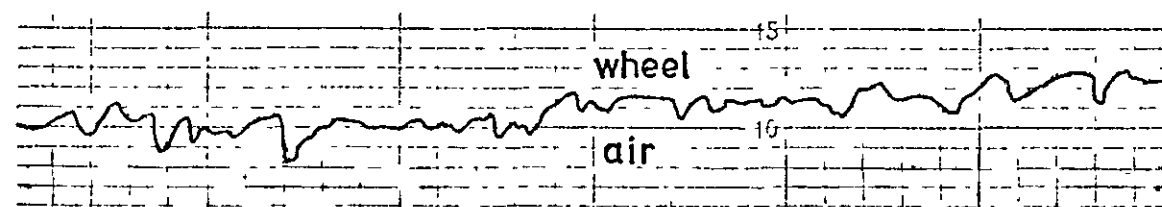
$\alpha = 15 \mu\text{m}$

$Ra = 1.13 \mu\text{m}$



$\alpha = 10 \mu\text{m}$

$Ra = .88 \mu\text{m}$



$\alpha = 5 \mu\text{m}$

$Ra = .75 \mu\text{m}$

h constant at .1 mm/rev

θ constant at 5°

Fig. 7.47 "Talysurf" traces of grinding wheel surface roughness Ra when dressing with a fixed diamond drag angle θ , constant cross-feed h and variable in-feed α .

test N° 5 : Wheel type:- A 60 KV : Diamond N° 63794/2 (worn)
 Vertical mag.: 1 scale div.=1.25 μm Horiz.mag.: 1 scale div.= 50 μm



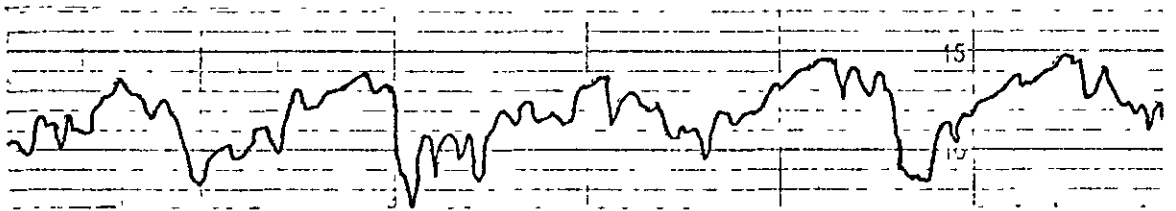
$\alpha = 25 \mu\text{m}$

$Ra = 1.95 \mu\text{m}$



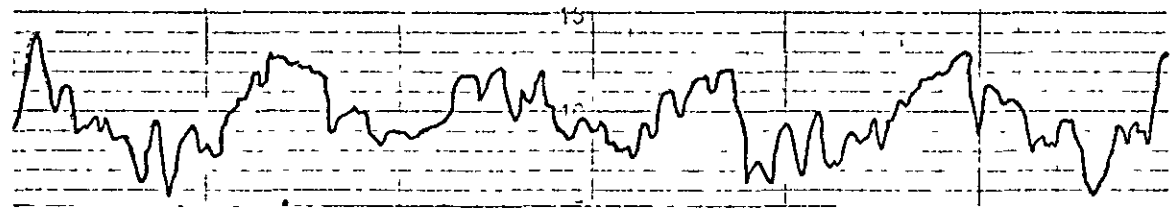
$\alpha = 20 \mu\text{m}$

$Ra = 1.75 \mu\text{m}$



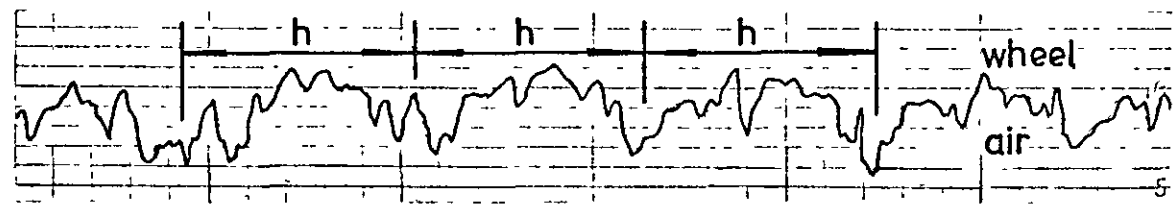
$\alpha = 15 \mu\text{m}$

$Ra = 1.60 \mu\text{m}$



$\alpha = 10 \mu\text{m}$

$Ra = 1.38 \mu\text{m}$



$\alpha = 5 \mu\text{m}$

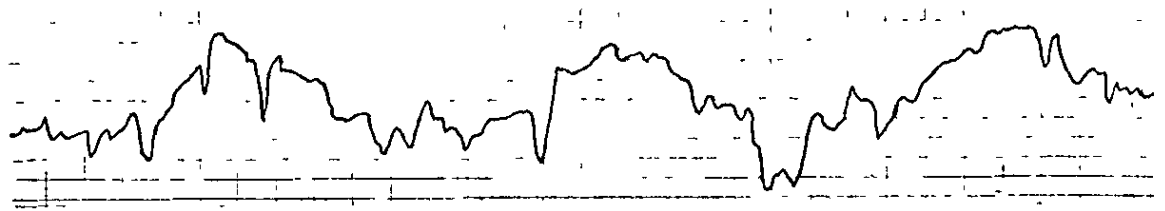
$Ra = 1.30 \mu\text{m}$

h constant at .3 mm/rev

θ constant at 10°

Fig. 7.48 "Talysurf" traces of grinding wheel surface roughness Ra when dressing with a fixed diamond drag angle θ , constant cross-feed h and variable in-feed α .

Test N° 5 : Wheel type:- A 60 KV :Diamond N° 63794/2 (worn)
 Vertical mag.: 1 scale div.=1.25 μm Horiz.mag.: 1 scale div.= 50 μm



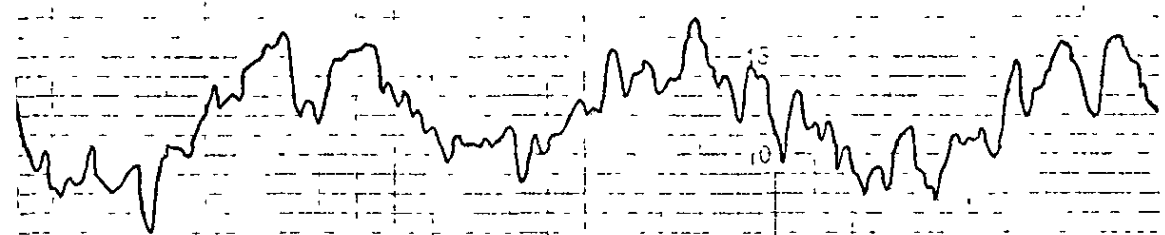
$\alpha = 25 \mu\text{m}$

$Ra = 2.63 \mu\text{m}$



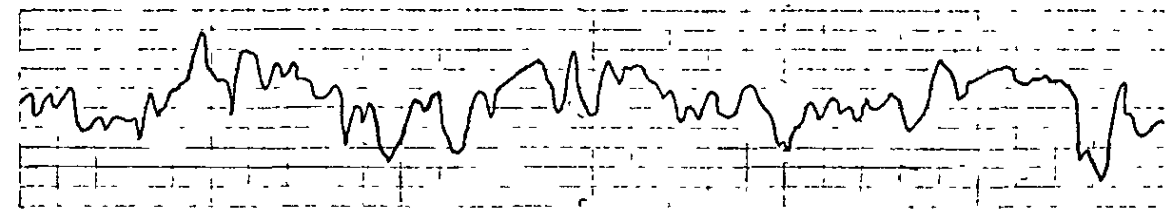
$\alpha = 20 \mu\text{m}$

$Ra = 2.25 \mu\text{m}$



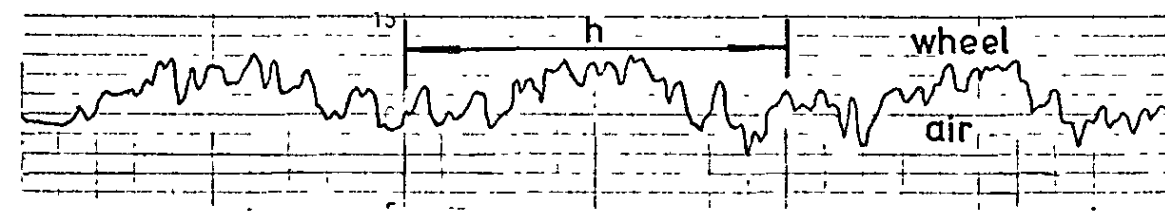
$\alpha = 15 \mu\text{m}$

$Ra = 2.38 \mu\text{m}$



$\alpha = 10 \mu\text{m}$

$Ra = 1.50 \mu\text{m}$



$\alpha = 5 \mu\text{m}$

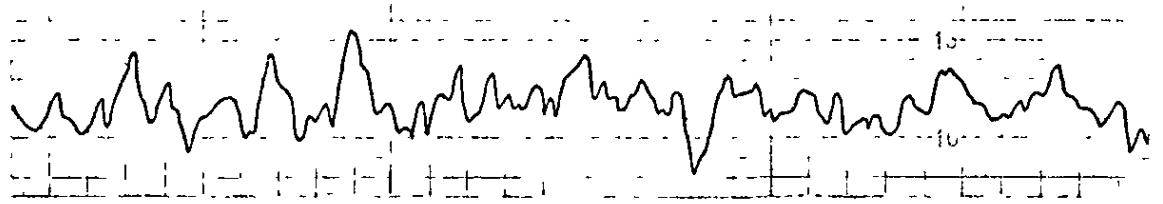
$Ra = 1.30 \mu\text{m}$

h constant at .5 mm/rev

θ constant at 15°

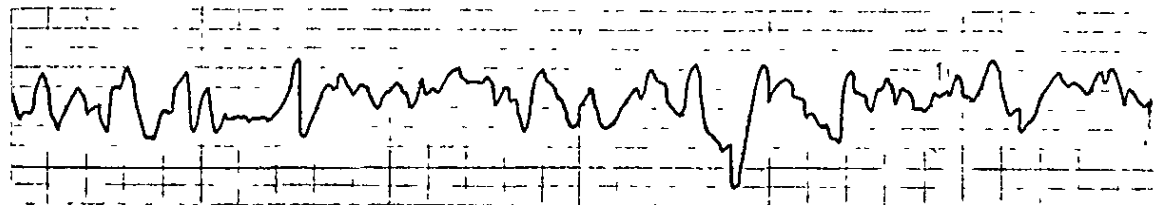
Fig. 7.49 "Talysurf" traces of grinding wheel surface roughness Ra when dressing with a fixed diamond drag angle θ , constant cross-feed h and variable in-feed a .

Test N° 6 : Wheel type:- A 46 KV :Diamond N° 63794/2 (worn)
 Vertical mag.: 1 scale div.=1.25 μm Horiz.mag.: 1 scale div.= 50 μm



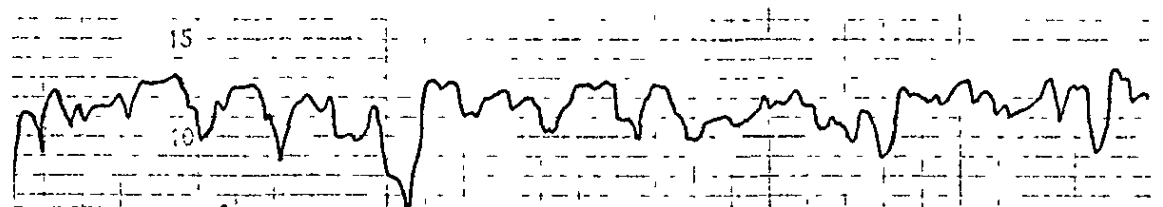
$\alpha = 25 \mu\text{m}$

$Ra = 1.30 \mu\text{m}$



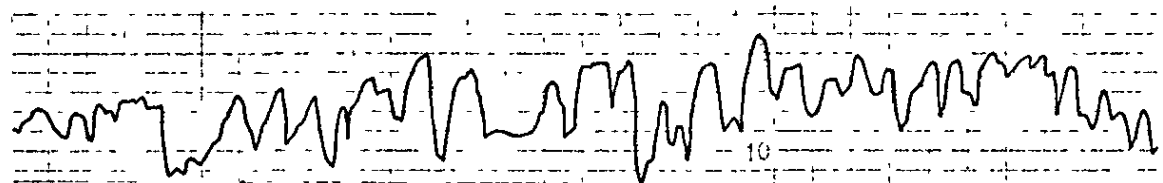
$\alpha = 20 \mu\text{m}$

$Ra = 1.13 \mu\text{m}$



$\alpha = 15 \mu\text{m}$

$Ra = 1.08 \mu\text{m}$



$\alpha = 10 \mu\text{m}$

$Ra = 1.38 \mu\text{m}$



$\alpha = 5 \mu\text{m}$

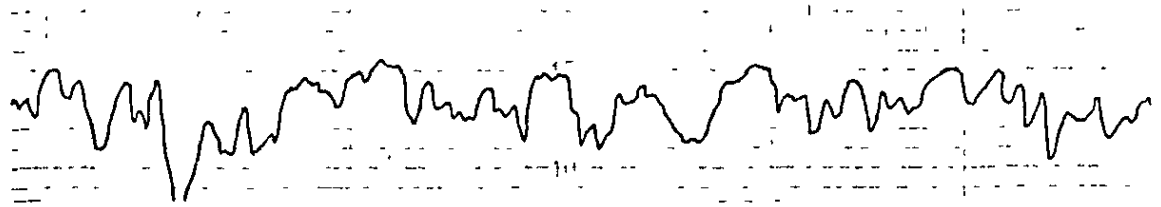
$Ra = 1.25 \mu\text{m}$

h constant at .1 mm/rev

θ constant at 5°

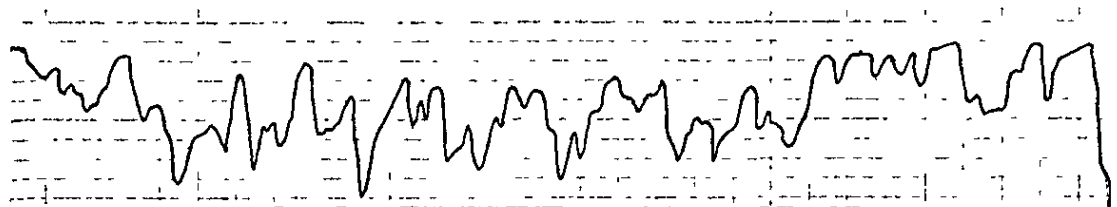
Fig. 7.50 "Talysurf" traces of grinding wheel surface roughness Ra when dressing with a fixed diamond drag angle θ , constant cross-feed h and variable in-feed α .

Test N° 6 : Wheel type:- A 46 KV :Diamond N° 63794/2 (worn)
 Vertical mag.: 1 scale div.=1.25 μm Horiz.mag.: 1 scale div.= 50 μm



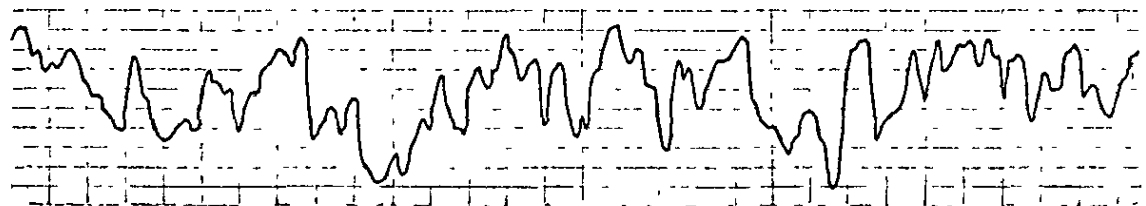
$\alpha = 25 \mu\text{m}$

$Ra = 1.88 \mu\text{m}$



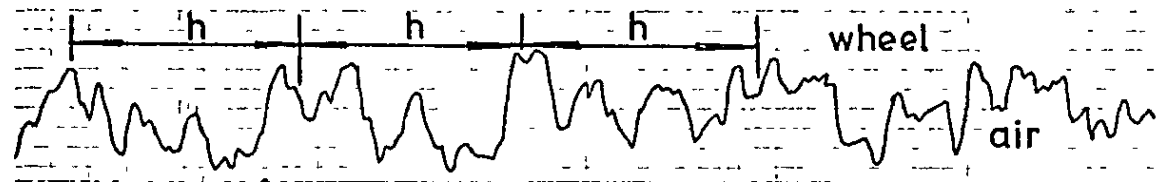
$\alpha = 20 \mu\text{m}$

$Ra = 1.80 \mu\text{m}$



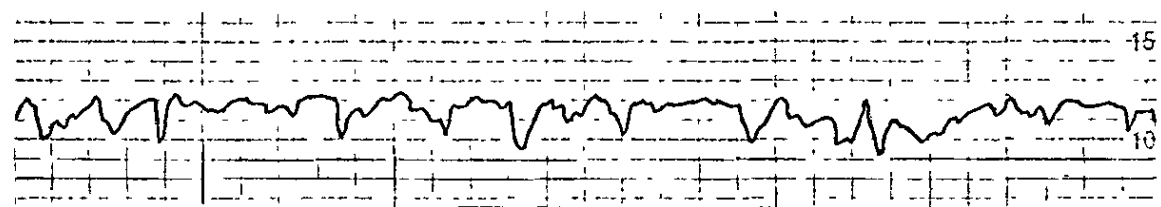
$\alpha = 15 \mu\text{m}$

$Ra = 1.70 \mu\text{m}$



$\alpha = 10 \mu\text{m}$

$Ra = 1.65 \mu\text{m}$



$\alpha = 5 \mu\text{m}$

$Ra = .95 \mu\text{m}$

h constant at .3 mm/rev

θ constant at 10°

Fig. 7.51 "Talysurf" traces of grinding wheel surface
roughness Ra when dressing with a fixed diamond drag
angle θ , constant cross-feed h and variable in-feed α .

Test N° 6 : Wheel type:- A 46 KV :Diamond N° 63794/2 (worn)

Vertical mag.: 1 scale div.=1.25 μm Horiz.mag.: 1 scale div.= 50 μm

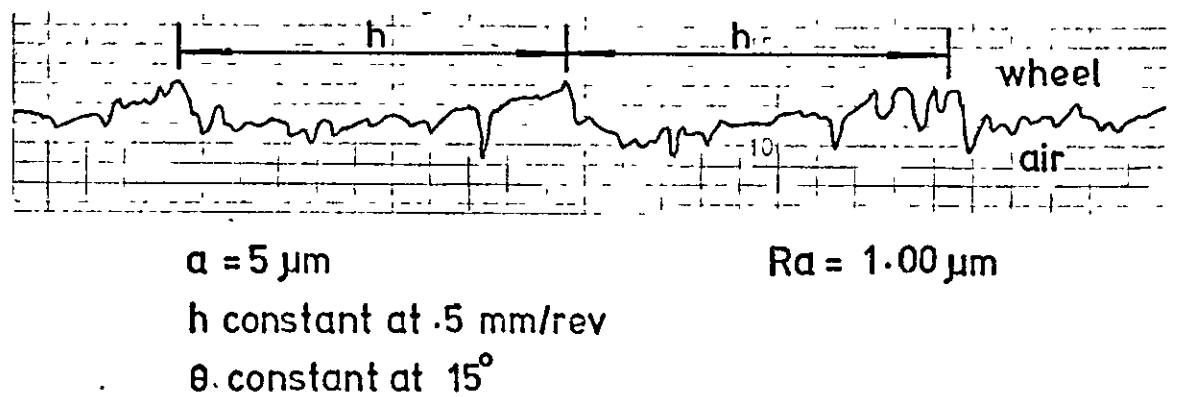
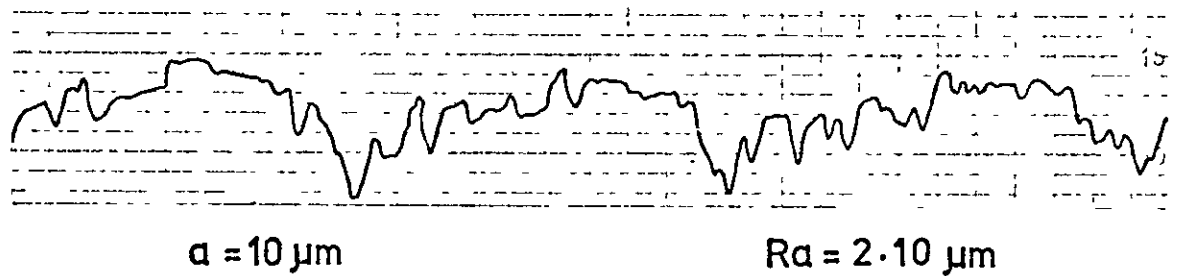
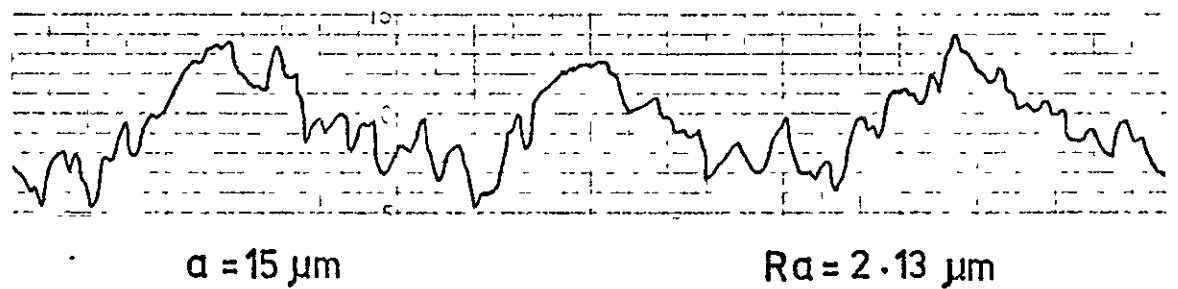
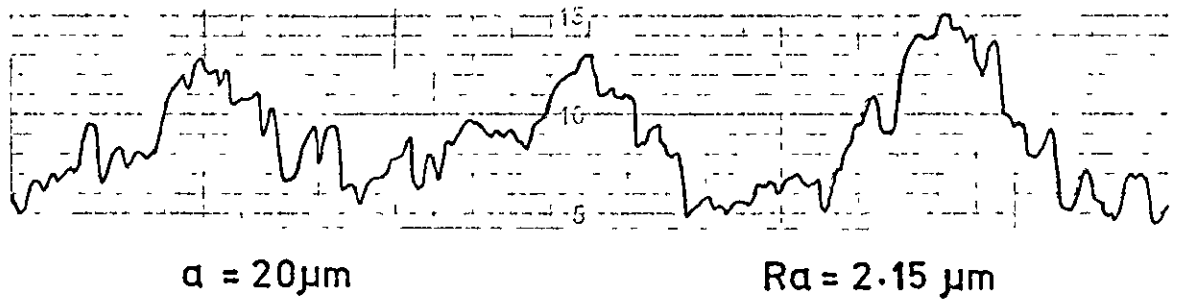
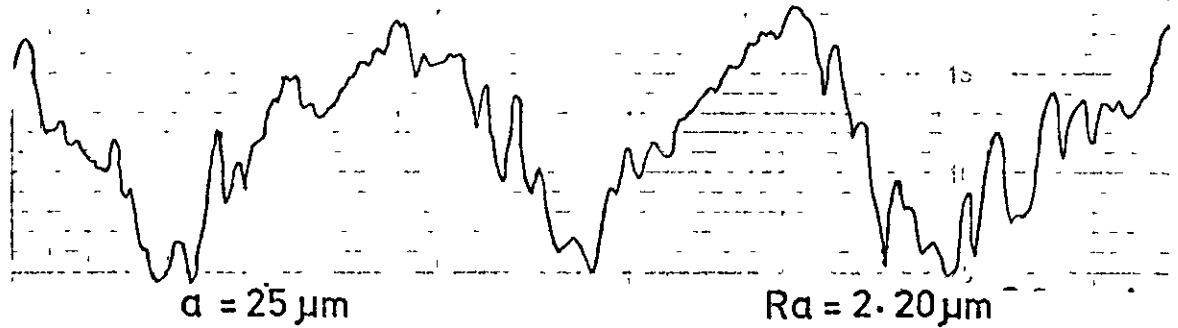


Fig. 7.52 "Talysurf" traces of grinding wheel surface roughness Ra when dressing with a fixed diamond drag angle θ , constant cross-feed h and variable in-feed α .

Test N° 7 : Wheel type:- 38A46-K5VBE : Diamond N° 63794/2 (worn)
 Vertical mag.: 1 scale div.=1.25 μm Horiz.mag.: 1 scale div.= 50 μm

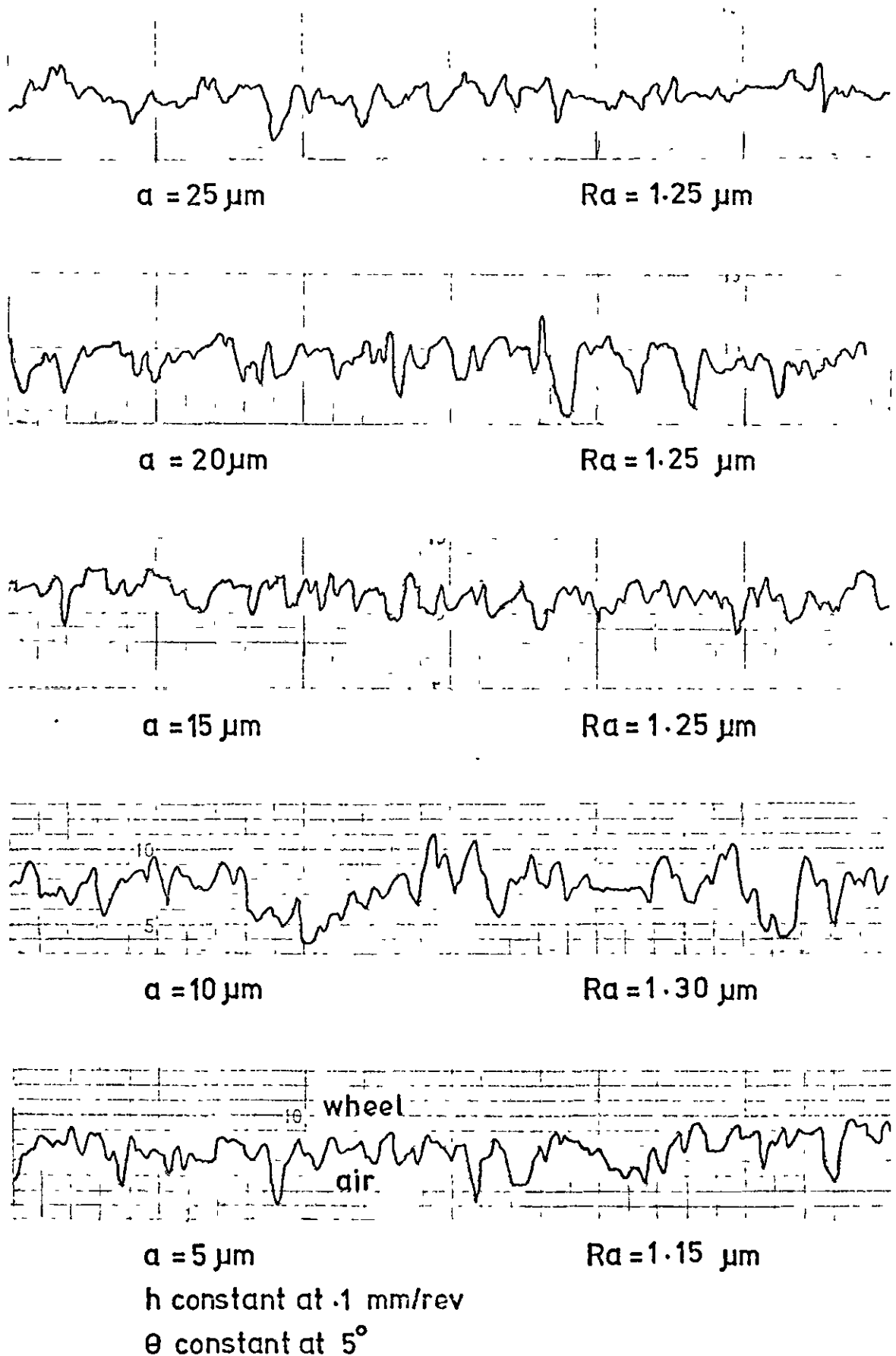


Fig. 7.53 "Talysurf" traces of grinding wheel surface roughness R_a when dressing with a fixed diamond drag angle θ , constant cross-feed h and variable in-feed a .

Test N°7 : Wheel type:-38 A 46-K5 VBE: Diamond N°63794/2 (worn)
 Vertical mag.: 1 scale div.=1.25 μm Horiz.mag. 1 scale div.=50 μm

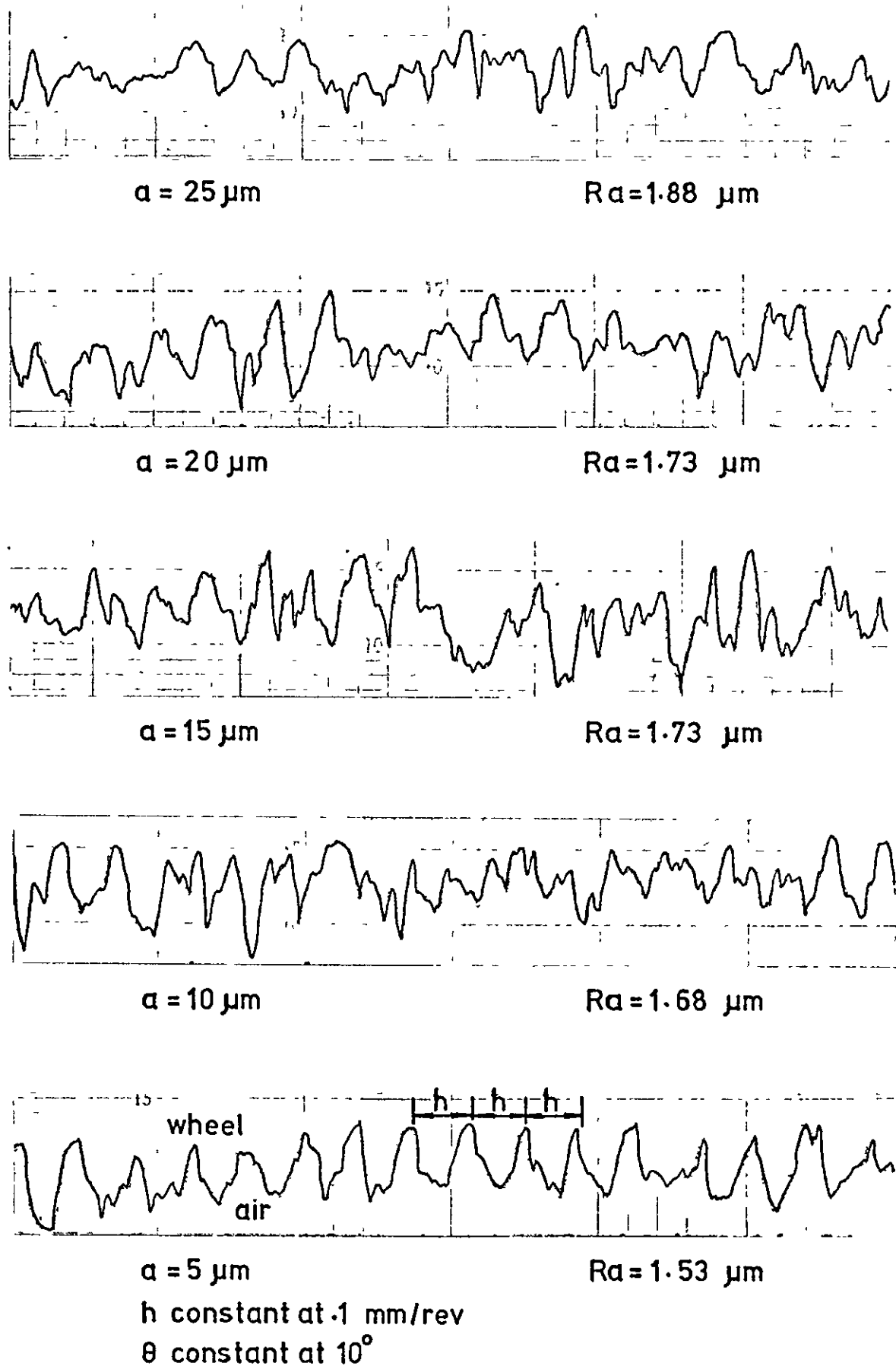


Fig. 7.54 "Talysurf" traces of grinding wheel surface
roughness Ra when dressing with a fixed diamond drag
angle θ , constant cross-feed h and variable in - feed a

Test N° 7 : Wheel type :- 38A46-K5VBE : Diamond N° 63794/2 (worn)
 Vertical mag. : 1 scale div. = 1.25 μm Horiz. mag. : 1 scale div. = 50 μm

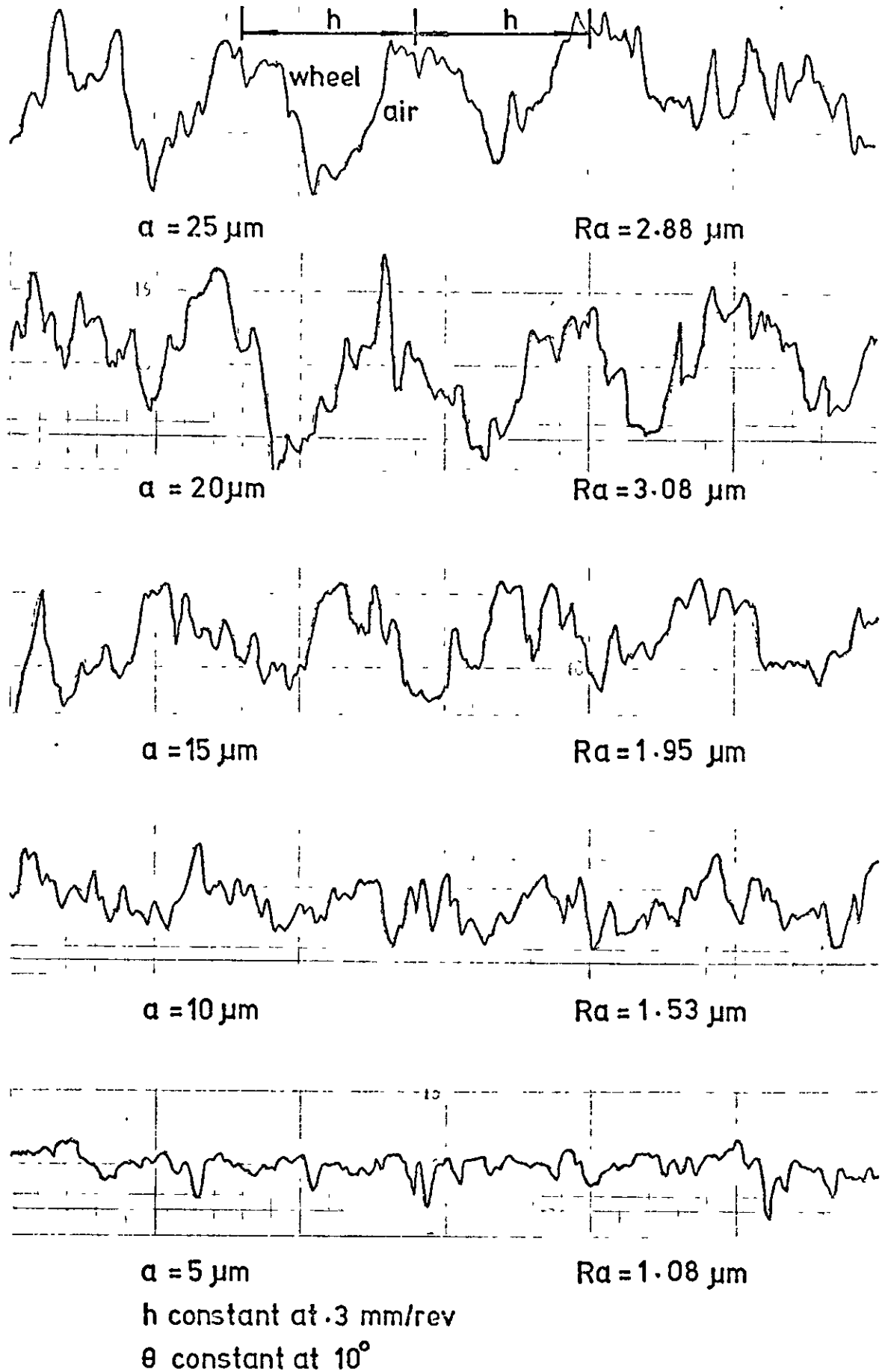


Fig. 7.55 "Talysurf" traces of grinding wheel surface roughness R_a when dressing with a fixed diamond drag angle θ , constant cross-feed h and variable in-feed α .

Test N° 7 : Wheel type: -38A46 - K5VBE : Diamond N° 63794/2 (worn)

Vertical mag.: 1 scale div. = 1.25 μm Horiz. mag.: 1 scale div. = 50 μm

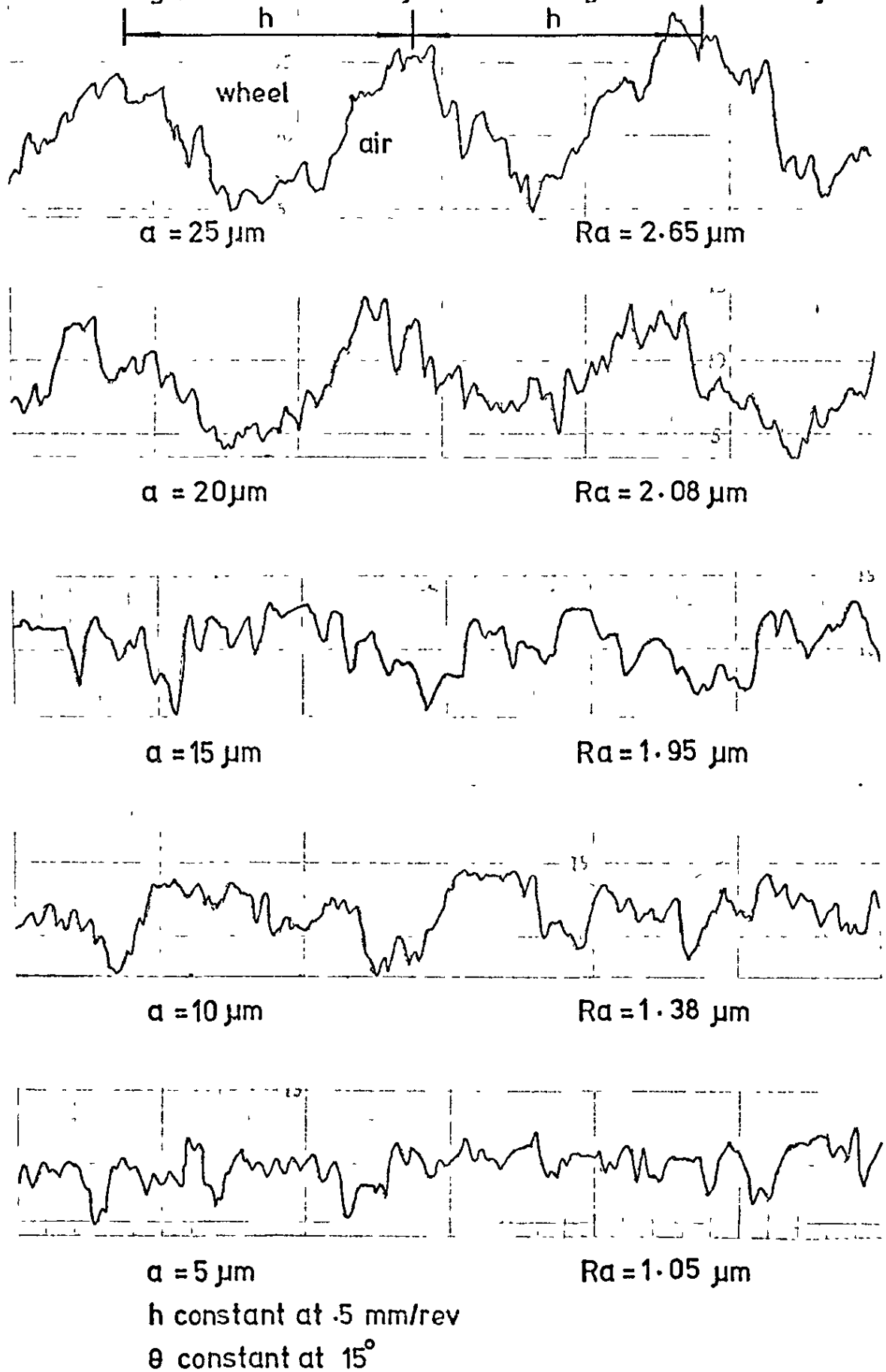
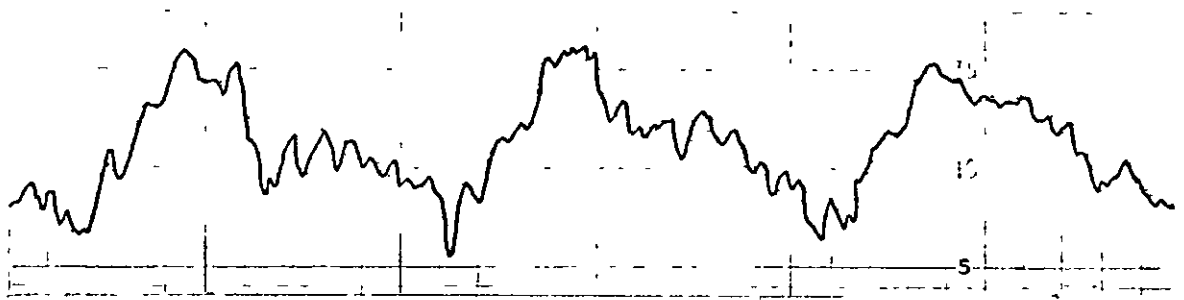


Fig. 7.56 "Talysurf" traces of grinding wheel surface roughness R_a when dressing with a fixed diamond drag angle θ , constant cross-feed h and variable in-feed α .

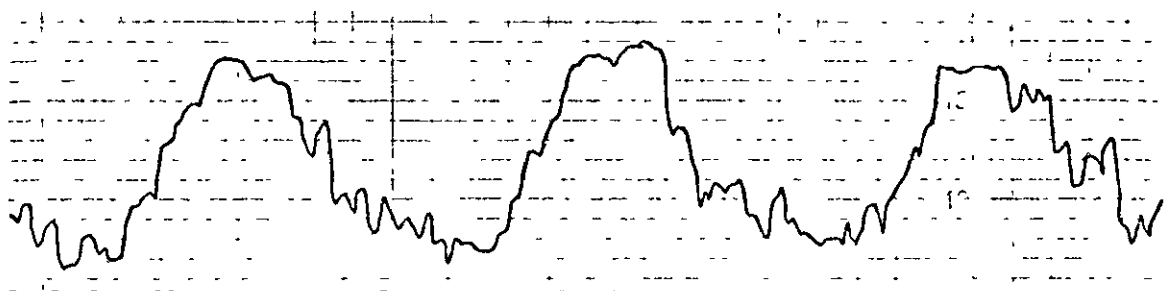
Test N^{os} 5, 6 and 7

Diamond N^o 63794/2 (worn)

Vertical mag.: 1 scale div. = 1.25 μm Horiz. mag.: 1 scale div. = 50 μm



Test N^o 7 Wheel type:- 38 A 46 -K5 VBE $R_a = 2.73 \mu\text{m}$



Test N^o 6 Wheel type:- A 46 KV $R_a = 3.75 \mu\text{m}$



Test N^o 5 Wheel type:- A 60 KV $R_a = 1.30 \mu\text{m}$

θ constant at 5°

a " " 25 μm

h " " .5 mm/rev

Fig. 7.57 "Talysurf traces of three grinding wheels dressed under the same conditions of in-feed, cross-feed and drag angle."

Test № 5
Diamond № 63794/2 (worn)
Wheel type A 60 KV

Key:-
Row 1. Ra actual (µm)
Row 2. Ra theoretical (µm)
Row 3. β theoretical (degrees)

| Drag angle 5° | | Cross-feed h mm/rev | | | | | | | | | |
|---------------|----|---------------------|------|------|------|------|-------|------|-------|------|-------|
| row | | .1 | | .2 | | .3 | | .4 | | .5 | |
| In-feed a µm | 5 | 1 | .75 | .77 | 1.00 | 1.09 | 1.30 | 1.30 | 1.55 | 1.48 | 1.00 |
| | | 2 | | | | | | | | | |
| | | 3 | 173 | | 175 | | 176 | | 176 | | 178 |
| | 10 | 1 | .88 | .88 | 1.13 | 1.09 | 1.35 | 1.31 | 1.70 | 1.75 | 1.20 |
| | | 2 | | | | | | | | | |
| | | 3 | 172 | | 175 | | 176 | | 176 | | 178 |
| | 15 | 1 | 1.13 | 1.09 | 1.20 | 1.09 | 1.20 | 1.31 | 1.63 | 1.75 | 1.55 |
| | | 2 | | | | | | | | | |
| | | 3 | 170 | | 175 | | 176 | | 176 | | 177 |
| | 20 | 1 | .88 | .88 | 1.13 | 1.09 | 1.25 | 1.31 | 1.55 | 1.53 | 1.30 |
| | | 2 | | | | | | | | | |
| | | 3 | 172 | | 175 | | 176 | | 176.5 | | 177.5 |
| | 25 | 1 | .88 | .88 | .95 | 1.09 | 1.50 | 1.47 | 1.38 | 1.31 | 1.38 |
| | | 2 | | | | | | | | | |
| | | 3 | 172 | | 175 | | 175.5 | | 177 | | 177.5 |

| Drag angle 10° | | Cross-feed h mm/rev | | | | | | | | | |
|----------------|----|---------------------|------|------|------|------|------|------|------|------|------|
| row | | .1 | | .2 | | .3 | | .4 | | .5 | |
| In-feed a µm | 5 | 1 | .88 | .88 | 1.00 | 1.09 | 1.30 | 1.30 | 1.33 | 1.48 | 1.55 |
| | | 2 | | | | | | | | | |
| | | 3 | 172 | | 175 | | 176 | | 176 | | 176 |
| | 10 | 1 | 1.20 | 1.20 | 1.33 | 1.31 | 1.38 | 1.31 | 1.50 | 1.75 | 1.75 |
| | | 2 | | | | | | | | | |
| | | 3 | 169 | | 174 | | 176 | | 176 | | 176 |
| | 15 | 1 | 1.05 | .99 | 1.25 | 1.31 | 1.60 | 1.64 | 2.13 | 2.18 | 2.30 |
| | | 2 | | | | | | | | | |
| | | 3 | 171 | | 174 | | 175 | | 175 | | 176 |
| | 20 | 1 | 1.00 | .99 | 1.20 | 1.31 | 1.75 | 1.64 | 2.20 | 2.18 | 2.25 |
| | | 2 | | | | | | | | | |
| | | 3 | 171 | | 174 | | 175 | | 175 | | 176 |
| | 25 | 1 | 1.20 | 1.20 | 1.38 | 1.31 | 1.95 | 1.64 | 2.13 | 2.18 | 1.75 |
| | | 2 | | | | | | | | | |
| | | 3 | 169 | | 174 | | 175 | | 175 | | 176 |

| Drag angle 15° | | Cross-feed h mm/rev | | | | | | | | | |
|----------------|----|---------------------|------|------|------|------|-------|------|------|------|------|
| row | | .1 | | .2 | | .3 | | .4 | | .5 | |
| In-feed a µm | 5 | 1 | 1.13 | 1.09 | 1.15 | 1.09 | 1.00 | .98 | 1.00 | .88 | 1.30 |
| | | 2 | | | | | | | | | |
| | | 3 | 170 | | 175 | | 177 | | 178 | | 177 |
| | 10 | 1 | 1.38 | 1.32 | 1.25 | 1.31 | 1.63 | 1.64 | 1.50 | 1.75 | 1.50 |
| | | 2 | | | | | | | | | |
| | | 3 | 168 | | 174 | | 175 | | 176 | | 177 |
| | 15 | 1 | 1.40 | 1.43 | 1.63 | 1.53 | 2.08 | 2.13 | 2.18 | 2.18 | 2.38 |
| | | 2 | | | | | | | | | |
| | | 3 | 167 | | 173 | | 173.5 | | 175 | | 176 |
| | 20 | 1 | 1.55 | 1.54 | 1.50 | 1.53 | 2.13 | 2.13 | 2.20 | 2.18 | 2.25 |
| | | 2 | | | | | | | | | |
| | | 3 | 166 | | 173 | | 173.5 | | 175 | | 176 |
| | 25 | 1 | 1.55 | 1.54 | 1.63 | 1.53 | 2.00 | 2.13 | 2.13 | 2.18 | 2.63 |
| | | 2 | | | | | | | | | |
| | | 3 | 166 | | 173 | | 173.5 | | 175 | | 175 |

Fig. 7.58
Table of actual and theoretical values of grinding wheel surface roughness Ra for different dressing conditions.

Wheel type:- A 60 KV

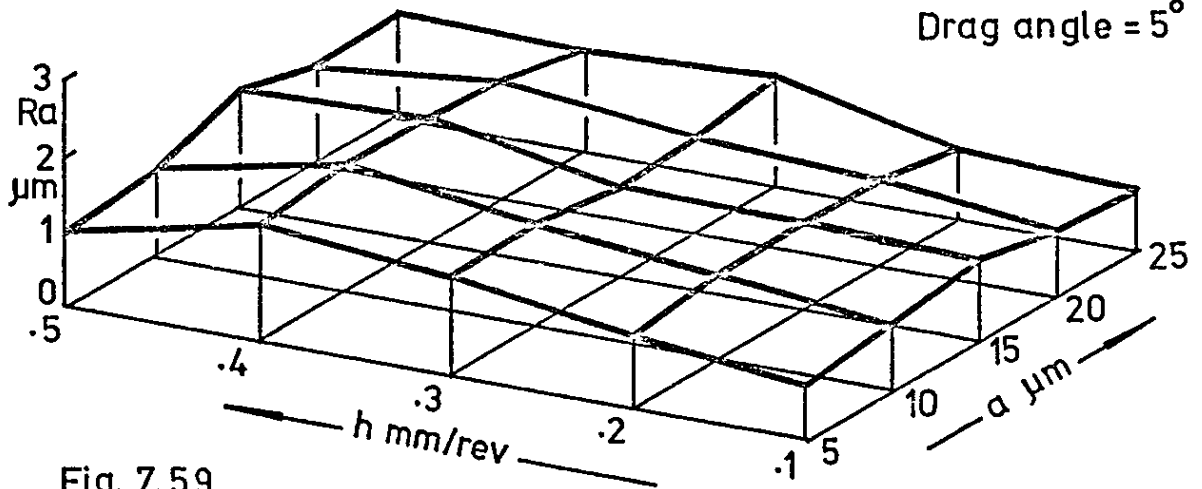
Drag angle = 5° 

Fig. 7.59

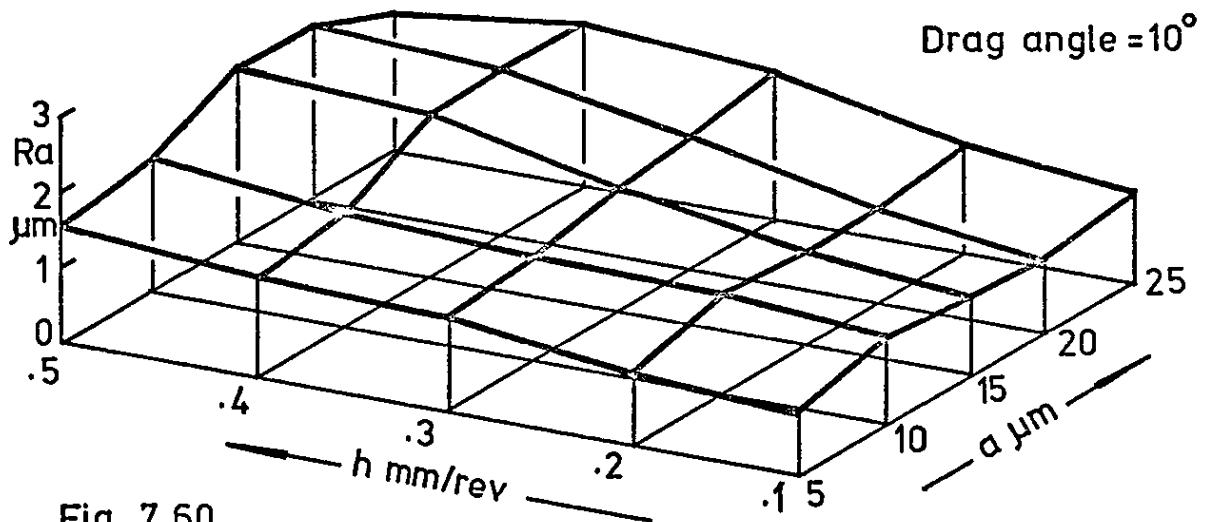


Fig. 7.60

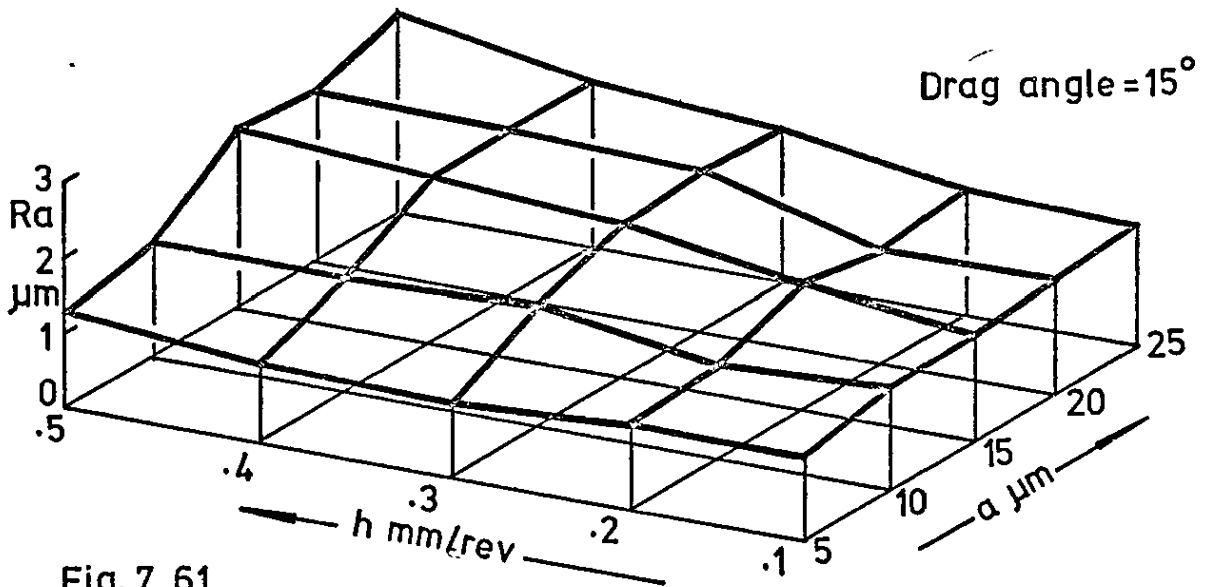


Fig. 7.61

Figs. 7.59 to 7.61 inc. Variation of grinding wheel surface roughness with depth of cut and traverse rate when dressing with a worn diamond set at different values of drag angle.

Test № 6
Diamond № 63794/2 (worn)
Wheel type A 46 KV

Key:-
Row 1. Ra actual (µm)
Row 2. Ra theoretical (µm)
Row 3. β theoretical (degrees)

| Drag angle 5° | | | Cross-feed h mm/rev | | | | | | | | | |
|---------------|----|---|---------------------|------|------|------|------|------|------|------|-------|------|
| row | | | .1 | | .2 | | .3 | | .4 | | .5 | |
| In-feed a μm | 5 | 1 | 1.25 | 1.32 | 1.03 | 1.09 | 1.45 | 1.46 | 1.45 | 1.46 | 1.00 | 1.09 |
| | | 2 | | | | | | | | | | |
| | | 3 | 168 | | 175 | | 175 | | 175 | | 178 | |
| | 10 | 1 | 1.38 | 1.32 | 1.05 | 1.09 | 1.68 | 1.64 | 1.88 | 2.18 | 1.90 | 1.91 |
| | | 2 | | | | | | | | | | |
| | | 3 | 168 | | 175 | | 175 | | 175 | | 176.5 | |
| | 15 | 1 | 1.08 | 1.09 | 1.55 | 1.53 | 1.65 | 1.64 | 2.38 | 2.18 | 3.20 | 3.28 |
| | | 2 | | | | | | | | | | |
| | | 3 | 170 | | 173 | | 175 | | 175 | | 174 | |
| | 20 | 1 | 1.13 | 1.09 | 1.45 | 1.31 | 1.55 | 1.64 | 2.00 | 2.18 | 2.95 | 3.28 |
| | | 2 | | | | | | | | | | |
| | | 3 | 170 | | 174 | | 175 | | 175 | | 174 | |
| | 25 | 1 | 1.30 | 1.32 | 1.33 | 1.31 | 1.65 | 1.64 | 2.10 | 2.18 | 3.75 | 3.82 |
| | | 2 | | | | | | | | | | |
| | | 3 | 168 | | 174 | | 175 | | 175 | | 173 | |

| Drag angle 10° | | | Cross-feed h mm/rev | | | | | | | | | |
|----------------|----|---|---------------------|------|------|------|------|------|-------|------|-------|------|
| row | | | .1 | | .2 | | .3 | | .4 | | .5 | |
| In-feed a μm | 5 | 1 | 1.05 | 1.09 | 1.15 | 1.09 | .95 | .98 | 1.00 | 1.03 | 1.20 | 1.09 |
| | | 2 | | | | | | | | | | |
| | | 3 | 170 | | 175 | | 177 | | 177.5 | | 178 | |
| | 10 | 1 | 1.05 | 1.09 | 1.40 | 1.31 | 1.65 | 1.64 | 1.78 | 1.75 | 1.83 | 1.91 |
| | | 2 | | | | | | | | | | |
| | | 3 | 170 | | 174 | | 175 | | 176 | | 176.5 | |
| | 15 | 1 | 1.00 | 1.09 | 1.45 | 1.53 | 1.70 | 1.64 | 2.38 | 2.18 | 2.25 | 2.18 |
| | | 2 | | | | | | | | | | |
| | | 3 | 170 | | 173 | | 175 | | 175 | | 176 | |
| | 20 | 1 | 1.20 | 1.20 | 1.58 | 1.53 | 1.80 | 1.97 | 2.78 | 2.62 | 2.73 | 2.73 |
| | | 2 | | | | | | | | | | |
| | | 3 | 169 | | 173 | | 174 | | 174 | | 175 | |
| | 25 | 1 | 1.50 | 1.54 | 1.75 | 1.75 | 1.88 | 1.97 | 2.50 | 2.62 | 2.78 | 2.73 |
| | | 2 | | | | | | | | | | |
| | | 3 | 166 | | 172 | | 174 | | 174 | | 175 | |

| Drag angle 15° | | | Cross-feed h mm/rev | | | | | | | | | |
|----------------|----|---|---------------------|------|------|------|------|------|-------|------|------|------|
| row | | | .1 | | .2 | | .3 | | .4 | | .5 | |
| In-feed a μm | 5 | 1 | 1.25 | 1.32 | 1.00 | 1.09 | 1.38 | 1.30 | 1.25 | 1.31 | 1.00 | 1.09 |
| | | 2 | | | | | | | | | | |
| | | 3 | 168 | | 175 | | 176 | | 177 | | 178 | |
| | 10 | 1 | 1.30 | 1.32 | 1.30 | 1.31 | 1.60 | 1.64 | 1.90 | 1.97 | 2.10 | 2.18 |
| | | 2 | | | | | | | | | | |
| | | 3 | 168 | | 174 | | 175 | | 175.5 | | 176 | |
| | 15 | 1 | 1.20 | 1.32 | 1.38 | 1.31 | 1.83 | 1.64 | 2.13 | 2.18 | 2.13 | 2.18 |
| | | 2 | | | | | | | | | | |
| | | 3 | 168 | | 174 | | 175 | | 175 | | 176 | |
| | 20 | 1 | 1.45 | 1.43 | 1.45 | 1.31 | 1.75 | 1.64 | 2.05 | 2.18 | 2.15 | 2.18 |
| | | 2 | | | | | | | | | | |
| | | 3 | 167 | | 174 | | 175 | | 175 | | 176 | |
| | 25 | 1 | 1.45 | 1.43 | 1.35 | 1.31 | 1.53 | 1.64 | 2.00 | 2.18 | 2.20 | 2.18 |
| | | 2 | | | | | | | | | | |
| | | 3 | 167 | | 174 | | 175 | | 175 | | 176 | |

Fig. 7.62

Table of actual and theoretical values of grinding wheel surface roughness Ra for different dressing conditions.

Test № 6

Wheel type:- A 46 KV
Drag angle = 5°

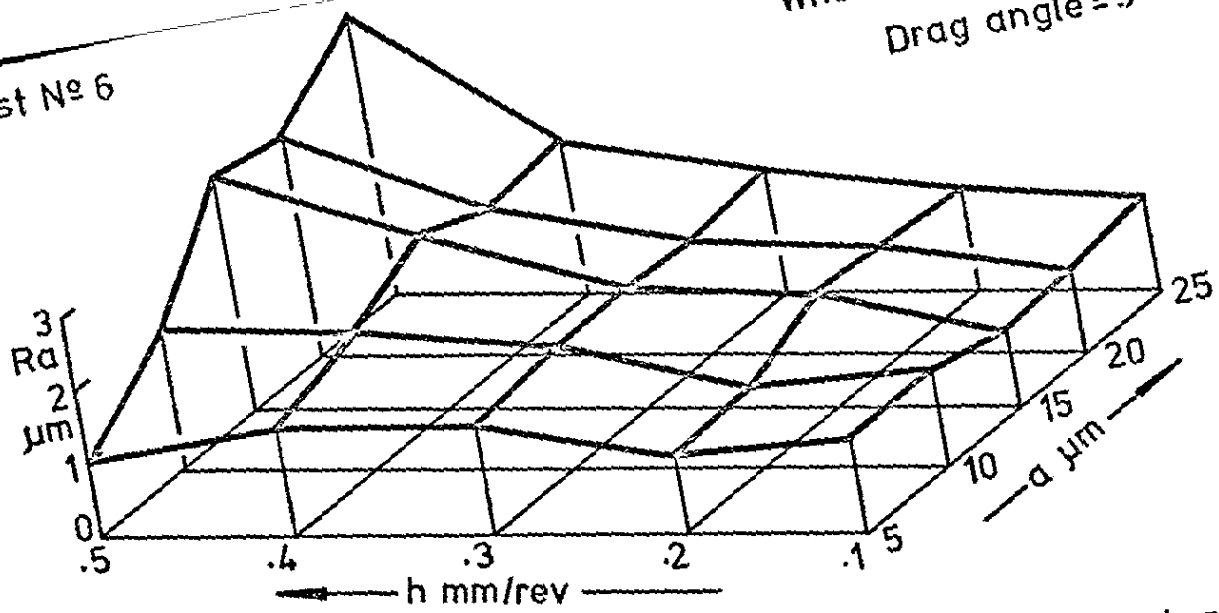


Fig. 7.63

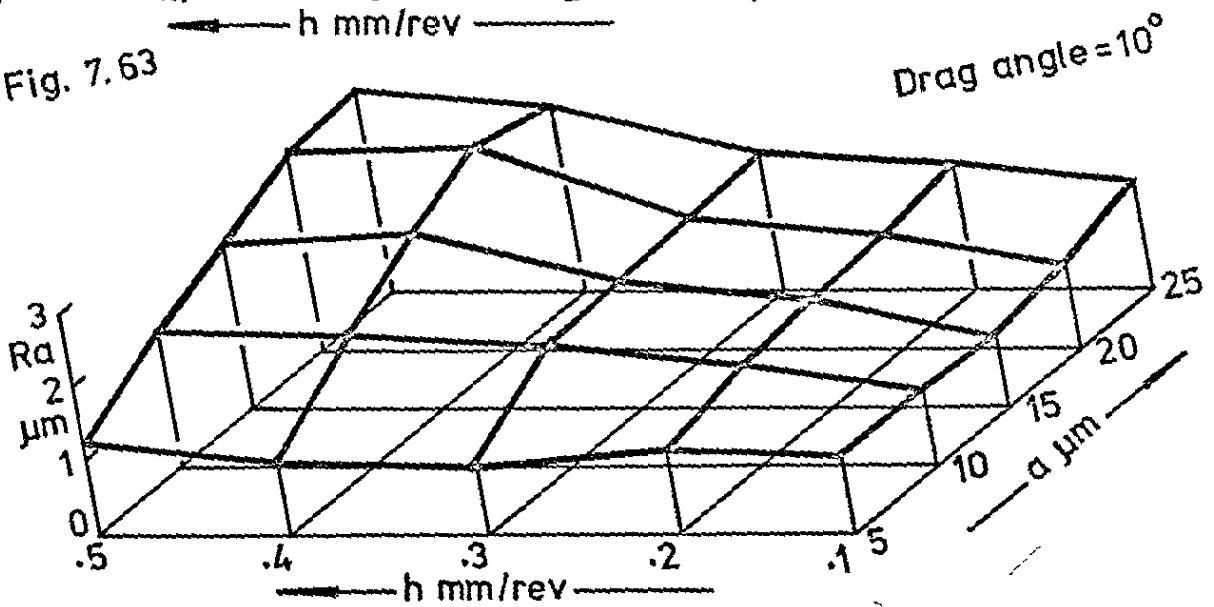


Fig. 7.64

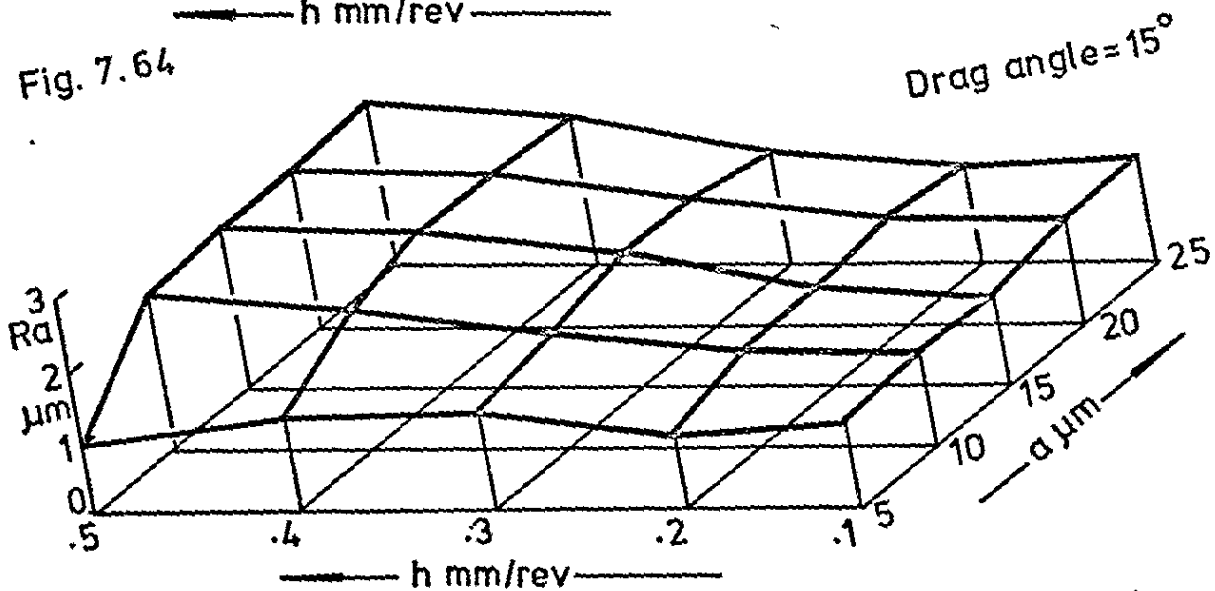


Fig. 7.65

Variation of grinding wheel surface roughness with depth of cut and traverse rate when dressing with a worn diamond set at different values of drag angle.

Test № 7
Diamond № 63794/2(worn)
Wheeltype 38 A 46 - K5 VBE

Key:-
Row 1. Ra actual (µm)
Row 2. Ra theoretical (µm)
Row 3. β theoretical (degrees)

| Drag angle 5° | | Cross-feed h mm/rev | | | | | | | | | |
|---------------|----|---------------------|------|------|------|------|-------|------|-------|------|------|
| row | | .1 | | .2 | | .3 | | .4 | | .5 | |
| In-feed a µm | 5 | 1 | 1.15 | 1.20 | 1.05 | 1.09 | 1.20 | 1.30 | 1.45 | 1.48 | 1.98 |
| | | 2 | | | | | | | | | |
| | | 3 | 169 | | 175 | | 176 | | 176 | | 177 |
| | 10 | 1 | 1.30 | 1.32 | 1.25 | 1.31 | 1.25 | 1.31 | 1.50 | 1.75 | 2.25 |
| | | 2 | | | | | | | | | |
| | | 3 | 168 | | 174 | | 176 | | 176 | | 176 |
| | 15 | 1 | 1.25 | 1.32 | 1.45 | 1.31 | 1.95 | 1.97 | 2.08 | 2.18 | 2.58 |
| | | 2 | | | | | | | | | |
| | | 3 | 168 | | 174 | | 174 | | 175 | | 175 |
| | 20 | 1 | 1.25 | 1.32 | 1.50 | 1.53 | 2.05 | 2.13 | 2.23 | 2.18 | 2.63 |
| | | 2 | | | | | | | | | |
| | | 3 | 168 | | 173 | | 173.5 | | 175 | | 175 |
| | 25 | 1 | 1.25 | 1.32 | 1.60 | 1.53 | 2.10 | 2.13 | 2.33 | 2.40 | 2.73 |
| | | 2 | | | | | | | | | |
| | | 3 | 168 | | 173 | | 173.5 | | 174.5 | | 175 |

| Drag angle 10° | | Cross-feed h mm/rev | | | | | | | | | |
|----------------|----|---------------------|------|------|------|------|-------|------|-------|------|-------|
| row | | .1 | | .2 | | .3 | | .4 | | .5 | |
| In-feed a µm | 5 | 1 | 1.53 | 1.46 | 1.25 | 1.31 | 1.08 | 1.15 | 1.10 | 1.09 | 1.20 |
| | | 2 | | | | | | | | | |
| | | 3 | 165 | | 174 | | 176.5 | | 177.5 | | 177.5 |
| | 10 | 1 | 1.68 | 1.65 | 1.48 | 1.53 | 1.53 | 1.64 | 1.68 | 1.75 | 1.58 |
| | | 2 | | | | | | | | | |
| | | 3 | 165 | | 173 | | 175 | | 176 | | 177 |
| | 15 | 1 | 1.73 | 1.76 | 1.55 | 1.53 | 1.95 | 1.97 | 1.95 | 1.97 | 2.13 |
| | | 2 | | | | | | | | | |
| | | 3 | 164 | | 173 | | 174 | | 175.5 | | 176 |
| | 20 | 1 | 1.73 | 1.76 | 1.83 | 1.75 | 3.08 | 2.95 | 2.38 | 2.40 | 2.83 |
| | | 2 | | | | | | | | | |
| | | 3 | 164 | | 172 | | 171 | | 174.5 | | 175 |
| | 25 | 1 | 1.88 | 1.87 | 2.08 | 2.19 | 2.88 | 2.95 | 3.38 | 3.50 | 3.70 |
| | | 2 | | | | | | | | | |
| | | 3 | 163 | | 170 | | 171 | | 172 | | 173 |

| Drag angle 15° | | Cross-feed h mm/rev | | | | | | | | | |
|----------------|----|---------------------|------|------|------|------|-------|------|-------|------|-------|
| row | | .1 | | .2 | | .3 | | .4 | | .5 | |
| In-feed a µm | 5 | 1 | 1.40 | 1.43 | 1.33 | 1.31 | 1.00 | .98 | 1.25 | 1.31 | 1.05 |
| | | 2 | | | | | | | | | |
| | | 3 | 167 | | 174 | | 177 | | 177 | | 178 |
| | 10 | 1 | 1.20 | 1.20 | 1.35 | 1.31 | 1.48 | 1.47 | 1.65 | 1.75 | 1.38 |
| | | 2 | | | | | | | | | |
| | | 3 | 169 | | 174 | | 175.5 | | 176 | | 177.5 |
| | 15 | 1 | 1.53 | 1.54 | 1.70 | 1.53 | 1.78 | 1.64 | 1.93 | 1.97 | 1.95 |
| | | 2 | | | | | | | | | |
| | | 3 | 166 | | 173 | | 175 | | 175.5 | | 176.5 |
| | 20 | 1 | 1.25 | 1.32 | 1.55 | 1.53 | 1.85 | 1.80 | 2.08 | 2.19 | 2.08 |
| | | 2 | | | | | | | | | |
| | | 3 | 168 | | 173 | | 174.5 | | 175 | | 176 |
| | 25 | 1 | 1.30 | 1.32 | 1.58 | 1.53 | 2.05 | 1.97 | 2.65 | 2.62 | 2.65 |
| | | 2 | | | | | | | | | |
| | | 3 | 168 | | 173 | | 174 | | 174 | | 175 |

Fig. 7.66

Table of actual and theoretical values of grinding wheel surface roughness Ra for different dressing conditions.

Test No 7

Wheel type :- 38 A 40

Drag angle = 5°

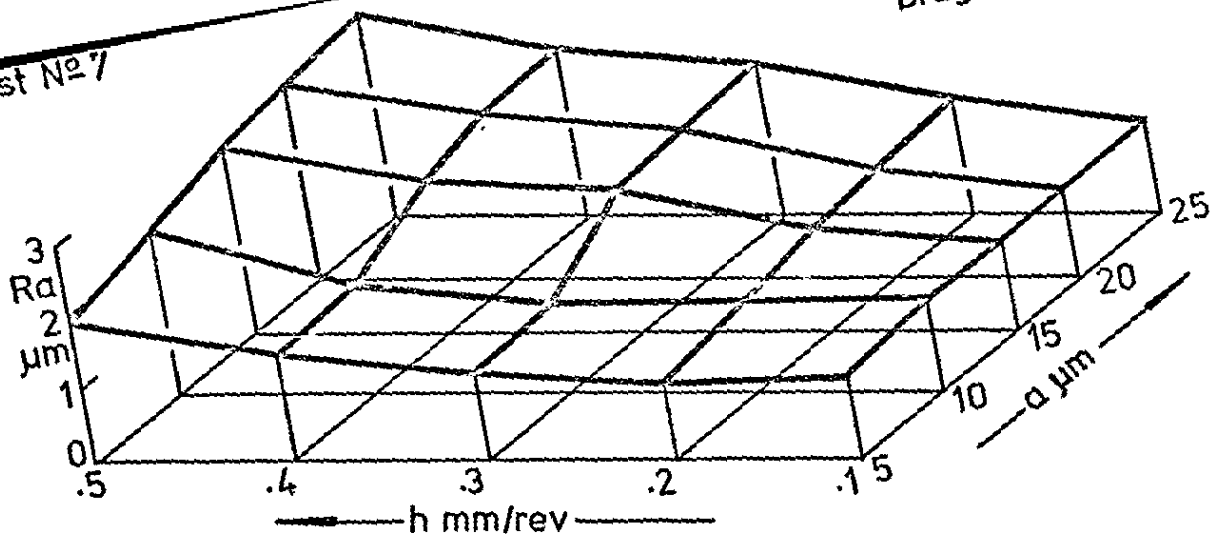


Fig. 7.67

Drag angle = 10°

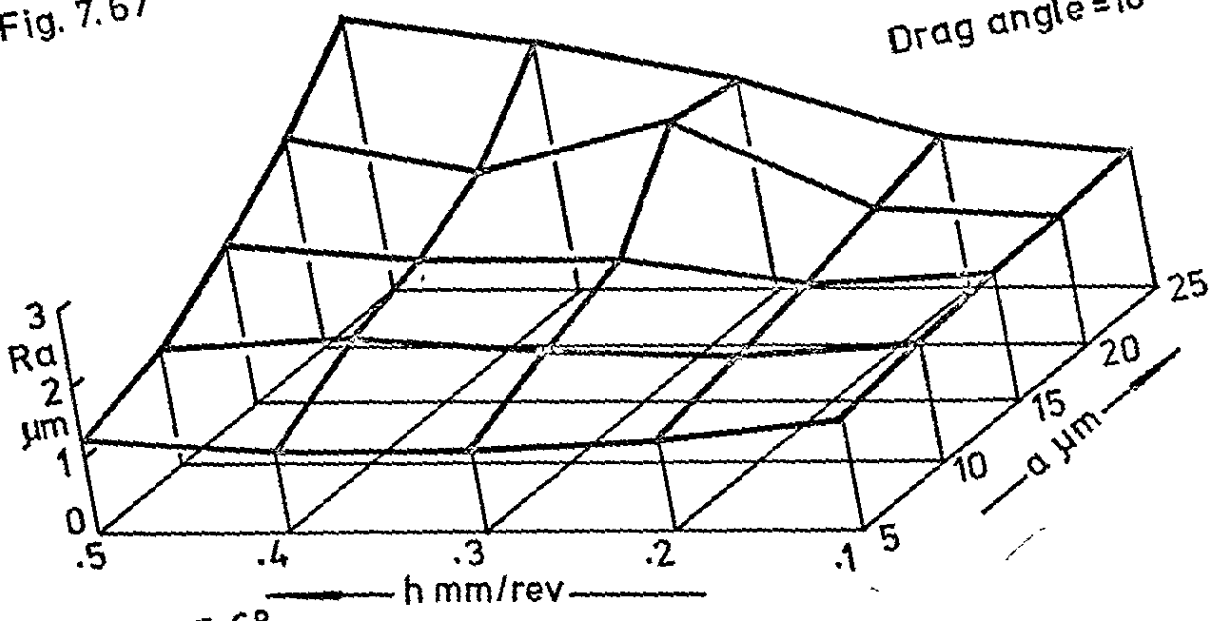


Fig. 7.68

Drag angle = 15°

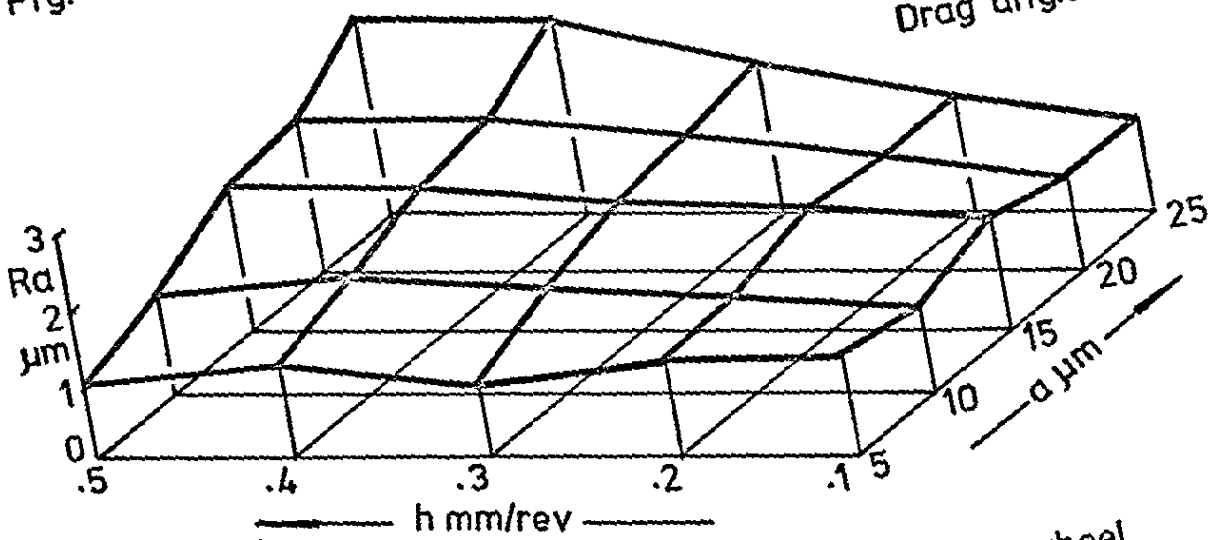
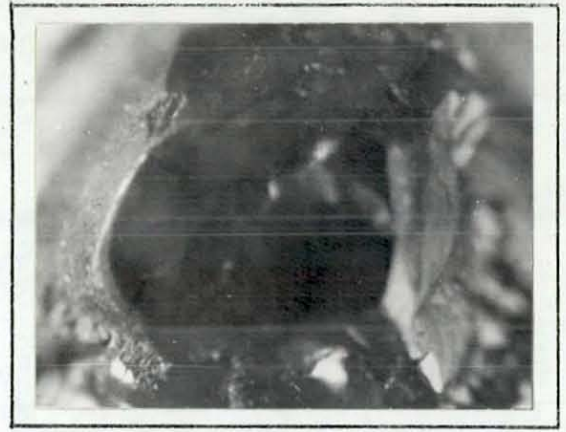


Fig. 7.69

Variation of grinding wheel surface roughness with depth of cut and traverse rate when dressing with a worn diamond set at different values of drag angle.

Test № 8

Pre - test front view of the
blunt dressing diamond



Diamond wear after dressing
wheel type 38 A 46 - K 5 VBE



Diamond wear after dressing
wheel type 32 A 60 - K 8 VBE



Diamond wear after dressing
wheel type A 46 KV

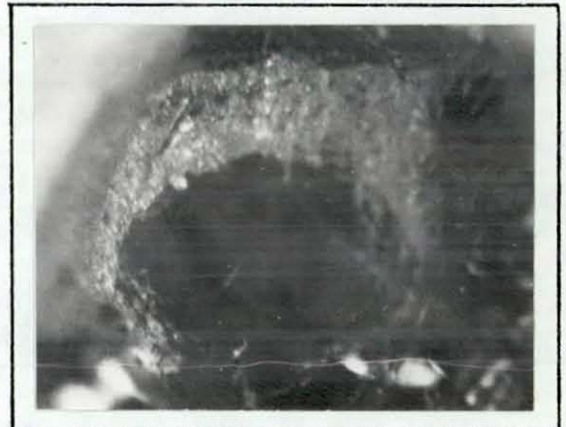


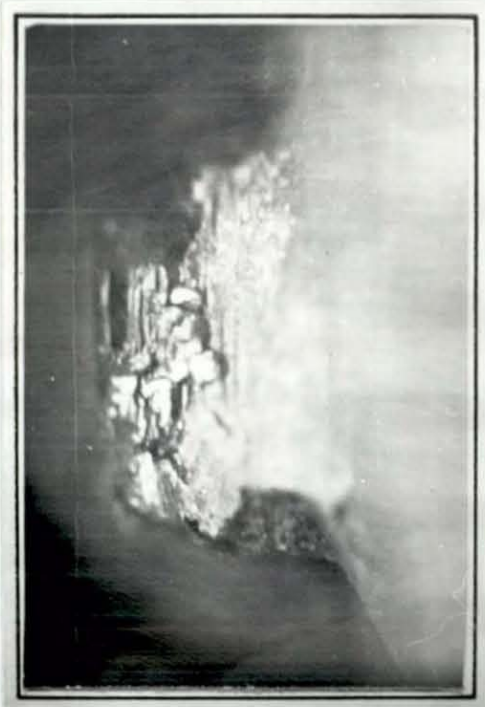
Fig. 7.70 Views of progressive wear of a blunt diamond used for dressing different grinding wheels.



PROFILE VIEWS

1.5mm

ISOMA
Projections
x25 mag.



1.64mm

PLAN VIEWS

Diamond wear after dressing wheel type A 60 KV
(End of test)

Fig. 7.71 Views of a diamond after the limit of
useful life for wheel dressing had been reached

Test N° 8 Wheel type :- 38 A 46 - K5VBE
 Diamond :- blunt - origin unknown Drag angle 5°

Key :-

— represents F_r

--- " F_t

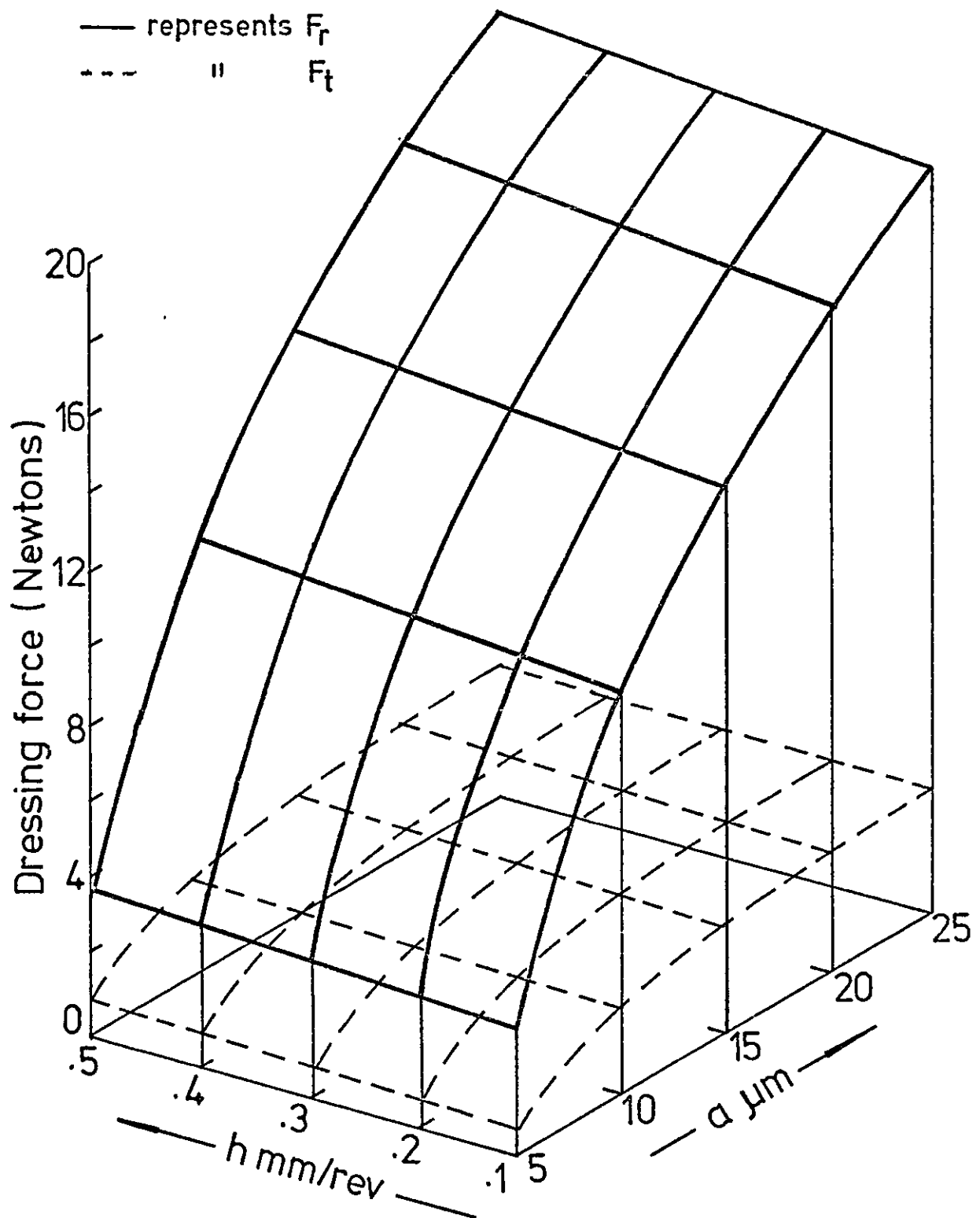


Fig. 7.72 Variation of dressing force (F_r & F_t components) with dressing depth of cut and traverse rate when dressing with a blunt diamond at a fixed drag angle

Test N° 8 Wheel type:- 32A60-K8VBE
 Diamond :- blunt-origin unknown Drag angle 5°

Key:-

— represents F_r

--- " F_t

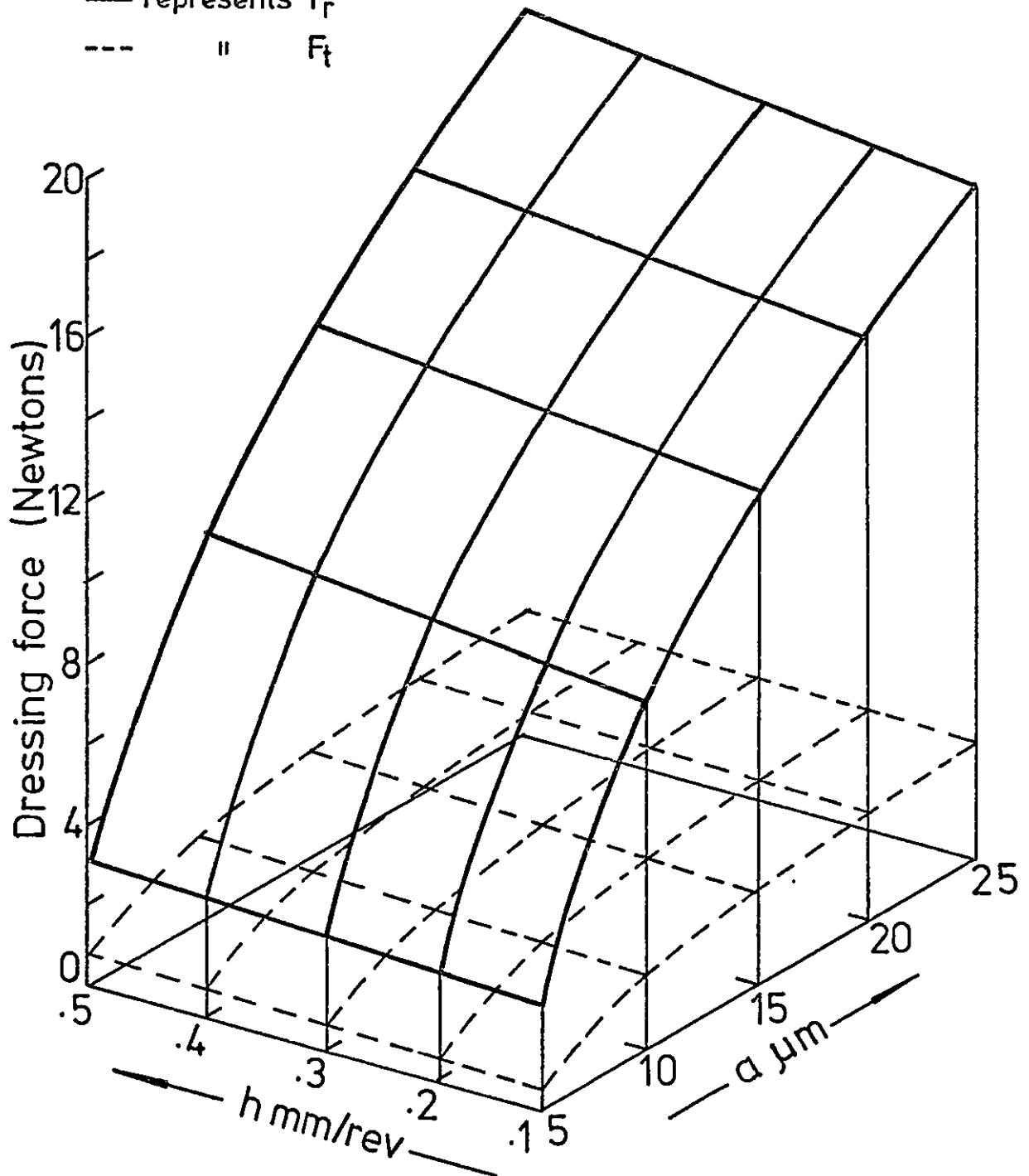


Fig. 7.73 Variation of dressing force (F_r & F_t components) with dressing depth of cut and traverse rate when dressing with a blunt diamond at a fixed drag angle

Test N° 8 Wheel type:- A 46 KV

Diamond:- blunt - origin unknown

Drag angle 5°

Key:-

— represents F_r

--- " F_t

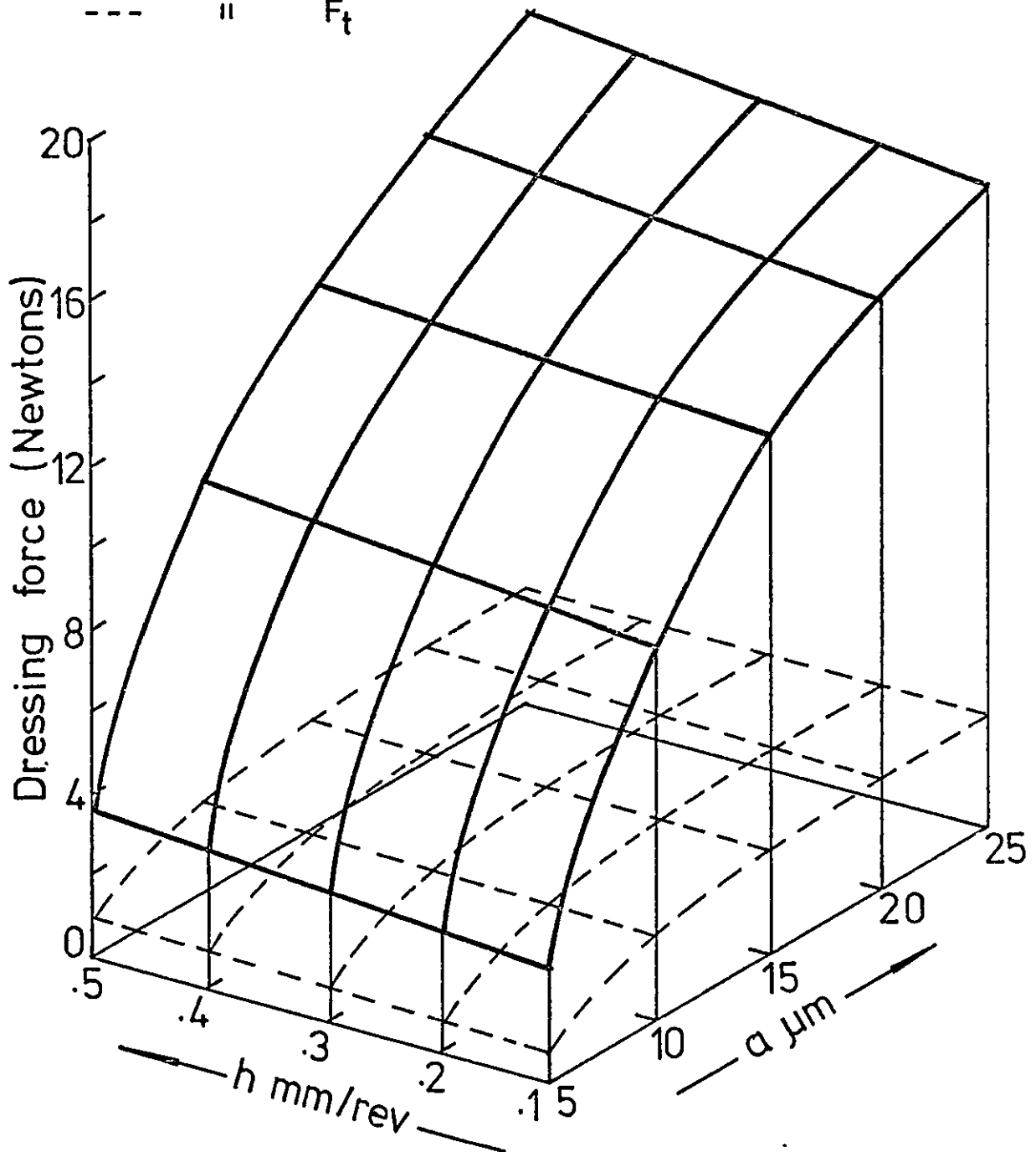


Fig. 7.74 Variation of dressing force (F_r & F_t components) with dressing depth of cut and traverse rate when dressing with a blunt diamond at a fixed drag angle

Test N° 3 Wheel type :- A 60 KV

Diamond :- blunt - origin unknown Drag angle 5°

Key :-

— represents F_r

--- " F_t

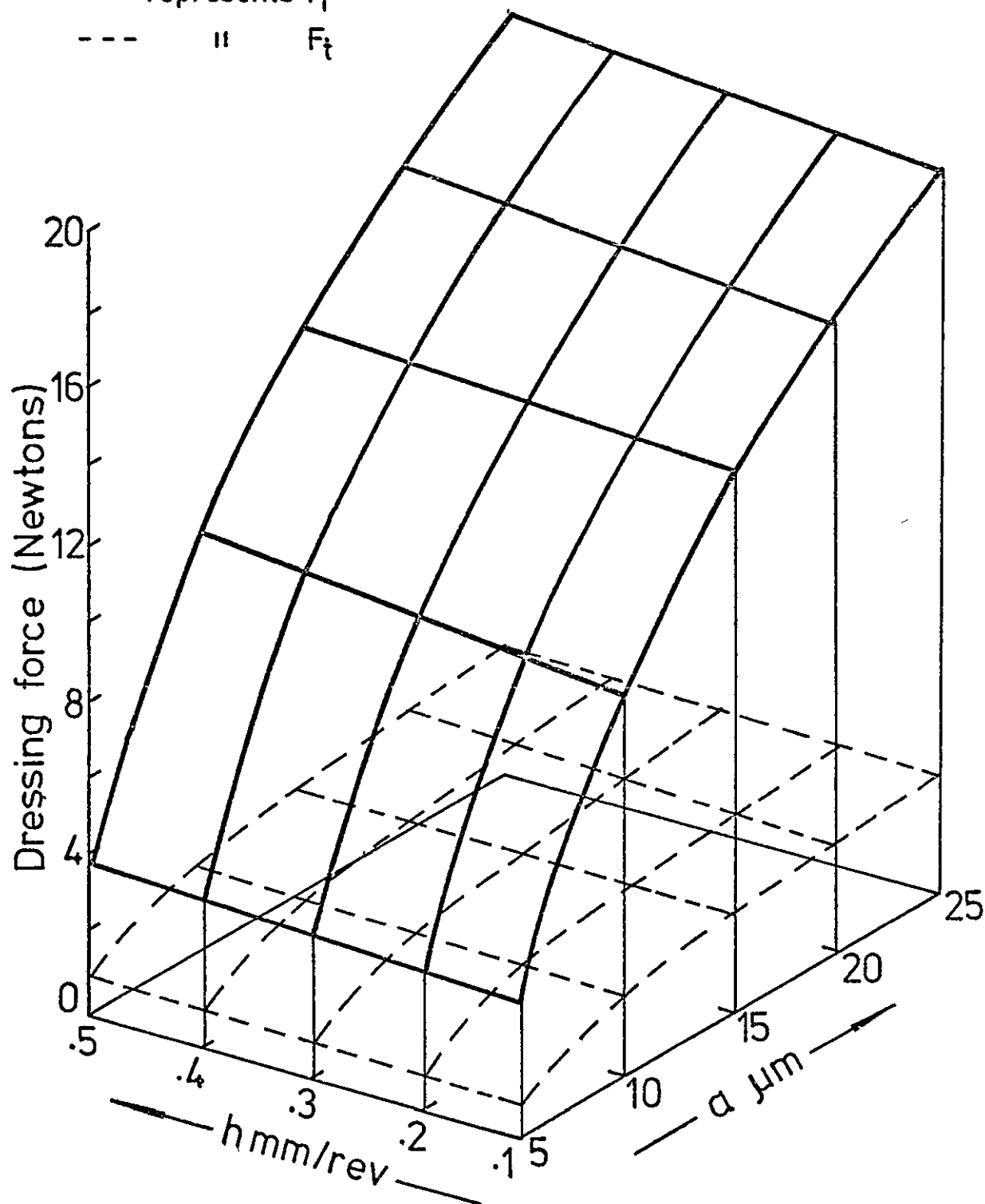


Fig. 7.75 Variation of dressing force (F_r & F_t components) with dressing depth of cut and traverse rate when dressing with a blunt diamond at a fixed drag angle

Test N° 8 : Wheel type:-- 38A46-K5VBE :Diamond blunt (origin unknown)

Vertical mag.: 1 scale div.=1.25 μm Horiz.mag.: 1 scale div.= 50 μm



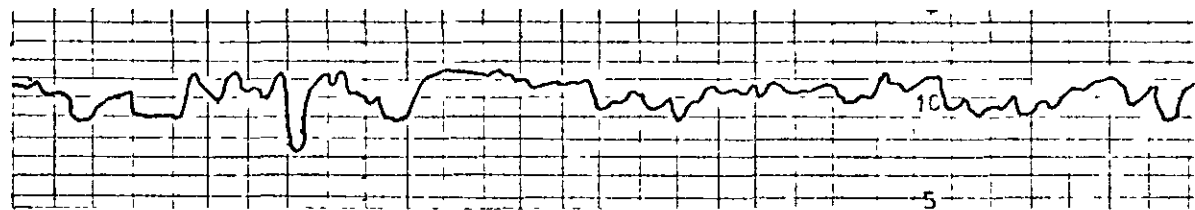
$\alpha = 25 \mu\text{m}$ $h = .5 \text{ mm/rev}$ $Ra = 1.30 \mu\text{m}$



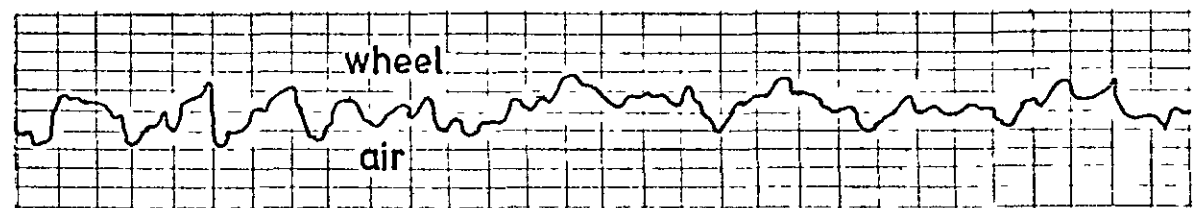
$\alpha = 20 \mu\text{m}$ $h = .4 \text{ mm/rev}$ $Ra = 1.30 \mu\text{m}$



$\alpha = 15 \mu\text{m}$ $h = .3 \text{ mm/rev}$ $Ra = 1.30 \mu\text{m}$



$\alpha = 10 \mu\text{m}$ $h = .2 \text{ mm/rev}$ $Ra = 1.15 \mu\text{m}$

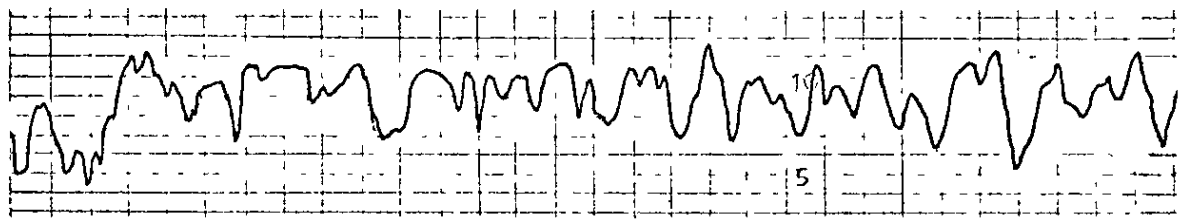


$\alpha = 5 \mu\text{m}$ $h = .1 \text{ mm/rev}$ $Ra = .78 \mu\text{m}$
 \propto constant at 5°

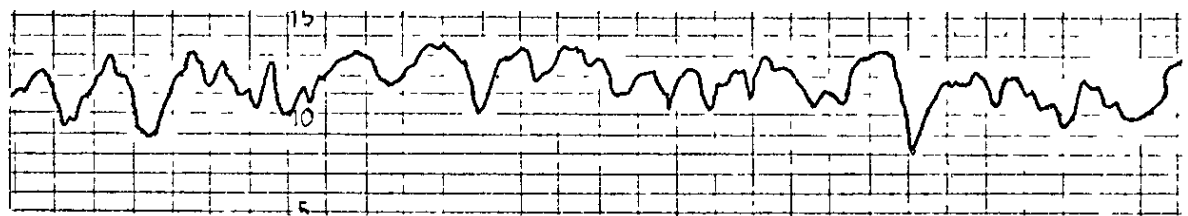
Fig. 7.76 "Talysurf" traces of grinding wheel surface roughness Ra when dressing with a fixed diamond drag angle \propto , variable cross-feed h and variable in-feed a .

Test N° 8 : Wheel type:- 32 A60-K8VBE: Diamond blunt (origin unknown)

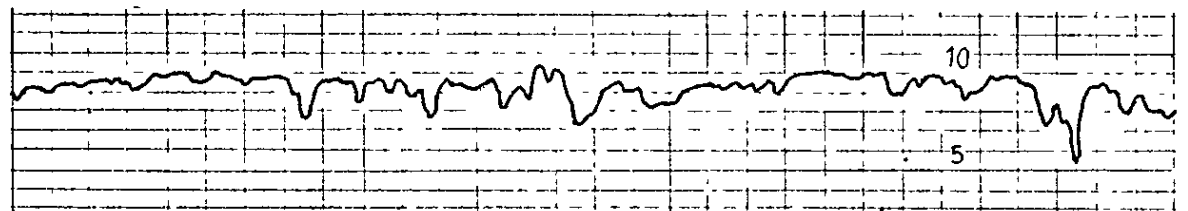
Vertical mag.: 1 scale div.=1.25 μm Horiz.mag.: 1 scale div.= 50 μm



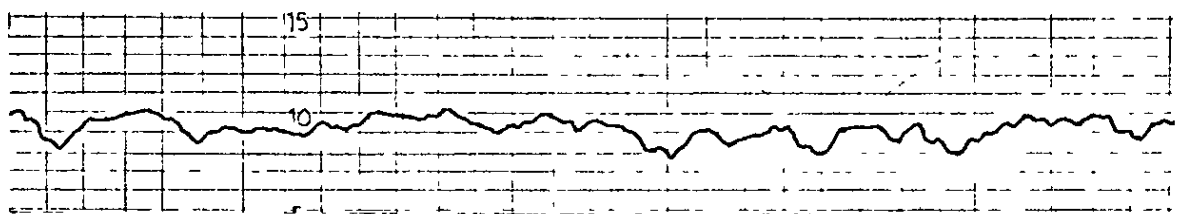
$\alpha = 25 \mu\text{m}$ $h = .5 \text{ mm/rev}$ $Ra = 1.25 \mu\text{m}$



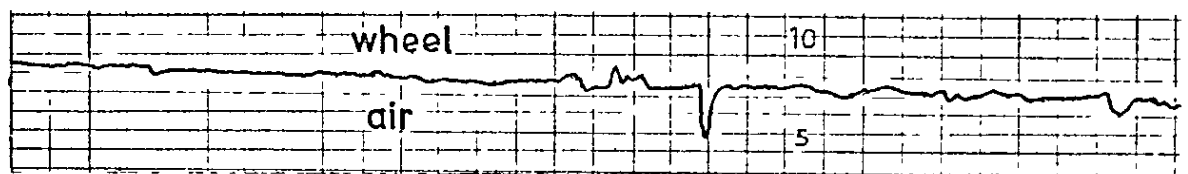
$\alpha = 20 \mu\text{m}$ $h = .4 \text{ mm/rev}$ $Ra = 1.20 \mu\text{m}$



$\alpha = 15 \mu\text{m}$ $h = .3 \text{ mm/rev}$ $Ra = .90 \mu\text{m}$



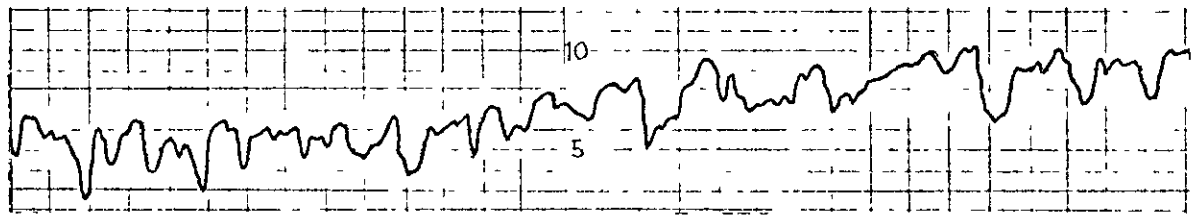
$\alpha = 10 \mu\text{m}$ $h = .2 \text{ mm/rev}$ $Ra = .55 \mu\text{m}$



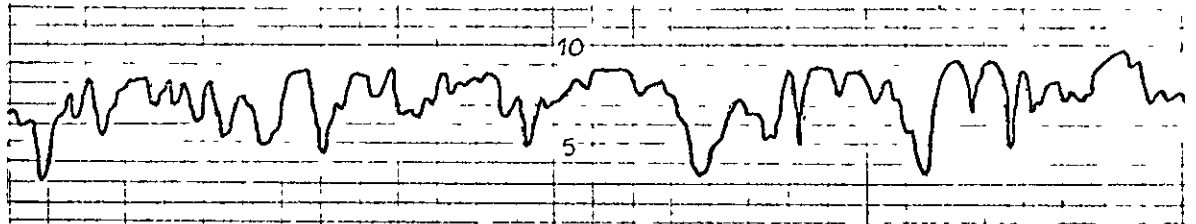
$\alpha = 5 \mu\text{m}$ $h = .1 \text{ mm/rev}$ $Ra = .35 \mu\text{m}$
 α constant at 5°

Fig. 7.77 "Talysurf" traces of grinding wheel surface roughness Ra when dressing with a fixed diamond drag angle α , variable cross-feed h and variable in-feed a .

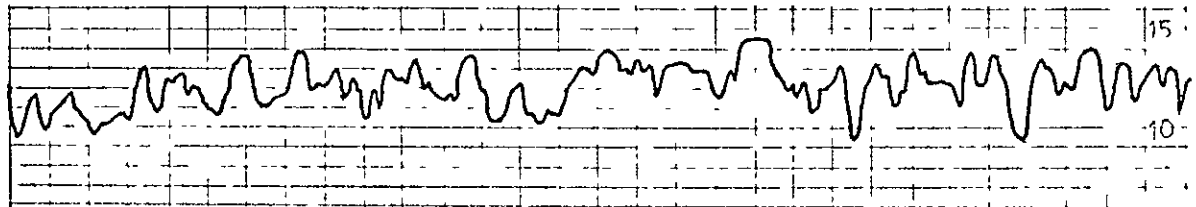
Test N° 8 : Wheel type :- A 46 KV : Diamond blunt (origin unknown)
 Vertical mag. : 1 scale div. = 1.25 μm Horiz. mag. : 1 scale div. = 50 μm



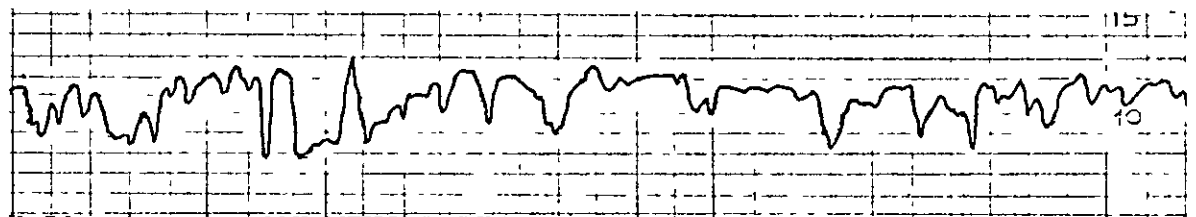
$a = 25 \mu\text{m}$ $h = .5 \text{ mm/rev}$ $Ra = 1.25 \mu\text{m}$



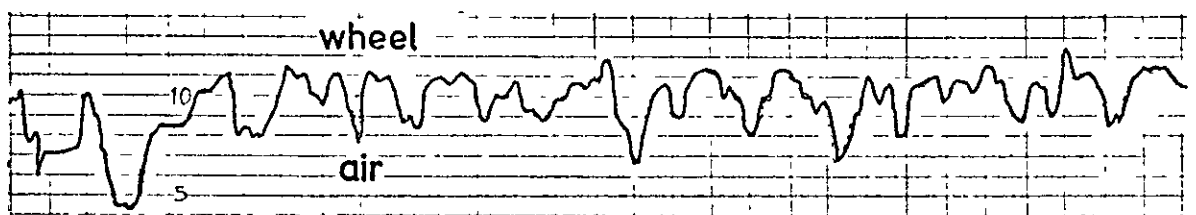
$a = 20 \mu\text{m}$ $h = .4 \text{ mm/rev}$ $Ra = 1.28 \mu\text{m}$



$a = 15 \mu\text{m}$ $h = .3 \text{ mm/rev}$ $Ra = 1.20 \mu\text{m}$



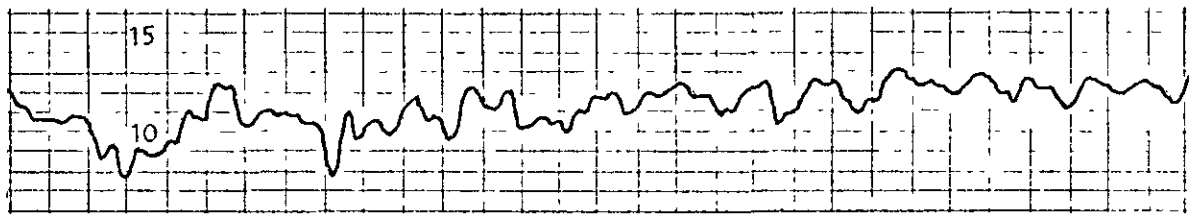
$a = 10 \mu\text{m}$ $h = .2 \text{ mm/rev}$ $Ra = 1.13 \mu\text{m}$



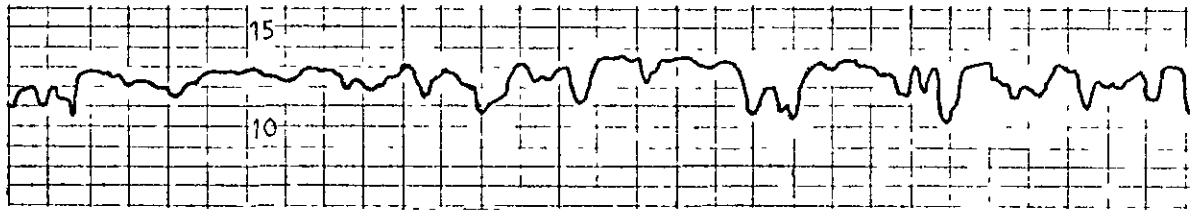
$a = 5 \mu\text{m}$ $h = .1 \text{ mm/rev}$ $Ra = 1.18 \mu\text{m}$
 α constant at 5°

Fig. 7.78 "Talysurf" traces of grinding wheel surface roughness Ra when dressing with a fixed diamond drag angle α , variable cross-feed h and variable in-feed a .

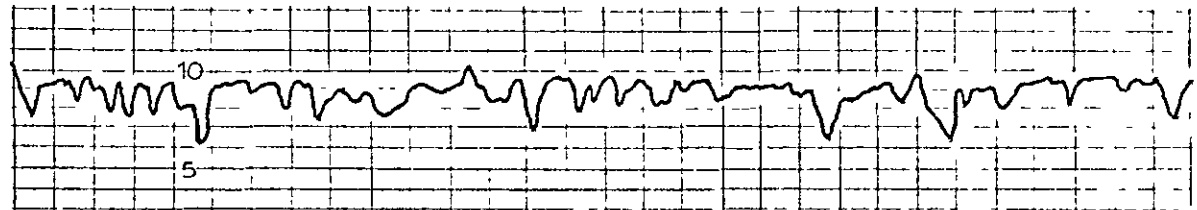
Test N° 8 : Wheel type:- A 60KV : Diamond blunt (origin unknown)
 Vertical mag.: 1 scale div.=1.25 μm Horiz.mag.: 1 scale div.= 50 μm



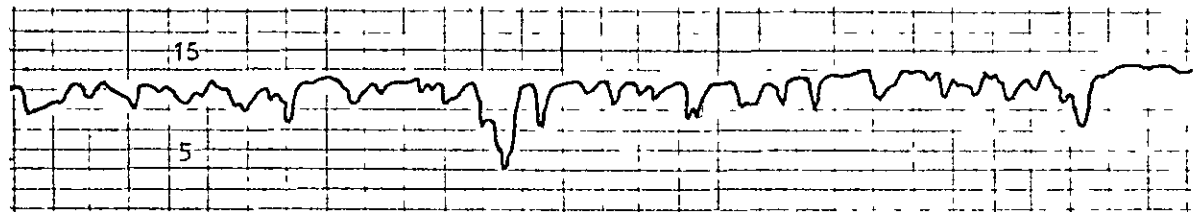
$a = 25 \mu\text{m}$ $h = .5 \text{ mm/rev}$ $Ra = .93 \mu\text{m}$



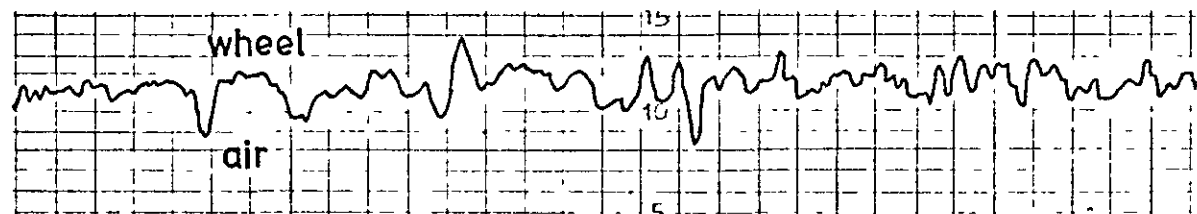
$a = 20 \mu\text{m}$ $h = .4 \text{ mm/rev}$ $Ra = .95 \mu\text{m}$



$a = 15 \mu\text{m}$ $h = .3 \text{ mm/rev}$ $Ra = .88 \mu\text{m}$



$a = 10 \mu\text{m}$ $h = .2 \text{ mm/rev}$ $Ra = .80 \mu\text{m}$



$a = 5 \mu\text{m}$ $h = .1 \text{ mm/rev}$ $Ra = .80 \mu\text{m}$
 α constant at 5°

Fig. 7.79 "Talysurf" traces of grinding wheel surface roughness Ra when dressing with a fixed diamond drag angle α , variable cross-feed h and variable in-feed a .

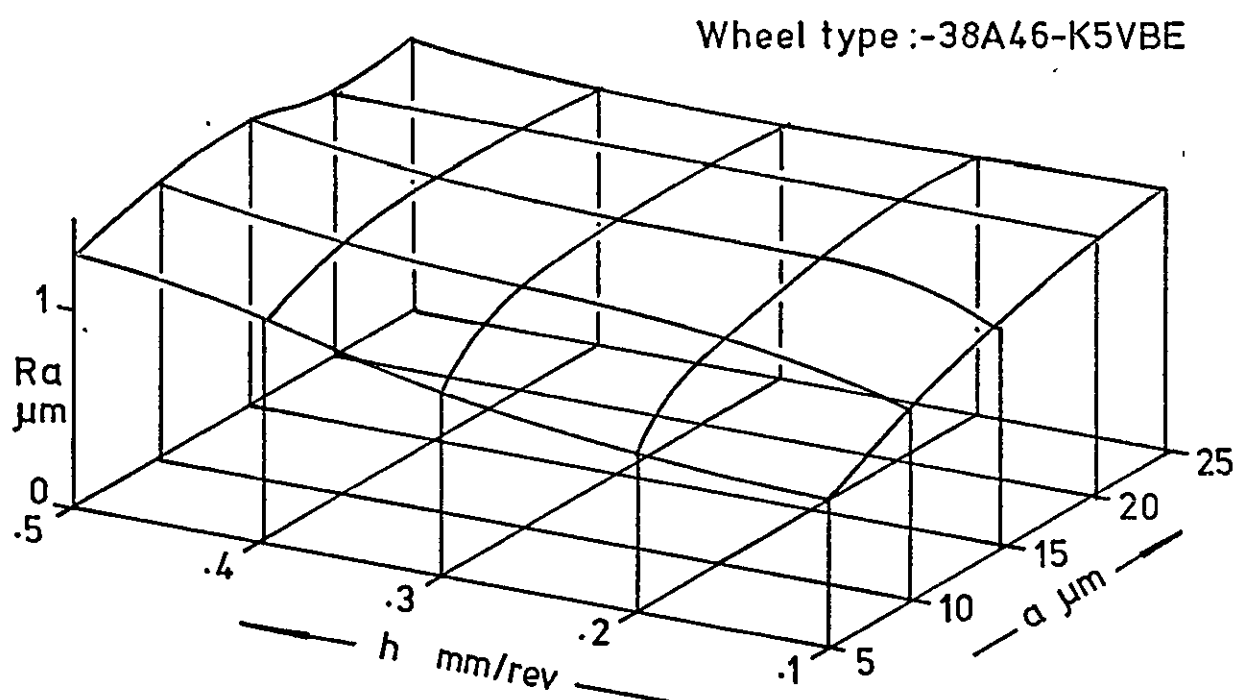
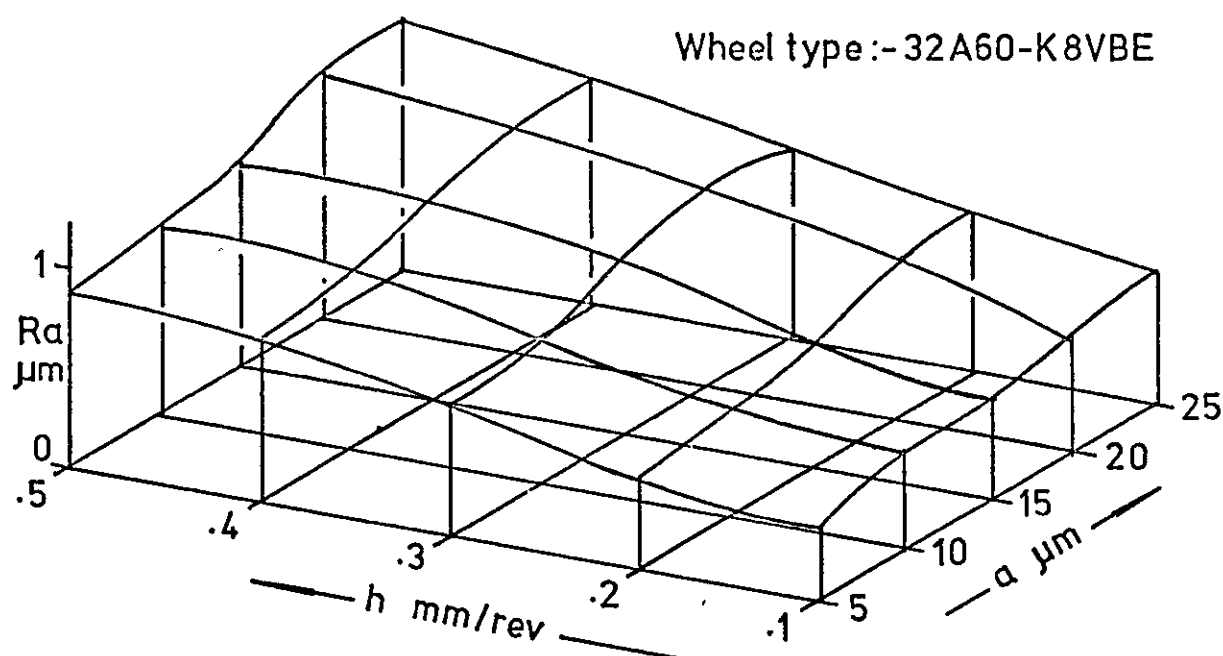


Fig. 7.80 Variation of wheel abrasive surface roughness R_a , with changes in dressing depth of cut a , & traverse rate h , when dressing various grinding wheels with a blunt diamond.

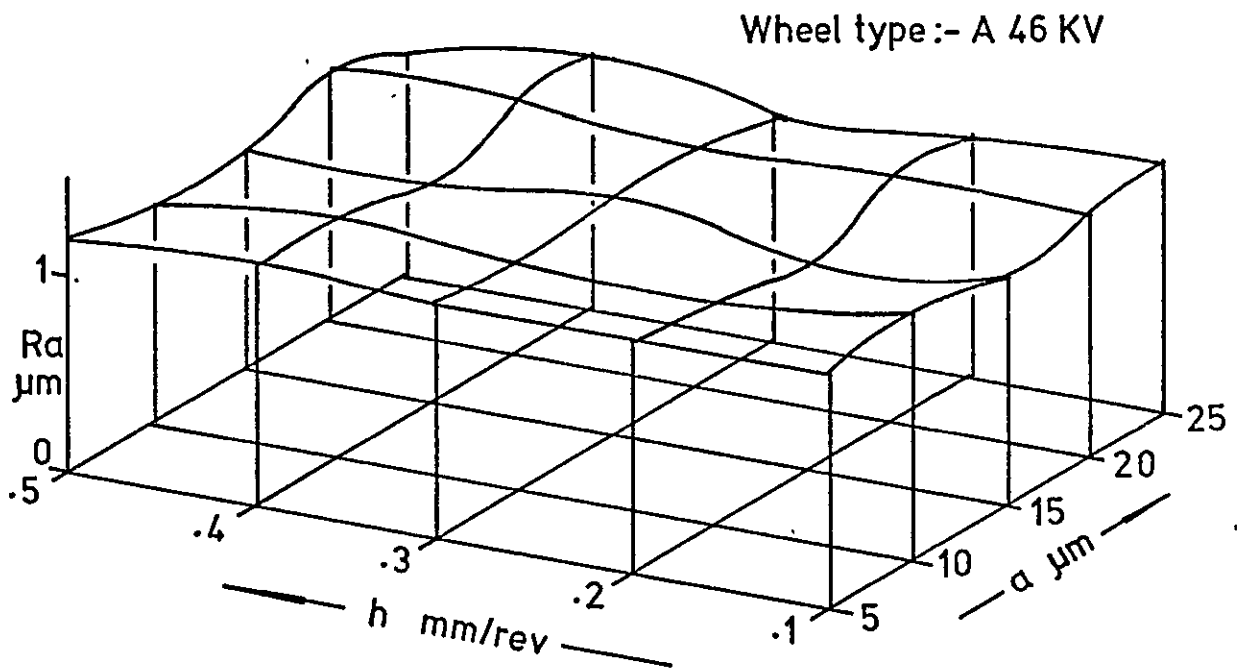
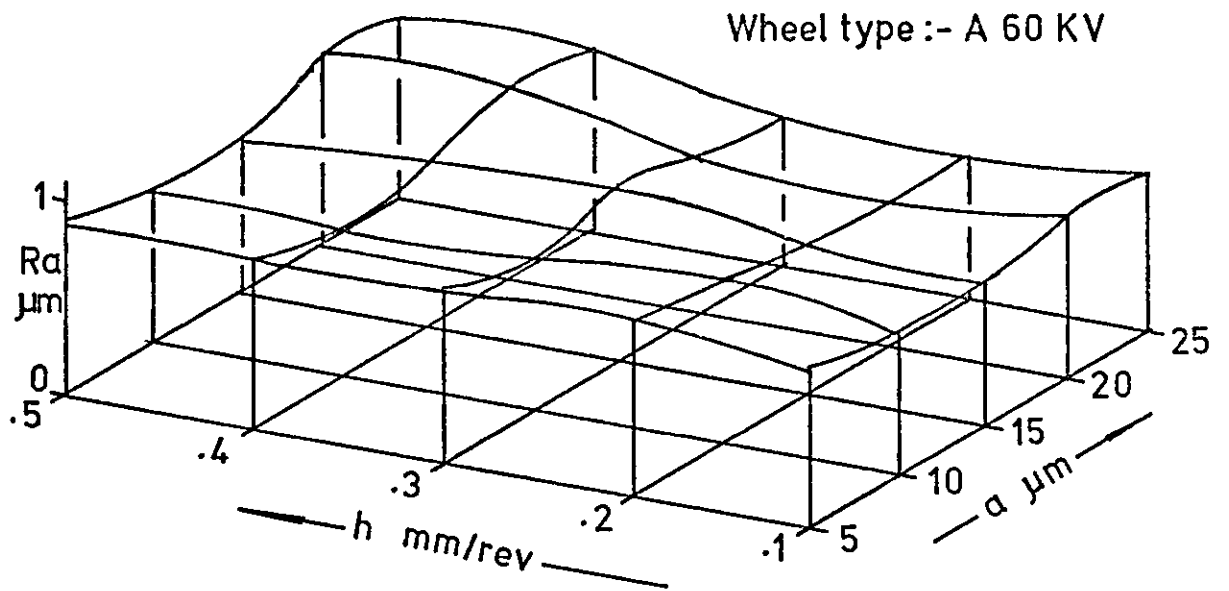


Fig. 7.81 Variation of wheel abrasive surface roughness R_a , with changes in dressing depth of cut a , & traverse rate h , when dressing various grinding wheels with a blunt diamond.

Test № 9
Diamond № 71784/4

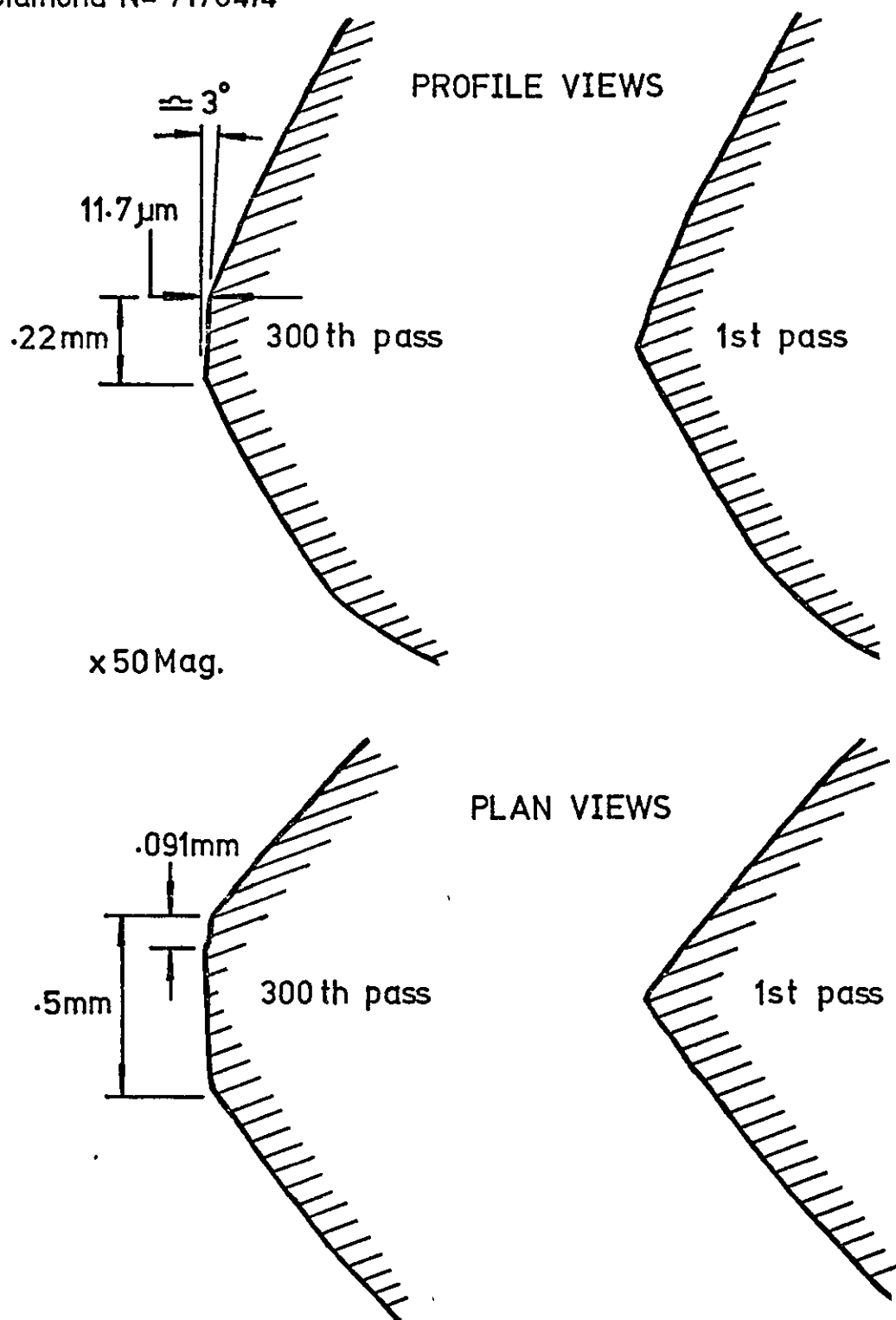


Fig.7.82 Profile and plan views of a diamond tool showing the degree of wear on completion of a dressing test.

Test N° 9

Diamond N° 71784/4

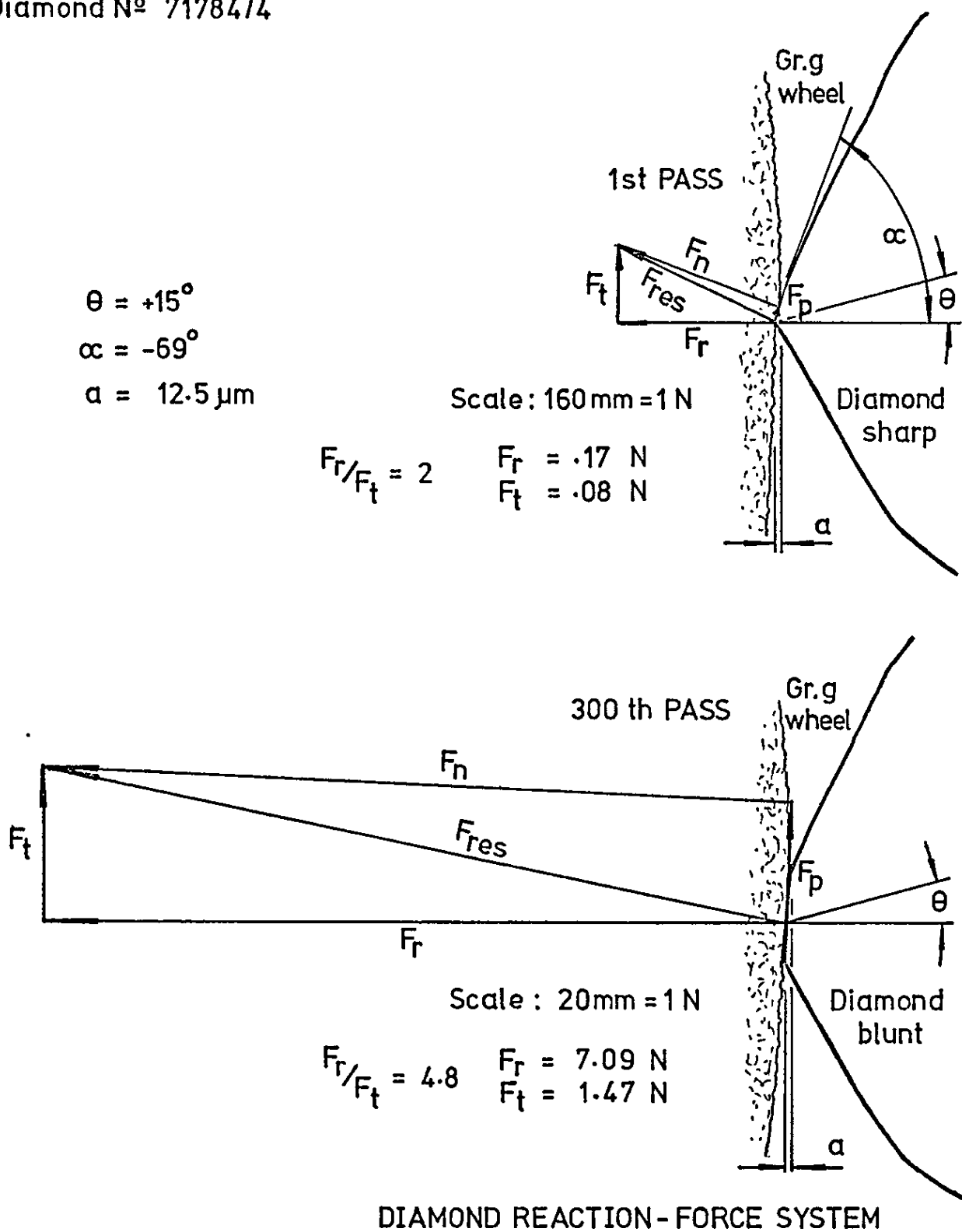


Fig. 7.83 Resolution of Dressing Force

| | | | | | | | | | |
|--|------|------|------|------|------|------|------|------|------|
| Table of pressure on the diamond tip for progressive diamond wear. | | | | | | | | | |
| Wear area mm ² | .033 | .066 | .109 | .174 | .277 | .302 | .323 | .340 | .348 |
| Force F_T N | .75 | 1.45 | 2.39 | 3.73 | 5.73 | 6.26 | 6.59 | 7.03 | 7.09 |
| Pressure N/mm ² | 22.7 | 22.0 | 21.9 | 21.4 | 20.7 | 20.7 | 20.4 | 20.7 | 20.4 |

Fig. 7.85

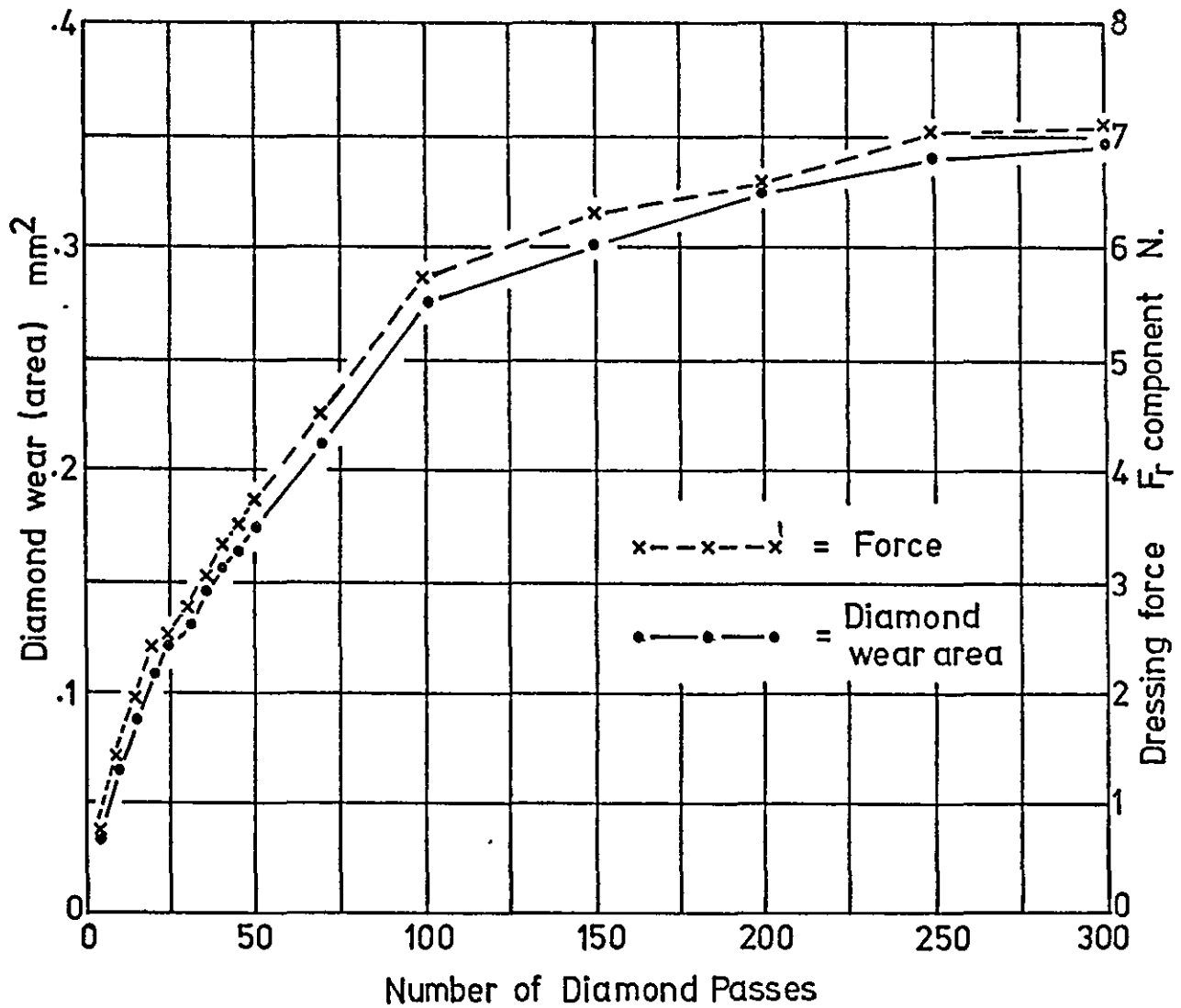
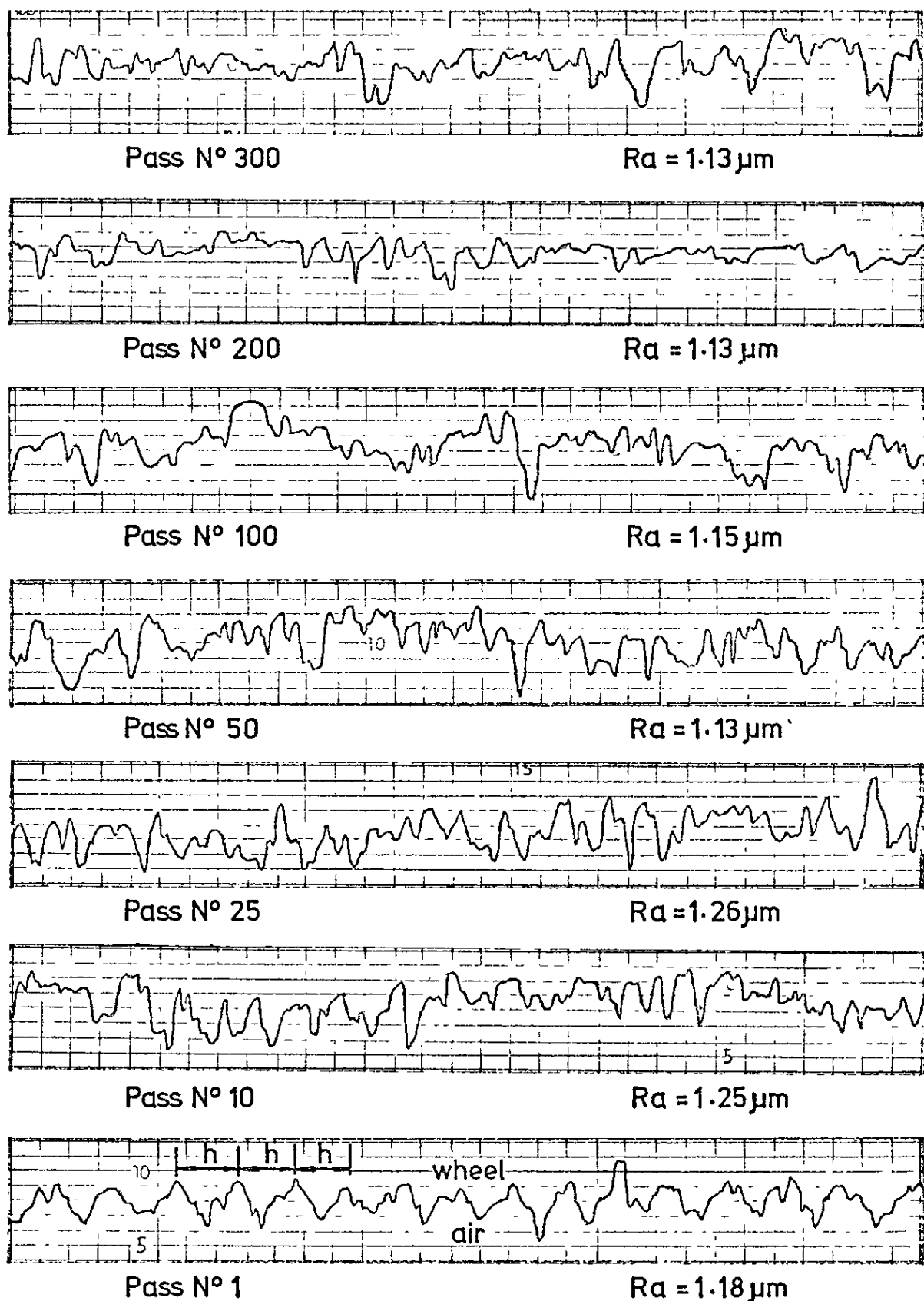


Fig. 7.84 Variation of diamond wear (area) and radial component of dressing force with number of diamond passes.

Test N° 9: Wheel type :- 38A46-K5VBE: Diamond N° 71784/4(sharp)
 Vertical mag.: 1 scale div. = $1.25\text{ }\mu\text{m}$ Horiz. mag.: 1 scale div. = $50\text{ }\mu\text{m}$



constant in-feed, $a = 12.5\text{ }\mu\text{m}$: constant cross-feed, $h = .1\text{ mm/rev}$
 constant drag angle, $\theta = 15^\circ$

Fig. 7.86 "Talysurf" traces showing the variation of grinding wheel surface roughness Ra with number of diamond passes when dressing.

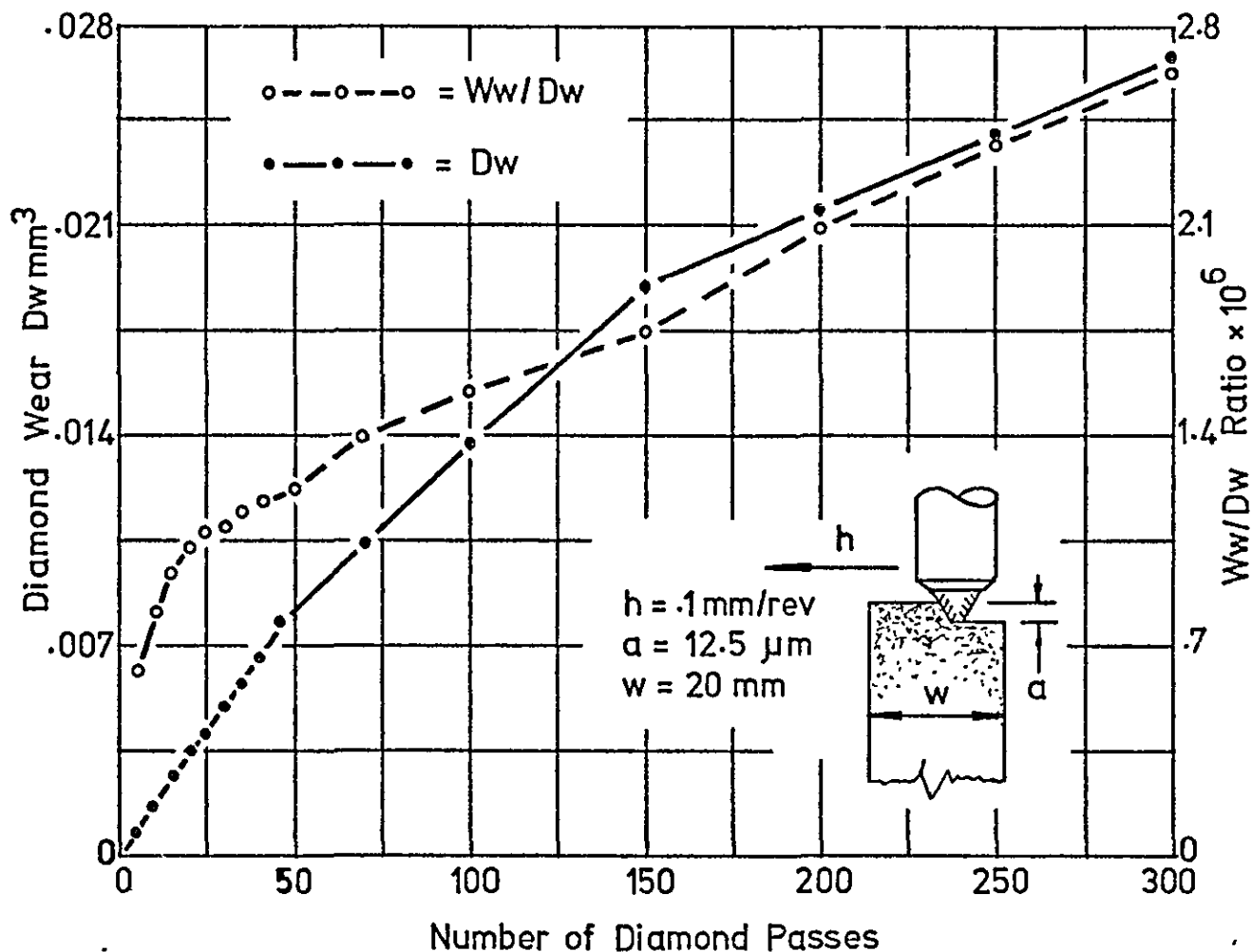


Fig.7.88 Variation of diamond wear and dressing ratio $(Ww/Dw)^*$ with number of diamond passes.

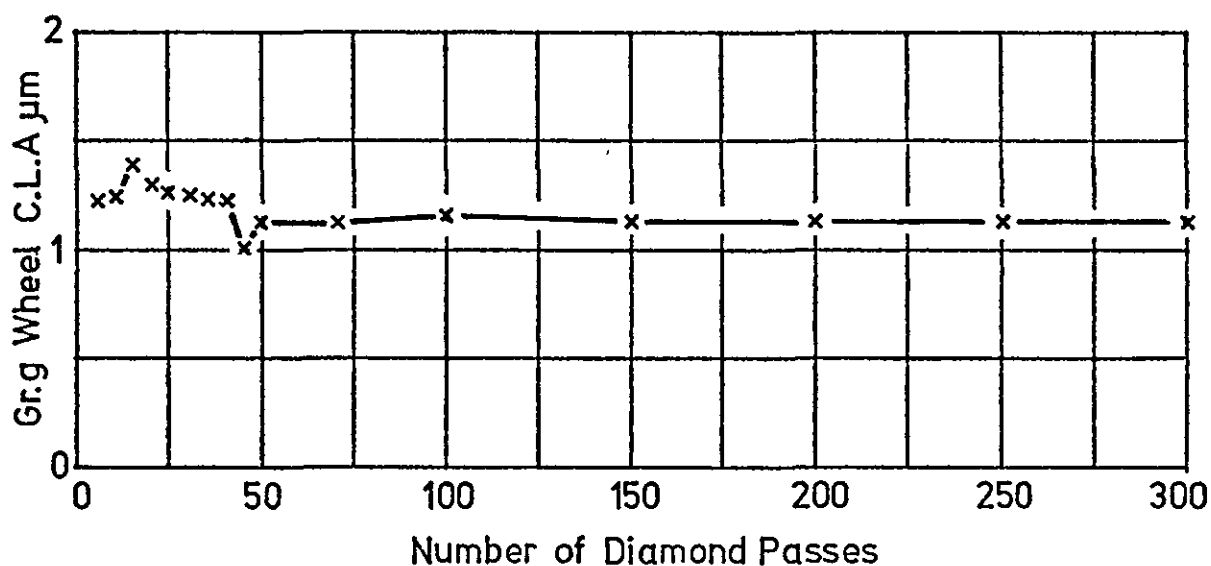


Fig.7.87 Variation of grinding wheel surface roughness with number of diamond passes

$$* \quad Ww/Dw = \frac{\text{Volume of wheel dressed away}}{\text{Volume of diamond worn away}} \quad \text{in same time}$$

Pre-test form of diamond N° 71784/2
used for Grinding Tests 1 to 18 inclusive

cross
feed
motion

β actual = 95°

PLAN VIEW
x50mag.

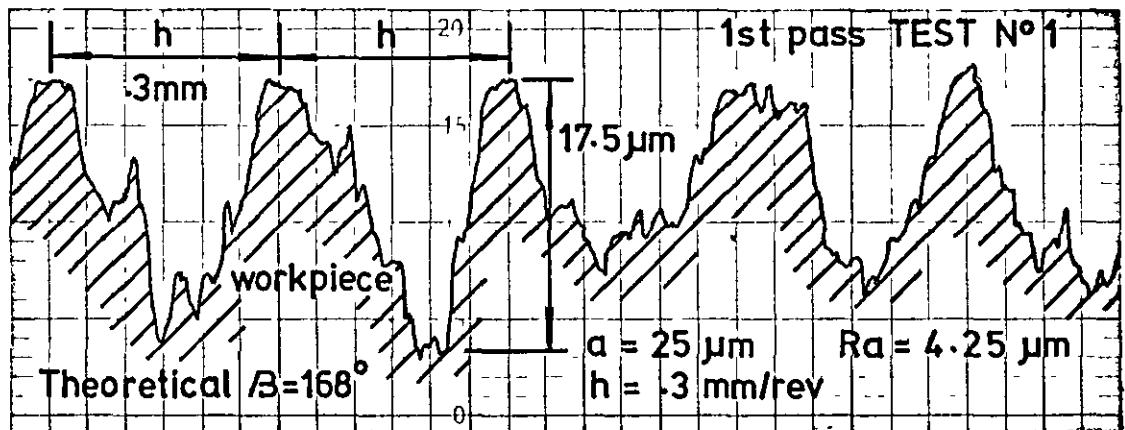


Fig. 7.89 Plan view of the dressing diamond
used for tests 1 to 18 inclusive, with a Talysurf
trace of a ground surface from test 1 showing
the influence of a , h and β .

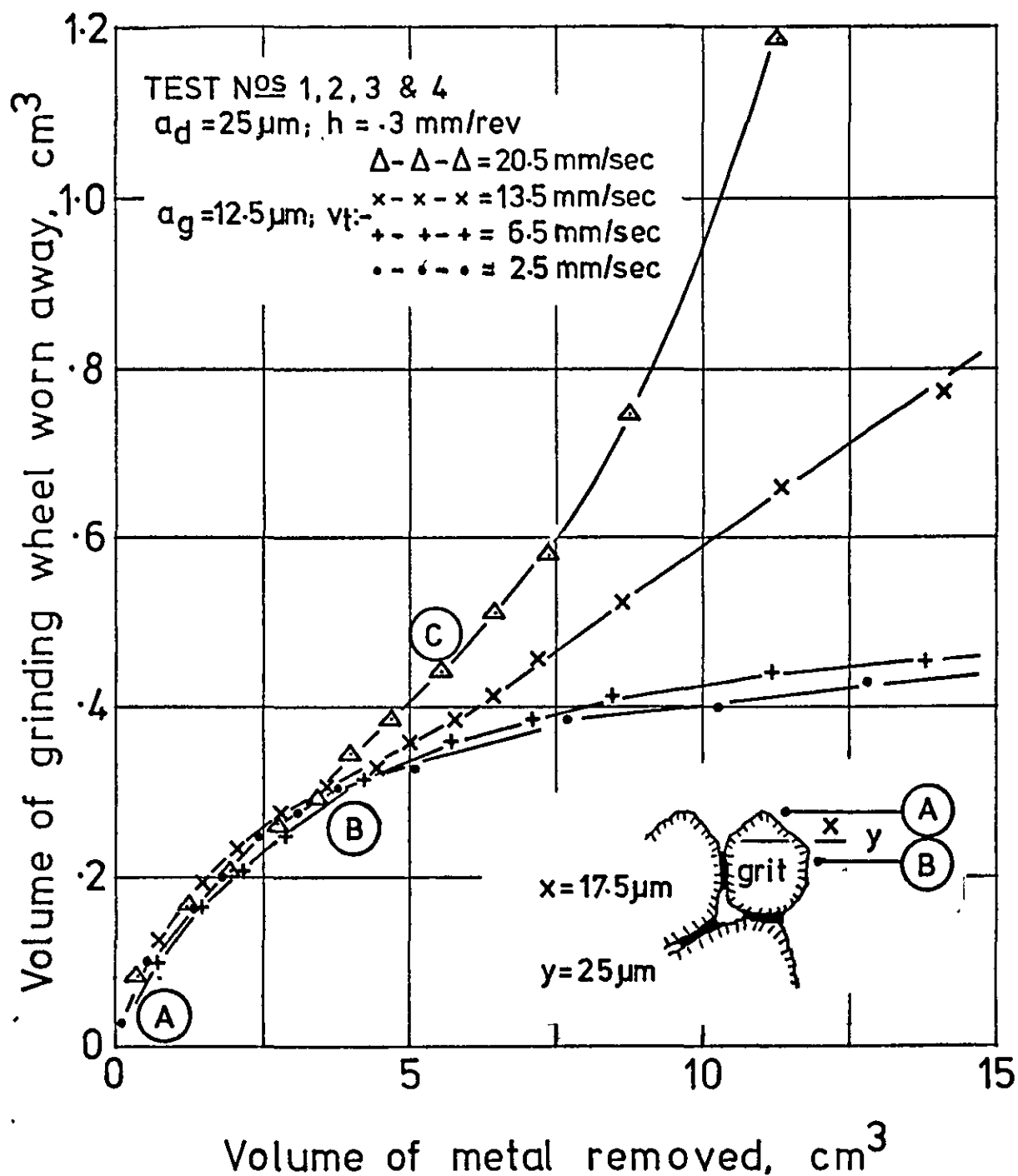


Fig. 7.90 Variation of grinding wheel wear with volume of metal removed for various traverse rates in grinding.

TEST N° 1

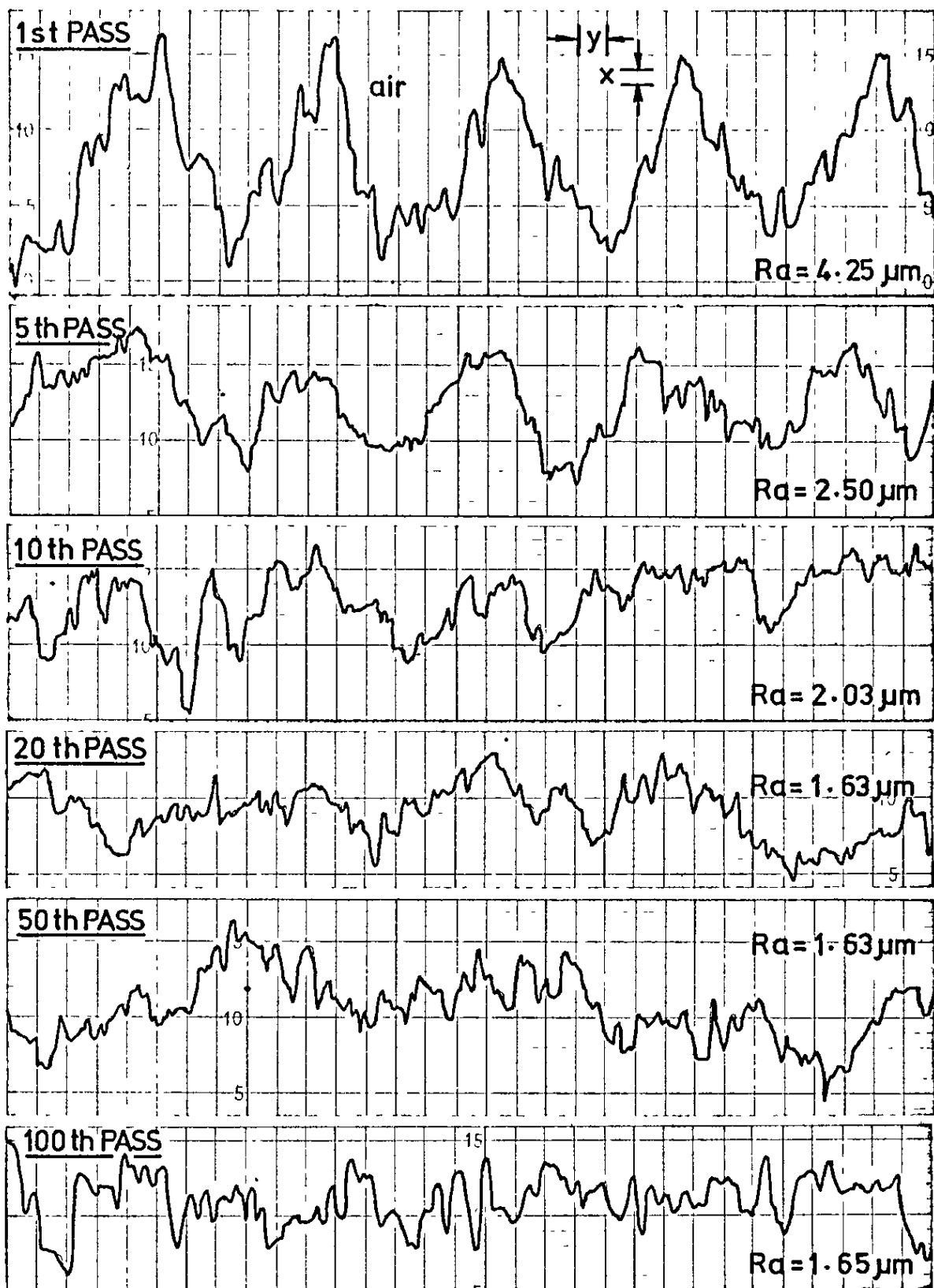
 $x = 1.25 \mu\text{m}$ $y = 50 \mu\text{m}$ 

Fig.7.91 “Talysurf” traces showing the variation of workpiece and grinding wheel surface roughness for the condition $v_t/nW = .75$

TEST N°4 $x = 1.25\mu\text{m}$ $y = 50\mu\text{m}$

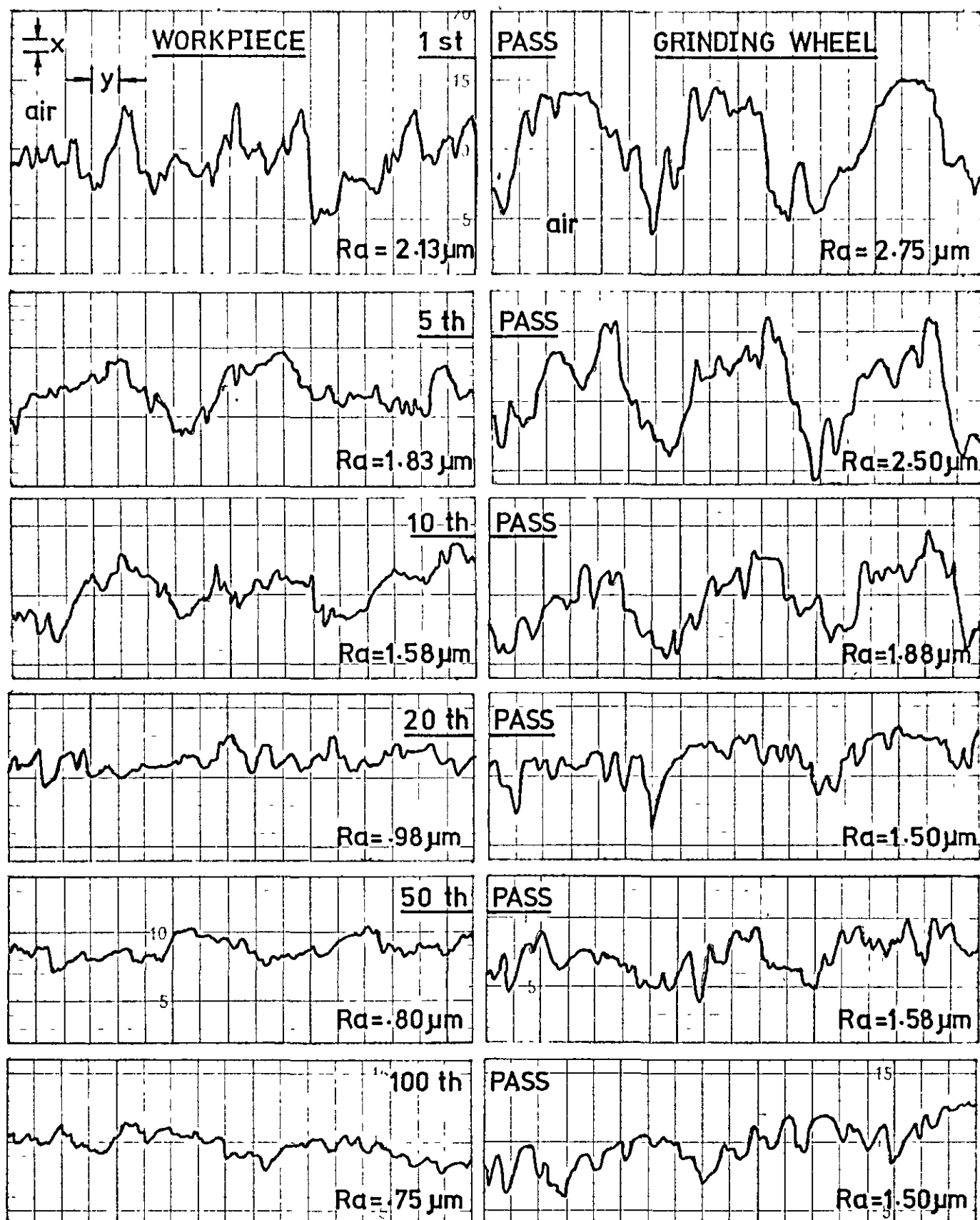


Fig.7.92 “Talysurf” traces showing the variation of workpiece and grinding wheel surface roughness for the condition $v_t/nW = .09$

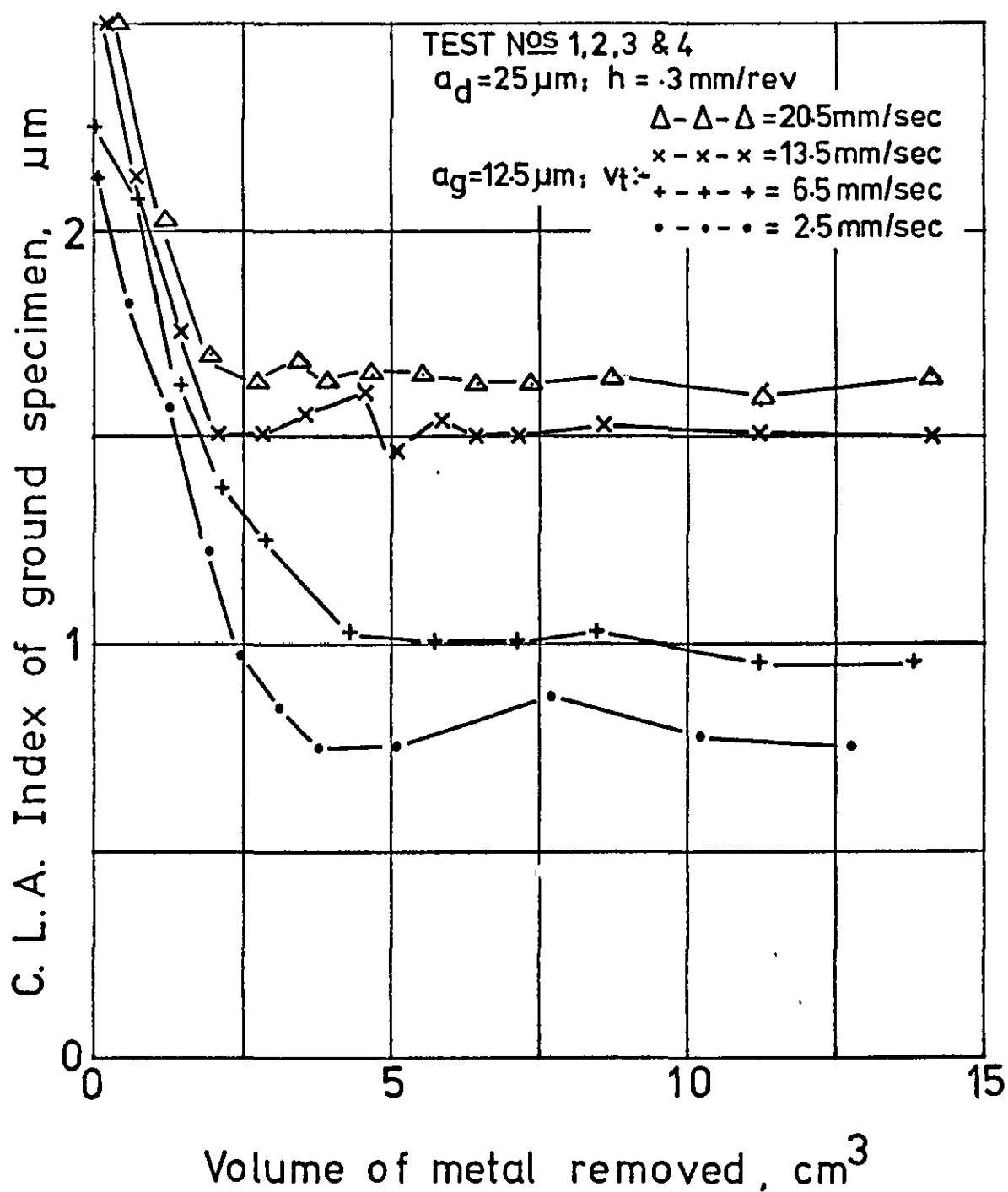


Fig. 7.93 Variation of workpiece surface roughness with volume of metal removed for various traverse rates in grinding.

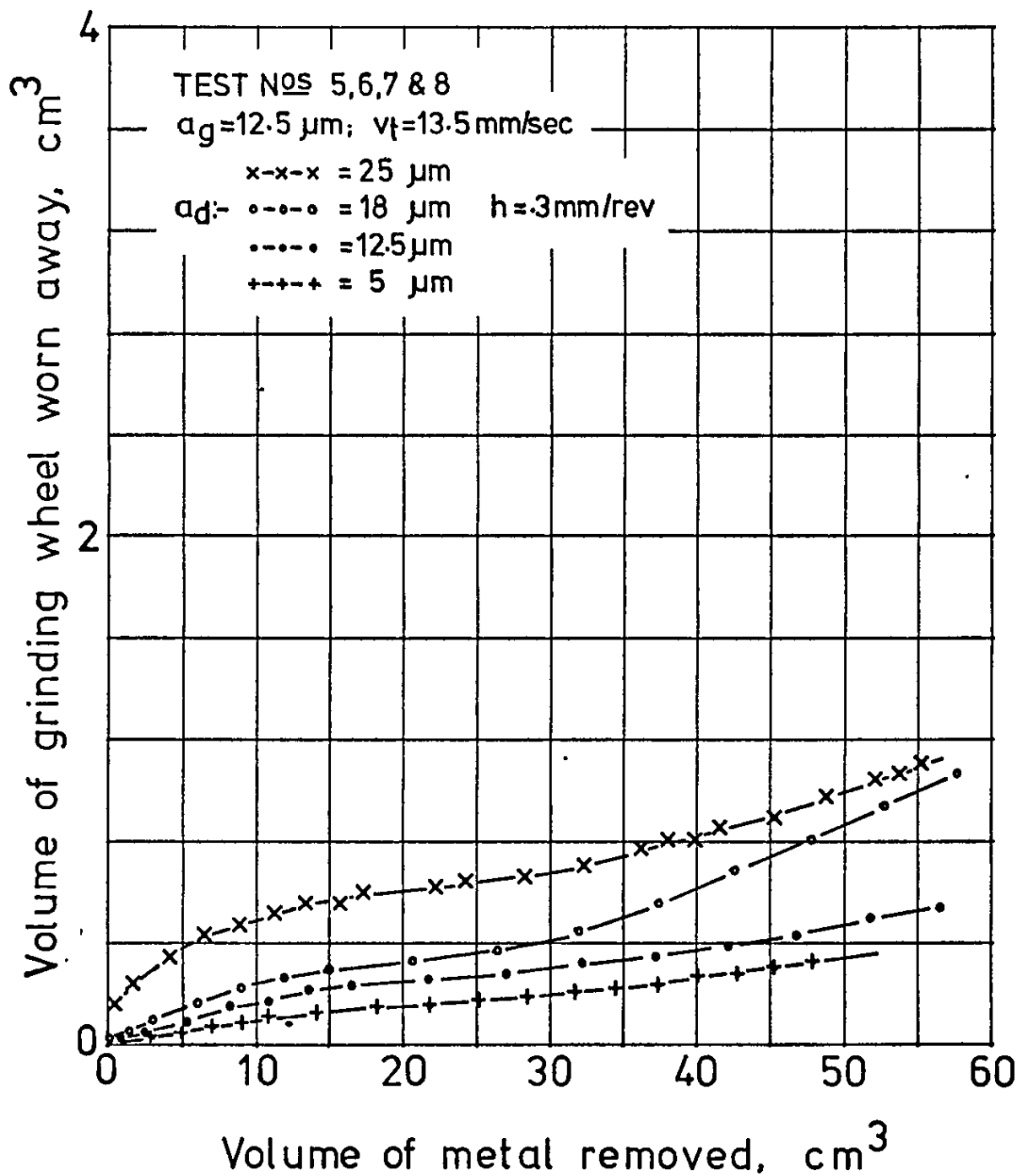


Fig. 7.94 Variation of grinding wheel wear with volume of metal removed for various wheel dressing conditions.

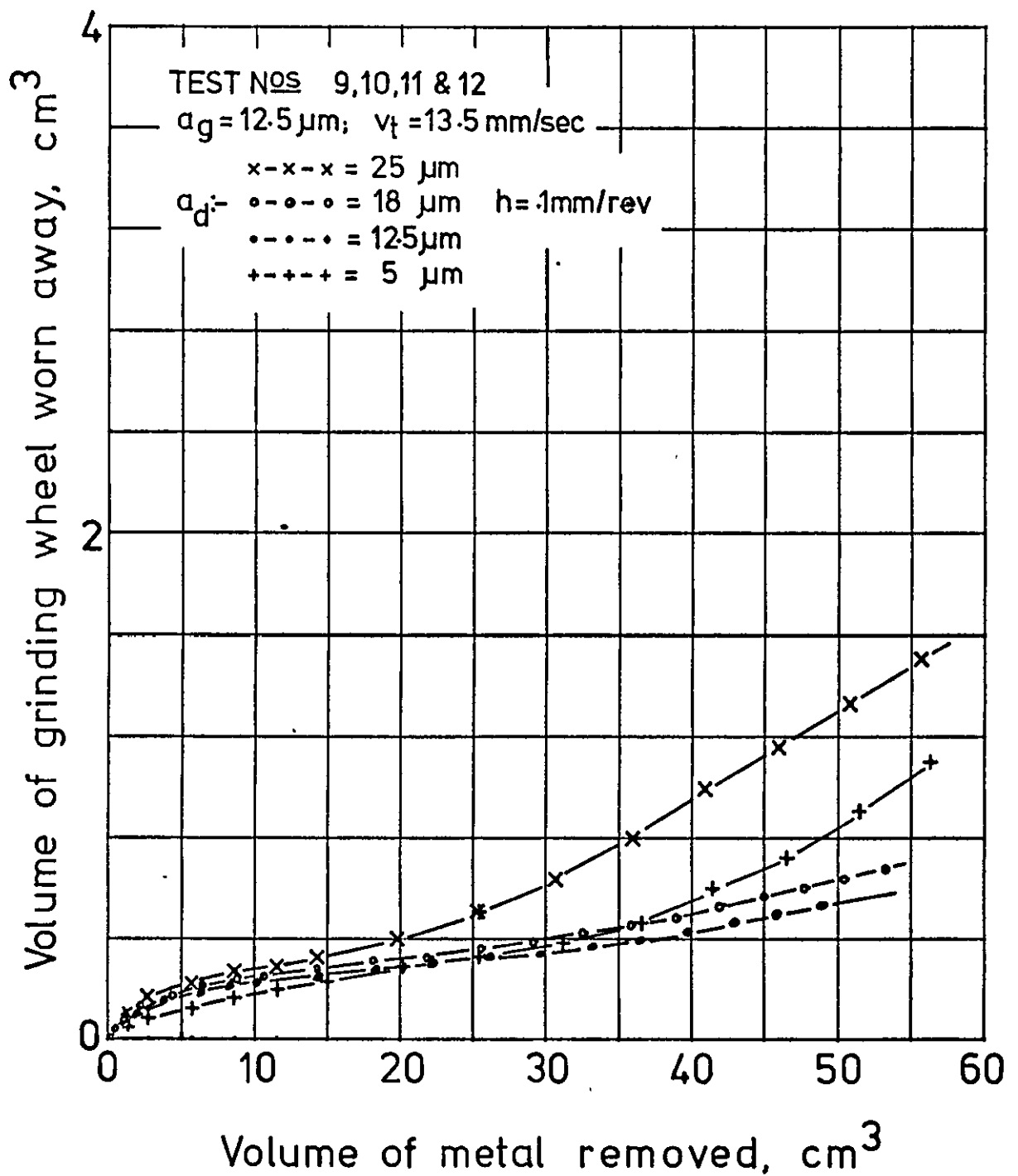


Fig. 7.95 Variation of grinding wheel wear with volume of metal removed for various wheel dressing conditions.

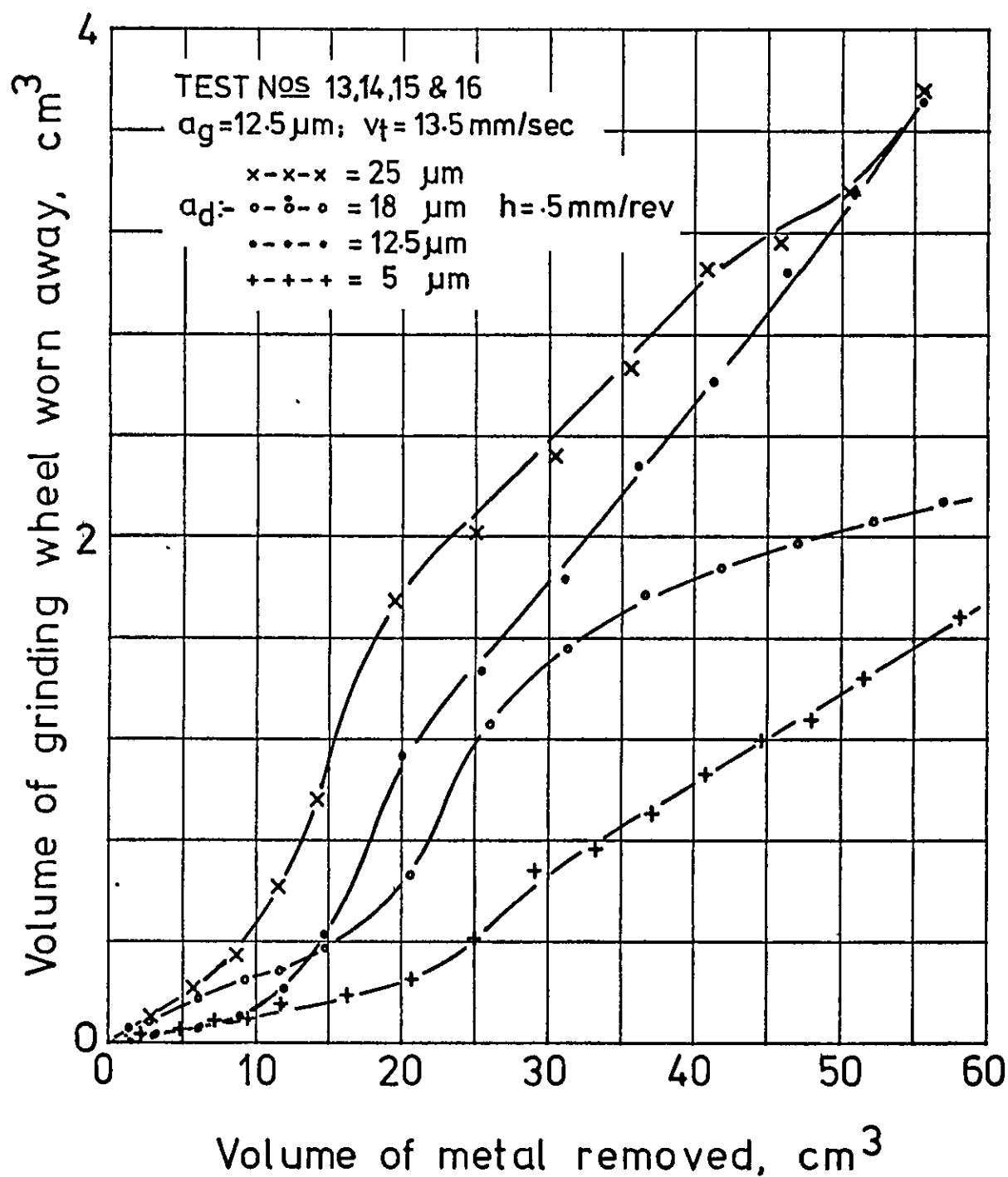


Fig. 7.96 Variation of grinding wheel wear with volume of metal removed for various wheel dressing conditions.

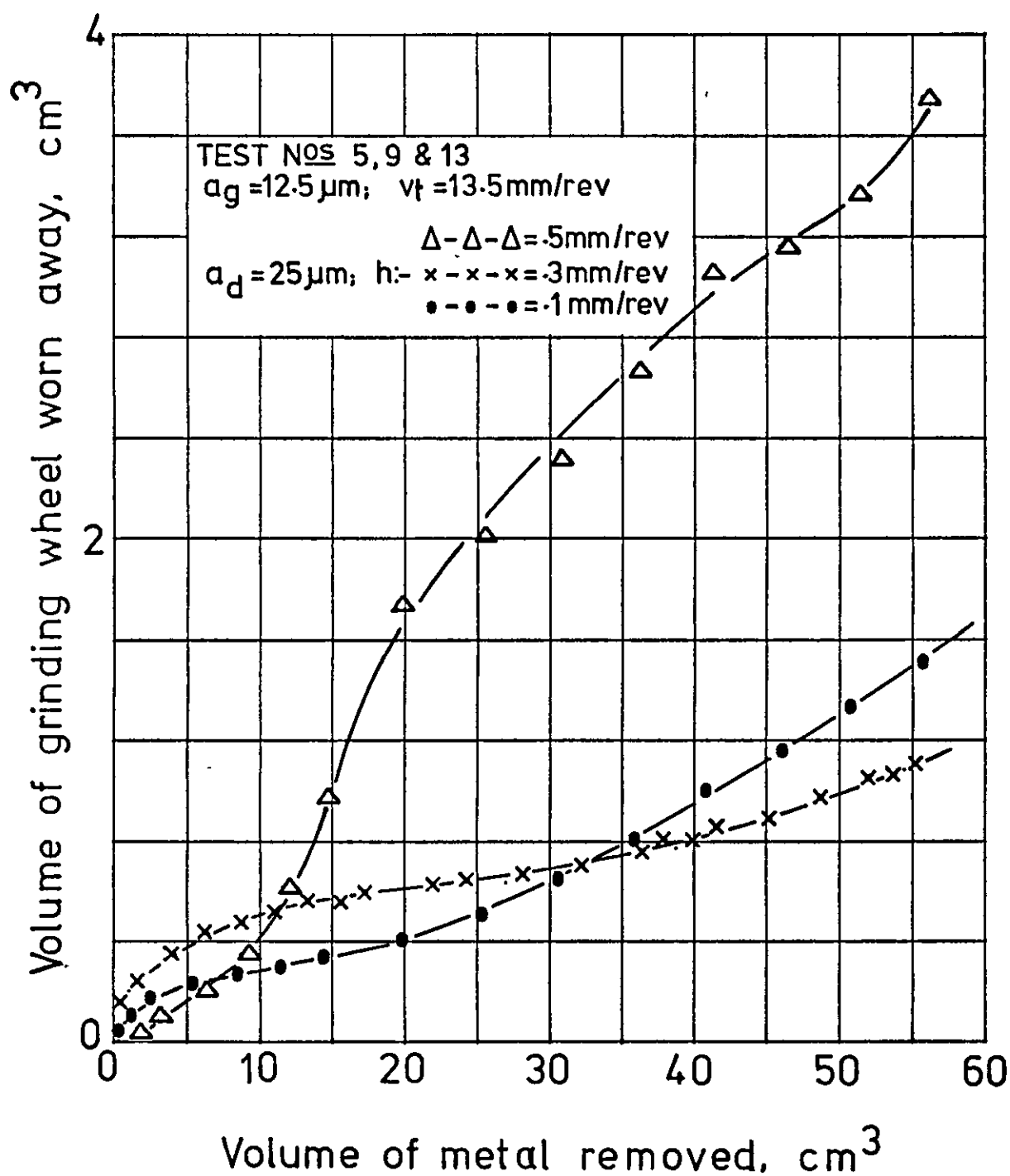


Fig. 7.97 Variation of grinding wheel wear with volume of metal removed for various wheel dressing conditions.

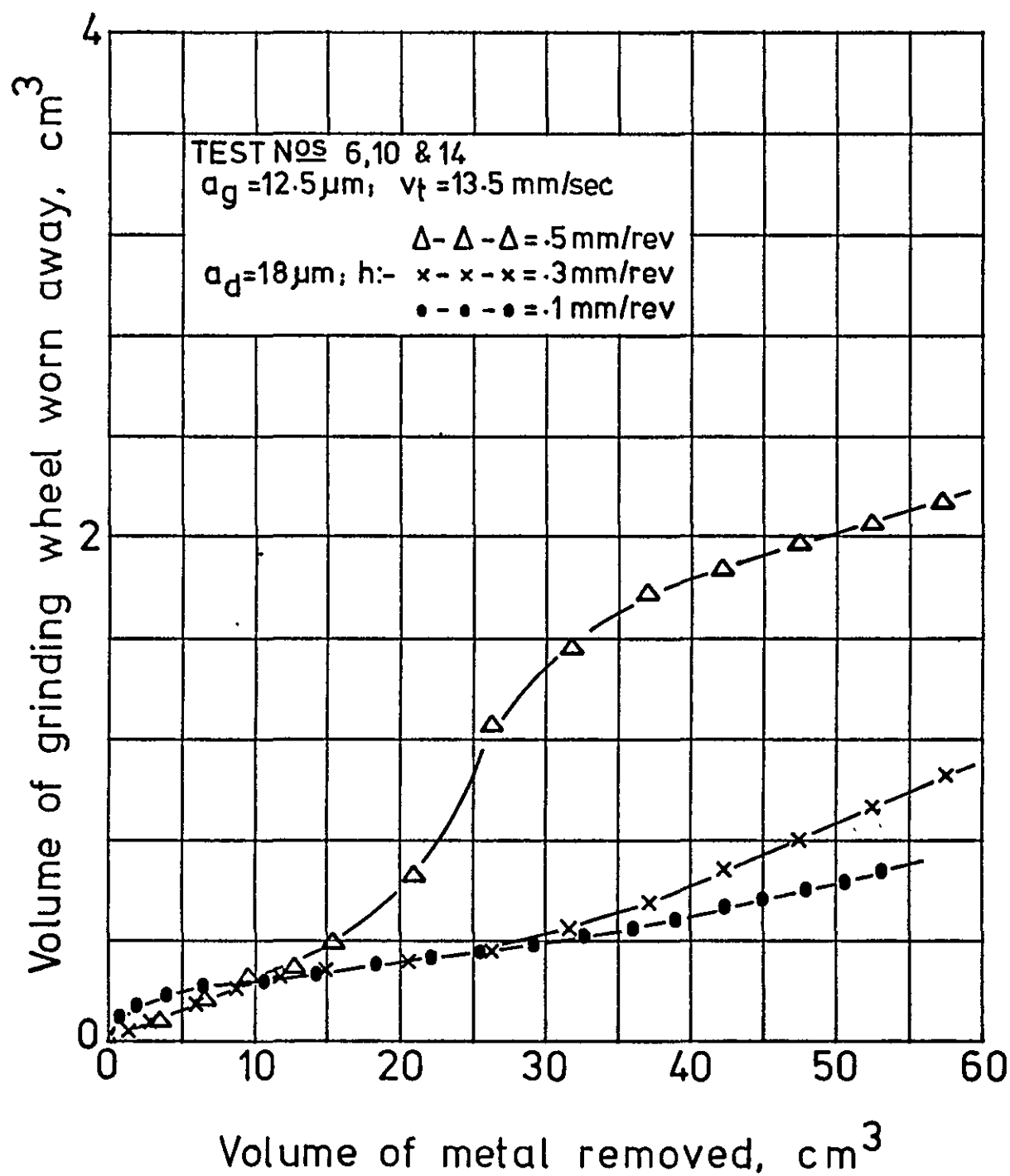


Fig. 7.98 Variation of grinding wheel wear with volume of metal removed for various wheel dressing conditions.

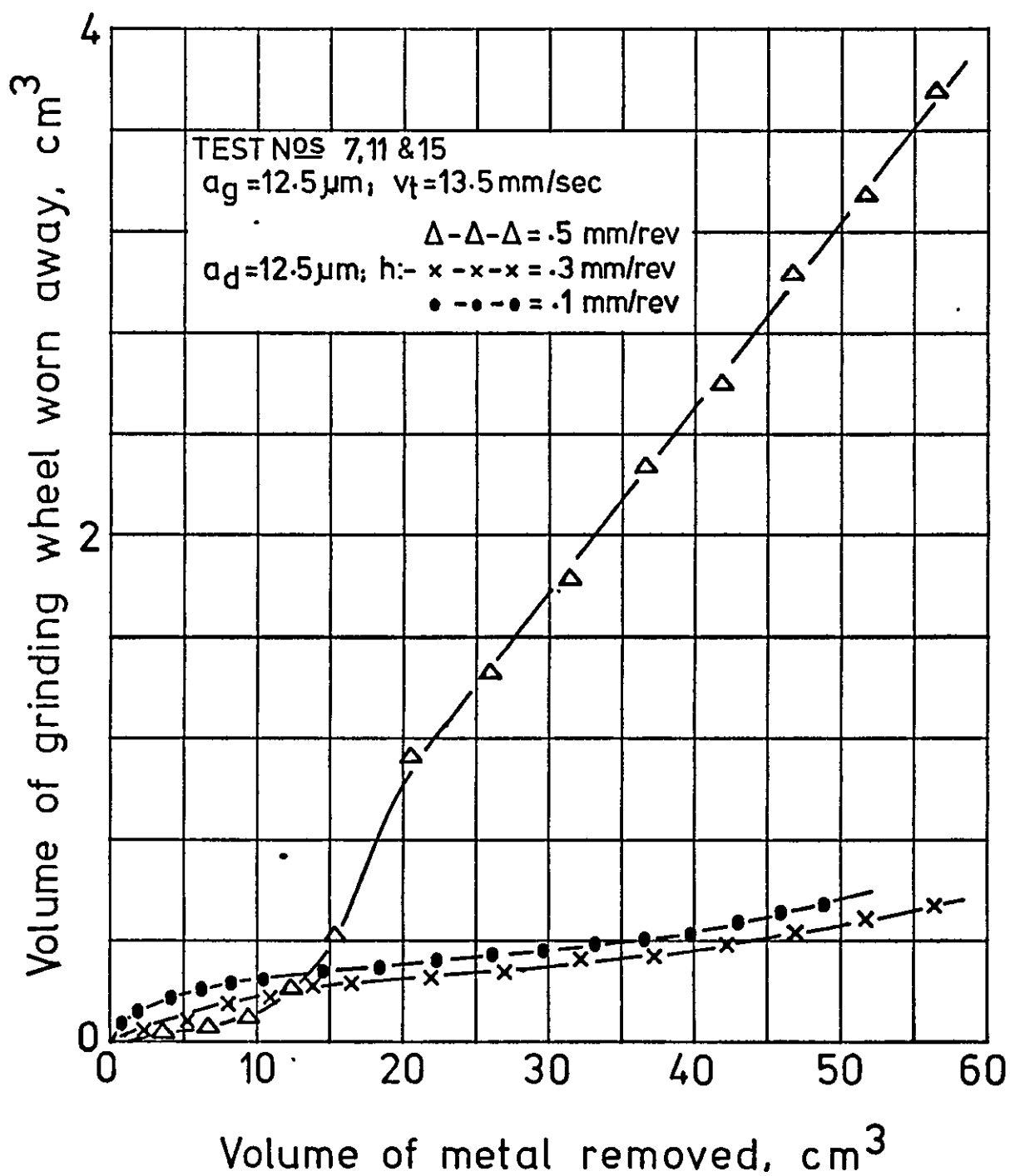


Fig. 7.99 Variation of grinding wheel wear with volume of metal removed for various wheel dressing conditions.

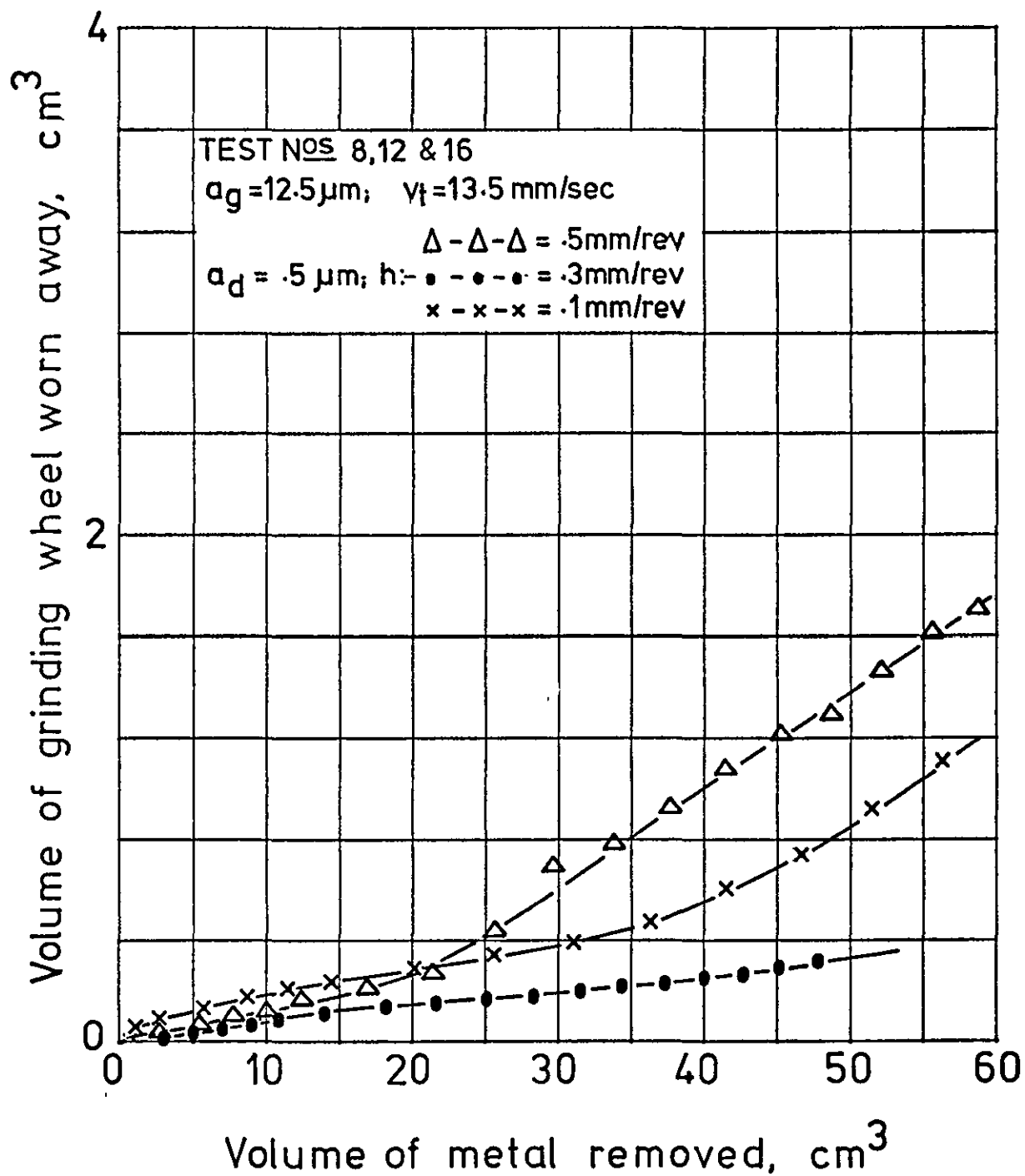


Fig. 7.100 Variation of grinding wheel wear with volume of metal removed for various wheel dressing conditions.

TEST N° 5

Dressing conditions :- $a_d = 25 \mu\text{m}$, $h = .3 \text{ mm/rev}$: $x = 1.25 \mu\text{m}$

Grinding conditions :- $a_g = 12.5 \mu\text{m}$, $v_t = 13.5 \text{ mm/sec}$: $y = 50 \mu\text{m}$

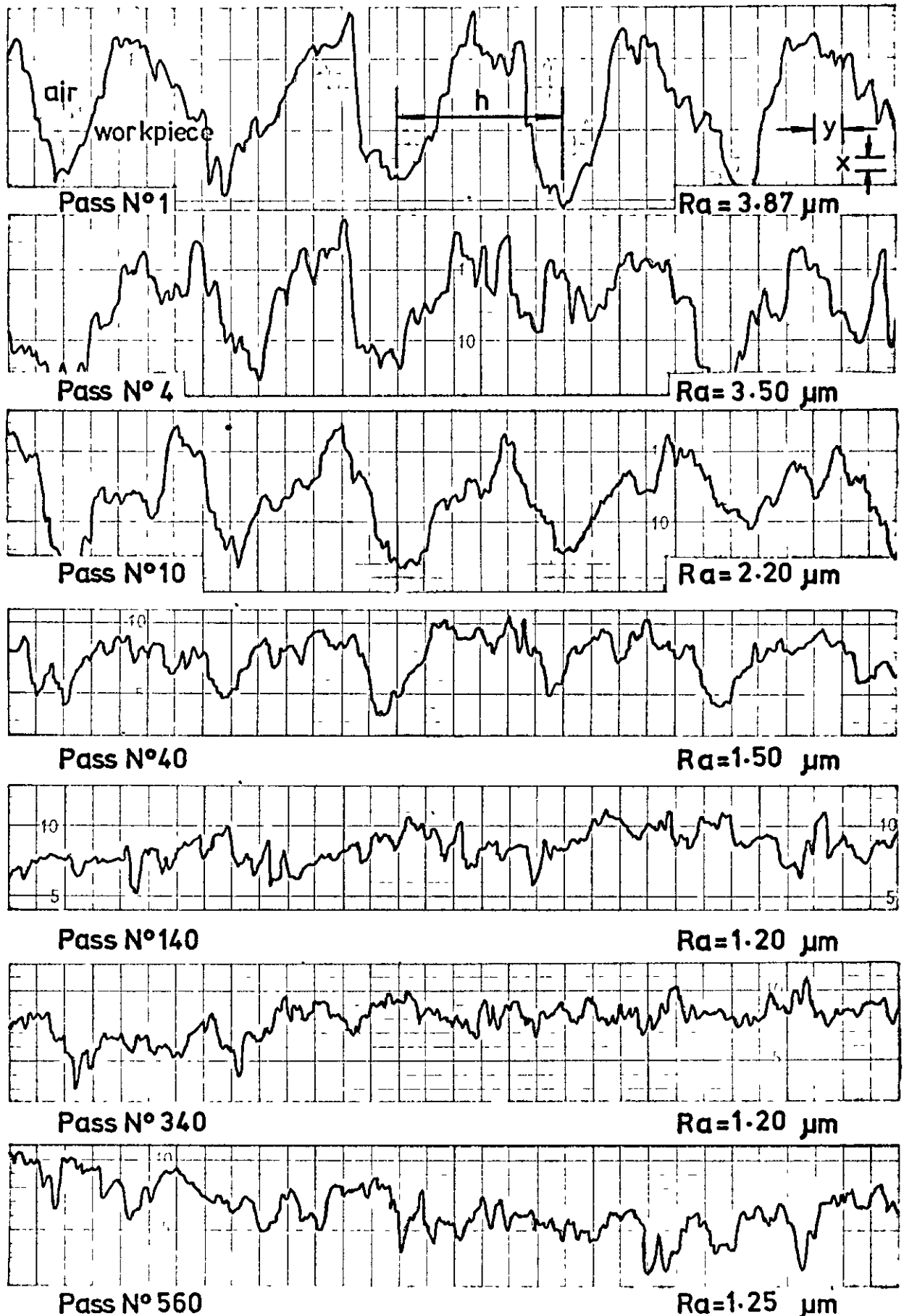
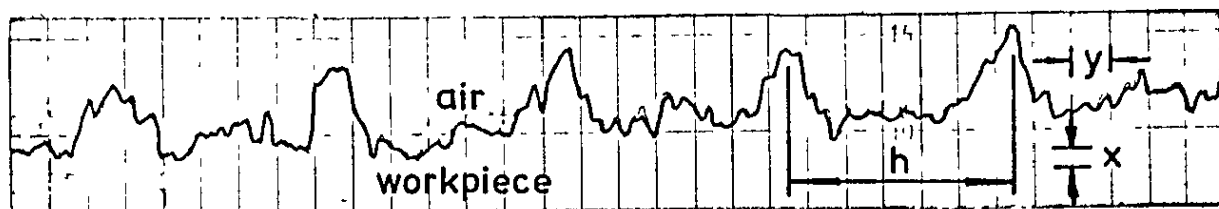


Fig. 7.101 "Talysurf" traces showing the variation of workpiece surface roughness for particular dressing and grinding conditions

TEST N° 8

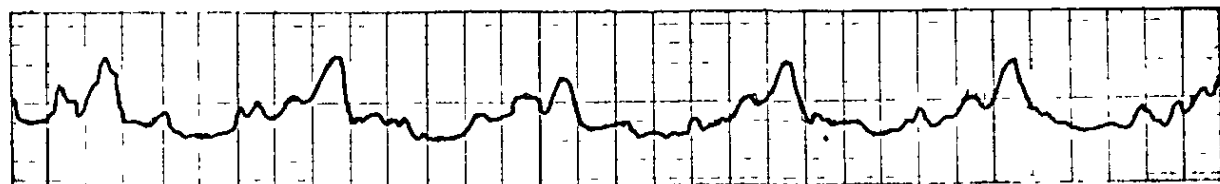
Dressing conditions :- $a_d = 5 \mu\text{m}$, $h = .3 \text{ mm/rev}$: $x = 1.25 \mu\text{m}$

Grinding conditions :- $a_g = 12.5 \mu\text{m}$, $v_t = 13.5 \text{ mm/sec}$: $y = 50 \mu\text{m}$



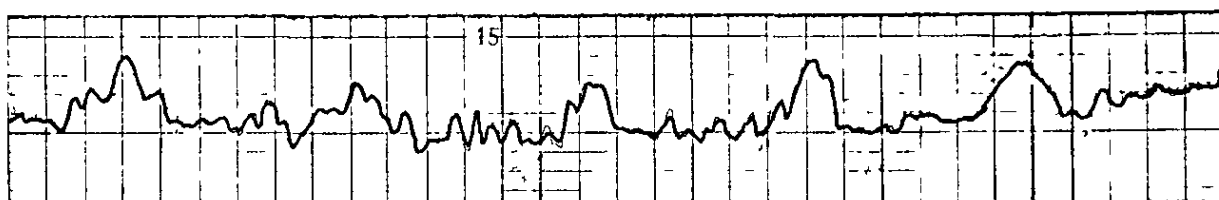
Pass N° 1

$Ra = 1.12 \mu\text{m}$



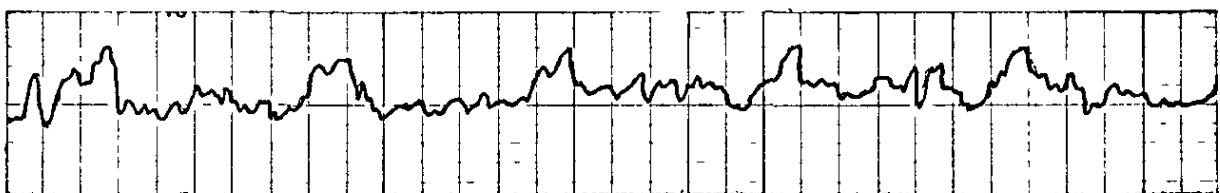
Pass N° 4

$Ra = .95 \mu\text{m}$



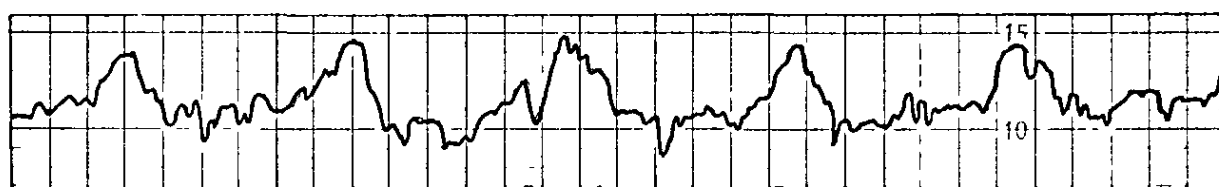
Pass N° 10

$Ra = .75 \mu\text{m}$



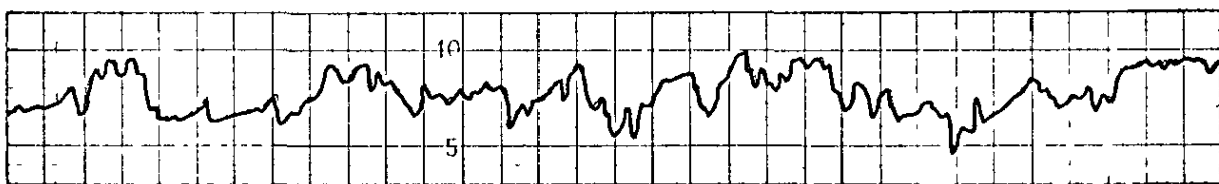
Pass N° 50

$Ra = .83 \mu\text{m}$



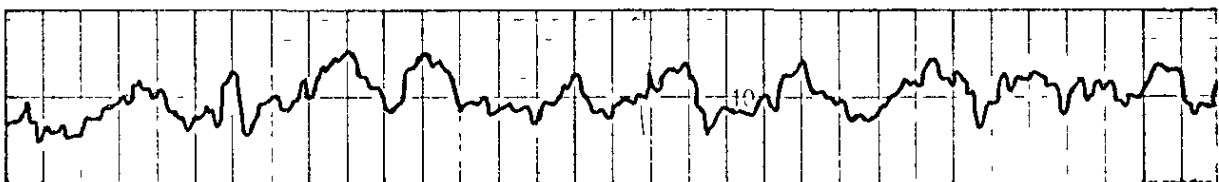
Pass N° 150

$Ra = 1.13 \mu\text{m}$



Pass N° 350

$Ra = 1.20 \mu\text{m}$



Pass N° 590

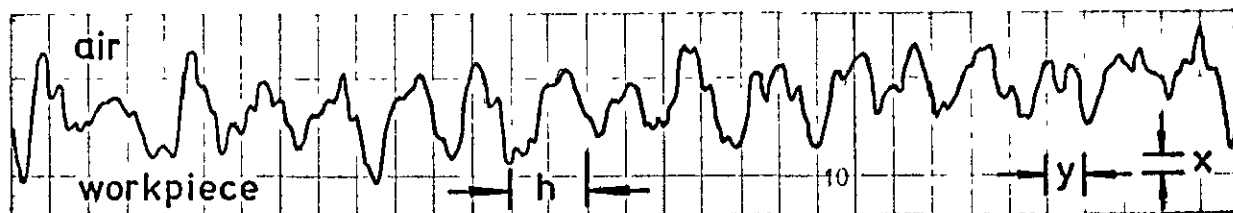
$Ra = 1.10 \mu\text{m}$

Fig.7.102 "Talysurf" traces showing the variation of workpiece surface roughness for particular dressing and grinding conditions

TEST N° 9

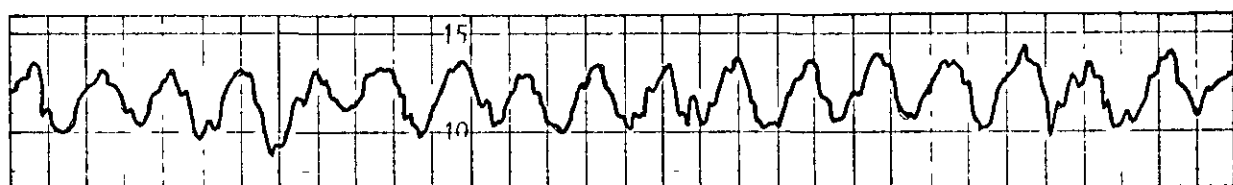
Dressing conditions :- $a_d = 25 \mu\text{m}$, $h = .1 \text{ mm/rev}$: $x = 1.25 \mu\text{m}$

Grinding conditions :- $a_g = 12.5 \mu\text{m}$, $v_t = 13.5 \text{ mm/sec}$: $y = 50 \mu\text{m}$



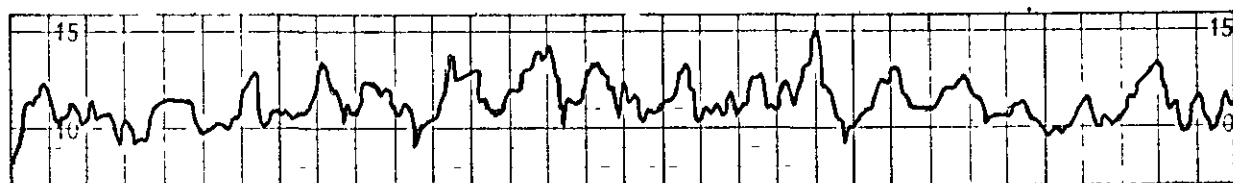
Pass N° 1

$Ra = 1.38 \mu\text{m}$



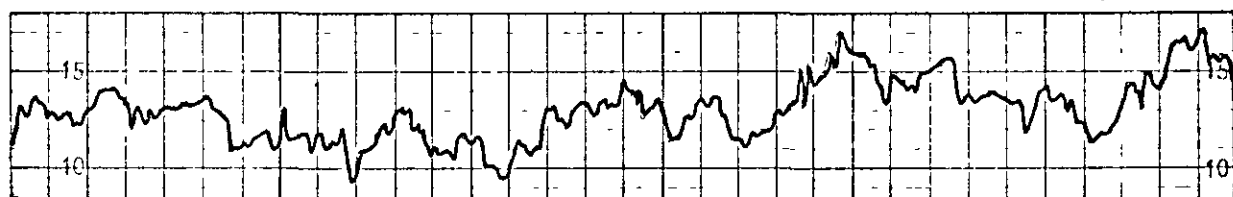
Pass N° 4

$Ra = 1.38 \mu\text{m}$



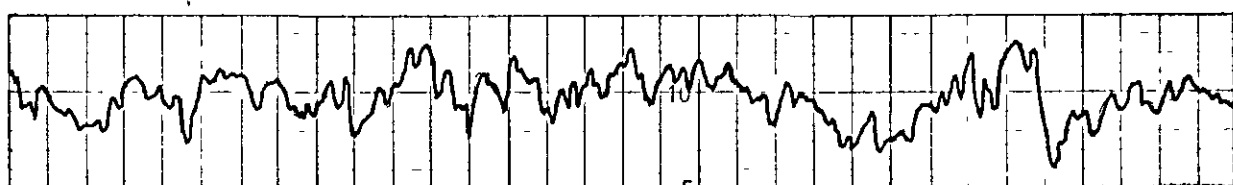
Pass N° 10

$Ra = 1.05 \mu\text{m}$



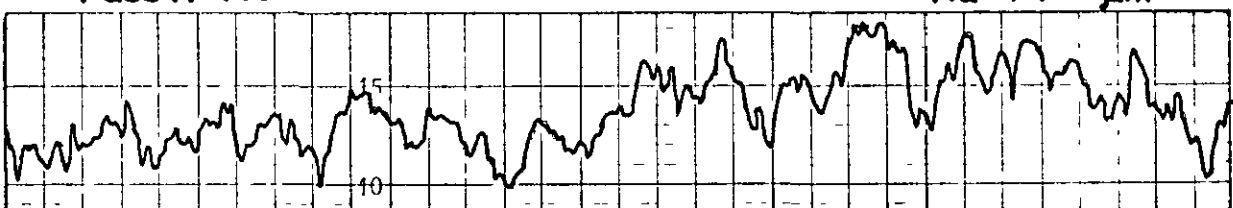
Pass N° 40

$Ra = 1.10 \mu\text{m}$



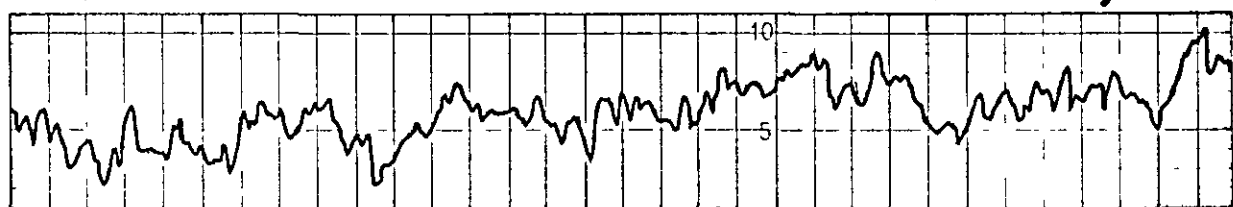
Pass N° 140

$Ra = 1.13 \mu\text{m}$



Pass N° 340

$Ra = 1.45 \mu\text{m}$



Pass N° 540

$Ra = 1.38 \mu\text{m}$

Fig. 7.103 "Taly surf" traces showing the variation of workpiece surface roughness for particular dressing and grinding conditions

TEST N°12

Dressing conditions :- $a_d = 5 \mu\text{m}$, $h = .1 \text{ mm/rev}$: $x = 1.25 \mu\text{m}$

Grinding conditions :- $a_g = 12.5 \mu\text{m}$, $v_t = 13.5 \text{ mm/sec}$: $y = 50 \mu\text{m}$

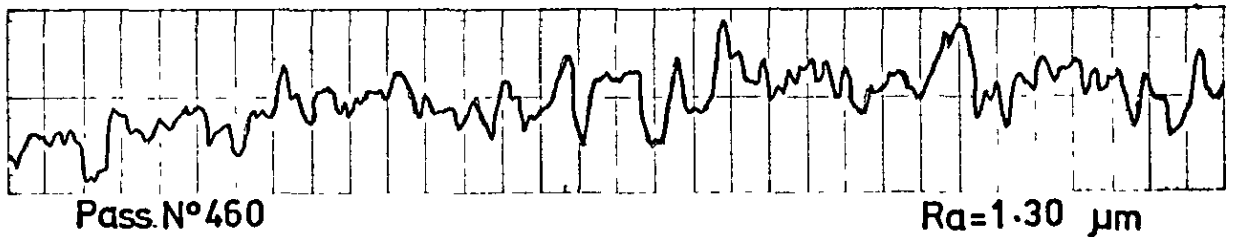
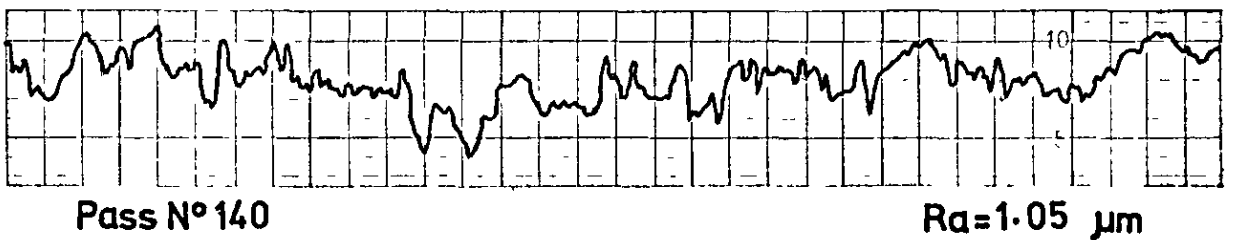
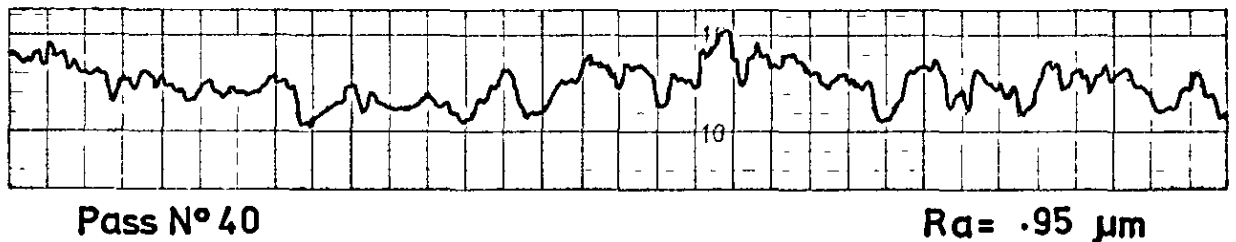
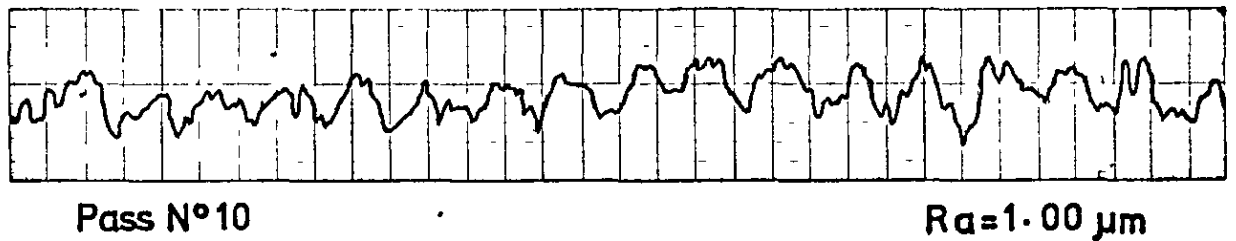
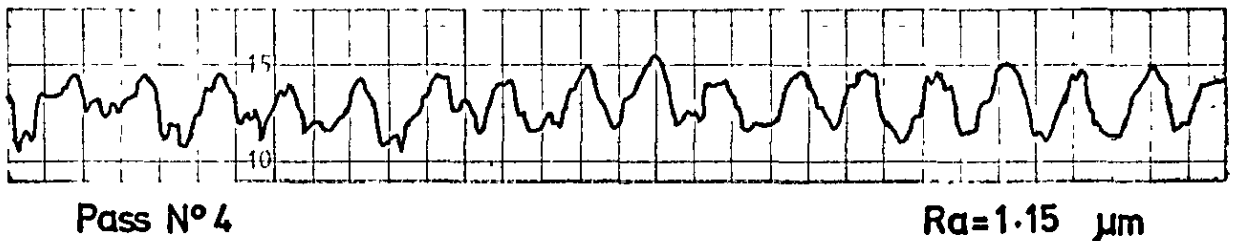
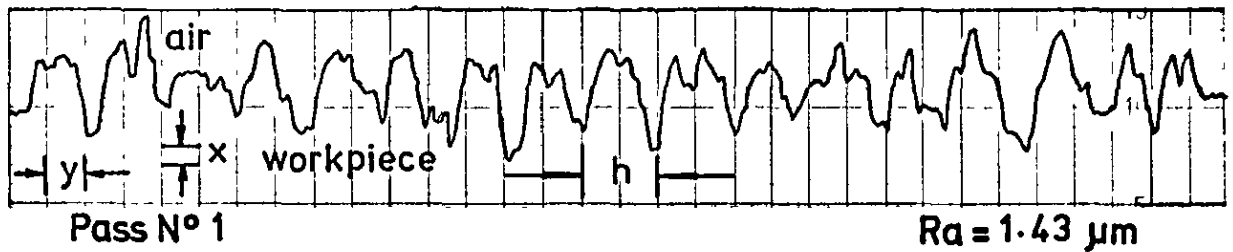


Fig.7.104 "Talysurf" traces showing the variation of workpiece surface roughness for particular dressing and grinding conditions

TEST N°13

Dressing conditions :- $a_d = 25 \mu\text{m}$, $h = .5 \text{ mm/rev}$: $x = 1.25 \mu\text{m}$

Grinding conditions :- $a_g = 12.5 \mu\text{m}$, $v_t = 13.5 \text{ mm/sec}$: $y = 50 \mu\text{m}$

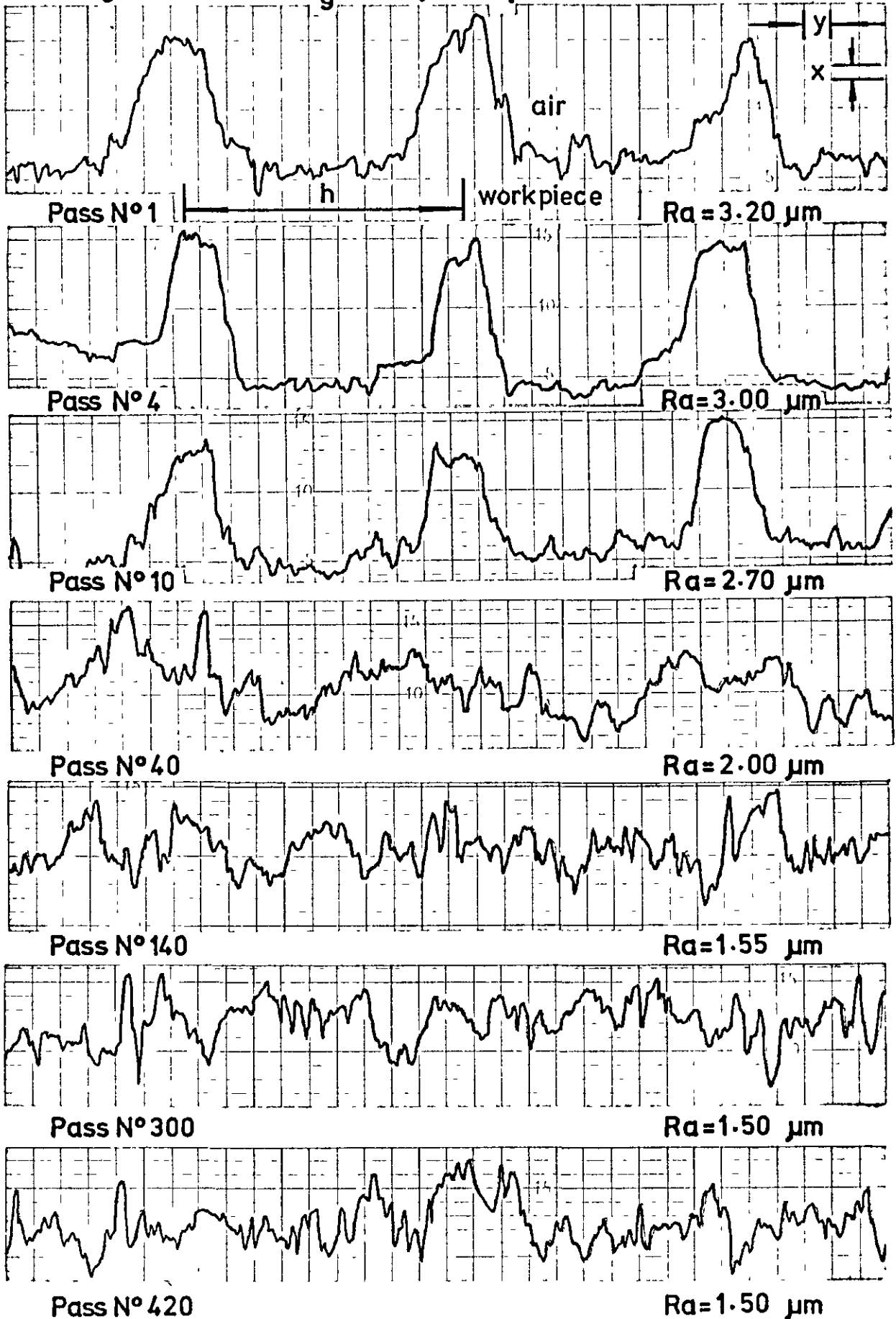


Fig.7.105 "Talysurf" traces showing the variation of workpiece surface roughness for particular dressing and grinding conditions

TEST N°16

Dressing conditions :- $a_d = 5 \mu\text{m}$, $h = .5 \text{ mm/rev}$: $x = 1.25 \mu\text{m}$

Grinding conditions :- $a_g = 12.5 \mu\text{m}$, $v_t = 13.5 \text{ mm/sec}$: $y = 50 \mu\text{m}$

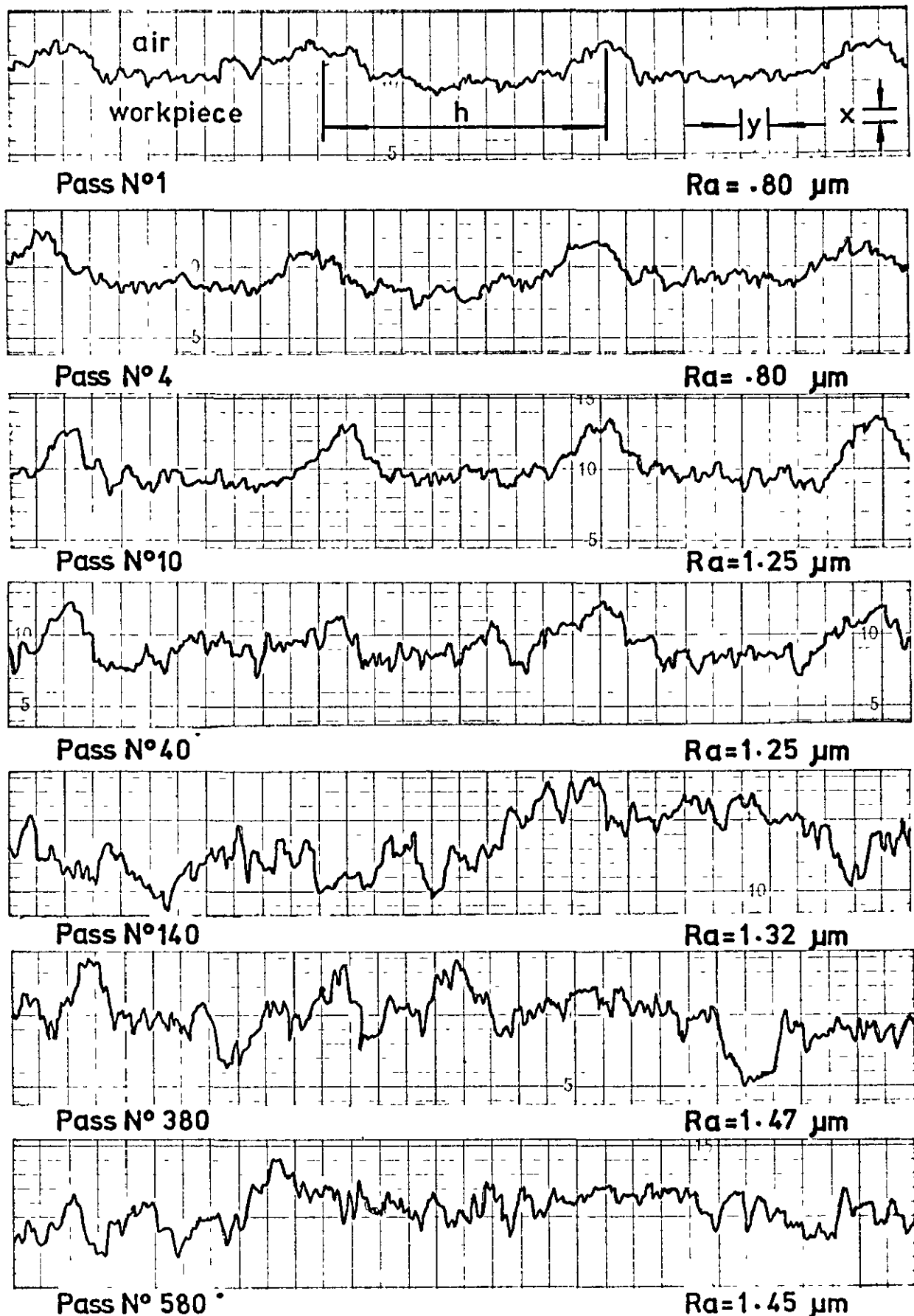


Fig.7.106 "Talysurf" traces showing the variation of workpiece surface roughness for particular dressing and grinding conditions

TEST N° 13

$a_d = 25 \text{ } \mu\text{m}$, $h = .5 \text{ mm/rev}$
 $a_g = 12.5 \text{ } \mu\text{m}$, $v_t = 13.5 \text{ mm/sec}$

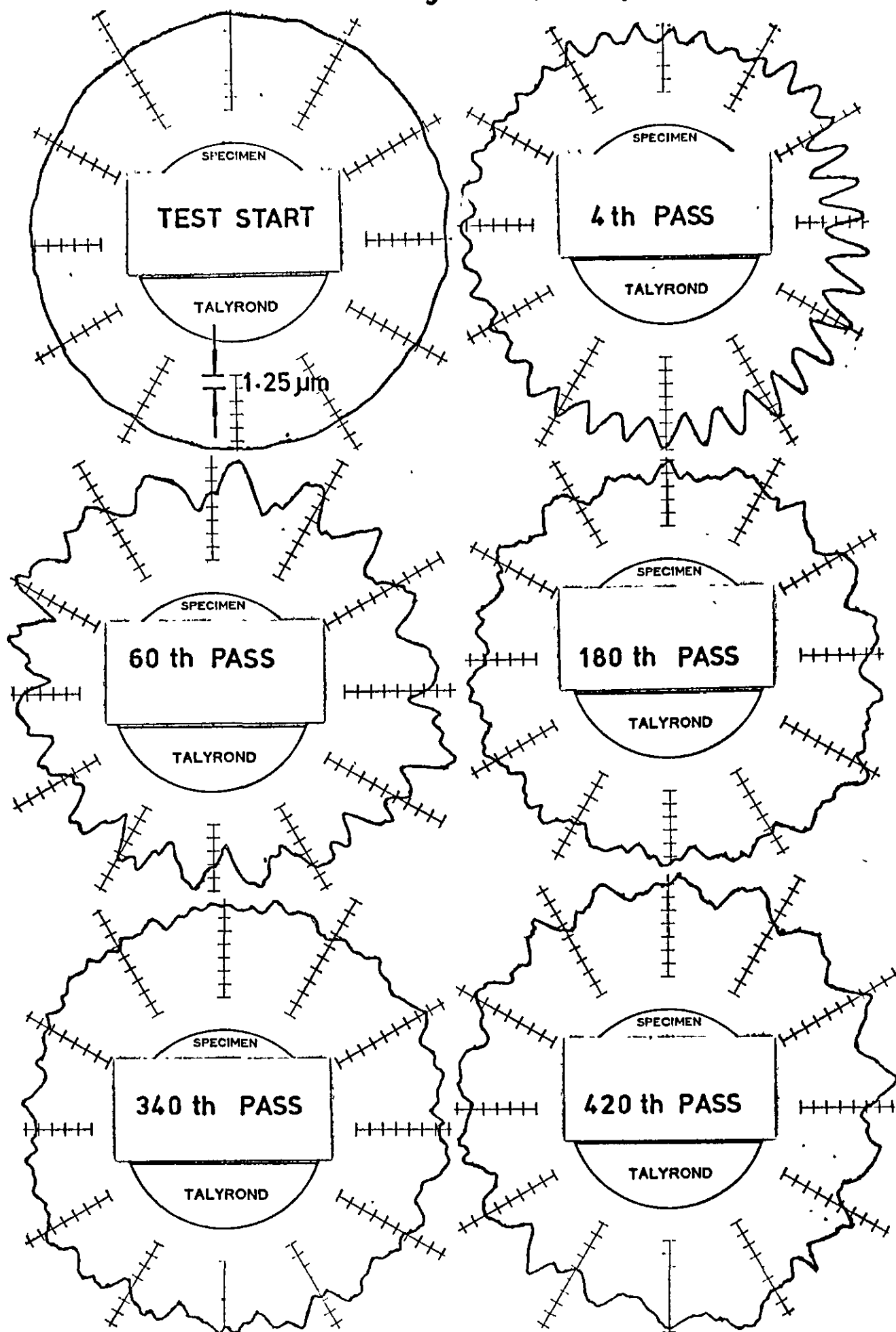


Fig. 7.107 "Talyrond" traces showing the variation of workpiece circularity with the number of grinding passes

TEST N°16

$a_d = 5 \text{ } \mu\text{m}$; $h = .5 \text{ mm/rev}$
 $a_g = 12.5 \text{ } \mu\text{m}$; $v_t = 13.5 \text{ mm/sec}$

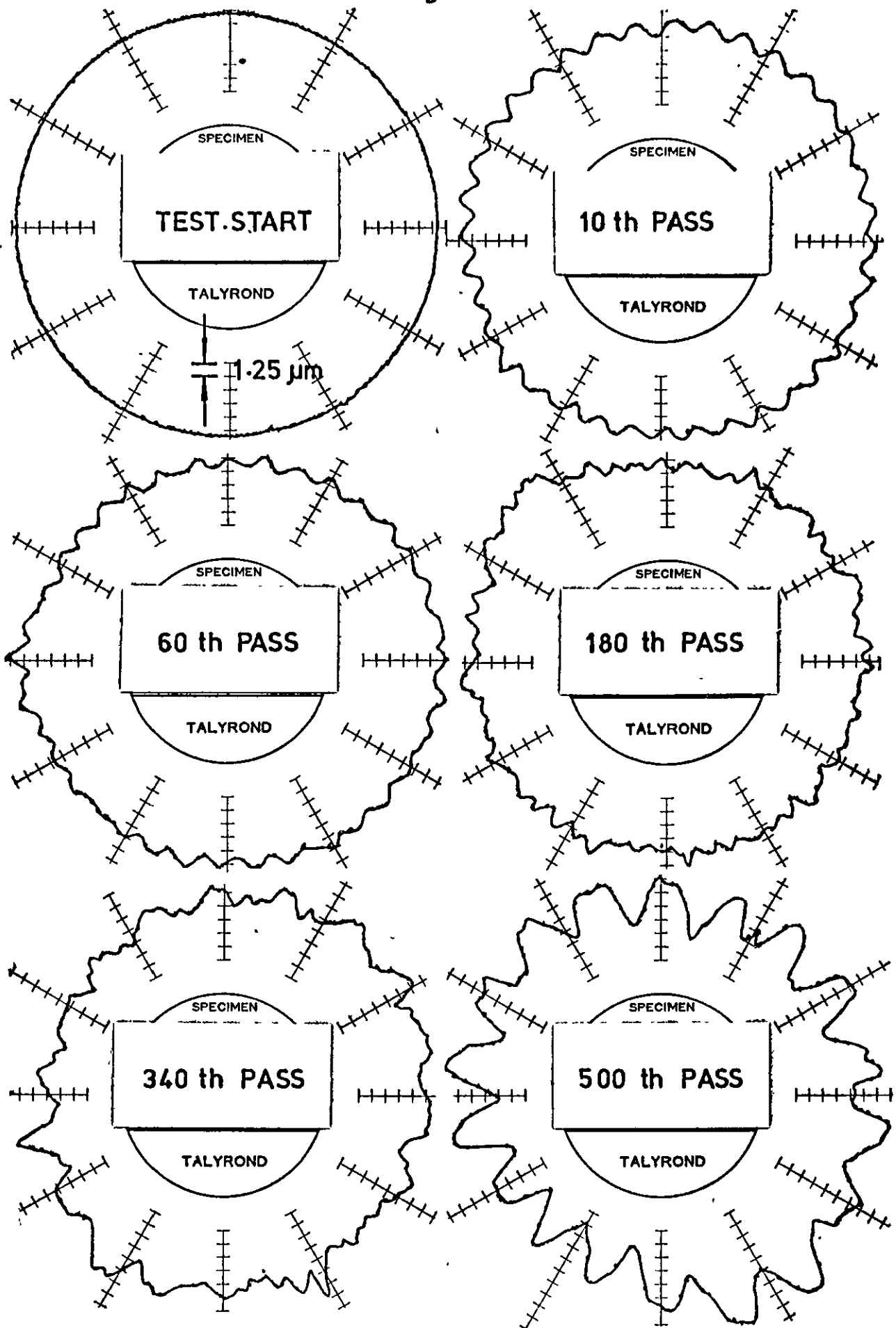


Fig.7.108 "Talyrond" traces showing the variation of workpiece circularity with the number of grinding passes

TEST N° 9

$a_d = 25 \text{ } \mu\text{m}$, $h = .1 \text{ mm/rev}$
 $a_g = 12.5 \text{ } \mu\text{m}$, $v_t = 13.5 \text{ mm/sec}$

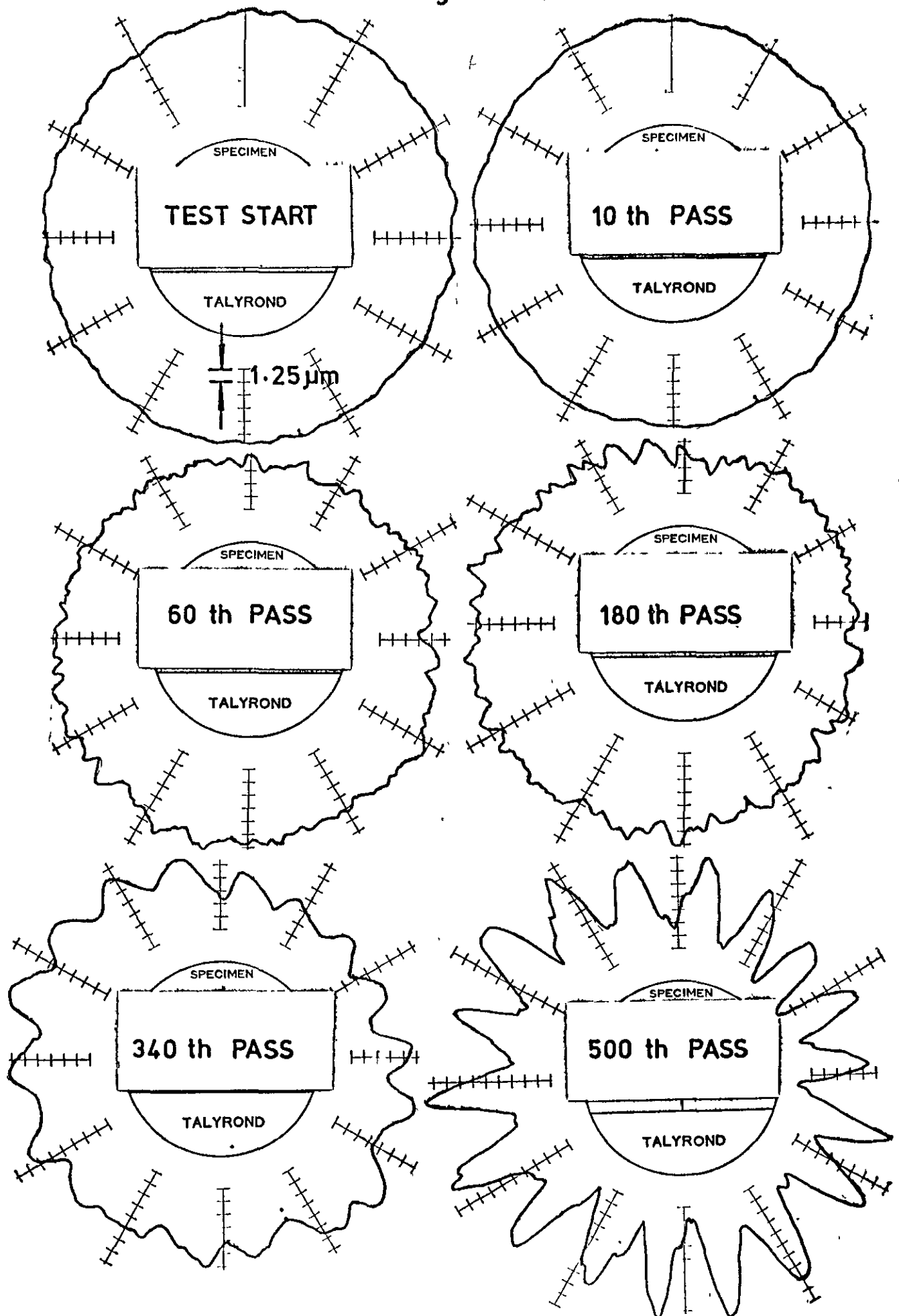


Fig. 7.109 "Talyrond" traces showing the variation of workplece circularity with the number of grinding passes

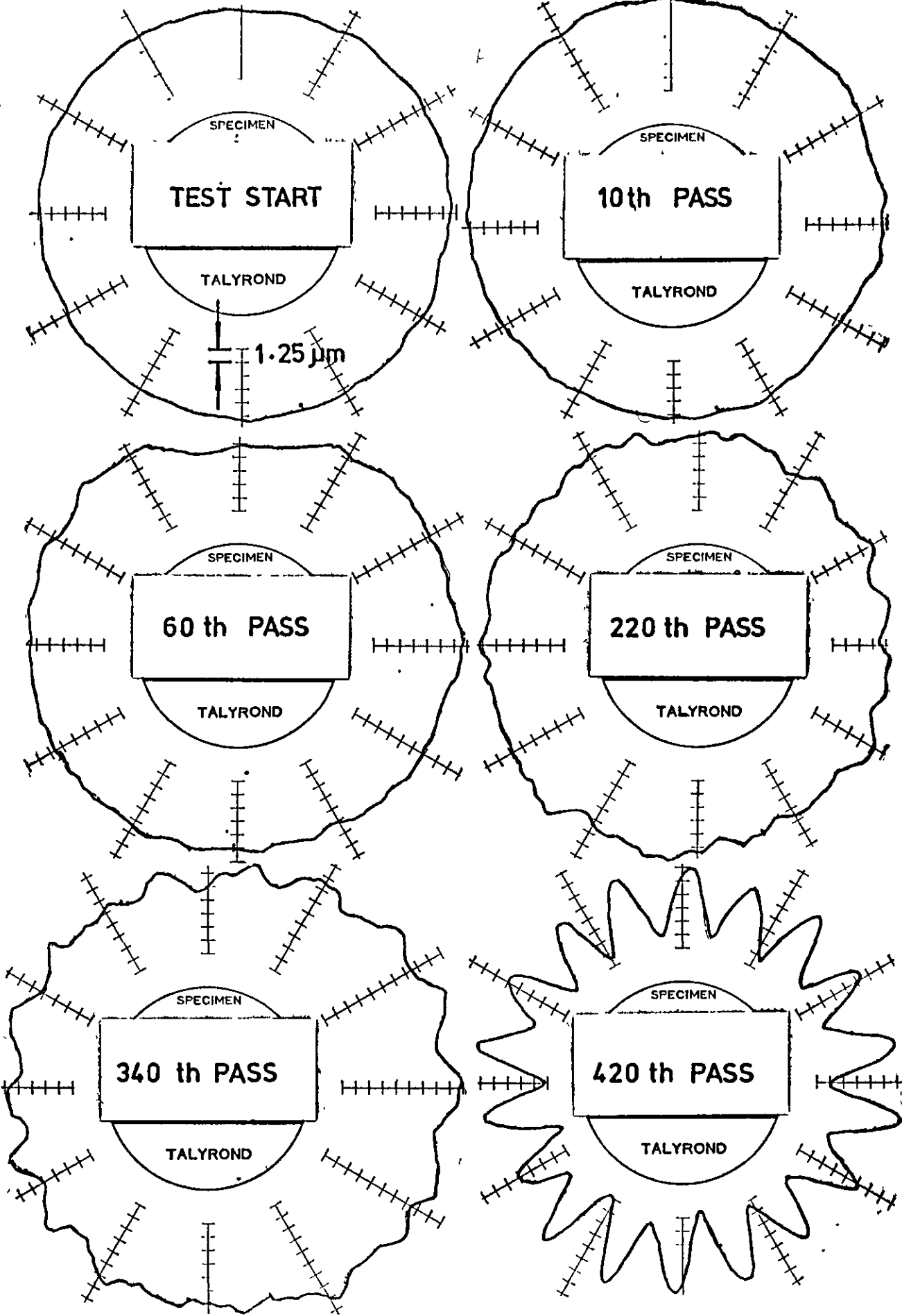


Fig. 7.110 "Talyrond" traces showing the variation of workpiece circularity with the number of grinding passes

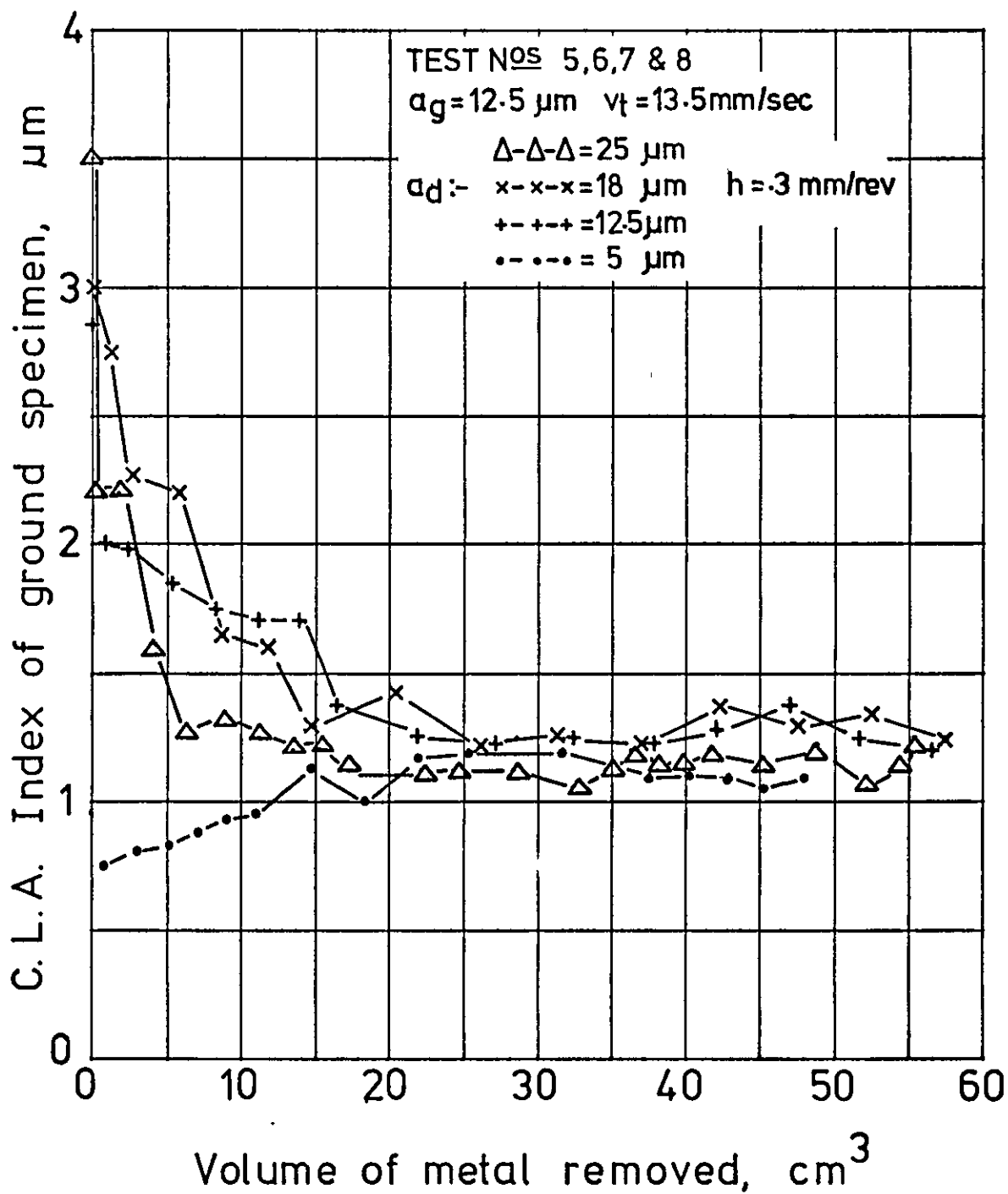


Fig. 7.111 Variation of workpiece surface roughness with volume of metal removed for various wheel dressing conditions.

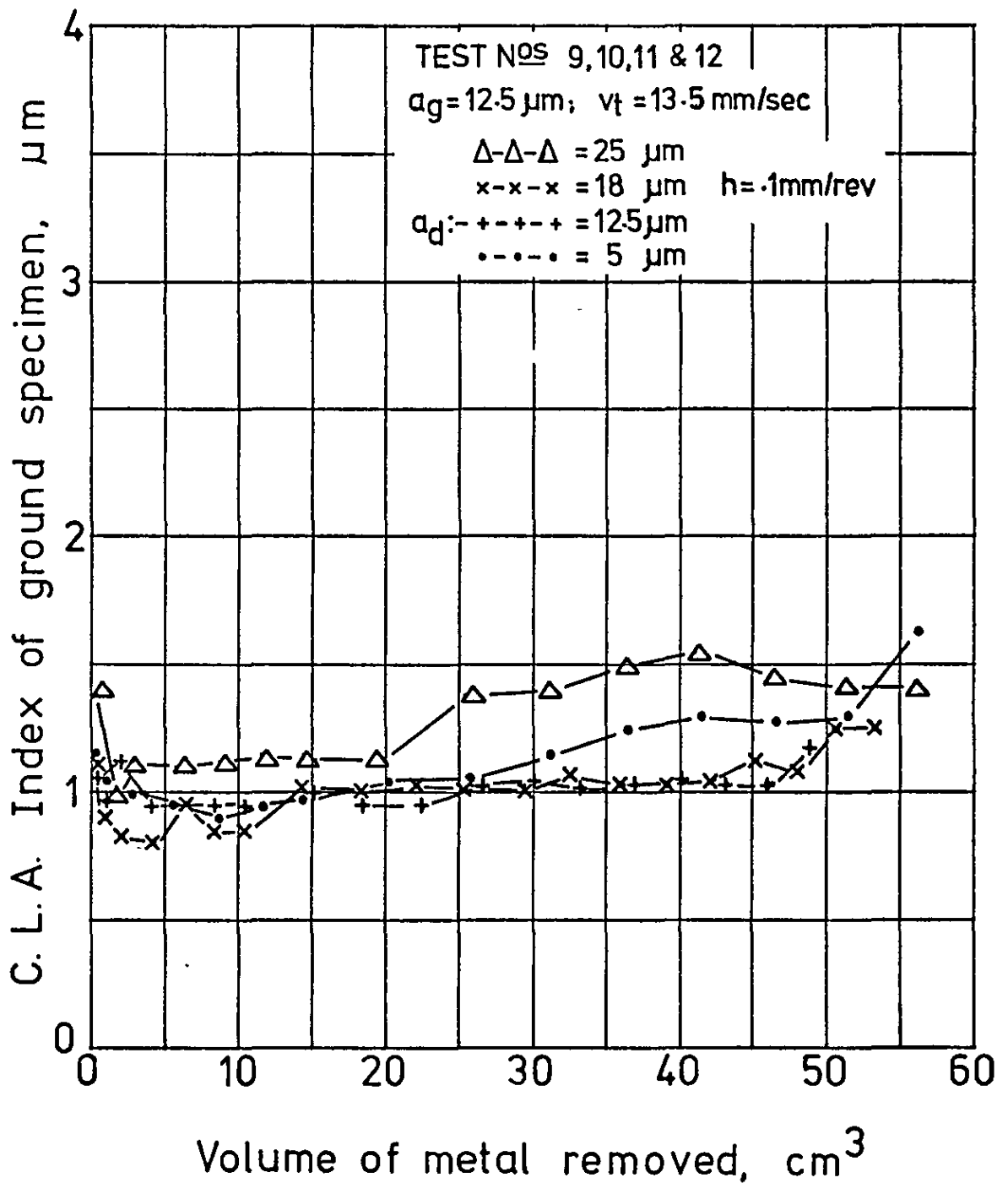


Fig. 7.112 Variation of workpiece surface roughness with volume of metal removed for various wheel dressing conditions.

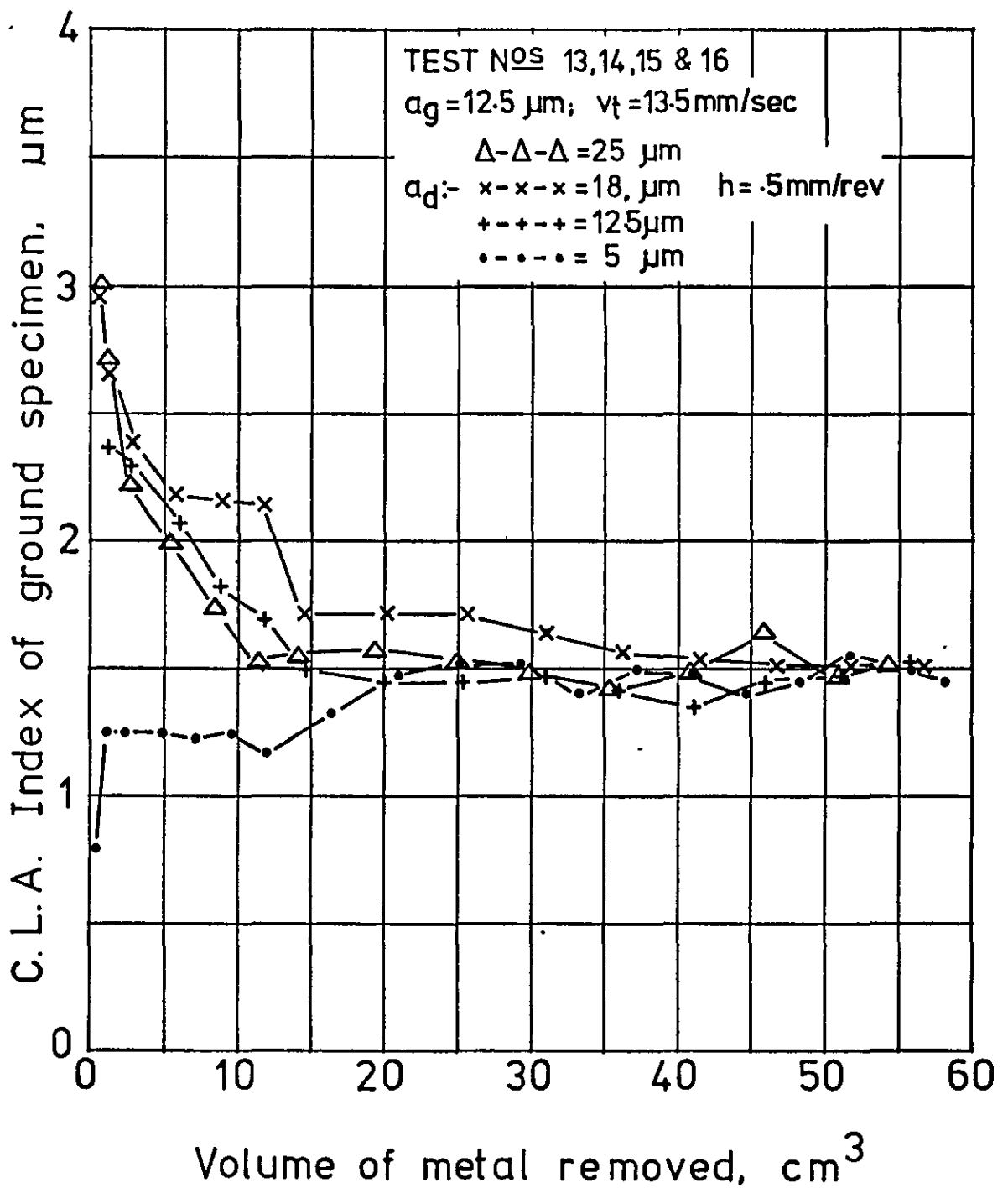


Fig. 7.113 Variation of workpiece surface roughness with volume of metal removed for various wheel dressing conditions.

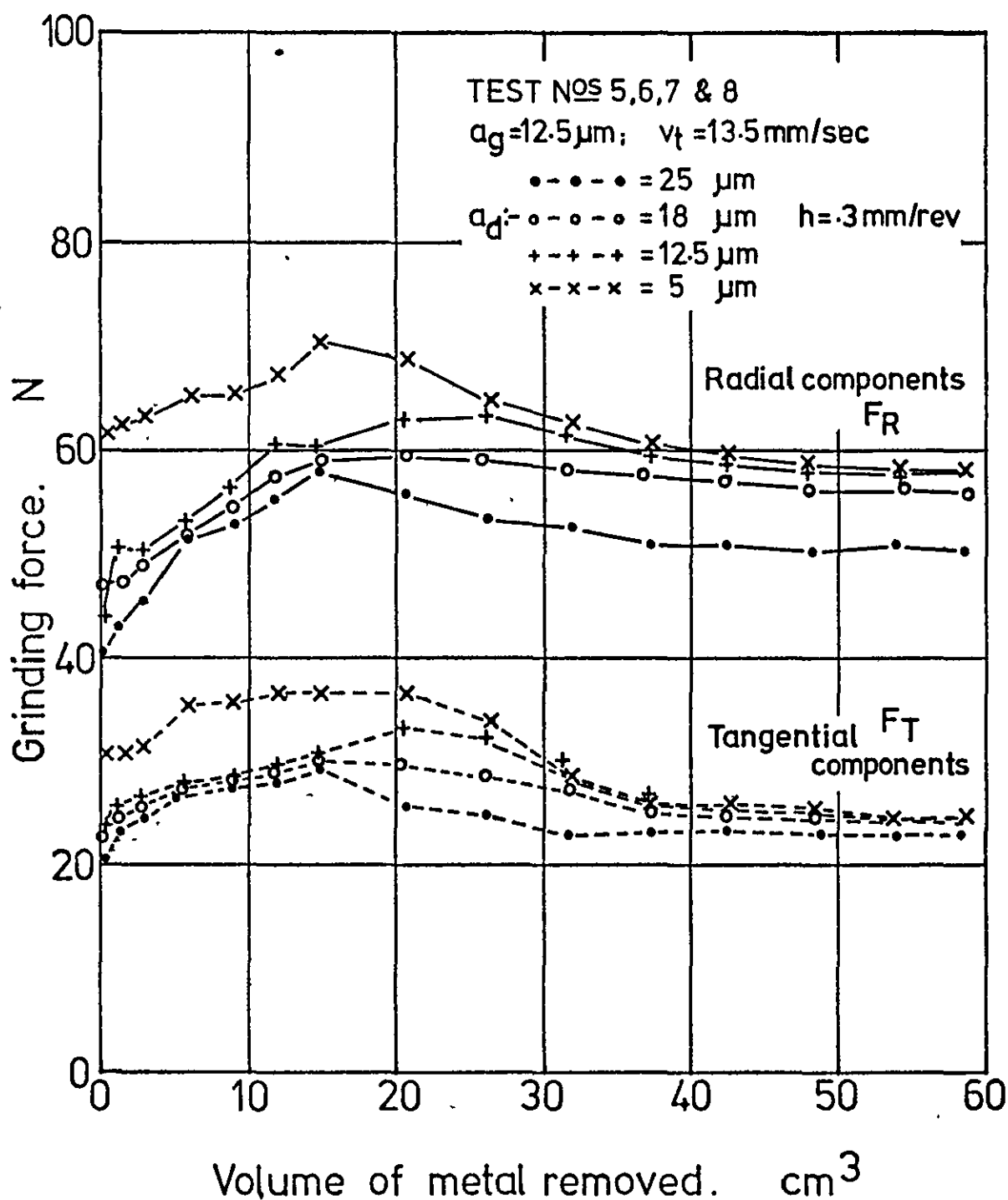


Fig. 7.114 Variation of grinding force with volume of metal removed for various wheel dressing conditions

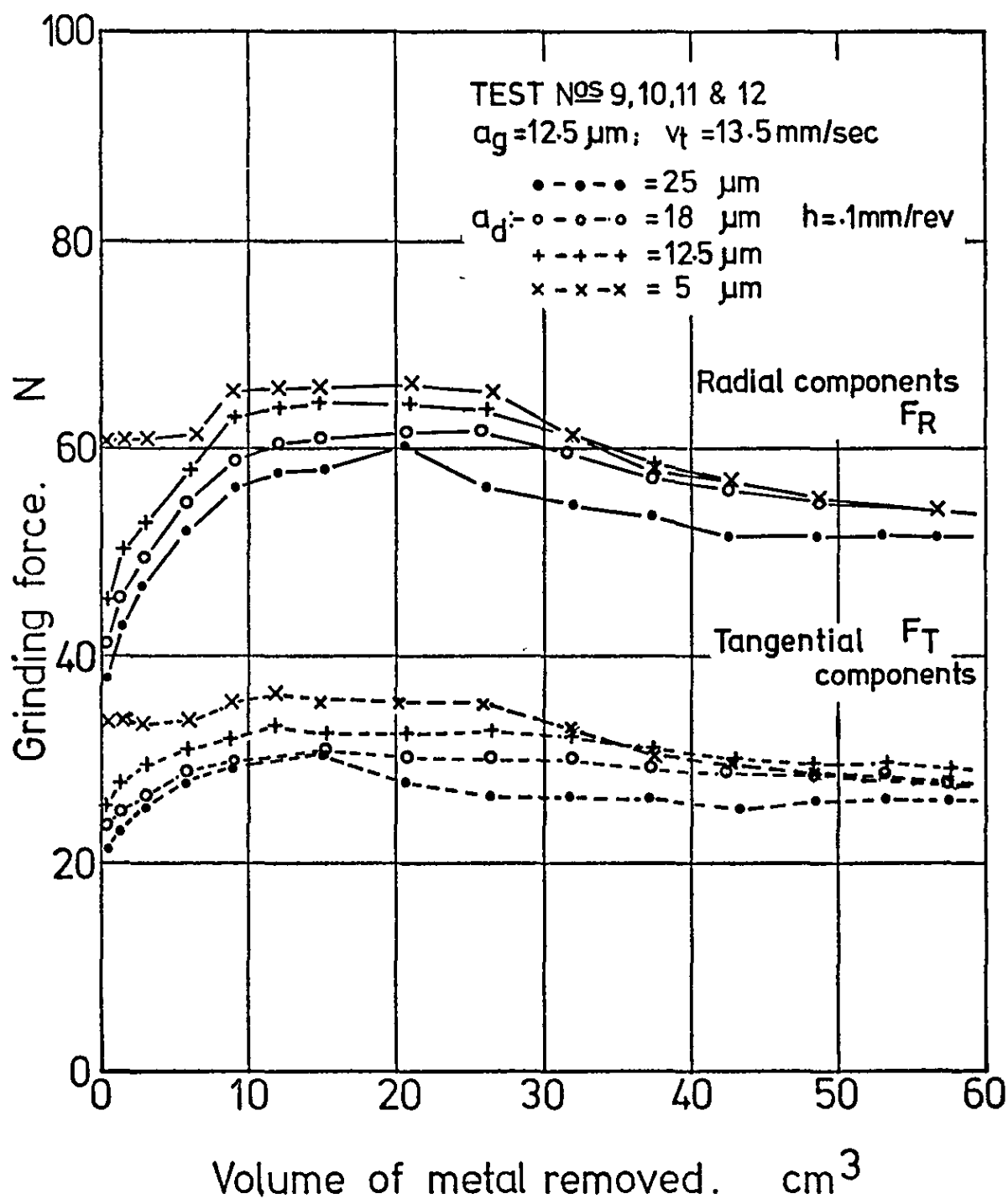


Fig. 7.115 Variation of grinding force
with volume of metal removed for
various wheel dressing conditions

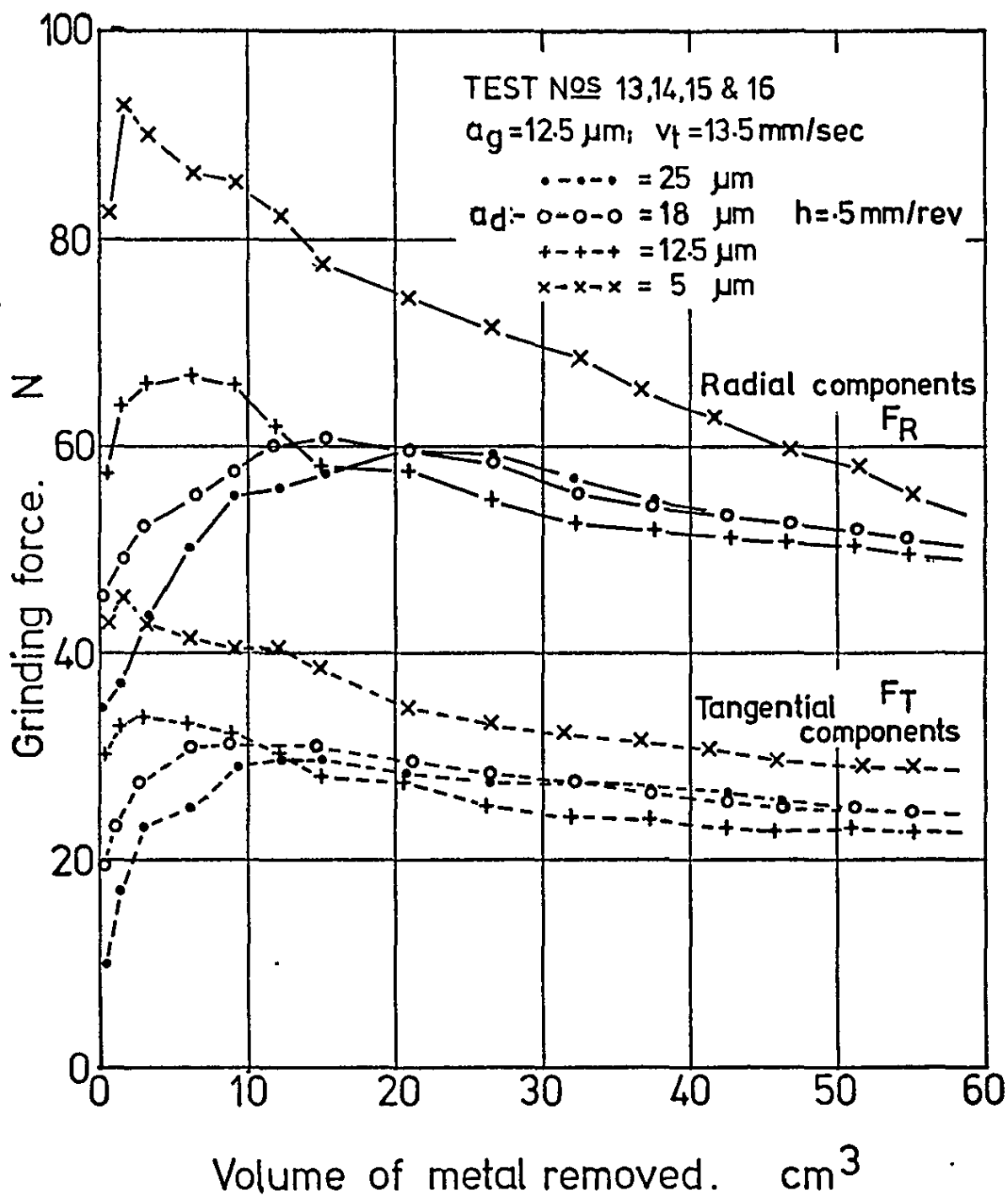


Fig. 7.116 Variation of grinding force with volume of metal removed for various wheel dressing conditions

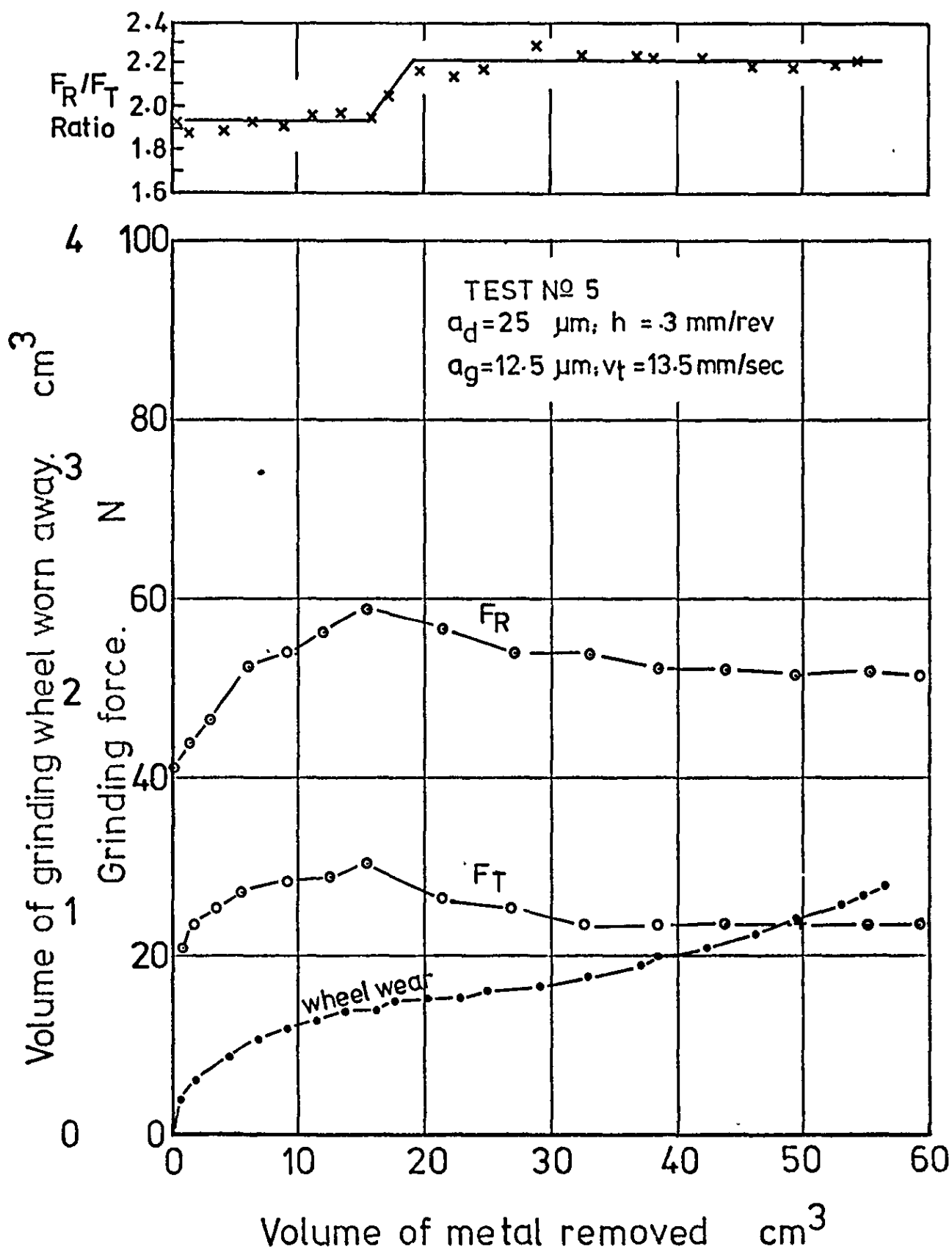


Fig. 7.117 Variation of grinding force and wheel wear with volume of metal removed for a particular wheel dressing condition.

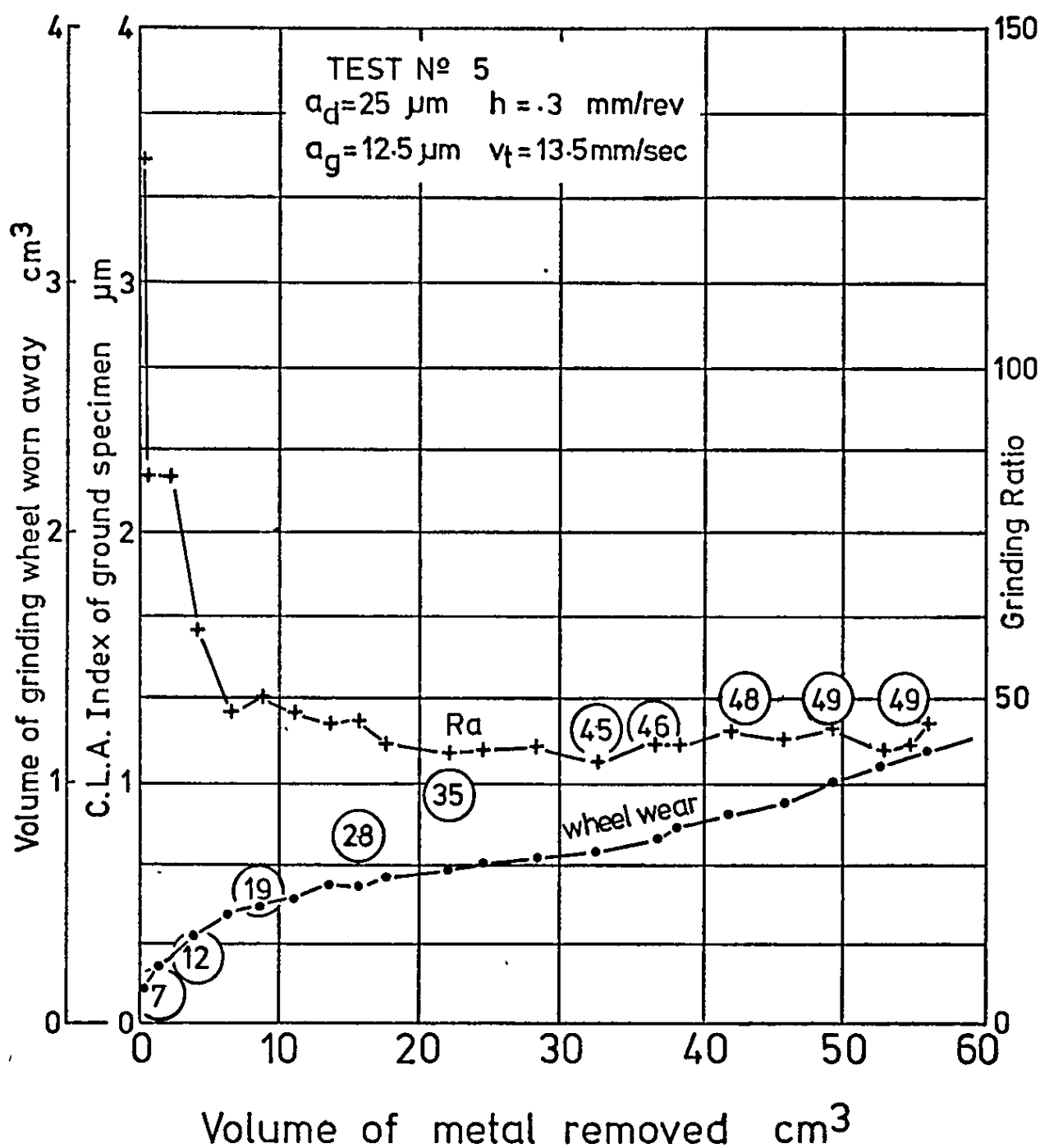


Fig.7.118 Variation of grinding wheel wear, workpiece surface roughness and grinding ratio with volume of metal removed for a particular wheel dressing condition.

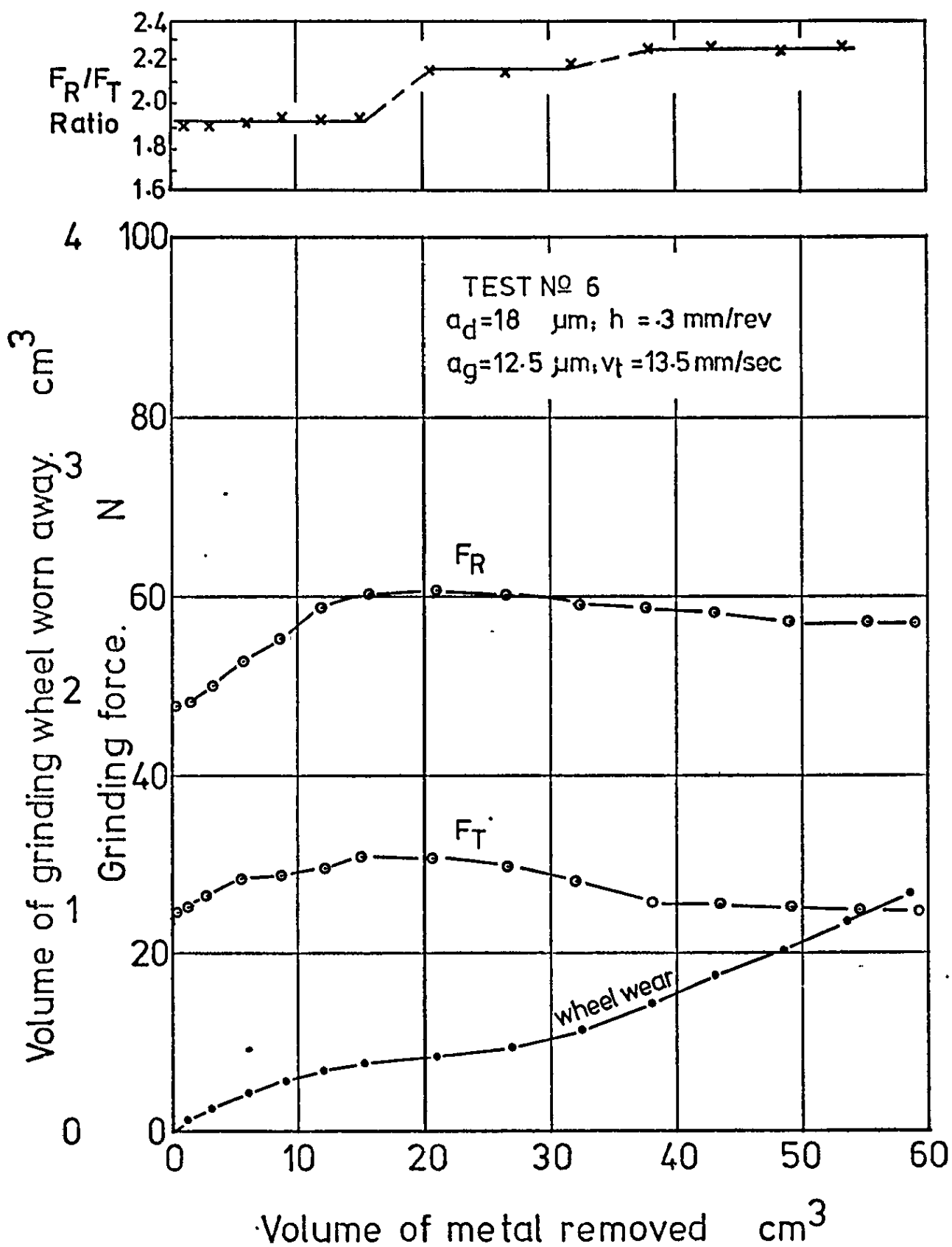


Fig. 7.119 Variation of grinding force and wheel wear with volume of metal removed for a particular wheel dressing condition.

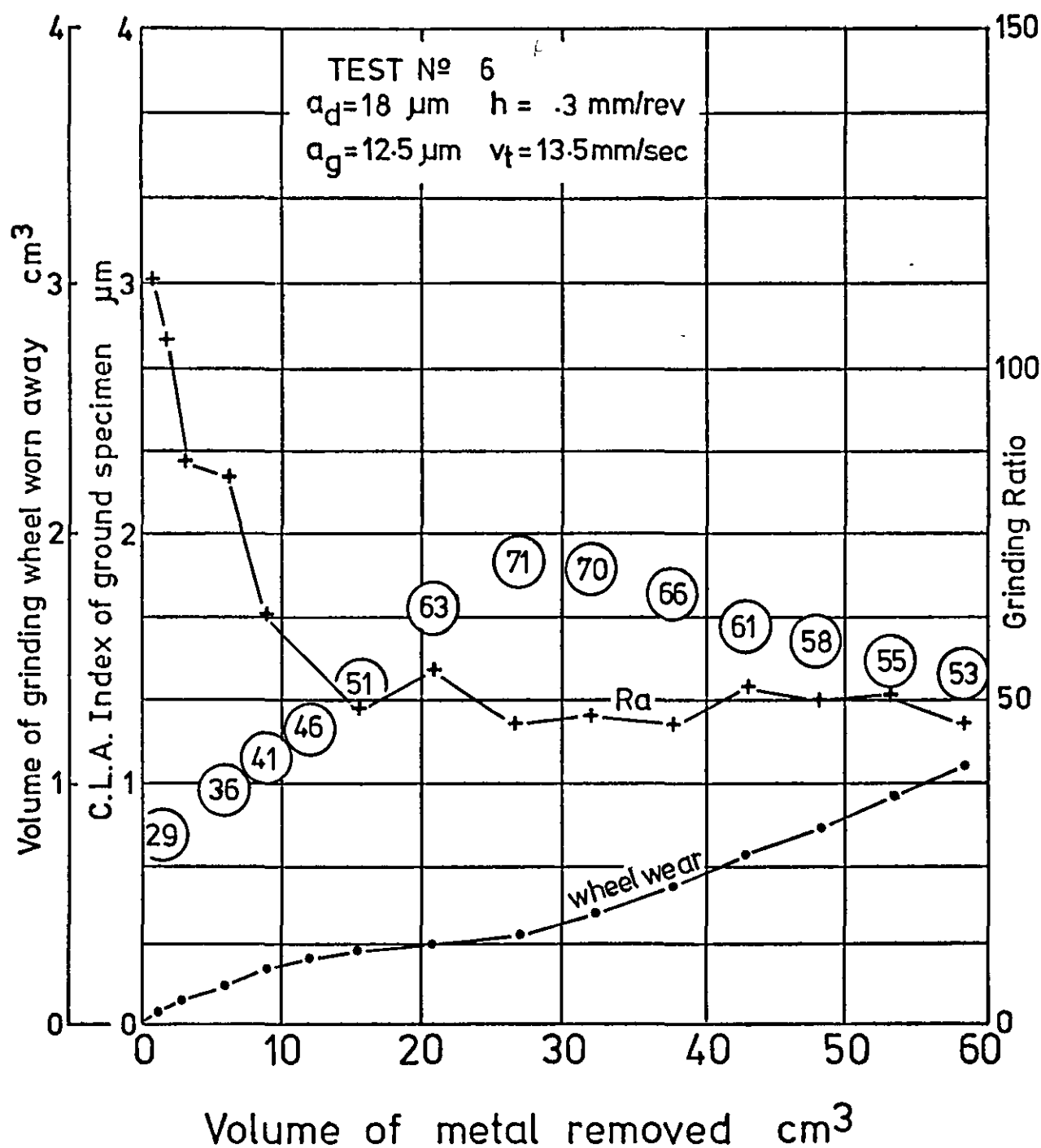


Fig. 7.120 Variation of grinding wheel wear, workpiece surface roughness and grinding ratio with volume of metal removed for a particular wheel dressing condition.

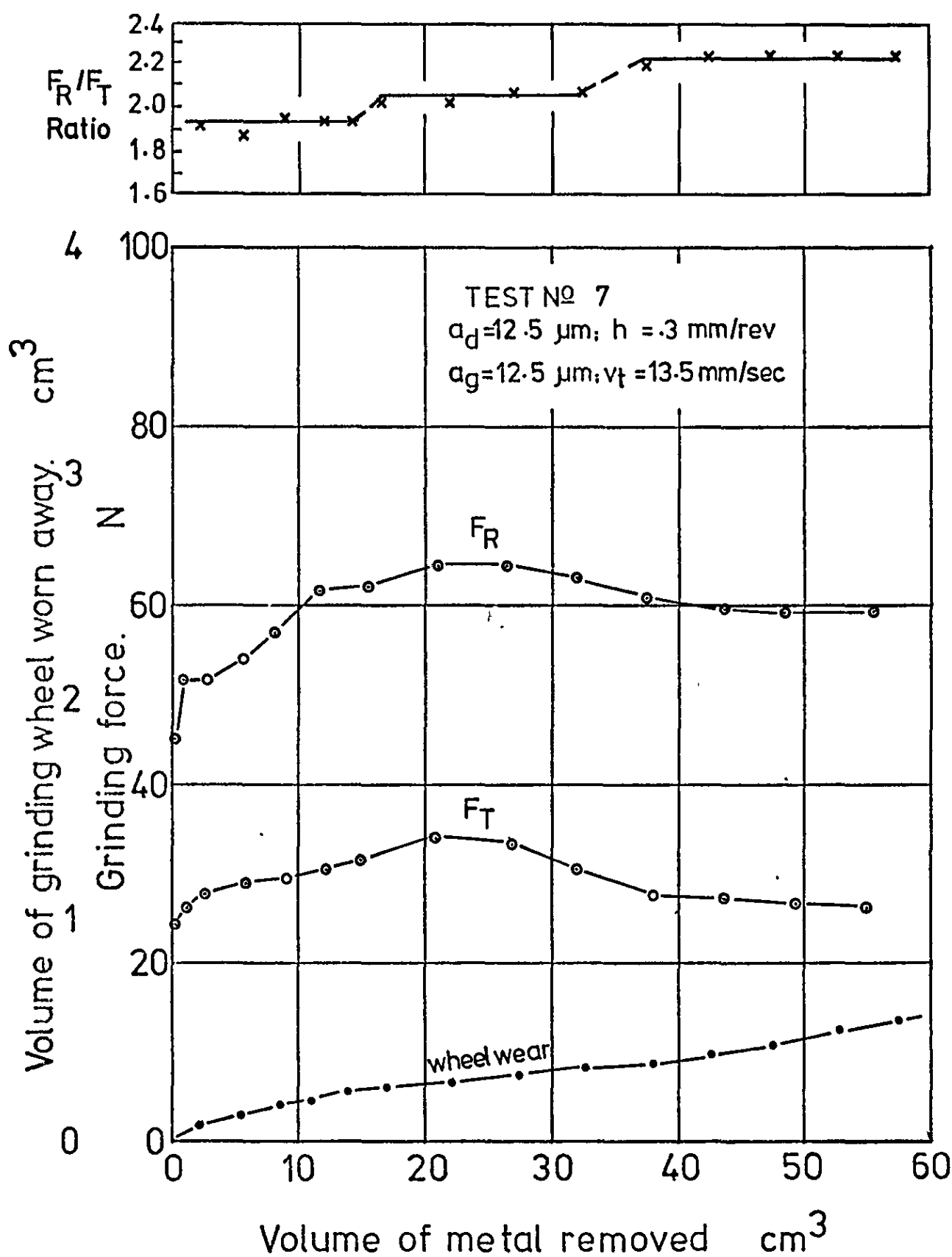


Fig. 7.121 Variation of grinding force and wheel wear with volume of metal removed for a particular wheel dressing condition.

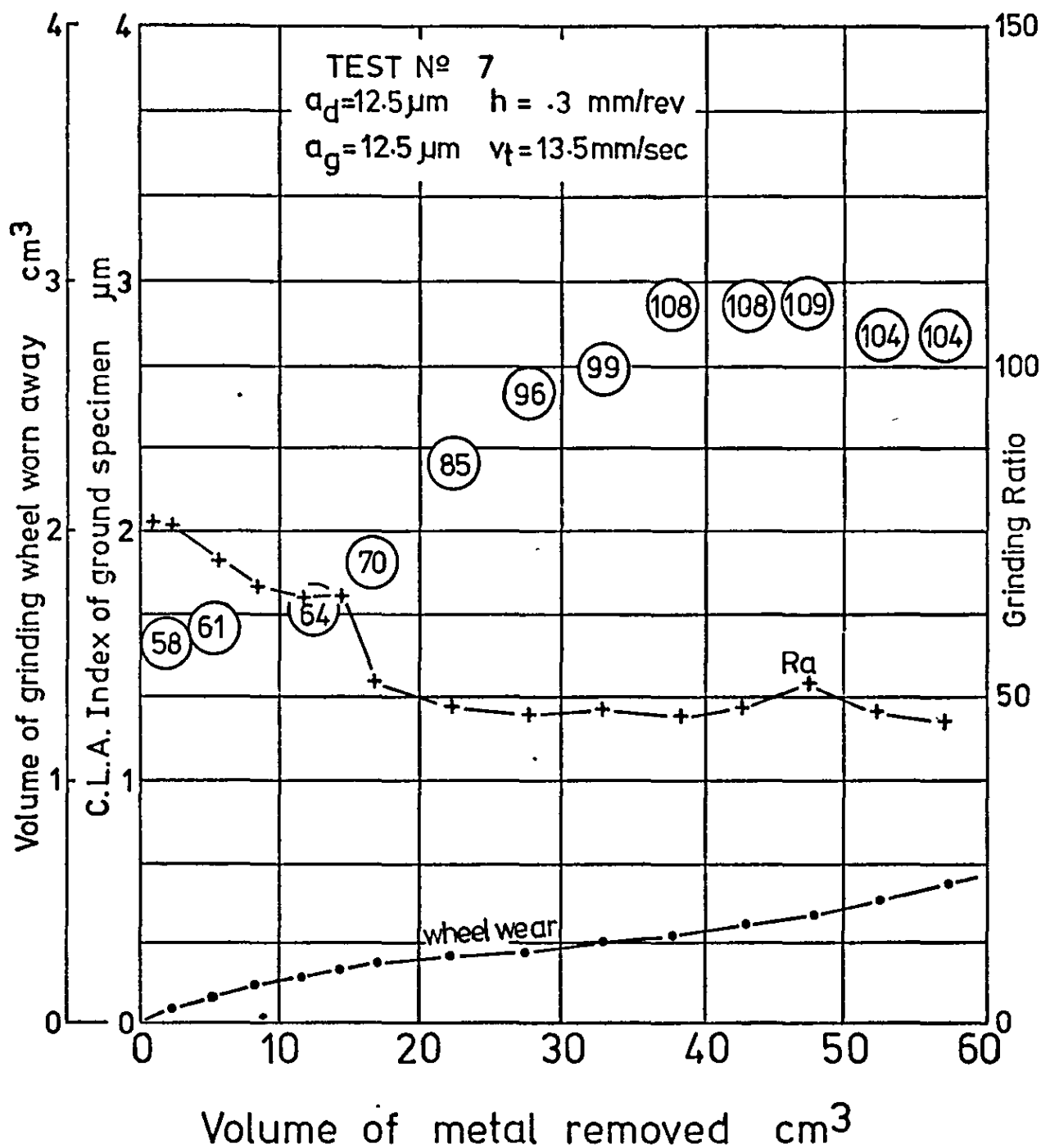


Fig. 7.122 Variation of grinding wheel wear, workpiece surface roughness and grinding ratio with volume of metal removed for a particular wheel dressing condition.

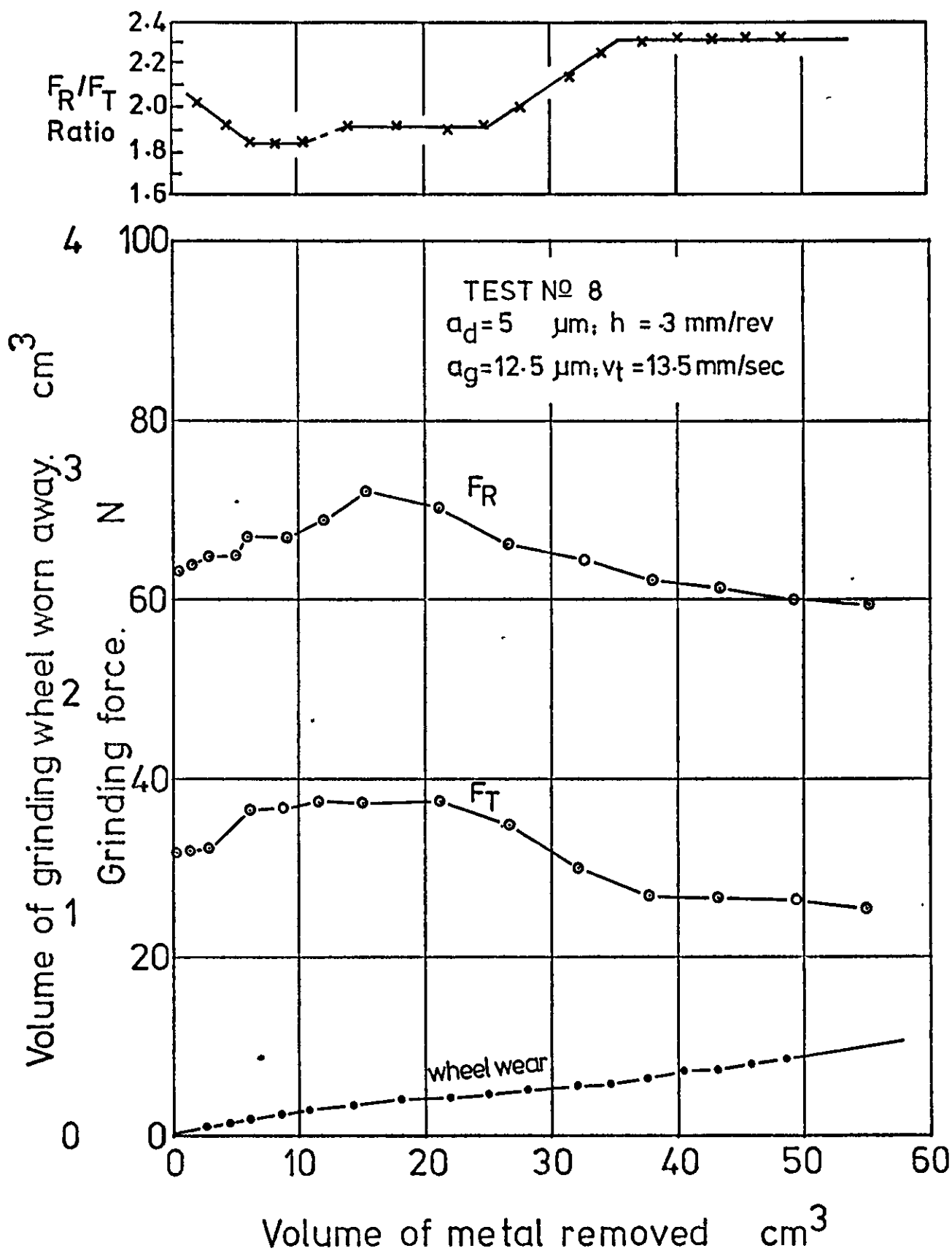


Fig. 7.123 Variation of grinding force and wheel wear with volume of metal removed for a particular wheel dressing condition.

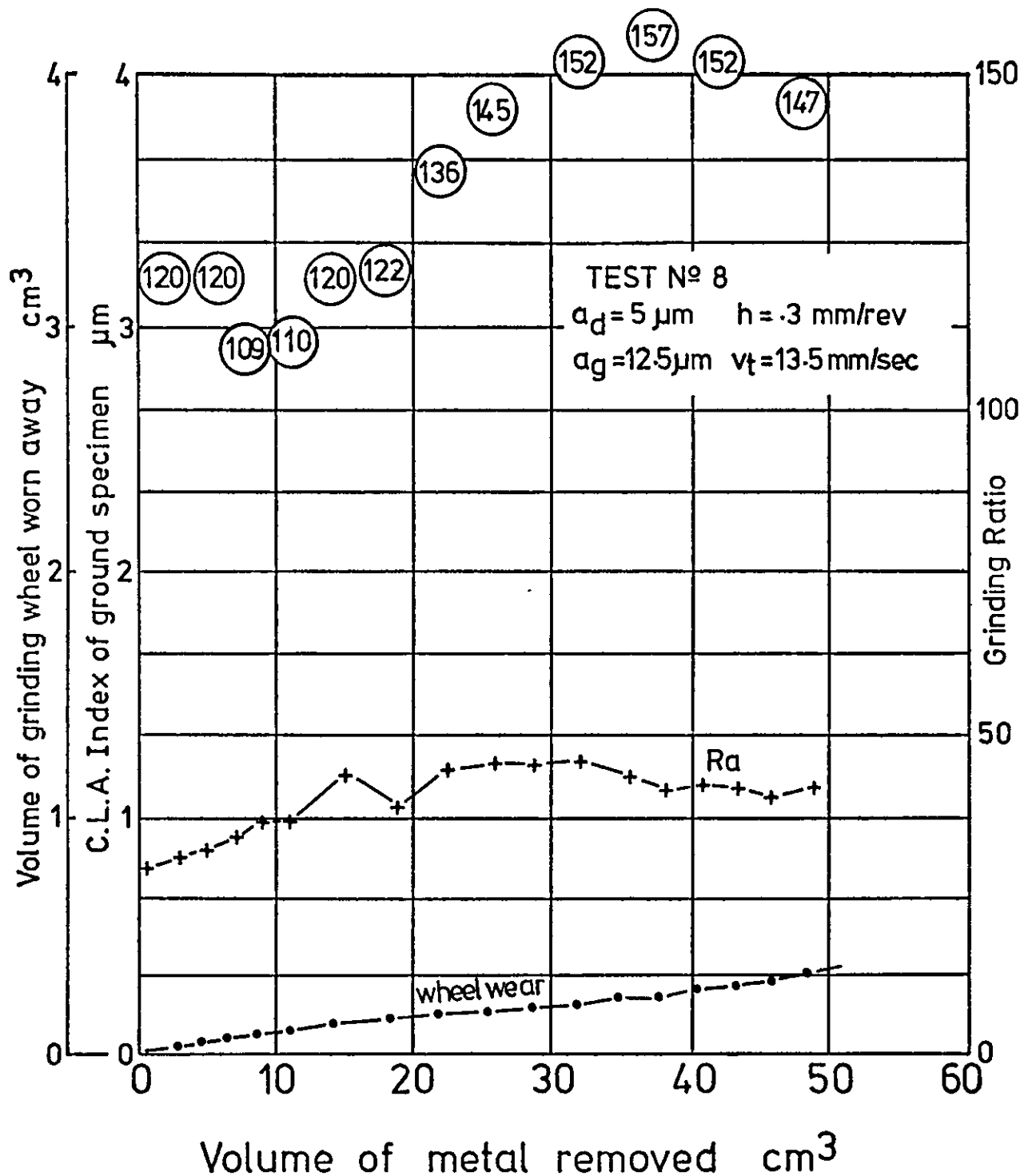


Fig.7.124 Variation of grinding wheel wear, workpiece surface roughness and grinding ratio with volume of metal removed for a particular wheel dressing condition.

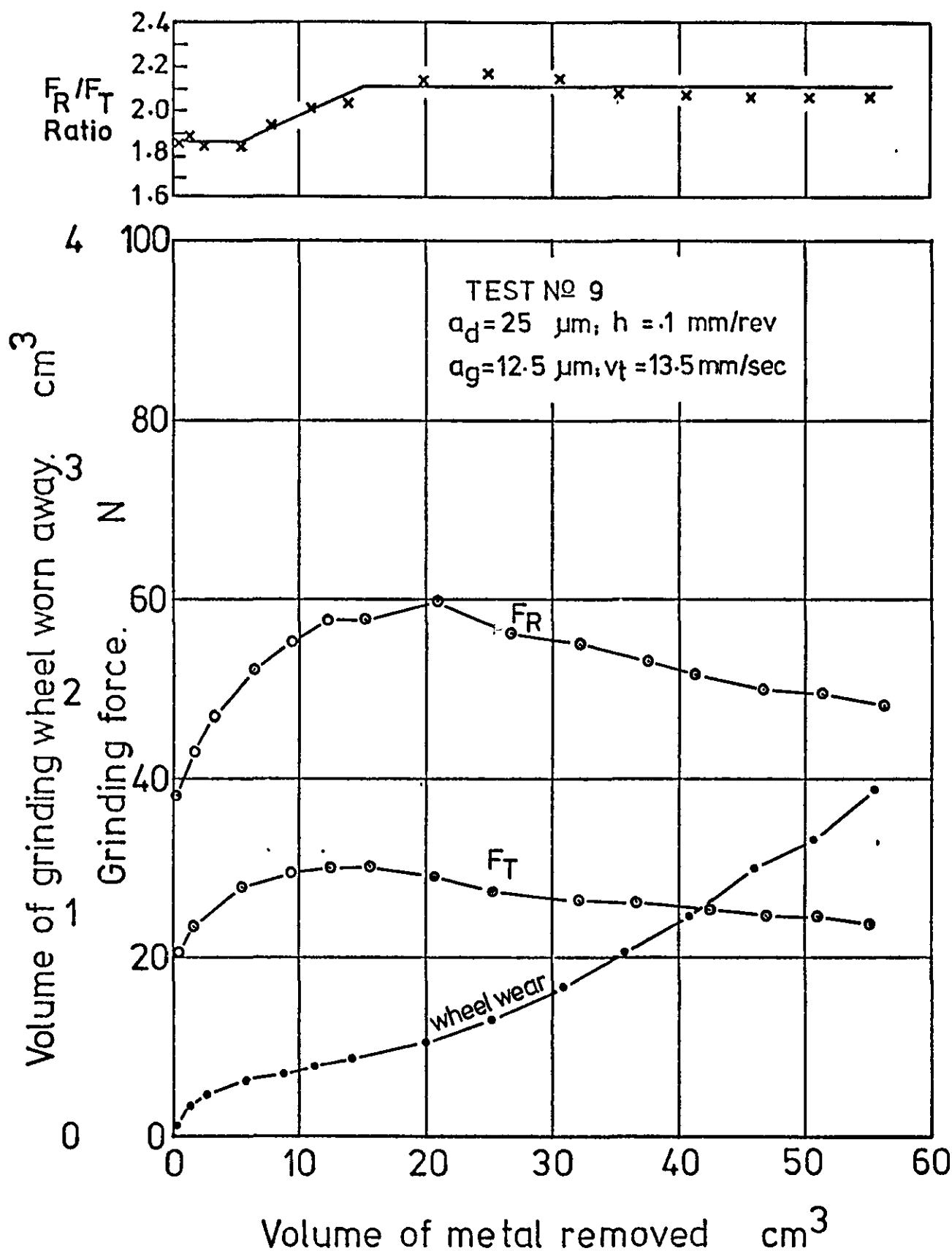


Fig. 7.125 Variation of grinding force and wheel wear with volume of metal removed for a particular wheel dressing condition.

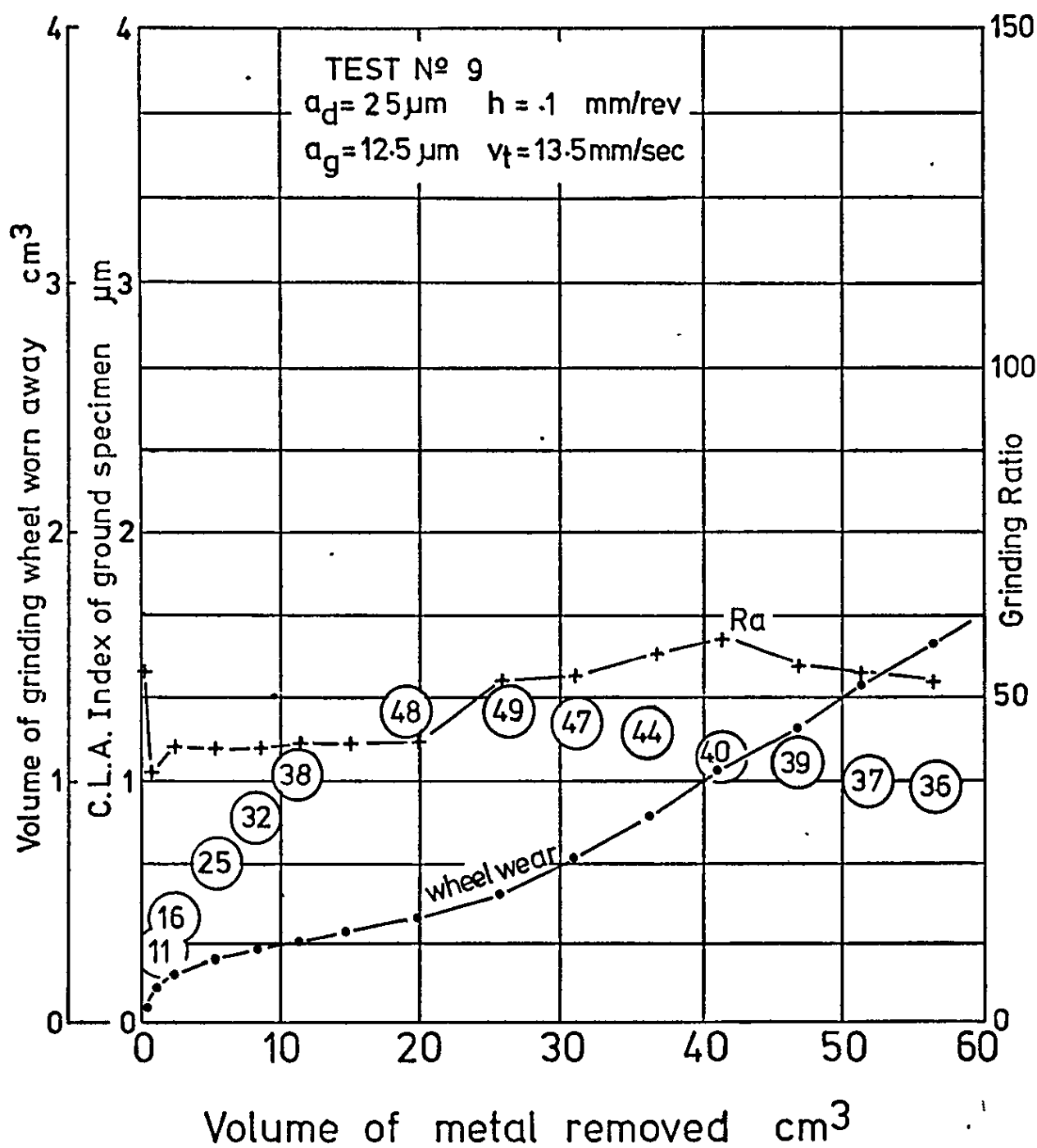


Fig.7.126 Variation of grinding wheel wear, workpiece surface roughness and grinding ratio with volume of metal removed for a particular wheel dressing condition.

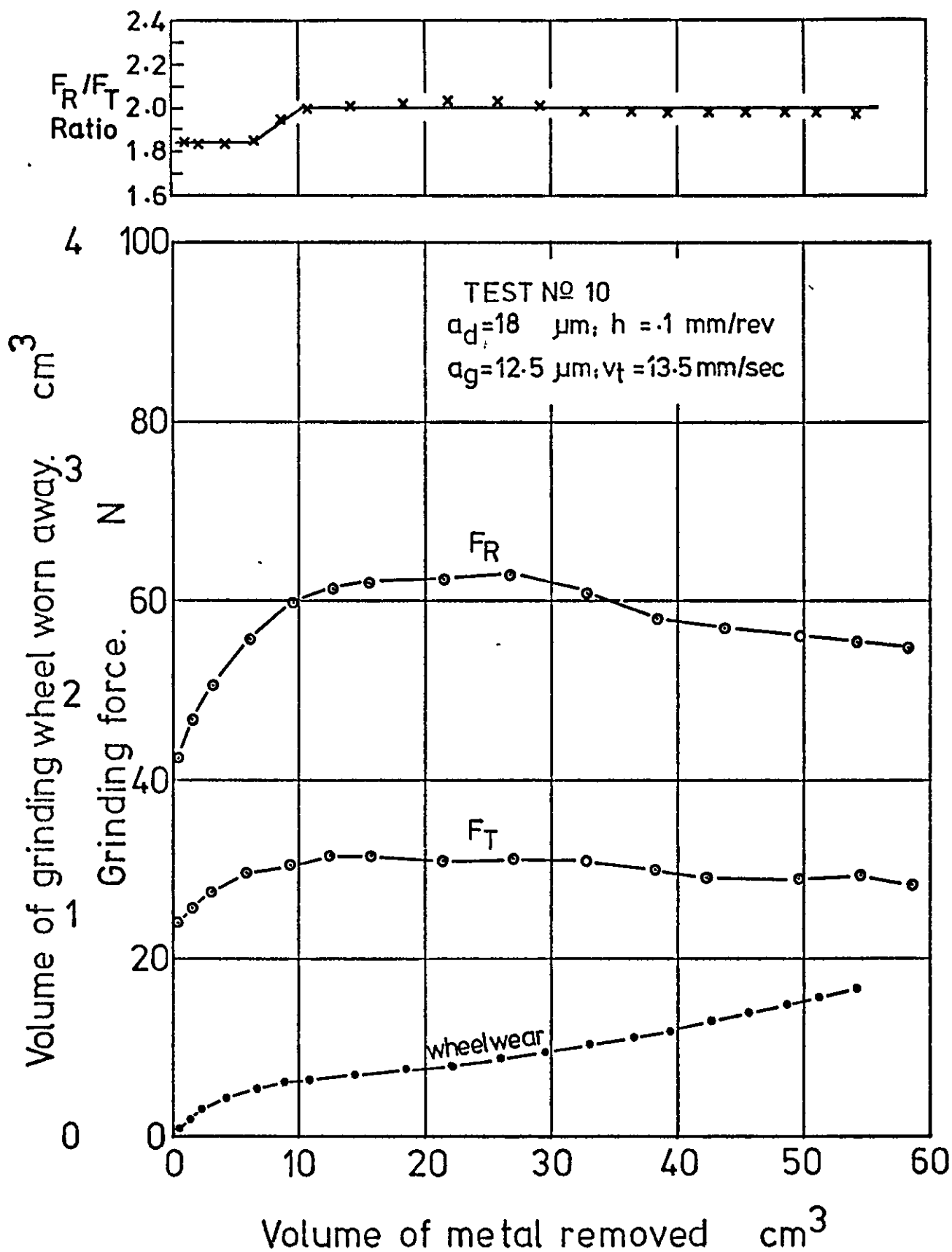


Fig.7.127 Variation of grinding force and wheel wear with volume of metal removed for a particular wheel dressing condition.

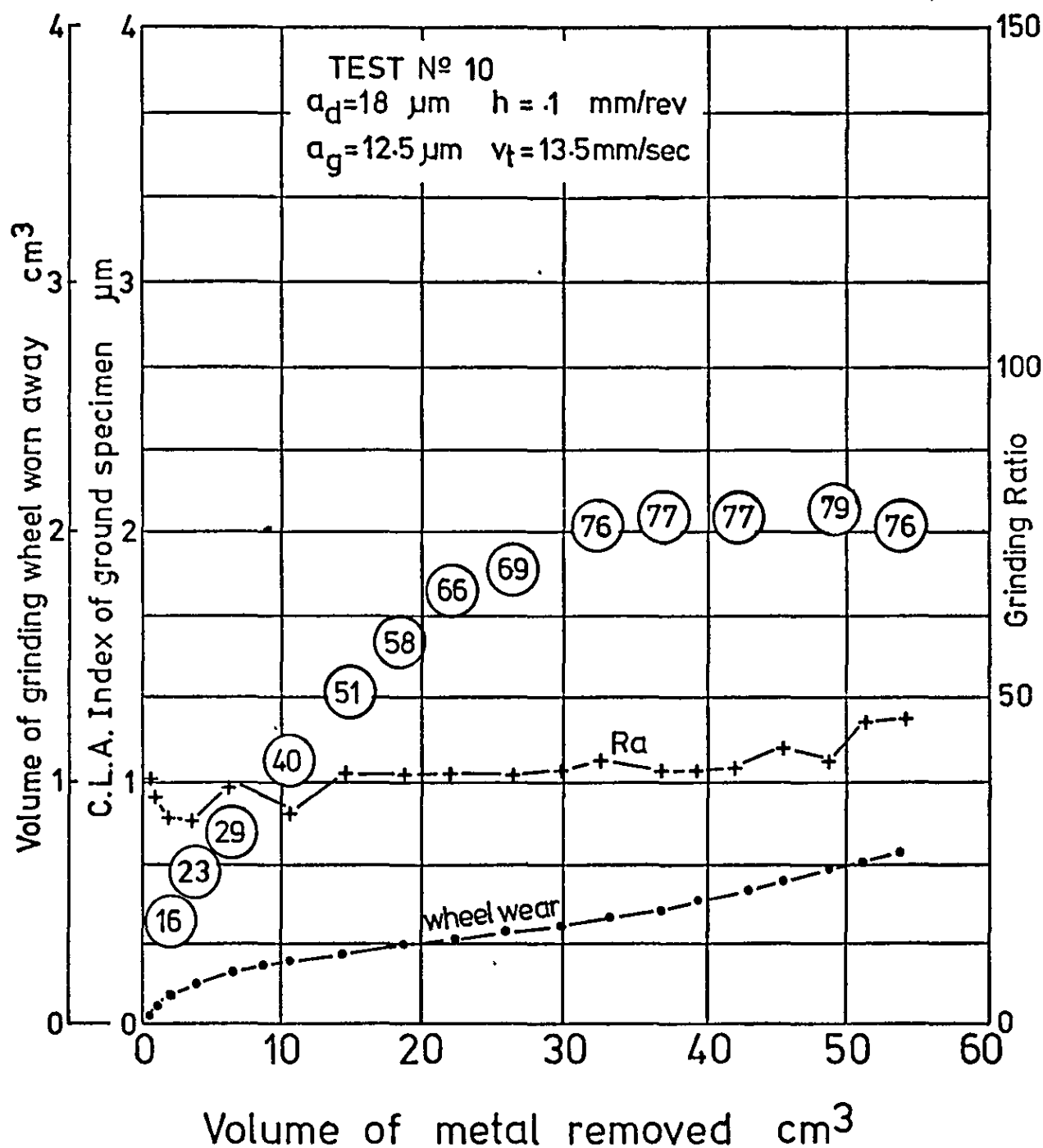


Fig.7.128 Variation of grinding wheel wear, workpiece surface roughness and grinding ratio with volume of metal removed for a particular wheel dressing condition.

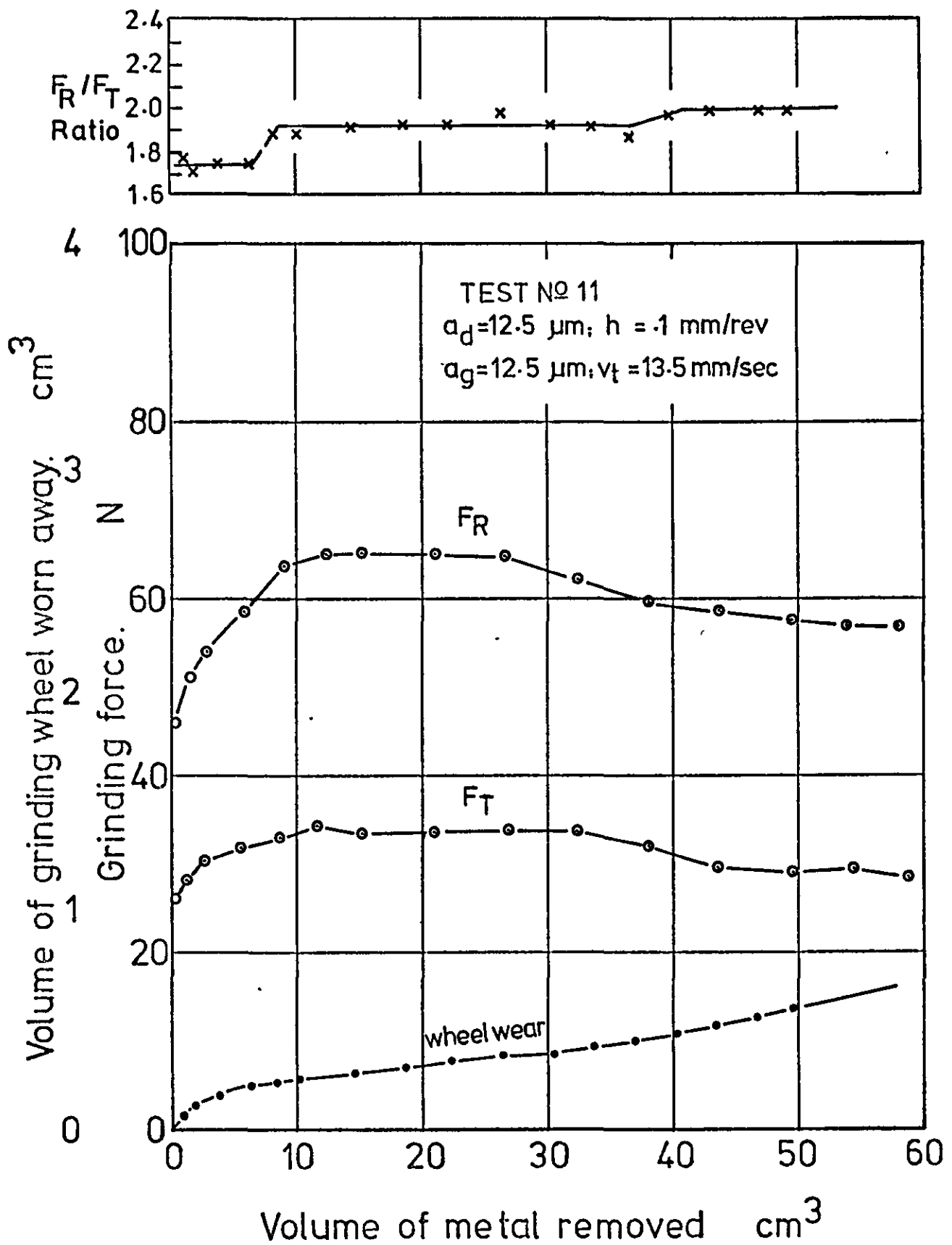


Fig. 7.129 Variation of grinding force and wheel wear with volume of metal removed for a particular wheel dressing condition.

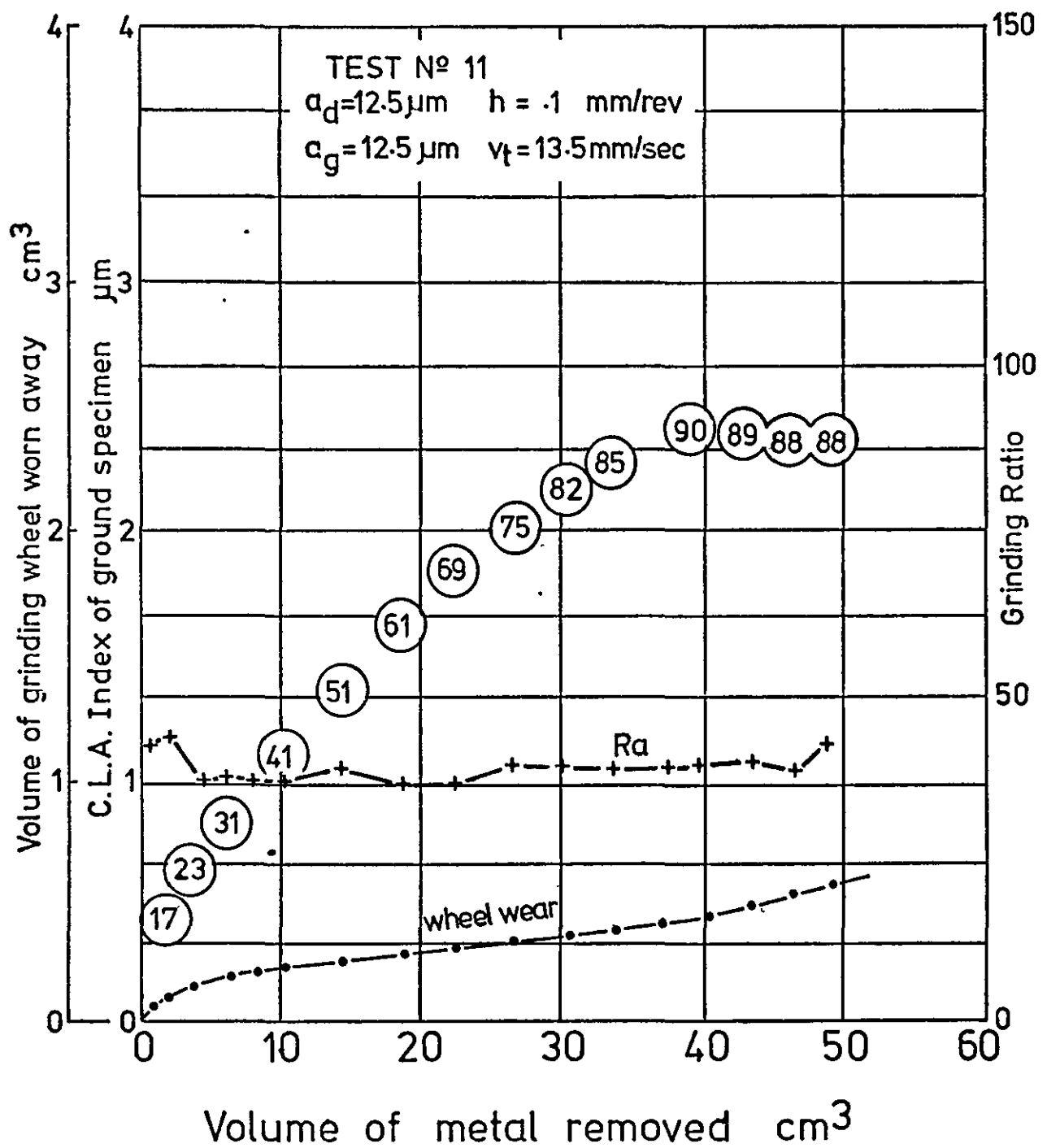


Fig.7.130 Variation of grinding wheel wear, workpiece surface roughness and grinding ratio with volume of metal removed for a particular wheel dressing condition.

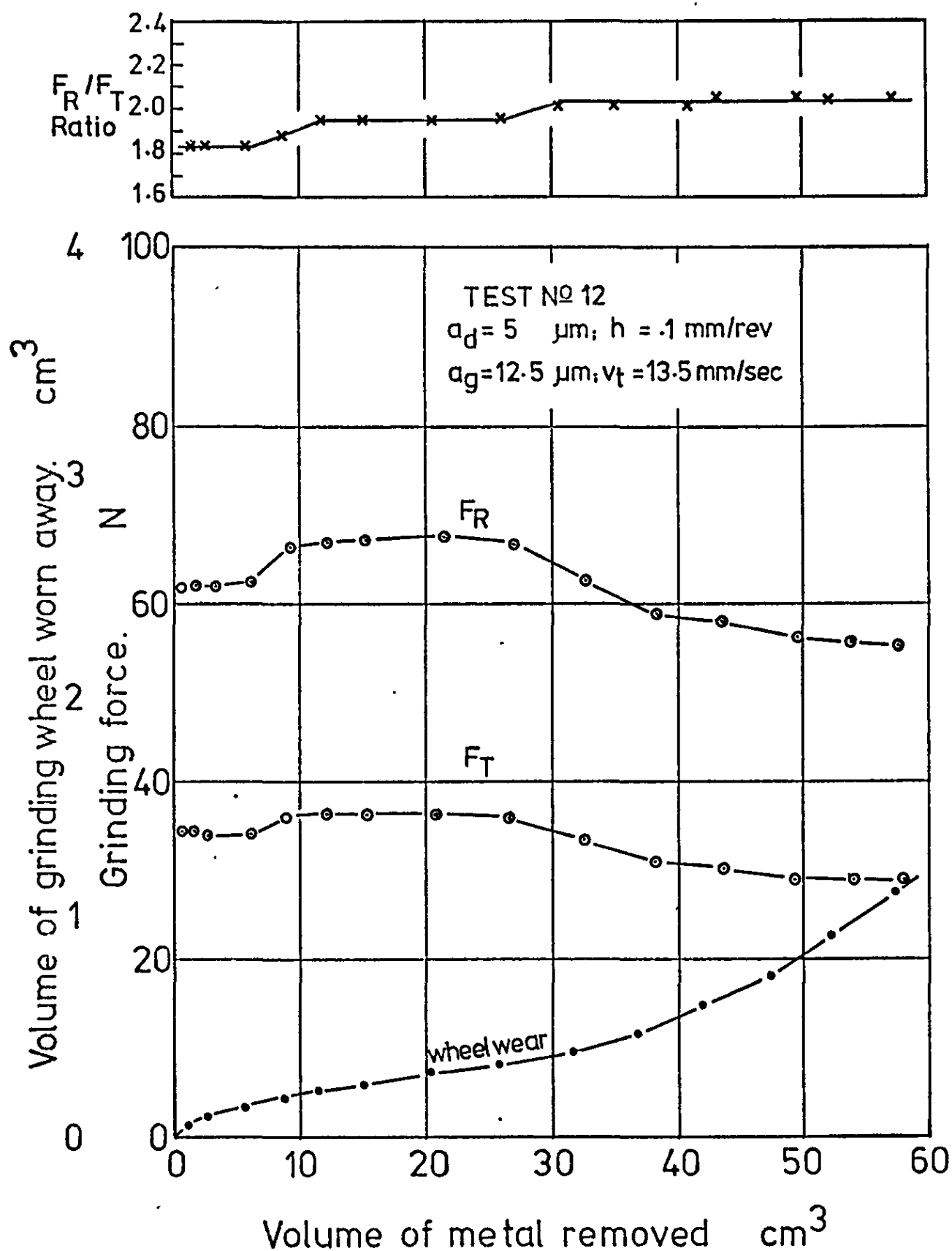


Fig.7.131 Variation of grinding force and wheel wear with volume of metal removed for a particular wheel dressing condition.

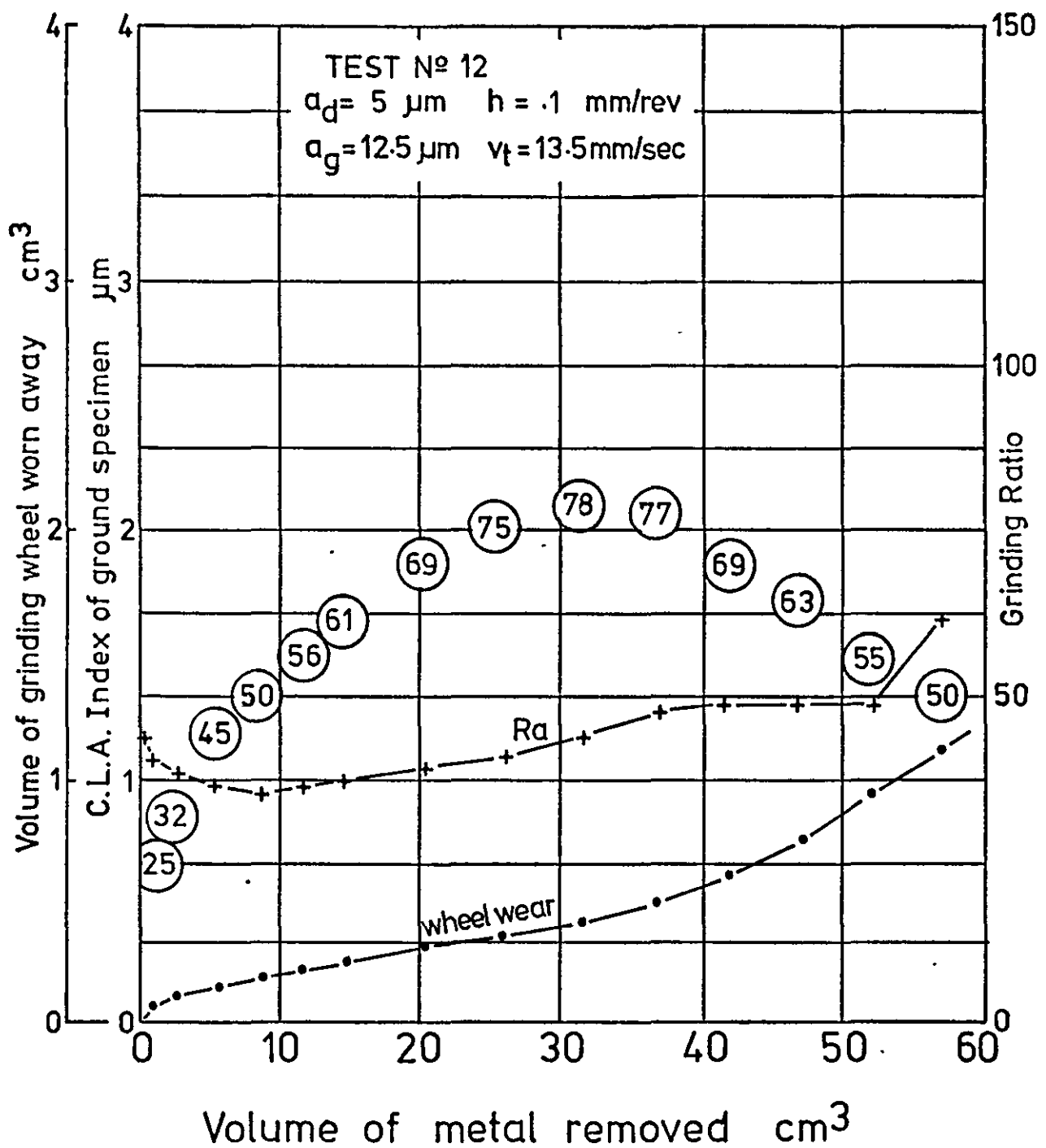


Fig.7.132 Variation of grinding wheel wear, workpiece surface roughness and grinding ratio with volume of metal removed for a particular wheel dressing condition.

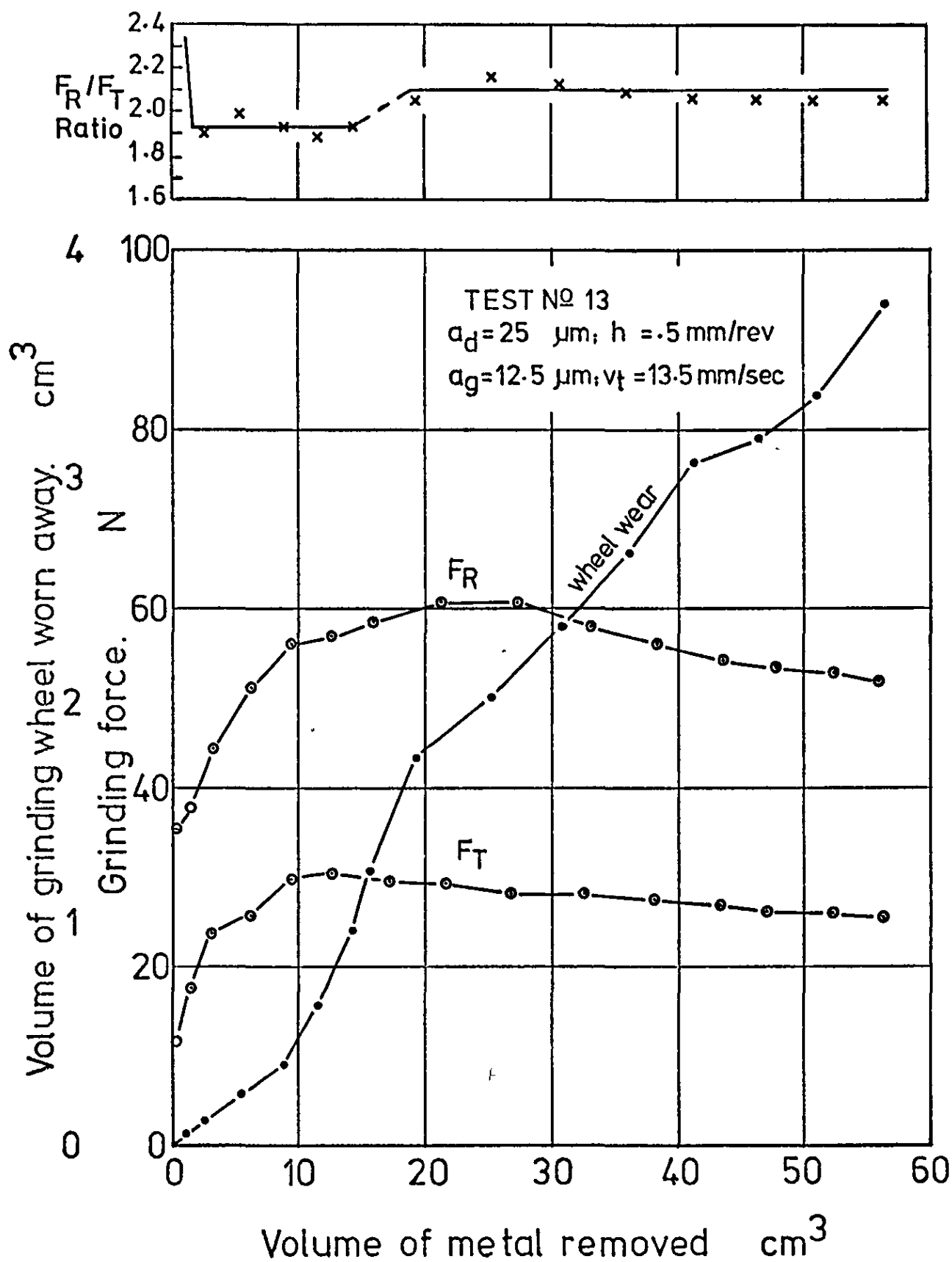


Fig.7.133 Variation of grinding force and wheel wear with volume of metal removed for a particular wheel dressing condition.

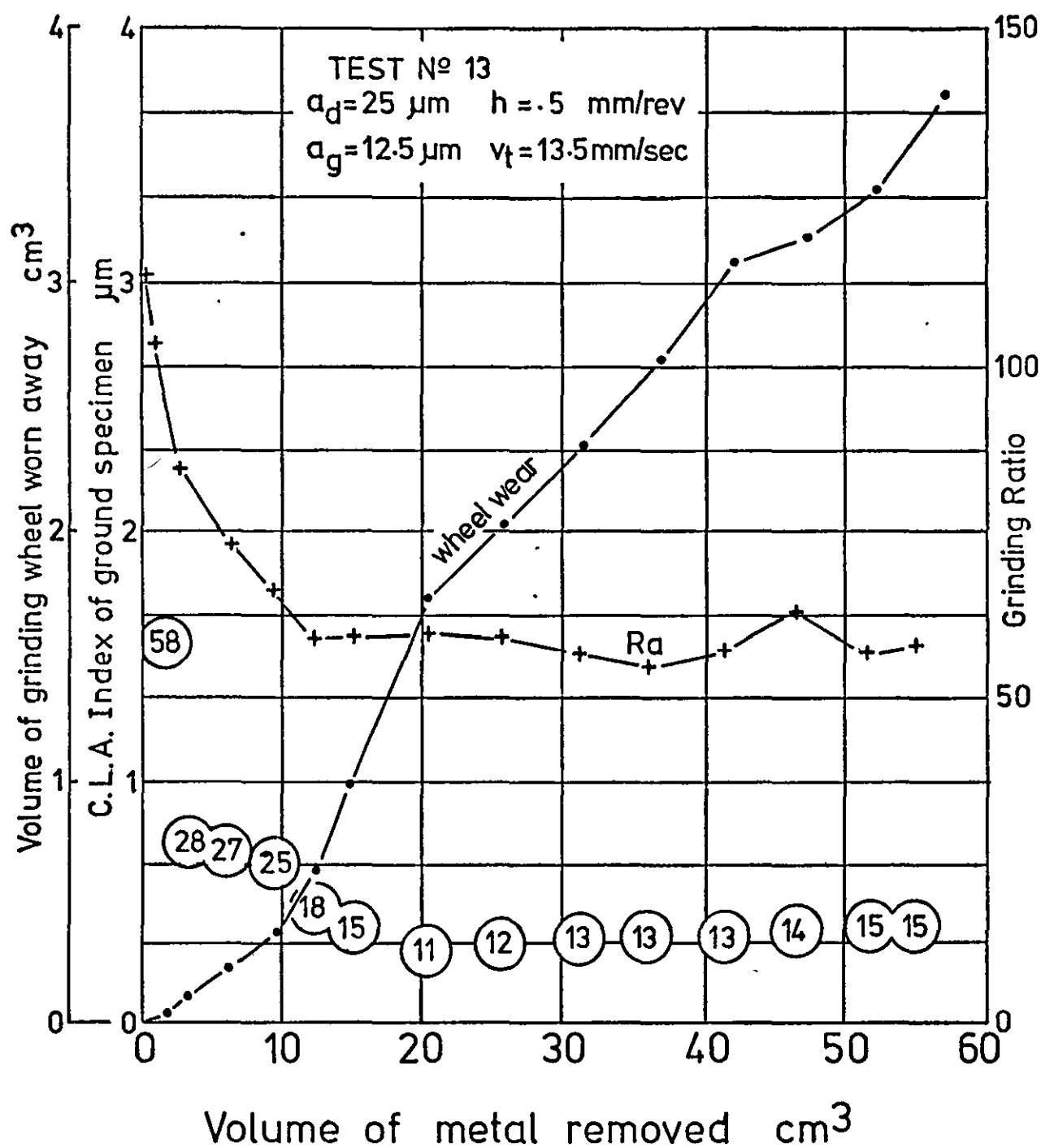


Fig.7.134 Variation of grinding wheel wear, workpiece surface roughness and grinding ratio with volume of metal removed for a particular wheel dressing condition.

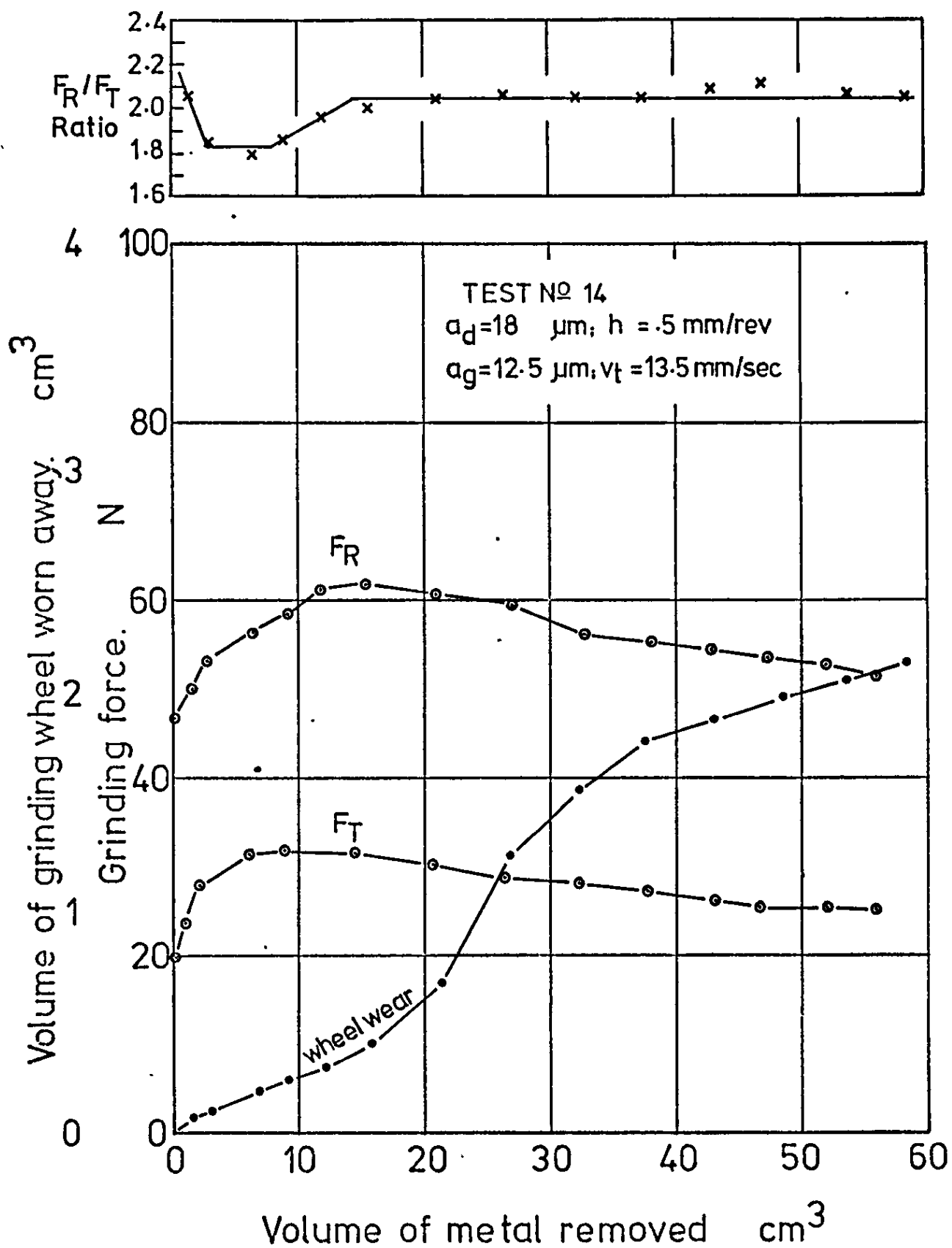


Fig.7.135 Variation of grinding force and wheel wear with volume of metal removed for a particular wheel dressing condition.

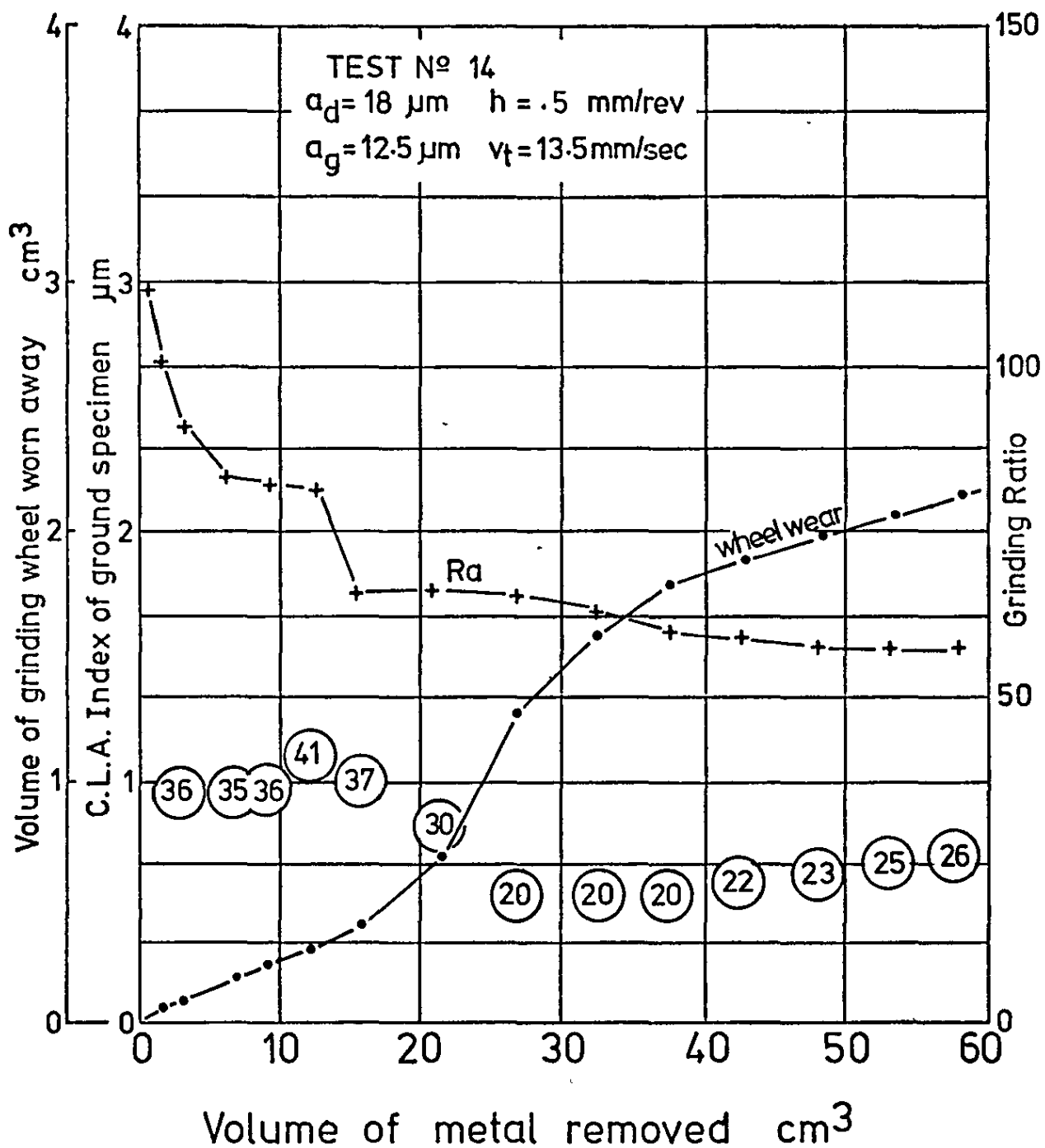


Fig.7.136 Variation of grinding wheel wear, workpiece surface roughness and grinding ratio with volume of metal removed for a particular wheel dressing condition.

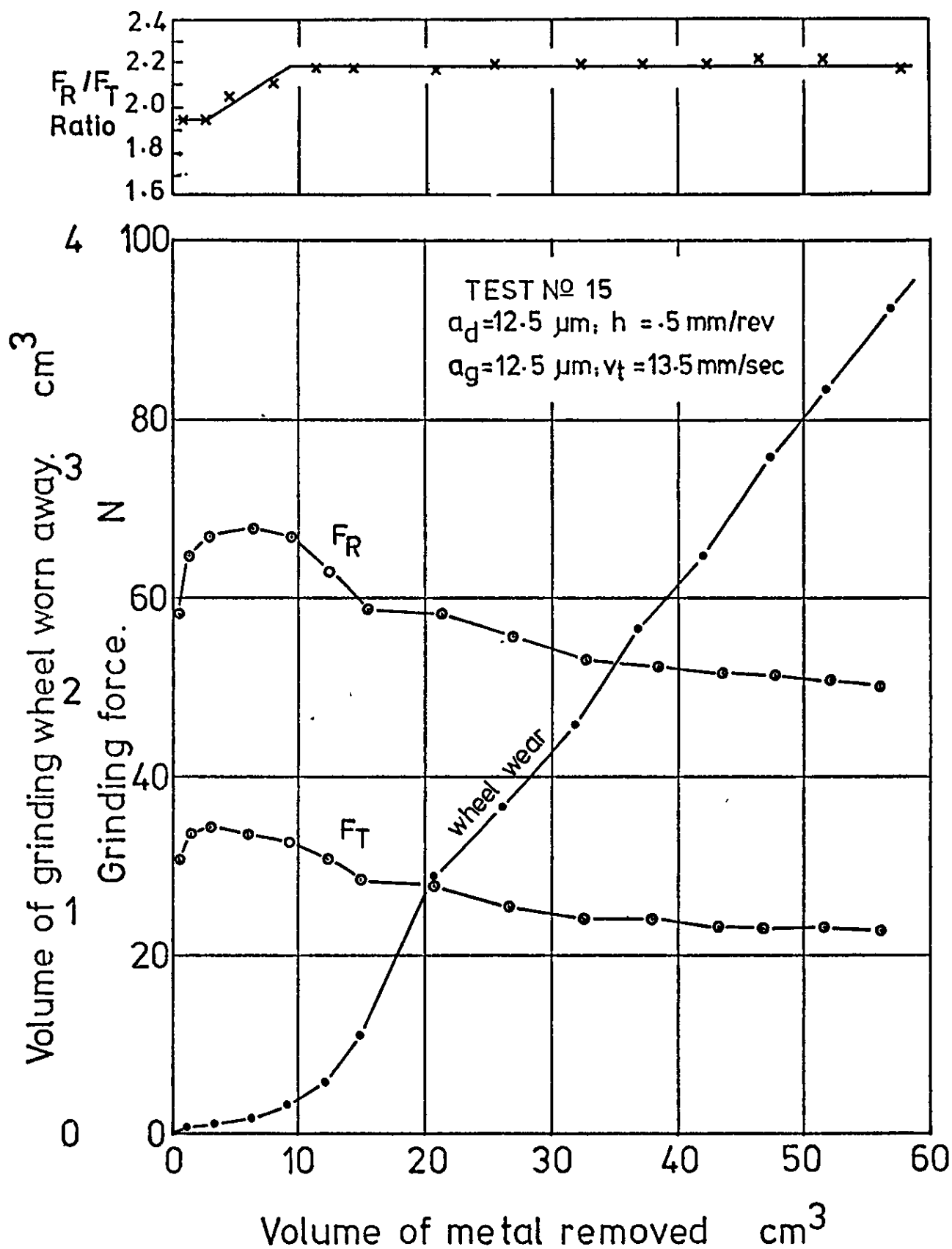


Fig.7.137 Variation of grinding force and wheel wear with volume of metal removed for a particular wheel dressing condition.

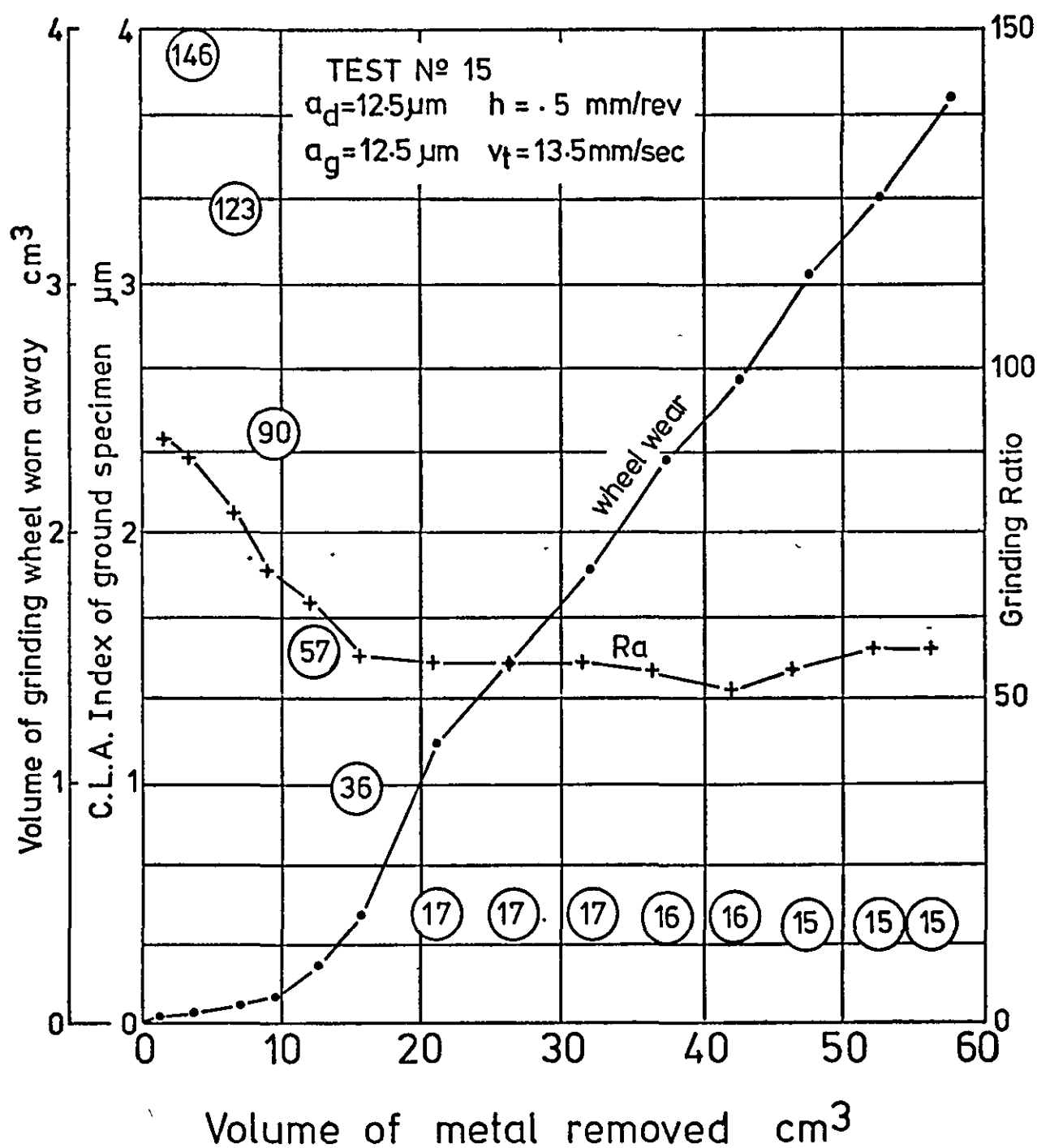


Fig. 7.138 Variation of grinding wheel wear, workpiece surface roughness and grinding ratio with volume of metal removed for a particular wheel dressing condition.

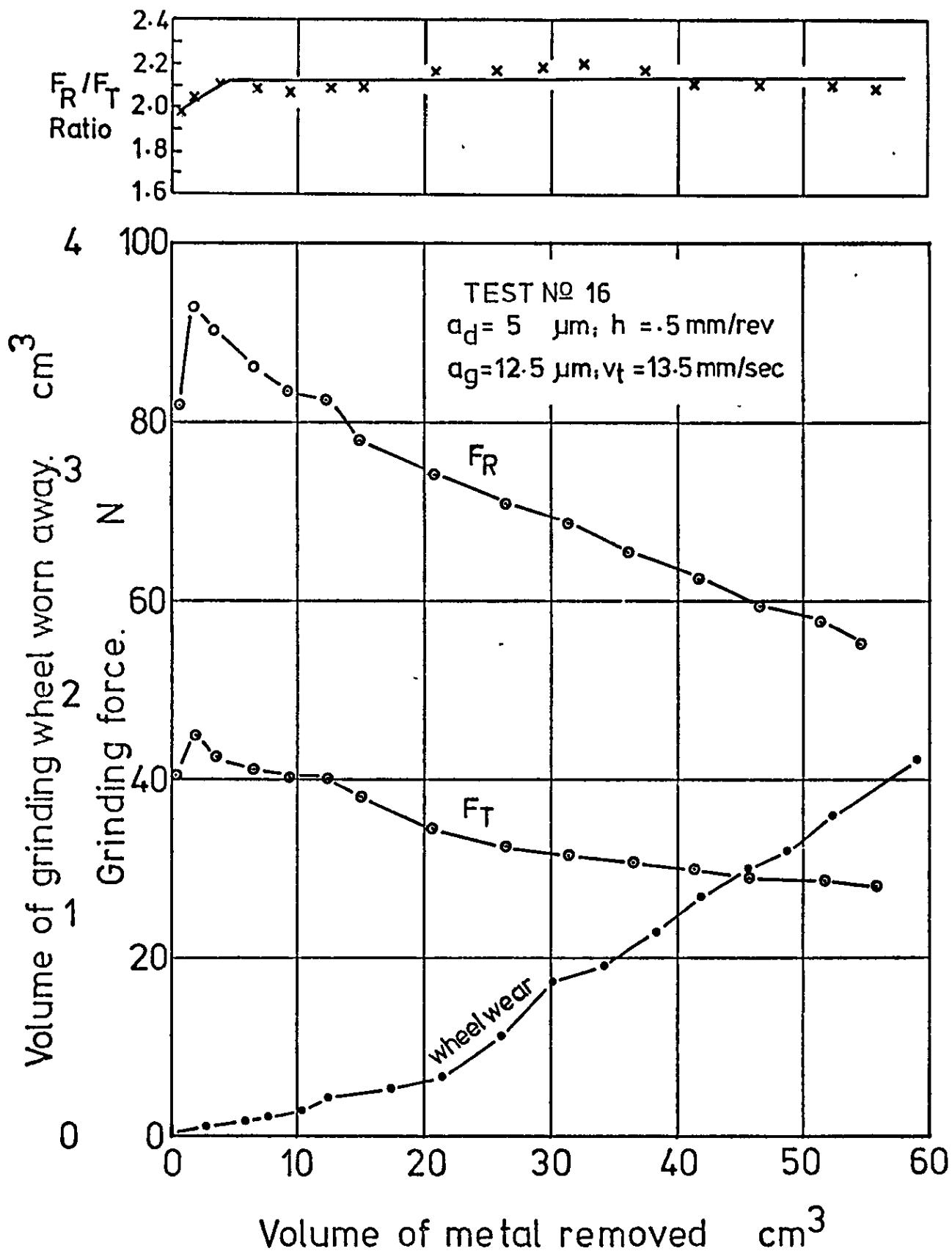


Fig. 7.139 Variation of grinding force and wheel wear with volume of metal removed for a particular wheel dressing condition.

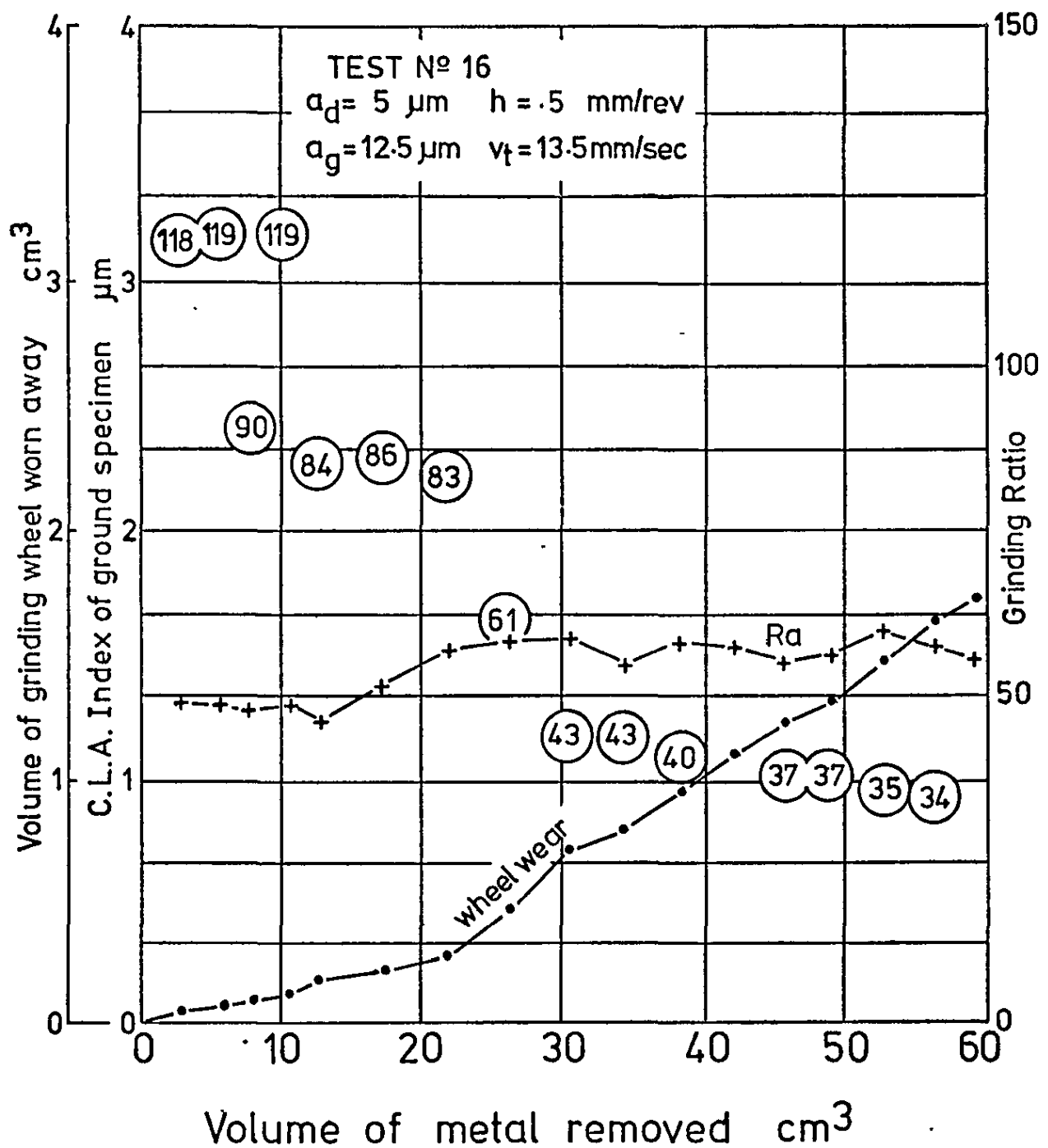


Fig. 7.140 Variation of grinding wheel wear, workpiece surface roughness and grinding ratio with volume of metal removed for a particular wheel dressing condition.

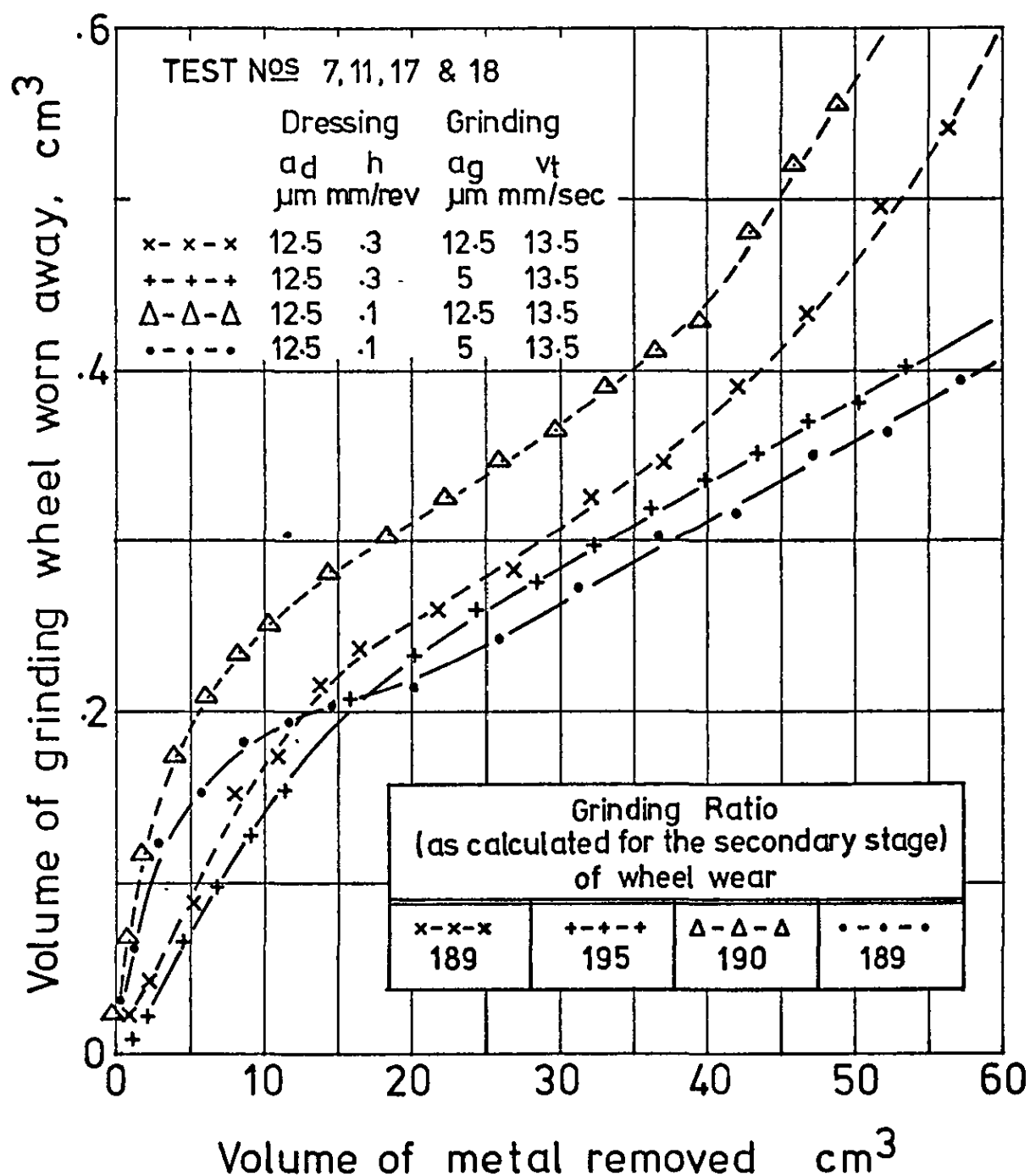


Fig. 7.141 Variation of grinding wheel wear with volume of metal removed for various wheel dressing and grinding conditions.

TEST N°17

 a_d h a_g v_t
 μm mm/rev μm mm/sec
 12.5 .3 5 13.5

TEST N°7

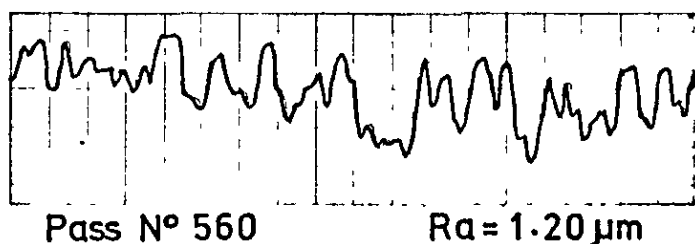
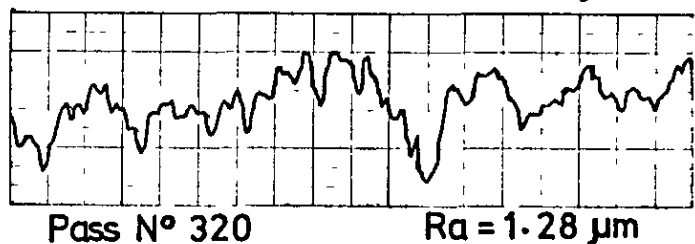
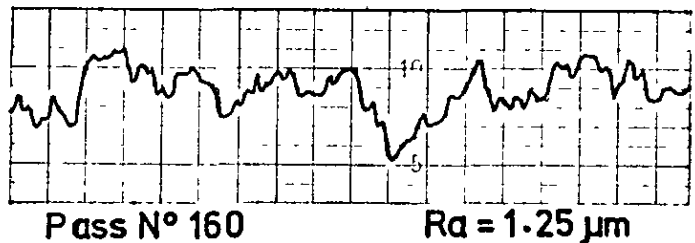
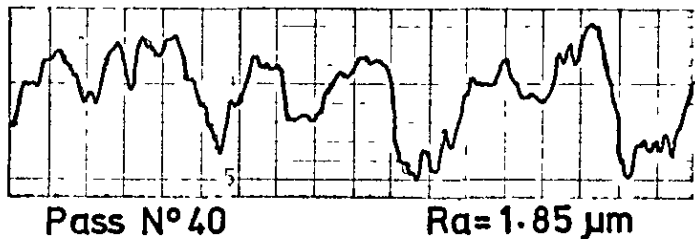
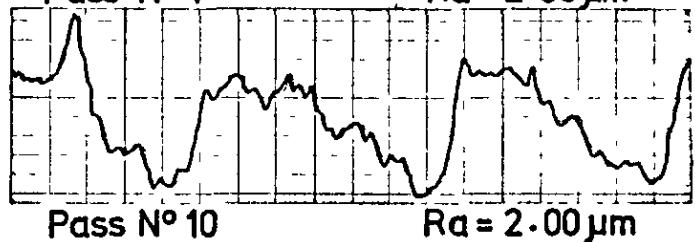
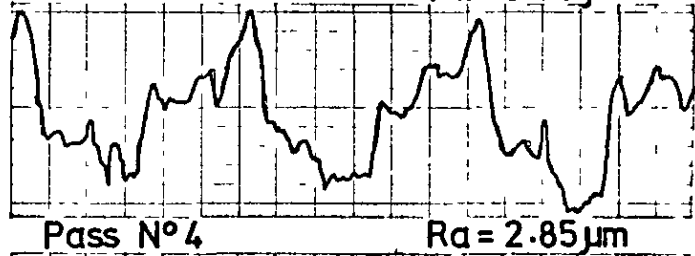
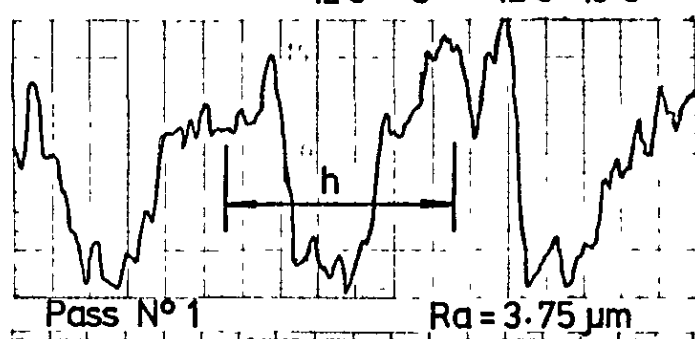
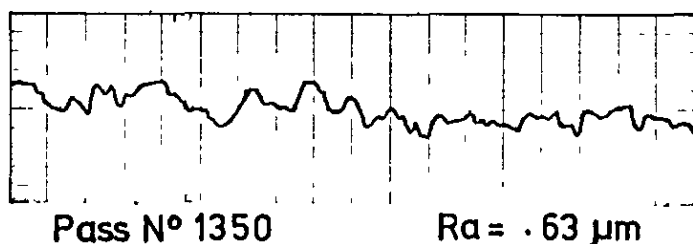
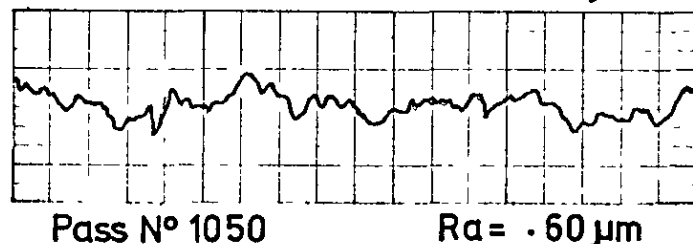
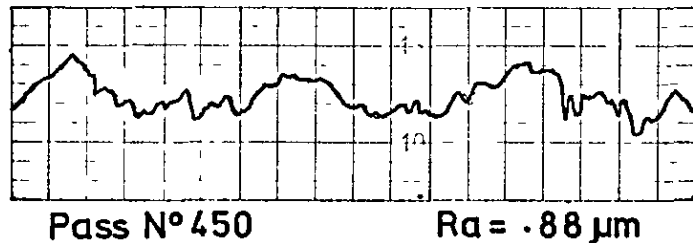
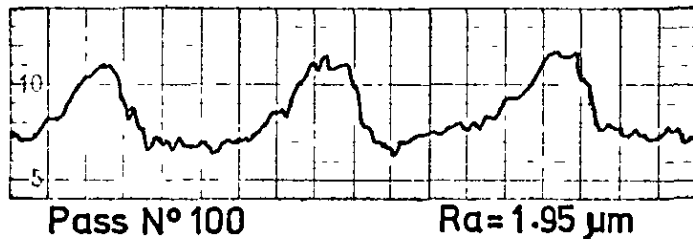
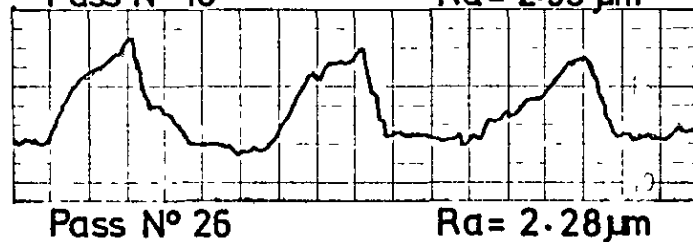
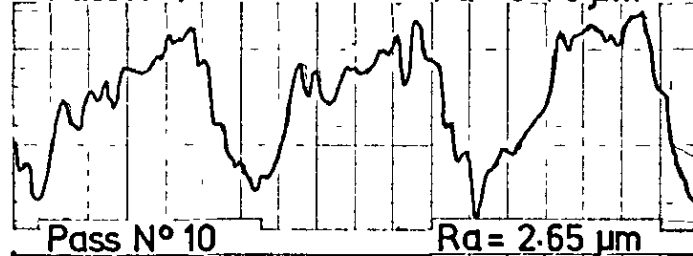
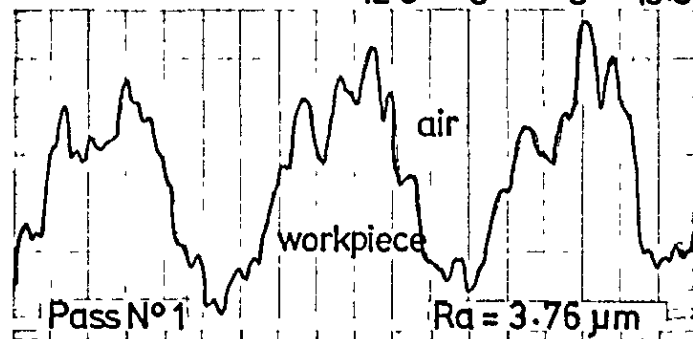
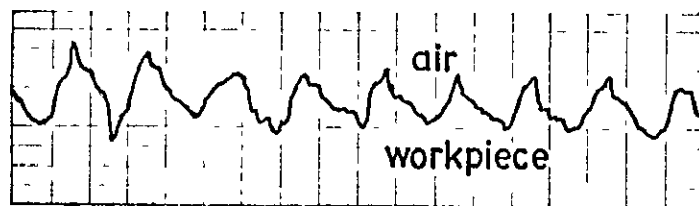
 a_d h a_g v_t
 μm mm/rev μm mm/sec
 12.5 .3 12.5 13.5


Fig. 7.142 "Taly surf" traces showing the variation of workpiece surface roughness for particular dressing and grinding conditions

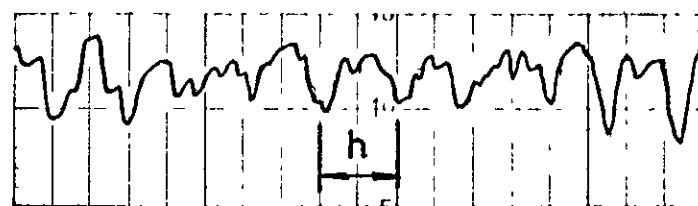
TEST N°18

 a_d h a_g v_t
 μm mm/rev μm mm/sec
 12.5 .1 5 13.5

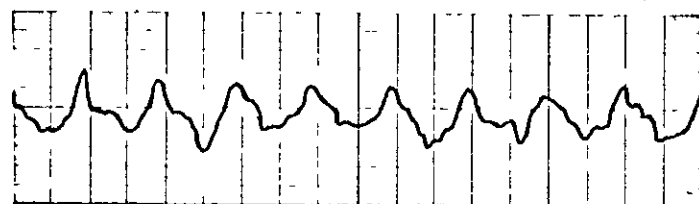
TEST N°11

 a_d h a_g v_t
 μm mm/rev μm mm/sec
 12.5 .1 12.5 13.5


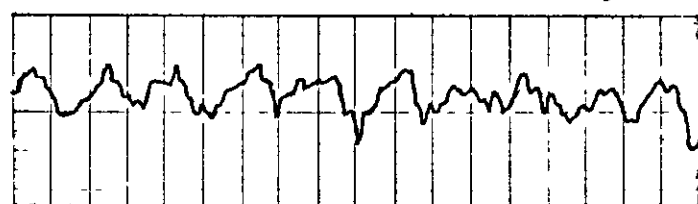
Pass N° 1

 $R_a = 1.35 \mu\text{m}$ 

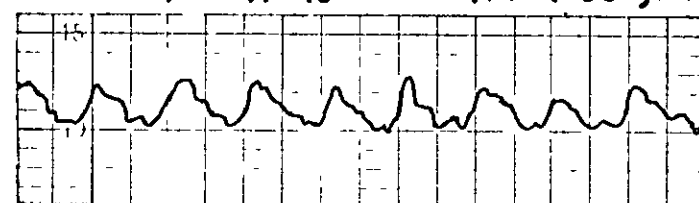
Pass N° 1

 $R_a = 1.35 \mu\text{m}$ 

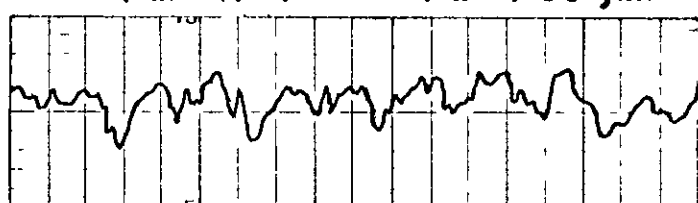
Pass N° 10

 $R_a = 1.05 \mu\text{m}$ 

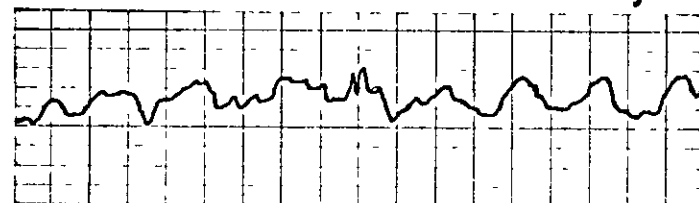
Pass N° 4

 $R_a = 1.08 \mu\text{m}$ 

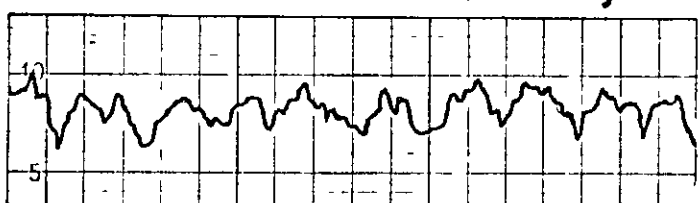
Pass N° 26

 $R_a = 0.85 \mu\text{m}$ 

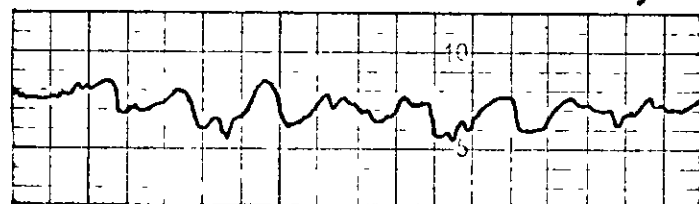
Pass N° 10

 $R_a = 0.98 \mu\text{m}$ 

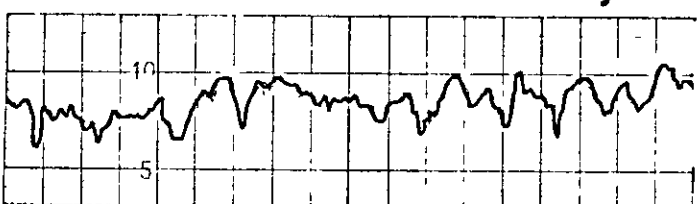
Pass N° 100

 $R_a = 0.75 \mu\text{m}$ 

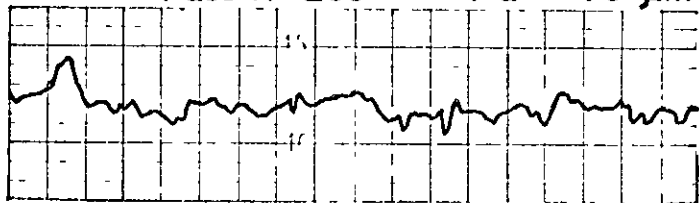
Pass N° 40

 $R_a = 0.95 \mu\text{m}$ 

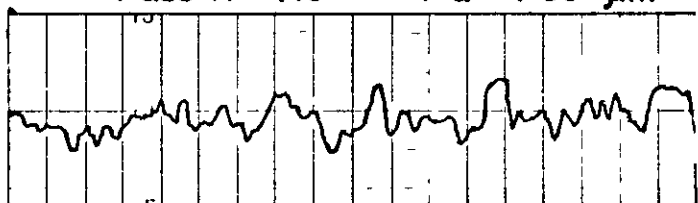
Pass N° 250

 $R_a = 0.70 \mu\text{m}$ 

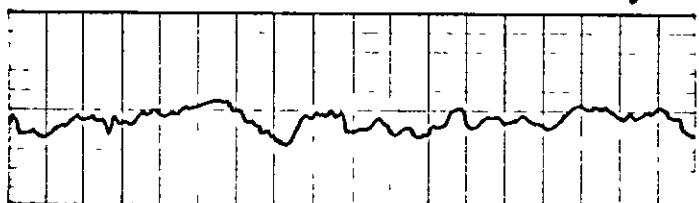
Pass N° 140

 $R_a = 1.00 \mu\text{m}$ 

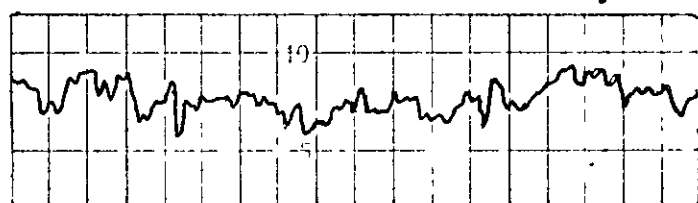
Pass N° 650

 $R_a = 0.73 \mu\text{m}$ 

Pass N° 340

 $R_a = 1.03 \mu\text{m}$ 

Pass N° 950

 $R_a = 0.63 \mu\text{m}$ 

Pass N° 540

 $R_a = 1.03 \mu\text{m}$

Fig. 7.143 "Talysurf" traces showing the variation of workpiece surface roughness for particular dressing and grinding conditions

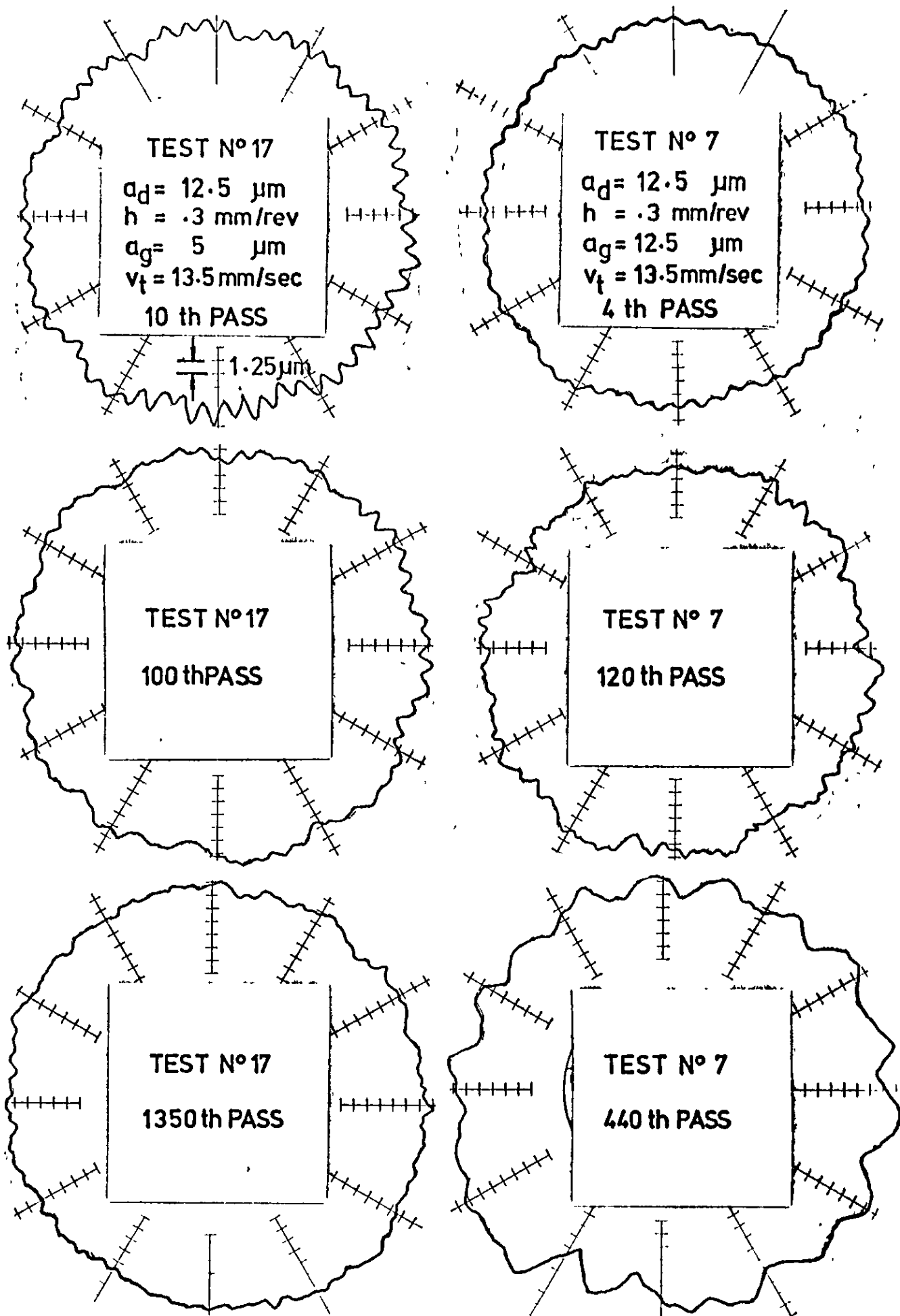


Fig. 7.144 Talyrond" traces showing the variation of workpiece circularity with the number of grinding passes

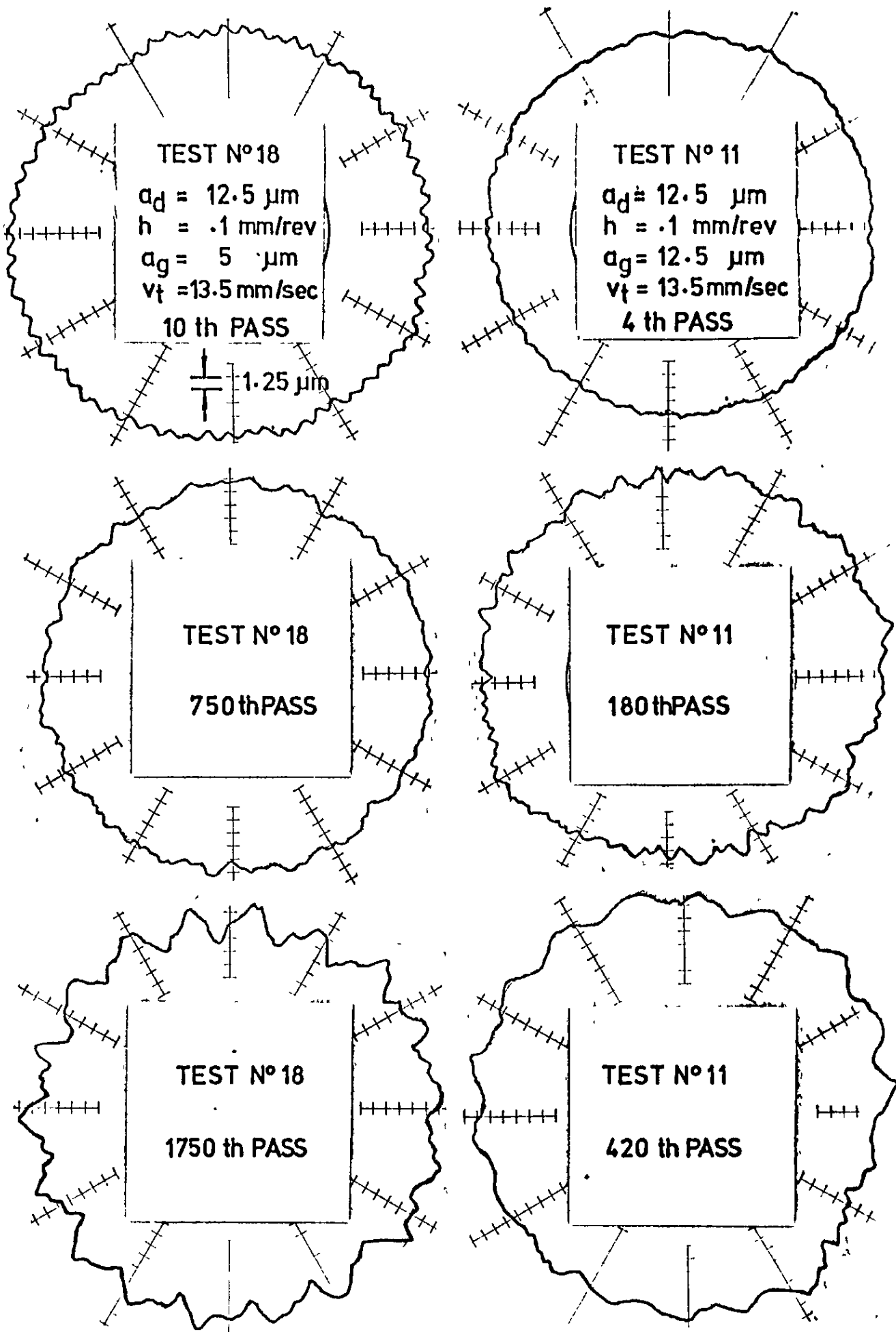


Fig.7.145 "Talyrond" traces showing the variation of workpiece circularity with the number of grinding passes

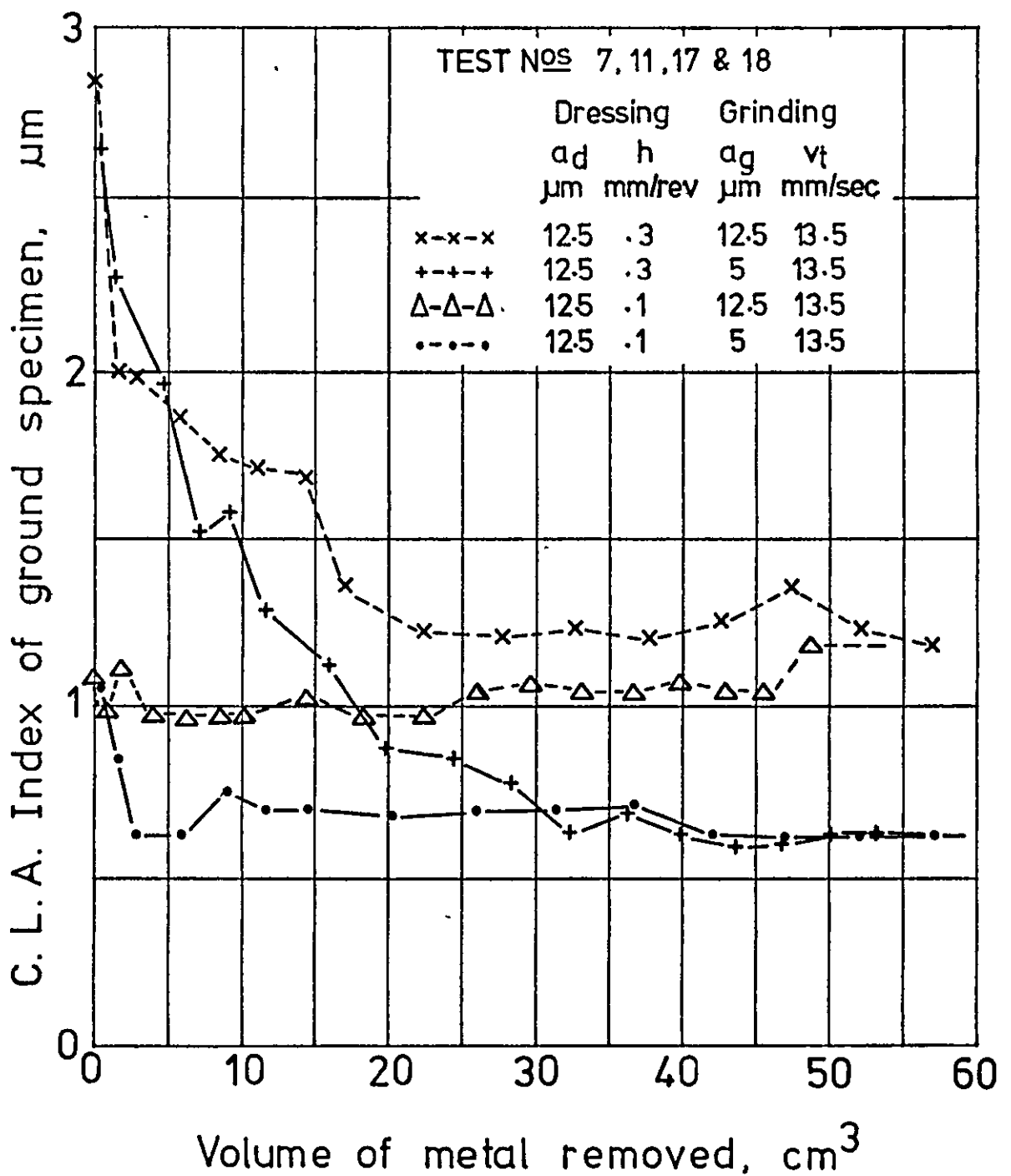
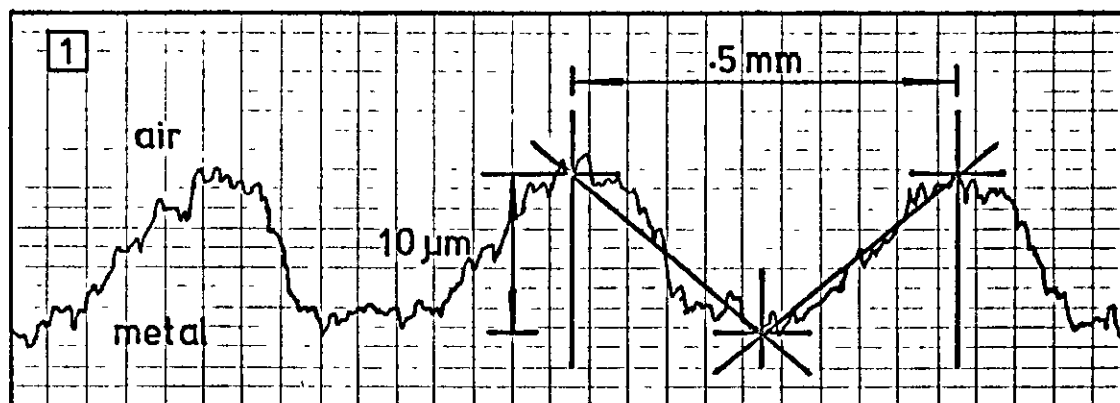
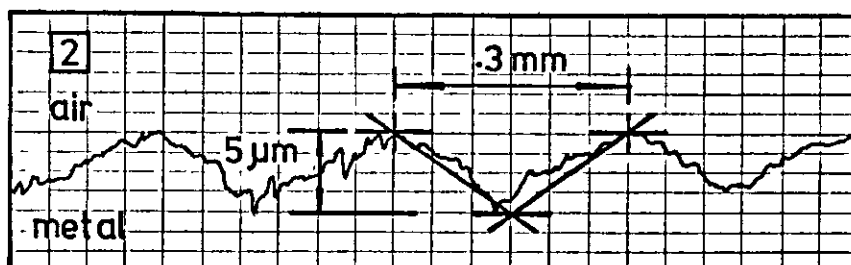


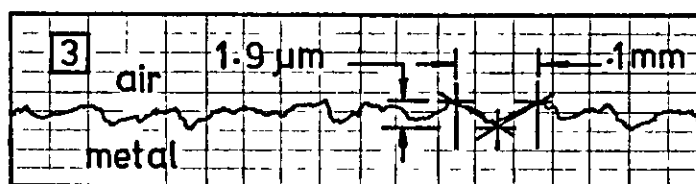
Fig. 7.146 Variation of workpiece surface roughness with volume of metal removed for various wheel dressing and grinding conditions.



"Talysurf"
traces of
three
workpiece
surfaces



Vertical Mag.
 $1.25 \mu\text{m}/\text{scale division}$
Horizontal Mag.
 $50 \mu\text{m}/\text{scale division}$



| Dressing Cross-Feed | .5 mm/rev | .3 mm/rev | .1 mm/rev |
|---------------------|-----------|-----------|-----------|
| Profile Number | 1 | 2 | 3 |

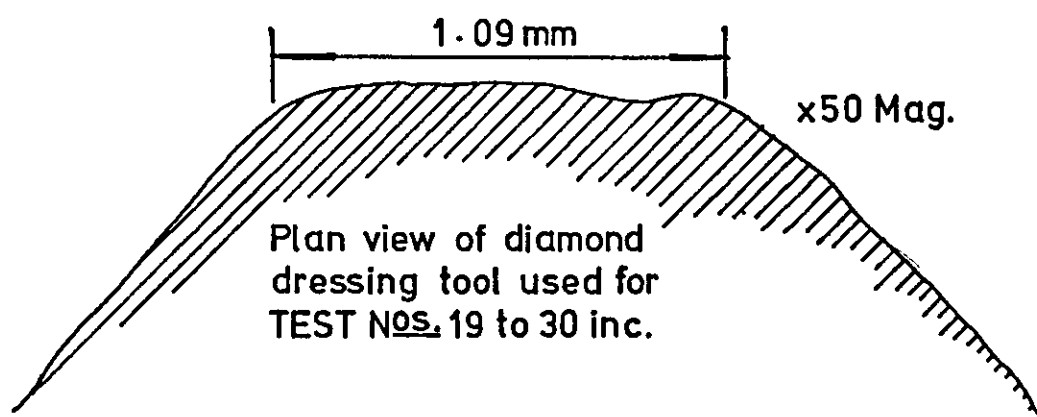
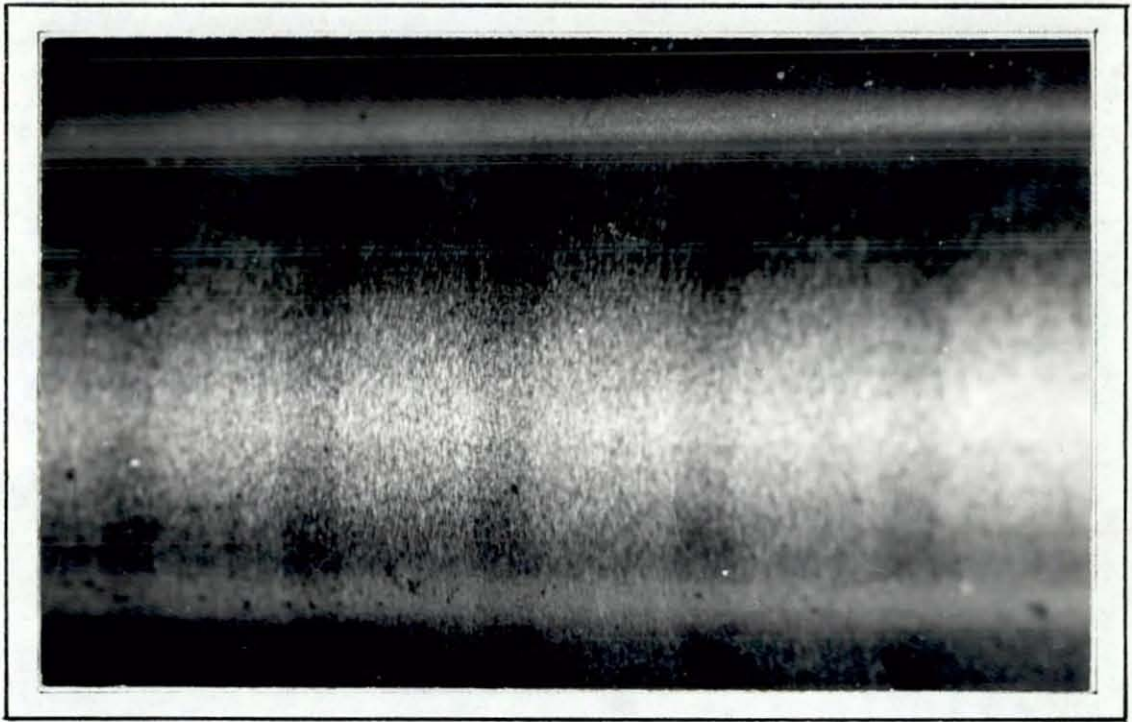
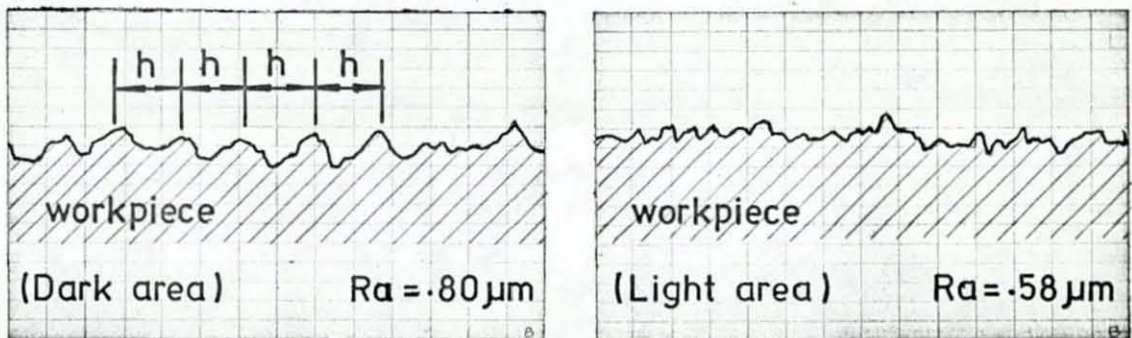


Fig. 7.147 "Talysurf" traces showing the influence of the dressing-feed on workpiece surface roughness, when "fine" grinding under conditions giving "no-interference."

NB. In the first instance, each profile can be approximated to a series of small triangles.



View of a cylindrically traverse ground surface showing the interference effect due to overlapping profiles



Talysurf traces of surface roughness

Fig. 7.148 An actual view of a cylindrically traverse ground workpiece surface with two Talysurf traces showing the changes of surface roughness caused by grinding overlap.

| v _t mm/sec | | | | | |
|----------------------------|--|-----------------------------------|--|-----------------------------------|--|
| 14 | | 12 | | 10 | |
| 7.5 | | 5 | | | |
| A+b=1.93 | | A+b=2.25 | | A+b=2.70 | |
| A+b=3.60 | | A+b=5.40 | | | |
| (1) — | | (1-b)v _t /n = (A-2) | | (1-b)v _t /n = (A-2) | |
| (2) bv _t /n = 1 | | bv _t /n=(A-1) | | bv _t /n=(A-1) | |
| COMMON TABLE | | | | | |
| h = .5 mm/rev | | | | | |
| (1) E = zero | | E = zero | | E = zero | |
| E = .1100 | | E = .3300 | | .3876 .4433 | |
| 10 Ra=2.50μm | | Ra=2.50μm | | Ra=2.50μm | |
| 4 Ra=1.00μm | | Ra=1.00μm | | Ra=1.00μm | |
| (2) E = .4433 | | E = .1100 | | E = .2767 | |
| E = .1100 | | E = .2200 | | E = .2733 | |
| .3300 .3867 | | .4433 | | | |
| 10 Ra=2.07μm | | Ra=2.04μm | | Ra=1.28μm | |
| 4 Ra=.83μm | | Ra=.82μm | | Ra=.51μm | |
| h = .3 mm/rev | | | | | |
| (1) E = zero | | E = zero | | E = zero | |
| E = .2660 | | E = .0993 | | .1987 .2980 | |
| 5 Ra=1.25μm | | Ra=1.25μm | | Ra=1.25μm | |
| 3.8 Ra=.95μm | | Ra=.95μm | | Ra=.95μm | |
| (2) E = .0993 | | E = .2660 | | E = .1327 | |
| E = .2320 | | E = .2660 | | E = .0973 | |
| .0993 .1987 | | .2980 | | | |
| 5 Ra=.78μm | | Ra=1.04μm | | Ra=.64μm | |
| 3.8 Ra=.59μm | | Ra=.79μm | | Ra=.49μm | |
| h = .1 mm/rev | | | | | |
| (1) E = zero | | E = zero | | E = zero | |
| E = .0220 | | E = .0107 | | .0553 .0660 | |
| 1.9 Ra=.48μm | | Ra=.48μm | | Ra=.48μm | |
| 1.3 Ra=.31μm | | Ra=.31μm | | Ra=.31μm | |
| (2) E = .0553 | | E = .0220 | | E = .0887 | |
| E = .0220 | | E = .0440 | | E = .0107 | |
| .0213 .0553 | | .0660 | | | |
| 1.9 Ra=.24μm | | Ra=.39μm | | Ra=.40μm | |
| 1.3 Ra=.17μm | | Ra=.27μm | | Ra=.27μm | |

Fig.7.149 Table of calculated parameters for grinding tests 19 to 30 inc..

TEST N° 19

$a = 25 \mu\text{m}$; $a^* = 10 \mu\text{m}$
 $h = .5 \text{ mm/rev}$; $v_t = 14 \text{ mm/sec}$
 $Ra = 2.00 \mu\text{m}$ $E/h = .88$

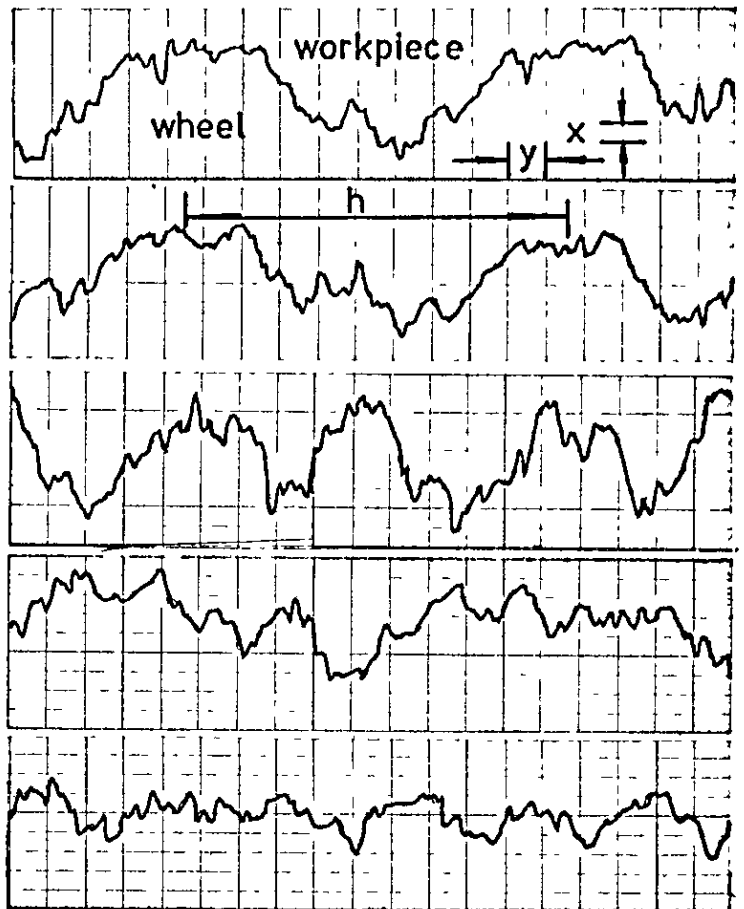
$a = 25 \mu\text{m}$; $a^* = 10 \mu\text{m}$
 $h = .5 \text{ mm/rev}$; $v_t = 12 \text{ mm/sec}$
 $Ra = 2.15 \mu\text{m}$ $E/h = .22$

$a = 25 \mu\text{m}$; $a^* = 10 \mu\text{m}$
 $h = .5 \text{ mm/rev}$; $v_t = 10 \text{ mm/sec}$
 $Ra = 2.00 \mu\text{m}$ $E/h = .55$

$a = 25 \mu\text{m}$; $a^* = 10 \mu\text{m}$
 $h = .5 \text{ mm/rev}$; $v_t = 7.5 \text{ mm/sec}$
 $Ra = 1.38 \mu\text{m}$

$a = 25 \mu\text{m}$; $a^* = 10 \mu\text{m}$
 $h = .5 \text{ mm/rev}$; $v_t = 5 \text{ mm/sec}$
 $Ra = 1.03 \mu\text{m}$

$x = 1.25 \mu\text{m}$; $y = 50 \mu\text{m}$



TEST N° 22

$a = 5 \mu\text{m}$; $a^* = 4 \mu\text{m}$
 $h = .5 \text{ mm/rev}$; $v_t = 14 \text{ mm/sec}$
 $Ra = 1.20 \mu\text{m}$ $E/h = .88$

$a = 5 \mu\text{m}$; $a^* = 4 \mu\text{m}$
 $h = .5 \text{ mm/rev}$; $v_t = 12 \text{ mm/sec}$
 $Ra = 1.18 \mu\text{m}$ $E/h = .22$

$a = 5 \mu\text{m}$; $a^* = 4 \mu\text{m}$
 $h = .5 \text{ mm/rev}$; $v_t = 10 \text{ mm/sec}$
 $Ra = .70 \mu\text{m}$ $E/h = .55$

$a = 5 \mu\text{m}$; $a^* = 4 \mu\text{m}$
 $h = .5 \text{ mm/rev}$; $v_t = 7.5 \text{ mm/sec}$
 $Ra = .65 \mu\text{m}$

$a = 5 \mu\text{m}$; $a^* = 4 \mu\text{m}$
 $h = .5 \text{ mm/rev}$; $v_t = 5 \text{ mm/sec}$
 $Ra = .55 \mu\text{m}$

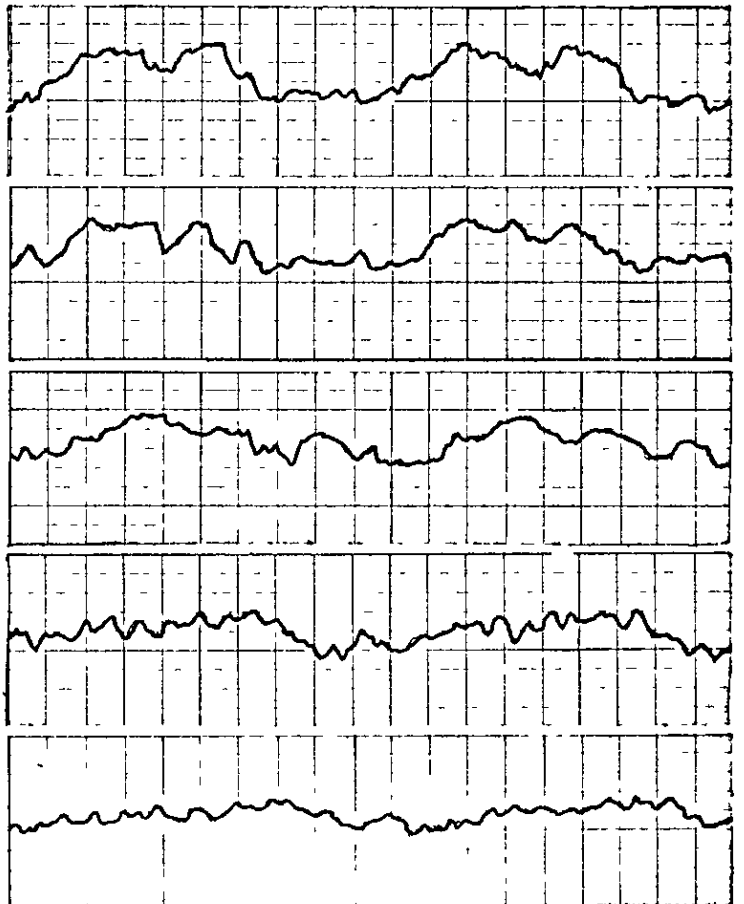


Fig. 7.150 Variation of workpiece surface roughness with grinding traverse rate for fine grinding

TEST N° 23

$a = 25 \mu\text{m}$; $a^* = 5 \mu\text{m}$
 $h = .3 \text{ mm/rev}$; $v_t = 14 \text{ mm/sec}$
 $Ra = 1.13 \mu\text{m}$ $E/h = .33$

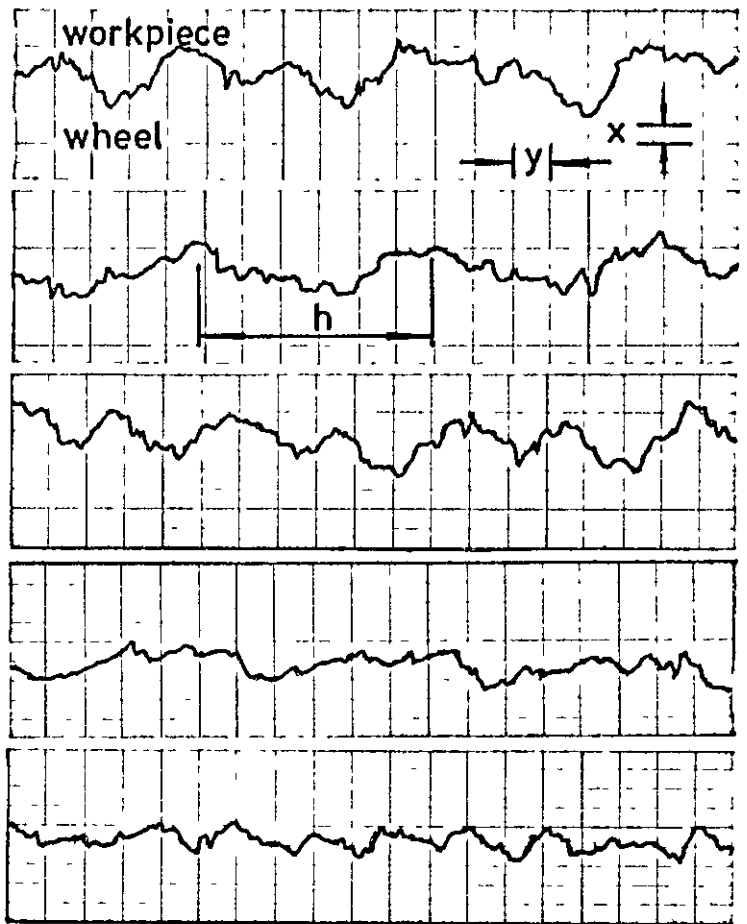
$a = 25 \mu\text{m}$; $a^* = 5 \mu\text{m}$
 $h = .3 \text{ mm/rev}$; $v_t = 12 \text{ mm/sec}$
 $Ra = .95 \mu\text{m}$ $E/h = .88$

$a = 25 \mu\text{m}$; $a^* = 5 \mu\text{m}$
 $h = .3 \text{ mm/rev}$; $v_t = 10 \text{ mm/sec}$
 $Ra = .98 \mu\text{m}$ $E/h = .44$

$a = 25 \mu\text{m}$; $a^* = 5 \mu\text{m}$
 $h = .3 \text{ mm/rev}$; $v_t = 7.5 \text{ mm/sec}$
 $Ra = .75 \mu\text{m}$

$a = 25 \mu\text{m}$; $a^* = 5 \mu\text{m}$
 $h = .3 \text{ mm/rev}$; $v_t = 5 \text{ mm/sec}$
 $Ra = .53 \mu\text{m}$

$x = 1.25 \mu\text{m}$; $y = 50 \mu\text{m}$



TEST N° 26

$a = 5 \mu\text{m}$; $a^* = 3.8 \mu\text{m}$
 $h = .3 \text{ mm/rev}$; $v_t = 14 \text{ mm/sec}$
 $Ra = .75 \mu\text{m}$ $E/h = .33$

$a = 5 \mu\text{m}$; $a^* = 3.8 \mu\text{m}$
 $h = .3 \text{ mm/rev}$; $v_t = 12 \text{ mm/sec}$
 $Ra = .78 \mu\text{m}$ $E/h = .88$

$a = 5 \mu\text{m}$; $a^* = 3.8 \mu\text{m}$
 $h = .3 \text{ mm/rev}$; $v_t = 10 \text{ mm/sec}$
 $Ra = .78 \mu\text{m}$ $E/h = .44$

$a = 5 \mu\text{m}$; $a^* = 3.8 \mu\text{m}$
 $h = .3 \text{ mm/rev}$; $v_t = 7.5 \text{ mm/sec}$
 $Ra = .63 \mu\text{m}$

$a = 5 \mu\text{m}$; $a^* = 3.8 \mu\text{m}$
 $h = .3 \text{ mm/rev}$; $v_t = 5 \text{ mm/sec}$
 $Ra = .53 \mu\text{m}$

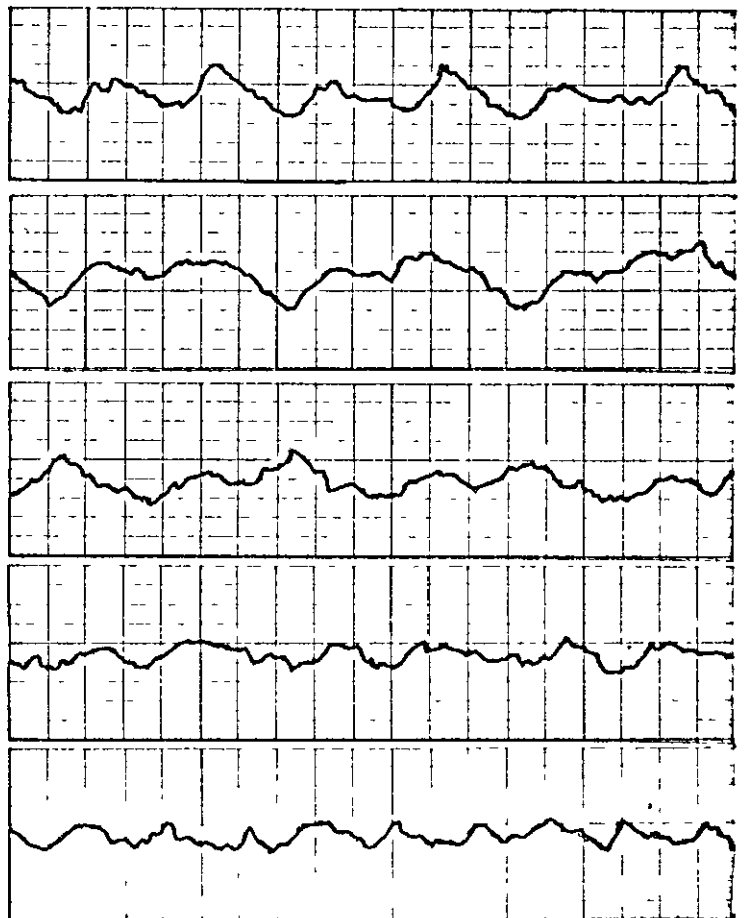


Fig. 7.151 Variation of workpiece surface roughness with grinding traverse rate for fine grinding

TEST N° 27

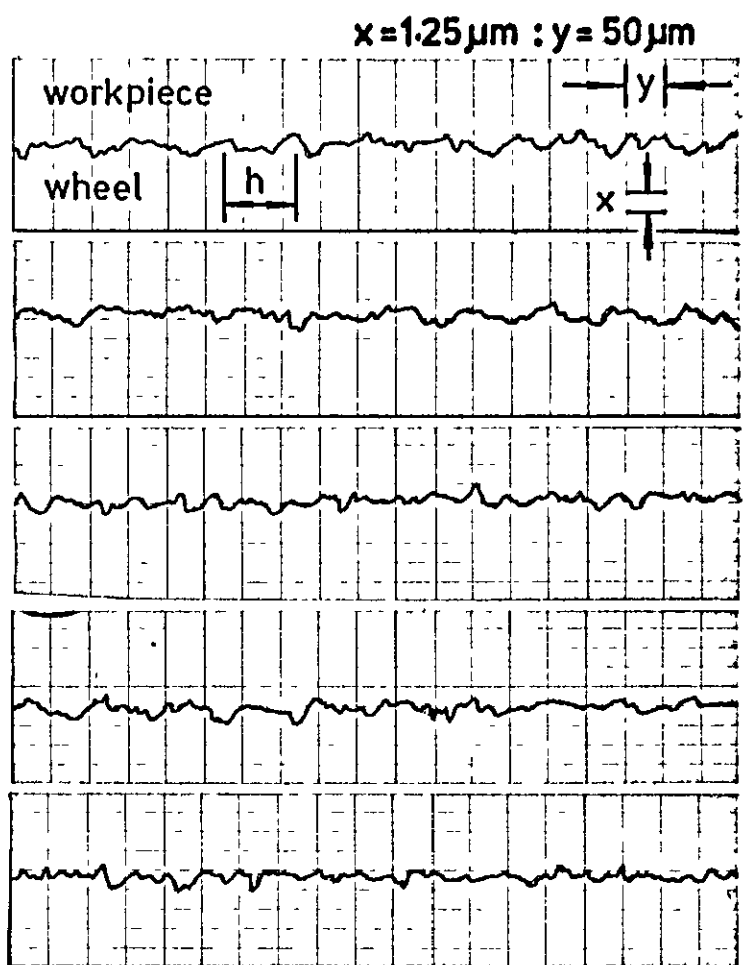
$a = 25 \mu\text{m}$; $a^* = 1.9 \mu\text{m}$
 $h = .1 \text{ mm/rev}$, $v_t = 14 \text{ mm/sec}$
 $Ra = .38 \mu\text{m}$ $E/h = .55$

$a = 25 \mu\text{m}$; $a^* = 1.9 \mu\text{m}$
 $h = .1 \text{ mm/rev}$, $v_t = 12 \text{ mm/sec}$
 $Ra = .38 \mu\text{m}$ $E/h = .22$

$a = 25 \mu\text{m}$; $a^* = 1.9 \mu\text{m}$
 $h = .1 \text{ mm/rev}$, $v_t = 10 \text{ mm/sec}$
 $Ra = .35 \mu\text{m}$ $E/h = .88$

$a = 25 \mu\text{m}$; $a^* = 1.9 \mu\text{m}$
 $h = .1 \text{ mm/rev}$, $v_t = 7.5 \text{ mm/sec}$
 $Ra = .33 \mu\text{m}$

$a = 25 \mu\text{m}$; $a^* = 1.9 \mu\text{m}$
 $h = .1 \text{ mm/rev}$, $v_t = 5 \text{ mm/sec}$
 $Ra = .30 \mu\text{m}$



TEST N° 30

$a = 5 \mu\text{m}$; $a^* = 1.3 \mu\text{m}$
 $h = .1 \text{ mm/rev}$, $v_t = 14 \text{ mm/sec}$
 $Ra = .30 \mu\text{m}$ $E/h = .55$

$a = 5 \mu\text{m}$; $a^* = 1.3 \mu\text{m}$
 $h = .1 \text{ mm/rev}$, $v_t = 12 \text{ mm/sec}$
 $Ra = .30 \mu\text{m}$ $E/h = .22$

$a = 5 \mu\text{m}$; $a^* = 1.3 \mu\text{m}$
 $h = .1 \text{ mm/rev}$, $v_t = 10 \text{ mm/sec}$
 $Ra = .25 \mu\text{m}$ $E/h = .88$

$a = 5 \mu\text{m}$; $a^* = 1.3 \mu\text{m}$
 $h = .1 \text{ mm/rev}$, $v_t = 7.5 \text{ mm/sec}$
 $Ra = .23 \mu\text{m}$

$a = 5 \mu\text{m}$; $a^* = 1.3 \mu\text{m}$
 $h = .1 \text{ mm/rev}$, $v_t = 5 \text{ mm/sec}$
 $Ra = .20 \mu\text{m}$

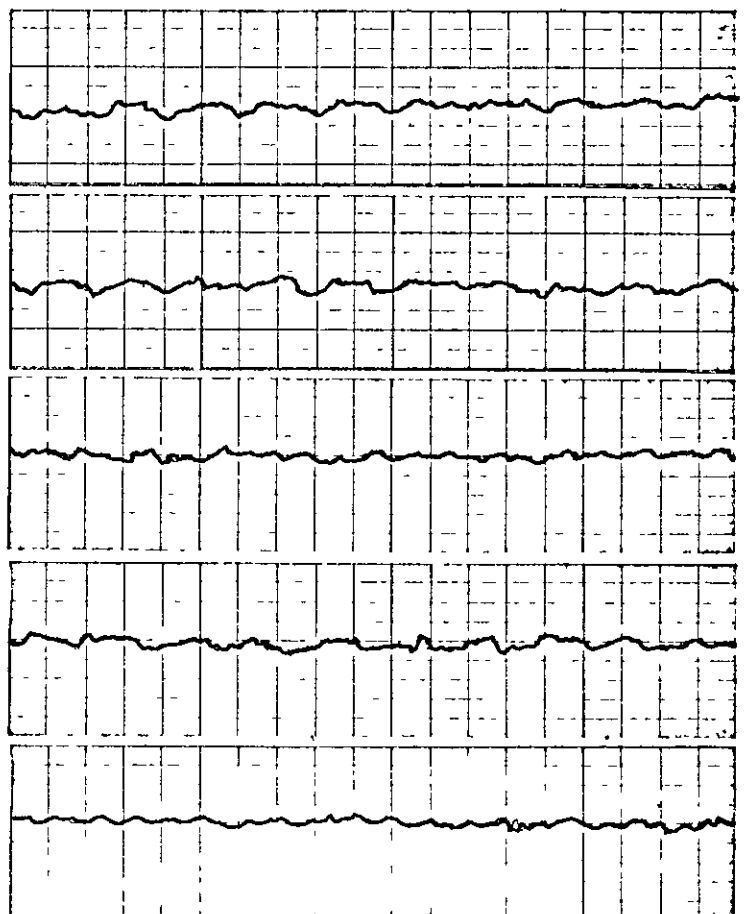


Fig. 7.152 Variation of workpiece surface roughness with grinding traverse rate for fine grinding

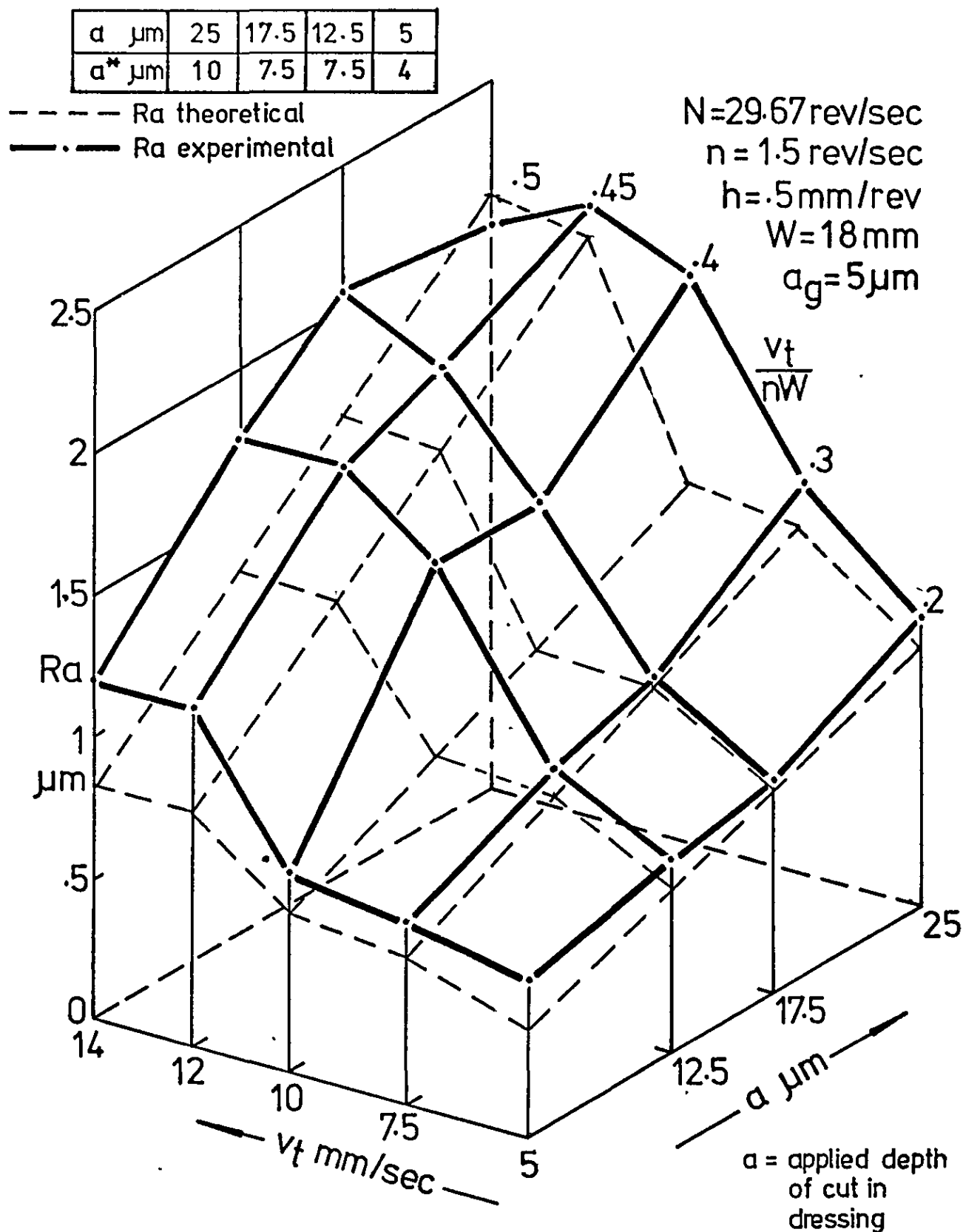


Fig.7.153 Variation of workpiece surface roughness R_a , for changes in the parameters v_t and a (dressing), N, n, W, a (grinding) and h remaining constant

| | | | | |
|----------------------------|----|------|------|-----|
| $a \text{ } \mu\text{m}$ | 25 | 17.5 | 12.5 | 5 |
| $a^* \text{ } \mu\text{m}$ | 5 | 5 | 3.8 | 3.8 |

- - - - - R_a theoretical
 — — — — — R_a experimental

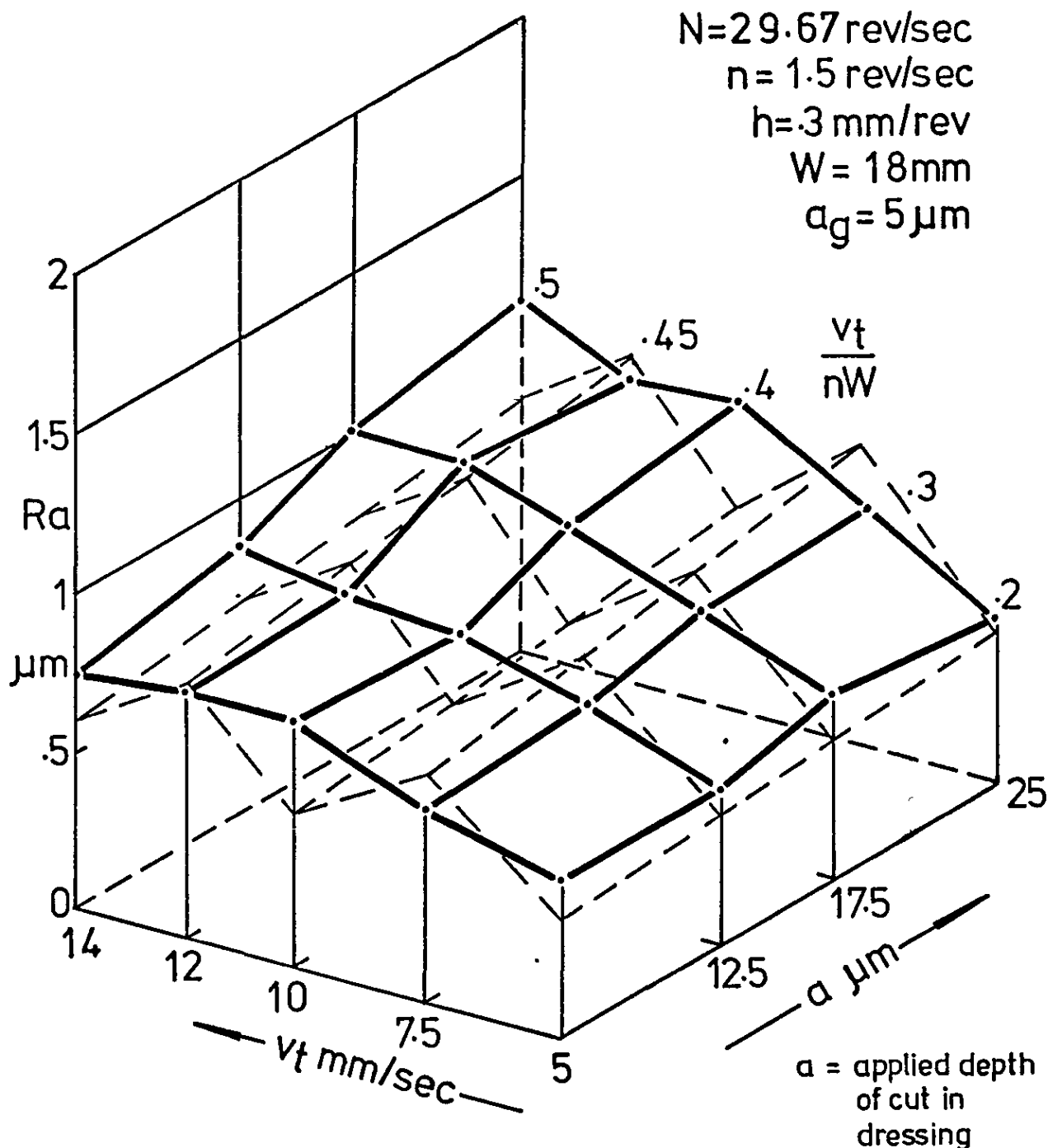


Fig. 7.154 Variation of workpiece surface roughness R_a , for changes in the parameters v_t and a (dressing), N, n, W, a (grinding) and h remaining constant

| | | | | |
|----------------------------|-----|------|------|-----|
| $a \text{ } \mu\text{m}$ | 25 | 17.5 | 12.5 | 5 |
| $a^* \text{ } \mu\text{m}$ | 1.9 | 1.9 | 1.3 | 1.3 |

--- Ra theoretical
 -.- Ra experimental

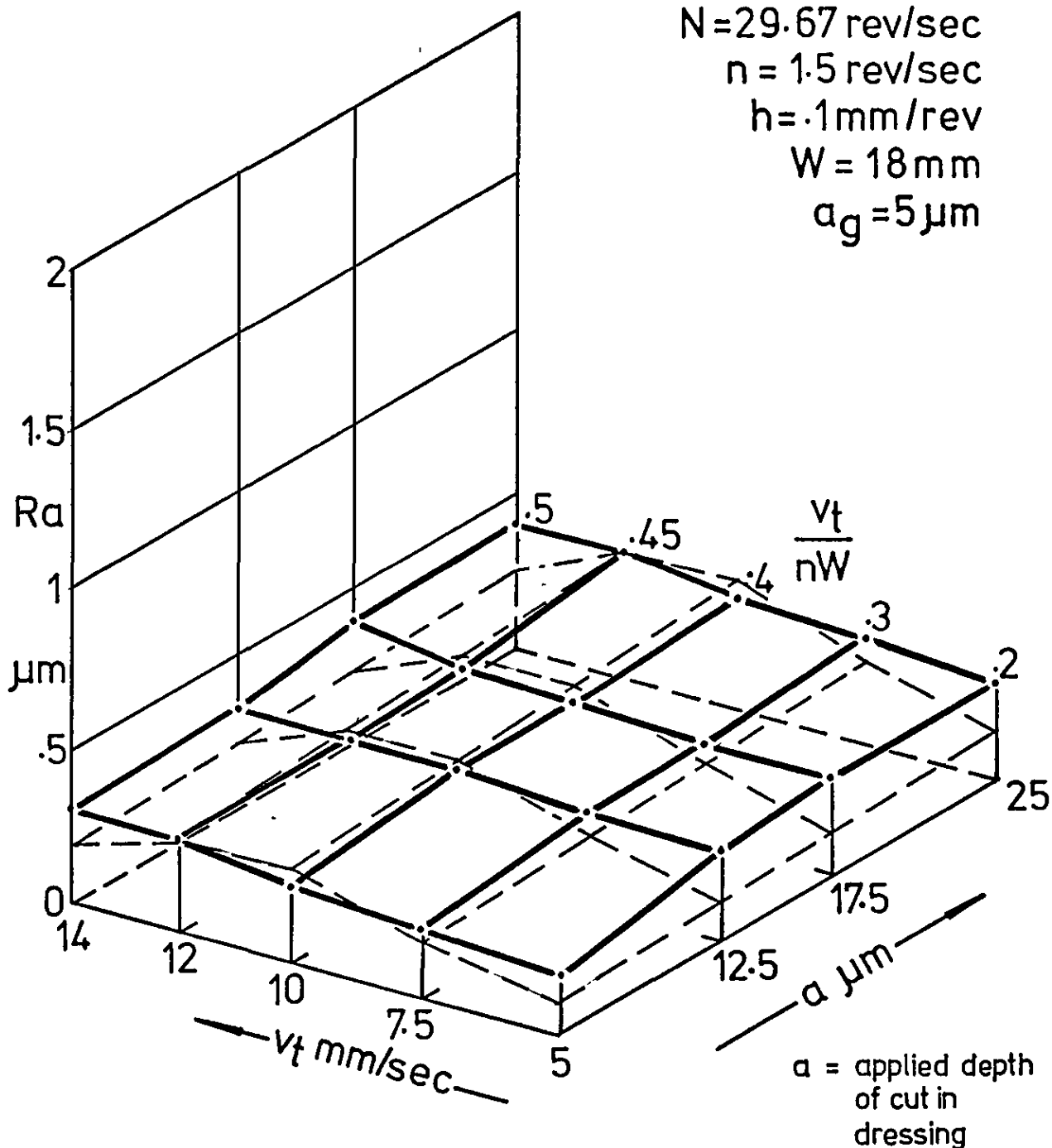


Fig. 7.155 Variation of workpiece surface roughness R_a , for changes in the parameters v_t and a (dressing), N, n, W, a (grinding) and h remaining constant

TEST N^os 19 & 22

$h = .5 \text{ mm/rev}$: $a_g = 5 \mu\text{m}$

$a = 5 \mu\text{m}$

$a = 25 \mu\text{m}$

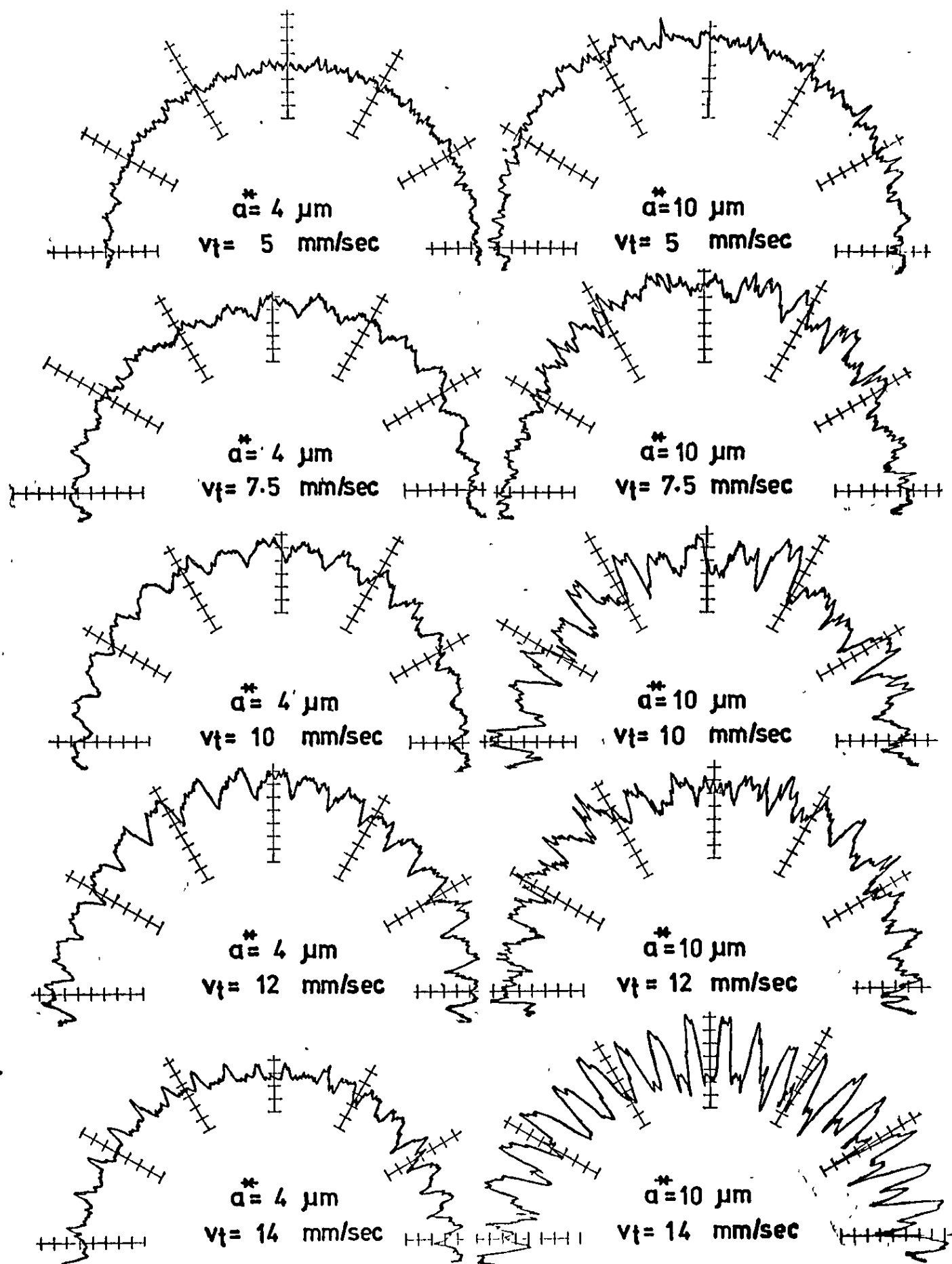
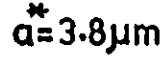


Fig. 7.156

Variation of workpiece circularity with grinding traverse rate for fine grinding

$a = 5 \mu m$

 $a = 25 \mu m$ 

$v_t = 5 \text{ mm/sec}$

 $a^* = 5 \text{ } \mu\text{m}$

$v_t = 5 \text{ mm/sec}$

$$a^* = 3.8 \mu\text{m}$$

$v_t = 7.5 \text{ mm/sec}$

$$a^* = 5 \text{ } \mu\text{m}$$

$v_t = 7.5 \text{ mm/sec}$

$$a^* = 3.8 \mu m$$

$v_t = 10 \text{ mm/sec}$

$$a^* = 5 \text{ } \mu\text{m}$$

$v_t = 10 \text{ mm/sec}$

$$a^* = 3.8 \mu m$$

$v_t = 12 \text{ mm/sec}$

$$a^* = 5 \text{ } \mu\text{m}$$

$v_t = 12 \text{ mm/sec}$

$$a^* = 3.8 \mu\text{m}$$

$v_t = 14$ mm/sec

$$a^* = 5 \text{ } \mu\text{m}$$

$v_t = 14 \text{ mm/sec}$

Fig. 7.157 Variation of workpiece circularity with grinding traverse rate for fine grinding

TEST N^os 27 & 30 $h = .1 \text{ mm/rev}$: $a_g = 5 \mu\text{m}$
 $a = 5 \mu\text{m}$ $a = 25 \mu\text{m}$

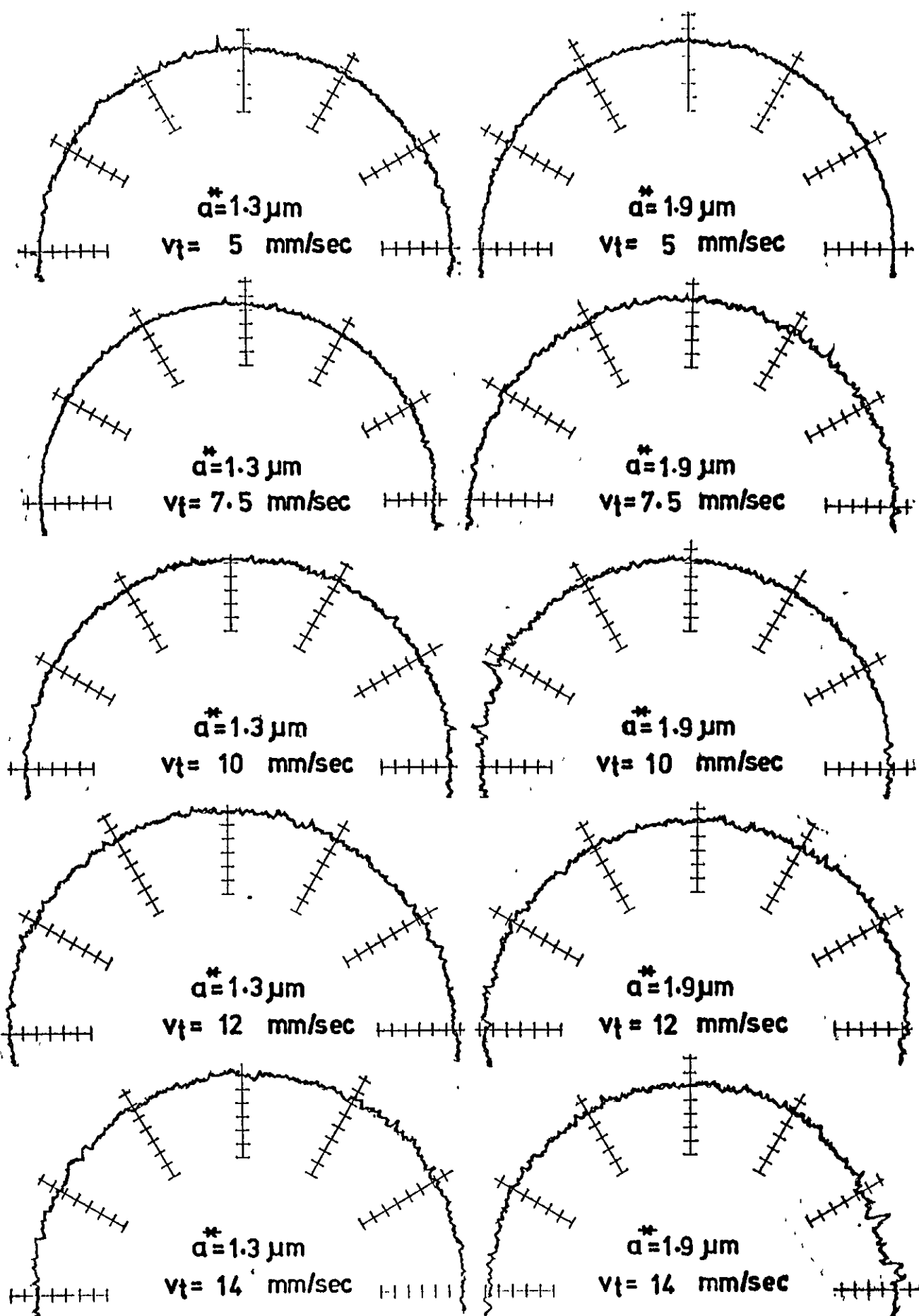


Fig. 7.158 Variation of workpiece circularity with grinding traverse rate for fine grinding

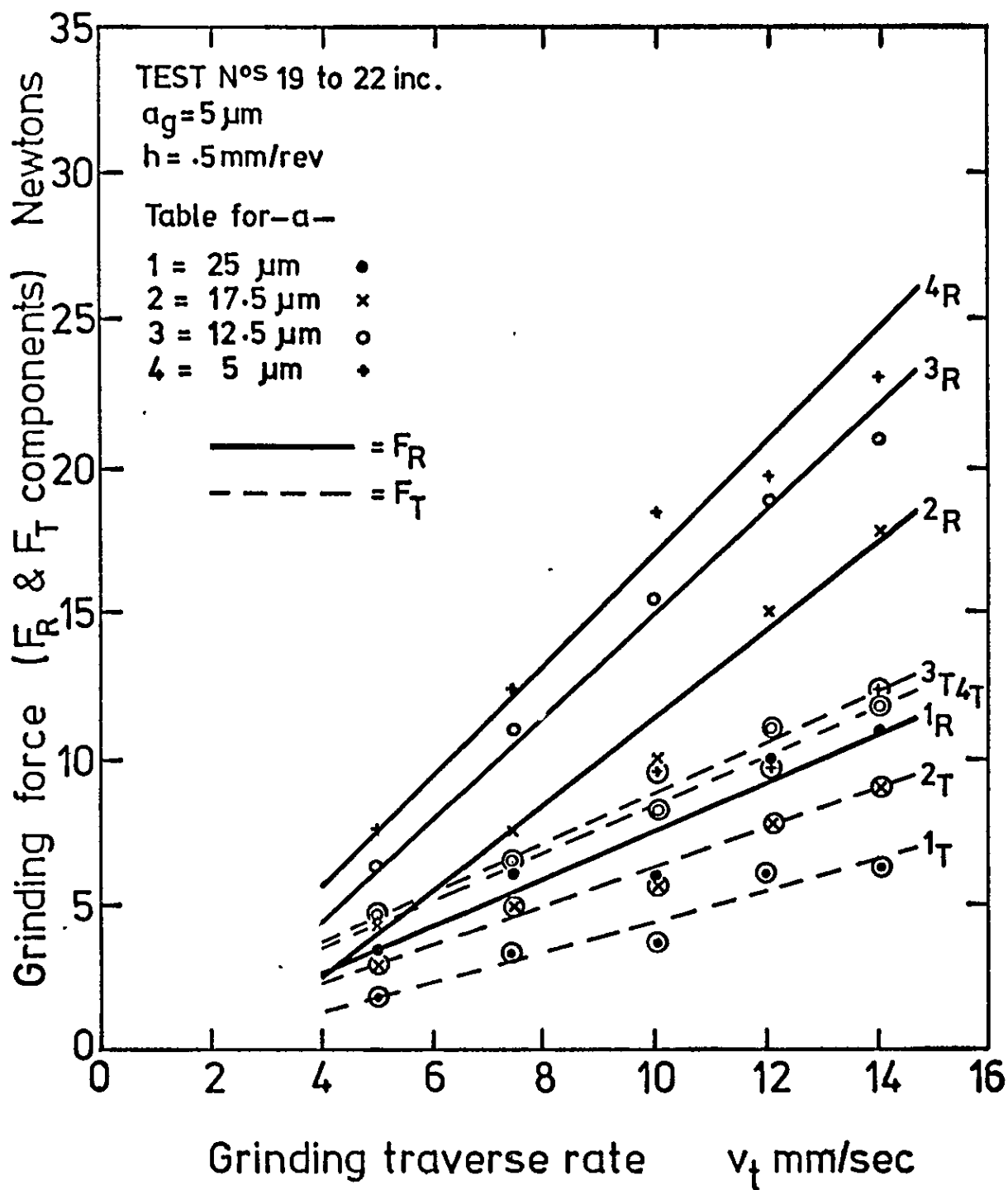


Fig. 7.159 Variation of grinding force
with traverse rate for fine grinding

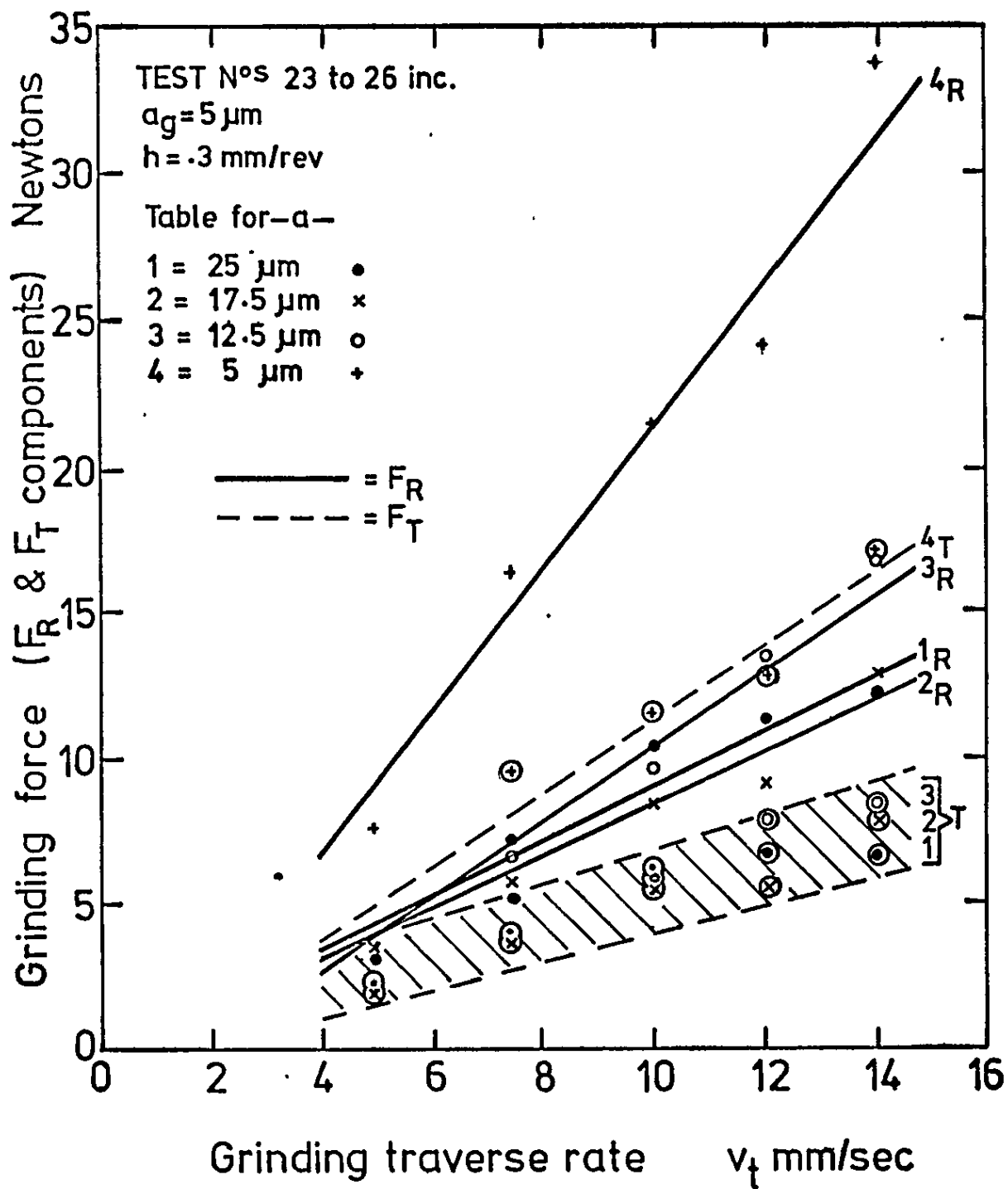


Fig.7.160 Variation of grinding force
with traverse rate for fine grinding

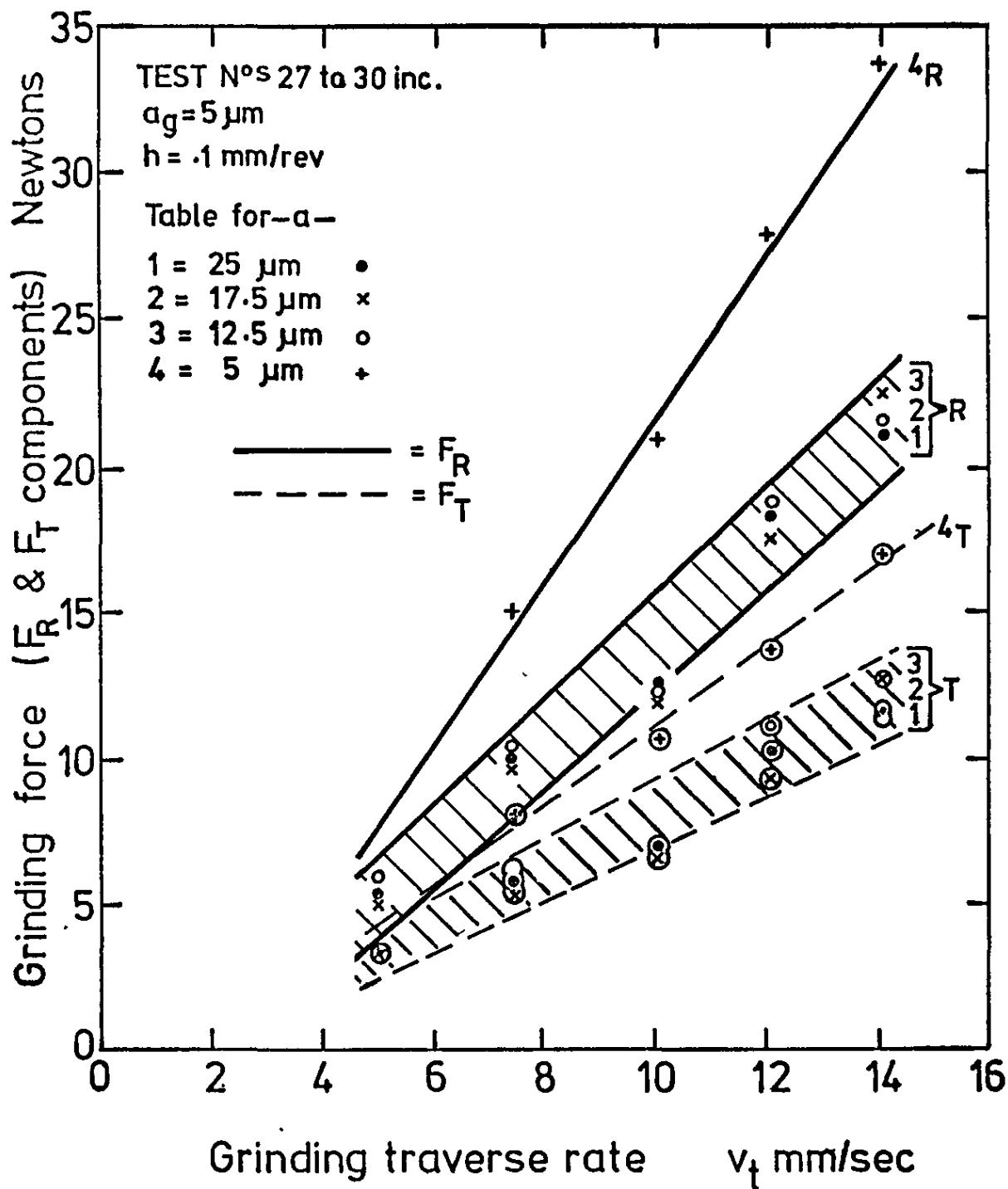


Fig.7.161 Variation of grinding force
with traverse rate for fine grinding

CHAPTER 8

GENERAL CONCLUSIONS

The following conclusions have been drawn, with reference to the materials and test conditions used in the investigation:-

WHEEL DRESSING

1. Dressing force has been shown to be an extremely useful parameter for assessing the relative importance of the variables associated with dressing, and as a means of analysing the dressing process itself. Ref: Chapter 7, test 4 pp 152 to 156. See figs. 7.22 to 7.24 inc.
2. The radial component of force was predominant, with a value of between 2 and 7 times that of the tangential component, and the axial component of force was least significant with a value of between .025 and .1 times that of the radial component. Ref: Chapter 7, statement 7.3 pp 171 to 173.
3. The rake angle of the diamond tool had greater influence on the dressing process than the drag angle, and affected both dressing force and rate of wear of the diamond tool. Ref: Chapter 7, tests 1 to 3 inc., pp 145 to 152. See figs. 7.1 to 7.18.
4. A small range of values of rake angle existed in which diamond wear and dressing force were a minimum for initially sharp diamonds of different geometry, i.e. -69° to -74° . Ref: Chapter 7, tests 1 to 3 inc., pp 145 to 152. See figs. 7.1, 7.12 and 7.13.
5. A relationship existed between the radial component of dressing force during dressing, and the amount of wear on the dressing diamond. Ref: Chapter 7, test 9 pp 169 to 170. See figs. 7.84 and 7.85.

WHEEL DRESSING cont.

6. A linear relationship existed between the cross-feed and dressing force, whilst a non-linear relationship existed between the in-feed and dressing force, the exact laws depending upon the prevailing dressing conditions. Ref: Chapter 7, tests 4 to 7 inc., pp 153 to 155. See figs. 7.22, 7.23, 7.24, 7.44, 7.45 and 7.46.
7. The cross-feed in dressing had greater influence on grinding wheel surface roughness than the in-feed. Ref: Chapter 7, tests 4 to 7 inc., pp 155 to 158 and 161 to 163. See figs. 7.35 and 7.54.

ROUGH GRINDING

1. Grinding wheel performance was influenced to a greater extent by the dressing cross-feed rate than by the dressing depth of cut, with optimum conditions occurring for values of h equal to the mean grit diameter, i.e. .3 mm. Ref: Chapter 7, tests 5 to 16 inc., pp 186 to 187 and p 191.
2. The initial rate of wheel breakdown when grinding was directly influenced by the dressing conditions. Ref: Chapter 7, tests 5 to 16 inc., pp 182 to 187. See figs. 7.94 to 7.100.
3. Adverse dressing conditions caused initial wheel breakdown to a depth greater than the as-dressed depth of cut. Ref: Chapter 7, tests 17 and 18, pp 193 to 194.
4. The workpiece surface finish was influenced by the dressing conditions during the primary stage of wheel wear only, with the final value being solely dependent on the variables associated with the grinding process. Ref: Chapter 7, tests 1 to 18 inc., p 181, pp 187 to 188 and 194 to 195.

ROUGH GRINDING cont.

5. As wheel wear progressed, the grinding forces tended towards the same values, irrespective of the wheel dressing conditions. This trend was similar to that observed in the case of the workpiece surface finish. Ref: Chapter 7, tests 5 to 16 inc., see figs. 7.114 to 7.139 inc.

FINE GRINDING

1. In the absence of spark-out, the workpiece surface finish has been shown to be a function of the dressing cross-feed rate, diamond shape and grinding wheel overlap. Ref: Chapter 7, tests 19 to 30 inc., pp 195 to 199. See figs. 7.148 to 7.150 inc.
2. The above relationship can be represented by equations which predict the workpiece surface roughness for known dressing and grinding conditions with a fair degree of accuracy. Ref: Chapter 3, pp 60 to 88. See figs. 3.22 to 3.24 inc. Chapter 7, See figs. 7.149 and 7.153 to 7.155 inc.
3. Improved surface finish was obtained at the expense of higher grinding forces. Ref: Chapter 7, tests 19 to 30 inc., pp 200 to 201. See figs. 7.159 to 7.161 inc.

CHAPTER 9

SUGGESTIONS FOR FURTHER WORK

Several further possible avenues of research, resulting from the findings of this work, are suggested:-

1. To investigate further, the influence of the diamond rake angle on diamond wear and dressing stability, when using shaped diamonds as opposed to those in their natural state. This parameter may seriously affect the efficiency of those processes using shaped diamonds, where the dressed form of the wheel is critical, particularly when using wheels having large face widths.
2. To investigate the above parameter when using a wide range of grinding wheels having different combinations of grit size and bond hardness, since they may modify the already established influence on the dressing process.
3. To establish more precisely the relationship between the dressing-diamond shape (angle β), the dressing in-feed and cross-feed, and the grinding variables, for a wider range of conditions.

BIBLIOGRAPHY

- | <u>Ref. No</u> | <u>Contents</u> |
|----------------|---|
| 1. | PHAAL C. Private communication The Industrial Diamond Information Bureau, London. (1972). |
| 2. | PAHLITZSCH G. and APPUN J. Effects of truing conditions on circular grinding. Industrial Diamond Review Vol. 14 (1954). pp. 185-189 Sept. pp 212-217 Oct. |
| 3. | PAHLITZSCH G. and THOEING W. New researches into the truing process in grinding. Industrial Diamond Review Vol.19 (1959). pp 97-99 May. pp 115-118 June. pp 128-130 July. |
| 4. | PATTINSON E.J. and CHISHOLM A.W.J. The effect of dressing techniques on grinding wheel wear. Proc. Intern. Conf. Manuf. Tech. Michigan (1967). p 106. |
| 5. | PAHLITZSCH G. The influence of the crystallographic orientation on the wear of truing diamonds. Industrial Diamond Review. Vol. 20 (1960). pp 31-37. |
| 6. | BACKER W.R. and KRABACHER E.J. New techniques in metal-cutting research. Trans. ASME. Vol. 78 (1956) pp 1497-1505. |
| 7. | HILL M.R. and MOFFATT V.L. The industrial application of grinding processes. Report N2 B/SR/8280 Dept. of Eng. Prodn., University of Birmingham (1972). |
| 8. | BHATEJA C.P. The influence of dressing on the performance of grinding wheels. Ph. D. Thesis. University of Salford (1970). |

9. ANON. The truing and dressing of grinding wheels. A publication by The Carborundum Company Limited, Trafford Park, Manchester. (1961).
10. Properties of diamonds. De Beers Industrial Diamond Division. London. (1972).
11. DENNING R.M. Amer. Min. Vol. 30 (1953) p 108
Vol. 40 (1955). p 186.
12. WILKS E.M. and WILKS J. The resistance of diamonds to abrasion. J. Phys. D: Appl. Phys. Vol. 5 (1972) pp 1902-1918.
13. BUSCH D.M. The dressing of grinding wheels with diamond dressing tools. Maschinenmarkt Vol. 75 No 82 (1969). pp 1807-1810. (Translated into English).
14. SMITH N.R. Industrial applications of the diamond. 1st Edit. London. Hutchinson (1965) pp 48-79.
15. BURLS J. Industrial diamonds and their applications in metalworking. Engineers Digest Vol. 33 No 3 (1972). pp 61-67.
16. GAUGER R. Diamond tools for dressing grinding wheels. Industrial Diamond Review. Vol. 28. (1968) pp 14-19.
17. SELBY J.S. Dressing abrasive grinding wheels with diamond tools. De Beers Industrial Diamond Division. Diamond information. Ll2.
18. BHATEJA C.P., PATTINSON E.J. and CHISHOLM A.W.J. The influence of dressing on the performance of grinding wheels. Annals of the C.I.R.P. Vol. 21 No 1 (1972) pp 81-82.

19. VICKERSTAFF T.J. Diamond dressing - its effect on work surface roughness. Industrial Diamond Review. Vol. 30 (1970) pp. 260-267.
20. LINDSAY R.P. Dressing and its effects on grinding performance. Amer. Soc. of Tool Manuf.. Engrs. Technical Paper MR69-568 (1969).
21. JONES and SHIPMAN. Precision grinding techniques. Publication № PG4.
22. ALDEN G. Operation of grinding wheels in machine grinding. Trans. Amer. Soc. Mech. Engrs. Vol. 35 (1914) p. 451.
23. GUEST J.J. Grinding Machinery. London. Edward Arnold & C . (1914)
24. BACKER W.R., MARSHALL E.R. AND SHAW M.C. The size effect in metal cutting. Trans. A.S.M.E. Vol. 74 (1952) pp. 61-72.
25. REICHENBACH G.S., MAYER J.E., KALPAKCIOGLU S. and SHAW M.C. The role of chip thickness in grinding. Trans. A.S.M.E. Vol. 78 (1956) pp. 847-859.
26. HAHN R.S. On the nature of the grinding process. Pergamon Press. Proc. of the 3rd M.T.D.R. Conf. Birmingham (Sept. 1962) pp. 129-164.
27. HAHN R.S. On the mechanics of the grinding process under plunge-cut conditions. J. Eng. for Industry. Trans. A.S.M.E. Vol. 88 (1966) pp. 72-80.
28. GRISBROOK H. Cutting points on the surface of a grinding wheel and chip produced. Advances in Machine Tool Design and Research. Oxford. Pergamon Press Ltd. (1962) p. 155.

29. TAKENO N. and NAGOAKA S. Electromicroscope observation of abrasive grain in precision grinding operation. Bull. - Japan. Soc. Prec. Eng. Vol. 1. Pt. 3. (1965) pp. 150-161.
30. TANAKA Y., TSUWA H. and KAWAMURA S. Rubbing of abrasive grains in grinding process. Bull. Japan. Soc. Prec. Eng. Vol. 1. Pt. 3. (1965) pp. 177-181.
31. SHONAZAKI T. and SHIGEMATU H. Mechanics of rubbing and biting and cutting edge on work surface in grinding process. Bull. Japan. Soc. Prec. Eng. Vol. 2. Pt. 1. (1966) pp. 8-13.
32. TAKENAKA N. A study on the grinding action by single grit. Annals of the C.L.R.P. Vol. 13. Pt. 2. (1966) pp. 183-190.
33. SATO K. Progress of researches on grinding mechanics in Japan. Bull. Japan. Soc. Prec. Eng. Vol. 2. No 1 (1966) pp. 1-7.
34. KRABACHER E.J. Factors influencing the performance of grinding wheels. Journal of Eng. for Ind. Trans. A.S.M.E. Vol. 81. (1951) pp. 187-200
35. TARASOV L.P. The theory of grinding -1
Grinding and Finishing. (Sept. 1967) pp. 20-24.
36. YOSHIKOWA H. and SATA T. Study on wear on grinding wheels -1, bond fracture in grinding wheels. Journal of Eng. for Ind. Trans. A.S.M.E. Vol. 85 (1963) pp. 39- 43.
37. TSUWA H. An investigation of grinding wheel cutting edges. Journal of Eng. for Ind. Trans. A.S.M.E. Vol. 86 (1964) pp. 371-382.
38. EISS, Jr. N.S. Fracture of abrasive grain in

- grinding. Journal of Eng. for Ind. Trans. A.S.M.E. (1966) Paper No 66-WA/Prod-3.
39. KING A.G. Ceramic tool wear. Trans. A.S.M.E. (May 1963) Paper No 63-Prod-11 .
40. DUWELL E.J., HONG I.S. and Mc DONALD W.J. The role of chemical reactions in the preparation of metal surfaces by abrasion. Wear. Vol. 9. (1966) pp. 417-424.
41. BUTTERY T.C. and ARCHARD J.F. Some microscopical investigations of grinding and abrasive wear. Journal of Microscopy. Vol. 94. Pt. 1. (Aug. 1971) pp. 13-24.
42. MARSHALL E.R. and SHAW M.C. Forces in dry surface grinding. Trans. A.S.M.E. Vol. 74. (1952) pp. 51-59.
43. BACKER W.R. and MERCHANT M.E. On the basic mechanics of the grinding process. Trans. A.S.M.E. Vol. 80 No 1. (1958) pp. 141-148.
44. GRISBROOK H. Precision grinding research. The Journal of the Inst. of Prod, Engrs. Vol. 39. No 5 (1960) pp. 251-269 & pp. 341-346.
45. GRISBROOK H., HOLLIER R.H. and VARLEY P.G. Related patterns of grinding forces, wheel wear and surface finish. Int. Journal of Prod. Res. Vol. 1. Pt. 3. (1962) pp. 57-74.
46. ONO K. Analysis on the grinding force. Bull. Japan. Soc. Grinding Engrs. Vol. 1. (1961) pp. 19-22.
47. KOBAYASHI A. On the grinding force. Bull. Japan.

Soc. Grinding Engrs. Vol. 1. (1961) pp. 13-17.

48. YANG C.T. Design of surface grinding dynamometers. Journal of Eng. for Ind. Trans. A.S.M.E. Vol. 90. (1968) pp. 127-133.
49. LANDBERG P. Experiments on grinding. Microtecnic. Vol. XI. Nº 1. (1957) pp. 18-26.
50. HAHN R.S. and LINDSAY R.P. The influence of process variables on material removal, surface integrity, surface finish and vibration in grinding. 10th International M.T.D.R. Conf. Manchester. (Sept. 1969).
51. LINDSAY R.P. and HAHN R.S. On the basic relationships between grinding parameters. Annals of the C.I.R.P. Vol. XVI (1971) pp. 657-666.
52. KORNBERGER Z. and KOZIARSKI A. Cutting characteristics of grinding wheels dressed by different methods. Machinery and Production Engineering. Vol. 118. Nº 3046 (1971) pp. 490-494.
53. BHATEJA C.P., CHISHOLM A.W.J. and PATTINSON E.J. The influence of grinding wheel wear and dressing on the quality of ground surfaces. Proceedings of the Int. Grd. Conf. Pittsburgh. U.S.A. (1972) pp. 685-707.
54. BAUL R.M., GRAHAM D. and SCOTT W. Characterisation of the working surface of abrasive wheels. Tribology. (Aug. 1972) pp. 169-176.
55. TSUWA H. and YASUI H. Micro-structure of dressed abrasive cutting edges. Proceedings of the Int. Grd. Conf. Pittsburgh U.S.A. (1972) pp. 142-160.
56. MALKIN S. and ANDERSON R.B. Active grains and

- dressing particles in grinding. Proceedings of the Int. Grd. Conf. Pittsburgh U.S.A. (1972) pp. 161-181.
57. PACITTI V. and RUBENSTEIN C. The influence of the dressing depth of cut on the performance of a single point diamond dressed alumina grinding wheel. Int. J. Mach. Tool Des. Res. Vol. 12. (1972) pp. 267-279.
58. NICOLLS M.O. The measurement of surface finish. De Beers Industrial Diamond Division.
59. STEEDS W. Engineering materials, machine tools and processes. 4th Ed. London. Longmans, Green & Co. (1964) p. 352.
60. GROSZMANN F.K. and RUBENSTEIN C. A low force three-component tool dynamometer and its application to grinding research. Proceedings of the 7th Int. Mach. Tool Design Res. Conf. Birmingham. (1966) pp. 415-436.
61. POTMA T. Strain gauges. Theory and application. 1st Ed. Eindhoven, The Netherlands. N.V. Philips. London. Iliffe Books Ltd. (1967) p. 23.
62. PAHLITZSCH G. Present state of the technique and research in the field of precision grinding. Microtechnic. Vol. 17. № 6. (1963) p. 245.
63. PEKLENIK J. A proposal for a physical hardness grading system for grinding wheels. Advances in Machine Tool Design and Research. Oxford. Pergamon Press Ltd. (1965).
64. PEKLENIK J., LANE R.D. and SHAW M.C. Comparison of static and dynamic hardness of grinding wheels. Journal of Eng. for Ind., Series B., Trans. A.S.M.E. Vol. 86. (1964) p. 295.

65. COLWELL L.V., LANE R.D. and SODERLUND N.K. On determining the hardness of grinding wheels - 1. Journal of Eng. for Ind., Series B, Trans. A.S.M.E. Vol. 84. (1962) p. 113.
66. GRAHAM W. and RUBENSTEIN C. Forces and wheel wear in grinding. Proceedings of the Diamond Conference, Bristol. (July 1968).
67. TIMOSHENKO S. Strength of materials. Part 1, Elementary theory and problems. 3rd Ed. New York. D. Van Nostrand Company, Inc. (1965) p. 381.
68. ROARK R.J. Formulas for stress and strain. 4th Ed. New York. McGraw-Hill. (1965) pp. 172-173.

Surface Texture.

This describes the overall condition of the surface and can be broken down as follows:-

"Primary Texture"

Primary texture or roughness is that part of surface texture which can best be defined as the marks left by the action of the production process used, e.g., grinding. The primary texture can be measured by various constants, see fig. A1.

Ra. (CLA,AA). Average arithmetic roughness. Also known as Centre Line Average (British) and Arithmetic Average (American). CLA and AA are usually quoted in micro-inches, and Ra in micro-metres. Ra is a mean value of the roughness.

Rp. Smoothing depth (distance between the highest point and the mean line.) Rp generally results from the condition of the cutting tool, i.e., a grinding wheel.

Rt. Maximum roughness within the tracing stroke (highest point to lowest point). An example of the cause of Rt and its magnitude would be the grit and its size as used in a grinding wheel.

RMS. Root-Mean-Square. This is an average geometric roughness and was an American standard. RMS, which gives a numerical value approximately 11% higher than that of Ra, became obsolete in 1955.

"Secondary Texture"

Secondary texture is that part of the surface texture which underlies the roughness. All types of machine vibrations, e.g., spindle deflection and imbalance can be the cause. It is generally described as waviness and designated W.

"Lay"

The production process used will form patterns on the surface. The predominant pattern direction is known as the "lay" and this is the direction in which most surface roughness measurements are taken.

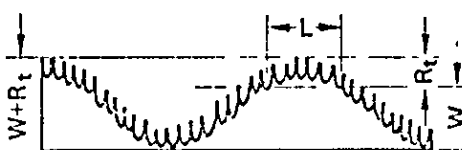
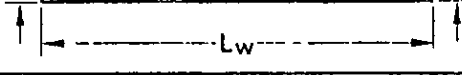


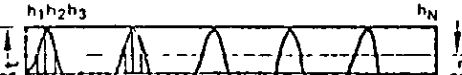
Before a value of Arithmetical Average, Ra, can be calculated for a particular profile, it is necessary to calculate the value of the centre-line, Rp, which passes through the dressed profile. Consider fig. A1. It can be seen that the centre-line is that line which divides the enveloped profile such that the sum of the areas above the centre line is equal to the sum of the areas below the centre line.

By definition:-

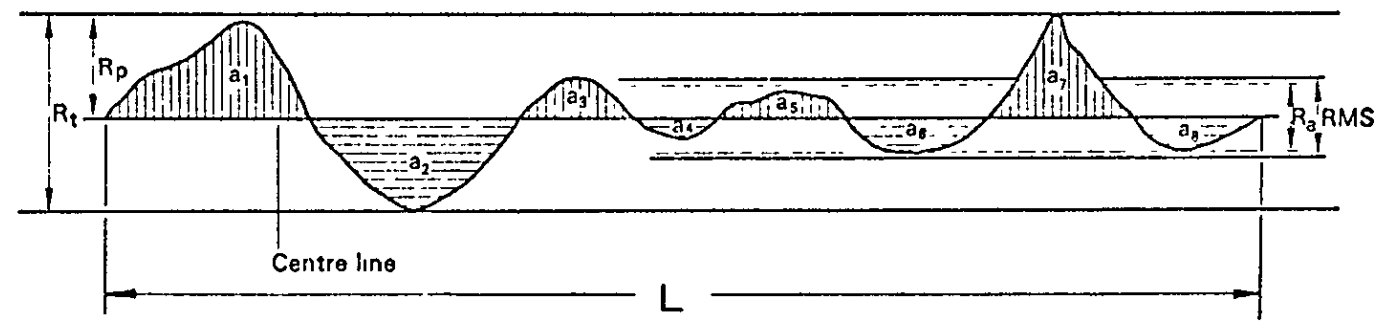
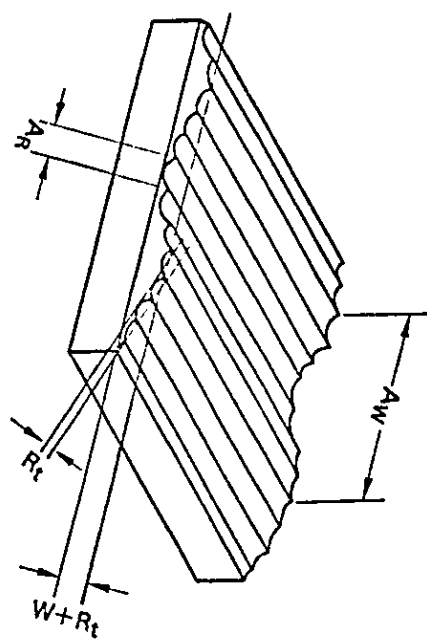
$$R_p = \frac{1}{L} \int_0^L |y_i| dx = \frac{y_1 + y_2 + \dots + y_{N'}}{N'}$$

$$\begin{aligned} R_a &= \frac{1}{L} \int_0^L |h_i| dx = \frac{|h_1| + |h_2| + \dots + |h_{N'}|}{N'} \\ &= \frac{A_1 + A_2 + \dots + A_{N'}}{L} \end{aligned}$$

Surface measurement parameters

| Nominal description | Profile description | Symbol | Definition | Unit |
|------------------------|---|--------------|---|----------|
| Waviness and roughness |  | $W + R_t$ | Total profile depth measured over L_w | μm |
| Waviness |  | W | $W + R_t$ Less average roughness depth | μm |
| Roughness |  | R_t | Total roughness depth over L | μm |
| Smoothing depth |  | R_p | $\frac{1}{L} \int_0^L y_i dx \approx \frac{y_1 + y_2 + \dots + y_N}{N}$ | μm |
| Arithmetical Average |  | R_a | $\frac{1}{L} \int_0^L h_i dx \approx \frac{ h_1 + h_2 + \dots + h_N }{N}$ | μm |
| | | $= CLA = AA$ | $1 \mu m = 40 \text{ Microinch}$ | μin |

The various components of a surface:
 R_t — Roughness (Primary Texture)
 A_w — Waviness (Secondary Texture)
 A_r — Roughness Spacing
 $W + R_t$ — Waviness + Roughness



The various parameters R_a , R_p , R_t and RMS are illustrated. It may be seen that the centre-line is that line which divides the areas such that $A_1 + A_3 + \dots + A_7 = A_2 + A_4 + \dots + A_8$.

Fig. A1 Surface Finish Parameters

APPENDIX II

1. DERIVATION OF R_a FOR WHEEL ABRASIVE SURFACE ROUGHNESS UNDER DIFFERENT DRESSING CONDITIONS

Assumptions made:-

1. The grinding wheel is considered as a homogenous structure.
2. The diamond dressing tool is considered to have a geometrically uniform profile.
3. The dressed wheel takes on the same shape as the diamond tool producing it.
4. There is negligible waviness in the dressed profile.

Dressing parameters:-

| | |
|---|---------------|
| h = dressing lead of the diamond | mm/rev |
| a = diamond depth of cut | μm |
| B = included angle of the diamond | degrees |
| w = width of the diamond wear flat | mm |
| x = diamond width at a depth of cut " a " | mm |

Dependency of the parameters.

| | |
|-------------------------------------|--------------------------------|
| Parameters selected by the operator | a and h |
| Natural parameters | B and w |
| Dependent parameter | x (fn of a, B and w) |

Calculation of R_a .

Case 1. (hypothetical) $(w = 0; h = x)$

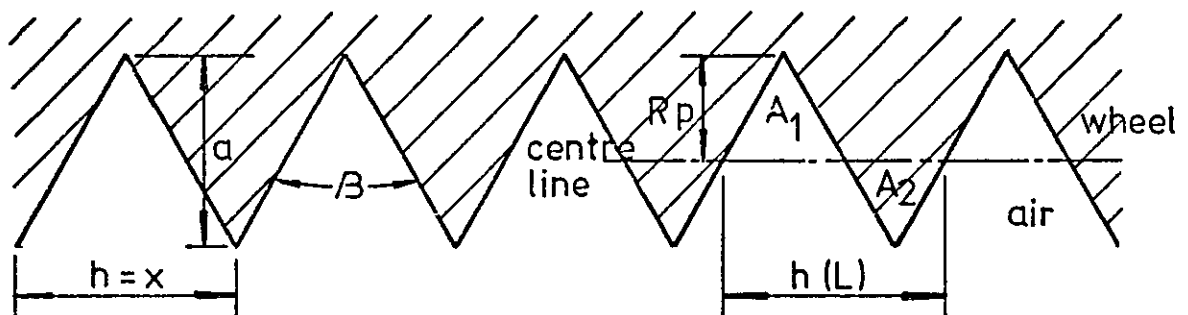


Fig. 3.1

Consider fig. 3.1

Calculation of R_p .

$$\text{Area } A_1 = R_p^2 \tan \frac{\beta}{2}$$

$$\text{Area } A_2 = (a - R_p)^2 \tan \frac{\beta}{2}$$

$$\text{Now } A_1 = A_2$$

$$\therefore R_p^2 \tan \frac{\beta}{2} = (a - R_p)^2 \tan \frac{\beta}{2}$$

$$\therefore R_p^2 = a^2 - 2aR_p + R_p^2$$

$$\therefore 2aR_p = a^2$$

$$\therefore R_p = \frac{a^2}{2a} = \frac{a}{2} \quad \dots(3.1)$$

Calculation of R_a

$$R_a = \frac{A_1 + A_2}{L} \quad (\text{where } L = h)$$

$$\begin{aligned} \therefore R_a &= \frac{1}{h} \left(2R_p^2 \tan \frac{\beta}{2} \right) \\ &= \frac{2}{h} \left(\frac{a^2}{4} \tan \frac{\beta}{2} \right) \end{aligned}$$

$$\therefore R_a = \frac{a^2}{2h} \tan \frac{\beta}{2} \quad \dots(3.2)$$

Simplifying R_a in terms of a .

$$\text{Now } h = 2a \tan \frac{\beta}{2}$$

Substituting for h in equation (3.2).

$$\therefore R_a = \frac{a}{4} \quad \dots(3.3)$$

Equation (3.3) gives the basic form of R_a in terms of a . This is a hypothetical case, where the diamond dressing tool is considered to be "sharp" ($w = 0$), and the dressing lead h , is equal to the diamond width, x , at a depth of cut, a .

The following cases can be checked against equation (3.3) for their truth.

Case 2.

($x < h$)

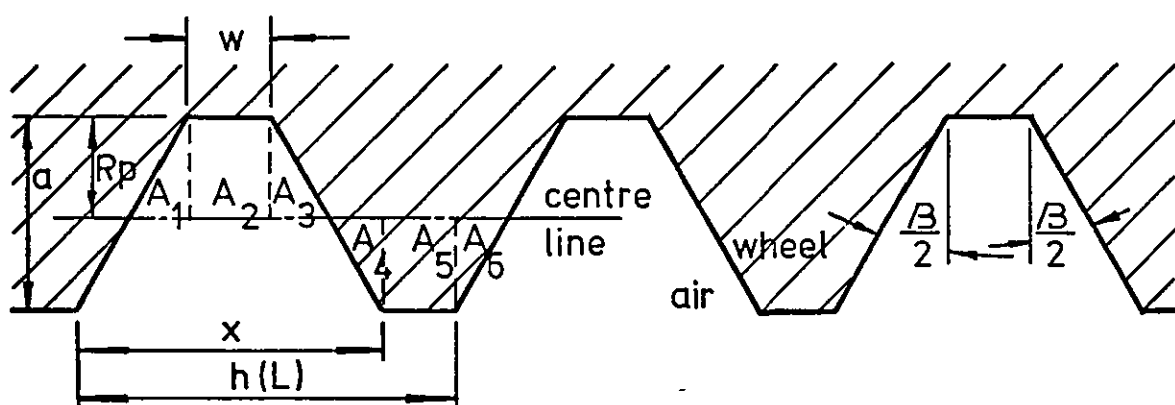


Fig. 3.2

Consider fig. 3.2

Calculation of R_p

$$\text{Area } A_1 = R_p \tan \frac{\beta}{2} \cdot \frac{R_p}{2} = \frac{R_p^2}{2} \tan \frac{\beta}{2}$$

$$\text{Area } A_2 = w R_p$$

$$\text{Area } A_3 = A_1 = \frac{R_p^2}{2} \tan \frac{\beta}{2}$$

$$\text{Area } A_4 = (a - R_p) \tan \frac{\beta}{2} \cdot \frac{(a - R_p)}{2} = \frac{(a - R_p)^2}{2} \tan \frac{\beta}{2}$$

$$\text{Area } A_5 = (a - R_p) (h - [2 R_p \tan \frac{\beta}{2} + w + 2(a - R_p) \tan \frac{\beta}{2}])$$

$$\text{Area } A_6 = A_4 = \frac{(a - R_p)^2}{2} \tan \frac{\beta}{2}$$

$$\text{Now } A_1 + A_2 + A_3 = A_4 + A_5 + A_6$$

$$\therefore R_p^2 \tan \frac{\beta}{2} + w R_p = (a - R_p)^2 \tan \frac{\beta}{2} + (a - R_p)(h - [2 R_p \tan \frac{\beta}{2} + w + 2(a - R_p) \tan \frac{\beta}{2}])$$

Considering the right-hand side of the equation

$$\begin{aligned} \text{R.H.S} &= (a^2 - 2aR_p + R_p^2) \tan \frac{\beta}{2} + (a - R_p)(h - w - 2a \tan \frac{\beta}{2}) \\ &= a^2 \tan \frac{\beta}{2} - 2aR_p \tan \frac{\beta}{2} + R_p^2 \tan \frac{\beta}{2} + ah - aw \\ &\quad - 2a^2 \tan \frac{\beta}{2} - hR_p + wR_p + 2aR_p \tan \frac{\beta}{2} \\ &= R_p^2 \tan \frac{\beta}{2} - a^2 \tan \frac{\beta}{2} + ah - aw - hR_p + wR_p \end{aligned}$$

Equating the R.H.S to the L.H.S

$$\begin{aligned} R_p^2 \tan \frac{\beta}{2} + w R_p &= R_p^2 \tan \frac{\beta}{2} - a^2 \tan \frac{\beta}{2} + ah - aw \\ &\quad - hR_p + wR_p \end{aligned}$$

$$\therefore a^2 \tan \frac{\beta}{2} + aw - ah = -hR_p$$

$$\therefore hR_p = a(h - w - a \tan \frac{\beta}{2})$$

$$\therefore R_p = \frac{a}{h} (h - w - a \tan \frac{\beta}{2}) \quad \dots(3.4)$$

Calculation of R_a .

$$R_a = \frac{A_1 + A_2 + A_3 + A_4 + A_5 + A_6}{L} \quad (\text{where } L = h)$$

$$\therefore R_a = \frac{2}{h} (R_p^2 \tan \frac{\beta}{2} + w R_p)$$

$$\begin{aligned} \therefore R_a &= \frac{2}{h} \left(\left[\frac{a}{h} (h - w - a \tan \frac{\beta}{2}) \right]^2 \tan \frac{\beta}{2} \right. \\ &\quad \left. + \left[\frac{a}{h} (h - w - a \tan \frac{\beta}{2}) w \right] \right) \end{aligned}$$

$$\therefore Ra = \frac{2a}{h^2} \left(\frac{a}{h} \tan \frac{\beta}{2} (h - w - a \tan \frac{\beta}{2})^2 + w(h - w - a \tan \frac{\beta}{2}) \right) \dots (3.5)$$

CHECK. when $w = 0$ and $h = 2a \tan \frac{\beta}{2}$

$$\begin{aligned} Ra &= \frac{2a}{4a^2 \tan^2 \frac{\beta}{2}} \left(\frac{a}{2a \tan \frac{\beta}{2}} \right. \\ &\quad \times \left(2a \tan \frac{\beta}{2} - a \tan \frac{\beta}{2} \right)^2 \tan \frac{\beta}{2} + 0 \Big) \\ &= \frac{a^3 \tan^3 \frac{\beta}{2}}{4a^2 \tan^3 \frac{\beta}{2}} \end{aligned}$$

$$\therefore Ra = \frac{a}{4}$$

Case 3.

($x = h$)

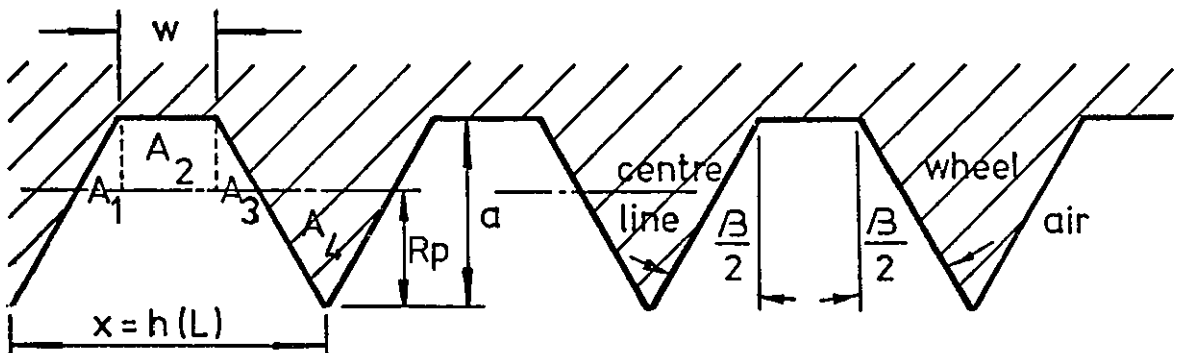


Fig. 3.3

Consider fig. 3.3

Calculation of R_p

$$\text{Area } A_1 = \frac{(a - R_p)^2}{2} \tan \frac{\beta}{2}$$

$$\text{Area } A_2 = w(a - R_p)$$

$$\text{Area } A_3 = A_1 = \frac{(a - Rp)^2}{2} \tan \frac{\beta}{2}$$

$$\text{Area } A_4 = Rp^2 \tan \frac{\beta}{2}$$

$$\text{Now } A_1 + A_2 + A_3 = A_4$$

$$\therefore (a - Rp)^2 \tan \frac{\beta}{2} + w(a - Rp) = Rp^2 \tan \frac{\beta}{2}$$

Considering the left-hand side of the equation

$$\begin{aligned} \text{L.H.S} &= a^2 \tan \frac{\beta}{2} - 2aRp \tan \frac{\beta}{2} + Rp^2 \tan \frac{\beta}{2} \\ &+ wa - wRp \end{aligned}$$

Equating the L.H.S to the R.H.S

$$a^2 \tan \frac{\beta}{2} + wa = Rp(w + 2a \tan \frac{\beta}{2})$$

$$\therefore Rp = \frac{a^2 \tan \frac{\beta}{2} + wa}{w + 2a \tan \frac{\beta}{2}} \quad \dots (3.6)$$

Calculation of Ra

$$Ra = \frac{A_1 + A_2 + A_3 + A_4}{L} \quad (\text{where } L = h)$$

$$\therefore Ra = \frac{2}{h} (Rp^2 \tan \frac{\beta}{2})$$

$$\therefore Ra = \frac{2}{h} \left(\frac{a^2 \tan \frac{\beta}{2} + wa}{w + 2a \tan \frac{\beta}{2}} \right)^2 \tan \frac{\beta}{2}$$

$$\text{Now } h = w + 2a \tan \frac{\beta}{2}$$

$$\therefore Ra = \frac{2}{h^3} (a^2 \tan \frac{\beta}{2} + wa)^2 \tan \frac{\beta}{2} \quad \dots (3.7)$$

CHECK. when $w = 0$; $h = 2 a \tan \frac{\beta}{2}$

$$\therefore Ra = \frac{2}{8a^3 \tan^3 \frac{\beta}{2}} (a^4 \tan^2 \frac{\beta}{2}) \tan \frac{\beta}{2}$$

$$\therefore Ra = \frac{a}{4}$$

Case 4.

($x > h$)

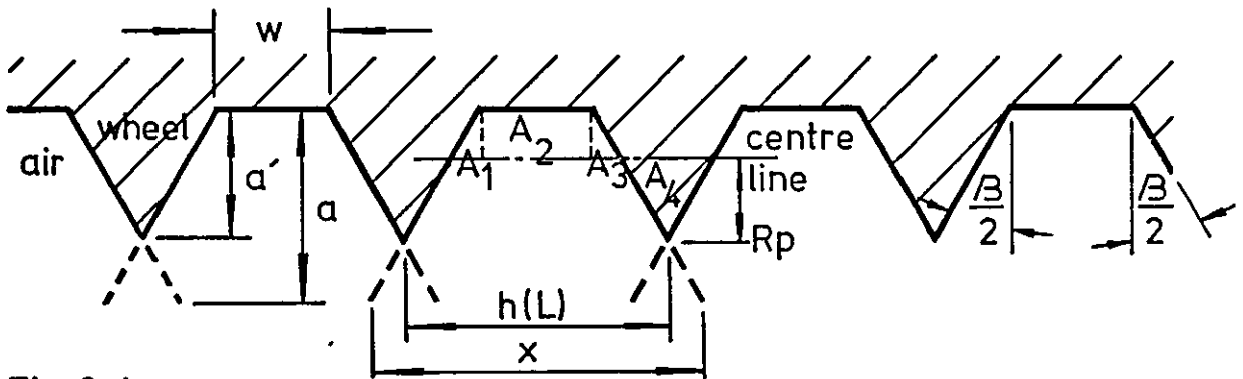


Fig. 3.4

a = apparent depth of cut

a' = actual depth of cut

Consider fig. 3.4

Calculation of R_p

$$\text{Area } A_1 = \frac{(a' - R_p)^2}{2} \tan \frac{\beta}{2}$$

$$\text{Area } A_2 = w(a' - R_p)$$

$$\text{Area } A_3 = A_1 = \frac{(a' - R_p)^2}{2} \tan \frac{\beta}{2}$$

$$\text{Area } A_4 = R_p^2 \tan \frac{\beta}{2}$$

$$\text{Now } A_1 + A_2 + A_3 = A_4$$

$$\therefore (a' - R_p)^2 \tan \frac{\beta}{2} + w(a' - R_p) = R_p^2 \tan \frac{\beta}{2}$$

Considering the left-hand side of the equation

$$\begin{aligned} \text{L.H.S} &= (a')^2 \tan \frac{\beta}{2} - 2 a' R_p \tan \frac{\beta}{2} + R_p^2 \tan \frac{\beta}{2} \\ &+ w a' - w R_p \end{aligned}$$

Equating the L.H.S to the R.H.S

$$\begin{aligned} (a')^2 \tan \frac{\beta}{2} + w a' &= R_p (w + 2 a' \tan \frac{\beta}{2}) \\ \therefore R_p &= \frac{(a')^2 \tan \frac{\beta}{2} + w a'}{w + 2 a' \tan \frac{\beta}{2}} \quad \dots (3.8) \end{aligned}$$

Calculation of R_a

$$\begin{aligned} R_a &= \frac{A_1 + A_2 + A_3 + A_4}{L} \quad (\text{where } L = h) \\ \therefore R_a &= \frac{2}{h} (R_p^2 \tan \frac{\beta}{2}) \\ \therefore R_a &= \frac{2}{h} \left(\frac{(a')^2 \tan \frac{\beta}{2} + w a'}{w + 2 a' \tan \frac{\beta}{2}} \right)^2 \tan \frac{\beta}{2} \\ \text{Now } h &= w + 2 a' \tan \frac{\beta}{2} \quad \text{and} \quad a' = \frac{(h-w)}{2} \cot \frac{\beta}{2} \\ \therefore R_a &= \frac{2}{h^3} \left(\left[\frac{(h-w)}{2} \cot \frac{\beta}{2} \right]^2 \tan \frac{\beta}{2} \right. \\ &\quad \left. + w \frac{(h-w)}{2} \cot \frac{\beta}{2} \right)^2 \tan \frac{\beta}{2} \\ \therefore R_a &= \frac{2}{h^3} \left(\cot \frac{\beta}{2} \left[\frac{h^2}{4} - \frac{hw}{2} + \frac{w^2}{4} + \frac{hw}{2} - \frac{w^2}{2} \right] \right)^2 \tan \frac{\beta}{2} \end{aligned}$$

$$\therefore Ra = \frac{2}{h^3} \cot \frac{\beta}{2} \left(\frac{h^2}{4} - \frac{w^2}{4} \right)^2$$

$$\therefore Ra = \frac{1}{8h^3} \cot \frac{\beta}{2} (h^4 - 2h^2 w^2 + w^4) \quad \dots\dots (3.9)$$

CHECK when $w = 0$

$$Ra = \frac{1}{8h^3} \cot \frac{\beta}{2} (h^4) = \frac{h}{8} \cot \frac{\beta}{2}$$

$$\text{Now } h = 2 a' \tan \frac{\beta}{2} \quad (\text{when } w = 0)$$

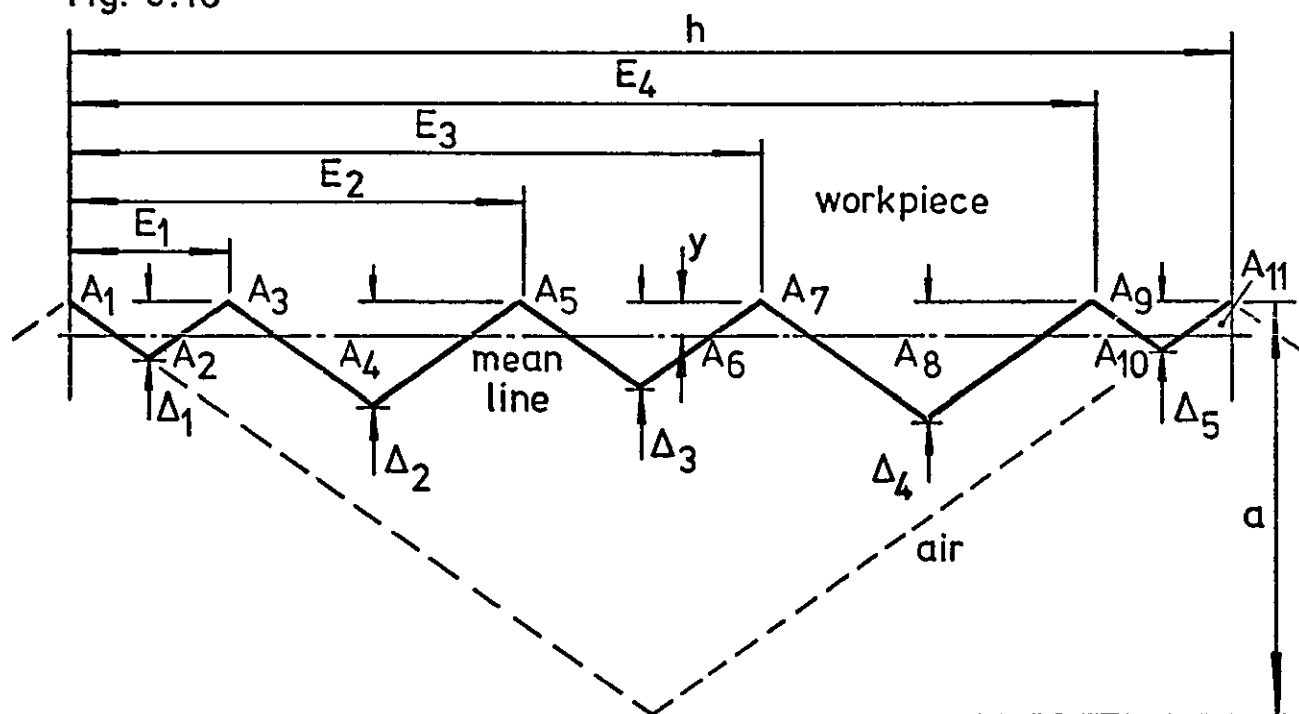
$$\therefore Ra = \frac{2}{8} a' \cot \frac{\beta}{2} \tan \frac{\beta}{2} = \frac{a'}{4}$$

2. DERIVATION OF Ra FOR WORKPIECE SURFACE ROUGHNESS WHEN GROUND UNDER CYLINDRICAL TRAVERSE GRINDING CONDITIONS.

Fig. 3.16 depicts a portion of the ground workpiece surface profile, with interference occurring. Let the term "value of interference", be denoted by the symbol E , and the peak to valley height of each triangular form be denoted by the symbol Δ .

Consider fig. 3.16 :-

Fig. 3.16



Consider fig. 3.16

$$\Delta_j = E_j \cdot \frac{a}{h} \quad (\text{for } j^{\text{th}} \text{ value}) \quad \dots \dots (3.42)$$

From equn.(3.42)

$$\Delta_1 = \frac{E_1 a}{h}$$

$$\Delta_2 = \frac{(E_2 - E_1) a}{h}$$

$$\Delta_3 = \frac{(E_3 - E_2) a}{h}$$

$$\Delta_4 = \frac{(E_4 - E_3) a}{h}$$

$$\Delta_5 = \frac{(h - E_4) a}{h}$$

Calculation of Areas

$$\text{Area } A_1 = \frac{y}{2} \cdot \frac{yh}{2a} = \frac{y^2 h}{4a}$$

$$\text{Area } A_2 = (\Delta_1 - y) \cdot \frac{(\Delta_1 - y) h}{2a} = \frac{h (\Delta_1 - y)^2}{2a}$$

$$\text{Area } A_3 = 2 A_1 = \frac{y^2 h}{2a}$$

$$\text{Area } A_4 = (\Delta_2 - y) \cdot \frac{(\Delta_2 - y) h}{2a} = \frac{h (\Delta_2 - y)^2}{2a}$$

$$\text{Area } A_5 = 2 A_1 = \frac{y^2 h}{2a}$$

$$\text{Area } A_6 = (\Delta_3 - y) \cdot \frac{(\Delta_3 - y) h}{2a} = \frac{h (\Delta_3 - y)^2}{2a}$$

$$\text{Area } A_7 = 2 A_1 = \frac{y^2 h}{2a}$$

$$\text{Area } A_8 = (\Delta_4 - y) \cdot \frac{(\Delta_4 - y) h}{2a} = \frac{h (\Delta_4 - y)^2}{2a}$$

$$\text{Area } A_9 = 2 A_1 = \frac{y^2 h}{2a}$$

$$\text{Area } A_{10} = (\Delta_5 - y) \cdot \frac{(\Delta_5 - y) h}{2a} = \frac{h (\Delta_5 - y)^2}{2a}$$

$$\text{Area } A_{11} = A_1 = \frac{y^2 h}{4a}$$

Calculation of Mean Line

The mean line is positioned such that :-

$$A_1 + A_3 + A_5 + A_7 + A_9 + A_{11} = A_2 + A_4 + A_6 + A_8 + A_{10}$$

Hence

$$5\left(\frac{y^2 h}{2a}\right) = \frac{h}{2a} \left\{ (\Delta_1 - y)^2 + (\Delta_2 - y)^2 + (\Delta_3 - y)^2 + (\Delta_4 - y)^2 + (\Delta_5 - y)^2 \right\}$$

Expanding the R.H.S

$$\begin{aligned} \text{R.H.S} &= \frac{h}{2a} \left\{ \Delta_1^2 - 2\Delta_1 y + y^2 + \Delta_2^2 - 2\Delta_2 y + y^2 + \Delta_3^2 - 2\Delta_3 y + y^2 + \Delta_4^2 - 2\Delta_4 y + y^2 + \Delta_5^2 - 2\Delta_5 y + y^2 \right\} \\ &= \frac{h}{2a} \left\{ 5y^2 - 2y(\Delta_1 + \Delta_2 + \Delta_3 + \Delta_4 + \Delta_5) + \Delta_1^2 + \Delta_2^2 + \Delta_3^2 + \Delta_4^2 + \Delta_5^2 \right\} \end{aligned}$$

Substituting for Δ in terms of E

$$\begin{aligned} \therefore \text{R.H.S} &= \frac{h}{2a} \left\{ 5y^2 - 2y \left(\frac{E_1 a}{h} + \frac{(E_2 - E_1)a}{h} + \frac{(E_3 - E_2)a}{h} + \frac{(E_4 - E_3)a}{h} + \frac{(h - E_4)a}{h} \right) + \frac{a^2}{h^2} \left(E_1^2 + (E_2 - E_1)^2 + (E_3 - E_2)^2 + (E_4 - E_3)^2 + (h - E_4)^2 \right) \right\} \end{aligned}$$

$$\begin{aligned} \therefore \text{R.H.S} &= \frac{h}{2a} \left\{ 5y^2 - \frac{2ya}{h} \left(E_1 + E_2 - E_1 + E_3 - E_2 + E_4 - E_3 - E_4 + h \right) + \frac{a^2}{h^2} \left(E_1^2 + E_2^2 - 2E_2 E_1 + E_1^2 + E_3^2 - 2E_3 E_2 + E_2^2 + E_4^2 - 2E_4 E_3 + E_3^2 + h^2 - 2h E_4 + E_4^2 \right) \right\} \end{aligned}$$

$$\therefore \text{R.H.S} = \frac{h}{2a} \left\{ 5y^2 - 2ay + \frac{2a^2}{h^2} \left((E_1^2 + E_2^2 + E_3^2 + E_4^2) - (E_2E_1 + E_3E_2 + E_4E_3) - hE_4 + \frac{h^2}{2} \right) \right\}$$

Equating the R.H.S to the L.H.S

$$\therefore \frac{5y^2h}{2a} = \frac{5y^2h}{2a} - yh + \frac{a}{h} \left\{ (E_1^2 + E_2^2 + E_3^2 + E_4^2) - (E_2E_1 + E_3E_2 + E_4E_3) - hE_4 + \frac{h^2}{2} \right\}$$

$$\therefore y = \frac{a}{h} \left\{ (E_1^2 + E_2^2 + E_3^2 + E_4^2) - (E_2E_1 + E_3E_2 + E_4E_3) - hE_4 + \frac{h^2}{2} \right\}$$

Calculation of Ra

$$\text{Now } Ra = \frac{\text{Total area above and below mean line}}{h}$$

$$\begin{aligned} \therefore Ra &= \frac{2 \times \text{Area above mean line}}{h} && \text{(by definition)} \\ &= \frac{2}{h} \times \frac{5y^2h}{2a} = \frac{5y^2}{a} && \dots (3.43) \end{aligned}$$

Substituting for y in equn.(3.43)

$$\therefore Ra = \frac{5a}{h^4} \left\{ (E_1^2 + E_2^2 + E_3^2 + E_4^2) - (E_2E_1 + E_3E_2 + E_4E_3) - hE_4 + \frac{h^2}{2} \right\}^2$$

From the above equation a general form of Ra can be written:-

Let there be M values of interference E.
(where M = number of non-repeated values.)

Hence

$$Ra = \frac{(M+1)a^*}{h^4} \left[\sum_{j=1}^{j=M} (E_j)^2 - \sum_{j=2}^{j=M} (E_j E_{j-1}) - h E_M + \frac{h^2}{2} \right]^2 \quad \dots (3.44)$$

If a^*, h and values of E are in mm, then Ra will be in mm.

CHECK for Ra_{max} put M and E = 0

$$\therefore Ra = \frac{(0+1)a^*}{h^4} \left[0 - 0 - h0 + \frac{h^2}{2} \right]^2$$

$$\therefore Ra = \frac{a^*}{h^4} \cdot \frac{h^4}{4}$$

$$\therefore Ra = \frac{a^*}{4}$$

Equation 3.44 will under certain circumstances give over estimated values of workpiece surface roughness Ra. Such values are caused by an incorrect positioning of the mean line when the ratio $E/h < .25$, with maximum errors occurring when $M = 1$. For increased values of M, the error is reduced.

In such cases allowances can be made for the over estimated vales of Ra, since the error is constant irrespective of the value of a^* .

An error table is shown overleaf.

| E/h | .05 | .10 | .15 | .20 | .25 | .30 | .35 | .40 | .45 | .50 | .55 | .60 | .65 | .70 | .75 | .80 | .85 | .90 | .95 |
|--|-------------------|-------------------|--------------------|--------------------|------|------|------|------|------|------|------|------|------|------|------|--------------------|--------------------|-------------------|-------------------|
| Ra (arbitrary units) | | | | | | | | | | | | | | | | | | | |
| True value | 2.48 | 2.40 | 2.23 | 2.13 | 1.93 | 1.68 | 1.48 | 1.35 | 1.28 | 1.25 | 1.28 | 1.35 | 1.48 | 1.68 | 1.93 | 2.13 | 2.23 | 2.40 | 2.48 |
| Eqn.3.44 value | 4.09 | 3.36 | 2.77 | 2.31 | 1.95 | 1.68 | 1.48 | 1.35 | 1.28 | 1.25 | 1.28 | 1.35 | 1.48 | 1.68 | 1.95 | 2.31 | 2.77 | 3.36 | 4.09 |
| Excess value | 1.6 | .96 | .54 | .18 | .02 | 0 | 0 | 0 | 0 | 0 | 0 | 0 | 0 | 0 | .02 | .18 | .54 | .96 | 1.6 |
| % age error in excess | 65 | 40 | 24 | 9 | 1 | 0 | 0 | 0 | 0 | 0 | 0 | 0 | 0 | 0 | 1 | 9 | 24 | 40 | 65 |
| %age reduction in Ra due to grinding overlap | X 1 | X 4 | X 11 | X 15 | | | | | | | | | | | | X 15 | X 11 | X 4 | X 1 |

~~X~~ NB. The conditions giving the greatest over estimates of workpiece surface roughness also give the least actual reductions in Ra , and are therefore non-preferred.

APPENDIX III

COMPUTATION OF VALUES OF GRINDING WHEEL SURFACE ROUGHNESS R_a , EMBRACING EQUATIONS 3.5, 3.7 AND 3.9. IN CHAPTER 3.

Programme executed on a HEWLETT-PACKARD 9810A Calculator.

| | | | | |
|-----------|------------|-----------|-----------|-----------|
| 0000--LEL | 0040--FMT | 0080--NTO | 0120-- + | 0160-- 2 |
| 0001-- D | 0041--FMT | 0081-- 8 | 0121--NFP | 0161-- 3 |
| 0002--FMT | 0042-- E | 0082--LEL | 0122-- 7 | 0162--NFP |
| 0003--FMT | 0043-- H | 0083-- L | 0123--LEV | 0163-- 6 |
| 0004-- C | 0044--NTO | 0084--NFP | 0124-- - | 0164-- 8 |
| 0005-- 0 | 0045-- E | 0085-- 5 | 0125-- DH | 0165--NFP |
| 0006-- H | 0046-- 0 | 0086-- UP | 0126--NTO | 0166-- 7 |
| 0007--YTO | 0047--CNT | 0087-- 2 | 0127-- 0 | 0167--NTO |
| 0008--NTO | 0048-- 0 | 0088--DIV | 0128-- 1 | 0168--DIV |
| 0009-- A | 0049--FMT | 0089-- 3H | 0129-- 1 | 0169--GTO |
| 0010-- H | 0050--STP | 0090-- 0 | 0130--NFP | 0170--LEL |
| 0011--NTO | 0051--FMT- | 0091-- UP | 0131-- 5 | 0171-- 7 |
| 0012--CNT | 0052--NTO- | 0092--NFP | 0132-- UP | 0172--LEL |
| 0013--YTO | 0053-- 6 | 0093-- 6 | 0133-- 2 | 0173-- 0 |
| 0014--NTO | 0054--FMT | 0094-- " | 0134--DIV | 0174--NFP |
| 0015-- 0 | 0055--FMT- | 0095-- 2 | 0135-- DH | 0175-- 5 |
| 0016-- 0 | 0056-- E - | 0096-- 1 | 0136-- 0 | 0176-- UP |
| 0017-- E | 0057-- H - | 0097--NFP | 0137-- UP | 0177-- 2 |
| 0018--FMT | 0058--NTO- | 0098-- 6 | 0138--NFP | 0178--DIV |
| 0019--STP | 0059-- E - | 0099-- + | 0139-- 0 | 0179-- DH |
| 0020--PNT | 0060-- 0 - | 0100--NFP | 0140-- 1 | 0180-- 0 |
| 0021--PNT | 0061--CNT | 0101-- 7 | 0141-- 1 | 0181--1 3 |
| 0022--NTO | 0062-- H | 0102--DIV | 0142--NTO | 0182-- 07 |
| 0023-- 9 | 0063--FMT | 0103--GTO | 0143-- 1 | 0183--NFP |
| 0024--LEL | 0064--STP | 0104--LEL | 0144--NFP | 0184-- 7 |
| 0025-- A | 0065--PNT | 0105-- 2 | 0145-- 2 | 0185-- UP |
| 0026--FMT | 0066--NTO | 0106--CNT | 0146-- 1 | 0186--NFP |
| 0027--FMT | 0067-- 7 | 0107--NFP | 0147--NFP | 0187-- 6 |
| 0028-- E | 0068--FMT | 0108-- 5 | 0148-- 7 | 0188--1 1 |
| 0029-- H | 0069--FMT | 0109-- UP | 0149--DIV | 0189--GTO |
| 0030--NTO | 0070-- E | 0110-- 2 | 0150--NFP | 0190--LEL |
| 0031-- E | 0071-- H | 0111--DIV | 0151-- 0 | 0191-- H |
| 0032-- 0 | 0072--NTO | 0112-- DH | 0152-- 1 | 0192--CNT |
| 0033--CNT | 0073-- E | 0113-- 0 | 0153-- 1 | 0193-- - |
| 0034-- 2 | 0074-- 0 | 0114-- UP | 0154-- UP | 0194-- DH |
| 0035--FMT | 0075--CNT | 0115--NFP | 0155--NFP | 0195--NTO |
| 0036--STP | 0076--IND | 0116-- 6 | 0156-- 0 | 0196-- 0 |
| 0037--PNT | 0077--FMT | 0117-- 1 | 0157-- 2 | 0197-- 2 |
| 0038--NTO | 0078--STP | 0118--NFP | 0158-- DH | 0198--DIV |
| 0039-- 5 | 0079--PNT | 0119-- 8 | 0159-- + | 0199--NFP |

| | | | | |
|-----------|-----------|-----------|-----------|-----------|
| 0200-- 7 | 0247-- C | 0294--LBL | 0341--N=Y | 0380--FMT |
| 0201--N=0 | 0248--CNT | 0295-- H | 0342--GTO | 0381--STP |
| 0202--DIV | 0249--CNT | 0296--LBL | 0343--LBL | 0382--PNT |
| 0203-- DN | 0250--CNT | 0297-- E | 0344-- I | 0383--XTO |
| 0204--XTO | 0251-- . | 0298--LFP | 0345--CNT | 0384-- E |
| 0205-- 0 | 0252-- 0 | 0299-- 6 | 0346-- 7 | 0385--GTO |
| 0206-- 1 | 0253-- 0 | 0300--GTO | 0347--N=Y | 0386--LBL |
| 0207-- 2 | 0254-- 1 | 0301--LBL | 0348--GTO | 0387-- L |
| 0208--NFF | 0255--DIV | 0302-- H | 0349--LBL | 0388--LBL |
| 0209-- 7 | 0256-- DN | 0303--LBL | 0350-- J | 0389-- J |
| 0210-- UP | 0257--PNT | 0304-- F | 0351--CNT | 0390--FMT |
| 0211-- 4 | 0258--PNT | 0305--NFP | 0352-- 8 | 0391--FMT |
| 0212--DIV | 0259--XTO | 0306-- 7 | 0353--N=Y | 0392-- E |
| 0213--NFP | 0260-- 1 | 0307--GTO | 0354--GTO | 0393-- H |
| 0214-- 8 | 0261-- 0 | 0308--LBL | 0355--LBL | 0394--XTO |
| 0215-- UP | 0262--NFP | 0309-- H | 0356-- I | 0395-- E |
| 0216-- 2 | 0263-- 9 | 0310--LBL | 0357--CNT | 0396-- 0 |
| 0217--DIV | 0264-- UP | 0311-- G | 0358--LBL | 0397--CNT |
| 0218-- DN | 0265-- 5 | 0312--NFP | 0359-- + | 0398-- H |
| 0219-- + | 0266--N=Y | 0313-- 2 | 0360--FMT | 0399--FMT |
| 0220--NFP | 0267--GTO | 0314--GTO | 0361--FMT | 0400--STP |
| 0221-- 8 | 0268--LBL | 0315--LBL | 0362-- E | 0401--XTO |
| 0222--N=0 | 0269-- H | 0316-- H | 0363-- H | 0402-- 7 |
| 0223-- UP | 0270--CNT | 0317--LBL | 0364--XTO | 0403--PNT |
| 0224-- 4 | 0271-- E | 0318-- H | 0365-- E | 0404--GTO |
| 0225--DIV | 0272--N=Y | 0319-- UP | 0366-- 0 | 0405--LBL |
| 0226--NFP | 0273--GTO | 0320--NFP | 0367--CNT | 0406-- L |
| 0227-- 7 | 0274--LBL | 0321-- 1 | 0368-- 2 | 0407--LBL |
| 0228--DIV | 0275-- E | 0322-- 0 | 0369--FMT | 0408-- I |
| 0229-- DN | 0276--CNT | 0323--NEY | 0370--STP | 0409--FMT |
| 0230-- + | 0277-- 7 | 0324-- I | 0371--PNT | 0410--FMT |
| 0231--NFP | 0278--N=Y | 0325--FMT | 0372--XTO | 0411-- E |
| 0232-- 0 | 0279--GTO | 0326-- UP | 0373-- 5 | 0412-- H |
| 0233-- 1 | 0280--LBL | 0327--FMT | 0374--GTO | 0413--XTO |
| 0234-- 2 | 0281-- F | 0328-- DN | 0375--LBL | 0414-- E |
| 0235-- N | 0282--CNT | 0329--FMT | 0376-- L | 0415-- 0 |
| 0236--GTO | 0283-- 8 | 0330-- UP | 0377--LBL | 0416--CNT |
| 0237--LBL | 0284--N=1 | 0331--NFP | 0378-- I | 0417--IND |
| 0238-- C | 0285--GTO | 0332-- 9 | 0379--FMT | 0418--FMT |
| 0239--LBL | 0286--LBL | 0333-- UP | 0380--FMT | 0419--STP |
| 0240-- M | 0287-- G | 0334-- 5 | 0381-- E | 0420--PNT |
| 0241-- 0 | 0288--CNT | 0335--N=Y | 0382-- H | 0421--XTO |
| 0242-- UF | 0289--LBL | 0336--GTO | 0383--XTO | 0422-- 8 |
| 0243--GTO | 0290-- H | 0337--LBL | 0384-- E | 0423--GTO |
| 0244--LBL | 0291--NFP | 0338-- + | 0385-- 0 | 0424--LBL |
| 0245-- C | 0292-- 5 | 0339--CNT | 0386--CNT | 0425-- L |
| 0246--LBL | 0293--GTO | 0340-- 6 | 0387-- A | 0426--END |

Specimen calculations of Ra(wheel) for $\beta = 90^\circ$
NB. Values of $a(A)$, $h(H)$ and $w(W)$ are in mm, and Ra in μm .

| | | |
|------------------------------------|-----------------------------------|-----------------------------------|
| CONSTANT SLOPE 6.000+ | CONSTANT SLOPE 6.000+ | CONSTANT SLOPE 6.000+ |
| ENTER B 90.000+ | ENTER B 90.000+ | ENTER B 90.000+ |
| ENTER A 0.005+ | ENTER A 0.005+ | ENTER A 0.005+ |
| ENTER H 0.500+ | ENTER H 0.300+ | ENTER H 0.100+ |
| ENTER W 0.000+ <u>0.008</u> | ENTER W 0.000+ <u>0.161</u> | ENTER W 0.000+ <u>0.451</u> |
| ENTER A 0.010+ <u>0.384</u> | ENTER A 0.010+ <u>0.623</u> | ENTER A 0.010+ <u>1.620</u> |
| ENTER A 0.015+ <u>0.047</u> | ENTER A 0.015+ <u>1.354</u> | ENTER A 0.015+ <u>3.251</u> |
| ENTER A 0.020+ <u>1.475</u> | ENTER A 0.020+ <u>2.323</u> | ENTER A 0.020+ <u>5.120</u> |
| ENTER A 0.025+ <u>2.255</u> | ENTER A 0.025+ <u>3.501</u> | ENTER A 0.025+ <u>7.031</u> |
| CONSTANT SLOPE 6.000+ | CONSTANT SLOPE 6.000+ | CONSTANT SLOPE 6.000+ |
| ENTER B 90.000+ | ENTER B 90.000+ | ENTER B 90.000+ |
| ENTER A 0.005+ | ENTER A 0.005+ | ENTER A 0.005+ |
| ENTER H 0.500+ | ENTER H 0.300+ | ENTER H 0.100+ |
| ENTER W 0.250+ <u>2.474</u> | ENTER W 0.250+ <u>1.254</u> | ENTER W 0.250+ <u>0.000</u> |
| ENTER A 0.010+ <u>4.692</u> | ENTER A 0.010+ <u>2.234</u> | ENTER A 0.010+ <u>0.000</u> |
| ENTER A 0.015+ <u>7.249</u> | ENTER A 0.015+ <u>2.917</u> | ENTER A 0.015+ <u>0.000</u> |
| ENTER A 0.020+ <u>4.439</u> | ENTER A 0.020+ <u>3.100</u> | ENTER A 0.020+ <u>0.000</u> |
| ENTER A 0.025+ <u>11.250</u> | ENTER A 0.025+ <u>3.501</u> | ENTER A 0.025+ <u>0.000</u> |

Specimen calculations of Ra (wheel) for $\beta = 150^\circ$
NB. Values of a(A), h(H) and w(W) are in mm, and Ra in μm .

| | | |
|--|--|--|
| CONSTANT SLOPE 6.000+ ENTER B 150.000+ ENTER A 0.005+ ENTER H 0.500+ ENTER W 0.000+ <u>0.346</u> ENTER A 0.010+ <u>1.278</u> ENTER A 0.015+ <u>2.649</u> ENTER A 0.020+ <u>4.322</u> ENTER A 0.025+ <u>6.173</u> | CONSTANT SLOPE 6.000+ ENTER B 150.000+ ENTER A 0.005+ ENTER H 0.300+ ENTER W 0.000+ <u>0.547</u> ENTER A 0.010+ <u>1.998</u> ENTER A 0.015+ <u>3.704</u> ENTER A 0.020+ <u>5.616</u> ENTER A 0.025+ <u>7.782</u> | CONSTANT SLOPE 6.000+ ENTER B 150.000+ ENTER A 0.005+ ENTER H 0.100+ ENTER W 0.000+ <u>1.235</u> ENTER A 0.010+ <u>2.932</u> ENTER A 0.015+ <u>3.349</u> ENTER A 0.020+ <u>3.349</u> ENTER A 0.025+ <u>3.349</u> |
| CONSTANT SLOPE 6.000+ ENTER B 150.000+ ENTER A 0.005+ ENTER H 0.500+ ENTER W 0.250+ <u>2.393</u> ENTER A 0.010+ <u>4.524</u> ENTER A 0.015+ <u>6.326</u> ENTER A 0.020+ <u>7.749</u> ENTER A 0.025+ <u>8.751</u> | CONSTANT SLOPE 6.000+ ENTER B 150.000+ ENTER A 0.005+ ENTER H 0.300+ ENTER W 0.250+ <u>0.877</u> ENTER A 0.010+ <u>0.938</u> ENTER A 0.015+ <u>0.938</u> ENTER A 0.020+ <u>0.938</u> ENTER A 0.025+ <u>0.938</u> | CONSTANT SLOPE 6.000+ ENTER B 150.000+ ENTER A 0.005+ ENTER H 0.100+ ENTER W 0.250+ <u>0.940</u> ENTER A 0.010+ <u>0.940</u> ENTER A 0.015+ <u>0.940</u> ENTER A 0.020+ <u>0.940</u> ENTER A 0.025+ <u>0.940</u> |

APPENDIX IV

COMPUTATION OF VALUES OF SURFACE INTERFERENCE AND WORKPIECE SURFACE ROUGHNESS R_a , EMBRACING EQUATIONS 3.13 TO 3.44 INC. IN CHAPTER 3.

Programme executed on a HEWLETT-PACKARD 9810A Calculator.

| | | | | |
|-----------|-----------|-----------|-----------|-----------|
| 0000--FMT | 0040-- M | 0080--CNT | 0120-- 1 | 0170--YTO |
| 0001--FMT | 0045-- M | 0089-- M | 0133-- 7 | 0177-- E |
| 0002-- I | 0046--DIV | 0090-- M | 0134--XTO | 0178--CNT |
| 0003-- N | 0047--YTO | 0091--FMT | 0135-- 1 | 0179-- 0 |
| 0004-- M | 0048--CLP | 0092--STP | 0136-- 8 | 0180-- 0 |
| 0005--1.2 | 0049--FMT | 0093--PNT | 0137--XTO | 0181--CNT |
| 0006--XTO | 0050--STP | 0094--PNT | 0138-- 1 | 0182-- 2 |
| 0007--CNT | 0051--PNT | 0095--XTO | 0139-- 9 | 0183--CNT |
| 0008-- D | 0052--PNT | 0096-- 7 | 0140--CNT | 0184-- F |
| 0009-- A | 0053--XTO | 0097--CNT | 0141-- 2 | 0185-- 0 |
| 0010--XTO | 0054-- 3 | 0098-- 1 | 0142-- 6 | 0186-- 0 |
| 0011-- A | 0055--FMT | 0099-- 1 | 0143--XTO | 0187--CNT |
| 0012--CLP | 0056--FMT | 0100--XTO | 0144-- 2 | 0188-- N |
| 0013--CLP | 0057--IND | 0101-- 8 | 0145-- 0 | 0189--CNT |
| 0014-- N | 0058--CNT | 0102--XFP | 0146--XTO | 0190--INT |
| 0015--CNT | 0059-- M | 0103-- 1 | 0147-- 2 | 0191--CNT |
| 0016-- 0 | 0060-- M | 0104-- UP | 0148-- 1 | 0192-- U |
| 0017--DIV | 0061--CLP | 0105--XFP | 0149--CNT | 0193-- 0 |
| 0018--YTO | 0062--FMT | 0106-- 2 | 0150--FMT | 0194-- 0 |
| 0019--CLP | 0063--STP | 0107--DIV | 0151--FMT | 0195-- 0 |
| 0020--FMT | 0064--PNT | 0108-- DN | 0152-- E | 0196--YTO |
| 0021--STP | 0065--FMT | 0109--XTO | 0153-- N | 0197-- 1 |
| 0022--PNT | 0066--XTO | 0110-- 9 | 0154--XTO | 0198--YTO |
| 0023--PNT | 0067-- 4 | 0111--XTO | 0155-- E | 0199-- E |
| 0024--XTO | 0068--FMT | 0112-- 1 | 0156-- 0 | 0200--YTO |
| 0025-- 1 | 0069--FMT | 0113-- 0 | 0157--CNT | 0201-- E |
| 0026--FMT | 0070-- H | 0114-- UP | 0158-- 1 | 0202-- N |
| 0027--FMT | 0071--CNT | 0115--XFP | 0159--CNT | 0203--YTO |
| 0028-- M | 0072-- M | 0116-- 9 | 0160-- F | 0204-- E |
| 0029--CNT | 0073-- N | 0117-- 1 | 0161-- 0 | 0205--FMT |
| 0030-- 0 | 0074--DIV | 0118-- DN | 0162-- 0 | 0206--STP |
| 0031--DIV | 0075-- 0 | 0119--XTO | 0163--CNT | 0207--PNT |
| 0032--YTO | 0076-- E | 0120-- 1 | 0164-- H | 0208--FMT |
| 0033--CLP | 0077--INT | 0121-- 1 | 0165--CNT | 0209-- UP |
| 0034--FMT | 0078--CLP | 0122--CNT | 0166--INT | 0210-- 2 |
| 0035--STP | 0079--FMT | 0123-- 2 | 0167--CNT | 0211--X Y |
| 0036--PNT | 0080--STP | 0124-- 5 | 0168--YTO | 0212--GTO |
| 0037--PNT | 0081--PNT | 0125--XTO | 0169-- A | 0213--LBL |
| 0038--XTO | 0082--PNT | 0126-- 1 | 0170-- M | 0214-- A |
| 0039-- 2 | 0083--XTO | 0127-- 6 | 0171-- E | 0215--CNT |
| 0040--FMT | 0084-- A | 0128--CNT | 0172--CNT | 0216--X Y |
| 0041--FMT | 0085--FMT | 0129-- 3 | 0173--YTO | 0217--GTO |
| 0042--INT | 0086--FMT | 0130-- 6 | 0174-- E | 0218--LBL |
| 0043--CNT | 0087-- 0 | 0131--XTO | 0175-- N | 0219-- B |

| | | | | |
|-----------|-----------|-----------|-----------|-----------|
| 0220--CNT | 0270-- 6 | 0330--CNT | 0390-- 6 | 0450-- 0 |
| 0221--LBL | 0271--HFP | 0331--INT | 0391-- - | 0451--FMT |
| 0222-- A | 0272-- 3 | 0332--CNT | 0392-- DN | 0452--PMT |
| 0223--FMT | 0273-- UP | 0333-- 0 | 0393-- UP | 0453--PMT |
| 0224--FMT | 0274--HFP | 0334-- a | 0394--INT | 0454--INT |
| 0225-- H | 0275-- 2 | 0335-- a | 0395-- - | 0455--INT |
| 0226--CNT | 0276--DIV | 0336-- . | 0396-- DN | 0456--INT |
| 0227--INT | 0277--HFP | 0337--CNT | 0397--INT | 0457--INT |
| 0228--CNT | 0278-- 6 | 0338--YTO | 0398-- 1 | 0458-- 1 |
| 0229--YTO | 0279--DIV | 0339-- E | 0399-- 7 | 0459-- 3 |
| 0230-- A | 0280--HFP | 0340-- N | 0400-- 1 | 0460-- UP |
| 0231-- M | 0281--IND | 0341--YTO | 0401-- 9 | 0461-- 1 |
| 0232-- E | 0282-- 1 | 0342-- E | 0402-- 7 | 0462-- - |
| 0233--CNT | 0283-- 6 | 0343--FMT | 0403--HFR | 0463-- DN |
| 0234--YTO | 0284-- - | 0344--LBL | 0404-- 9 | 0464--INT |
| 0235-- E | 0285-- DN | 0345-- 1 | 0405-- UP | 0465-- 1 |
| 0236-- H | 0286-- UP | 0346-- 6 | 0406--HFP | 0466-- 4 |
| 0237--YTO | 0287--INT | 0347-- 1 | 0407-- 1 | 0467-- UP |
| 0238-- E | 0288-- - | 0348-- 6 | 0408-- 0 | 0468-- 1 |
| 0239--FMT | 0289-- DN | 0349-- UP | 0409-- + | 0469-- - |
| 0240--CNT | 0290-- 6 | 0350-- 1 | 0410-- DN | 0470-- DN |
| 0241--GTO | 0291-- 6 | 0351-- 6 | 0411--INT | 0471--INT |
| 0242--LBL | 0292-- - | 0352-- 1 | 0412-- 9 | 0472-- 1 |
| 0243-- C | 0293-- DN | 0353-- + | 0413-- UP | 0473-- 5 |
| 0244--LBL | 0294-- 7 | 0354-- DN | 0414--HFP | 0474--HFR |
| 0245-- C | 0295--HFP | 0355-- 1 | 0415-- 1 | 0475-- 1 |
| 0246--HFP | 0296-- 9 | 0356-- 6 | 0416-- 1 | 0476-- 2 |
| 0247-- 1 | 0297-- UP | 0357-- 1 | 0417-- 1 | 0477-- UP |
| 0248-- 6 | 0298--HFP | 0358-- 7 | 0418-- 1 | 0478-- 1 |
| 0249-- UP | 0299-- 1 | 0359-- UP | 0419-- 1 | 0479-- 1 |
| 0250-- 1 | 0300-- + | 0360-- 1 | 0420--GTO | 0480--GTO |
| 0251-- + | 0301-- DN | 0361-- 1 | 0421--CNT | 0481--LBL |
| 0252-- DN | 0302--INT | 0362-- 1 | 0422--H=Y | 0482-- H |
| 0253--INT | 0303-- 9 | 0363-- 1 | 0423--GTO | 0483--CNT |
| 0254-- 1 | 0304-- 9 | 0364-- 1 | 0424--LBL | 0484-- 1 |
| 0255-- 6 | 0305-- 1 | 0365-- 1 | 0425-- E | 0485--GTO |
| 0256--HFP | 0306-- 1 | 0366-- 1 | 0426--CNT | 0486--LBL |
| 0257-- 1 | 0307-- 0 | 0367-- + | 0427-- 1 | 0487-- G |
| 0258-- 7 | 0308-- + | 0368-- DN | 0428-- 1 | 0488--CNT |
| 0259-- UP | 0309-- 9 | 0369-- 1 | 0429-- 1 | 0489--GTO |
| 0260-- 1 | 0310--INT | 0370-- 1 | 0430-- 1 | 0490--LBL |
| 0261-- + | 0311-- 9 | 0371-- 7 | 0431-- 1 | 0491-- 1 |
| 0262-- DN | 0312-- UP | 0372--HFP | 0432-- D | 0492-- H |
| 0263--INT | 0313--HFP | 0373-- 9 | 0433-- 1 | 0493--LBL |
| 0264-- 1 | 0314-- 1 | 0374-- UP | 0434-- 1 | 0494-- H |
| 0265-- 7 | 0315-- 1 | 0375--INT | 0435--HFR | 0495-- 3 |
| 0266--HFP | 0316-- 1 | 0376-- - | 0436-- 4 | 0496--FMT |
| 0267-- 9 | 0317--GTO | 0377-- DN | 0437-- UP | 0497--FMT |
| 0268-- UP | 0318--LBL | 0378--INT | 0438-- 1 | 0498-- 0 |
| 0269--INT | 0319-- C | 0379--IND | 0439-- 1 | 0499--INT |
| 0270-- - | 0320--CNT | 0380-- 1 | 0440-- 3 | 0500-- E |
| 0271-- 1 | 0321--H=Y | 0381-- 6 | 0441--DIV | 0501-- 0 |
| 0272--KEY | 0322--GTO | 0382--HFP | 0442-- DN | 0502-- L |
| 0273-- - | 0323--LBL | 0383-- 3 | 0443--INT | 0503-- A |
| 0274-- DN | 0324-- C | 0384-- UP | 0444-- 1 | 0504-- a |
| 0275--INT | 0325--CNT | 0385--HFR | 0445--FMT | 0505--FMT |
| 0276--IND | 0326--H=Y | 0386-- 2 | 0446-- 1 | 0506--FMT |
| 0277-- 1 | 0327--GTO | 0387--DIV | 0447-- 2 | 0507--GTO |
| | 0328--LBL | 0388--HFP | 0448-- 1 | 0508--LBL |
| | 0329-- D | 0389-- 6 | 0449-- 1 | 0509--INT |
| | 0330--CNT | 0390--DIV | 0450-- 1 | 0510--INT |
| | 0331--LBL | 0391--HFP | 0451-- + | 0511--INT |
| | 0332-- B | 0392--IND | | 0512--INT |
| | 0333--FMT | 0393-- 1 | | 0513--INT |
| | 0334--FMT | | | 0514--INT |
| | 0335-- H | | | 0515--INT |

| | | | | |
|-----------|-----------|-----------|-----------|-----------|
| 0510--LNT | 0560--A | 0620--DH | 0680--N Y | 0740--LNT |
| 0511--LBL | 0565--L | 0627--NTO | 0685--GTO | 0742--N Y |
| 0512--F | 0570--1 H | 0628--2 | 0686--LBL | 0744--GTO |
| 0513--FMT | 0571--E | 0629--8 | 0687--M | 0745--LBL |
| 0514--FMT | 0572--YTO | 0630--NFP | 0688--CNT | 0746--7 |
| 0515--C | 0573--CNT | 0631--1 | 0689--LBL | 0747--LBL |
| 0516--A | 0574--O | 0632--8 | 0690--L | 0748--7 |
| 0517--YTO | 0575--F | 0633--UP | 0691--FMT | 0749--FMT |
| 0518--E | 0576--CNT | 0634--1 | 0692--FMT | 0750--FMT |
| 0519--CNT | 0577--I | 0635--4 | 0693--C | 0751--C |
| 0520--CNT | 0578--H | 0636--DH | 0694--A | 0752--A |
| 0521--3 | 0579--NTO | 0637--NTO | 0695--YTO | 0753--YTO |
| 0522--CLP | 0580--F | 0638--1 | 0696--E | 0754--E |
| 0523--IND | 0581--. | 0639--8 | 0697--CNT | 0755--CNT |
| 0524--M | 0582--E | 0640--NFP | 0698--CNT | 0756--2 |
| 0525--DIV | 0583--CLP | 0641--IND | 0699--1 | 0757--CLP |
| 0526--INT | 0584--FMT | 0642--2 | 0700--CNT | 0758--IND |
| 0527--GFL | 0585--GTO | 0643--8 | 0701--CNT | 0759--M |
| 0528--N Y | 0586--LBL | 0644--UP | 0702--CNT | 0760--DIV |
| 0529--A | 0587--J | 0645--NFP | 0703--IND | 0761--INT |
| 0530--+ | 0588--LBL | 0646--IND | 0704--M | 0762--SFL |
| 0531--B | 0589--J | 0647--1 | 0705--DIV | 0763--N Y |
| 0532--PSE | 0590--NFP | 0648--8 | 0706--INT | 0764--A |
| 0533--CLP | 0591--2 | 0649--+ | 0707--SFL | 0765--+ |
| 0534--B | 0592--2 | 0650--NFP | 0708--A | 0766--B |
| 0535--INT | 0593--UP | 0651--2 | 0709--D | 0767--PSE |
| 0536--DIV | 0594--1 | 0652--4 | 0710--E | 0768--CLP |
| 0537--M | 0595--+ | 0653--+ | 0711--G | 0769--N Y |
| 0538--CNT | 0596--DH | 0654--DH | 0712--. | 0770--1 |
| 0539--CNT | 0597--NTO | 0655--UP | 0713--CNT | 0771--. |
| 0540--CNT | 0598--2 | 0656--INT | 0714--I | 0772--B |
| 0541--CNT | 0599--2 | 0657--. | 0715--CNT | 0773--PSE |
| 0542--CNT | 0600--UP | 0658--DH | 0716--CNT | 0774--INT |
| 0543--CNT | 0601--NFP | 0659--NTO | 0717--CNT | 0775--DI" |
| 0544--CNT | 0602--1 | 0660--2 | 0718--CNT | 0776--M |
| 0545--CNT | 0603--4 | 0661--4 | 0719--CNT | 0777--CNT |
| 0546--CNT | 0604--N Y | 0662--UP | 0720--N Y | 0778--CNT |
| 0547--N Y | 0605--GTO | 0663--NFP | 0721--A | 0779--CNT |
| 0548--1 | 0606--LBL | 0664--6 | 0722--. | 0780--N Y |
| 0549--PSE | 0607--YTO | 0665--H | 0723--1 | 0781--A |
| 0550--CLP | 0608--CNT | 0666--DH | 0724--PSE | 0782--. |
| 0551--FMT | 0609--N Y | 0667--PNT | 0725--CLR | 0783--2 |
| 0552--1 | 0610--GTO | 0668--CNT | 0726--FMT | 0784--PSE |
| 0553--NTO | 0611--LBL | 0669--CNT | 0727--GTO | 0785--CLP |
| 0554--1 | 0612--K | 0670--GTO | 0728--LBL | 0786--FMT |
| 0555--4 | 0613--CNT | 0671--LBL | 0729--I | 0787--LBL |
| 0556--LBL | 0614--N Y | 0672--J | 0730--CNT | 0788--H |
| 0557--I | 0615--GTO | 0673--CNT | 0731--LBL | 0789--8 |
| 0558--8 | 0616--LBL | 0674--LBL | 0732--M | 0790--NTO |
| 0559--NTO | 0617--F | 0675--G | 0733--NFP | 0791--2 |
| 0560--2 | 0618--LBL | 0676--NFP | 0734--1 | 0792--3 |
| 0561--2 | 0619--F | 0677--1 | 0735--2 | 0793--NTO |
| 0562--NTO | 0620--NFP | 0678--3 | 0736--UP | 0794--2 |
| 0563--2 | 0621--2 | 0679--N Y | 0737--2 | 0795--5 |
| 0564--4 | 0622--8 | 0680--GTO | 0738--N Y | 0796--FMT |
| 0565--FMT | 0623--UP | 0681--LBL | 0739--GTO | 0797--FMT |
| 0566--FMT | 0624--1 | 0682--L | 0740--LBL | 0798--INT |
| 0567--INT | 0625--+ | 0683--CNT | 0741--F | 0799--6 |

| | | | | |
|-------------|-----------|-----------|-------------|-------------|
| 0800-- L | 0850--WFP | 0916--LNT | 0974--WTO | 1032-- E |
| 0801--1 : : | 0859-- 1 | 0917--CNT | 0975-- 6 | 1033-- H |
| 0802-- E | 0860-- 9 | 0918--N Y | 0976-- 2 | 1034--WTO |
| 0803--YTO | 0861-- UP | 0919-- A | 0977--WTO | 1035-- E |
| 0804--CNT | 0862-- 1 | 0920-- - | 0978-- 6 | 1036-- o |
| 0805-- 0 | 0863-- + | 0921-- 1 | 0979-- 3 | 1037--CNT |
| 0806-- F | 0864-- DN | 0922--PSE | 0980--WTO | 1038--INT |
| 0807--CNT | 0865--WTO | 0923--CLP | 0981-- 6 | 1039-- A |
| 0808-- I | 0866-- 1 | 0924--FMT | 0982-- 4 | 1040-- L |
| 0809-- H | 0867-- 9 | 0925--GTO | 0983--WTO | 1041--1 : : |
| 0810--WTO | 0868--WFP | 0926--LBL | 0984-- 6 | 1042-- E |
| 0811-- F | 0869--IND | 0927-- I | 0985-- 5 | 1043--YTO |
| 0812-- . | 0870-- 2 | 0928--CNT | 0986--WTO | 1044--CNT |
| 0813-- E | 0871-- 1 | 0929--LBL | 0987-- 6 | 1045-- 0 |
| 0814--CLP | 0872-- UP | 0930--YTO | 0988-- 6 | 1046-- F |
| 0815--FMT | 0873--WFP | 0931-- 0 | 0989--FMT | 1047--CNT |
| 0816--LBL | 0874--IND | 0932--WTO | 0990--FMT | 1048-- E |
| 0817-- n | 0875-- 1 | 0933-- 4 | 0991-- E | 1049--CNT |
| 0818--WFP | 0876-- 9 | 0934-- 8 | 0992-- H | 1050-- I |
| 0819-- 2 | 0877-- + | 0935--WTO | 0993--WTO | 1051-- H |
| 0820-- 3 | 0878--WFP | 0936-- 4 | 0994-- E | 1052--CNT |
| 0821-- UP | 0879-- 2 | 0937-- 9 | 0995-- o | 1053-- C |
| 0822-- 1 | 0880-- 5 | 0938--WTO | 0996--CNT | 1054-- 0 |
| 0823-- + | 0881-- + | 0939-- 5 | 0997-- L | 1055-- o |
| 0824-- DN | 0882-- DN | 0940-- 0 | 0998-- M | 1056-- o |
| 0825--WTO | 0883-- UP | 0941--WTO | 0999--WTO | 1057-- E |
| 0826-- 2 | 0884--INT | 0942-- 5 | 1000-- . | 1058-- C |
| 0827-- 2 | 0885-- - | 0943-- 1 | 1001--CNT | 1059--WTO |
| 0828-- UP | 0886-- DN | 0944--WTO | 1002-- F | 1060--CLR |
| 0829--WFP | 0887--WTO | 0945-- 5 | 1003-- 0 | 1061-- 0 |
| 0830-- 1 | 0888-- 2 | 0946-- 2 | 1004-- o | 1062-- n |
| 0831-- 5 | 0889-- 5 | 0947--WTO | 1005--CNT | 1063-- D |
| 0832--N Y | 0890-- UP | 0948-- 5 | 1006-- E | 1064-- E |
| 0833--GTO | 0891--WFP | 0949-- 3 | 1007-- H | 1065-- o |
| 0834--LBL | 0892-- e | 0950--WTO | 1008-- 0 | 1066--FMT |
| 0835-- b | 0893-- N | 0951-- 5 | 1009-- H | 1067-- 0 |
| 0836--CNT | 0894-- DN | 0952-- 4 | 1010-- o | 1068--WTO |
| 0837--N Y | 0895--FMT | 0953--WTO | 1011-- E | 1069-- 5 |
| 0838--GTO | 0896--CNT | 0954-- 5 | 1012-- n | 1070-- 0 |
| 0839--LBL | 0897--CNT | 0955-- 5 | 1013-- E | 1071--CNT |
| 0840-- o | 0898--GTO | 0956--WTO | 1014-- A | 1072-- 4 |
| 0841--CNT | 0899--LEL | 0957-- 5 | 1015--WTO | 1073-- 7 |
| 0842--N Y | 0900-- n | 0958-- 6 | 1016--CNT | 1074--WTO |
| 0843--GTO | 0901--CNT | 0959--WTO | 1017--INT | 1075-- C |
| 0844--LBL | 0902--LBL | 0960-- 5 | 1018-- A | 1076-- 0 |
| 0845-- o | 0903-- b | 0961-- 7 | 1019-- L | 1077--LBL |
| 0846--LBL | 0904--FMT | 0962--WTO | 1020--1 : : | 1078--WTO |
| 0847-- o | 0905--FMT | 0963-- 5 | 1021-- E | 1079--WFP |
| 0848--WFP | 0906--CLP | 0964-- 8 | 1022--YTO | 1080-- 5 |
| 0849-- 2 | 0907-- B | 0965--WTO | 1023--FMT | 1081-- 8 |
| 0850-- 1 | 0908--INT | 0966-- 5 | 1024--STP | 1082-- UP |
| 0851-- UP | 0909--DIV | 0967-- 9 | 1025--PNT | 1083-- 1 |
| 0852-- 1 | 0910-- A | 0968--WTO | 1026--PNT | 1084-- + |
| 0853-- + | 0911--CNT | 0969-- 6 | 1027--WTO | 1085-- DN |
| 0854-- DN | 0912--CNT | 0970-- 0 | 1028-- 5 | 1086--WTO |
| 0855--WTO | 0913--CNT | 0971--WTO | 1029-- 9 | 1087-- 5 |
| 0856-- 2 | 0914--CNT | 0972-- 6 | 1030--FMT | 1088-- 8 |
| 0857-- 1 | 0915--CNT | 0973-- 1 | 1031--FMT | 1089-- UP |

| | | | | |
|-----------|-----------|-----------|-----------|-----------|
| 1090--XFP | 1150-- 6 | 1210-- 0 | 1276--XTO | 1330-- DN |
| 1091-- 5 | 1151-- 0 | 1211--XTO | 1277-- 5 | 1331--XSO |
| 1092-- 9 | 1152-- UP | 1212-- 6 | 1278-- 5 | 1332--XTO |
| 1093--X Y | 1153-- 1 | 1213-- 3 | 1279--GTO | 1333-- 6 |
| 1094--GTO | 1154-- + | 1214--LDL | 1274--LBL | 1334-- 6 |
| 1095--LEL | 1155-- DN | 1215--XSO | 1275--XSO | 1335--XFP |
| 1096--1 X | 1156--XTO | 1216--XFP | 1276--CNT | 1336-- 5 |
| 1097--CNT | 1157-- 6 | 1217-- 6 | 1277--LBL | 1337-- 9 |
| 1098--X Y | 1158-- 0 | 1218-- 2 | 1278-- 1 | 1338-- UP |
| 1099--GTO | 1159-- UP | 1219-- UP | 1279--XFP | 1339-- 1 |
| 1100--LBL | 1160-- 5 | 1220-- 1 | 1280-- 5 | 1340-- + |
| 1101--INT | 1161-- 7 | 1221-- + | 1281-- 9 | 1341--XFP |
| 1102--CNT | 1162--X Y | 1222-- DN | 1282-- UP | 1342-- 7 |
| 1103--X=Y | 1163--GTO | 1223--XTO | 1283-- 4 | 1343-- 0 |
| 1104--GTO | 1164--LBL | 1224-- 6 | 1284-- 7 | 1344-- 1 |
| 1105--LBL | 1165--XFP | 1225-- 2 | 1285-- + | 1345-- 0 |
| 1106--INT | 1166--CNT | 1226--XFP | 1286-- DN | 1346-- 0 |
| 1107--LBL | 1167--X=Y | 1227-- 6 | 1287--XTO | 1347-- 1 |
| 1108--INT | 1168--GTO | 1228-- 0 | 1288-- 6 | 1348--XFP |
| 1109--XFP | 1169--LDL | 1229-- UP | 1289-- 4 | 1349-- 6 |
| 1110-- 6 | 1170-- YE | 1230-- 1 | 1290--XFP | 1350-- UP |
| 1111-- 9 | 1171--CNT | 1231-- + | 1291--IND | 1351-- 1 |
| 1112-- UP | 1172--X Y | 1232-- DN | 1292-- 6 | 1352-- 0 |
| 1113-- 1 | 1173--GTO | 1233--XTO | 1293-- 4 | 1353-- 0 |
| 1114-- + | 1174--LBL | 1234-- 6 | 1294-- UP | 1354-- DN |
| 1115-- DN | 1175-- YE | 1235-- 0 | 1295--XFP | 1355--XSO |
| 1116--XTO | 1176--LEL | 1236-- UP | 1296-- 6 | 1356--XSO |
| 1117-- 6 | 1177-- YE | 1237-- 5 | 1297-- 0 | 1357--DIV |
| 1118-- 6 | 1178--XFP | 1238-- 7 | 1298-- 1 | 1358--XFP |
| 1119--STP | 1179--IND | 1239--X Y | 1299-- 0 | 1359-- 6 |
| 1120--FMT | 1180-- 6 | 1240--GTO | 1300-- 0 | 1360-- 6 |
| 1121-- UP | 1181-- 0 | 1241--LBL | 1301-- 0 | 1361-- 0 |
| 1122-- 1 | 1182--XSO | 1242-- 1 | 1302-- DN | 1362-- 1 |
| 1123-- 0 | 1183-- UP | 1243--CNT | 1303--XTO | 1363-- 0 |
| 1124-- 6 | 1184--XFP | 1244--X=Y | 1304-- 6 | 1364-- 0 |
| 1125-- 7 | 1185-- 6 | 1245--GTO | 1305-- 5 | 1365-- 0 |
| 1126-- DN | 1186-- 1 | 1246--LDL | 1306--XFP | 1366--DIV |
| 1127--XTO | 1187-- + | 1247-- 2 | 1307-- 6 | 1367-- DN |
| 1128--IND | 1188-- DN | 1248--CNT | 1308-- UP | 1368--FMT |
| 1129-- 6 | 1189--XTO | 1249--X Y | 1309-- 1 | 1369--FMT |
| 1130-- 0 | 1190-- 6 | 1250--GTO | 1310-- 0 | 1370--CLP |
| 1131--GTO | 1191-- 1 | 1251--LBL | 1311-- 0 | 1371-- 0 |
| 1132--LBL | 1192--GTO | 1252-- 2 | 1312-- 1 | 1372-- R |
| 1133--XTO | 1193--LBL | 1253--LBL | 1313-- DN | 1373--CNT |
| 1134--CNT | 1194--IND | 1254-- 2 | 1314--XSO | 1374--CNT |
| 1135--LBL | 1195--CNT | 1255--XFP | 1315-- UP | 1375--CNT |
| 1136--1 X | 1196--LBL | 1256--IND | 1316-- 2 | 1376-- M |
| 1137-- 4 | 1197--XFP | 1257-- 6 | 1317--DIV | 1377-- I |
| 1138-- 7 | 1198-- 4 | 1258-- 2 | 1318--XFP | 1378-- C |
| 1139--XTO | 1199-- 6 | 1259-- UP | 1319-- 6 | 1379-- 0 |
| 1140-- 6 | 1200--XTO | 1260--XFP | 1320-- 1 | 1380-- 0 |
| 1141-- 6 | 1201-- 6 | 1261--IND | 1321-- + | 1381-- 0 |
| 1142--CNT | 1202-- 2 | 1262-- 6 | 1322--XFP | 1382-- E |
| 1143-- 6 | 1203--CNT | 1263-- 0 | 1323-- 6 | 1383--XTO |
| 1144--XTO | 1204-- 4 | 1264-- 0 | 1324-- 3 | 1384-- 0 |
| 1145-- 6 | 1205-- 7 | 1265--XFP | 1325-- - | 1385-- E |
| 1146-- 1 | 1206--XTO | 1266-- 6 | 1326--XFP | 1386--XTO |
| 1147--LBL | 1207-- 6 | 1267-- 3 | 1327-- 6 | 1387--FMT |
| 1148--IND | 1208-- 0 | 1268-- + | 1328-- 5 | 1388--FMT |
| 1149--XFP | 1209--CNT | 1269-- DN | 1329-- - | 1389--STP |
| | | | | 1390--LMB |

Specimen calculations of interference E, showing the repetition
of values of E for each band of width v_t/n .

(where $M=n$, $V=v$, $H=h$, $W=w$ and $L=l$)

| INPUT DATA | | BAND NUMBER | BAND NUMBER |
|------------------|----------|-------------|-------------|
| H P S | 29.0000+ | 3.0000 | 10.0000 |
| | | 0.0033 | 0.0033 |
| H P S | 1.2000+ | 0.1667 | 0.1667 |
| | | 0.2500 | 0.2500 |
| | | 0.3333 | 0.3333 |
| V MM S | 6.0000+ | BAND NUMBER | BAND NUMBER |
| | | 4.0000 | 11.0000 |
| H MM PEV | 0.5000+ | 0.0033 | 0.0033 |
| | | 0.1667 | 0.1667 |
| | | 0.2500 | 0.2500 |
| | | 0.3333 | 0.3333 |
| H MM | 25.0000+ | BAND NUMBER | BAND NUMBER |
| | | 5.0000 | 12.0000 |
| L MM | 75.0000+ | 0.0033 | 0.0033 |
| | | 0.1667 | 0.1667 |
| | | 0.2500 | 0.2500 |
| | | 0.3333 | 0.3333 |
| ENTER 1 FOR H V | | BAND NUMBER | BAND NUMBER |
| CHNL SENSE OF 2 | | 6.0000 | 13.0000 |
| FOR H V OPPOSITE | | 0.0033 | 0.0033 |
| SENSE | 2.0000+ | 0.1667 | 0.1667 |
| | | 0.2500 | 0.2500 |
| H V OPP. SENSE | | 0.3333 | 0.3333 |
| BAND WIDTHS | 16.0000 | BAND NUMBER | BAND NUMBER |
| | | 7.0000 | 14.0000 |
| A+B | 5.0000 | 0.0033 | 0.0033 |
| | | 0.1667 | 0.1667 |
| | | 0.2500 | 0.2500 |
| | | 0.3333 | 0.3333 |
| CASE 1 MM V=A | | BAND NUMBER | BAND NUMBER |
| CFG. I (A-1) | | 8.0000 | 15.0000 |
| BAND NUMBER | 1.0000 | 0.0033 | 0.0033 |
| | | 0.1667 | 0.1667 |
| | 0.0033 | 0.2500 | 0.2500 |
| | 0.1667 | 0.3333 | 0.3333 |
| | 0.2500 | BAND NUMBER | BAND NUMBER |
| | 0.3333 | 9.0000 | 16.0000 |
| BAND NUMBER | 2.0000 | 0.0033 | 0.0033 |
| | | 0.1667 | 0.1667 |
| | 0.0033 | 0.2500 | 0.2500 |
| | 0.1667 | 0.3333 | 0.3333 |

Specimen calculations of interference E, showing how the workpiece can have two values of surface roughness Ra for each band of width v_t/n .

| | |
|------------------|-------------|
| INPUT DATA | BAND NUMBER |
| | 1.0000 |
| H P S | 0.2692 |
| 27.0000- | BAND NUMBER |
| | 2.0000 |
| H P S | 0.2692 |
| 1.3000+ | BAND NUMBER |
| | 3.0000 |
| V MM S | 0.2692 |
| 7.0000- | BAND NUMBER |
| | 4.0000 |
| H MM PEV | 0.2692 |
| 0.5000+ | BAND NUMBER |
| | 0.2692 |
| M MM | 0.2692 |
| 20.0000- | BAND NUMBER |
| | 1A-1 |
| L MM | BAND NUMBER |
| 17.0000- | 1.0000 |
| ENTER 1 FOR H V | 0.2692 |
| SAME SENSE OF 2 | 0.5085 |
| FOR H V OPPOSITE | BAND NUMBER |
| SENSE | 2.0000 |
| 2.0000+ | 0.2692 |
| | 0.5085 |
| H V OFF. SENSE | BAND NUMBER |
| BAND WIDTHS | 3.0000 |
| 4.0000 | 0.2692 |
| | 0.5085 |
| A/P | BAND NUMBER |
| 3.7143 | 4.0000 |
| CASE 2 | 0.2692 |
| MM " = 1A+B1 | 0.5085 |
| 11-DIV M 1A-21 | |

NB. Equation (3.46) may produce incorrect values of workpiece surface roughness Ra, under the following circumstances :-

1. When repeated values of interference are used more than once.

2. When very small values of interference E, or values of E close together are used, causing an incorrect value of M to be entered into the equation.

Specimen calculations of workpiece surface roughness Ra. $V_t \rightarrow$
 $h \rightarrow$

| | | |
|---|---|---|
| INPUT DATA | INPUT DATA | INPUT DATA |
| H P S 29.6667+ | H P S 29.6667+ | H P S 29.6667+ |
| H P S 1.0000+ | H P S 1.0000+ | H P S 1.0000+ |
| V MM S <u>2.5000+</u> | V MM S <u>10.0000+</u> | V MM S <u>20.0000+</u> |
| W MM 25.0000+ | W MM 25.0000+ | W MM 25.0000+ |
| H MM PEV 0.5000+ | H MM PEV 0.5000+ | H MM PEV 0.5000+ |
| H MM 0.0100+ | H MM 0.0100+ | H MM 0.0100+ |
| ENTER 1 FOR H V SAME SENSE OR 2 FOR H V OPPOSITE SENSE 1.0000+ | ENTER 1 FOR H V SAME SENSE OR 2 FOR H V OPPOSITE SENSE 1.0000+ | ENTER 1 FOR H V SAME SENSE OR 2 FOR H V OPPOSITE SENSE 1.0000+ |
| H V SAME SENSE A+B 10.0000 | H V SAME SENSE A+B 2.5000 | H V SAME SENSE A+B 1.2500 |
| CASE 1 MM V=A DEG. I 1A-11 | CASE 2 MM V=A+B 11-BIV M 1A-21 | CASE 3 MM V=A+B 11 |
| VALUES OF INTF.E 0.1667 0.3333 0.5000 0.1666 0.3333 0.4999 0.1666 0.3332 0.4999 ENTER LMT. FOR E NONREPEAT VALUES 3.0000+ | VALUES OF INTF.E 0.1667 ENTER LMT. FOR E NONREPEAT VALUES 1.0000+ | VALUES OF INTF.E 0.1667 ENTER LMT. FOR E NONREPEAT VALUES 1.0000+ |
| ENTER VALUES OF E IN CORRECT ORDER 0.1667+ 0.3333+ 0.5000+ | ENTER VALUES OF E IN CORRECT ORDER 0.1667+ | ENTER VALUES OF E IN CORRECT ORDER 0.1667+ |
| RA MICROMETRES <u>1.1111</u> | RA MICROMETRES <u>1.5410</u> | RA MICROMETRES <u>1.5410</u> |

Specimen calculations of workpiece surface roughness Ra.

$V_t \Rightarrow$
 $h \Leftarrow$

| INPUT DATA | INPUT DATA | INPUT DATA |
|---|---|---|
| H P S 29.6667+ | H P S 29.6667+ | H P S 29.6667+ |
| H P S 1.0000- | H P S 1.0000+ | H P S 1.0000= |
| W MM S <u>2.5000+</u> | W MM S <u>10.0000+</u> | W MM S <u>20.0000+</u> |
| W MM 25.0000- | W MM 25.0000+ | W MM 25.0000= |
| H MM PEV 0.5000- | H MM PEV 0.5000+ | H MM PEV 0.5000= |
| A MM 0.0100+ | A MM 0.0100+ | A MM 0.0100= |
| ENTER 1 FOR H V SAME SENSE OR 2 FOR H V OPPOSITE SENSE 2.0000+ | ENTER 1 FOR H V SAME SENSE OR 2 FOR H V OPPOSITE SENSE 2.0000- | ENTER 1 FOR H V SAME SENSE OR 2 FOR H V OPPOSITE SENSE 2.0000= |
| H V OPP. SENSE A+B 10.0000 | H V OPP. SENSE A+B 2.5000 | H V OPP. SENSE A+B 1.2500 |
| CASE 1 MM V=A DEL. I (A-1) | CASE 2 MM V=(A+B) 11-B:V M (A-2) | CASE 3 MM V=(A+B) BY P (1) |
| VALUES OF INTF.E 0.3334 0.1667 0.0001 0.3334 0.1668 0.0001 0.3335 0.1668 0.0002 ENTER LMT. FOR E NONREPEAT VALUES 2.0000- | VALUES OF INTF.E 0.3334 0.1667 0.0001 0.3334 0.1668 0.0001 0.3335 0.1668 0.0002 ENTER LMT. FOR E NONREPEAT VALUES 1.0000- | VALUES OF INTF.E 0.3334 0.1667 0.0001 0.3334 0.1668 0.0001 0.3335 0.1668 0.0002 ENTER LMT. FOR E NONREPEAT VALUES 1.0000= |
| ENTER VALUES OF E IN CORRECT ORDER 0.1667+ 0.3334+ | ENTER VALUES OF E IN CORRECT ORDER 0.3334+ | ENTER VALUES OF E IN CORRECT ORDER 0.3334= |
| RA MICROMETRES <u>0.013</u> | RA MICROMETRES <u>1.5037</u> | RA MICROMETRES <u>1.5437</u> |

Specimen calculations of workpiece surface roughness Ra. $V_t \rightarrow$
 $h \rightarrow$

| | | |
|---|---|---|
| INPUT DATA | INPUT DATA | INPUT DATA |
| H P S 29.6667+ | H P S 29.6667+ | H P S 29.6667- |
| H P S 1.0000+ | H P S 1.0000+ | H P S 1.0000- |
| V MM S 2.5000+ | V MM S 10.0000- | V MM S 20.0000- |
| H MM 25.0000+ | H MM 25.0000+ | H MM 25.0000+ |
| H MM PEV 0.5000+ | H MM PEV 0.5000+ | H MM PEV 0.5000+ |
| A MM 0.0020+ | A MM 0.0020+ | A MM 0.0020+ |
| ENTER 1 FOR H V SAME SENSE OR 2 FOR H V OPPOSITE SENSE 1.0000- | ENTER 1 FOR H V SAME SENSE OR 2 FOR H V OPPOSITE SENSE 1.0000+ | ENTER 1 FOR H V SAME SENSE OR 2 FOR H V OPPOSITE SENSE 1.0000+ |
| H V SAME SENSE AND 10.0000 | H V SAME SENSE AND 2.5000 | H V SAME SENSE AND 1.2500 |
| ENTER 1 FOR H V=A AND I (A-1) | ENTER 2 FOR V=(A+B) I=B/H (A-2) | ENTER 3 FOR V=(A+B) I=B/H (1) |
| VALUES OF INTF.E 0.1667 0.3333 0.5000 0.1666 0.3333 0.4999 0.1666 0.3332 0.4999 ENTER LMT. FOR E NONREPEAT VALUES 2.0000+ | VALUES OF INTF.E 0.1667 ENTER LMT. FOR E NONREPEAT VALUES 1.0000+ | VALUES OF INTF.E 0.1667 ENTER LMT. FOR E NONREPEAT VALUES 1.0000- |
| ENTER VALUES OF E IN CORRECT ORDER 0.1667+ 0.3333+ 0.5000- | ENTER VALUES OF E IN CORRECT ORDER 0.1667+ | ENTER VALUES OF E IN CORRECT ORDER 0.1667+ |
| H MICROMETERS 0.3332 | H MICROMETERS 0.3006 | H MICROMETERS 0.3006 |

Specimen calculations of workpiece surface roughness Ra. $V_t \rightarrow$
 $h \leftarrow$

| | | |
|--|--|--|
| INPUT DATA | INPUT DATA | INPUT DATA |
| H P S 29.6667+ | H P S 29.6667+ | H P S 29.6667+ |
| H P S 1.0000+ | H P S 1.0000+ | H P S 1.0000+ |
| V MM S <u>2.5000+</u> | V MM S <u>10.0000+</u> | V MM S <u>20.0000+</u> |
| H MM 25.0000+ | H MM 25.0000+ | H MM 25.0000+ |
| H MM PEV 0.5000+ | H MM PEV 0.5000+ | H MM PEV 0.5000+ |
| H MM 0.0020+ | H MM 0.0020+ | H MM 0.0020+ |
| ENTER 1 FOR H V SAME SENSE OR 2 FOR H V OPPOSITE SENSE 2.0000+ | ENTER 1 FOR H V SAME SENSE OR 2 FOR H V OPPOSITE SENSE 2.0000+ | ENTER 1 FOR H V SAME SENSE OR 2 FOR H V OPPOSITE SENSE 2.0000+ |
| H V-OPP. SENSE A+B 10.0000 | H V-OPP. SENSE A+B 2.5000 | H V-OPP. SENSE A+B 1.2500 |
| CASE 1 MM V=A NEG. I (A-1) | CASE 2 MM V=A+B 11-ENV H (A-2) | CASE 3 MM V=A+B ENV H (1) |
| VALUES OF INTF.E 0.3334 0.1667 0.0001 0.3334 0.1668 0.0001 0.3335 0.1668 0.0002 | VALUES OF INTF.E 0.3334 0.0001 0.3334 0.1668 0.0002 | VALUES OF INTF.E 0.3334 0.0001 0.3334 0.1668 0.0002 |
| ENTER LMT. FOR E NONREPEAT VALUES 2.0000+ | ENTER LMT. FOR E NONREPEAT VALUES 1.0000+ | ENTER LMT. FOR E NONREPEAT VALUES 1.0000+ |
| ENTER VALUES OF E IN CORRECT ORDER 0.1667+ 0.3334+ | ENTER VALUES OF E IN CORRECT ORDER 0.3334+ | ENTER VALUES OF E IN CORRECT ORDER 0.3334+ |
| RA MICROMETRES <u>0.1667</u> | RA MICROMETRES <u>0.3087</u> | RA MICROMETRES <u>0.3087</u> |

APPENDIX V

DETERMINATION OF SYSTEM PARAMETERS FOR THE THREE COMPONENT DRESSING FORCE DYNAMOMETER

1. CALCULATION OF THE FORCE-SENSING RING DIMENSIONS.

These calculations are based on the following value of stiffness k:-

F_r AXIS (initially)

F_a AXIS $k = 880 \text{ N/mm}$

F_t AXIS

For a thin ring subjected to diametral loading, the deflection measured in the direction of the applied load is given by⁶⁷

$$\delta = \frac{.149 P R^3}{E I} \quad \text{mm}$$

where

δ = deflection of the ring along the line of action of the applied load mm

P = applied load N

R = mean radius of the ring (radius to the neutral axis) mm

E = Young's Modulus of Elasticity (210,000 N/mm² for steel) N/mm²

I = Second Moment of Area of the ring mm⁴

also

$$R = \frac{D_1 + D_2}{4} \quad \text{mm}$$

$$I = \frac{b(D_1 - D_2)^3}{96} \quad \text{mm}^4$$

where

D_1 = outside diameter of the ring mm

D_2 = inside diameter of the ring mm

b = width of the ring mm

Substituting in the deflection equation above for P , R and I in terms of D_1 , D_2 and b .

$$\delta = \frac{.2235 P}{E b} \left[\frac{D_1 + D_2}{D_1 - D_2} \right]^3 \text{ mm}$$

Re-arranging the above equation to give an expression for stiffness k .

$$\frac{P}{\delta} = k = 4.4742 E b \left[\frac{D_1 - D_2}{D_1 + D_2} \right]^3 \text{ N/mm}$$

The strain-ring dimensions were calculated using the above expression.

F_r axis

One ring of stiffness 880 N/mm (see fig. 5.7)

D_1 30.5 mm D_2 28.2 mm b 10 mm

F_a and F_t axes

Two rings per axis of stiffness 440 N/mm (see fig. 5.8)

D_1 20.3 mm D_2 18.8 mm b 8.9 mm

2. CALCULATION OF THE SYSTEM NATURAL FREQUENCIES

$$f = \frac{1}{2\pi} \sqrt{\frac{k}{M}} \quad \text{Hz}$$

where

f = Natural frequency Hz
 k = system stiffness N/m
 M = system mass kg

F_r axis

$$M = .638 \text{ kg}$$

$$k = 3.336 \text{ MN/m} \quad (\text{actual}) \quad \text{stiffness increased from } 880 \text{ kN/m}$$

$$f = 364 \text{ Hz}$$

F_a axis

$$M = .638 \text{ kg}$$

$$k = 853.1 \text{ kN/m} \quad (\text{actual})$$

$$f = \underline{184} \text{ Hz}$$

F_t axis

$$M = .638 \text{ kg}$$

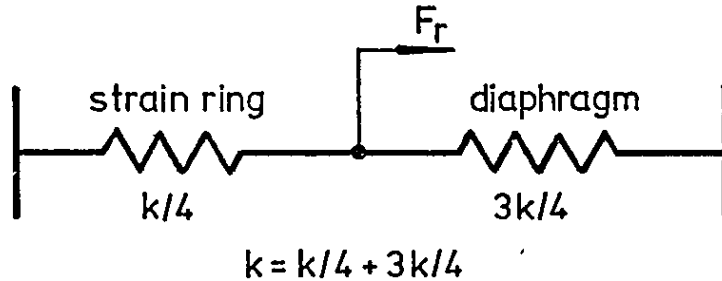
$$k = 1.079 \text{ MN/m} \quad (\text{actual})$$

$$f = \underline{207} \text{ Hz}$$

3. CALCULATION OF THE STRAIN DEVELOPED IN THE FORCE MEASURING SYSTEM, AND THE CORRESPONDING ELECTRICAL SIGNAL.

Specimen calculations for the Fr Axis.

Considering a force of 1 Newton applied to the system.



Hence the force acting on the strain ring = .25 N.

For a thin ring subjected to diametral loading, the bending stress acting at the inner and outer fibres is given by⁶⁸

$$\sigma = \frac{6 M}{b t^2} \quad \text{N/mm}^2$$

where

t = wall thickness of the ring mm

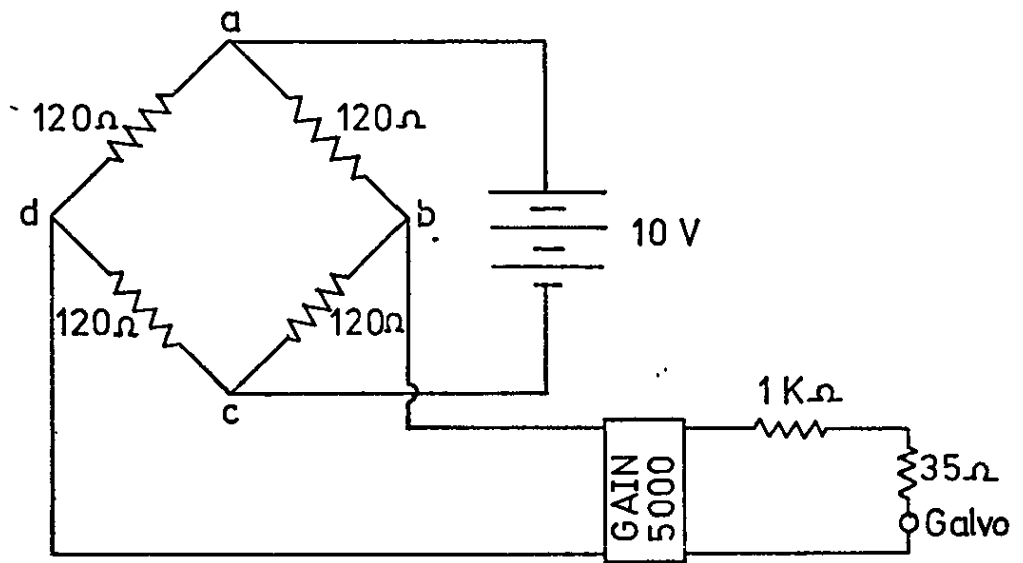
M = bending moment considered at any point around the ring N.mm

At the strain gauge fixing points (see fig. 5.12), the bending moment is given by

$$M = \pm .1817 PR \quad \text{N.mm}$$

Hence the strain at the inner and outer fibres of the ring where the strain gauges are mounted is given by

$$e = \frac{1.09 PR}{b t^2 E}$$



For the above Wheatstone Bridge Circuit the voltage across d-b is given by

$$V_{db} = e U G \quad \text{Volts}$$

where

U = bridge voltage (constant at 10 V.)

and G = gauge factor (2.095 for the gauges used.)

Hence the voltage across d-b is

$$V_{db} = \frac{1.09 P R U G}{b t^2 E} \quad \text{Volts}$$

For a force of 1 Newton applied to the system, V_{db} is

$$\begin{aligned} & \frac{1.09 \times .25 \times 14.68 \times 10 \times 2.095}{10 \times 1.15 \times 1.15 \times 210,000} \quad \text{Volts} \\ & = 30 \mu\text{V} \end{aligned}$$

With a gain of 5,000:

$$V_{db} = 150 \text{ mV}$$

Hence the current through the galvanometer circuit is

$$\frac{150 \times 10^{-3}}{1035} \text{ A} = 145 \mu\text{A}$$

and the voltage drop across the galvanometer is

$$150 \times 10^{-3} - (145 \times 10^{-6} \times 10^3) \text{ V} = 5 \text{ mV}$$

For the galvanometer used, the sensitivity is 1.75mV/mm, giving a trace width of

$$\frac{5}{1.75} \text{ mm} = 2.85 \text{ mm}$$

Hence the theoretical trace sensitivity of the Fr axis is

$$2.85 \text{ mm/N}$$

From the calibration chart (see fig. 5.I7) the actual trace sensitivity is

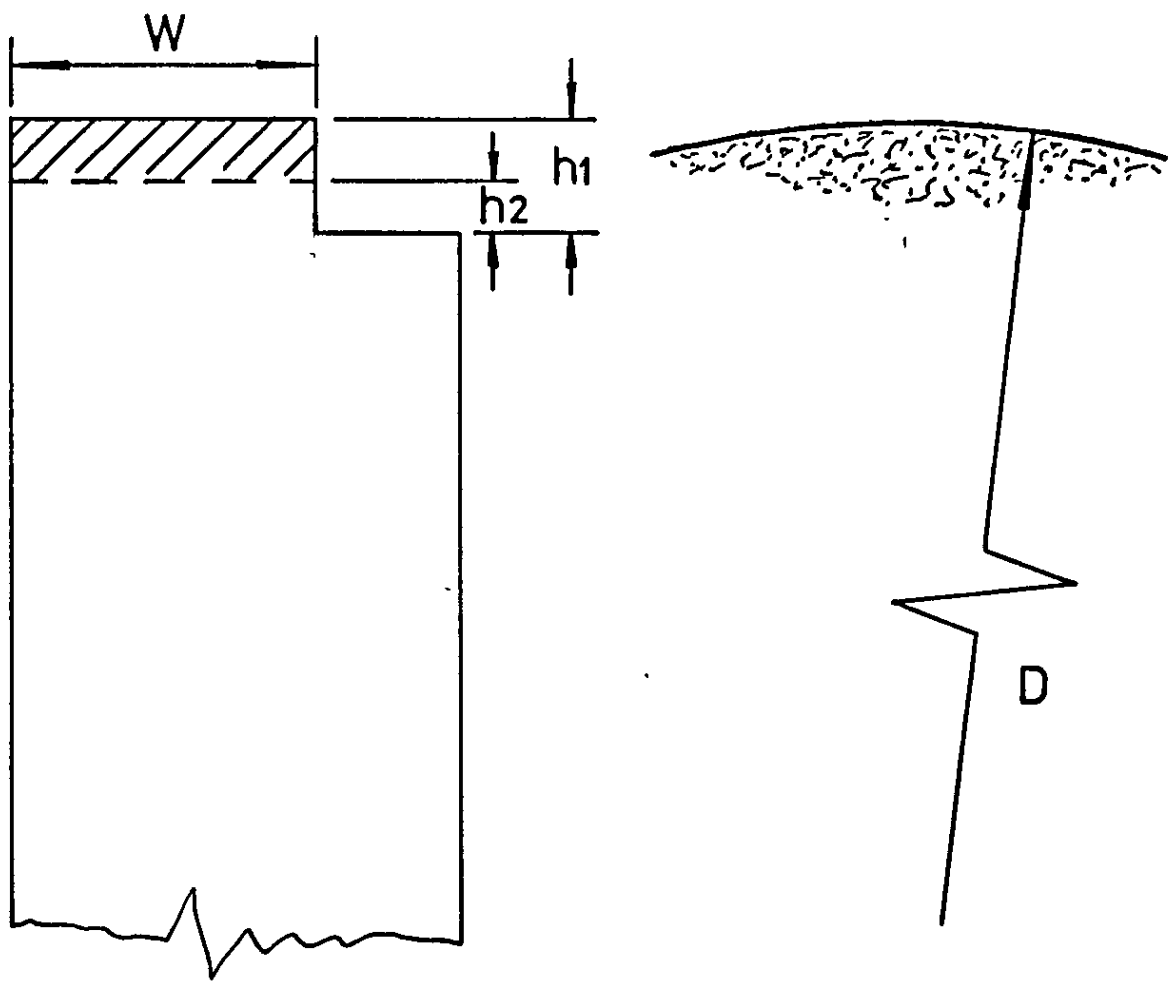
$$2.5 \text{ mm/N}$$

Similar calculations for the Fa and Ft axes were calculated.

APPENDIX VI

DRESSING TEST RESULTS

(TABULATED FORM)



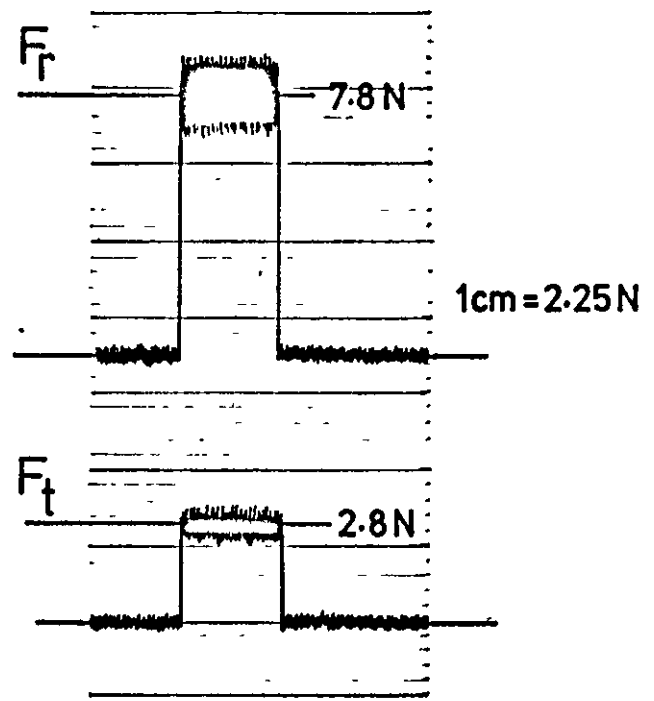
Volume of wheel worn away

$$= \pi D W (h_1 - h_2) \text{ cubic units}$$

Calculation of the volume of grinding wheel
dressed away or worn away by grinding

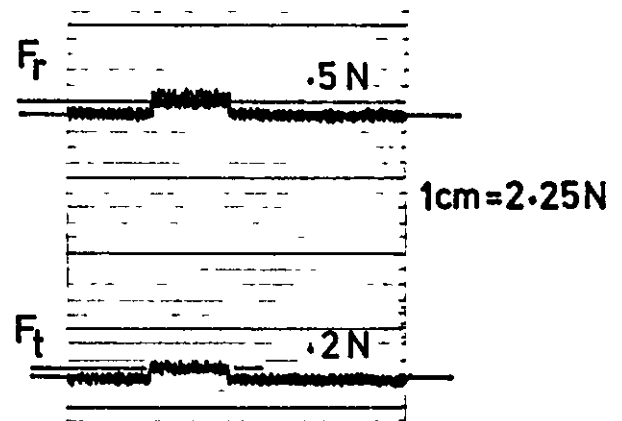
$\theta = +15^\circ$
 $a = 25 \mu\text{m}$
 $h = .5 \text{ mm/rev}$

$F_r = 7.8 \text{ N}$
 $F_t = 2.8 \text{ N}$



$\theta = +15$
 $a = 5 \mu\text{m}$
 $h = .5 \text{ mm/rev}$

$F_r = .5 \text{ N}$
 $F_t = .2 \text{ N}$



Specimen dressing force readings

TEST NO :- 1

DIAMOND NO :- 63794/1 1.00K wt.

IN-FEED :- 12.5 μ m (.0005 in.)

CROSS-FEED :- .5 mm/rev (.020 in/rev)

WHEEL TYPE :- A 46 KV

ϕ :- 305 mm

SPEED:- 1800rev/min

DRESSING PASS NO :-

| DRAG ANGLE (Degrees): | | DRESSING PASS No :- | ϕ:- 305 mm SPEED:- 1800rev/min | | | |
|-------------------------|-------|--------------------------------|-----------------------------------|------|------|------|
| | | | 1 | 2 | 3 | 4 |
| DRAG ANGLE (Degrees): | + 15° | F _r | 1.45 | 1.52 | 1.59 | 1.59 |
| | | F _t | .55 | .55 | .63 | .66 |
| | | F _r /F _t | 2.63 | 2.76 | 2.52 | 2.40 |
| | + 10° | F _r | 1.04 | 1.18 | 1.32 | 1.45 |
| | | F _t | .41 | .48 | .55 | .62 |
| | | F _r /F _t | 2.53 | 2.45 | 2.40 | 2.33 |
| | + 5° | F _r | .90 | 1.32 | 1.45 | 1.94 |
| | | F _t | .34 | .41 | .48 | .62 |
| | | F _r /F _t | 2.64 | 3.21 | 3.02 | 3.12 |
| | 0° | F _r | 2.22 | 2.16 | 2.57 | 2.91 |
| | | F _t | .69 | .69 | .76 | .77 |
| | | F _r /F _t | 3.21 | 3.13 | 3.38 | 3.77 |
| | - 5° | F _r | 3.12 | 2.86 | 3.47 | 2.98 |
| | | F _t | .76 | .83 | .90 | .83 |
| | | F _r /F _t | 4.10 | 3.44 | 3.85 | 3.59 |
| | - 10° | F _r | 2.98 | 3.47 | 3.82 | 3.12 |
| | | F _t | .69 | .90 | .94 | .83 |
| | | F _r /F _t | 4.31 | 3.85 | 4.06 | 3.75 |
| | - 15° | F _r | 3.19 | 2.98 | 3.82 | 3.83 |
| | | F _t | 1.04 | .69 | .83 | .83 |
| | | F _r /F _t | 3.06 | 4.31 | 4.60 | 4.61 |

TEST NO :- 2

DIAMOND NO :- 63794/1 1.00K wt.

IN-FEED :- 12.5 μ m (.0005 in.)

CROSS-FEED :- .1 mm/rev (.004 in/rev)

WHEEL TYPE :- A 46 KV

ϕ :- 305 mm

SPEED:- 1800rev/min

DRESSING PASS NO :-

| ϕ :- 305 mm SPEED:- 1800rev/min | | DRESSING PASS N ^o :- | | | | |
|---|-------|---------------------------------|------|------|------|------|
| | | 1 | 2 | 3 | 4 | |
| DRAG ANGLE (Degrees): | + 15° | F_r | 1.11 | 1.56 | 1.56 | 1.14 |
| | | F_t | .33 | .44 | .44 | .36 |
| | | F_r/F_t | 3.33 | 3.50 | 3.53 | 3.15 |
| | + 10° | F_r | 1.43 | 1.61 | 1.57 | 1.45 |
| | | F_t | .41 | .44 | .44 | .41 |
| | | F_r/F_t | 3.48 | 3.61 | 3.53 | 3.50 |
| | + 5° | F_r | 1.47 | 1.45 | 1.61 | 1.45 |
| | | F_t | .39 | .39 | .41 | .39 |
| | | F_r/F_t | 3.80 | 3.70 | 3.91 | 3.65 |
| | 0° | F_r | 1.81 | 1.83 | 1.78 | 2.00 |
| | | F_t | .42 | .43 | .42 | .46 |
| | | F_r/F_t | 4.33 | 4.30 | 4.25 | 4.31 |
| | - 5° | F_r | 1.88 | 2.11 | 2.22 | 2.22 |
| | | F_t | .37 | .41 | .42 | .44 |
| | | F_r/F_t | 4.90 | 5.10 | 5.33 | 5.00 |
| | - 10° | F_r | 2.43 | 2.53 | 2.39 | 2.43 |
| | | F_t | .44 | .48 | .45 | .44 |
| | | F_r/F_t | 5.46 | 5.30 | 5.33 | 5.46 |
| | - 15° | F_r | 2.64 | 2.71 | 2.67 | 2.59 |
| | | F_t | .50 | .50 | .49 | .46 |
| | | F_r/F_t | 5.27 | 5.41 | 5.40 | 5.63 |

TEST NO:- 2 cont.

DIAMOND NO :- 63794/1 1.00K wt.

IN-FEED :- 12.5 μ m (.0005 in.)

CROSS-FEED :- .1 mm/rev (.004 in/rev)

WHEEL TYPE:- A 46 KV

ϕ :- 305 mm

SPEED:- 1800rev/min

DRESSING PASS NO :-

| | | 5 | 6 | 7 | 8 |
|--|-------------|------|------|------|------|
| DRAG ANGLE (Degrees) : DRESSING FORCE COMPONENTS (Newtons) | + 15° F_r | 1.11 | 1.58 | 1.58 | 1.57 |
| | F_t | .36 | .46 | .46 | .47 |
| | F_r/F_t | 3.07 | 3.40 | 3.41 | 3.35 |
| | + 10° F_r | 1.49 | 1.46 | 1.50 | 1.46 |
| | F_t | .43 | .41 | .41 | .41 |
| | F_r/F_t | 3.50 | 3.55 | 3.69 | 3.55 |
| | + 5° F_r | 1.46 | 1.70 | 1.81 | 1.53 |
| | F_t | .39 | .44 | .45 | .39 |
| | F_r/F_t | 3.70 | 3.81 | 4.00 | 3.92 |
| | 0° F_r | 1.89 | 1.95 | 1.95 | 1.74 |
| | F_t | .44 | .45 | .45 | .39 |
| | F_r/F_t | 4.32 | 4.35 | 4.33 | 4.45 |
| | - 5° F_r | 2.36 | 2.22 | 2.09 | 2.71 |
| | F_t | .45 | .44 | .41 | .52 |
| | F_r/F_t | 5.21 | 5.00 | 5.10 | 5.21 |
| | - 10° F_r | 2.56 | 2.57 | 2.78 | 3.34 |
| | F_t | .46 | .46 | .49 | .58 |
| | F_r/F_t | 5.57 | 5.53 | 5.62 | 5.70 |
| | - 15° F_r | 2.39 | 2.31 | 3.22 | 3.34 |
| | F_t | .42 | .44 | .56 | .57 |
| | F_r/F_t | 5.73 | 5.24 | 5.76 | 5.83 |

TEST NO:- 2 cont.

DIAMOND NO :- 63794/1 1.00K wt.

IN-FEED :- 12.5 μ m (.0005 in.)

CROSS-FEED :- .1 mm/rev (.004 in/rev)

WHEEL TYPE:- A 46 KV

ϕ :- 305 mm

SPEED:- 1800rev/min

DRESSING PASS NO :-

| ϕ :- 305 mm SPEED:-1800rev/min | | DRESSING PASS № :- | | | | |
|--|-------|--------------------|------|------|------|------|
| | | 9 | 10 | 11 | 12 | |
| DRAG ANGLE (Degrees): | + 15° | F_r | 1.61 | 1.56 | 1.60 | 1.47 |
| | | F_t | .48 | .47 | .47 | .44 |
| | | F_r/F_t | 3.36 | 3.33 | 3.39 | 3.31 |
| | + 10° | F_r | 1.56 | 1.58 | 1.56 | 1.64 |
| | | F_t | .44 | .44 | .44 | .47 |
| | | F_r/F_t | 3.49 | 3.59 | 3.50 | 3.49 |
| | + 5° | F_r | 1.74 | 1.70 | 1.67 | 1.81 |
| | | F_t | .44 | .43 | .44 | .48 |
| | | F_r/F_t | 3.95 | 3.89 | 3.75 | 3.77 |
| | 0° | F_r | 2.11 | 2.06 | 2.09 | 2.04 |
| | | F_t | .48 | .47 | .48 | .47 |
| | | F_r/F_t | 4.39 | 4.35 | 4.34 | 4.31 |
| | - 5° | F_r | 2.72 | 2.64 | 2.72 | 2.50 |
| | | F_t | .51 | .49 | .50 | .47 |
| | | F_r/F_t | 5.30 | 5.32 | 5.40 | 5.29 |
| | - 10° | F_r | 3.39 | 3.00 | 3.06 | 3.06 |
| | | F_t | .59 | .54 | .54 | .53 |
| | | F_r/F_t | 5.70 | 5.59 | 5.64 | 5.70 |
| | - 15° | F_r | 3.81 | 3.73 | 3.61 | 3.68 |
| | | F_t | .64 | .63 | .62 | .62 |
| | | F_r/F_t | 5.95 | 5.94 | 5.78 | 5.90 |

TEST N^o :- 2 cont.

DIAMOND N^o :- 63794/1 1.00K wt.

IN-FEED :- 12.5 μ m (.0005 in.)

CROSS-FEED :- .1 mm/rev (.004 in/rev)

WHEEL TYPE :- A 46 KV

ϕ :- 305 mm

SPEED :- 1800rev/min

DRESSING PASS N^o :-

| | | 13 | 14 | 15 | |
|-------------------------|-------|-----------|------|------|------|
| DRAG ANGLE (Degrees): | + 15° | F_r | 1.42 | 1.45 | 1.53 |
| | | F_t | .44 | .44 | .45 |
| | | F_r/F_t | 3.19 | 3.25 | 3.36 |
| | + 10° | F_r | 1.64 | 1.58 | 1.70 |
| | | F_t | .47 | .46 | .47 |
| | | F_r/F_t | 3.51 | 3.41 | 3.62 |
| | + 5° | F_r | 1.72 | 1.88 | 2.00 |
| | | F_t | .43 | .49 | .52 |
| | | F_r/F_t | 3.98 | 3.85 | 3.86 |
| | 0° | F_r | 2.02 | 2.11 | 2.10 |
| | | F_t | .48 | .49 | .49 |
| | | F_r/F_t | 4.15 | 4.34 | 4.25 |
| | - 5° | F_r | 2.22 | 2.29 | 2.78 |
| | | F_t | .44 | .45 | .52 |
| | | F_r/F_t | 5.00 | 5.06 | 5.30 |
| | - 10° | F_r | 2.99 | 3.06 | 3.61 |
| | | F_t | .53 | .54 | .62 |
| | | F_r/F_t | 5.60 | 5.60 | 5.80 |
| | - 15° | F_r | 3.68 | 3.61 | 3.48 |
| | | F_t | .61 | .61 | .58 |
| | | F_r/F_t | 6.00 | 5.88 | 5.95 |

TEST NO 3

DIAMOND NO :- 71784/2

IN-FEED :- 12.5 μ m (.0005 in)

CROSS-FEED :- .1mm/rev (.004in/rev)

WHEEL ϕ 305 mm

SPEED 1800 rev/min

GRINDING WHEEL TYPE :-

| WHEEL ϕ 305 mm SPEED 1800 rev/min | | GRINDING WHEEL TYPE :- | | | | |
|---|-------|------------------------|-------|-----------|-----------|------|
| | | A 60KV | A46KV | 38A46K5V- | 32A60K8V- | |
| DRAG ANGLE(Degrees): DRESSING FORCE COMPONENTS(Newtons) | + 15° | F_r | .70 | .90 | .50 | .50 |
| | | F_t | .22 | .30 | .15 | .15 |
| | | F_r/F_t | 3.18 | 3.00 | 3.33 | 3.33 |
| | + 10° | F_r | 1.39 | 1.93 | 1.61 | 1.58 |
| | | F_t | .27 | .41 | .33 | .33 |
| | | F_r/F_t | 5.14 | 4.70 | 4.87 | 4.78 |
| | + 5° | F_r | 2.08 | 2.25 | 1.76 | 1.75 |
| | | F_t | .38 | .51 | .34 | .30 |
| | | F_r/F_t | 5.47 | 4.41 | 5.17 | 5.83 |
| | 0° | F_r | 2.34 | 2.52 | 2.18 | 1.83 |
| | | F_t | .48 | .55 | .37 | .31 |
| | | F_r/F_t | 4.87 | 4.58 | 5.78 | 5.90 |
| | - 5° | F_r | 2.36 | 2.78 | 2.25 | 1.97 |
| | | F_t | .41 | .54 | .38 | .32 |
| | | F_r/F_t | 5.75 | 5.14 | 5.80 | 6.00 |
| | - 10° | F_r | 2.44 | 2.79 | 2.25 | 1.97 |
| | | F_t | .40 | .40 | .32 | .27 |
| | | F_r/F_t | 6.10 | 6.97 | 7.00 | 7.10 |
| | - 15° | F_r | 2.48 | 2.25 | 1.83 | 1.62 |
| | | F_t | .38 | .33 | .28 | .23 |
| | | F_r/F_t | 6.52 | 6.81 | 6.51 | 6.88 |

TEST NO 3 cont.

DIAMOND NO :- 70795/2

IN-FEED :- 12.5 μ m (.0005 in)

CROSS-FEED :- .1mm/rev (.004in/rev)

WHEEL ϕ 305 mm
SPEED 1800 rev/min

GRINDING WHEEL TYPE :-

| WHEEL ϕ 305 mm SPEED 1800 rev/min | | GRINDING WHEEL TYPE :- | | | | |
|---|-------|------------------------|-------|-----------|-----------|------|
| | | A 60KV | A46KV | 38A46K5V- | 32A60K8V- | |
| DRAG ANGLE (Degrees): DRESSING FORCE COMPONENTS (Newtons) | + 15° | F_r | 1.54 | 1.68 | 1.11 | .95 |
| | | F_t | .39 | .42 | .35 | .31 |
| | | F_r/F_t | 3.96 | 4.00 | 3.20 | 3.09 |
| | + 10° | F_r | 1.33 | 1.36 | 1.04 | .82 |
| | | F_t | .37 | .37 | .35 | .29 |
| | | F_r/F_t | 3.56 | 3.68 | 3.00 | 2.81 |
| | + 5° | F_r | 1.25 | 1.22 | .96 | .68 |
| | | F_t | .38 | .35 | .33 | .26 |
| | | F_r/F_t | 3.33 | 3.49 | 2.88 | 2.58 |
| | 0° | F_r | 1.25 | 1.37 | .88 | .67 |
| | | F_t | .36 | .36 | .31 | .25 |
| | | F_r/F_t | 3.50 | 3.80 | 2.86 | 2.67 |
| | - 5° | F_r | 1.47 | 1.74 | 1.22 | 1.33 |
| | | F_t | .37 | .41 | .32 | .38 |
| | | F_r/F_t | 3.93 | 4.22 | 3.83 | 3.56 |
| | - 10° | F_r | 1.68 | 2.52 | 1.33 | 2.04 |
| | | F_t | .38 | .45 | .32 | .39 |
| | | F_r/F_t | 4.48 | 5.56 | 4.17 | 5.25 |
| | - 15° | F_r | 1.97 | 2.52 | 1.63 | 1.77 |
| | | F_t | .39 | .43 | .33 | .33 |
| | | F_r/F_t | 5.00 | 5.84 | 4.88 | 5.29 |

TEST NO:- 4

DIAMOND NO:- 63794/2

WHEEL TYPE:-32A60- ϕ :-305mm SPEED 1800 rev/min

DRAG ANGLE:- 5° K8VBE

| F _a F _r & F _t (Newtons) | | | | | Ra [C.L.A] (μm) | | IN-FEED (μm & in.) | | | | | CROSS-FEED (mm/rev & in/rev) | | | | | | | | | | | | | | | | | | | | | | | | | | | | | | | | | | | | | | | | | | | | | | | | | | | | | | | | | | | | | | | | | | | | | | | | | | | | | | | | | | | | | | | | | | | | | | | | | | | | | | | | | | | | | | | | | | | | | | | | | | | | | | | | | | | | | | | | | | | | | | | | | | | | | | | | | | | | | | | | | | | | | | | | | | | | | | | | | | | | | | | | | | | | | | | |
|--|--|----|--|---|-------------------|---|---------------------|---|----|---|-------|---|----|---|-------|---|----|---|-------|---|---|---|---------------|---|----|---|--------|---|------|---|------|---|------|---|------|---|------|---|--|---|--|---|--|---|--|---|--|---|--|---|--|---|--|---|--|---|--|---|--|---|--|---|--|---|--|---|--|---|--|---|--|---|--|---|--|---|--|---|--|---|--|---|--|---|--|---|--|---|--|---|--|---|--|---|--|---|--|---|--|---|--|---|--|---|--|---|--|---|--|---|--|---|--|---|--|---|--|---|--|---|--|---|--|---|--|---|--|---|--|---|--|---|--|---|--|---|--|---|--|---|--|---|--|---|--|---|--|---|--|---|--|---|--|---|--|---|--|---|--|---|--|---|--|---|--|---|--|---|--|---|--|---|--|---|--|---|--|---|--|---|--|---|--|---|--|---|--|---|--|---|--|---|--|---|--|---|--|---|--|---|--|--|--|
| | | | | | | | .0008 | | 20 | | .0006 | | 15 | | .0004 | | 10 | | .0002 | | 5 | | in. mm/rev | | μm | | in/rev | | .004 | | .008 | | .012 | | .016 | | .020 | | | | | | | | | | | | | | | | | | | | | | | | | | | | | | | | | | | | | | | | | | | | | | | | | | | | | | | | | | | | | | | | | | | | | | | | | | | | | | | | | | | | | | | | | | | | | | | | | | | | | | | | | | | | | | | | | | | | | | | | | | | | | | | | | | | | | | | | | | | | | | | | | | | | | | | | | | | | | | | | | | | | | | |
| | | | | | | | | | | | | | | | | | | | | | | | | | | | | | | | | | | | | | | | | | | | | | | | | | | | | | | | | | | | | | | | | | | | | | | | | | | | | | | | | | | | | | | | | | | | | | | | | | | | | | | | | | | | | | | | | | | | | | | | | | | | | | | | | | | | | | | | | | | | | | | | | | | | | | | | | | | | | | | | | | | | | | | | | | | | | | | | | | | | | | | | | | | | | | | | | | | | | | | | | | | | |
| .0010 | | 25 | | F _a F _r F _t F _r / F _t R _a | | F _a F _r F _t F _r / F _t R _a | | F _a F _r F _t F _r / F _t R _a | | F _a F _r F _t F _r / F _t R _a | | F _a F _r F _t F _r / F _t R _a | | F _a F _r F _t F _r / F _t R _a | | F _a F _r F _t F _r / F _t R _a | | F _a F _r F _t F _r / F _t R _a | | F _a F _r F _t F _r / F _t R _a | | F _a F _r F _t F _r / F _t R _a | | F _a F _r F _t F _r / F _t R _a | | F _a F _r F _t F _r / F _t R _a | | F _a F _r F _t F _r / F _t R _a | | F _a F _r F _t F _r / F _t R _a | | F _a F _r F _t F _r / F _t R _a | | F _a F _r F _t F _r / F _t R _a | | F _a F _r F _t F _r / F _t R _a | | F _a F _r F _t F _r / F _t R _a | | F _a F _r F _t F _r / F _t R _a | | F _a F _r F _t F _r / F _t R _a | | F _a F _r F _t F _r / F _t R _a | | F _a F _r F _t F _r / F _t R _a | | F _a F _r F _t F _r / F _t R _a | | F _a F _r F _t F _r / F _t R _a | | F _a F _r F _t F _r / F _t R _a | | F _a F _r F _t F _r / F _t R _a | | F _a F _r F _t F _r / F _t R _a | | F _a F _r F _t F _r / F _t R _a | | F _a F _r F _t F _r / F _t R _a | | F _a F _r F _t F _r / F _t R _a | | F _a F _r F _t F _r / F _t R _a | | F _a F _r F _t F _r / F _t R _a | | F _a F _r F _t F _r / F _t R _a | | F _a F _r F _t F _r / F _t R _a | | F _a F _r F _t F _r / F _t R _a | | F _a F _r F _t F _r / F _t R _a | | F _a F _r F _t F _r / F _t R _a | | F _a F _r F _t F _r / F _t R _a | | F _a F _r F _t F _r / F _t R _a | | F _a F _r F _t F _r / F _t R _a | | F _a F _r F _t F _r / F _t R _a | | F _a F _r F _t F _r / F _t R _a | | F _a F _r F _t F _r / F _t R _a | | F _a F _r F _t F _r / F _t R _a | | F _a F _r F _t F _r / F _t R _a | | F _a F _r F _t F _r / F _t R _a | | F _a F _r F _t F _r / F _t R _a | | F _a F _r F _t F _r / F _t R _a | | F _a F _r F _t F _r / F _t R _a | | F _a F _r F _t F _r / F _t R _a | | F _a F _r F _t F _r / F _t R _a | | F _a F _r F _t F _r / F _t R _a | | F _a F _r F _t F _r / F _t R _a | | F _a F _r F _t F _r / F _t R _a | | F _a F _r F _t F _r / F _t R _a | | F _a F _r F _t F _r / F _t R _a | | F _a F _r F _t F _r / F _t R _a | | F _a F _r F _t F _r / F _t R _a | | F _a F _r F _t F _r / F _t R _a | | F _a F _r F _t F _r / F _t R _a | | F _a F _r F _t F _r / F _t R _a | | F _a F _r F _t F _r / F _t R _a | | F _a F _r F _t F _r / F _t R _a | | F _a F _r F _t F _r / F _t R _a | | F _a F _r F _t F _r / F _t R _a | | F _a F _r F _t F _r / F _t R _a | | F _a F _r F _t F _r / F _t R _a | | F _a F _r F _t F _r / F _t R _a | | F _a F _r F _t F _r / F _t R _a | | F _a F _r F _t F _r / F _t R _a | | F _a F _r F _t F _r / F _t R _a | | F _a F _r F _t F _r / F _t R _a | | F _a F _r F _t F _r / F _t R _a | | F _a F _r F _t F _r / F _t R _a | | F _a F _r F _t F _r / F _t R _a | | F _a F _r F _t F _r / F _t R _a | | F _a F _r F _t F _r / F _t R _a | | F _a F _r F _t F _r / F _t R _a | | F _a F _r F _t F _r / F _t R _a | | F _a F _r F _t F _r / F _t R _a | | F _a F _r F _t F _r / F _t R _a | | F _a F _r F _t F _r / F _t R _a | | F _a F _r F _t F _r / F _t R _a | | F _a F _r F _t F _r / F _t R _a | | F _a F _r F _t F _r / F _t R _a | | F _a F _r F _t F _r / F _t R _a | | F _a F _r F _t F _r / F _t R _a | | F _a F _r F _t F _r / F _t R _a | | F _a F _r F _t F _r / F _t R _a | | F _a F _r F _t F _r / F _t R _a | | F _a F _r F _t F _r / F _t R _a | | F _a F _r F _t F _r / F _t R _a | | F _a F _r F _t F _r / F _t R _a | | F _a F _r F _t F _r / F _t R _a | | F _a F _r F _t F _r / F _t R _a | | F _a F _r F _t F _r / F _t R _a | | F _a F _r F _t F _r / F _t R _a | | F _a F _r F _t F _r / F _t R _a | | F _a F _r F _t F _r / F _t R _a | | F _a F _r F _t F _r | |

TEST NO:- 4 cont.

DIAMOND NO:- 63794/2

WHEEL TYPE:- 32A60- ϕ :-305mm SPEED 1800 rev/minDRAG ANGLE:- 10° K8VBE

| Ra [C.L.A] (μm) | | | | | CROSS-FEED (mm/rev & in/rev) | | | | | | |
|--|-------|----|---------------------------------|---------------------------------|------------------------------|------|------|------|------|------|------|
| | | | | | in/rev | | .004 | .008 | .012 | .016 | .020 |
| | | | | | mm/rev | .1 | .2 | .3 | .4 | .5 | |
| F _a F _r & F _t (Newtons) | .0002 | | 5 | F _a | — | — | — | — | — | | |
| | | | | F _r | .19 | .24 | .35 | .53 | .53 | | |
| | | | | F _t | .08 | .10 | .13 | .21 | .20 | | |
| | | | | F _r / F _t | 2.33 | 2.43 | 2.78 | 2.53 | 2.68 | | |
| | | | | R _a | 1.00 | 1.25 | 1.55 | 1.50 | 1.50 | | |
| | .0004 | | 10 | F _a | — | — | — | — | — | | |
| | | | | F _r | .72 | 1.06 | 1.25 | 1.53 | 1.86 | | |
| | | | | F _t | .25 | .37 | .42 | .61 | .64 | | |
| | | | | F _r / F _t | 2.89 | 2.83 | 2.96 | 2.80 | 2.90 | | |
| | | | | R _a | 1.33 | 1.55 | 2.00 | 1.70 | 1.88 | | |
| | .0006 | | 15 | F _a | .04 | .05 | .04 | .04 | .06 | | |
| | | | | F _r | 1.08 | 1.56 | 2.03 | 2.56 | 3.00 | | |
| | | | | F _t | .35 | .61 | .61 | .75 | .89 | | |
| | | | | F _r / F _t | 3.10 | 3.14 | 3.31 | 3.41 | 3.39 | | |
| | | | | R _a | 1.25 | 1.75 | 2.13 | 2.05 | 1.93 | | |
| | .0008 | | 20 | F _a | .10 | .10 | .13 | .11 | .11 | | |
| | | | | F _r | 1.31 | 2.00 | 2.50 | 3.14 | 3.66 | | |
| | | | | F _t | .40 | .64 | .75 | .95 | 1.08 | | |
| | | | | F _r / F _t | 3.25 | 3.13 | 3.32 | 3.30 | 3.40 | | |
| | | | | R _a | 1.63 | 1.75 | 2.38 | 1.98 | 2.08 | | |
| .0010 | | 25 | F _a | .15 | .14 | .14 | .15 | .14 | | | |
| | | | F _r | 1.54 | 2.28 | 2.86 | 3.56 | 4.04 | | | |
| | | | F _t | .49 | .75 | .84 | 1.06 | 1.18 | | | |
| | | | F _r / F _t | 3.17 | 3.04 | 3.41 | 3.35 | 3.42 | | | |
| | | | R _a | 1.70 | 1.80 | 2.63 | 1.98 | 2.70 | | | |

TEST NO:- 4 cont.

DIAMOND NO:- 63794/2

WHEEL TYPE:- 32 A 60- ϕ :-305mm SPEED 1800 rev/min

DRAG ANGLE:- 15° K8VBE

| Ra [C.L.A] (μm) | | | CROSS-FEED (mm/rev & in/rev) | | | | | |
|--|---|---|------------------------------|------|------|------|------|------|
| | | | in/rev | | | | | |
| | | | mm/rev | .004 | .008 | .012 | .016 | .020 |
| | | | in. | .1 | .2 | .3 | .4 | .5 |
| | | | μm | | | | | |
| | | | 5 | | | | | |
| F _a F _r & F _t (Newtons) | .0002 | F _a F _r F _t F _r / F _t R _a | | | | | | |
| | | | | | | | | |
| | | | | | | | | |
| | | | | | | | | |
| | | | | | | | | |
| | .0004 | F _a F _r F _t F _r / F _t R _a | | | | | | |
| | | | | | | | | |
| | | | | | | | | |
| | | | | | | | | |
| | | | | | | | | |
| | .0006 | F _a F _r F _t F _r / F _t R _a | | | | | | |
| | | | | | | | | |
| | | | | | | | | |
| | | | | | | | | |
| | | | | | | | | |
| | .0008 | F _a F _r F _t F _r / F _t R _a | | | | | | |
| | | | | | | | | |
| | | | | | | | | |
| | | | | | | | | |
| | | | | | | | | |
| .0010 | F _a F _r F _t F _r / F _t R _a | | | | | | | |
| | | | | | | | | |
| | | | | | | | | |
| | | | | | | | | |
| | | | | | | | | |

TEST NO:- 5

DIAMOND NO:- 63794/2

WHEEL TYPE:- A 60 KV ϕ :-305mm SPEED 1800 rev/minDRAG ANGLE:- 5°

| F _d F _r & F _t (Newtons) | | | | | Ra [C.L.A] (μm) | | | | |
|--|-------|--------------------------------|--------------------------------|--------|------------------------------|-------|-------|-------|------|
| | | | | | IN-FEED (μm & in.) | | | | |
| | | | | | CROSS-FEED (mm/rev & in/rev) | | | | |
| F _d F _r & F _t | | in. μm | mm/rev | in/rev | .004 | .008 | .012 | .016 | .020 |
| | | | | | .1 | .2 | .3 | .4 | .5 |
| F _d F _r & F _t | .0002 | 5 | F _d | _____ | _____ | _____ | _____ | _____ | |
| | | | F _r | 1.25 | 1.70 | 2.14 | 2.64 | 3.34 | |
| | | | F _t | .42 | .53 | .71 | .88 | 1.04 | |
| | | | F _r /F _t | 3.00 | 3.21 | 3.02 | 3.02 | 3.20 | |
| | | | R _a | .75 | 1.00 | 1.30 | 1.55 | 1.00 | |
| | .0004 | 10 | F _d | _____ | _____ | _____ | _____ | _____ | |
| | | | F _r | 2.64 | 2.85 | 3.75 | 4.11 | 4.66 | |
| | | | F _t | .78 | .86 | 1.18 | 1.22 | 1.45 | |
| | | | F _r /F _t | 3.41 | 3.33 | 3.19 | 3.38 | 3.22 | |
| | | | R _a | .88 | 1.13 | 1.35 | 1.70 | 1.20 | |
| | .0006 | 15 | F _d | .25 | .28 | .28 | .33 | .33 | |
| | | | F _r | 5.03 | 5.70 | 6.46 | 7.23 | 8.34 | |
| | | | F _t | 1.48 | 1.69 | 1.90 | 2.16 | 2.46 | |
| | | | F _r /F _t | 3.39 | 3.37 | 3.41 | 3.35 | 3.39 | |
| | | | R _a | 1.13 | 1.20 | 1.20 | 1.63 | 1.55 | |
| | .0008 | 20 | F _d | .39 | .47 | .53 | .53 | .56 | |
| | | | F _r | 6.45 | 7.23 | 8.19 | 9.37 | 10.43 | |
| | | | F _t | 1.87 | 2.08 | 2.35 | 2.66 | 3.01 | |
| | | | F _r /F _t | 3.46 | 3.47 | 3.49 | 3.52 | 3.47 | |
| | | | R _a | .88 | 1.13 | 1.25 | 1.55 | 1.30 | |
| .0010 | 25 | F _d | .56 | .61 | .61 | .70 | .70 | | |
| | | F _r | 7.23 | 8.52 | 9.79 | 11.12 | 12.70 | | |
| | | F _t | 2.02 | 2.42 | 2.78 | 2.95 | 3.34 | | |
| | | F _r /F _t | 3.57 | 3.52 | 3.52 | 3.77 | 3.81 | | |
| | | R _a | .88 | .95 | 1.50 | 1.38 | 1.38 | | |

TEST NO:- 5 cont.

DIAMOND NO:- 63794/2

WHEEL TYPE:- A 60 KV ϕ :-305mm SPEED 1800 rev/min

DRAG ANGLE:- 10°

| F _a F _r & F _t (Newtons) | | | | | Ra [C.L.A] (μm) | | | | | CROSS-FEED (mm/rev & in/rev) | | | | | | | |
|--|--|--|--|--|-------------------|--|--|--|--|------------------------------|-------|--------|-------|-------|--------|--|--|
| | | | | | | | | | | in. | | mm/rev | | | in/rev | | |
| | | | | | | | | | | μm | | | | | | | |
| | | | | | | | | | | .004 | .008 | .012 | .016 | .020 | | | |
| | | | | | | | | | | .1 | .2 | .3 | .4 | .5 | | | |
| | | | | | | | | | | _____ | _____ | _____ | _____ | _____ | | | |
| | | | | | | | | | | .79 | .83 | 1.18 | 1.39 | 1.86 | | | |
| | | | | | | | | | | .25 | .26 | .36 | .40 | .56 | | | |
| | | | | | | | | | | 3.20 | 3.16 | 3.27 | 3.48 | 3.35 | | | |
| | | | | | | | | | | .88 | 1.00 | 1.30 | 1.33 | 1.55 | | | |
| | | | | | | | | | | _____ | _____ | _____ | _____ | _____ | | | |
| | | | | | | | | | | 2.59 | 3.27 | 3.50 | 4.17 | 4.73 | | | |
| | | | | | | | | | | .75 | .94 | .99 | 1.19 | 1.32 | | | |
| | | | | | | | | | | 3.44 | 3.47 | 3.55 | 3.50 | 3.57 | | | |
| | | | | | | | | | | 1.20 | 1.33 | 1.38 | 1.50 | 1.75 | | | |
| | | | | | | | | | | .19 | .22 | .22 | .24 | .25 | | | |
| | | | | | | | | | | 4.56 | 5.37 | 6.12 | 7.23 | 8.12 | | | |
| | | | | | | | | | | 1.34 | 1.55 | 1.70 | 2.02 | 2.42 | | | |
| | | | | | | | | | | 3.40 | 3.45 | 3.60 | 3.59 | 3.51 | | | |
| | | | | | | | | | | 1.05 | 1.25 | 1.60 | 2.13 | 2.30 | | | |
| | | | | | | | | | | .36 | .39 | .39 | .44 | .46 | | | |
| | | | | | | | | | | 6.26 | 7.12 | 8.16 | 9.04 | 10.06 | | | |
| | | | | | | | | | | 1.74 | 2.00 | 2.25 | 2.44 | 2.73 | | | |
| | | | | | | | | | | 3.60 | 3.55 | 3.62 | 3.71 | 3.69 | | | |
| | | | | | | | | | | 1.00 | 1.20 | 1.75 | 2.20 | 2.25 | | | |
| | | | | | | | | | | .56 | .61 | .61 | .64 | .65 | | | |
| | | | | | | | | | | 7.23 | 8.28 | 9.31 | 10.29 | 11.40 | | | |
| | | | | | | | | | | 2.04 | 2.36 | 2.60 | 2.76 | 2.99 | | | |
| | | | | | | | | | | 3.55 | 3.51 | 3.58 | 3.73 | 3.81 | | | |
| | | | | | | | | | | 1.20 | 1.38 | 1.95 | 2.13 | 1.75 | | | |

TEST NO:- 5 cont.

DIAMOND NO:- 63794/2

WHEEL TYPE:- A 60 KV ϕ :-305mm SPEED 1800 rev/min

DRAG ANGLE:- 15°

| F _a F _r & F _t (Newtons) | | Ra [C.L.A] (μm) | | IN-FEED (μm & in.) | | CROSS-FEED (mm/rev & in/rev) | | | | | |
|--|--|-------------------|--|---------------------------------|------|---------------------------------|------|--------|------|------|------|
| | | | | | | in/rev | | mm/rev | | | |
| | | | | | | in. | μm | .004 | .008 | .012 | .016 |
| | | | | | | .1 | .2 | .3 | .4 | .5 | |
| F _a F _r & F _t (Newtons) | | .0002 | | 5 | | F _a | — | — | — | — | — |
| | | | | | | F _r | .72 | .78 | .89 | .90 | 1.22 |
| | | | | | | F _t | .23 | .24 | .28 | .28 | .39 |
| | | | | | | F _r / F _t | 3.17 | 3.20 | 3.19 | 3.22 | 3.15 |
| | | | | | | R _a | 1.13 | 1.15 | 1.00 | 1.00 | 1.30 |
| | | .0004 | | 10 | | F _a | — | — | — | — | — |
| | | | | | | F _r | 2.34 | 2.39 | 2.68 | 2.84 | 3.23 |
| | | | | | | F _t | .71 | .71 | .79 | .84 | .96 |
| | | | | | | F _r / F _t | 3.31 | 3.37 | 3.41 | 3.39 | 3.38 |
| | | | | | | R _a | 1.38 | 1.25 | 1.63 | 1.50 | 1.50 |
| | | .0006 | | 15 | | F _a | .19 | .21 | .26 | .25 | .28 |
| | | | | | | F _r | 3.24 | 3.53 | 4.17 | 4.42 | 5.12 |
| | | | | | | F _t | .94 | 1.01 | 1.18 | 1.25 | 1.45 |
| | | | | | | F _r / F _t | 3.45 | 3.51 | 3.55 | 3.54 | 3.52 |
| | | | | | | R _a | 1.40 | 1.63 | 2.08 | 2.18 | 2.38 |
| | | .0008 | | 20 | | F _a | .36 | .36 | .38 | .42 | .42 |
| | | | | | | F _r | 5.00 | 5.52 | 6.14 | 6.71 | 7.28 |
| | | | | | | F _t | 1.45 | 1.57 | 1.68 | 1.86 | 2.03 |
| | | | | | | F _r / F _t | 3.46 | 3.52 | 3.65 | 3.61 | 3.58 |
| | | | | | | R _a | 1.55 | 1.50 | 2.13 | 2.20 | 2.25 |
| .0010 | | 25 | | F _a | .58 | .50 | .49 | .53 | .53 | | |
| | | | | F _r | 6.12 | 6.84 | 7.62 | 8.20 | 9.04 | | |
| | | | | F _t | 1.70 | 1.90 | 1.99 | 2.27 | 2.54 | | |
| | | | | F _r / F _t | 3.60 | 3.59 | 3.83 | 3.62 | 3.56 | | |
| | | | | R _a | 1.55 | 1.63 | 2.00 | 2.13 | 2.63 | | |

TEST NO:- 6

DIAMOND NO:- 63794/2

WHEEL TYPE:- A46KV ϕ :-305mm SPEED 1800 rev/minDRAG ANGLE:- 5°

| Ra [C.L.A] (μ m) | | | | | CROSS-FEED (mm/rev & in/rev) | | | | | | |
|--|-------|---------------------------------|---------------------------------|------|------------------------------|------|-------|-------|------|--|--|
| | | | | | in/rev | | | | | | |
| | | | | | .004 | .008 | .012 | .016 | .020 | | |
| | | | | | .1 | .2 | .3 | .4 | .5 | | |
| F _a F _r & F _t (Newtons) | .0002 | 5 | F _a | | | | | | | | |
| | | | F _r | 1.25 | 1.60 | 1.81 | 2.10 | 2.31 | | | |
| | | | F _t | .43 | .54 | .67 | .72 | .78 | | | |
| | | | F _r / F _t | 2.90 | 2.95 | 2.71 | 2.90 | 2.96 | | | |
| | | | R _a | 1.25 | 1.03 | 1.45 | 1.45 | 1.00 | | | |
| | .0004 | 10 | F _a | .15 | .18 | .14 | .14 | .15 | | | |
| | | | F _r | 2.22 | 3.09 | 3.89 | 4.60 | 5.21 | | | |
| | | | F _t | .77 | .98 | 1.26 | 1.53 | 1.64 | | | |
| | | | F _r / F _t | 2.90 | 3.15 | 3.10 | 3.00 | 3.17 | | | |
| | | | R _a | 1.38 | 1.05 | 1.68 | 1.88 | 1.90 | | | |
| | .0006 | 15 | F _a | .17 | .14 | .19 | .14 | .15 | | | |
| | | | F _r | 2.59 | 4.17 | 5.64 | 6.76 | 8.24 | | | |
| | | | F _t | .83 | 1.30 | 1.73 | 2.14 | 2.74 | | | |
| | | | F _r / F _t | 3.10 | 3.20 | 3.27 | 3.15 | 3.01 | | | |
| | | | R _a | 1.08 | 1.55 | 1.65 | 2.38 | 3.20 | | | |
| | .0008 | 20 | F _a | .19 | .21 | .19 | .22 | .19 | | | |
| | | | F _r | 3.06 | 5.09 | 6.78 | 9.12 | 10.99 | | | |
| | | | F _t | .94 | 1.54 | 2.05 | 2.80 | 3.28 | | | |
| | | | F _r / F _t | 3.25 | 3.30 | 3.31 | 3.26 | 3.35 | | | |
| | | | R _a | 1.13 | 1.45 | 1.55 | 2.00 | 2.95 | | | |
| .0010 | 25 | F _a | .22 | .25 | .21 | .22 | .23 | | | | |
| | | F _r | 3.22 | 5.34 | 7.90 | 9.90 | 12.51 | | | | |
| | | F _t | .91 | 1.56 | 2.28 | 2.91 | 3.67 | | | | |
| | | F _r / F _t | 3.53 | 3.42 | 3.46 | 3.40 | 3.41 | | | | |
| | | R _a | 1.30 | 1.33 | 1.65 | 2.10 | 3.75 | | | | |

TEST NO:- 6 cont.

DIAMOND NO:- 63794/2

WHEEL TYPE:- A46 KV ϕ :-305mm SPEED 1800 rev/minDRAG ANGLE:- 10°

| F _a F _r & F _t (Newtons) | | Ra [C.L.A] (μm) | | CROSS-FEED (mm/rev & in/rev) | | | | | |
|--|--|-------------------|----|---------------------------------|-------|--------|-------|-------|-------|
| | | | | in/rev | | mm/rev | | | |
| | | | | .004 | .008 | .012 | .016 | .020 | |
| | | in. | μm | mm/rev | | | | | |
| | | .0002 | 5 | F _a | _____ | _____ | _____ | _____ | _____ |
| | | | | F _r | .67 | .75 | 1.26 | 1.47 | 1.65 |
| | | | | F _t | .26 | .28 | .48 | .54 | .60 |
| | | | | F _r / F _t | 2.53 | 2.70 | 2.65 | 2.70 | 2.77 |
| | | | | R _a | 1.05 | 1.15 | .95 | 1.00 | 1.20 |
| | | .0004 | 10 | F _a | .10 | .11 | .11 | .13 | .11 |
| | | | | F _r | 1.53 | 2.28 | 2.42 | 3.27 | 3.56 |
| | | | | F _t | .56 | .80 | .86 | 1.11 | 1.24 |
| | | | | F _r / F _t | 2.71 | 2.85 | 2.80 | 2.93 | 2.87 |
| | | | | R _a | 1.05 | 1.40 | 1.65 | 1.78 | 1.83 |
| | | .0006 | 15 | F _a | .17 | .19 | .18 | .19 | .21 |
| | | | | F _r | 2.65 | 3.67 | 4.39 | 5.50 | 6.03 |
| | | | | F _t | .88 | 1.16 | 1.47 | 1.72 | 2.02 |
| | | | | F _r / F _t | 3.01 | 3.15 | 3.00 | 3.20 | 2.99 |
| | | | | R _a | 1.00 | 1.45 | 1.70 | 2.38 | 2.25 |
| | | .0008 | 20 | F _a | .24 | .24 | .25 | .25 | .26 |
| | | | | F _r | 3.60 | 4.74 | 6.14 | 7.51 | 8.70 |
| | | | | F _t | 1.15 | 1.50 | 1.98 | 2.33 | 2.69 |
| | | | | F _r / F _t | 3.12 | 3.15 | 3.10 | 3.22 | 3.23 |
| | | | | R _a | 1.20 | 1.58 | 1.80 | 2.78 | 2.73 |
| | | .0010 | 25 | F _a | .26 | .28 | .27 | .31 | .33 |
| | | | | F _r | 4.11 | 5.75 | 7.17 | 9.04 | 10.61 |
| | | | | F _t | 1.29 | 1.87 | 2.31 | 2.87 | 3.31 |
| | | | | F _r / F _t | 3.18 | 3.07 | 3.10 | 3.15 | 3.20 |
| | | | | R _a | 1.50 | 1.75 | 1.88 | 2.50 | 2.78 |

TEST NO:- 6 cont.

DIAMOND NO:- 63794/2

WHEEL TYPE:- A46KV ϕ :-305mm SPEED 1800 rev/min

DRAG ANGLE:- 15°

| F _a F _r & F _t (Newtons) | | | | Ra [C.L.A] (μm) | | CROSS-FEED (mm/rev & in/rev) | | | | |
|---|-------|---------------------------------|---------------------------------|-------------------|-------|------------------------------|-------|-------|------|------|
| | | | | | | | | | | |
| | | | | | | | | | | |
| IN-FEED (μm & in.) | | in. μm | | in/rev mm/rev | | .004 | .008 | .012 | .016 | .020 |
| | | | | | | .1 | .2 | .3 | .4 | .5 |
| F _a F _r F _t F _r / F _t R _a | .0002 | 5 | F _a | _____ | _____ | _____ | _____ | _____ | | |
| | | | F _r | 1.04 | 1.25 | 1.61 | 1.75 | 1.97 | | |
| | | | F _t | .39 | .46 | .51 | .56 | .64 | | |
| | | | F _r / F _t | 2.65 | 2.73 | 3.14 | 3.15 | 3.09 | | |
| | | | R _a | 1.25 | 1.00 | 1.38 | 1.25 | 1.00 | | |
| | .0004 | 10 | F _a | .04 | .06 | .07 | .08 | .08 | | |
| | | | F _r | 2.32 | 3.17 | 3.84 | 4.34 | 4.93 | | |
| | | | F _t | .79 | 1.10 | 1.32 | 1.45 | 1.56 | | |
| | | | F _r / F _t | 2.95 | 2.87 | 2.91 | 2.98 | 3.16 | | |
| | | | R _a | 1.30 | 1.30 | 1.60 | 1.90 | 2.10 | | |
| | .0006 | 15 | F _a | .09 | .08 | .10 | .11 | .12 | | |
| | | | F _r | 2.86 | 3.84 | 4.45 | 5.49 | 6.07 | | |
| | | | F _t | .89 | 1.18 | 1.48 | 1.66 | 1.98 | | |
| | | | F _r / F _t | 3.22 | 3.25 | 3.01 | 3.31 | 3.07 | | |
| | | | R _a | 1.20 | 1.38 | 1.83 | 2.13 | 2.13 | | |
| | .0008 | 20 | F _a | .15 | .17 | .17 | .18 | .19 | | |
| | | | F _r | 3.85 | 4.99 | 6.13 | 7.51 | 8.48 | | |
| | | | F _t | 1.21 | 1.53 | 1.86 | 2.29 | 2.60 | | |
| | | | F _r / F _t | 3.18 | 3.26 | 3.30 | 3.28 | 3.26 | | |
| | | | R _a | 1.45 | 1.45 | 1.75 | 2.05 | 2.15 | | |
| .0010 | 25 | F _a | .22 | .22 | .25 | .26 | .28 | | | |
| | | F _r | 4.61 | 6.12 | 7.42 | 8.63 | 9.80 | | | |
| | | F _t | 1.42 | 1.87 | 2.22 | 2.62 | 2.96 | | | |
| | | F _r / F _t | 3.26 | 3.28 | 3.35 | 3.29 | 3.31 | | | |
| | | R _a | 1.45 | 1.35 | 1.53 | 2.00 | 2.20 | | | |

TEST NO:- 7

DIAMOND NO:- 63794/2

WHEEL TYPE:- 38 A 46- ϕ :-305mm SPEED 1800 rev/min

DRAG ANGLE:- 5°

K5VBE

| Ra [C.L.A] (μm) | | | | | CROSS-FEED (mm/rev & in/rev) | | | | | | | | | | | |
|--|---------------------|-------|---------------------------------|---------------------------------|------------------------------|-------|--------|-------|--------|--------|--------|--------|--------|----|--------|----|
| | | | | | in/rev | | mm/rev | | | in/rev | | mm/rev | | | | |
| | | | | | .004 | .008 | .012 | .016 | .020 | .1 | .2 | .3 | .4 | .5 | | |
| F _a F _r & F _t (Newtons) | | | | | in. | | μm | | in/rev | | mm/rev | | in/rev | | mm/rev | |
| | | | | | .0002 | .0004 | .0006 | .0008 | .0010 | 5 | 10 | 15 | 20 | 25 | 5 | 10 |
| F _a F _r & F _t (Newtons) | IN-FEED (μm & in.) | .0002 | 5 | F _a | _____ | | | | | | | | | | | |
| | | | | F _r | .57 | .83 | 1.29 | 1.58 | 1.78 | | | | | | | |
| | | | | F _t | .19 | .28 | .42 | .51 | .57 | | | | | | | |
| | | | | F _r / F _t | 3.00 | 2.95 | 3.05 | 3.10 | 3.10 | | | | | | | |
| | | | | R _a | 1.15 | 1.05 | 1.20 | 1.45 | 1.98 | | | | | | | |
| | .0004 | 10 | F _a | _____ | | | | | | | | | | | | |
| | | | F _r | 1.47 | 2.25 | 2.79 | 3.73 | 4.39 | | | | | | | | |
| | | | F _t | .48 | .71 | .87 | 1.25 | 1.42 | | | | | | | | |
| | | | F _r / F _t | 3.10 | 3.15 | 3.20 | 2.98 | 3.10 | | | | | | | | |
| | | | R _a | 1.30 | 1.25 | 1.25 | 1.50 | 2.25 | | | | | | | | |
| | .0006 | 15 | F _a | .14 | .11 | .11 | .10 | .11 | | | | | | | | |
| | | | F _r | 2.18 | 3.20 | 4.17 | 4.98 | 6.51 | | | | | | | | |
| | | | F _t | .65 | .97 | 1.24 | 1.51 | 1.94 | | | | | | | | |
| | | | F _r / F _t | 3.37 | 3.29 | 3.37 | 3.30 | 3.35 | | | | | | | | |
| | | | R _a | 1.25 | 1.45 | 1.95 | 2.08 | 2.58 | | | | | | | | |
| | .0008 | 20 | F _a | .22 | .24 | .21 | .22 | .24 | | | | | | | | |
| | | | F _r | 3.00 | 4.23 | 5.64 | 6.89 | 7.94 | | | | | | | | |
| | | | F _t | .88 | 1.28 | 1.66 | 2.06 | 2.32 | | | | | | | | |
| | | | F _r / F _t | 3.40 | 3.31 | 3.40 | 3.35 | 3.42 | | | | | | | | |
| | | | R _a | 1.25 | 1.50 | 2.05 | 2.23 | 2.63 | | | | | | | | |
| | .0010 | 25 | F _a | .26 | .26 | .28 | .28 | .29 | | | | | | | | |
| | | | F _r | 3.42 | 5.21 | 6.23 | 7.98 | 9.24 | | | | | | | | |
| | | | F _t | .97 | 1.51 | 1.81 | 2.37 | 2.68 | | | | | | | | |
| | | | F _r / F _t | 3.51 | 3.46 | 3.44 | 3.37 | 3.45 | | | | | | | | |
| | | | R _a | 1.25 | 1.60 | 2.10 | 2.33 | 2.73 | | | | | | | | |

TEST NO:- 7 cont.

DIAMOND NO:- 63794/2

WHEEL TYPE:- 38A 46 - ϕ :-305mm SPEED 1800 rev/min

DRAG ANGLE:-10° K5VBE

| F _a F _r & F _t (Newtons) | | | | | Ra [C.L.A] (μm) | | | | | CROSS-FEED (mm/rev & in/rev) | | | | | | | | | |
|--|----------------|----------------|---------------------------------|----------------|-------------------|--|---|--|----------------|------------------------------|----------------|---------------------------------|----------------|----------------|---------------------------------|----------------|----|----|----|
| | | | | | | | | | | in/rev | | mm/rev | | | in. | | | μm | |
| | | | | | | | | | | .004 | .008 | .012 | .016 | .020 | .1 | .2 | .3 | .4 | .5 |
| IN-FEED (μm & in.) | | | | | .0002 | | 5 | | F _a | F _r | F _t | F _r / F _t | R _a | | | | | | |
| | | | | | | | | | F _a | F _r | F _t | F _r / F _t | R _a | | | | | | |
| | | | | | .0004 | | | | | 10 | | F _a | F _r | F _t | F _r / F _t | R _a | | | |
| | | | | | | | | | | | | F _a | F _r | F _t | F _r / F _t | R _a | | | |
| | | | | | | | | | | | | F _a | F _r | F _t | F _r / F _t | R _a | | | |
| | | | | | | | | | | | | F _a | F _r | F _t | F _r / F _t | R _a | | | |
| | | | | | | | | | | | | F _a | F _r | F _t | F _r / F _t | R _a | | | |
| | | | | | .0006 | | | | | 15 | | F _a | F _r | F _t | F _r / F _t | R _a | | | |
| | | | | | | | | | | | | F _a | F _r | F _t | F _r / F _t | R _a | | | |
| | | | | | | | | | | | | F _a | F _r | F _t | F _r / F _t | R _a | | | |
| | | | | | | | | | | | | F _a | F _r | F _t | F _r / F _t | R _a | | | |
| | | | | | | | | | | | | F _a | F _r | F _t | F _r / F _t | R _a | | | |
| | | | | | .0008 | | | | | 20 | | F _a | F _r | F _t | F _r / F _t | R _a | | | |
| | | | | | | | | | | | | F _a | F _r | F _t | F _r / F _t | R _a | | | |
| | | | | | | | | | | | | F _a | F _r | F _t | F _r / F _t | R _a | | | |
| | | | | | | | | | | | | F _a | F _r | F _t | F _r / F _t | R _a | | | |
| | | | | | | | | | | | | F _a | F _r | F _t | F _r / F _t | R _a | | | |
| | | | | | .0010 | | | | | 25 | | F _a | F _r | F _t | F _r / F _t | R _a | | | |
| | | | | | | | | | | | | F _a | F _r | F _t | F _r / F _t | R _a | | | |
| | | | | | | | | | | | | F _a | F _r | F _t | F _r / F _t | R _a | | | |
| F _a | F _r | F _t | F _r / F _t | R _a | | | | | | | | | | | | | | | |
| F _a | F _r | F _t | F _r / F _t | R _a | | | | | | | | | | | | | | | |
| | | | | | | | | | | | | | | | | | | | |

TEST NO:- 7cont.

DIAMOND NO:- 63794/2

WHEEL TYPE:- 38A46 - ϕ :-305mm SPEED 1800 rev/min

DRAG ANGLE:-15° K5VBE

| F _a F _r & F _t (Newtons) | | Ra [C.L.A] (μm) | | IN-FEED (μm & in.) | | CROSS-FEED (mm/rev & in/rev) | | | | |
|--|-------|--------------------------------|--------------------------------|---------------------|-------|------------------------------|-------|--------|------|------|
| | | | | | | in/rev | | mm/rev | | |
| | | | | | | .004 | .008 | .012 | .016 | .020 |
| | | in. | μm | mm/rev | .1 | .2 | .3 | .4 | .5 | |
| F _a F _r F _t F _r /F _t R _a | .0002 | 5 | F _a | _____ | _____ | _____ | _____ | _____ | | |
| | | | F _r | .17 | .56 | .79 | 1.24 | 1.39 | | |
| | | | F _t | .06 | .19 | .26 | .40 | .46 | | |
| | | | F _r /F _t | 2.98 | 2.95 | 3.00 | 3.07 | 3.05 | | |
| | | | R _a | 1.40 | 1.33 | 1.00 | 1.25 | 1.05 | | |
| | .0004 | 10 | F _a | _____ | _____ | _____ | _____ | _____ | | |
| | | | F _r | 1.47 | 1.67 | 2.20 | 2.46 | 2.75 | | |
| | | | F _t | .47 | .55 | .68 | .79 | .89 | | |
| | | | F _r /F _t | 3.13 | 3.01 | 3.24 | 3.11 | 3.08 | | |
| | | | R _a | 1.20 | 1.35 | 1.48 | 1.65 | 1.38 | | |
| | .0006 | 15 | F _a | .08 | .07 | .08 | .10 | .10 | | |
| | | | F _r | 1.95 | 2.45 | 3.06 | 3.63 | 3.98 | | |
| | | | F _t | .59 | .74 | .94 | 1.08 | 1.20 | | |
| | | | F _r /F _t | 3.29 | 3.31 | 3.26 | 3.35 | 3.31 | | |
| | | | R _a | 1.53 | 1.70 | 1.78 | 1.93 | 1.95 | | |
| | .0008 | 20 | F _a | .11 | .11 | .11 | .13 | .11 | | |
| | | | F _r | 2.34 | 2.96 | 3.61 | 4.00 | 4.61 | | |
| | | | F _t | .68 | .86 | 1.08 | 1.17 | 1.36 | | |
| | | | F _r /F _t | 3.41 | 3.42 | 3.35 | 3.41 | 3.39 | | |
| | | | R _a | 1.25 | 1.55 | 1.85 | 2.08 | 2.08 | | |
| .0010 | 25 | F _a | .15 | .17 | .15 | .14 | .15 | | | |
| | | F _r | 2.59 | 3.11 | 3.93 | 4.45 | 5.14 | | | |
| | | F _t | .74 | .90 | 1.12 | 1.25 | 1.53 | | | |
| | | F _r /F _t | 3.51 | 3.47 | 3.50 | 3.55 | 3.35 | | | |
| | | R _a | 1.30 | 1.58 | 2.05 | 2.65 | 2.65 | | | |

TEST NO:- 8

DIAMOND NO:- (Origin unknown) blunt; single-point

WHEEL TYPE:-38A46-K5VBE ϕ :-292mm SPEED 1800 rev/min

DRAG ANGLE:- $+5^\circ$

| | | | | CROSS-FEED (mm/rev & in/rev) | | | | |
|--|----------------|------------------------|---------------------------------|------------------------------|---------------------------------|---------|--|--|
| | | | | in/rev | | | | |
| | | | | mm/rev | | | | |
| F _a F _r & F _t (Newtons) | | Ra [C.L.A] (μ m) | | in. | | μ m | | |
| | | | | | | | | |
| IN-FEED (μ m & in.) | | .0002 | | 5 | | | | |
| | | | | | | | | |
| F _a | F _r | F _t | F _r / F _t | Ra | | | | |
| | | | | | | | | |
| | | | | | | | | |
| | | | | | | | | |
| | | | | | | | | |
| .0004 | 10 | F _a | F _r | F _t | F _r / F _t | Ra | | |
| | | | | | | | | |
| | | | | | | | | |
| | | | | | | | | |
| | | | | | | | | |
| .0006 | 15 | F _a | F _r | F _t | F _r / F _t | Ra | | |
| | | | | | | | | |
| | | | | | | | | |
| | | | | | | | | |
| | | | | | | | | |
| .0008 | 20 | F _a | F _r | F _t | F _r / F _t | Ra | | |
| | | | | | | | | |
| | | | | | | | | |
| | | | | | | | | |
| | | | | | | | | |
| .0010 | 25 | F _a | F _r | F _t | F _r / F _t | Ra | | |
| | | | | | | | | |
| | | | | | | | | |
| | | | | | | | | |
| | | | | | | | | |

TEST NO:- 8 cont.

DIAMOND NO:- (Origin unknown) blunt; single-point

WHEEL TYPE:-32 A60-K8VBE ϕ :-287 mm SPEED 1800 rev/min

DRAG ANGLE:- $+5^\circ$

| F _a F _r & F _t (Newtons) | | | Ra [C.L.A] (μm) | | CROSS-FEED (mm/rev & in/rev) | | | | | |
|--|----|--------------------------------|-------------------|-------|--------------------------------|-------|-------|-------|-------|-------|
| | | | | | in/rev | | | | | |
| | | | | | mm/rev | .004 | .008 | .012 | .016 | .020 |
| | | | in. | μm | | .1 | .2 | .3 | .4 | .5 |
| | | | .0002 | 5 | F _a | _____ | _____ | _____ | _____ | _____ |
| | | | | | F _r | 2.59 | 2.61 | 2.92 | 2.92 | 3.06 |
| | | | | | F _t | .58 | .60 | .68 | .63 | .71 |
| | | | | | F _r /F _t | 4.50 | 4.36 | 4.32 | 4.61 | 4.29 |
| | | | | | R _a | .35 | .45 | .63 | .80 | .88 |
| | | | .0004 | 10 | F _a | _____ | _____ | _____ | _____ | _____ |
| | | | | | F _r | 8.62 | 8.81 | 9.15 | 9.50 | 9.67 |
| | | | | | F _t | 1.79 | 1.81 | 1.93 | 2.00 | 2.10 |
| | | | | | F _r /F _t | 4.81 | 4.87 | 4.75 | 4.75 | 4.61 |
| | | | | | R _a | .48 | .55 | .68 | .83 | .93 |
| | | | .0006 | 15 | F _a | _____ | _____ | _____ | _____ | _____ |
| | | | | | F _r | 12.23 | 12.51 | 12.84 | 13.07 | 13.01 |
| | | | | | F _t | 2.40 | 2.36 | 2.58 | 2.66 | 2.74 |
| | | | | | F _r /F _t | 5.09 | 5.30 | 4.98 | 4.91 | 4.75 |
| | | | | | R _a | .48 | .63 | .90 | 1.00 | 1.00 |
| | | | .0008 | 20 | F _a | _____ | _____ | _____ | _____ | _____ |
| | | | | | F _r | 14.32 | 14.76 | 15.01 | 15.07 | 15.29 |
| | | | | | F _t | 2.67 | 2.64 | 2.88 | 2.76 | 2.90 |
| | | | | | F _r /F _t | 5.35 | 5.59 | 5.21 | 5.47 | 5.28 |
| | | | | | R _a | .58 | .85 | 1.03 | 1.20 | 1.25 |
| .0010 | 25 | F _a | _____ | _____ | _____ | _____ | _____ | | | |
| | | F _r | 16.40 | 17.10 | 16.96 | 17.51 | 18.07 | | | |
| | | F _t | 2.78 | 2.84 | 2.77 | 3.03 | 3.06 | | | |
| | | F _r /F _t | 5.89 | 6.02 | 6.13 | 5.78 | 5.90 | | | |
| | | R _a | .70 | .80 | 1.00 | 1.13 | 1.25 | | | |

TEST NO:- 8 cont.

DIAMOND NO:- (Origin unknown) blunt; single-point

WHEEL TYPE:- A 46 KV ϕ :- 278mm SPEED 1800 rev/min

DRAG ANGLE:- +5°

| F _a F _r & F _t (Newtons) | | | | | Ra [C.L.A] (μm) | | CROSS-FEED (mm/rev & in/rev) | | | | | | |
|--|-------|---------------------------------|---------------------------------|-------|-------------------|-------|------------------------------|-------|--------|-------|-------|-------|-------|
| | | | | | | | in/rev | | mm/rev | | | | |
| | | | | | | | .004 | .008 | .012 | .016 | .020 | .1 | .2 |
| IN-FEED (μm & in.) | .0002 | 5 | F _a | _____ | _____ | _____ | _____ | _____ | _____ | _____ | _____ | _____ | |
| | | | F _r | 2.78 | 3.00 | 3.34 | 3.42 | 3.60 | _____ | _____ | _____ | _____ | _____ |
| | | | F _t | .65 | .68 | .80 | .81 | .84 | _____ | _____ | _____ | _____ | _____ |
| | | | F _r / F _t | 4.30 | 4.42 | 4.15 | 4.20 | 4.28 | _____ | _____ | _____ | _____ | _____ |
| | | | R _a | 1.18 | 1.23 | 1.18 | 1.23 | 1.18 | _____ | _____ | _____ | _____ | _____ |
| | .0004 | 10 | F _a | _____ | _____ | _____ | _____ | _____ | _____ | _____ | _____ | _____ | |
| | | | F _r | 9.17 | 9.73 | 10.04 | 10.29 | 10.17 | _____ | _____ | _____ | _____ | _____ |
| | | | F _t | 2.00 | 2.11 | 2.21 | 2.34 | 2.30 | _____ | _____ | _____ | _____ | _____ |
| | | | F _r / F _t | 4.60 | 4.61 | 4.55 | 4.40 | 4.43 | _____ | _____ | _____ | _____ | _____ |
| | | | R _a | 1.25 | 1.13 | 1.15 | 1.23 | 1.08 | _____ | _____ | _____ | _____ | _____ |
| | .0006 | 15 | F _a | _____ | _____ | _____ | _____ | _____ | _____ | _____ | _____ | _____ | |
| | | | F _r | 12.79 | 12.79 | 13.07 | 13.34 | 13.37 | _____ | _____ | _____ | _____ | _____ |
| | | | F _t | 2.46 | 2.50 | 2.51 | 2.54 | 2.63 | _____ | _____ | _____ | _____ | _____ |
| | | | F _r / F _t | 5.20 | 5.12 | 5.21 | 5.25 | 5.08 | _____ | _____ | _____ | _____ | _____ |
| | | | R _a | 1.13 | 1.03 | 1.20 | 1.10 | 1.10 | _____ | _____ | _____ | _____ | _____ |
| | .0008 | 20 | F _a | _____ | _____ | _____ | _____ | _____ | _____ | _____ | _____ | _____ | |
| | | | F _r | 13.34 | 13.93 | 14.04 | 14.21 | 14.79 | _____ | _____ | _____ | _____ | _____ |
| | | | F _t | 2.47 | 2.57 | 2.66 | 2.54 | 2.73 | _____ | _____ | _____ | _____ | _____ |
| | | | F _r / F _t | 5.39 | 5.41 | 5.28 | 5.59 | 5.41 | _____ | _____ | _____ | _____ | _____ |
| | | | R _a | 1.20 | 1.25 | 1.20 | 1.28 | 1.25 | _____ | _____ | _____ | _____ | _____ |
| .0010 | 25 | F _a | _____ | _____ | _____ | _____ | _____ | _____ | _____ | _____ | _____ | | |
| | | F _r | 15.85 | 16.40 | 16.85 | 16.96 | 16.96 | _____ | _____ | _____ | _____ | _____ | |
| | | F _t | 2.70 | 2.69 | 2.84 | 2.84 | 2.77 | _____ | _____ | _____ | _____ | _____ | |
| | | F _r / F _t | 5.87 | 6.09 | 5.94 | 5.97 | 6.12 | _____ | _____ | _____ | _____ | _____ | |
| | | R _a | 1.28 | 1.20 | 1.15 | 1.25 | 1.13 | _____ | _____ | _____ | _____ | _____ | |

TEST NO:- 8 cont.

DIAMOND NO:- (Origin unknown) blunt; single-point

WHEEL TYPE:- A 60 KV ϕ :-295 mm SPEED 1800 rev/min

DRAG ANGLE:- $+5^\circ$

| F _a F _r & F _t (Newtons) | | Ra [C.L.A] (μm) | | IN-FEED (μm & in.) | | CROSS-FEED (mm/rev & in/rev) | | | | |
|--|----------------|---------------------------------|---------------------------------|---------------------|--------|------------------------------|-------|-------|-------|------|
| | | | | | | | | | | |
| | | | | | | | | | | |
| | | .0002 | 5 | mm/rev | in/rev | .004 | .008 | .012 | .016 | .020 |
| | | | | | | .1 | .2 | .3 | .4 | .5 |
| F _a | F _r | F _t | F _r / F _t | Ra | _____ | _____ | _____ | _____ | _____ | |
| | | | | | 3.48 | 3.34 | 3.71 | 3.84 | 3.84 | |
| | | | | | .81 | .83 | .87 | .93 | .95 | |
| | | | | | 4.30 | 4.02 | 4.26 | 4.13 | 4.04 | |
| | | | | | .80 | .88 | .85 | .85 | .83 | |
| | F _r | F _t | F _r / F _t | Ra | _____ | _____ | _____ | _____ | _____ | |
| | | | | | 9.73 | 10.43 | 10.56 | 10.45 | 11.06 | |
| | | | | | 2.03 | 2.05 | 2.30 | 2.27 | 2.30 | |
| | | | | | 4.80 | 5.10 | 4.60 | 4.60 | 4.80 | |
| | | | | | .70 | .80 | .75 | .73 | .75 | |
| | F _r | F _t | F _r / F _t | Ra | _____ | _____ | _____ | _____ | _____ | |
| | | | | | 13.90 | 14.18 | 13.96 | 14.26 | 14.60 | |
| | | | | | 2.44 | 2.44 | 2.41 | 2.50 | 2.61 | |
| | | | | | 5.70 | 5.80 | 5.80 | 5.70 | 5.60 | |
| | | | | | .70 | .75 | .88 | .83 | .85 | |
| | F _r | F _t | F _r / F _t | Ra | _____ | _____ | _____ | _____ | _____ | |
| | | | | | 16.12 | 16.65 | 16.74 | 16.96 | 17.10 | |
| | | | | | 2.78 | 2.78 | 2.79 | 2.95 | 3.05 | |
| | | | | | 5.80 | 6.00 | 6.00 | 5.75 | 5.60 | |
| | | | | | .80 | .83 | .88 | .95 | .98 | |
| F _r | F _t | F _r / F _t | Ra | _____ | _____ | _____ | _____ | _____ | | |
| | | | | 18.68 | 19.18 | 19.52 | 19.46 | 19.74 | | |
| | | | | 3.00 | 3.20 | 3.20 | 3.30 | 3.30 | | |
| | | | | 6.25 | 6.00 | 6.10 | 5.90 | 6.00 | | |
| | | | | .78 | .83 | .85 | .90 | .93 | | |

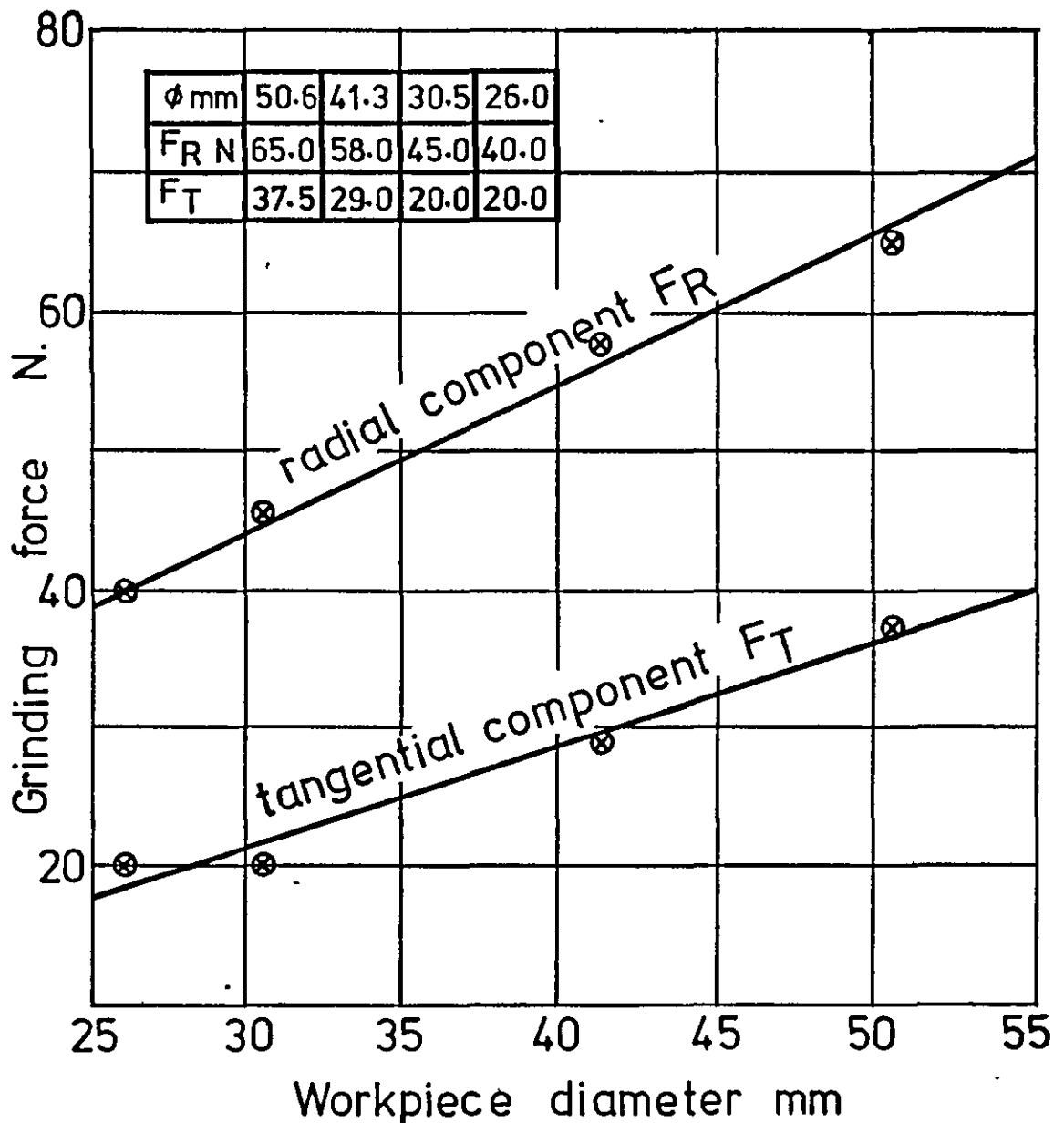
| DIAMOND N ^o :-71784/4 .90K wt | | | | | WHEEL TYPE :-38A46-K5VBE | | | | | Grd.width :-20 mm Step width :- 5 mm | | TEST N ^o :- 9 | | |
|--|--|--------------------------------|-----------|-------|--|--|--|-----------|-------|---|------|--------------------------|------------------------------------|-------------------------|
| PASS N ^o | GRINDING WHEEL WEAR | | | | DIAMOND TOOL WEAR | | | | | DRESSING FORCE (Newtons) | | Fr/Ft RATIO | Ww/Dw RATIO x10 ⁶ | WHEEL C.L.A. (μm) |
| | depth worn in x 10 ⁻⁴ | accum in x 10 ⁻⁴ | Volume Ww | | depth worn in x 10 ⁻⁴ | area worn in ² x 10 ⁻⁶ | depth x area in ³ x 10 ⁻¹⁰ | Volume Dw | | Fr | Ft | | | |
| 1 | — | — | — | — | 2 | 11.5 | 23 | 23 | — | .17 | .08 | 2.0 | — | 1.18 |
| 5 | 9 | 9 | .03 | .44 | 8 | 52 | 416 | 439 | .72 | .75 | .27 | 2.8 | .62 | 1.23 |
| 10 | 20 | 29 | .09 | 1.43 | 6 | 103 | 618 | 1057 | 1.73 | 1.45 | .56 | 2.8 | .82 | 1.25 |
| 15 | 22 | 51 | .15 | 2.52 | 4 | 138 | 552 | 1609 | 2.64 | 1.95 | .61 | 3.2 | .95 | 1.40 |
| 20 | 23 | 74 | .22 | 3.66 | 3 | 170 | 510 | 2119 | 3.47 | 2.39 | .80 | 3.0 | 1.05 | 1.30 |
| 25 | 19 | 93 | .28 | 4.59 | 2 | 190 | 380 | 2499 | 4.10 | 2.50 | .78 | 3.2 | 1.11 | 1.26 |
| 30 | 22 | 115 | .35 | 5.68 | 3 | 203 | 609 | 3108 | 5.09 | 2.78 | .79 | 3.5 | 1.11 | 1.25 |
| 35 | 23 | 138 | .42 | 6.82 | 2 | 226 | 452 | 3560 | 5.83 | 3.09 | .88 | 3.5 | 1.16 | 1.23 |
| 40 | 23 | 161 | .49 | 7.95 | 2 | 242 | 484 | 4044 | 6.63 | 3.34 | .93 | 3.6 | 1.19 | 1.23 |
| 45 | 25 | 186 | .56 | 9.19 | 3 | 252 | 756 | 4800 | 7.87 | 3.53 | .93 | 3.8 | 1.16 | 1.00 |
| 50 | 21 | 207 | .62 | 10.23 | 1 | 270 | 270 | 5070 | 8.31 | 3.73 | .98 | 3.8 | 1.23 | 1.13 |
| 70 | 97 | 304 | .92 | 15.02 | 4 | 330 | 1320 | 6390 | 10.47 | 4.50 | 1.13 | 4.0 | 1.43 | 1.13 |
| 100 | 145 | 449 | 1.35 | 22.18 | 5 | 430 | 2150 | 8540 | 13.99 | 5.73 | 1.27 | 4.5 | 1.58 | 1.15 |
| 150 | 254 | 703 | 2.12 | 34.73 | 7 | 469 | 3283 | 11823 | 19.37 | 6.26 | 1.42 | 4.4 | 1.79 | 1.13 |
| 200 | 256 | 959 | 2.89 | 47.38 | 3 | 501 | 1503 | 13326 | 21.84 | 6.59 | 1.37 | 4.8 | 2.16 | 1.13 |
| 250 | 244 | 1203 | 3.63 | 59.44 | 3 | 528 | 1584 | 14910 | 24.43 | 7.03 | 1.50 | 4.7 | 2.43 | 1.13 |
| 300 | 259 | 1462 | 4.41 | 72.23 | 3 | 540 | 1620 | 16530 | 27.09 | 7.09 | 1.47 | 4.8 | 2.66 | 1.13 |

APPENDIX VII

GRINDING TEST RESULTS

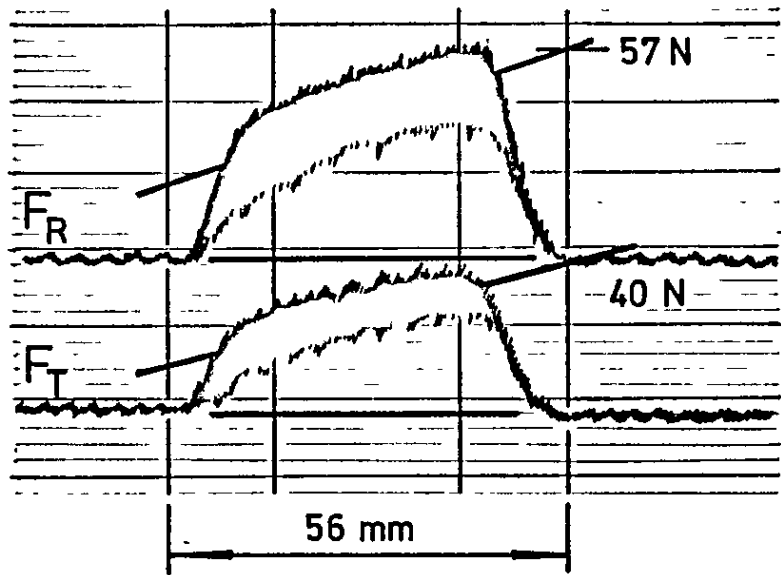
(TABULATED FORM)

Variation of grinding force with changes in workpiece diameter



A series of grinding tests were conducted to observe the effect of the change in workpiece diameter on grinding force. The results are shown above. Due to the observed reduction in force reading for a reduction in workpiece diameter, several of the main tests were repeated, using workpieces having a starting diameter of 50 mm. The variations in force readings were noted for similar volumes of metal removed, and were found to follow the same trend.

1cm = 20 N



Depth of cut $a_g = 12.5 \mu\text{m}$

Cross-feed $v_t = 13.5 \text{ mm/sec}$

Paper trace rate = 7.5 mm/sec

Workpiece length = 75.5 mm

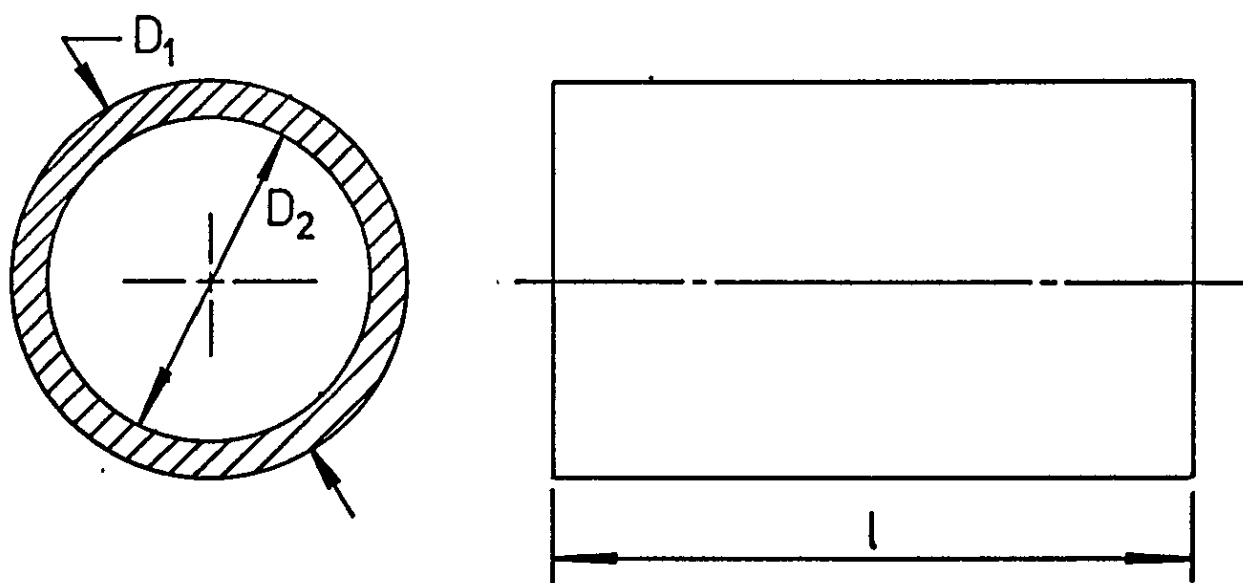
Grinding wheel width = 25 mm

$$\therefore \text{Active trace length} = \frac{7.5}{13.5} \times (75.5 + 25) \text{ mm}$$
$$\approx 56 \text{ mm}$$

From the trace $F_R = \underline{\underline{57 \text{ N}}}$

$F_T = \underline{\underline{40 \text{ N}}}$

Specimen grinding force readings



Volume of metal removed

$$= \pi \frac{(D_1 + D_2)}{2} \times \frac{(D_1 - D_2)}{2} \times l$$

$$= \pi l \frac{(D_1 + D_2)(D_1 - D_2)}{4}$$

$$= \pi l \frac{(D_1^2 - D_2^2)}{4} \text{ cubic units}$$

Calculation of the volume of metal removed
by grinding

TEST NO:- 1

DIAMOND NO:- 71784/2

DRESSING CONDITION:- IN-FEED 25 μ m CROSS-FEED .3 mm/revGRINDING CONDITION:- IN-FEED 12.5 μ m CROSS FEED 20.5mm/secWHEEL TYPE:- 32A60-K8VBE ϕ :-272 mm SPEED.- 1800 rev/minWORKPIECE MAT.L EN31 ϕ :- 50.8 mm length:- 77.3 mm

| PASS NO. | METAL cm^3 REMOVED | WHEEL cm^3 WEAR | GRINDING RATIO | WORKPIECE Ra μ m |
|----------|-----------------------------|--------------------------|----------------|----------------------|
| 5 | .39 | .08 | 4.8 | 2.50 |
| 10 | 1.17 | .16 | 7.3 | 2.03 |
| 15 | 1.95 | .21 | 9.3 | 1.70 |
| 20 | 2.73 | .26 | 10.5 | 1.63 |
| 25 | 3.43 | .29 | 11.8 | 1.70 |
| 30 | 3.97 | .34 | 11.7 | 1.63 |
| 35 | 4.67 | .39 | 12.0 | 1.65 |
| 40 | 5.52 | .44 | 12.5 | 1.65 |
| 45 | 6.44 | .51 | 12.6 | 1.63 |
| 50 | 7.36 | .58 | 12.7 | 1.63 |
| 60 | 8.73 | .71 | 12.3 | 1.65 |
| 80 | 11.24 | 1.18 | 9.5 | 1.58 |
| 100 | 14.09 | 1.65 | 8.5 | 1.65 |
| | | | | |

TEST NO:- 2

DIAMOND NO:- 71784/2

DRESSING CONDITION:- IN-FEED $25\mu\text{m}$ CROSS-FEED $.3\text{ mm/rev}$

GRINDING CONDITION:- IN-FEED $12.5\mu\text{m}$ CROSS FEED 13.5 mm/sec

WHEEL TYPE:- 32A60-K8VBE ϕ :- 272 mm SPEED:- 1800 rev/min

WORKPIECE MAT.L EN31 ϕ :- 48.4 mm length:- 77.3 mm

| PASS NO. | METAL cm^3 REMOVED | WHEEL cm^3 WEAR | GRINDING RATIO | WORKPIECE $\text{Ra } \mu\text{m}$ |
|----------|-----------------------------|--------------------------|----------------|------------------------------------|
| 1 | .33 | .08 | 4.1 | 2.50 |
| 5 | .74 | .12 | 6.2 | 2.13 |
| 10 | 1.49 | .19 | 7.8 | 1.75 |
| 15 | 2.08 | .23 | 9.1 | 1.50 |
| 20 | 2.82 | .28 | 10.1 | 1.50 |
| 25 | 3.55 | .30 | 11.9 | 1.55 |
| 30 | 4.45 | .33 | 13.5 | 1.63 |
| 35 | 5.03 | .36 | 14.0 | 1.45 |
| 40 | 5.77 | .39 | 14.8 | 1.55 |
| 45 | 6.42 | .41 | 15.7 | 1.50 |
| 50 | 7.15 | .46 | 15.6 | 1.50 |
| 60 | 8.61 | .52 | 16.6 | 1.53 |
| 80 | 11.34 | .66 | 17.2 | 1.50 |
| 100 | 14.12 | .77 | 18.3 | 1.50 |

TEST NO:- 3

DIAMOND NO:- 71784/2

DRESSING CONDITION:- IN-FEED $25\mu\text{m}$ CROSS-FEED .3 mm/rev

GRINDING CONDITION:- IN-FEED $12.5\mu\text{m}$ CROSS FEED 6.5mm/sec

WHEEL TYPE:- 32A60-K8VBE ϕ :-272 mm SPEED:- 1800 rev/min

WORKPIECE MAT.L EN31 ϕ :-45.9 mm length:- 77.3 mm

| PASS NO. | METAL REMOVED cm^3 | WHEEL WEAR cm^3 | GRINDING RATIO | WORKPIECE $R_a \mu\text{m}$ |
|----------|-----------------------------|--------------------------|----------------|-----------------------------|
| 1 | .07 | .03 | 2.3 | 2.25 |
| 5 | .78 | .10 | 7.8 | 2.08 |
| 10 | 1.48 | .16 | 9.3 | 1.63 |
| 15 | 2.18 | .21 | 10.4 | 1.38 |
| 20 | 2.88 | .25 | 11.5 | 1.25 |
| 30 | 4.28 | .32 | 13.4 | 1.03 |
| 40 | 5.74 | .36 | 15.9 | 1.00 |
| 50 | 7.12 | .39 | 18.3 | 1.00 |
| 60 | 8.49 | .41 | 20.7 | 1.03 |
| 80 | 11.21 | .44 | 25.5 | .85 |
| 100 | 13.84 | .45 | 30.8 | .85 |
| | | | | |
| | | | | |
| | | | | |

TEST NO:- 4

DIAMOND NO:- 71784/2

DRESSING CONDITION:- IN-FEED $25\mu\text{m}$ CROSS-FEED .3 mm/rev

GRINDING CONDITION:- IN-FEED $12.5\mu\text{m}$ CROSS FEED 2.5 mm/sec

WHEEL TYPE:- 32A60-K8VBE ϕ :-272 mm SPEED.- 1800 rev/min

WORKPIECE MAT.L EN31 ϕ :-43.3 mm length:- 77.3 mm

| PASS NO. | METAL REMOVED cm^3 | WHEEL WEAR cm^3 | GRINDING RATIO | WORKPIECE $R_a \mu\text{m}$ |
|----------|-----------------------------|--------------------------|----------------|-----------------------------|
| 1 | .13 | .03 | 4.5 | 2.13 |
| 5 | .60 | .10 | 6.0 | 1.83 |
| 10 | 1.26 | .16 | 7.9 | 1.58 |
| 15 | 1.93 | .21 | 9.2 | 1.23 |
| 20 | 2.46 | .25 | 9.8 | .98 |
| 25 | 3.12 | .28 | 11.1 | .85 |
| 30 | 3.77 | .30 | 12.6 | .75 |
| 40 | 5.08 | .33 | 15.4 | .75 |
| 60 | 7.68 | .39 | 19.7 | .88 |
| 80 | 10.25 | .40 | 25.6 | .78 |
| 100 | 12.78 | .43 | 29.7 | .75 |
| | | | | |
| | | | | |
| | | | | |

ROUGH GRINDING

TEST NO:- 5

DIAMOND NO:- 71784/2

DRESSING CONDITION:-IN-FEED 25 μ m CROSS-FEED .3 mm/rev

GRINDING CONDITION:-IN FEED 12.5 μ m CROSS-FEED 13.5 mm/sec

WHEEL TYPE:- 32A60-K8VBE ϕ :-305 mm nom. SPEED:-1800 rev/min

WORKPIECE MAT.L EN31 ϕ :- 39.5 mm length:-77.3 mm

| PASS NO. | METAL cm ³ REMOVED | WHEEL cm ³ WEAR | GR.D RATIO | WK.PCE. Ra μ m | F _R (N) | F _T (N) |
|----------|-------------------------------|----------------------------|------------|--------------------|--------------------|--------------------|
| 4 | — | .04 | — | 3.50 | | |
| 10 | .60 | .15 | 4.0 | 2.20 | 41.2 | 21.5 |
| 20 | 1.76 | .23 | 7.4 | 2.20 | 44.9 | 24.0 |
| 40 | 4.16 | .34 | 12.4 | 1.58 | 49.0 | 26.1 |
| 60 | 6.41 | .43 | 14.8 | 1.25 | 52.8 | 27.5 |
| 80 | 8.87 | .47 | 18.7 | 1.30 | 53.3 | 28.0 |
| 100 | 11.12 | .51 | 21.4 | 1.25 | 55.6 | 28.5 |
| 120 | 13.40 | .56 | 23.8 | 1.20 | 57.5 | 29.4 |
| 140 | 15.64 | .56 | 27.8 | 1.20 | 58.8 | 30.4 |
| 160 | 17.27 | .60 | 28.5 | 1.13 | 57.8 | 28.5 |
| 200 | 22.04 | .62 | 35.1 | 1.13 | 55.9 | 26.0 |
| 220 | 24.21 | .64 | 37.3 | 1.13 | 54.6 | 25.8 |
| 260 | 28.26 | .67 | 42.2 | 1.13 | 53.3 | 24.6 |
| 300 | 32.29 | .71 | 45.2 | 1.05 | 53.5 | 23.5 |
| 340 | 36.19 | .77 | 46.5 | 1.20 | 52.4 | 23.5 |
| 360 | 38.00 | .82 | 46.3 | 1.13 | 52.0 | 23.5 |
| 380 | 39.82 | .82 | 48.5 | 1.13 | 51.8 | 23.5 |
| 400 | 41.53 | .86 | 48.0 | 1.20 | 51.8 | 23.5 |
| 440 | 45.26 | .90 | 49.9 | 1.13 | 51.5 | 23.8 |
| 480 | 48.73 | .99 | 49.0 | 1.23 | 51.3 | 23.7 |
| 520 | 52.08 | 1.06 | 49.1 | 1.05 | 51.2 | 23.5 |
| 540 | 53.70 | 1.08 | 49.7 | 1.13 | 51.2 | 23.4 |
| 560 | 55.22 | 1.12 | 49.1 | 1.25 | 51.2 | 23.4 |

ROUGH GRINDING

TEST NO:- 6

DIAMOND NO:- 71784/2

DRESSING CONDITION:-IN-FEED 18 μm CROSS-FEED .3 mm/rev

GRINDING CONDITION:-IN FEED 12.5 μm CROSS-FEED 13.5 mm/sec

WHEEL TYPE:- 32A60-K8VBE ϕ :-305 mm nom. SPEED:-1800 rev/min

WORKPIECE MAT'L EN31 ϕ :-50.8 mm length:- 76.6 mm

| PASS NO. | METAL cm^3 REMOVED | WHEEL cm^3 WEAR | GR.D RATIO | WK.PCE. R_a μm | F_R (N) | F_T (N) |
|----------|-----------------------------|--------------------------|------------|-----------------------------|-----------|-----------|
| 4 | .38 | .01 | 29.0 | 3.00 | 48.0 | 24.0 |
| 10 | 1.31 | .04 | 30.7 | 2.75 | 48.4 | 25.5 |
| 20 | 2.86 | .08 | 32.9 | 2.28 | 49.7 | 26.5 |
| 40 | 5.84 | .16 | 36.4 | 2.20 | 51.9 | 27.8 |
| 60 | 8.80 | .21 | 40.7 | 1.65 | 54.5 | 28.3 |
| 80 | 11.80 | .25 | 45.6 | 1.60 | 58.0 | 29.5 |
| 100 | 14.70 | .29 | 50.7 | 1.30 | 60.0 | 30.4 |
| 140 | 20.47 | .32 | 63.1 | 1.43 | 61.0 | 28.4 |
| 180 | 26.13 | .36 | 71.2 | 1.23 | 60.4 | 28.4 |
| 220 | 31.67 | .45 | 69.8 | 1.25 | 59.0 | 27.1 |
| 260 | 37.15 | .56 | 66.1 | 1.23 | 58.5 | 26.0 |
| 300 | 42.31 | .69 | 61.2 | 1.38 | 58.0 | 25.8 |
| 340 | 47.48 | .82 | 57.8 | 1.30 | 57.0 | 25.5 |
| 380 | 52.40 | .95 | 55.0 | 1.35 | 57.0 | 25.3 |
| 420 | 57.40 | 1.08 | 53.1 | 1.25 | 56.8 | 24.7 |
| 460 | 62.11 | 1.20 | 51.4 | 1.33 | 56.6 | 24.6 |
| | | | | | | |
| | | | | | | |
| | | | | | | |
| | | | | | | |
| | | | | | | |
| | | | | | | |
| | | | | | | |

ROUGH GRINDING

TEST NO:- 7

DIAMOND NO:- 71784/2

DRESSING CONDITION:-IN-FEED 12.5 μm CROSS-FEED .3 mm/revGRINDING CONDITION:-IN FEED 125 μm CROSS-FEED 13.5 mm/secWHEEL TYPE:- 32A60-K8VBE ϕ :-305 mm nom. SPEED:-1800 rev/minWORKPIECE MAT.L EN31 ϕ :- 48.5 mm length:- 75.5 mm

| PASS NO. | METAL cm^3 REMOVED | WHEEL cm^3 WEAR | GR.D RATIO | WK.PCE. R_a μm | F_R (N) | F_T (N) |
|----------|-----------------------------|--------------------------|------------|-----------------------------|-----------|-----------|
| 4 | .14 | ——— | ——— | 2.85 | 45.0 | 24.0 |
| 10 | 1.02 | .02 | 47.9 | 2.00 | 51.4 | 26.0 |
| 20 | 2.47 | .04 | 58.0 | 1.98 | 51.5 | 27.0 |
| 40 | 5.36 | .08 | 61.7 | 1.85 | 53.2 | 28.3 |
| 60 | 8.21 | .15 | 54.5 | 1.75 | 56.5 | 29.0 |
| 80 | 11.03 | .17 | 63.5 | 1.70 | 60.0 | 30.8 |
| 100 | 13.83 | .21 | 63.9 | 1.70 | 61.0 | 31.4 |
| 120 | 16.51 | .23 | 69.5 | 1.38 | 63.2 | 31.6 |
| 160 | 21.88 | .25 | 84.5 | 1.25 | 64.0 | 32.0 |
| 200 | 27.06 | .28 | 96.0 | 1.23 | 64.0 | 31.1 |
| 240 | 32.25 | .32 | 99.4 | 1.25 | 62.5 | 30.2 |
| 280 | 37.25 | .34 | 107.7 | 1.23 | 61.0 | 27.8 |
| 320 | 42.21 | .39 | 108.2 | 1.28 | 60.0 | 27.0 |
| 360 | 46.92 | .43 | 108.5 | 1.38 | 59.0 | 26.5 |
| 400 | 51.62 | .49 | 103.6 | 1.25 | 59.0 | 26.2 |
| 440 | 56.43 | .54 | 104.4 | 1.20 | 59.0 | 26.0 |
| 480 | 60.94 | .58 | 104.5 | 1.23 | 58.9 | 25.8 |
| 520 | 65.22 | .64 | 100.5 | 1.20 | 58.9 | 25.8 |
| 560 | 69.38 | .69 | 100.3 | 1.20 | 59.0 | 25.8 |
| | | | | | | |
| | | | | | | |
| | | | | | | |
| | | | | | | |

ROUGH GRINDING

TEST NO:- 8

DIAMOND NO:- 71784/2

DRESSING CONDITION:-IN-FEED 5 μm CROSS-FEED 3 mm/rev

GRINDING CONDITION:-IN FEED 12.5 μm CROSS-FEED 13.5 mm/sec

WHEEL TYPE:- 32A60-K8VBE ϕ :-305 mm nom. SPEED:-1800 rev/min

WORKPIECE MAT.L EN31 ϕ :- 34.4 mm length:- 75.5 mm

| PASS NO. | METAL cm^3 REMOVED | WHEEL cm^3 WEAR | GR.D RATIO | WK.PCE. Ra μm | F_R (N) | F_T (N) |
|----------|-----------------------------|--------------------------|------------|-----------------------------------|-----------|-----------|
| 4 | .26 | ———— | ———— | .95 | 62.0 | 31.0 |
| 10 | .98 | .01 | 119.6 | .75 | 62.5 | 31.2 |
| 30 | 3.08 | .02 | 144.6 | .80 | 64.5 | 31.9 |
| 50 | 5.09 | .04 | 119.5 | .83 | 66.0 | 34.3 |
| 70 | 7.12 | .06 | 108.6 | .88 | 66.5 | 36.0 |
| 90 | 9.07 | .08 | 110.7 | .93 | 66.4 | 36.0 |
| 110 | 10.99 | .10 | 110.0 | .95 | 68.0 | 37.0 |
| 150 | 14.74 | .12 | 119.9 | 1.13 | 71.0 | 36.9 |
| 190 | 18.32 | .15 | 121.5 | 1.00 | 70.5 | 37.0 |
| 230 | 21.83 | .16 | 136.4 | 1.18 | 69.5 | 36.8 |
| 270 | 25.21 | .17 | 145.1 | 1.20 | 66.9 | 34.9 |
| 310 | 28.48 | .19 | 149.8 | 1.25 | 65.3 | 32.8 |
| 350 | 31.61 | .20 | 151.9 | 1.20 | 63.9 | 30.0 |
| 390 | 34.49 | .22 | 153.6 | 1.13 | 62.8 | 28.0 |
| 430 | 37.45 | .23 | 157.6 | 1.10 | 62.0 | 26.9 |
| 470 | 40.15 | .26 | 149.4 | 1.10 | 61.3 | 26.4 |
| 510 | 42.81 | .28 | 151.9 | 1.10 | 60.8 | 26.2 |
| 550 | 45.31 | .30 | 149.5 | 1.05 | 60.6 | 26.2 |
| 590 | 47.84 | .32 | 147.4 | 1.10 | 60.2 | 26.2 |
| | | | | | | |
| | | | | | | |
| | | | | | | |
| | | | | | | |

ROUGH GRINDING

TEST NO:- 9

DIAMOND NO:- 71784/2

DRESSING CONDITION:-IN-FEED 25 μm CROSS-FEED .1 mm/revGRINDING CONDITION:-IN FEED 12.5 μm CROSS-FEED 13.5 mm/secWHEEL TYPE:- 32A60-K8VBE ϕ :-305 mm nom. SPEED:-1800 rev/minWORKPIECE MAT.L EN31 ϕ :- 50.4 mm length:-75.5 mm

| PASS NO. | METAL cm^3 REMOVED | WHEEL cm^3 WEAR | GR.D RATIO | WK.PCE. R_a μm | F_R (N) | F_T (N) |
|----------|-----------------------------|--------------------------|------------|-----------------------------|-----------|-----------|
| 4 | .30 | .03 | 7.6 | 1.38 | | |
| 10 | 1.21 | .10 | 11.2 | 1.05 | 37.5 | 20.3 |
| 20 | 2.72 | .16 | 16.1 | 1.13 | 45.6 | 24.2 |
| 40 | 5.62 | .22 | 25.0 | 1.10 | 50.6 | 27.8 |
| 60 | 8.59 | .27 | 31.6 | 1.13 | 54.3 | 28.4 |
| 80 | 11.45 | .30 | 37.8 | 1.15 | 56.5 | 28.5 |
| 100 | 14.36 | .33 | 43.2 | 1.15 | 57.3 | 28.7 |
| 140 | 19.79 | .41 | 48.1 | 1.13 | 59.0 | 28.0 |
| 180 | 25.33 | .51 | 49.2 | 1.38 | 57.0 | 26.5 |
| 220 | 30.67 | .65 | 46.7 | 1.40 | 54.7 | 25.9 |
| 260 | 35.90 | .81 | 43.9 | 1.50 | 53.2 | 25.9 |
| 300 | 40.89 | 1.01 | 40.2 | 1.55 | 51.5 | 25.3 |
| 340 | 46.02 | 1.18 | 38.7 | 1.45 | 50.0 | 24.8 |
| 380 | 50.78 | 1.36 | 37.3 | 1.40 | 49.2 | 24.2 |
| 420 | 55.67 | 1.54 | 36.1 | 1.40 | 48.2 | 23.8 |
| 460 | 60.43 | 1.73 | 34.9 | 1.35 | 47.8 | 23.5 |
| 500 | 64.90 | 1.91 | 33.9 | 1.50 | 47.3 | 23.3 |
| 540 | 69.32 | 2.07 | 33.4 | 1.38 | 47.0 | 23.2 |
| | | | | | | |
| | | | | | | |
| | | | | | | |
| | | | | | | |
| | | | | | | |

ROUGH GRINDING

TEST NO:- 10

DIAMOND NO:- 71784/2

DRESSING CONDITION:-IN-FEED 18 μm CROSS-FEED .1 mm/revGRINDING CONDITION:-IN FEED 12.5 μm CROSS-FEED 13.5 mm/secWHEEL TYPE:- 32A60-K8VBE ϕ :-305 mm nom. SPEED:-1800 rev/minWORKPIECE MAT.L EN31 ϕ :- 36.4 mm length:-75.7 mm

| PASS NO. | METAL cm^3 REMOVED | WHEEL cm^3 WEAR | GR.D RATIO | WK.PCE. R_a μm | F_R (N) | F_T (N) |
|----------|-----------------------------|--------------------------|------------|-----------------------------|-----------|-----------|
| 4 | .43 | .04 | 9.0 | 1.13 | 42.3 | 24.2 |
| 10 | 1.04 | .09 | 11.5 | .90 | 46.0 | 25.0 |
| 20 | 2.13 | .13 | 15.9 | .83 | 48.8 | 26.6 |
| 40 | 4.23 | .18 | 23.3 | .80 | 52.5 | 28.7 |
| 60 | 6.36 | .22 | 28.7 | .95 | 56.0 | 30.4 |
| 80 | 8.40 | .24 | 35.0 | .85 | 58.4 | 30.4 |
| 100 | 10.47 | .25 | 40.4 | .85 | 60.5 | 30.6 |
| 140 | 14.41 | .28 | 50.5 | 1.00 | 61.9 | 31.2 |
| 180 | 18.33 | .31 | 58.0 | 1.00 | 62.0 | 31.0 |
| 220 | 22.13 | .33 | 65.6 | 1.03 | 62.1 | 30.8 |
| 260 | 25.76 | .37 | 69.3 | 1.03 | 62.5 | 30.9 |
| 300 | 29.31 | .39 | 73.6 | 1.03 | 61.7 | 31.0 |
| 340 | 32.78 | .43 | 75.8 | 1.05 | 60.9 | 31.0 |
| 380 | 36.09 | .46 | 77.3 | 1.03 | 59.0 | 30.1 |
| 420 | 39.16 | .50 | 78.1 | 1.03 | 57.4 | 29.5 |
| 460 | 42.26 | .54 | 77.4 | 1.05 | 57.0 | 29.2 |
| 500 | 45.48 | .58 | 78.4 | 1.13 | 56.3 | 28.8 |
| 540 | 47.98 | .61 | 78.7 | 1.08 | 56.0 | 28.8 |
| 580 | 50.65 | .65 | 77.7 | 1.13 | 55.9 | 29.0 |
| 620 | 53.22 | .69 | 76.4 | 1.13 | 55.3 | 29.0 |
| | | | | | | |
| | | | | | | |
| | | | | | | |

ROUGH GRINDING

TEST NO:- 11

DIAMOND NO:- 71784/2

DRESSING CONDITION:-IN-FEED 12.5 μm CROSS-FEED .1 mm/revGRINDING CONDITION:-IN FEED 12.5 μm CROSS-FEED 13.5 mm/secWHEEL TYPE:- 32A60-K8VBE ϕ :-305 mm nom. SPEED:-1800 rev/minWORKPIECE MAT.L EN31 ϕ :- 37 mm length:- 75.5 mm

| PASS NO. | METAL cm^3 REMOVED | WHEEL cm^3 WEAR | GR.D RATIO | WK.PCE. R_a μm | F_R (N) | F_T (N) |
|----------|-----------------------------|--------------------------|------------|-----------------------------|-----------|-----------|
| 4 | .22 | .02 | 10.3 | 1.08 | | |
| 10 | .88 | .06 | 13.4 | .98 | 48.0 | 27.0 |
| 20 | 1.94 | .11 | 16.7 | 1.00 | 51.0 | 30.0 |
| 40 | 4.07 | .17 | 23.4 | .95 | 55.2 | 31.5 |
| 60 | 6.35 | .20 | 30.5 | .95 | 58.2 | 33.5 |
| 80 | 8.36 | .23 | 35.7 | .95 | 62.0 | 33.0 |
| 100 | 10.40 | .25 | 41.5 | .95 | 63.8 | 34.0 |
| 140 | 14.46 | .28 | 51.3 | 1.00 | 65.0 | 33.9 |
| 180 | 18.44 | .30 | 60.8 | .95 | 65.0 | 33.7 |
| 220 | 22.30 | .32 | 68.7 | .95 | 65.0 | 33.6 |
| 260 | 26.04 | .34 | 75.3 | 1.03 | 65.0 | 33.0 |
| 300 | 29.66 | .36 | 81.5 | 1.05 | 63.8 | 33.4 |
| 340 | 33.16 | .39 | 85.0 | 1.03 | 62.3 | 33.2 |
| 380 | 36.53 | .41 | 88.8 | 1.03 | 60.0 | 32.2 |
| 420 | 39.78 | .44 | 90.2 | 1.05 | 59.2 | 30.5 |
| 460 | 42.91 | .48 | 89.4 | 1.03 | 58.5 | 29.5 |
| 500 | 45.91 | .51 | 88.4 | 1.03 | 57.8 | 29.0 |
| 540 | 48.80 | .55 | 88.1 | 1.03 | 57.3 | 28.8 |
| | | | | | | |
| | | | | | | |
| | | | | | | |
| | | | | | | |
| | | | | | | |

ROUGH GRINDING

TEST NO:- 12

DIAMOND NO:- 71784/2

DRESSING CONDITION:-IN-FEED 5 μm CROSS-FEED .1 mm/rev

GRINDING CONDITION:-IN FEED 12.5 μm CROSS-FEED 13.5 mm/sec

WHEEL TYPE:- 32A60-K8VBE ϕ :-305 mm nom. SPEED:-1800 rev/min

WORKPIECE MAT.L EN31 ϕ :- 50.8mm length:-75.7 mm

| PASS NO. | METAL cm^3 REMOVED | WHEEL cm^3 WEAR | GR.D RATIO | WK.PCE. R_a μm | F_R (N) | F_T (N) |
|----------|-----------------------------|--------------------------|------------|-----------------------------|-----------|-----------|
| 4 | .38 | .02 | 17.8 | 1.15 | | |
| 10 | 1.29 | .05 | 24.6 | 1.00 | 61.6 | 33.8 |
| 20 | 2.80 | .08 | 32.2 | 1.00 | 61.6 | 33.7 |
| 40 | 5.80 | .12 | 44.8 | .95 | 62.0 | 33.8 |
| 60 | 8.70 | .17 | 50.1 | .90 | 65.3 | 35.0 |
| 80 | 11.64 | .20 | 55.9 | .95 | 66.6 | 35.1 |
| 100 | 14.55 | .23 | 61.2 | .98 | 67.0 | 35.0 |
| 140 | 20.28 | .29 | 69.1 | 1.05 | 67.4 | 34.9 |
| 180 | 25.75 | .34 | 74.5 | 1.05 | 67.0 | 34.5 |
| 220 | 31.16 | .39 | 78.3 | 1.15 | 63.5 | 32.1 |
| 260 | 36.40 | .47 | 76.6 | 1.25 | 60.2 | 30.1 |
| 300 | 41.51 | .60 | 68.5 | 1.30 | 58.0 | 29.0 |
| 340 | 46.64 | .74 | 62.7 | 1.28 | 56.9 | 27.8 |
| 380 | 51.52 | .92 | 55.4 | 1.30 | 55.8 | 27.5 |
| 420 | 56.28 | 1.12 | 50.1 | 1.30 | 55.0 | 27.4 |
| 460 | 60.93 | 1.34 | 45.2 | 1.30 | 54.5 | 27.1 |
| | | | | | | |
| | | | | | | |
| | | | | | | |
| | | | | | | |
| | | | | | | |
| | | | | | | |
| | | | | | | |

ROUGH GRINDING

TEST NO:- 13

DIAMOND NO:- 71784/2

DRESSING CONDITION:-IN-FEED 25 μ m CROSS-FEED .5 mm/rev

GRINDING CONDITION:-IN FEED 12.5 μ m CROSS-FEED 13.5 mm/sec

WHEEL TYPE:- 32A60-K8VBE ϕ :-305 mm nom. SPEED:-1800 rev/min

WORKPIECE MAT.L EN31 ϕ :- 50.9 mm length:-76.2 mm

| PASS NO. | METAL cm ³ REMOVED | WHEEL cm ³ WEAR | GR.D RATIO | WK.PCE. Ra μ m | F _R (N) | F _T (N) |
|----------|-------------------------------|----------------------------|------------|--------------------|--------------------|--------------------|
| 4 | .31 | — | — | 3.00 | | |
| 10 | 1.24 | .02 | 58.2 | 2.70 | 35.0 | 11.0 |
| 20 | 2.77 | .10 | 27.7 | 2.20 | 43.0 | 22.5 |
| 40 | 5.75 | .20 | 27.4 | 2.00 | 49.8 | 25.0 |
| 60 | 8.70 | .35 | 24.4 | 1.75 | 54.5 | 28.5 |
| 80 | 11.54 | .62 | 18.3 | 1.50 | 56.5 | 30.0 |
| 100 | 14.21 | .97 | 14.6 | 1.52 | 57.3 | 30.0 |
| 140 | 19.47 | 1.78 | 10.9 | 1.55 | 60.0 | 29.5 |
| 180 | 25.06 | 2.05 | 12.2 | 1.52 | 60.6 | 28.2 |
| 220 | 30.45 | 2.37 | 12.8 | 1.47 | 59.0 | 28.0 |
| 260 | 35.67 | 2.72 | 13.1 | 1.42 | 57.0 | 27.5 |
| 300 | 40.84 | 3.12 | 13.1 | 1.50 | 54.8 | 26.9 |
| 340 | 45.89 | 3.23 | 14.2 | 1.62 | 53.8 | 26.5 |
| 380 | 50.84 | 3.44 | 14.8 | 1.45 | 52.6 | 26.0 |
| 420 | 55.61 | 3.84 | 14.5 | 1.50 | 52.0 | 25.8 |
| | | | | | | |
| | | | | | | |
| | | | | | | |
| | | | | | | |
| | | | | | | |
| | | | | | | |
| | | | | | | |
| | | | | | | |

ROUGH GRINDING

TEST NO:- 14

DIAMOND NO:- 71784/2

DRESSING CONDITION:-IN-FEED 18 μm CROSS-FEED .5 mm/rev

GRINDING CONDITION:-IN FEED 12.5 μm CROSS-FEED 13.5 mm/sec

WHEEL TYPE:- 32A60-K8VBE ϕ :-305 mm nom. SPEED:-1800 rev/min

WORKPIECE MAT.L EN31 ϕ :-50.7 mm length:-76.3 mm

| PASS NO. | METAL cm^3 REMOVED | WHEEL cm^3 WEAR | GR.D RATIO | WK.PCE. R_a μm | F_R (N) | F_T (N) |
|----------|-----------------------------|--------------------------|------------|-----------------------------|-----------|-----------|
| 4 | .38 | — | — | 3.00 | 46.0 | 20.0 |
| 10 | 1.38 | .04 | 34.5 | 2.65 | 48.4 | 23.8 |
| 20 | 2.99 | .08 | 35.8 | 2.37 | 51.5 | 27.8 |
| 40 | 5.88 | .16 | 35.2 | 2.17 | 55.0 | 30.9 |
| 60 | 8.97 | .25 | 35.5 | 2.15 | 57.0 | 31.2 |
| 80 | 11.88 | .29 | 40.5 | 2.12 | 61.0 | 31.2 |
| 100 | 14.71 | .39 | 36.9 | 1.70 | 61.0 | 31.0 |
| 140 | 20.35 | .67 | 30.3 | 1.70 | 60.5 | 30.0 |
| 180 | 25.76 | 1.27 | 20.1 | 1.70 | 59.4 | 29.0 |
| 220 | 31.13 | 1.59 | 19.5 | 1.62 | 56.8 | 27.8 |
| 260 | 36.38 | 1.80 | 20.1 | 1.55 | 55.3 | 27.2 |
| 300 | 41.56 | 1.91 | 21.8 | 1.52 | 54.1 | 26.0 |
| 340 | 46.81 | 2.01 | 23.2 | 1.50 | 53.3 | 25.4 |
| 380 | 51.83 | 2.09 | 24.7 | 1.50 | 52.5 | 25.4 |
| 420 | 56.68 | 2.18 | 25.9 | 1.50 | 51.5 | 25.0 |
| | | | | | | |
| | | | | | | |
| | | | | | | |
| | | | | | | |
| | | | | | | |
| | | | | | | |
| | | | | | | |
| | | | | | | |

ROUGH GRINDING

TEST NO:- 15

DIAMOND NO:- 71784/2

DRESSING CONDITION:-IN-FEED 12.5 μm CROSS-FEED .5 mm/revGRINDING CONDITION:-IN FEED 12.5 μm CROSS-FEED 13.5 mm/secWHEEL TYPE:- 32A60-K8VBE ϕ :-305 mm nom. SPEED:-1800 rev/minWORKPIECE MAT.L EN31 ϕ :- 50.9 mm length:- 76.2 mm

| PASS NO. | METAL cm^3 REMOVED | WHEEL cm^3 WEAR | GR.D RATIO | WK.PCE. R_a μm | F_R (N) | F_T (N) |
|----------|-----------------------------|--------------------------|------------|-----------------------------|-----------|-----------|
| 4 | .30 | — | — | 2.40 | 57.6 | 31.0 |
| 10 | 1.38 | — | — | 2.37 | 63.0 | 32.5 |
| 20 | 2.92 | .02 | 146.0 | 2.30 | 66.5 | 34.0 |
| 40 | 6.12 | .05 | 122.5 | 2.07 | 67.5 | 33.0 |
| 60 | 8.95 | .10 | 89.5 | 1.82 | 67.0 | 31.9 |
| 80 | 11.91 | .21 | 56.7 | 1.70 | 63.0 | 29.0 |
| 100 | 14.71 | .41 | 35.9 | 1.50 | 59.0 | 27.2 |
| 140 | 20.04 | 1.15 | 17.4 | 1.45 | 58.0 | 26.7 |
| 180 | 25.47 | 1.49 | 17.1 | 1.45 | 56.2 | 25.7 |
| 220 | 30.93 | 1.86 | 16.6 | 1.47 | 53.6 | 24.5 |
| 260 | 36.07 | 2.33 | 15.5 | 1.42 | 52.4 | 24.0 |
| 300 | 41.30 | 2.66 | 15.5 | 1.35 | 51.8 | 23.6 |
| 340 | 46.15 | 3.10 | 14.9 | 1.45 | 51.0 | 23.0 |
| 380 | 51.09 | 3.42 | 14.9 | 1.47 | 50.8 | 23.0 |
| 420 | 55.79 | 3.84 | 14.5 | 1.52 | 50.0 | 23.0 |
| | | | | | | |
| | | | | | | |
| | | | | | | |
| | | | | | | |
| | | | | | | |
| | | | | | | |
| | | | | | | |
| | | | | | | |
| | | | | | | |

ROUGH GRINDING

TEST NO:- 16

DIAMOND NO:- 71784/2

DRESSING CONDITION:-IN-FEED 5 μ m CROSS-FEED .5 mm/rev

GRINDING CONDITION:-IN FEED 125 μ m CROSS-FEED 13.5 mm/sec

WHEEL TYPE:- 32A60-K8VBE ϕ :-305 mm nom. SPEED:-1800 rev/min

WORKPIECE MAT.L EN31 ϕ :- 40.7 mm length:- 76.2 mm

| PASS NO. | METAL cm ³ REMOVED | WHEEL cm ³ WEAR | GR.D RATIO | WK.PCE. Ra μ m | F _R (N) | F _T (N) |
|----------|-------------------------------|----------------------------|------------|--------------------|--------------------|--------------------|
| 4 | .43 | — | — | .80 | 78.8 | 40.9 |
| 10 | 1.13 | .02 | 56.5 | 1.25 | 86.5 | 43.6 |
| 20 | 2.36 | .02 | 118.0 | 1.25 | 92.6 | 45.0 |
| 40 | 4.77 | .04 | 119.3 | 1.25 | 88.6 | 42.0 |
| 60 | 7.17 | .08 | 89.6 | 1.22 | 86.0 | 41.2 |
| 80 | 9.54 | .08 | 119.3 | 1.25 | 82.8 | 40.0 |
| 100 | 11.82 | .14 | 84.4 | 1.17 | 82.3 | 40.0 |
| 140 | 16.35 | .19 | 86.1 | 1.32 | 76.8 | 37.0 |
| 180 | 20.80 | .25 | 83.2 | 1.47 | 73.7 | 34.2 |
| 220 | 25.05 | .41 | 61.1 | 1.52 | 71.4 | 33.0 |
| 260 | 29.15 | .68 | 42.9 | 1.52 | 69.9 | 32.0 |
| 300 | 33.27 | .77 | 43.2 | 1.40 | 67.2 | 30.6 |
| 340 | 37.15 | .92 | 40.4 | 1.50 | 64.9 | 30.3 |
| 380 | 40.91 | 1.08 | 37.9 | 1.47 | 62.5 | 30.0 |
| 420 | 44.60 | 1.21 | 36.9 | 1.40 | 60.5 | 28.9 |
| 460 | 48.12 | 1.30 | 37.0 | 1.45 | 58.5 | 28.4 |
| 500 | 51.52 | 1.46 | 35.3 | 1.55 | 57.3 | 28.0 |
| 540 | 54.86 | 1.62 | 33.9 | 1.50 | 54.8 | 27.5 |
| 580 | 58.09 | 1.72 | 33.8 | 1.45 | 52.9 | 27.5 |
| | | | | | | |
| | | | | | | |
| | | | | | | |
| | | | | | | |

ROUGH GRINDING

TEST NO:- 17

DIAMOND NO:- 71784/2

DRESSING CONDITION:-IN-FEED 12.5 μ m CROSS-FEED .3 mm/rev

GRINDING CONDITION:-IN FEED 5 μ m CROSS-FEED 13.5 mm/sec

WHEEL TYPE:- 32A60-K8VBE ϕ :-305 mm nom. SPEED:-1800 rev/min

WORKPIECE MAT.L EN31 ϕ :- 39.3 mm length:- 76.6 mm

| PASS NO. | METAL cm ³ REMOVED | WHEEL cm ³ WEAR | GR.D RATIO | WK.PCE. Ra μ m | F _R (N) | F _T (N) |
|----------|-------------------------------|----------------------------|------------|--------------------|--------------------|--------------------|
| 10 | .36 | — | — | 2.65 | | |
| 26 | 1.14 | .01 | 114.0 | 2.28 | | |
| 50 | 2.21 | .02 | 110.5 | 2.00 | | |
| 100 | 4.57 | .06 | 76.2 | 1.95 | | |
| 150 | 6.90 | .10 | 69.0 | 1.53 | | |
| 200 | 9.14 | .13 | 70.3 | 1.58 | | |
| 250 | 11.41 | .15 | 74.0 | 1.28 | | |
| 350 | 15.85 | .21 | 75.5 | 1.13 | | |
| 450 | 20.17 | .23 | 87.7 | .88 | | |
| 550 | 24.37 | .26 | 93.7 | .85 | | |
| 650 | 28.44 | .28 | 101.6 | .78 | | |
| 750 | 32.36 | .30 | 107.9 | .63 | | |
| 850 | 36.14 | .32 | 112.9 | .70 | | |
| 950 | 39.81 | .33 | 120.6 | .63 | | |
| 1050 | 43.38 | .35 | 123.9 | .60 | | |
| 1150 | 46.83 | .37 | 126.6 | .60 | | |
| 1250 | 50.24 | .38 | 132.2 | .63 | | |
| 1350 | 53.40 | .40 | 133.5 | .63 | | |
| | | | | | | |
| | | | | | | |
| | | | | | | |
| | | | | | | |
| | | | | | | |

ROUGH GRINDING

TEST NO:- 18

DIAMOND NO:- 71784/2

DRESSING CONDITION:-IN-FEED 12.5 μ m CROSS-FEED .1 mm/rev

GRINDING CONDITION:-IN FEED 5 μ m CROSS-FEED 13.5 mm/sec

WHEEL TYPE:- 32A60-K8VBE ϕ :-305 mm nom. SPEED:-1800 rev/min

WORKPIECE MAT.L EN31 ϕ :- 50.7 mm length:- 76.2 mm

| PASS NO. | METAL cm ³ REMOVED | WHEEL cm ³ WEAR | GR.D RATIO | WK.PCE. Ra μ m | F _R (N) | F _T (N) |
|----------|-------------------------------|----------------------------|------------|--------------------|--------------------|--------------------|
| 10 | .46 | .03 | 15.3 | 1.05 | | |
| 26 | 1.46 | .06 | 24.3 | .85 | | |
| 50 | 2.92 | .12 | 24.3 | .75 | | |
| 100 | 5.86 | .15 | 39.1 | .75 | | |
| 150 | 8.81 | .18 | 48.9 | .75 | | |
| 200 | 11.71 | .19 | 61.6 | .70 | | |
| 250 | 14.66 | .20 | 73.3 | .70 | | |
| 350 | 20.32 | .21 | 96.7 | .68 | | |
| 450 | 25.94 | .24 | 108.1 | .70 | | |
| 550 | 31.36 | .27 | 116.1 | .70 | | |
| 650 | 36.81 | .30 | 122.7 | .73 | | |
| 750 | 42.13 | .31 | 135.9 | .63 | | |
| 850 | 47.32 | .35 | 135.2 | .63 | | |
| 950 | 52.32 | .36 | 145.3 | .63 | | |
| 1050 | 57.22 | .39 | 146.7 | .63 | | |
| 1150 | 62.05 | .42 | 147.7 | .68 | | |
| 1250 | 66.64 | .45 | 148.1 | .70 | | |
| 1350 | 71.22 | .48 | 148.4 | .68 | | |
| 1450 | 75.64 | .51 | 148.3 | .65 | | |
| 1550 | 79.89 | .54 | 147.9 | .80 | | |
| 1650 | 84.08 | .58 | 145.0 | .73 | | |
| 1750 | 88.17 | .62 | 142.2 | .75 | | |
| 1850 | 92.14 | .67 | 137.5 | .78 | | |

TEST NO:- 18 cont.

WORKPIECE MAT.L EN31 ϕ :- 50.7 mm length:- 76.2 mm

[illegible]

FINE GRINDING

TEST NOS 19 to 22
inclusive

DIAMOND NO:- 63794/2

WHEEL TYPE:- 32A60-K8VBE ϕ :-305mm nom. SPEED:-GRINDING IN-FEED:- $5\mu\text{m}(\text{radial})$ 1800 rev/min

| DRESSING ↓ CONDITION | WORK PIECE ϕ mm | CROSS FEED mm/sec | WORK PIECE Ra μm | F_R (N) | F_T (N) |
|---|----------------------------|-------------------------|-----------------------------------|--------------|--------------|
| TEST NO:-19 In-feed:- 25 μm Cross-feed:- .5 mm/rev | 50.8 | 14 | 2.00 | 11.0 | 6.4 |
| | " | 12 | 2.15 | 10.0 | 5.5 |
| | " | 10 | 2.00 | 6.0 | 3.8 |
| | " | 7.5 | 1.38 | 5.9 | 3.5 |
| | " | 5 | 1.03 | 3.6 | 2.0 |
| TEST NO:-20 In-feed:- 17.5 μm Cross-feed:- .5 mm/rev | 50.6 | 14 | 2.05 | 17.8 | 9.1 |
| | " | 12 | 1.88 | 15.0 | 7.8 |
| | " | 10 | 1.50 | 10.0 | 5.8 |
| | " | 7.5 | 1.00 | 7.6 | 5.0 |
| | " | 5 | .75 | 4.5 | 3.0 |
| TEST NO:-21 In-feed:- 12.5 μm Cross-feed:- .5mm/rev | 50.4 | 14 | 1.75 | 21.0 | 11.8 |
| | " | 12 | 1.75 | 19.0 | 11.0 |
| | " | 10 | 1.50 | 15.5 | 8.2 |
| | " | 7.5 | .88 | 11.0 | 6.5 |
| | " | 5 | .68 | 6.3 | 4.8 |
| TEST NO:-22 In-feed:- 5 μm Cross-feed:- .5 mm/rev | 50.2 | 14 | 1.20 | 23.2 | 12.0 |
| | " | 12 | 1.18 | 19.8 | 9.8 |
| | " | 10 | .70 | 18.6 | 9.6 |
| | " | 7.5 | .65 | 12.5 | 6.5 |
| | " | 5 | .55 | 7.8 | 3.9 |

FINE GRINDING

TEST NOS 23 to 26
inclusive

DIAMOND NO:- 63794/2

WHEEL TYPE:- 32A60-K8VBE ϕ :-305mm nom. SPEED:-GRINDING IN-FEED:- 5 μ m(radial) 1800 rev/min

| DRESSING ↓ CONDITION | WORK PIECE ϕ mm | CROSS FEED mm/sec | WORK PIECE Ra μ m | F _R (N) | F _T (N) |
|---|----------------------------|-------------------------|-----------------------------|-----------------------|-----------------------|
| TEST NO:- 23 In-feed:- 25 μ m Cross-feed:- .3 mm/rev | 50.0 | 14 | 1.13 | 12.4 | 6.8 |
| | " | 12 | .95 | 11.5 | 6.8 |
| | " | 10 | .98 | 10.5 | 6.3 |
| | " | 7.5 | .75 | 7.2 | 5.2 |
| | " | 5 | .53 | 3.0 | 2.0 |
| TEST NO:-24 In-feed:- 17.5 μ m Cross-feed:- .3 mm/rev | 49.8 | 14 | 1.00 | 13.0 | 8.0 |
| | " | 12 | 1.00 | 9.2 | 5.5 |
| | " | 10 | .90 | 8.5 | 5.2 |
| | " | 7.5 | .73 | 5.8 | 3.6 |
| | " | 5 | .58 | 3.2 | 1.8 |
| TEST NO:-25 In-feed:- 12.5 μ m Cross-feed:- .3 mm/rev | 49.6 | 14 | .83 | 17.0 | 8.8 |
| | " | 12 | .80 | 13.8 | 8.0 |
| | " | 10 | .73 | 9.8 | 5.5 |
| | " | 7.5 | .68 | 6.8 | 4.0 |
| | " | 5 | .50 | 3.5 | 2.0 |
| TEST NO:-26 In-feed:- 5 μ m Cross-feed:- .3 mm/rev | 49.4 | 14 | .75 | 34.0 | 17.2 |
| | " | 12 | .78 | 24.4 | 13.0 |
| | " | 10 | .78 | 21.7 | 11.8 |
| | " | 7.5 | .63 | 16.3 | 9.8 |
| | " | 5 | .53 | 7.8 | 4.3 |

FINE GRINDING

TEST NOS 27 to 30
inclusive

DIAMOND NO:- 63794/2

WHEEL TYPE:- 32A60-K8VBE ϕ :-305mm nom. SPEED:-GRINDING IN-FEED:- 5 μ m(radial)

1800 rev/min

| DRESSING ↓ CONDITION | WORK PIECE ϕ mm | CROSS FEED mm/sec | WORK PIECE Ra μ m | F _R (N) | F _T (N) |
|--|----------------------------|-------------------------|-----------------------------|-----------------------|-----------------------|
| TEST NO:-27 In-feed:- 25 μ m Cross-feed:- .1 mm/rev | 49.2 | 14 | .38 | 21.2 | 11.8 |
| | " | 12 | .38 | 18.5 | 10.2 |
| | " | 10 | .35 | 12.8 | 7.1 |
| | " | 7.5 | .33 | 10.0 | 5.2 |
| | " | 5 | .30 | 5.3 | 3.2 |
| TEST NO:- 28 In-feed:- 17.5 μ m Cross-feed:- .1 mm/rev | 49.0 | 14 | .38 | 22.8 | 12.8 |
| | " | 12 | .33 | 17.6 | 9.2 |
| | " | 10 | .33 | 12.0 | 6.5 |
| | " | 7.5 | .30 | 10.0 | 5.5 |
| | " | 5 | .30 | 5.2 | 3.2 |
| TEST NO:-29 In-feed:- 12.5 μ m Cross-feed:- .1mm/rev | 48.8 | 14 | .33 | 22.0 | 11.8 |
| | " | 12 | .33 | 19.0 | 11.4 |
| | " | 10 | .33 | 12.4 | 6.5 |
| | " | 7.5 | .30 | 10.1 | 5.5 |
| | " | 5 | .28 | 6.0 | 3.5 |
| TEST NO:-30 In-feed:- 5 μ m Cross-feed:- .1mm/rev | 48.6 | 14 | .30 | 34.0 | 17.2 |
| | " | 12 | .30 | 28.2 | 14.8 |
| | " | 10 | .25 | 21.0 | 10.8 |
| | " | 7.5 | .23 | 15.0 | 8.0 |
| | " | 5 | .20 | 6.3 | 3.5 |

